



# Template Directed Synthesis of Molecular Knots

by

Paul Christopher Mayers

Department of Chemistry  
University of Sheffield

Submitted to the University of Sheffield  
as partial fulfilment for the degree of  
Doctor of Philosophy

October 1997

*None but those who have  
experienced them can  
conceive of the enticements  
of science.*

Mary Shelley

## Acknowledgements

First and foremost, I would like to thank my supervisor Professor Chris Hunter. For the last three years, Chris has been a constant source of ideas, encouragement and enthusiasm. I thank him for giving me the opportunity to undertake this project and for all his help and advice as well as for being a really nice guy to work for.

The most important factor in the enjoyment of a PhD (apart from the chemistry?) is the group of people that one works with and the Hunter Group are no exception to this. The sheer number of people who have been part of the group during my time here precludes the possibility of mentioning everyone individually, so I would like to say a collective thankyou to everyone who I have had the chance to work with, whether it be for many years or just a few weeks. Without exception, everyone has made a unique contribution to a happy and interesting group. I must of course say a special thankyou to that select bunch of people who have helped me keep Club 197 and the various West Street eateries in business during the last three years.

I would also like to thank all the staff who are necessary to keep a department such as this running smoothly. Again, there are too many people to mention everyone individually, but special thanks are due to Carole for her constant deliveries of solvents and Denise for her constant (albeit sometimes rationed) supply of tea.

I would also like to thank my industrial supervisor Dr Gloria Breault and indeed everyone at Zeneca Pharmaceuticals whose help (and sometimes patience!) made my 3 month CASE placement a happy one. Special thanks are due to Joy and Trev for providing somewhere to live that was almost too good to leave.

I must also thank everyone who has contributed ideas or suggestions that have helped in any way. Special thanks to Dr Jim Thomas for teaching me all that I know about ruthenium chemistry and Dr Brian Taylor for all his help with the NMR aspects of the work.

Thanks are of course due to Zeneca Pharmaceuticals and EPSRC who provided the crucial funding for this work through a CASE award.

And finally, I must mention the sterling efforts of Fred, Daphne, Shaggy and especially Scooby-Doo himself without whom this thesis would never have come together - Scooby Snacks all round.....

# Summary

## Template Directed Synthesis of Molecular Knots

Paul C. Mayers

The Work described in this thesis was carried out in the Department of Chemistry, University of Sheffield between October 1994 and October 1997. Except where stated to the contrary, this thesis is the result of my own work and contains nothing which is the outcome of work completed in collaboration.

Chapter 1 introduces some important ideas involved in topology and their relationship to molecules both synthetic and naturally occurring. It includes a review of the literature related to the synthesis of topologically complex molecules with particular emphasis on template directed methods and attempts at the preparation of molecular knots. Chapter 2 then introduces my strategy for synthesising molecular knots utilising metal-ligand coordination and templating aromatic interactions.

Chapter 3 outlines the preparation of some octahedral metal complexes and describes attempted direct macrocyclisation reactions to give access to molecular knots.

Chapter 4 discusses some model complexes that have been used to investigate the templating aromatic interactions that form a key component of the design strategy. The influence of solvent and temperature on interactions between strongly polarised aromatic rings are reported.

Chapter 5 then outlines a successful new knot synthesis. Bipyridine oligomers containing appropriate spacers spontaneously fold into a knotted structure in the presence of a metal ion. Detailed characterisation of the molecular knots obtained is provided as well as a discussion of the importance of the oligomer structure and the metal ion. Chapter 6 outlines the potential of these products as topological building blocks for the preparation of a variety of knotted structures and describes attempts to prepare a novel knotted structure which we have termed an *overhand knot*. Finally, the preparation in moderate yield of a molecular trefoil knot is presented.

Full experimental details are given in Chapter 7.

# Summary

## Template Directed Synthesis of Molecular Knots

Paul C. Mayers

The Work described in this thesis was carried out in the Department of Chemistry, University of Sheffield between October 1994 and October 1997. Except where stated to the contrary, this thesis is the result of my own work and contains nothing which is the outcome of work completed in collaboration.

Chapter 1 introduces some important ideas involved in topology and their relationship to molecules both synthetic and naturally occurring. It includes a review of the literature related to the synthesis of topologically complex molecules with particular emphasis on template directed methods and attempts at the preparation of molecular knots. Chapter 2 then introduces my strategy for synthesising molecular knots utilising metal-ligand coordination and templating aromatic interactions.

Chapter 3 outlines the preparation of some octahedral metal complexes and describes attempted direct macrocyclisation reactions to give access to molecular knots.

Chapter 4 discusses some model complexes that have been used to investigate the templating aromatic interactions that form a key component of the design strategy. The influence of solvent and temperature on interactions between strongly polarised aromatic rings are reported.

Chapter 5 then outlines a successful new knot synthesis. Bipyridine oligomers containing appropriate spacers spontaneously fold into a knotted structure in the presence of a metal ion. Detailed characterisation of the molecular knots obtained is provided as well as a discussion of the importance of the oligomer structure and the metal ion. Chapter 6 outlines the potential of these products as topological building blocks for the preparation of a variety of knotted structures and describes attempts to prepare a novel knotted structure which we have termed an *overhand knot*. Finally, the preparation in moderate yield of a molecular trefoil knot is presented.

Full experimental details are given in Chapter 7.

# Table of Contents

Abbreviations	1
<b>Chapter One: Introduction</b>	
1.1 Chemical Topology and Topological Isomerism	
1.1.0 Isomerism in Organic Chemistry	3
1.1.1 An Introduction to Topology	4
1.1.2 Relation of Geometry to Chemical Isomerism	5
1.1.3 Chirality in Topological Isomers	5
1.2 Topological Targets for Chemical Synthesis	6
1.3 Topological Isomers in Nature	
1.3.0 DNA Knots and Catenanes	7
1.3.1 DNA Supercoiling	8
1.3.2 Knots in Proteins	9
1.3.3 Synthesis Using DNA Building Blocks	10
1.4 Early Attempts at Synthesis of Topologically Complex Molecules	
1.4.0 The First Statistical Catenane Synthesis	11
1.4.1 Possibilities for Extension to Molecular Knots	12
1.4.2 The First Statistical Rotaxane Synthesis	13
1.4.3 Improved Statistical Methods for the Preparation of Catenanes	14
1.4.4 Topological Isomers From a Molecular Möbius Strip	15
1.5. Tempered Synthesis	
1.5.0 Classification of Templates	17
1.5.1 Cyclisation Templates - Metal ions	17
1.5.2 Cyclisation Templates - Organic Molecules	19
1.6 Tempered Synthesis of Catenanes and Rotaxanes	
1.6.0 Covalent Templating of a Catenane	21
1.6.1 Metal Ion Tempered Catenane and Rotaxane Syntheses	22
1.6.2 Catenanes and Rotaxanes Tempered by Aromatic Interactions	24
1.6.3 Catenanes Tempered by Hydrogen Bonding	27
1.6.4 Other Tempered Syntheses of Rotaxanes and Catenanes	29

**1.7 Templat ed Synthesis of Molecular Knots**

1.7.0 Attempted Synthesis Using a Covalent Template	30
1.7.1 Attempted Templat ed Synthesis via a Möbius Strip	30
1.7.2 The "Hook and Ladder" Approach to a Templat ed Möbius Strip	31
1.7.3 A Metal Ion Templat ed Synthesis of a Molecular Trefoil Knot	32
1.7.4 Extension to More Complex Topologies	33
1.7.5 Composite Molecular Knots	35
1.7.6 A Trefoil Knot Templat ed by an Octahedral Metal Ion	36

**Chapter Two: Design Strategy****2.1 Approach**

2.1.0 Tris-Bipyridine Complexes	38
2.1.1 A Secondary Template Effect	39
2.1.2 Molecular Modelling and Final Design	40
2.2 Folding Strategy	43

**Chapter Three: Synthesis and Macrocyclisation of Metal Complexes****3.1 Synthesis of Building Blocks**

3.1.0 The Bipyridine Unit	45
3.1.1 The Bisphenol Unit	46

**3.2 Synthesis of Metal Complexes**

3.2.0 General Procedures	47
3.2.1 Synthesis of Ruthenium (II) Complexes	47
3.2.2 Synthesis of Iron (II) Complexes	48

**3.3 Attempted Macrocyclisation via Formation of Ether Links**

3.3.0 Model Reactions	50
3.3.1 Iron (II) Complexes	51
3.3.2 Ruthenium (II) Complexes	52

**3.4 Macrocyclisation via Formation of Ester Links**

3.4.0 Model Reactions	53
3.4.1 Ruthenium (II) Complexes	54
3.4.2 Iron (II) Complexes	59

**3.5 Conclusions**65

**Chapter Four: Model Studies of  $\pi$ - $\pi$  Interactions****4.1. Development of a Model System**

4.1.0 Background	67
4.1.1 Previous Studies	67
4.1.2 Design of a Model System	68
4.1.3 Synthesis of Simple Model Complexes	68
4.1.4 Conformation-Induced Differences in Chemical Shift	70
4.1.5 2D NMR Studies	73
4.1.6 Molecular Modelling	74
4.1.7 Prediction of Chemical Shifts	75
4.1.8 Temperature Dependent Effects	76
4.1.9 Summary	76

**4.2 Solvent Dependence of  $\pi$ - $\pi$  Interactions**

4.2.0 Changes in Chemical Shift	77
4.2.1 2D NMR Studies	79

**4.3 A Model System Incorporating Bisphenol Units**

4.3.0 Conformation-Induced Chemical Shifts	80
4.3.1 2D NMR Studies	81

**4.4 Conclusions**82**Chapter Five: The Linear Oligomer Strategy****5.1 Introduction**84**5.2 Synthesis of an Ether-Linked Oligomer**

5.2.0 Synthesis of Mono-Protected Building Blocks	84
5.2.1 Attempted Oligomer Synthesis via SN2 Reactions	86
5.2.2 Oligomer Synthesis Using Mitsunobu Conditions	87
5.2.3 Oligomer Synthesis Using Modified Mitsunobu Conditions	88

**5.3 Oligomers With Other Linker Units**

5.3.0 Attempted Synthesis of an Ester Linked Oligomer	90
5.3.1 Synthesis of a Mixed Ether-Ester Linked Oligomer	91

<b>5.4 Folding of the Ether Linked Oligomer</b>	
5.4.0 Folding Around Iron (II)	92
5.4.1 NMR Structure Determination	94
5.4.2 Summary of Folding Around Iron (II)	99
5.4.3 Folding Around Zinc (II)	100
5.4.4 NMR Structure Determination	100
5.4.5 Effects of Terminal Groups	103
5.4.6 Other Metal Ions	104
<b>5.5 Folding of The Mixed Ether-Ester Linked Oligomer</b>	105
<b>5.6 Prediction of NMR Shifts</b>	107
<b>5.7 Conclusions</b>	108
<b>Chapter Six: Synthesis of Molecular Knots</b>	
<b>6.1 Introduction</b>	110
<b>6.2 Design of Bond-forming Reactions</b>	
6.2.0 Ether Links	111
6.2.1 Ester Links	112
6.2.2 Stability Studies of Complex 105	113
6.2.3 Development of a New Carbodiimide Coupling Reagent	114
6.2.4 Model Reaction with EDC•PF <sub>6</sub>	115
<b>6.3 Synthesis of a Stopper Group</b>	
6.3.0 A Benzoic Acid Derived Stopper Group	116
6.3.1 A 9-Fluorenecarboxylic Acid Derived Stopper Group	119
<b>6.4 Towards the Synthesis of an Overhand Knot</b>	
6.4.0 Preparation of the Topologically Trivial Isomer	121
6.4.1 Attempted Synthesis of an Overhand Knot	122
6.4.2 Conclusions and Future Possibilities	125
<b>6.5 Macrocyclisation to a Trefoil Knot</b>	126
<b>6.6 Conclusions</b>	129

**Chapter Seven: Experimental**

<b>7.1 General</b>	
<b>7.1.0 Instrumentation</b>	131
<b>7.1.1 Materials</b>	132
<b>7.2 Synthetic Procedures</b>	133
<b>References</b>	179
<b>Appendices</b>	190

## Abbreviations

ADDP	1,1'-Azo(dicarbonyl)dipiperidine
AIBN	$\alpha,\alpha'$ -Azoisobutyronitrile
bipy	2,2'-Bipyridine
Bn	Benzyl
COSY	Correlated spectroscopy
DCC	1,1'-Dicyclohexylcarbodiimide
DEAD	Diethylazodicarboxylate
DMAP	4-(Dimethylamino)pyridine
DME	1,2-Dimethoxyethane
DMF	N,N-Dimethylformamide
DMSO	Dimethylsulphoxide
dppp	1,3-Bis(diphenylphosphino)propane
EDC	1-(3-Dimethylaminopropyl)-1'-ethyl carbodiimide hydrochloride
EDC•PF <sub>6</sub>	1-(3-Dimethylaminopropyl)-1'-ethyl carbodiimide hexafluorophosphate
EDTA	Ethylenediaminetetraacetic acid
ES	Electrospray (mass spectrometry)
FAB	Fast atom bombardment (mass spectrometry)
MS	Mass spectrometry
NBS	N-bromosuccinimide
NMR	Nuclear magnetic resonance
NOE	Nuclear Overhauser enhancement
ROESY	Rotating frame Overhauser enhancement spectroscopy
RT	Room temperature
TBAF	Tetra <i>n</i> -butyl ammonium fluoride
TBDMS	<i>Tert</i> -butyldimethylsilyl
TBP	Tri <i>n</i> -butyl phosphine
Tf	Trifluoromethanesulphonate (triflate)
TFA	Trifluoroacetic acid
THF	Tetrahydrofuran
TLC	Thin layer chromatography
TPP	Triphenylphosphine
Ts	p-Toluenesulphonate (tosylate)

---

---

# *Chapter 1*

---

## **Introduction**

## 1.1 Chemical Topology and Topological Isomerism

### 1.1.0 Isomerism in Organic Chemistry

Traditionally, chemists have described the structure of organic molecules in terms of the number and types of atoms they contain and the sequence and nature of bonding between those atoms. It was soon realised that two molecules could contain the same atoms linked in a different sequence and such a pair of molecules are described as constitutional isomers - for example, *n*-butane and *iso*-butane. Somewhat later, it became clear that even when molecules contained the same atoms and bonds, it was still possible for isomers to exist. Variations in the arrangement around a bond with restricted rotation lead to *cis-trans* isomerism<sup>1</sup> (formerly called *geometric* isomerism) - for example (E)- and (Z)-2-butene - while variation in the spatial arrangement around an atom or other centre can lead to optically active stereoisomers (e.g. (R)- and (S)-alanine)<sup>2</sup> (Figure 1.1).

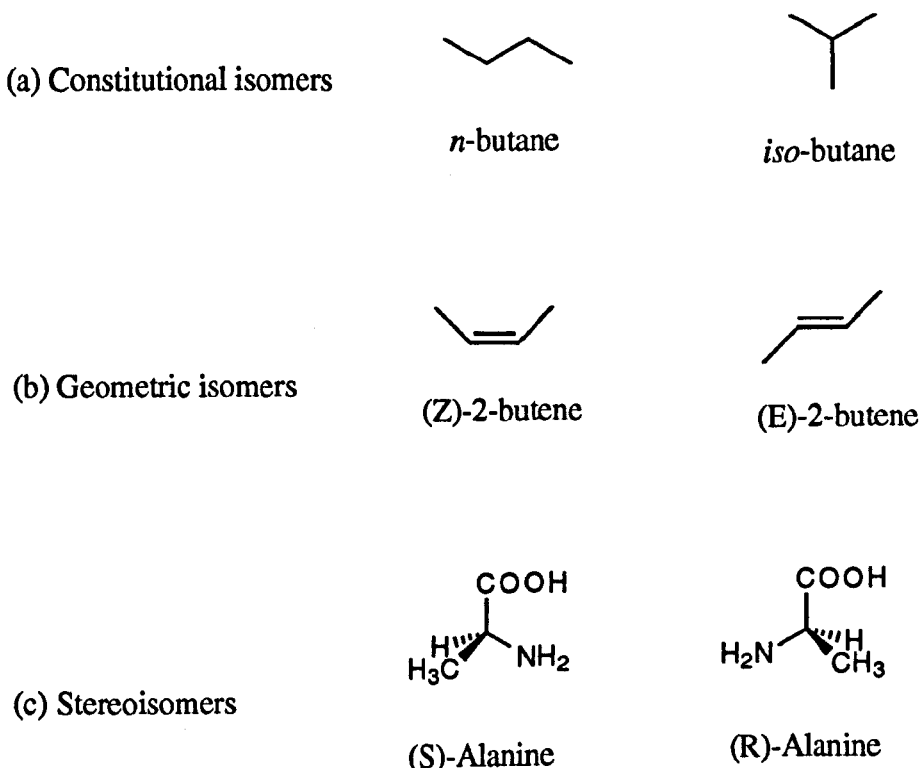


Figure 1.1. Simple forms of isomerism in organic molecules.

Over the years, many forms of isomerism have been identified as the range of molecules prepared has become more complex, but almost all are variants upon one of these fundamental types. The first molecule whose structure could not be absolutely described by considering all the factors outlined above was reported by Frisch and Wasserman in 1961<sup>3</sup>. They synthesised a molecule consisting of two interlocked rings

which they termed a catenane (from the Latin *catena* - "chain"), outlined schematically in Figure 1.2. The two rings in the linked catenane structure did not differ in any way from the unlinked rings in terms of the atoms or bonds they contained, yet clearly the two systems were chemically distinct. It was to describe this difference that the term "topological isomerism" was introduced. The two structures were then said to be *topological isomers*. The synthesis and study of such "topologically complex" molecules is often referred to as *topological stereochemistry*.<sup>4</sup>

Before going on to discuss topology in chemistry, it is worth briefly considering some of the basic ideas underlying the mathematics of topology.

### 1.1.1 An Introduction to Topology

Topology is an area of mathematics that allows one to decide upon the equivalence or inequivalence of two geometric forms.<sup>5</sup> It is important at this stage to separate the two distinct ideas of Euclidean and topological geometries. It is the concepts of Euclidean geometry that we are most familiar with in the everyday world - properties such as size, length, angles, etc. which we use to describe a given object. For example, let us consider some of the simple objects in Figure 1.3. In Euclidean geometry, squares 1 and 2 which have the same side lengths and areas would be said to be equivalent (or *congruent* in mathematical terminology). Square 3 which differs in size is not equivalent but is said to be *similar*. Clearly, triangle 4 and circle 5 are entirely different objects.

In topological geometry however, we consider different properties. To understand these, consider the object of interest on the surface of a rubber sheet.<sup>6</sup> Properties of interest in topological geometry are those that remain unchanged during any twisting or stretching of the rubber sheet - in general, this can be considered to be the connectivity of the object : lengths, angles and size are no longer considered. If we now look again at the objects in Figure 1.3, we can see that in terms of topology they are all equivalent since given complete freedom to distort lengths and angles, any one object can be transformed into any other - indeed, they are all simply different representations of the same topological object , a closed curve.

When considering the transformation of any object into another in topological geometry, one may consider the object to be totally flexible with no restriction on length and angle changes. However, connectivity is a property that must remain unchanged. A line cannot be broken or a line may not pass through another during the deformation.

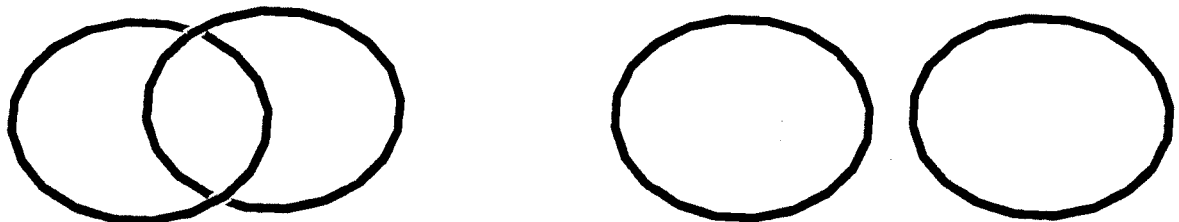


**Figure 1.2.** Schematic of a catenane and unlinked rings.

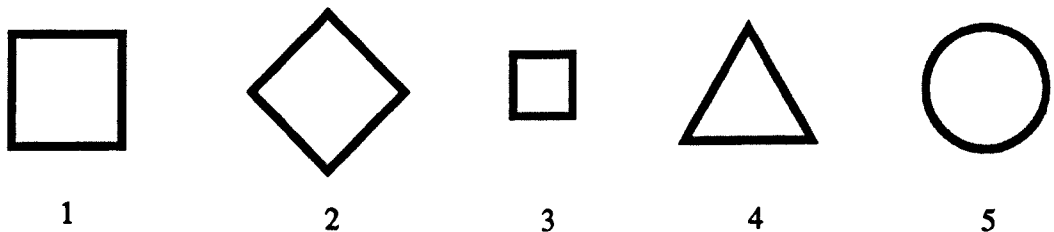


**Figure 1.3.** Some simple objects for the consideration of Euclidean and topological geometry.

### 1.1.2 Relation of Geometry to Chemical Isomerism.

If we apply these rules to the schematic catenane in Figure 1.2, it is clear that the two structures cannot be interconverted by a continuous deformation and the two systems are topologically distinct. This can also be seen for the circle and knot in Figure 1.4, both of which are closed curves yet are topologically distinct.

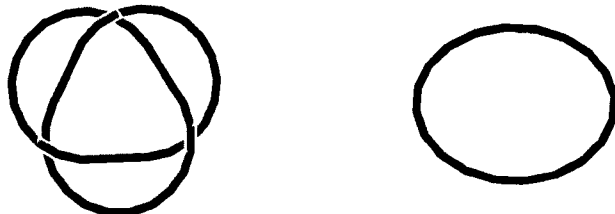


**Figure 1.4.** Two topologically distinct closed curve structures.

So, we can now see that while normal chemical isomerism such as stereoisomers arise from the consideration of Euclidean properties (bond types, angles), to classify topological isomers we must consider topological geometry.

### 1.1.3 Chirality in Topological Isomers

Although we have already referred to the synthesis and study of topologically complex molecules as *topological stereochemistry*, the use of the word stereochemistry must not be taken to imply that such molecules are inherently chiral. Some simple systems, for example catenanes, are achiral although they can be made chiral by defining a "direction" around each of the rings (Figure 1.5). Also, while the trefoil knot is indeed chiral, the closely related figure-of-eight knot is achiral (Figure 1.6). Examples of such molecules have been prepared and resolved and their chirality proven as will be discussed in due course.

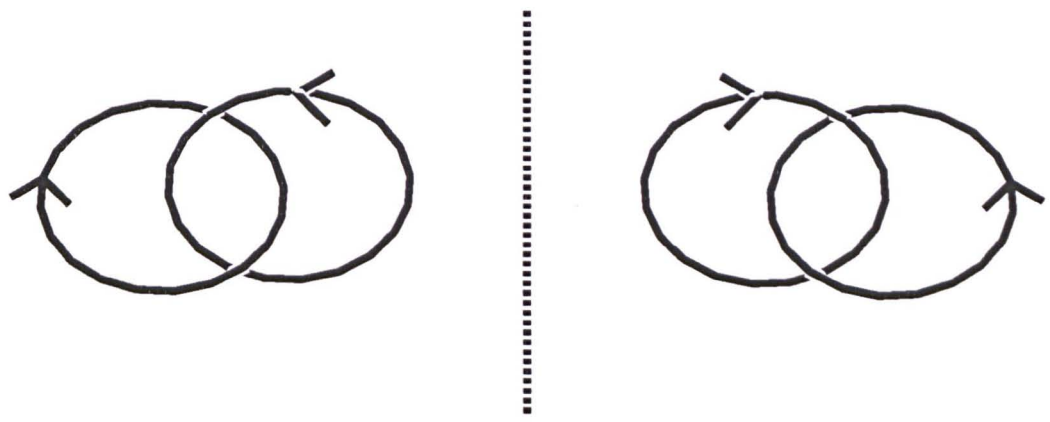


**Figure 1.5.** A chiral catenane and its non-superimposable mirror image.

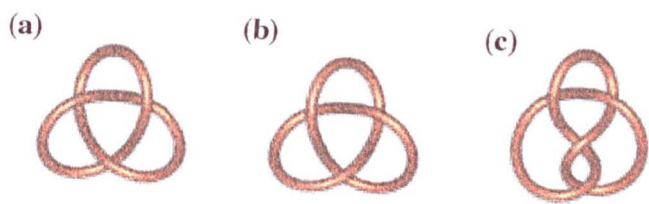


**Figure 1.6.** Right-handed (a) and left-handed (b) trefoil knots along with the achiral figure-of-eight knot (c)

## 1.2 Topological Targets for Chemical Synthesis

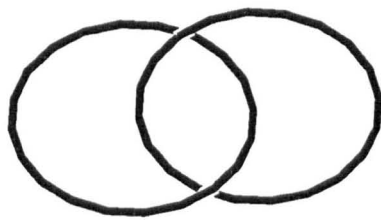
Now that we have defined the properties which distinguish topological isomers, let us consider some of the past, present and future target topologies for organic synthesis. The synthesis and properties of such interlocked and intertwined structures has recently been thoroughly reviewed by Stoddart and Amabilino.<sup>7</sup> Some possible targets are outlined schematically in Figure 1.7.

We have already discussed Frisch and Wasserman's catenane. Although the existence of the catenated product was only inferred from spectroscopic data and not actually isolated, the catenane has certainly become a readily accessible synthetic target in recent years.

A closely related structure is the rotaxane. Here, the two components - the macrocycle and a linear strand - are held together by virtue of a bulky "stopper" group that prevents unthreading occurring. It must be noted that since the rules of topological geometry apply only to closed systems, it is therefore not possible to define the topology of a rotaxane in the precise mathematical sense. However, because of its obvious relationship to the catenane, the rotaxane is nonetheless best classified as a topological isomer of the corresponding free macrocycle and linear molecule.

Another target readily prepared is the related pseudo-rotaxane. This differs from the rotaxane in that no bulky groups are present to prevent unthreading. Although the components are rapidly equilibrating, the pseudo-rotaxane structure is favoured due to favourable non-covalent interactions between the two components.

Also of interest are the large class of knotted structures, the simplest example of which (and indeed until very recently, the only example of a molecular knot prepared) is the illustrated trefoil knot. Two new targets that we have identified are the "overhand knot" - related to a trefoil knot in the same way that a rotaxane is related to a catenane - and the corresponding pseudo-overhand knot - again, related to the overhand knot in the same way that a pseudo rotaxane is related to a rotaxane. Currently, the synthesis of neither system has been reported.



[2]-catenane



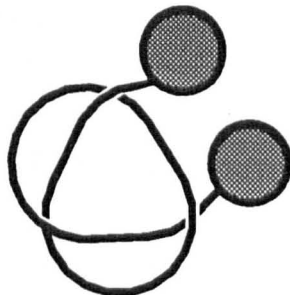
rotaxane



pseudo-rotaxane



Trefoil knot



overhand knot



pseudo-overhand knot

**Figure 1.7.** Schematics of some topologically complex target molecules.

## 1.3 Topological Isomers in Nature

### 1.3.0 DNA Knots and Catenanes

Although examples of synthetic topological isomers are still somewhat rare, there are numerous examples of such structures in nature. It was during the 1960s - a time which also coincided with the first serious attempts at the preparation of synthetic systems - that the first examples of topological complexity were discovered in DNA molecules. Although knots are relatively rare, catenated structures are common. The first DNA catenane was discovered in the mitochondria of human cells in 1967 by Vinograd,<sup>8,9</sup> while DNA knots were first observed somewhat later - 1976 for the first single stranded DNA knot from bacteriophage fd and 1981 for the first double stranded DNA knot from bacteriophage P2 DNA both discovered by Wang and co-workers.<sup>10, 11</sup> Some examples of such structures are illustrated in the electron micrographs shown in Figure 1.8.

Although at first it appeared that knotted and catenated DNA molecules were nothing more than curiosities, it quickly became apparent that these structures had important implications for the biological function of DNA. Catenanes can form during the replication of circular DNA molecules, and this has been observed in a number of biological systems - for example in the animal virus SV40.<sup>14</sup> Clearly if parent and daughter molecules are interlocked in a catenane, the replication process cannot proceed as expected. To solve this problem, it was discovered that nature has a class of enzymes called *topoisomerases* that are capable of effecting topological transformations upon DNA molecules to overcome such problems.<sup>15</sup> These enzymes are divided into two classes - type I and type II. Type I enzymes can carry out transformations that require the breaking of only one strand of DNA while type II enzymes effect reactions that require the breaking of two strands. Some of the possible transformations are illustrated in Figure 1.9.<sup>16</sup>

Since in our discussion of topology we have seen that for simple objects changes in Euclidean properties cannot produce a change in topology, it is apparent that the mechanism of action of such enzymes must involve the breaking of a DNA strand followed by the passage of another strand through the gap so formed, followed by a resealing process (Figure 1.10).<sup>17</sup> Enzymes that can control such a process are obviously rather complex and a detailed structure of the active site and hence an understanding of how such an operation occurs has yet to be obtained.

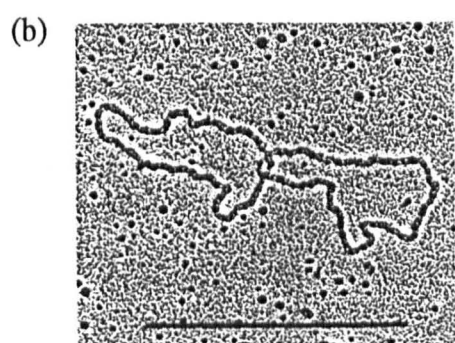
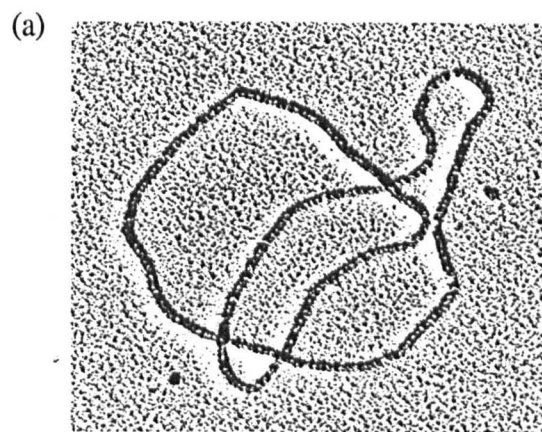


**Figure 1.8.** Electron micrographs of (a) knotted<sup>12</sup> and (b) catenated<sup>13</sup> DNA molecules.

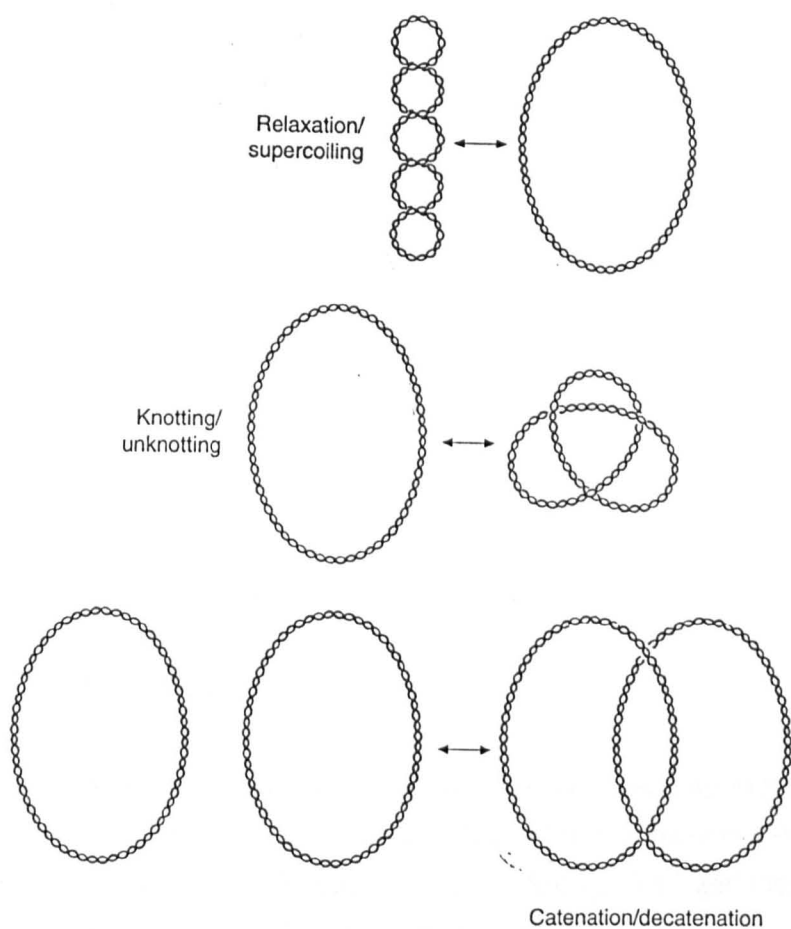


**Figure 1.9.** Some topological transformations of double stranded DNA effected by topoisomerase II enzymes.

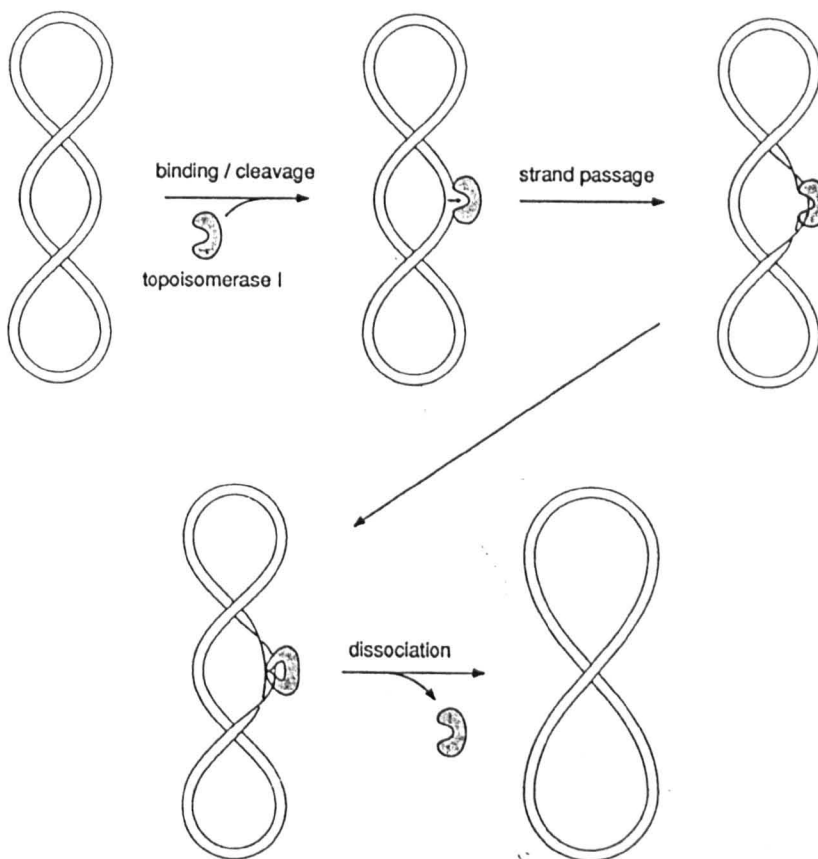


**Figure 1.10. Proposed mechanism of action of topoisomerase enzymes.**

### 1.3.1 DNA Supercoiling

Topology and topoisomerases play an even more important role in the biology of DNA via a process known as *supercoiling*. If one considers taking a circular double stranded DNA, cutting both strands, twisting through 360° and then resealing the strands it may appear that exactly the same structure has been reformed. However, the product is in fact a topological isomer of the initial material. As a consequence, the overall 3-dimensional DNA structure may be significantly changed. In fact, highly supercoiled DNA (i.e. DNA containing a large number of such twists) adopts a very compact structure rather than the fairly open structure that would otherwise exist. In this way, the availability of the DNA molecule for replication or transcription can be controlled via its topology.<sup>18, 19</sup>

Given this variety of functions for the topoisomerase enzymes, it is not surprising that they are vitally important within the cell. In fact, *all* cells contain such enzymes and if their function is inhibited, the cell dies. This has made both type I and type II topoisomerases attractive drug targets.<sup>20, 21</sup> For example, a number of antibacterial drugs have been shown to target bacterial topoisomerases and inhibit various stages of the cutting - strand passage - resealing process. Drugs that target eukaryotic topoisomerases are highly cytotoxic and include many anti-cancer drugs.

### 1.3.2 Knots in Proteins

While DNA exhibits a large number of knotted and catenated structures, until very recently there were no reports of similar phenomena in proteins. Clearly since protein formation involves the reversible folding of a linear polypeptide molecule, closed structures such as catenane or trefoil knots are not possible. However, it seems not unreasonable that a polypeptide may fold into an open knotted structure. As we have already discussed, a precise mathematical definition of such a system is not possible, so the identification of these structural motifs is somewhat subjective.

The first claims of knotted protein structures were made by Liang and Mislow in 1994 following a search of crystallographic structures in the Brookhaven Protein Data Bank.<sup>22, 23</sup> They claimed that a number of proteins exhibited knotted substructures, for example ascorbate oxidase illustrated in Figure 1.11. However, it is clear that such structures are not really knots. It is certainly not the polypeptide chain itself that adopts any sort of knotted conformation, but rather that links between various points on the chain via metal-histidine interactions and disulphide links allow one to trace out a topologically significant connectivity. It seemed that proteins may not adopt "real" knotted structures at all until in 1996 Takusagawa reported the structure of (S)-adenosylmethionine synthetase (MAT) containing a true knot (Figure 1.12).<sup>24</sup>

Such structures may have important implications concerning the nature of the series of events that occur during protein synthesis. For example, some inter-peptide interactions cannot occur immediately the relevant section of polypeptide chain has been synthesised and a global folding process must occur only after the whole polypeptide chain has been formed.

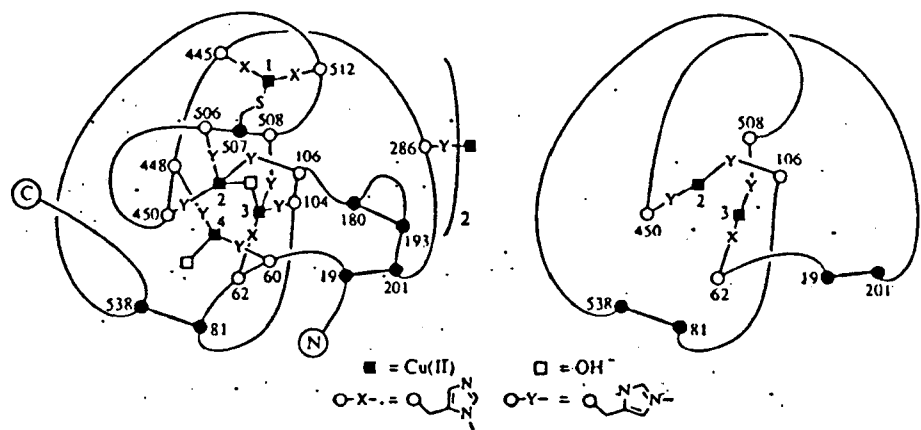


**Figure 1.11.** Schematic of ascorbate oxidase with the "knotted" section expanded.  
Bold lines represent disulphide linkages.

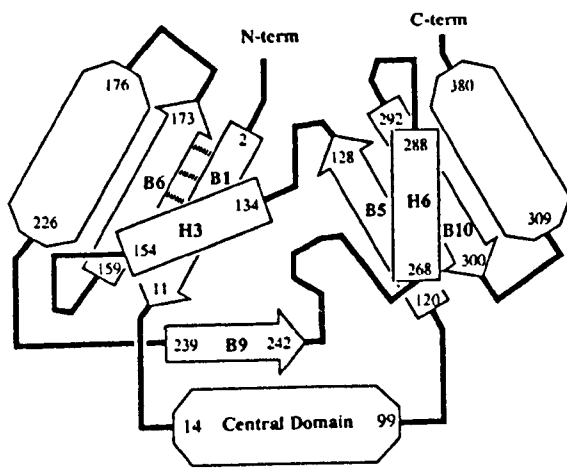


**Figure 1.12.** Schematic of the open knot structure of the polypeptide chain of MAT.

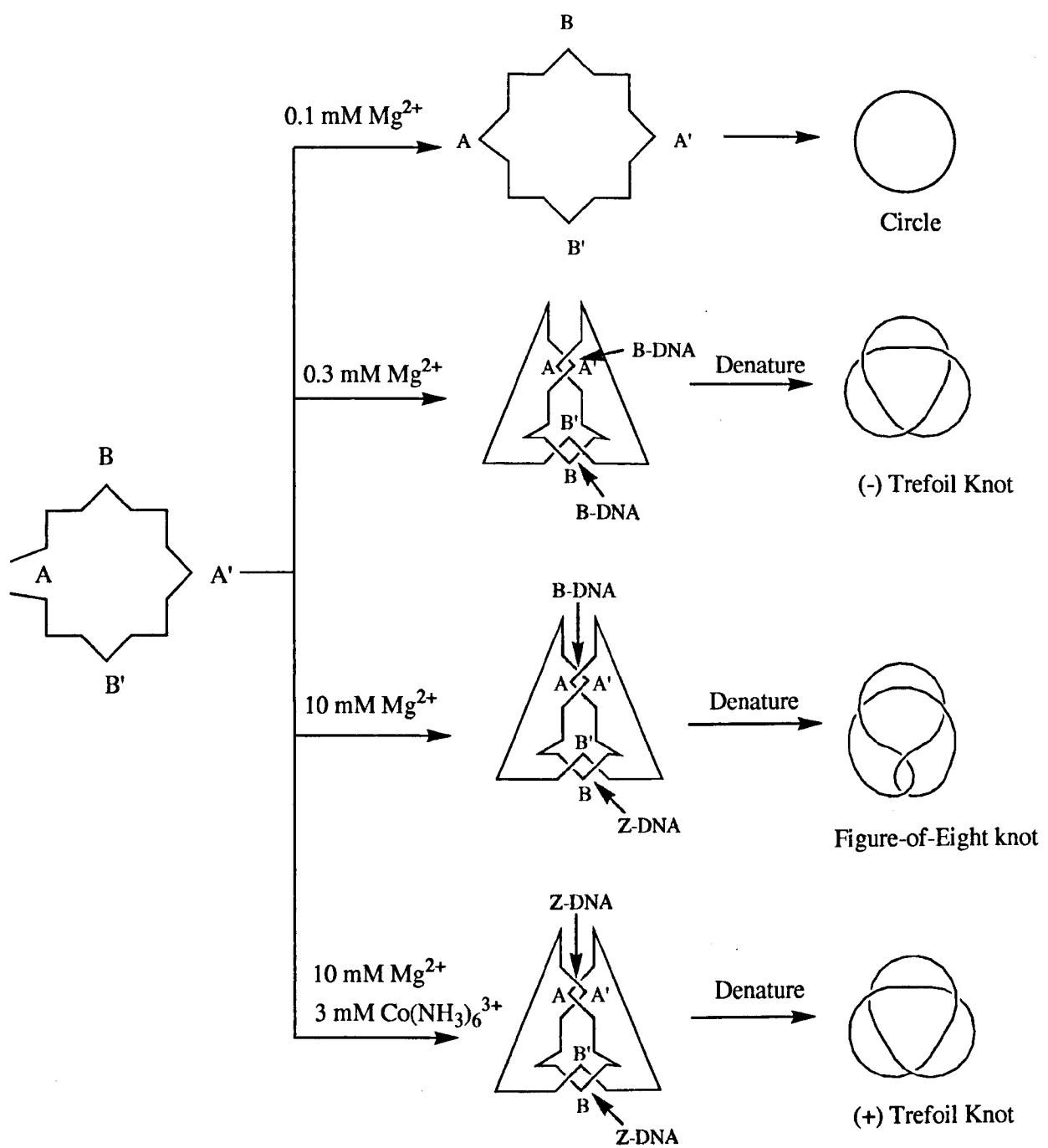


**Figure 1.13.** Seeman's synthesis of trefoil knotted and figure-of-eight knotted DNA molecules.

### 1.3.3 Synthesis Using DNA Building Blocks

As well as naturally occurring topologically complex structures in DNA, linear DNA molecules have been used by Nadrian Seeman as building blocks in designed syntheses of topologically complex molecules. These syntheses utilise the fact that DNA can form double helical structures in a designed manner by control of base sequences which also enable the design of right-handed (B-DNA) and left-handed (Z-DNA) helix sequences. Figure 1.13 illustrates schematically how Seeman has used a single strand of DNA containing 104 nucleotides to prepare a circle, both left- and right-handed trefoil knots and a figure-of-eight knot.<sup>25</sup> A-A' and B-B' represent 11 or 12 base-pair complementary sequences that have been designed to produce specific sections of double helix. The A and B sequences are joined by oligo-T linkers. Addition of various concentrations of Mg<sup>2+</sup> and Co(NH<sub>3</sub>)<sub>6</sub><sup>3+</sup> can induce the formation of either B-DNA or Z-DNA helices in various parts of the structure and hence can lead to the differing products formed.

In addition to DNA knots, Seeman has used similar techniques to assemble extremely complex structures from multiple strands of DNA such as a DNA cube<sup>26</sup> and a truncated octahedron<sup>27</sup> (Figure 1.14).

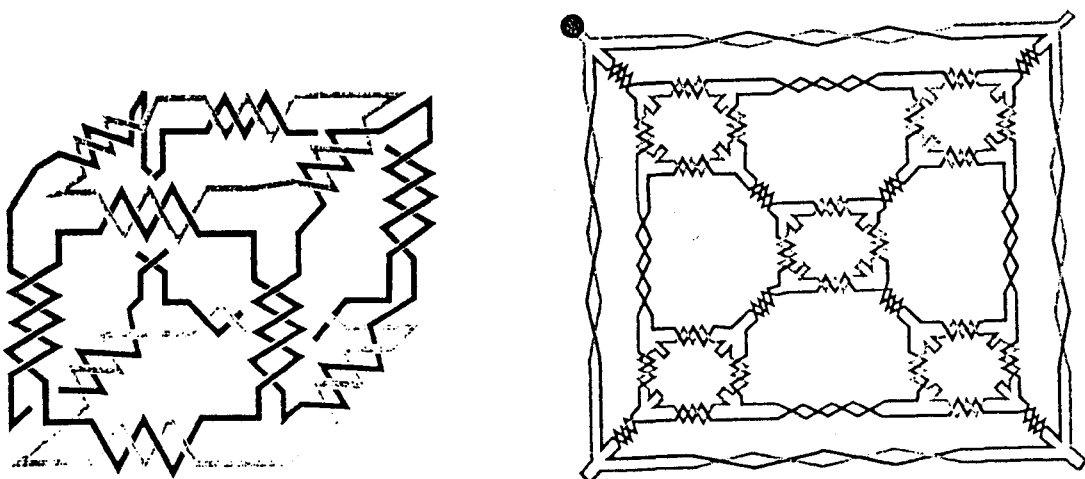


**Figure 1.14.** Schematic representation of Seeman's DNA cube and truncated octahedron.

## 1.4 Early Attempts at Synthesis of Topologically Complex Molecules

### 1.4.0 The First Statistical Catenane Synthesis

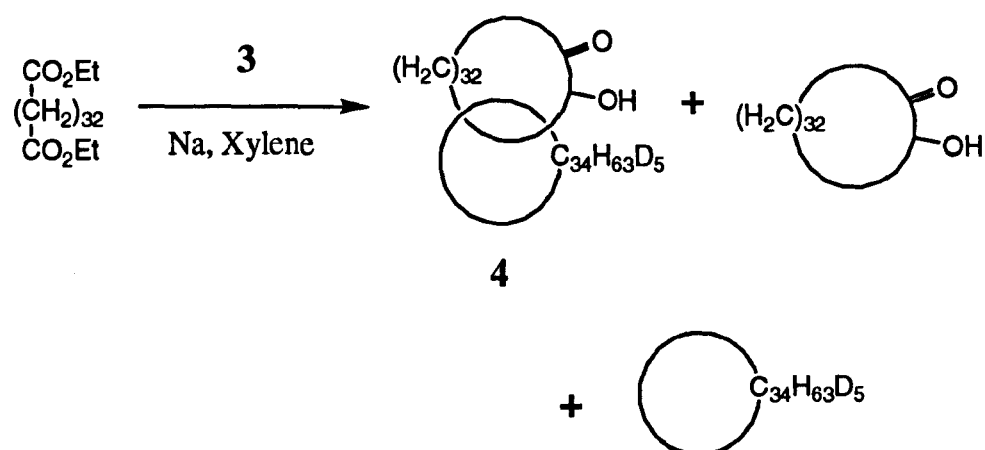
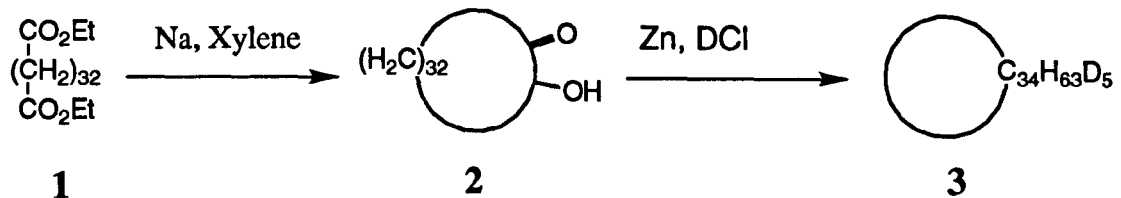
In 1960, Van Gulick and Wasserman independently began to consider the problem of the synthesis of two linked rings - a system for which they both proposed the name catenane. Van Gulick's discussion of the problem was surprisingly never published at the time although it has been much referenced by other workers in the field. His manuscript was reputedly rejected for "not being chemistry"<sup>28</sup> although it was finally published in 1993!<sup>29</sup> Wasserman went on to publish a low yielding catenane synthesis in late 1960 as outlined in Scheme 1.1 (a).<sup>3</sup>

Diester **1** was subjected to an acyloin condensation followed by a Clemmensen reduction in DCl to give the deuterium labelled cyclic hydrocarbon **3**. A further molecule of diester **1** was then cyclised in the presence of **3** and produced a mixture of products which by a random threading of **1** through **3** during the cyclisation contained some catenane **4**. The yield was very low and the presence of **4** could only be inferred spectroscopically as outlined below. Such low yields from so called *statistical reactions* are in marked contrasts to the almost quantitative yields in the *templated reactions* that will be discussed later.

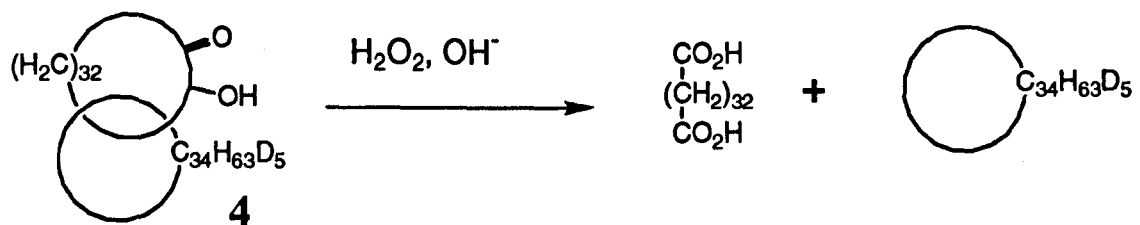
Wasserman's proof of structure consisted of chromatographing the crude product on silica. Pentane was used to elute the non-polar cyclic hydrocarbon while the more polar acyloin functionality remained on the silica. When the product remaining on the column was removed, it was shown by IR spectroscopy to still contain deuterium - evidence for the mechanical linking of the deuterated and acyloin rings. Further evidence came from oxidative cleavage of the acyloin function in the product followed by chromatography. Now after eluting with pentane, the product remaining on the silica was shown to contain no deuterium. This was attributed to cleavage of the catenane as shown in Scheme 1.1 (b).

Wasserman calculated that for a simple cycloalkane, a ring of at least C<sub>20</sub> would be required before another alkane chain could thread through it.<sup>30</sup> The larger the ring, the easier the threading but the lower the cyclisation yield. His initial system was a compromise using two 34-membered rings. His early terminology was to denote this a 34,34-catenane, although later - with the advent of multi-ring systems - such compounds came to be called simply [2]-catenanes. The number in square brackets denotes the number of interlocked rings.

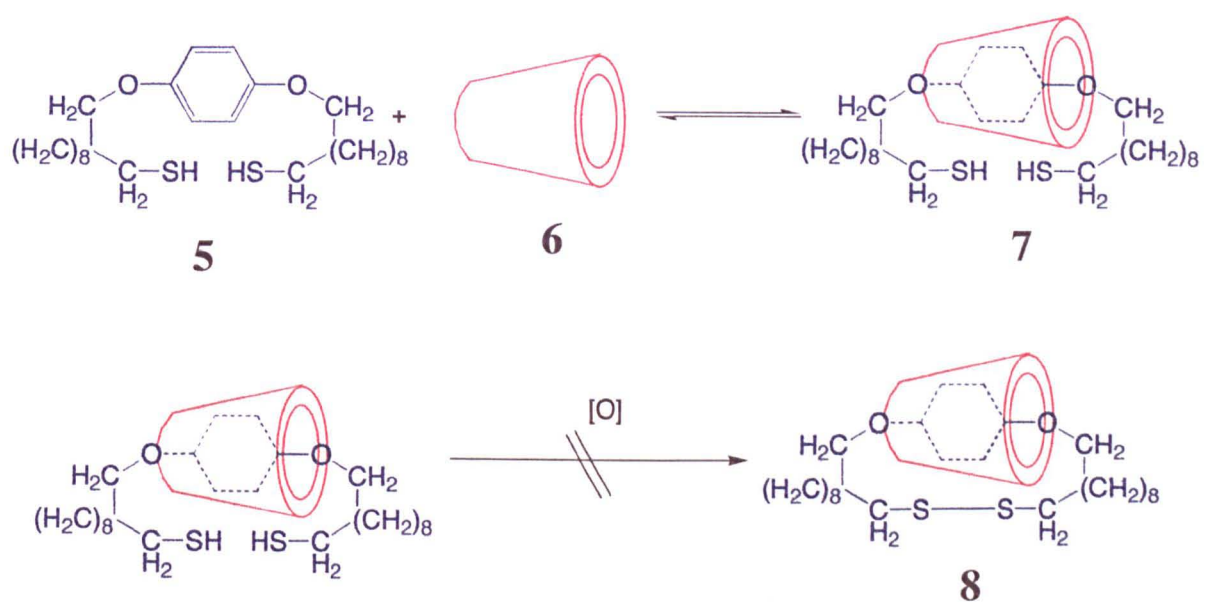
(a)



(b)



Scheme 1.1. (a) Wasserman's statistical catenane synthesis, 1960. (b) A structural proof of catenane formation based upon cleavage of the product.



**Scheme 1.2.** Lüttringhaus' attempted catenane synthesis, 1958.

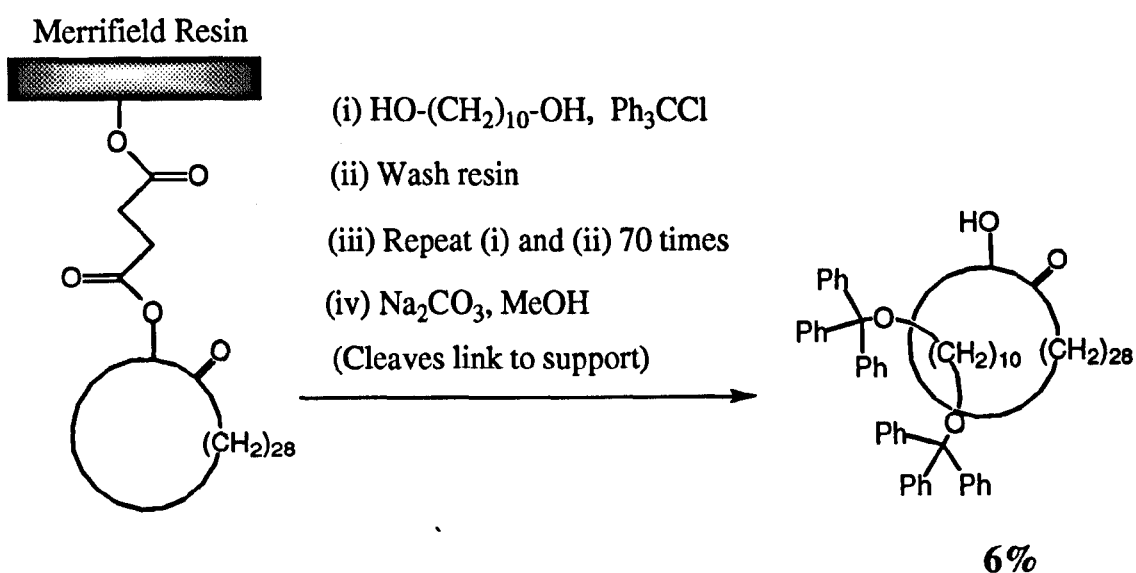
Although this was the first evidence for the formation of a catenane, it was certainly not the first attempted synthesis to appear in the literature. As early as 1958, Lüttringhaus and co-workers had published the attempted synthesis outlined in Scheme 1.2.<sup>31</sup> This utilised the fact that the aromatic ring of **5** formed an inclusion complex with cyclodextrin **6**. In theory, intramolecular oxidative coupling of the thiols should give catenane **8**. However, only starting material was ever isolated. In many ways, this attempted synthesis was ahead of its time, utilising the ideas of templated synthesis that were not to appear for many years. Also, it is worth noting that inadvertently Lüttringhaus had prepared the first example of a pseudo-rotaxane - molecules that were to become synthetic targets in their own right many years later.

#### 1.4.1 Possibilities For Extension to Molecular Knots.

In a 1961 paper, Wasserman also considered the possibility of a statistical approach to a molecular knot.<sup>32</sup> He calculated that at least a C<sub>50</sub> chain would be required and prepared a C<sub>66</sub> diester which he subjected to a similar acyloin condensation to that used successfully in his catenane synthesis. Not surprisingly, no results were ever published, and one can envisage many problems associated with such a scheme. The desired product could only ever be produced in a very low yield, and the spectroscopic proof used in the catenane characterisation was not applicable to this system. As Wasserman appreciated, the only hope of identifying a knot in the product mixture was to utilise the fact that a trefoil knot exhibits chirality. However, since both enantiomers would form in equal amounts, the product would still be optically inactive. This left the proposal of adding an optically active species that would bind to the knot to produce diastereoisomers for chromatographic separation or spectroscopic identification. Again, no results were forthcoming, and it seems that the yield of knot was simply too low to have any hope of detecting it among the products. A further 30 years would pass before the first synthetic knot was isolated and characterised.

### 1.4.2 The First Statistical Rotaxane Synthesis

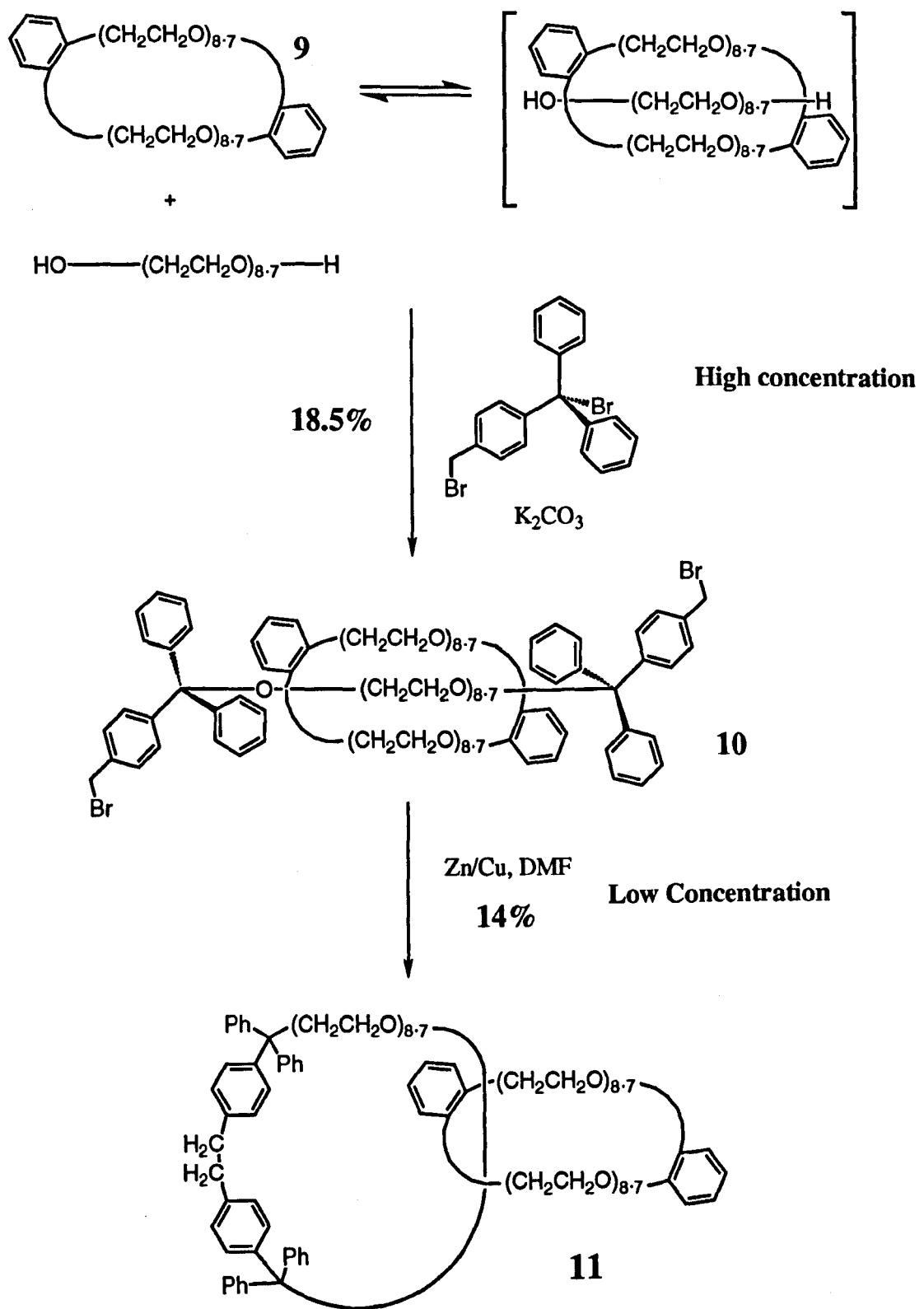
Although a molecular knot was to remain beyond the scope of such early work, the 1960s did also see the first successful rotaxane synthesis. In 1967 Harrison and Harrison reported the synthesis of a rotaxane in 6% yield using the statistical threading approach outlined in Scheme 1.3.<sup>33</sup> This ingenious route partly surmounted the problem of a low yield in statistical reactions by repeating the threading and capping step 70 times! Although they proposed the name “hooplane” for such systems, rotaxane - from the Latin *rota* (wheel) and *axis* (axle) - is the term that has become generally accepted.



Scheme 1.3. Harrison and Harrison's rotaxane synthesis, 1967.

### 1.4.3 Improved Statistical Methods for the Preparation of Catenanes

The work of Zilkha and Agam<sup>34, 35</sup> in the mid-1970s saw the only real improvement in the yields of catenanes by the statistical method. They realised that the conditions favouring the required threading processes (i.e. high concentration) were inconsistent with those conditions favouring macrocyclisation (low concentration). To overcome this problem in their catenane synthesis (Scheme 1.4) they divided the synthesis into two stages. They prepared a mixture of crown ethers, dibenzo-58.2-crown-19.4 **9** from PEG 400 (polyethylene glycol with an average molecular weight of 400). In a high concentration reaction, a further molecule of PEG 400 was stoppered using two derivatised trityl groups in the presence of the crown macrocycle to give rotaxane **10** in 18.5% yield. It has been suggested that this yield may be so high due to a small degree of templating by favourable electrostatic interactions between the crown macrocycle and the threaded polyethylene glycol chain.<sup>7</sup> **10** was isolated and then subjected to a high dilution macrocyclisation to yield catenane **11** in 14% yield, an overall 2.6% yield of catenane. They called this method the Double-Stage approach, and the synthesis still represents one of the few examples of the direct conversion of a rotaxane into a catenane.



**Scheme 1.4.** Zilkha and Agam's rotaxane and catenane synthesis using the 'Double-stage' method

#### 1.4.4 Topological Isomers From a Molecular Möbius Strip

Another idea for an approach to topologically complex molecules that can be classified generally as a statistical route is that of using a molecular Möbius strip. A Möbius strip is a topological object possessing only one surface prepared by taking a strip, introducing a twist and sealing the ends together (Figure 1.15).

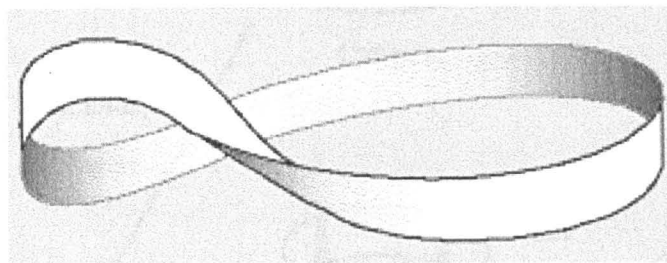
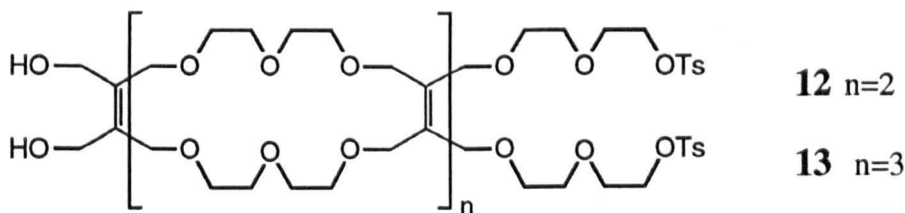
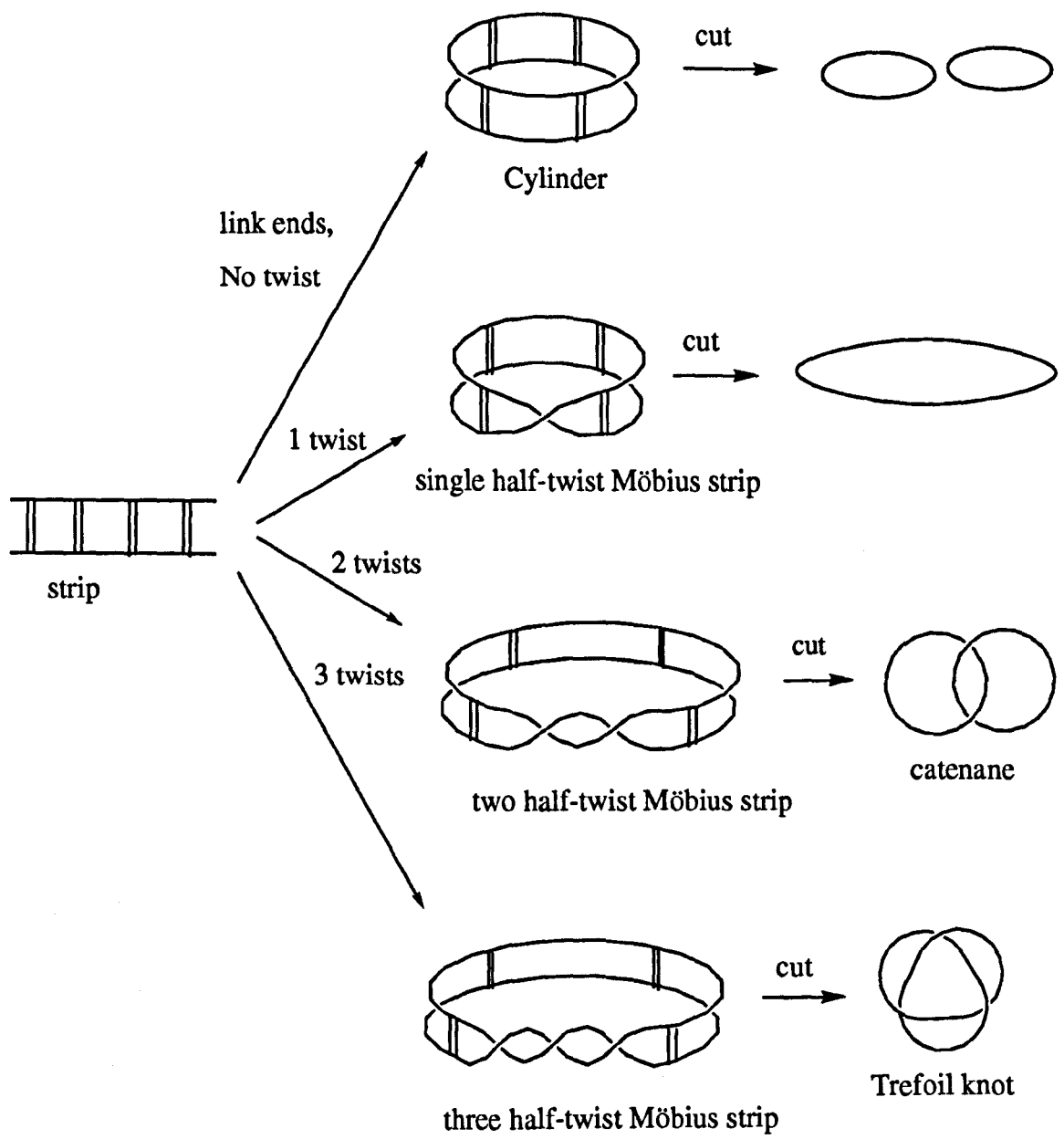


**Figure 1.15.** A Möbius Strip.

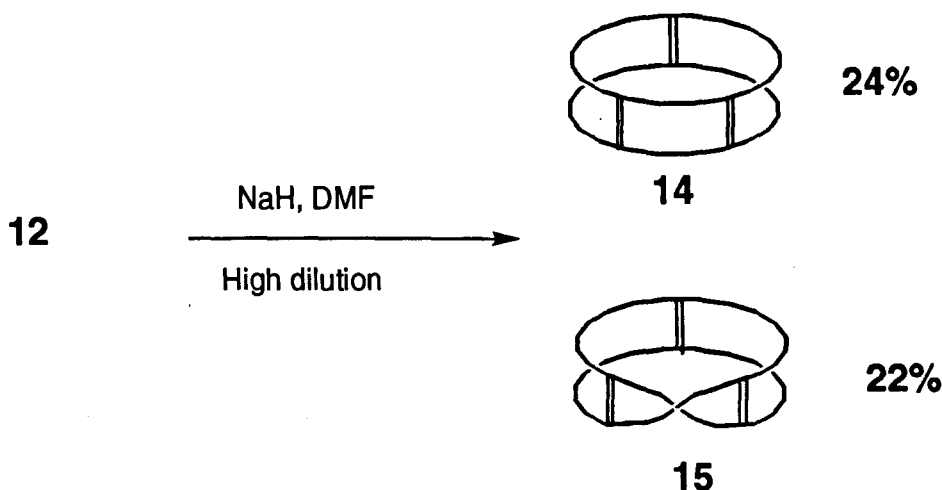
The idea that such a strategy could give access to a molecular knot was suggested by Frisch and Wasserman in 1961.<sup>32</sup> In fact, if a Möbius strip with various numbers of twists is cut down its centre, a whole range of interesting topologies could be accessible, some of the simpler possibilities being illustrated in Scheme 1.5.<sup>4</sup>



Much experimental work towards realising these possibilities has been carried out by Walba and co-workers who have synthesised a number of molecular strips such as **12** and **13** based upon tetra(hydroxymethyl)ethene (THYME) polyethers.<sup>36</sup> They have subjected such molecules to high dilution macrocyclisation reactions and identified some of the products formed (Scheme 1.6)

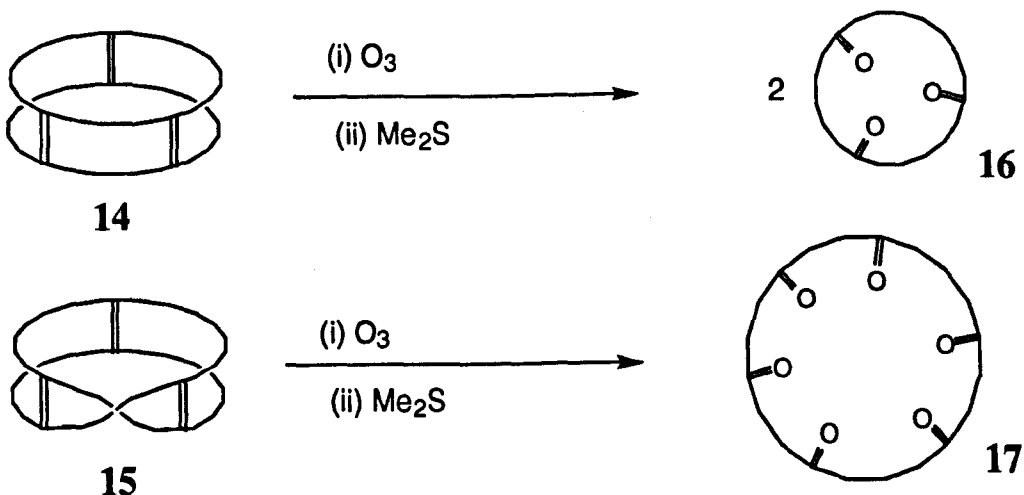


**Scheme 1.5.** Some topologies theoretically accessible from a molecular Möbius strip

**Scheme 1.6.** Cyclisation of a molecular strip.

Cyclisation of **12** yielded two products identified as the cylinder **14** and the single half-twist Möbius strip **15**. Walba has demonstrated that “cutting” of the strip down its centre can be achieved in the chemical sense via ozonolysis of the THYME double bonds (Scheme 1.7).<sup>37</sup> Cylinder **14** gave two molecules of triketone **16** and the half-twist Möbius strip **15** gave the hexaketone macrocycle **17**.

So far, the double and triple half-twist Möbius strips required for the formation of a catenane and trefoil knot respectively have not been characterised. It seems that the chance of so many twists occurring during the cyclisation reaction is remote. Other workers have attempted to incorporate units that template the formation of a half-twist in such systems and these attempts will be considered later during the discussion of templated synthesis.

**Scheme 1.7.** Cutting of a Möbius strip and its untwisted topological isomer.

## 1.5 Templat ed Synthesis

### 1.5.0 Classification of Templates

When Watson and Crick elucidated the structure of the DNA double helix in 1953, it was soon realised that when DNA replicated, one strand acted as a “template” for the formation of a new molecule.<sup>38</sup> Since that time, chemists have developed many systems whose synthesis depends on a template effect. So, how do we define a template? A good definition was given by Busch in 1993:

*“A chemical template organises an assembly of atoms with respect to one or more geometric loci in order to achieve a particular linking of atoms.”<sup>39</sup>*

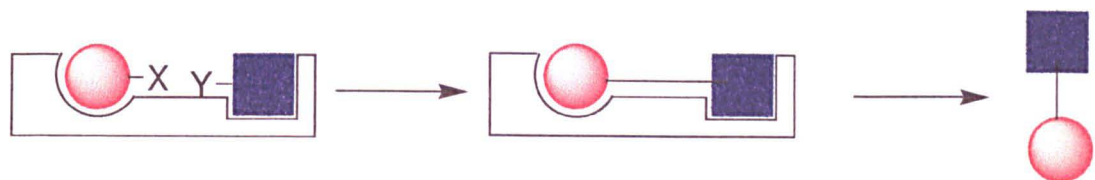
In other words, we can use a template to preorganise the geometric arrangement, orientation or conformation of molecules such that when new covalent bonds form between them, they do so in a precise and controlled manner.

Bonding between template and substrate(s) is often via weak non-covalent interactions although some systems do use covalent bonds that can be readily cleaved or form reversibly. There are many different forms of template, giving access to different types of molecule. A convenient subdivision for our purpose is that used by Sanders in a recent review (Figure 1.16).<sup>40</sup> For our purpose of the synthesis of topologically complex molecules, it is clearly interweaving and cyclisation templates that are of greatest importance, so linear type templates leading to phenomena such as artificial enzymes and self-replicating systems will not be considered here.<sup>41</sup>

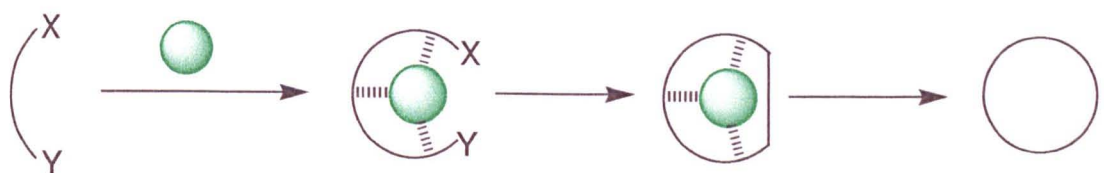
### 1.5.1 Cyclisation Templates - Metal Ions

By far the most common class of templated macrocyclisations are those templated by metal ions. It was the discovery that metal ions can act in such a manner during the 1960s that began the serious study of template effects in synthesis. A good early example is Pedersen’s crown ether synthesis in 1967.<sup>42</sup> His initial yields were very low, but Greene *et al* obtained much improved results during the early 1970s. His general route is illustrated in Scheme 1.8.<sup>43</sup>

(a) Linear



(b) Cyclisation



(c) Interweaving

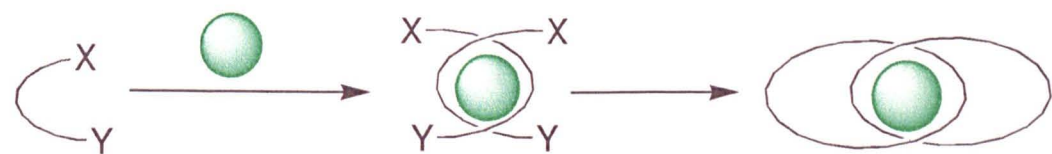
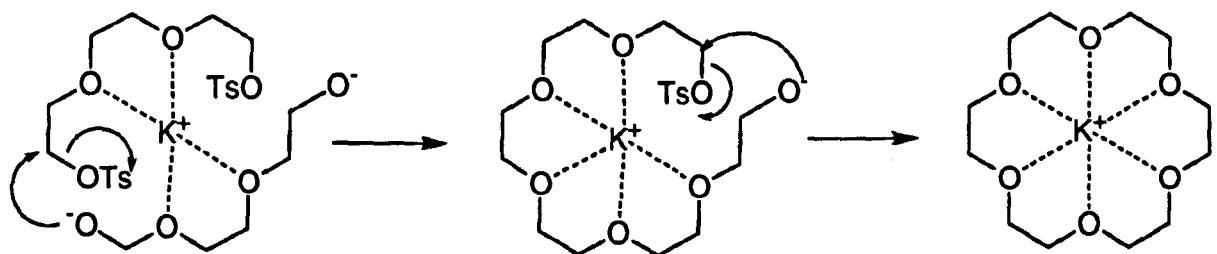


**Figure 1.16.** Subdivision of template classes according to Sanders et al.

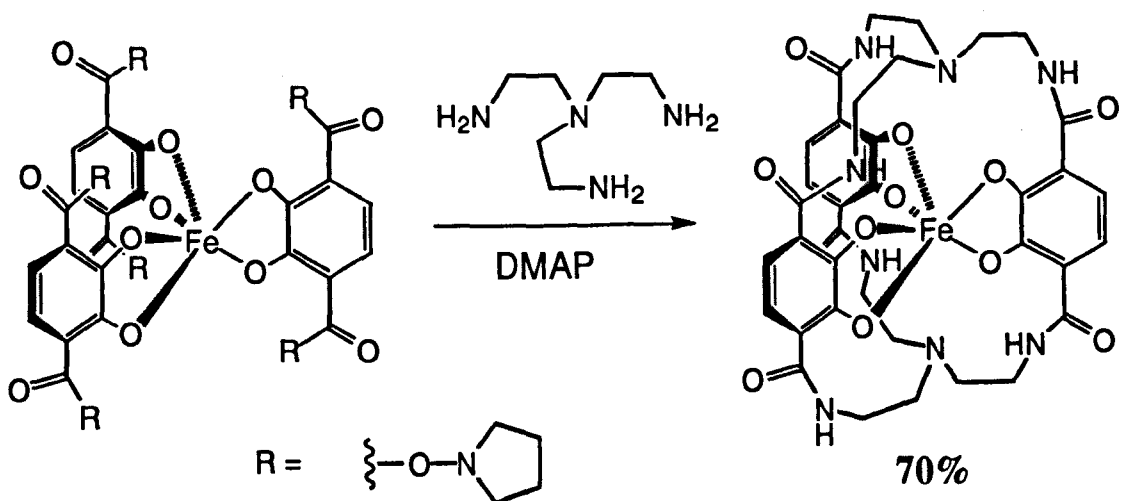


**Scheme 1.8.** Greene's improved 18-crown-6 synthesis and a proposed mechanism for a template effect provided by  $K^+$ .

He found that if tetra-*n*-butylammonium hydroxide was used as base, mainly polymer was obtained along with only a very low yield of the expected crown ether. However, if *t*BuOK was substituted as base, the yield increased dramatically, to as high as 93% and the product was isolated coordinated to potassium as its tosylate salt. He proposed the templated mechanism outlined in Scheme 1.8. It seems likely that the first tosylate displacement reaction may occur before complexation to potassium ion, since the formation of a termolecular complex would be entropically disfavoured.

The metal template effect has now been used in countless examples of macrocycle synthesis, too numerous to mention, often to build up complex molecules. Removing the metal ion after the synthesis to obtain the free macrocycle is often problematical, and this represents the only real drawback of this very useful technique.

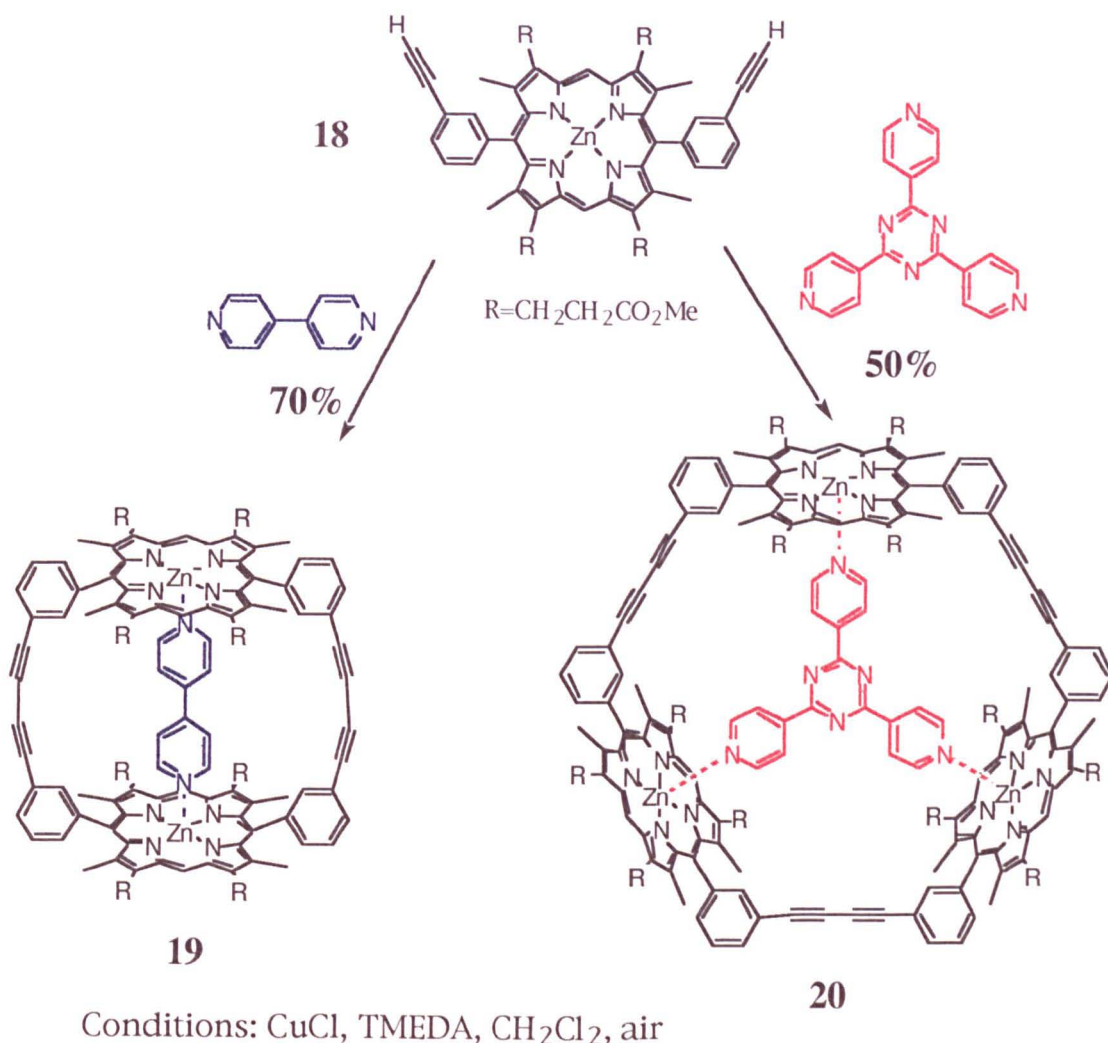
The method is not limited to simple “2-dimensional” macrocycles. It has also been used extensively to build up complex “cage” molecules to totally encapsulate a metal ion - for example, Raymond’s iron sequestering agent (Scheme 1.9).<sup>44</sup> In the absence of iron (II), and using high dilution conditions to minimise polymerisation, it is possible to obtain only a 3.5% yield of macrocycle - a spectacular example of the success of templated synthesis.



**Scheme 1.9.** *Templated synthesis of Raymond’s iron sequestering agent.*

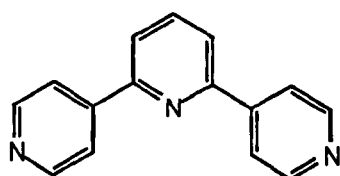
### 1.5.2 Cyclisation Templates - Organic Molecules

Although metal ions are by far the most common templates for macrocyclisation reactions, other methods do exist. Sanders has prepared a number of porphyrin-based macrocycles using a neutral organic molecule to provide a template effect.<sup>45, 46</sup> He found that the porphyrin monomer **18** could be cyclised in good yield to either dimer **19** or trimer **20** depending upon the presence of a small organic molecule to provide the relevant template effect (Scheme 1.10).



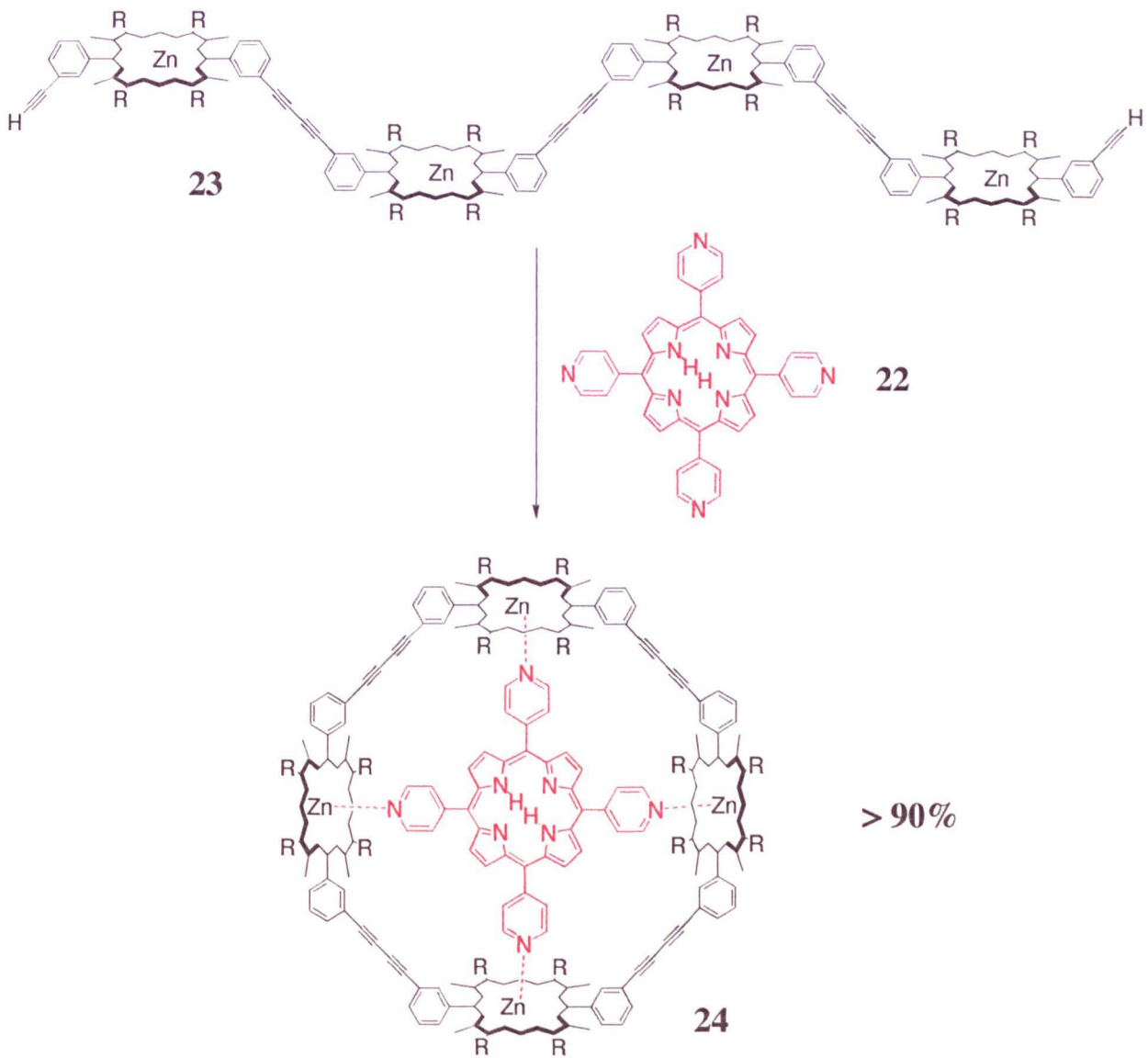
**Scheme 1.10.** Sanders' templated synthesis of porphyrin macrocycles.

**19** is formed as would be expected - 4,4'-bipyridine acts as a positive template producing a three-fold increase in yield, and fits well into the cavity produced. However, Sanders suggests that tripyridyltriazine plays a rather different role in the formation of the trimer **20**. It seems to increase the yield of trimer (by a factor of 1.5) by inhibiting the formation of dimer, which is more dominant in the absence of template. It is therefore best considered as acting as a *negative* template for dimer formation. Further evidence for this proposal comes from obtaining a similar trimer yield in the presence of 2,6-dipyridylpyridine **21** which is clearly not capable of acting as a true trimer template since it lacks the third binding site.



**21**

The technique has also been extended to prepare cyclic tetramer **24** using the tetrapyridylporphyrin **22** as a template.<sup>40</sup> Although this produces a poor yield in direct reaction of the monomer, it does produce a near quantitative yield for cyclisation of the linear tetramer **23** (Scheme 1.11).



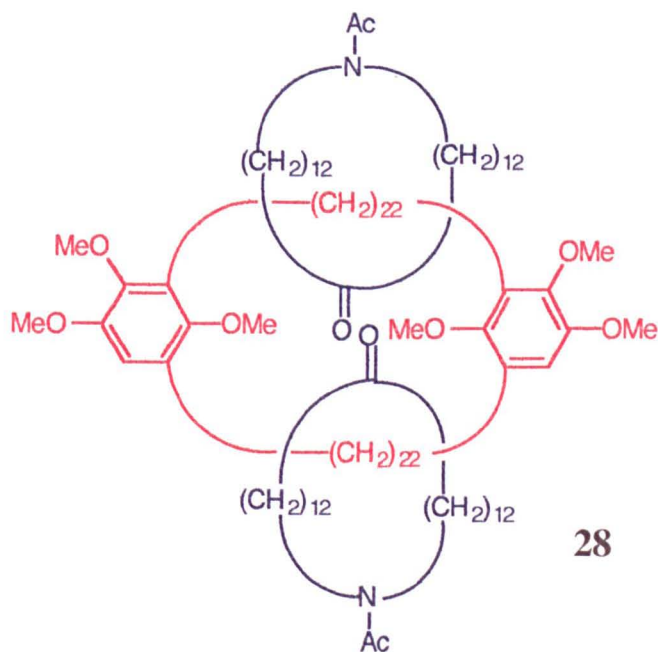
**Scheme 1.11.** Sanders' templated cyclic tetramer synthesis.

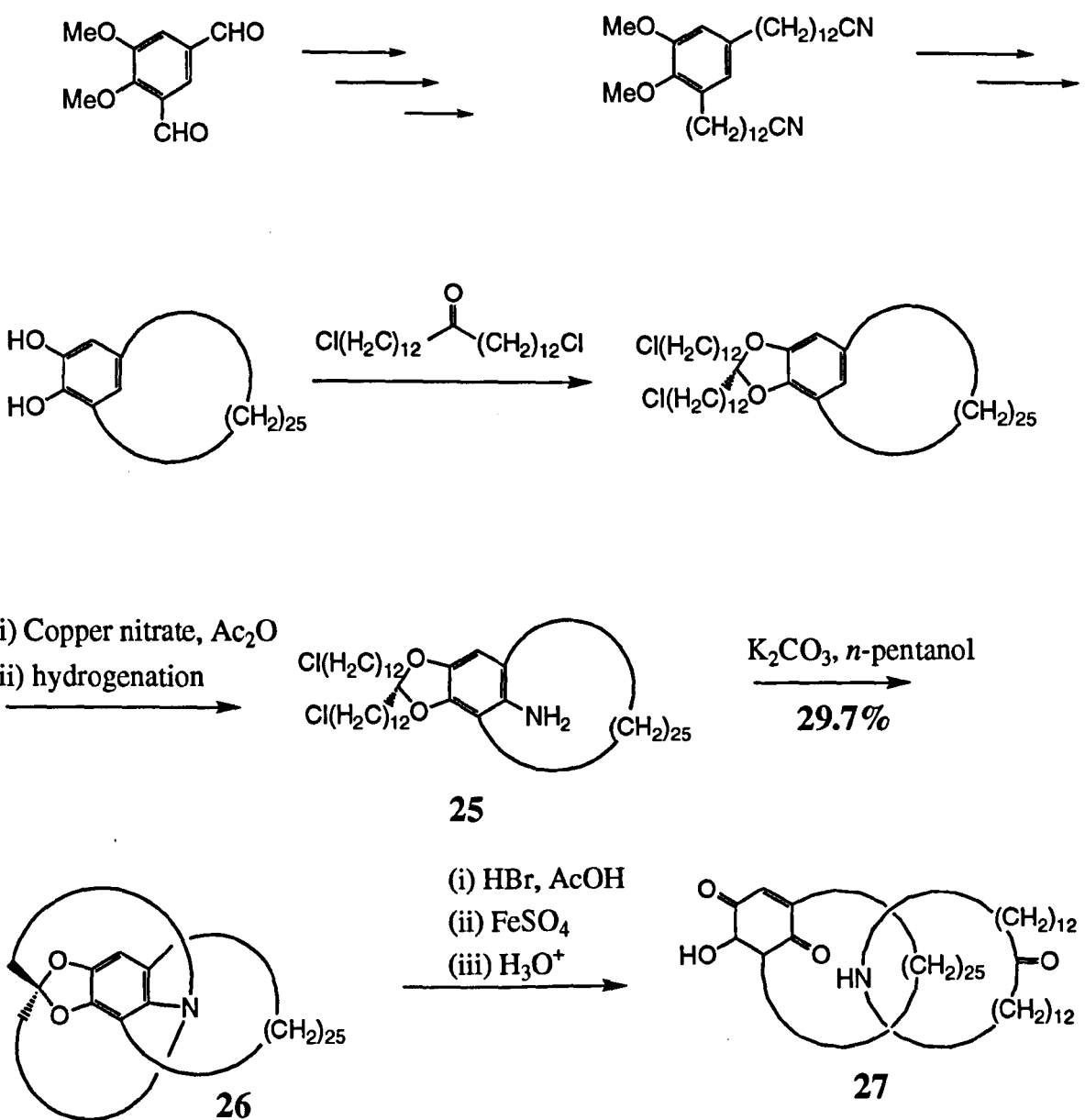
## 1.6 Tempered Synthesis of Catenanes and Rotaxanes

### 1.6.0 Covalent Templating of a Catenane

As we have already seen, the first catenane synthesis was demonstrated by Wasserman in 1960. Four years later, Schill and Lüttringhaus published the first *templated* catenane synthesis.<sup>47</sup> Their design used a covalent template effect rather than just random threading to ensure that the two rings produced were interlocked. The main points of their rather lengthy synthesis are illustrated in Scheme 1.12. The key intermediate is the dichloride **25**. Cyclisation via intramolecular alkylation of the amine is constrained by the tetrahedral geometry of the acetal carbon to give only the catenane precursor **26**. The core of the molecule is therefore acting as a template to ensure that cyclisation gives the required topology. The final steps of the synthesis involving acetal hydrolysis and cleavage of the aryl-nitrogen bond are trivial to give the catenated structure **27** which was characterised as its N-acetyl derivative.

This methodology has also been extended to the synthesis of [3]-catenane **28**<sup>48</sup> and an unsuccessful trefoil knot synthesis that will be discussed shortly.





**Scheme 1.12.** Schill and Lüttringhaus' covalently templated catenane synthesis, 1964.

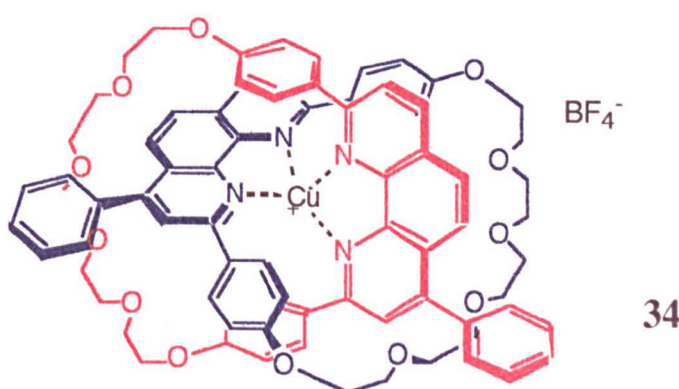
### 1.6.1 Metal Ion Tempted Catenane and Rotaxane Syntheses

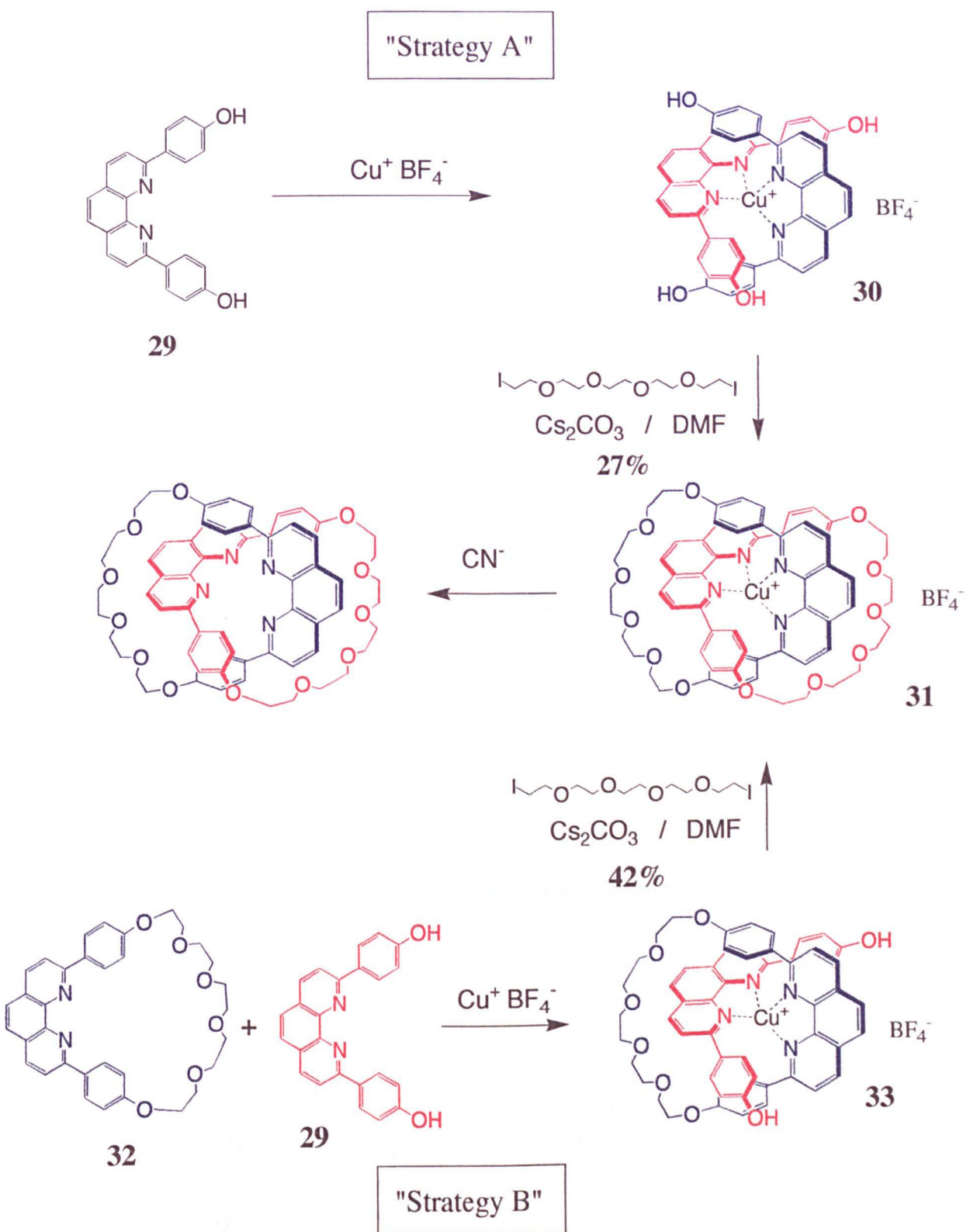
During the 1980s, the group of Jean-Pierre Sauvage in Strasbourg developed a metal-ion templating strategy,<sup>49</sup> which initially gave access to catenanes and rotaxanes, and has since been expanded to give the first synthetic molecular trefoil knot.<sup>50</sup> The catenane synthesis is illustrated by two different methods (Scheme 1.13).

In Strategy “A” the phenanthroline unit **29** is coordinated to Cu(I) which provides a template effect due to its tetrahedral geometry. Macrocyclisation of complex **30** under high dilution conditions gave the required catenane **31** in 27% yield. Strategy “B” is simply a variant on this. Here, the macrocycle **32** is preformed. Upon mixing **32**, **29** and Cu(I), the complex **33** is formed. Complexation of two **32** units to Cu(I) cannot occur due to steric reasons, and since the reaction is an equilibrium process, the end result is that **33** is formed quantitatively. Macrocyclisation of **33** gives catenane **31** in 42% yield. This higher yield is reflective of the fact that only one macrocyclisation is required in the catenane formation step. The overall yield from acyclic starting material is roughly equal for both strategies.

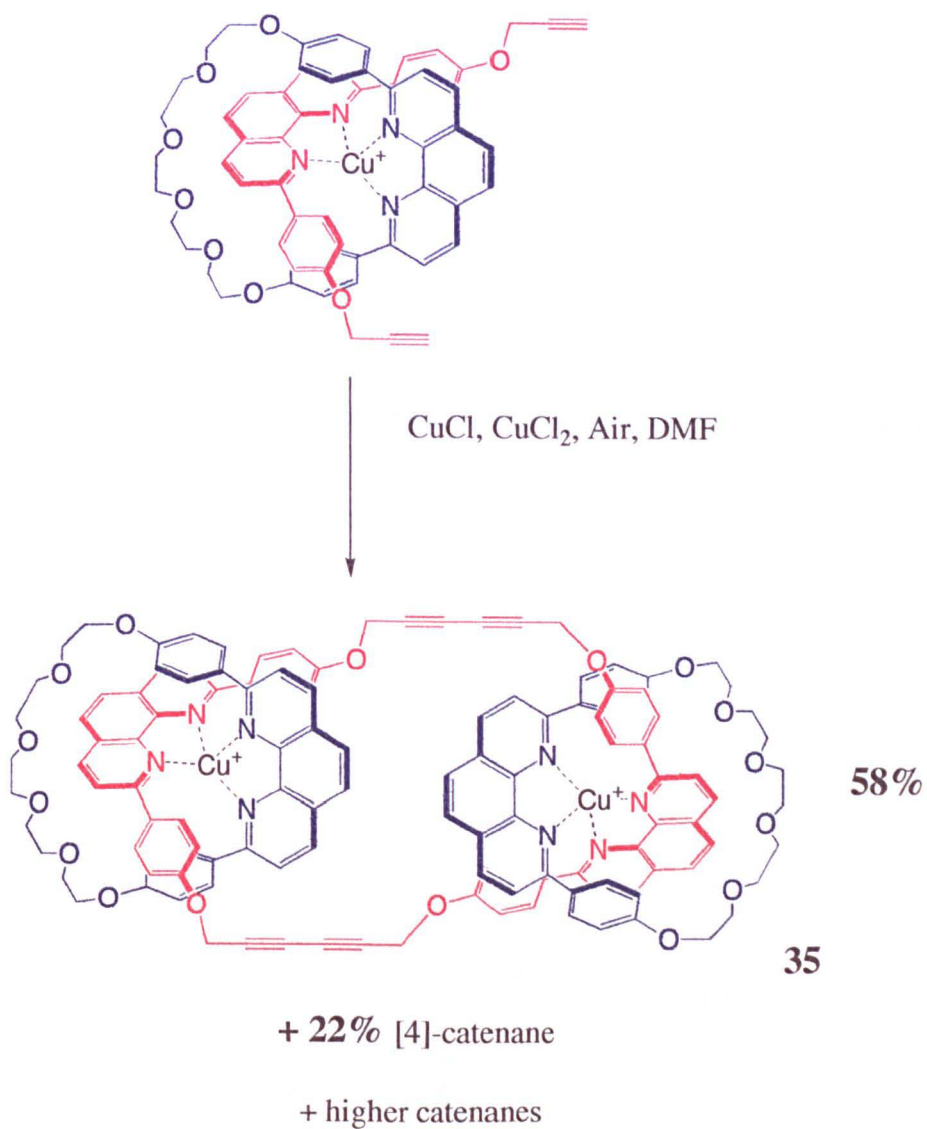
Although the Cu(I) ion provides an *interweaving* template effect to ensure that the two macrocycles that form are interlocked, it must be noted that the macrocyclisation reactions themselves are *not* templated in the strictest sense, although favourable electrostatic contacts between the edge of the phenanthroline units and the polyethylene glycol chain may provide a weak directing effect. The reaction is therefore carried out under high dilution conditions to maximise intramolecular cyclisation and reduce any intermolecular reactions.

Sauvage has already extended this strategy to prepare a number of other systems. For example, as mentioned earlier, when it is possible to define a direction around the rings, a catenane becomes chiral. The catenane **34** made by the same strategy has indeed been demonstrated to be chiral by NMR experiments.<sup>51</sup>

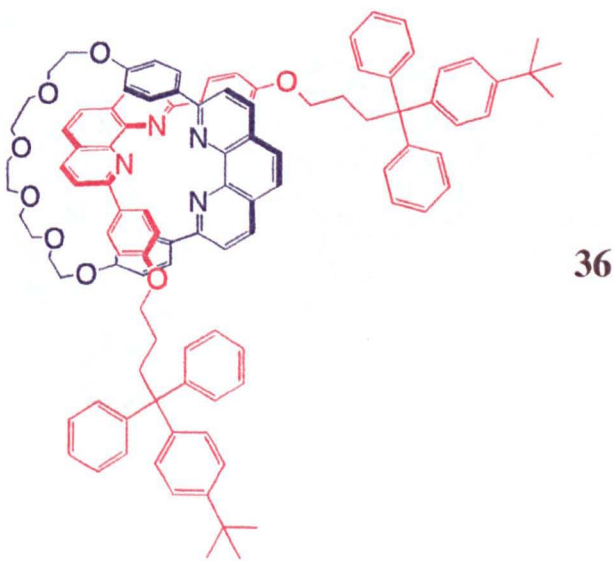




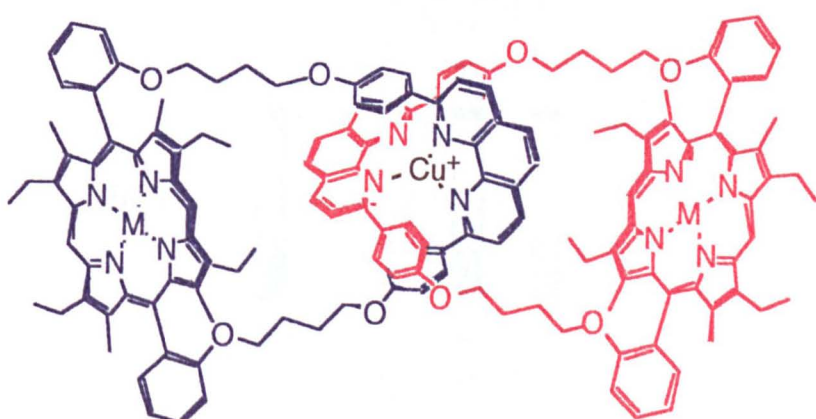
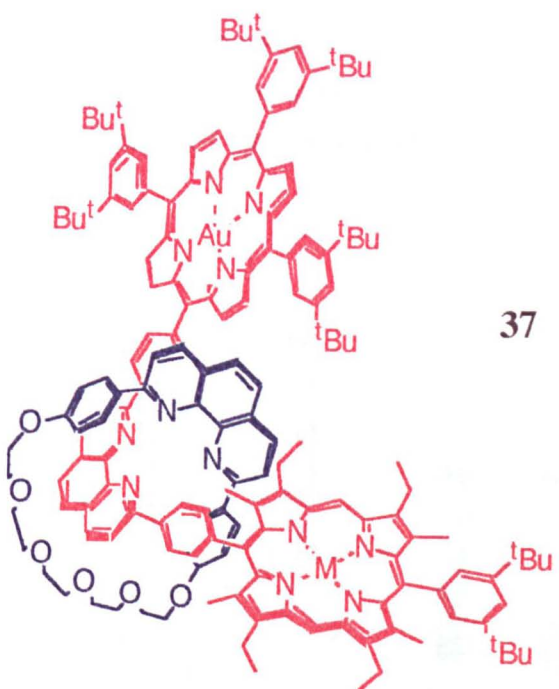
**Scheme 1.13.** Sauvage's templated catenane synthesis.



**Scheme 1.14** Sauvage's [3]- and higher catenane synthesis.



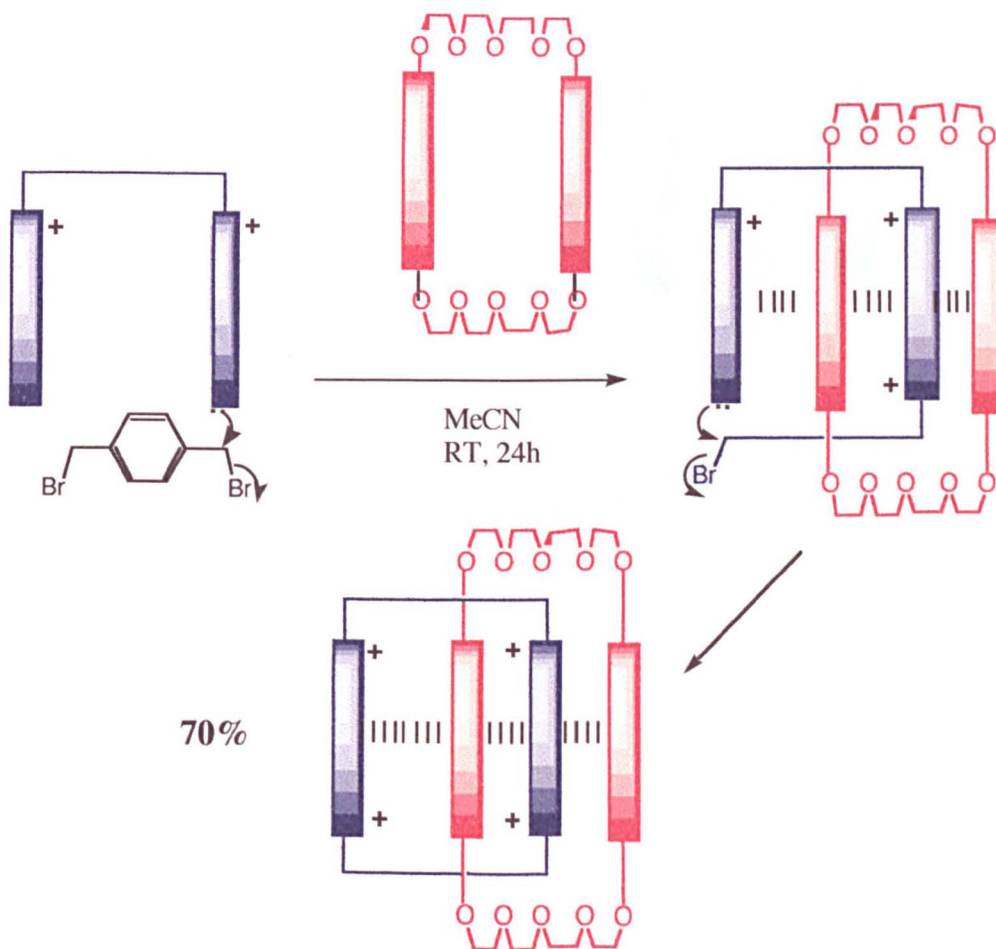
Sauvage has also gone on to prepare [3]-catenanes such as **35**<sup>52</sup> (Scheme 1.14) and has spectroscopically identified higher catenanes up to a [7]-catenane as byproducts.<sup>53</sup> This type of template effect has also yielded a number of rotaxanes, the first of which was **36** reported by Gibson in 1991.<sup>54</sup> Sauvage has also reported a number of rotaxanes containing interesting stopper groups such as porphyrin-stoppered **37**<sup>55</sup> and more recently a compound featuring C<sub>60</sub> (buckminsterfullerene) stoppers.<sup>56</sup> In these compounds, as well as playing a mechanical role in preventing unthreading, the stoppers confer interesting electrochemical or photochemical activity upon the molecules. Pseudo rotaxanes have also been reported<sup>57</sup> as have functional catenanes containing redox active components intended for the study of electron transfer effects such as porphyrin-catenane **38**.<sup>58</sup>



### 1.6.2 Catenanes and Rotaxanes Tempered by Aromatic Interactions

A second distinct template effect developed during the 1980s was due to the group of J. Fraser Stoddart at Birmingham. He has used  $\pi$ - $\pi$  stacking interactions to provide the template effects that have enabled a host of catenanes and rotaxanes to be prepared.<sup>59</sup> The key building blocks are illustrated by the two complexes shown in Figure 1.17 which were first made in 1986.<sup>60, 61</sup> In addition to stacking interactions, Stoddart suggests that the complexes are further stabilised by hydrogen bonding between the  $\alpha$ -protons of the paraquat unit and oxygen atoms of the crown ether as well as by electrostatic interactions involving the hydroquinone oxygens.<sup>7</sup>

The bipyridinium ring (schematically represented as the blue rectangle) and the 1,4-dialkoxybenzene ring (the red rectangle) form  $\pi$ -stacked structures in a wide variety of complexes. This interaction is used to provide a template effect throughout Stoddart's work, and is well illustrated in the [2]-catenane synthesis in Scheme 1.15 which gives a superb 70% overall yield of catenane.<sup>62</sup> The broken lines represent the templating  $\pi$ - $\pi$  stacking interactions.



**Scheme 1.15.** Stoddart's [2]-catenane synthesis.

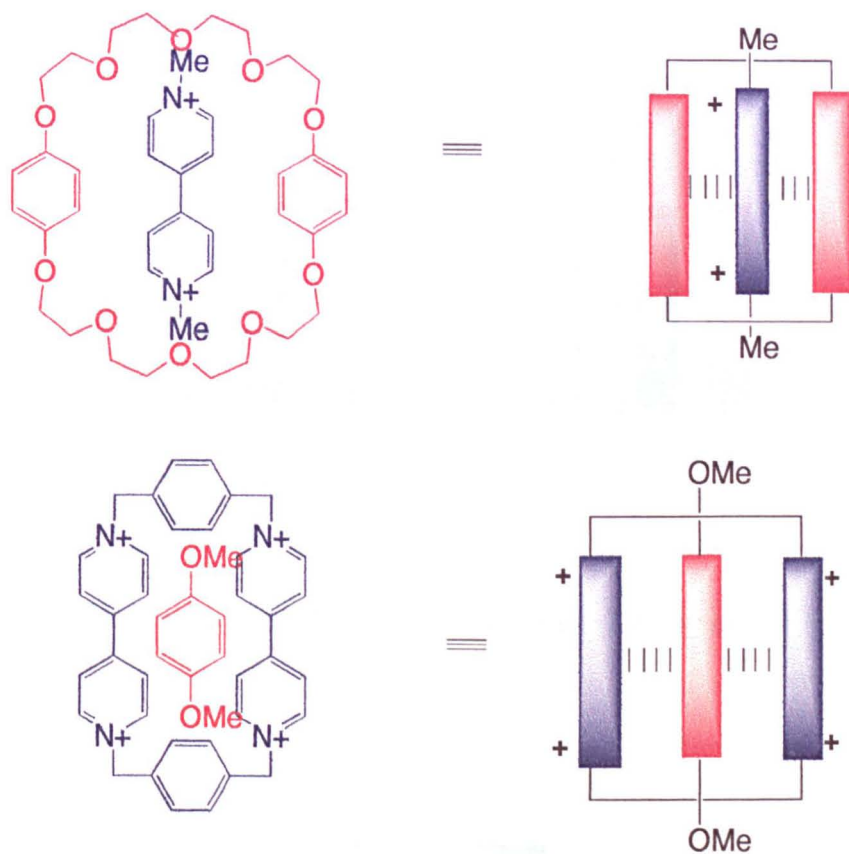


**Figure 1.17.** Stoddart's early complexes and a useful schematic representation.

These interactions have also allowed access to a [3]-catenane (Figure 1.18)<sup>63</sup> and numerous rotaxanes,<sup>64</sup> for example the one illustrated in Figure 1.19, using virtually identical techniques. Three distinct routes have been reported for such a rotaxane synthesis - The threading approach where the linear component is threaded through the pre-formed macrocycle and then stoppered, the slippage approach where the pre-stoppered strand can slip through the macrocycle at elevated temperature but cannot slip out again at room temperature and the clipping approach where the macrocycle is formed around the stoppered strand (Figure 1.20).<sup>65</sup>

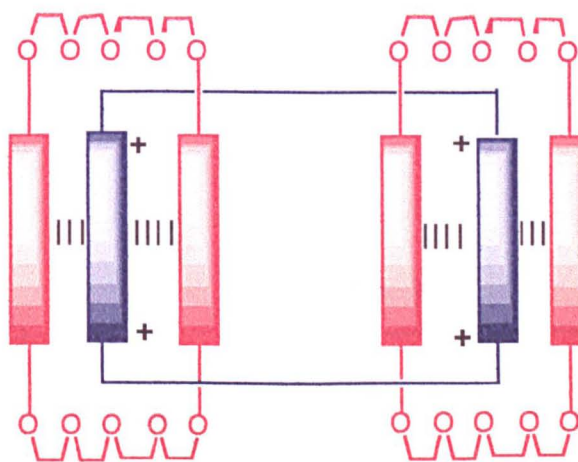


**Figure 1.18.** Stoddart's [3]-catenane. See Figure 1.17 for details of schematics.

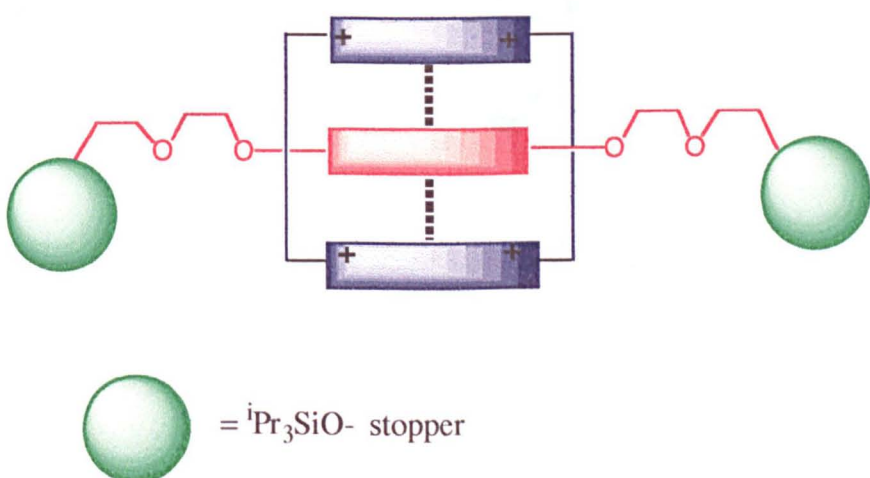


**Figure 1.19.** Schematic of Stoddart's rotaxane.

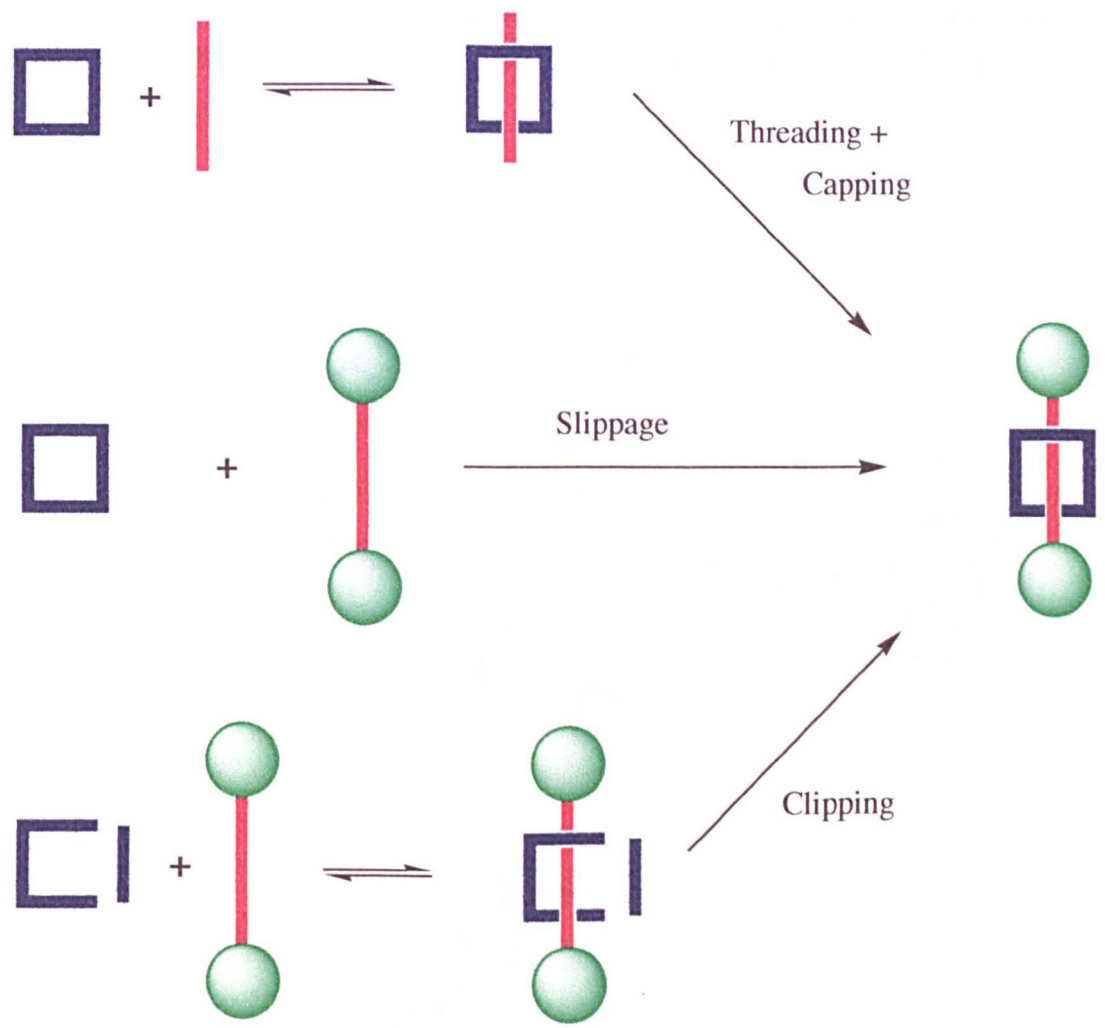
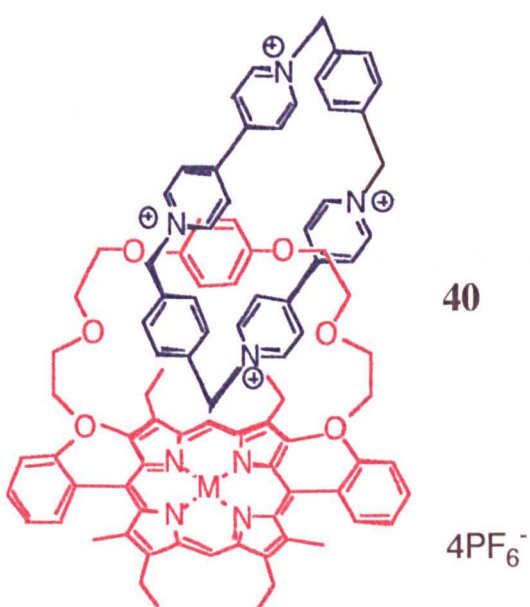
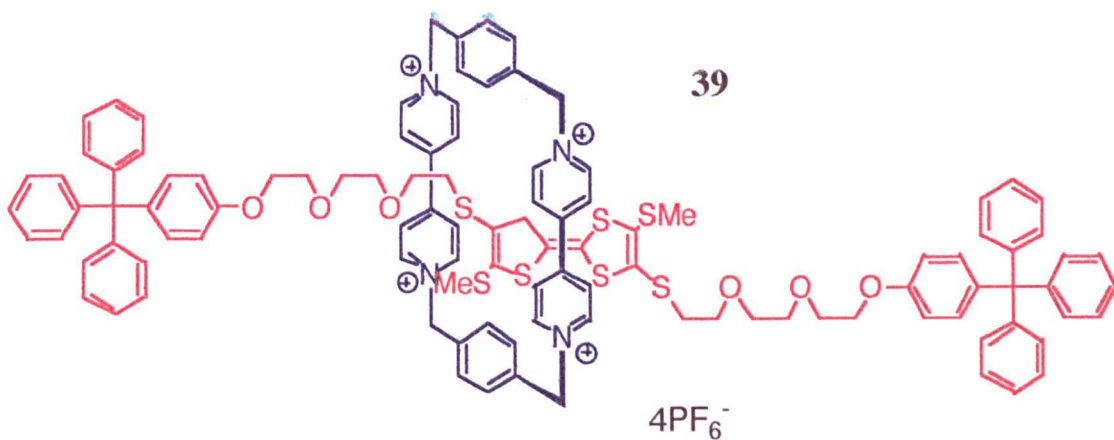


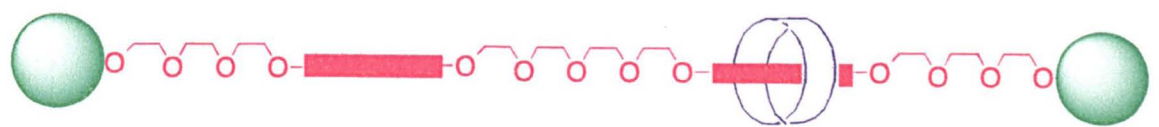
**Figure 1.20.** Schematics of three alternative routes to a [2]-rotaxane.

An extension of the same idea has led to some quite complex systems, for which one can begin to envisage potential applications in the emerging field of molecular devices. The same methodology has allowed access to the “molecular shuttle” and the “molecular train set” (Figure 1.21).<sup>66</sup> Modification of the electronic properties of the aromatic ring “stations” has led to recent reports of molecular switches.<sup>67</sup>

Identical types of interactions have also been used by other workers to prepare many different molecules too numerous to mention. For example **39**, a similar rotaxane based upon tetrathiafulvene reported by Becher *et al* and porphyrin-containing catenane **40** reported by Gunter *et al*.



(a)



(b)

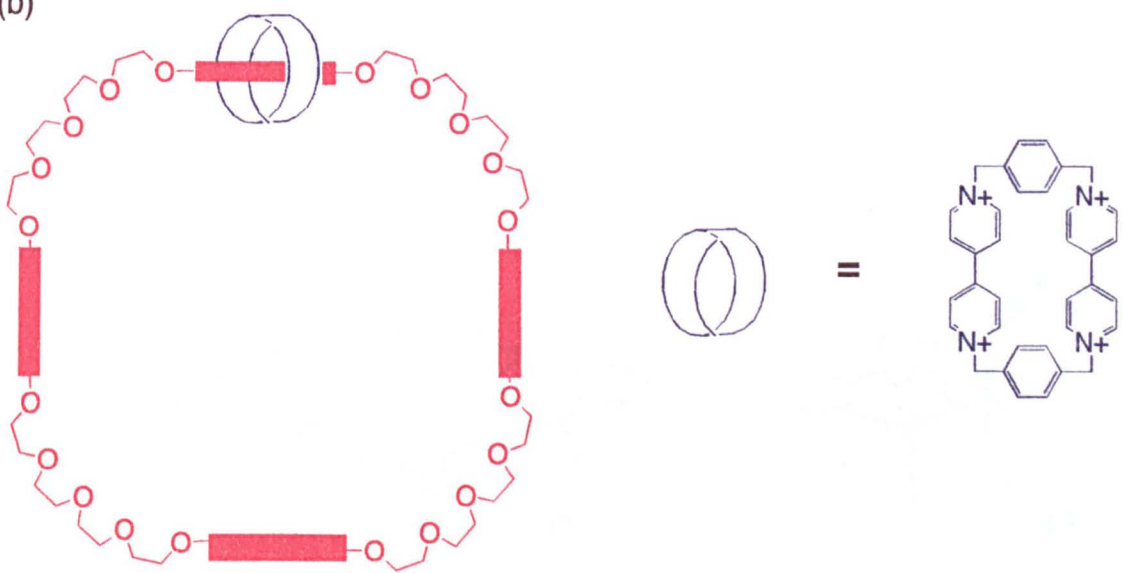
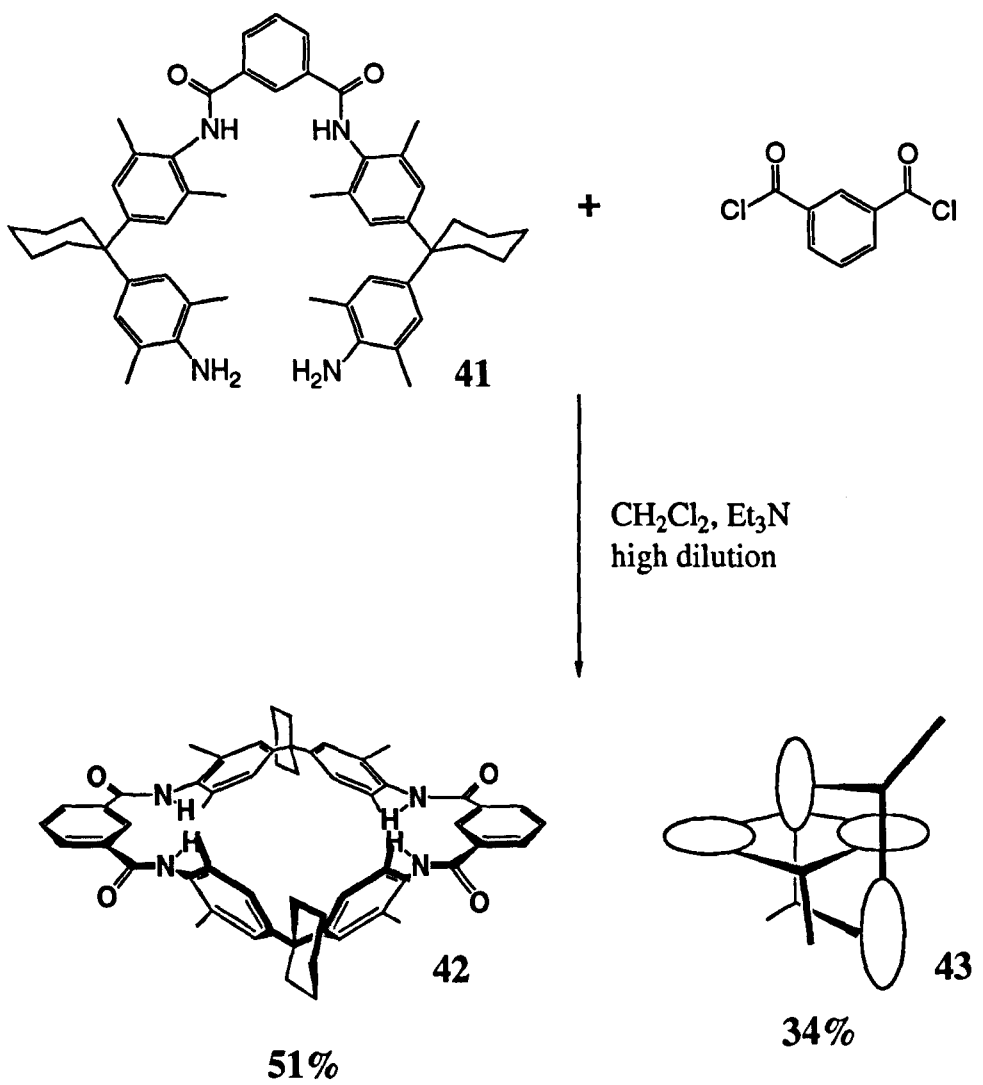


**Figure 1.21.** (a) Stoddart's "molecular shuttle" and (b) "molecular train set".

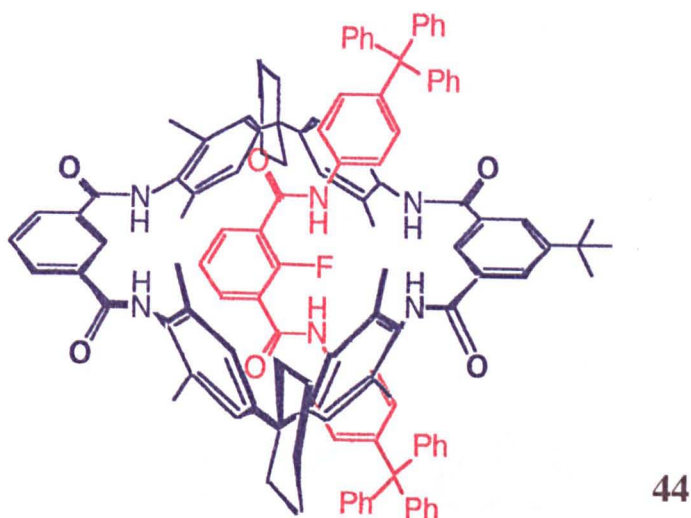


**Scheme 1.16.** Hunter's catenane synthesis.

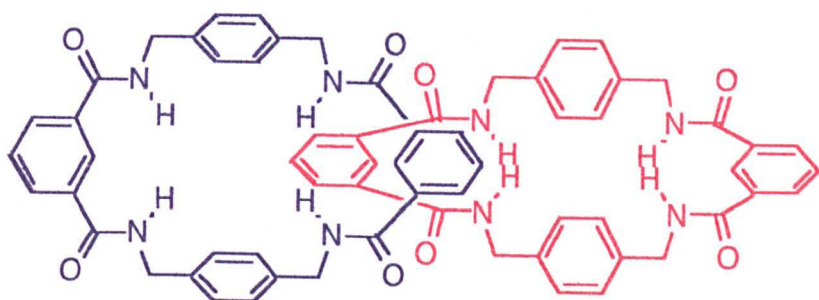
### 1.6.3 Catenanes Tempered by Hydrogen Bonding

A final source of non-covalent interactions for a template effect is hydrogen bonding. The first example of a catenane templated by hydrogen bonding was reported by Hunter in 1992 as shown in Scheme 1.16.<sup>70-72</sup> Upon cyclisation, **41** and isophthaloyl dichloride gave not only the expected macrocycle **42** in 51% yield but also the [2]-catenane **43** in 34% yield.

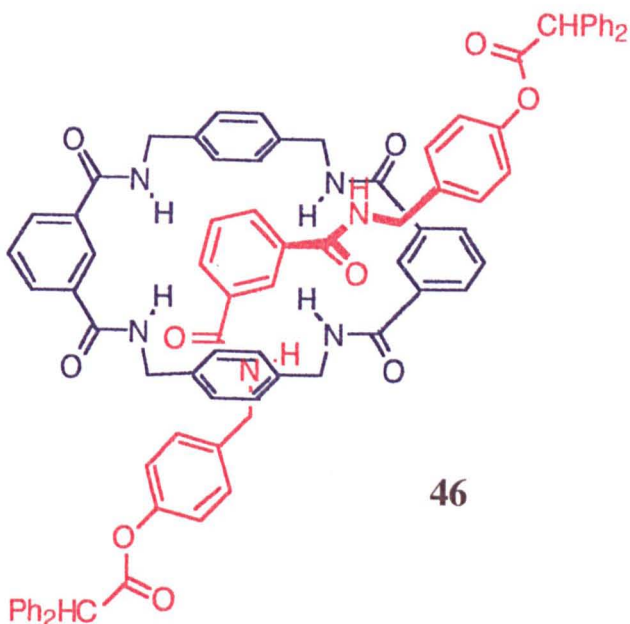
Later, Vögtle reported a number of structurally similar catenanes bearing various substituents and with heterocycles such as furan replacing the 1,3-disubstituted aromatic rings.<sup>73, 74</sup> He has also gone on to use the same methodology to prepare rotaxanes such as **44**.<sup>75</sup>



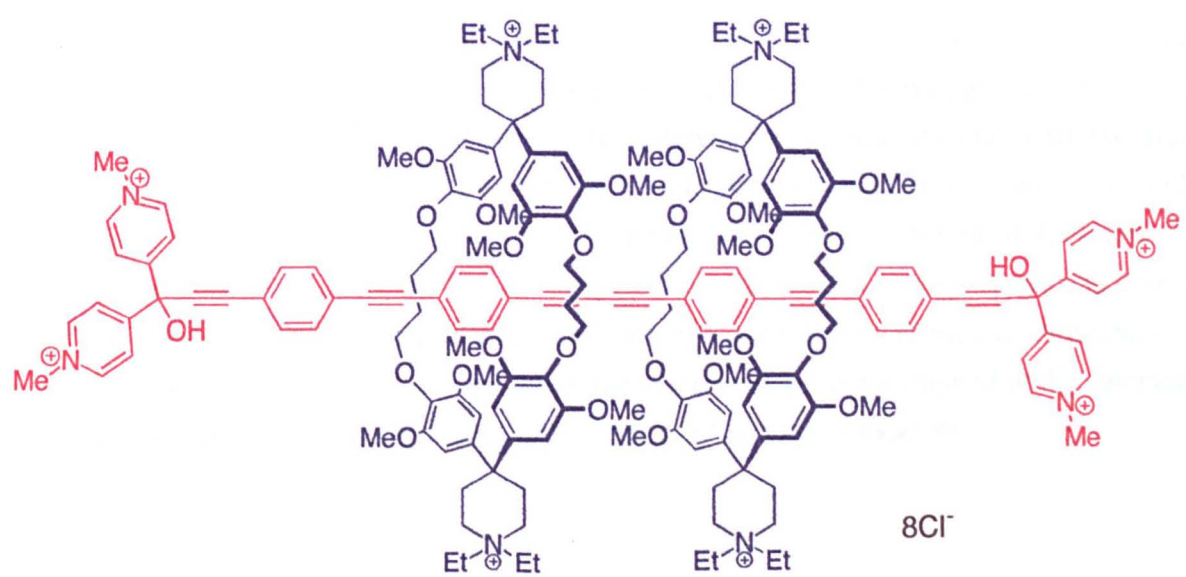
David Leigh has recently reported the self-assembly of [2]-catenane **45** from two commercially available compounds directed by similar interactions. **45** is formed in a remarkable 20% yield from the assembly of eight separate components.<sup>76</sup> The assembly is so efficient that the simple macrocyclic target molecule required as a receptor for carbon dioxide cannot be prepared directly. Leigh has recently published a strategy based upon the preparation and subsequent cleavage of rotaxane **46** to access the non-catenated macrocycle.<sup>77</sup>



**45**



**46**

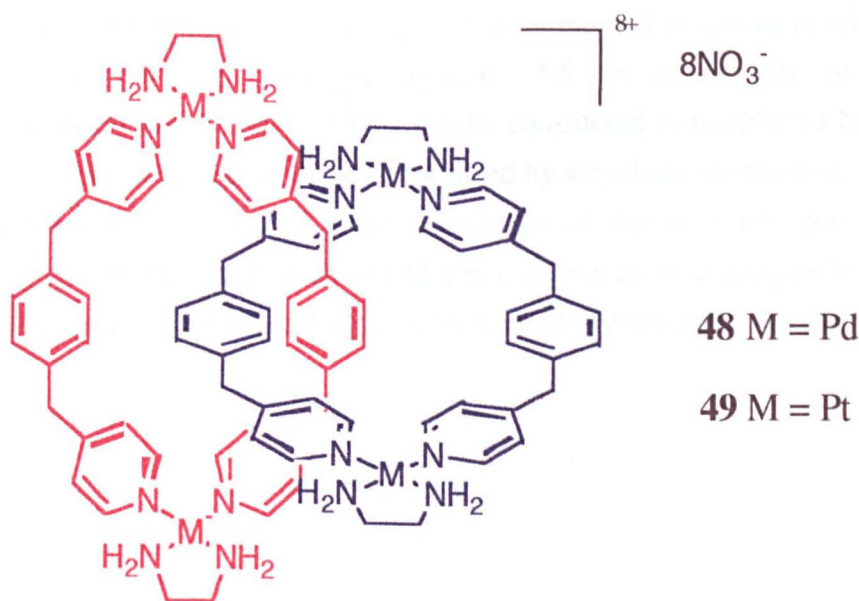


47

### 1.6.4 Other Templated Syntheses of Rotaxanes and Catenanes

Many other templated syntheses have been reported that rely on some sort of template effect although the actual templating interactions may be less readily classified than those discussed earlier. For example, Anderson's synthesis of water-soluble [3]-rotaxane **47** relies upon the hydrophobic effect to template the threading process in reasonable yield.<sup>78</sup>

Also of interest are Fujita's catenanes **48** and **49**<sup>79</sup> which represent one of the few examples of the incorporation of a metal ion into the cyclic components of a catenane structure. Again, aromatic interactions provide the molecular recognition to favour catenane formation. Where M = Pd, the catenane is in equilibrium with the free macrocycle and the amount of catenane present depends on concentration. At high concentration, **48** exists almost entirely in the form of catenane. When M = Pt, a more kinetically inert metal ion, the free macrocycles are stable at room temperature and do not equilibrate to catenane **49**. However, upon heating in highly polar media, catenane can form. Upon cooling to room temperature, the macrocycles remain trapped in the catenane structure which has led Fujita to term this system a "molecular lock".<sup>80</sup>



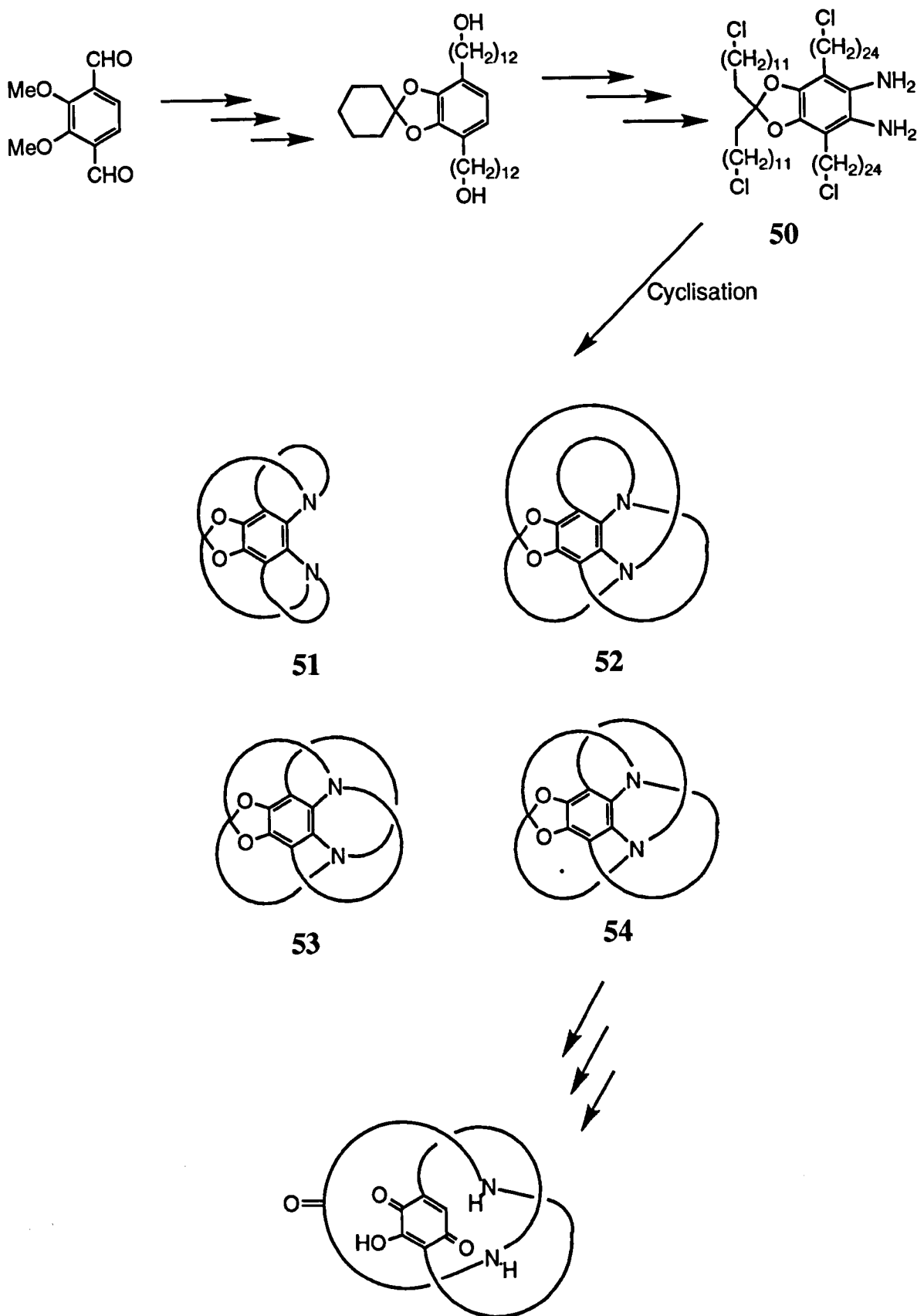
## 1.7 Templated Synthesis of Molecular Knots

### 1.7.0 Attempted Synthesis Using a Covalent Template

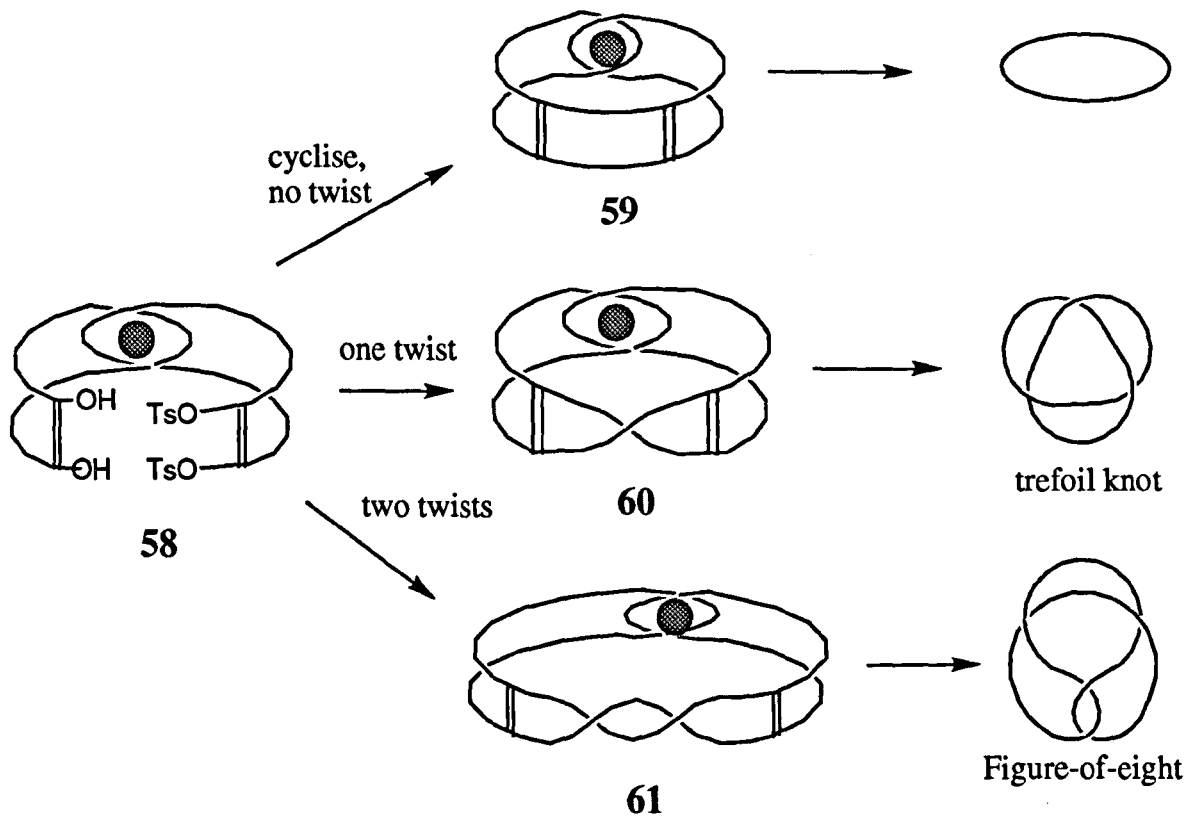
We have already discussed Schill and Lüttringhaus' covalently templated catenane syntheses. Schill also attempted to extend this methodology to a trefoil knot as outlined in Scheme 1.17.<sup>81</sup> Here, the key intermediate is **50**. Again, the geometry of the tetrahedral acetal carbon is constrained such that the possible products from intramolecular cyclisation are limited. There are four possible products that could arise from complete intramolecular cyclisation of **50**. Of these, **54** is the precursor of a trefoil knot via the acetal hydrolysis and aryl-nitrogen bond cleavage discussed earlier. In his attempted synthesis, Schill obtained three products in a total yield of 1.7% from this cyclisation but could not confidently assign structures. It is unclear whether **54** was produced or not. It seems that too many low yielding steps were required in this synthesis.

### 1.7.1 Attempted Templated Synthesis via a Möbius Strip

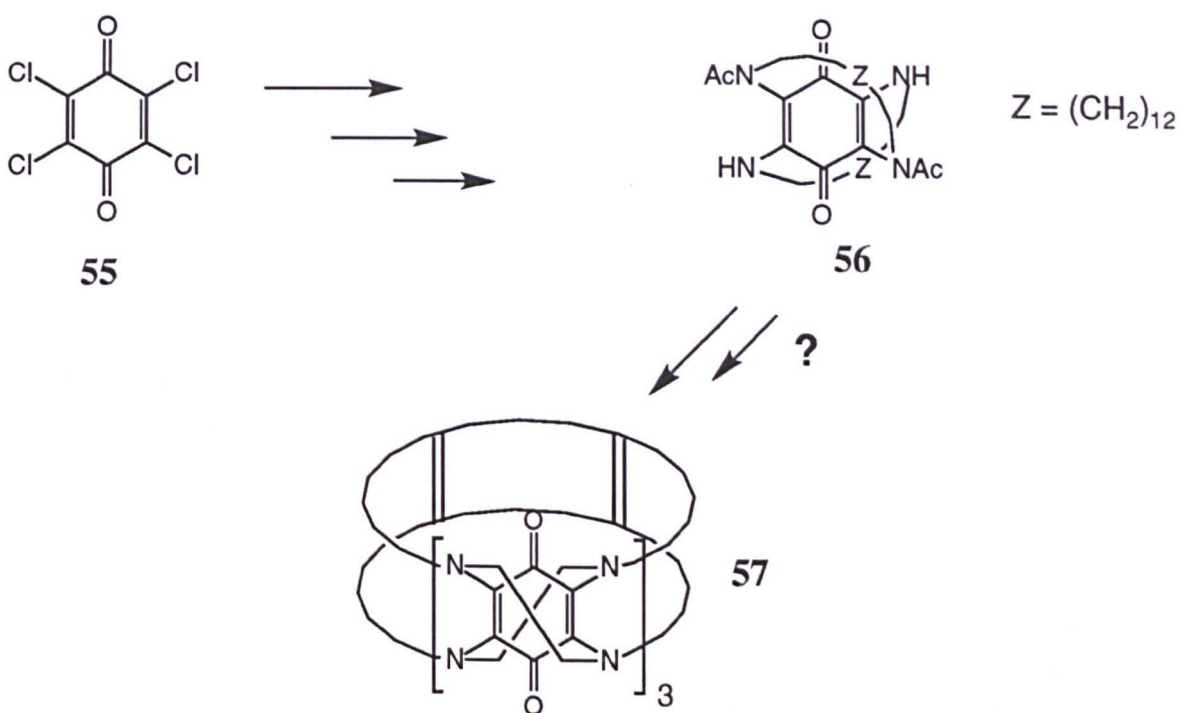
We have also discussed attempted strategies using molecular Möbius strips to obtain topologically complex molecules. We observed that such methods must be considered to be statistical in nature since only random chance can result in the formation of the twists required to give objects with complex topologies upon cleavage. Schill attempted to template a half-twist using a covalent method as shown in scheme 1.18. He prepared the doubly bridged system **56** in a number of steps from tetrachlorobenzoquinone **55**.<sup>82, 83</sup> This can be considered to template a half-twist, such that if three units were linked together followed by a cyclisation reaction, the triple half-twist Möbius strip **57** would result. Cleavage of the aryl-nitrogen bonds would effectively cut the strip in half and yield a trefoil knot as discussed earlier. No positive results were ever published, and again it seems that just too many low yielding steps are required.



**Scheme 1.17.** Schill's attempted trefoil knot synthesis.



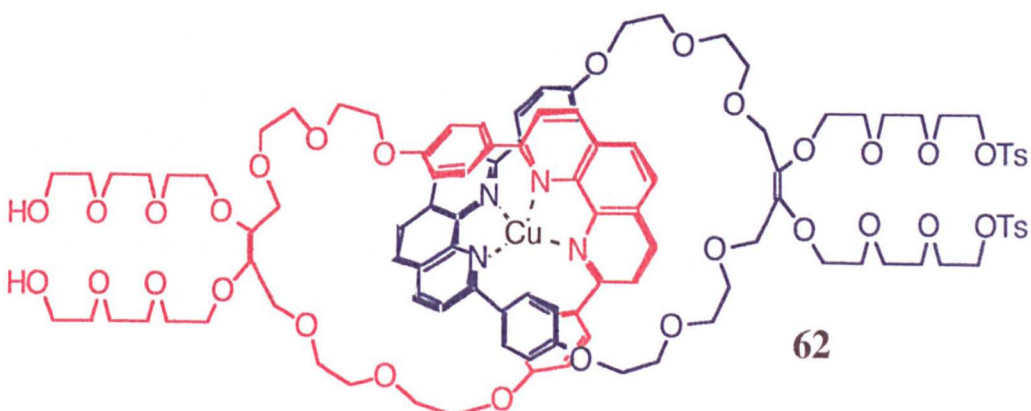
**Scheme 1.19.** Walba's "hook and ladder" approach to a template effect.



**Scheme 1.18.** Schill's attempted templated synthesis of a triple half-twist Möbius strip.

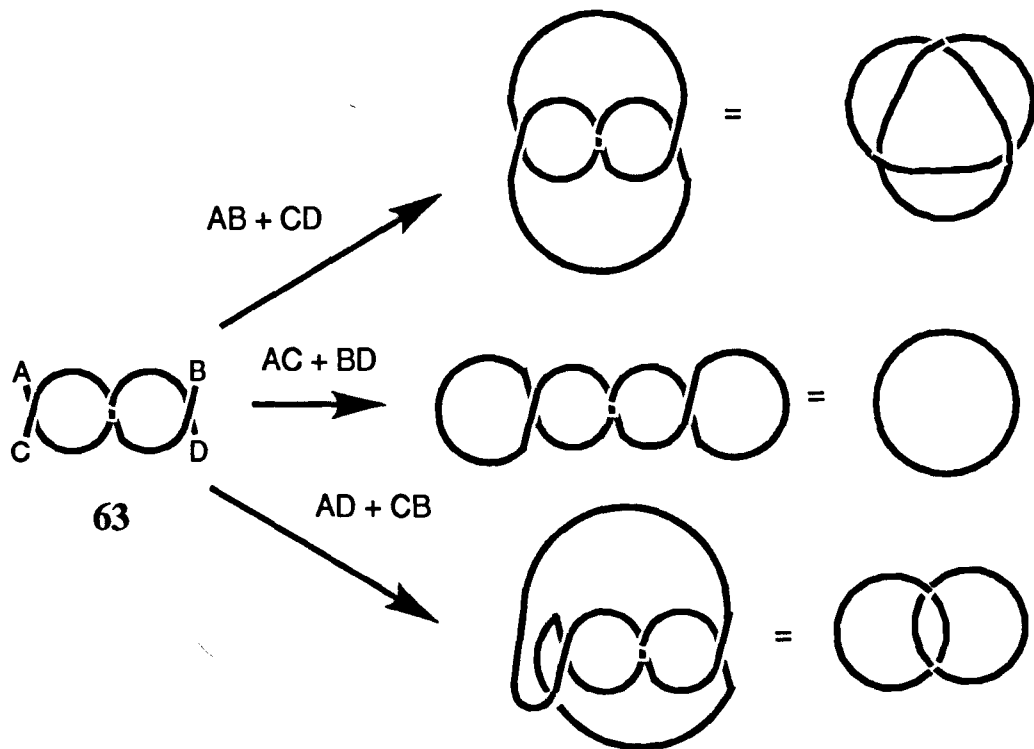
### 1.7.2 The “Hook and Ladder” Approach to a Templatized Möbius Strip

A further scheme for at least a partial templating of twists in a molecular strip is illustrated by the so called “hook and ladder” approach developed by Walba (Scheme 1.19).<sup>84</sup> Now only one half-twist has to be introduced in the random cyclisation of **58** in order to get the knot precursor **60**. If two half-twists could be introduced, then **61** would be a precursor for a figure-of-eight knot - a structure for which no other synthetic route has been proposed. Experimental work along these lines has recently been completed by Walba and co-workers, but only untwisted **59** was isolated and characterised from the cyclisation of **62**.<sup>85</sup>



### 1.7.3 A Metal Ion Tempered Synthesis of a Molecular Trefoil Knot

So far, we have discussed the approach to catenanes, rotaxanes and various structures derived from them, using a number of different templating strategies. The ultimate extension of this came in 1989 when Sauvage published the synthesis of a molecular trefoil knot.<sup>50</sup> Such a synthesis was really unthinkable without a template effect of some sort, and it was an ingenious extension of the catenane template that we have already seen that provided the answer. A schematic of Sauvage's approach is shown in Scheme 1.20.



**Scheme 1.20.** Sauvage's approach to a trefoil knot template.

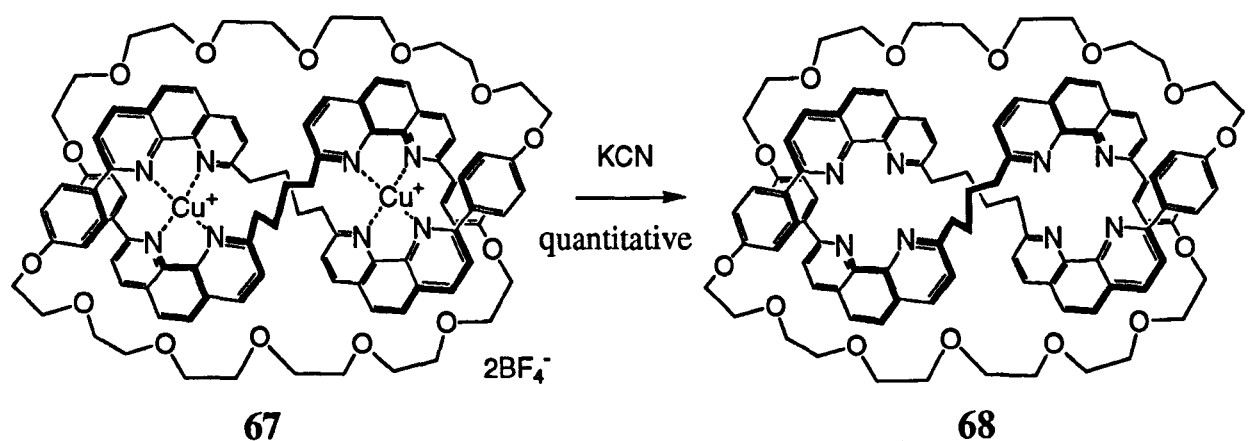
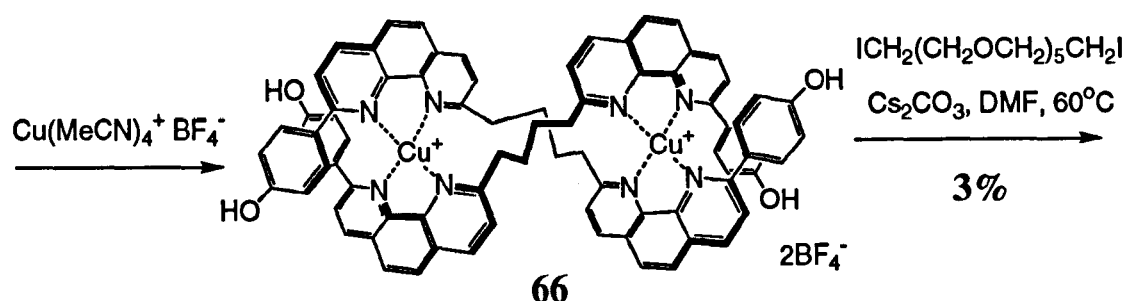
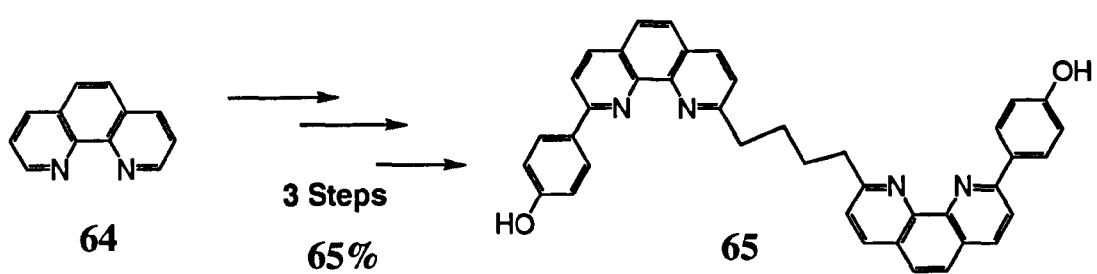
If a double helical structure **63** consisting of two strands with functionalised ends could be prepared and then a macrocyclisation reaction used to link those ends intramolecularly, three possible products could arise as shown in Scheme 1.20. One of those products is a trefoil knot. A model of this system reveals that the connection leading to the catenane is very strained, and the connections to give the knot do indeed seem to be more favourable than those leading to the simple macrocycle.

Double helical structures templated by metal ions have been observed in Lehn's group<sup>86</sup>, so a logical extension of this combined with Sauvage's experience of templated catenane synthesis led after many unsuccessful attempts to the synthetic sequence in Scheme 1.21. The bisphenanthroline unit **65** was prepared readily in 65% overall yield from commercial 1,10-phenanthroline **64** in 3 steps. Addition of  $\text{Cu}(\text{MeCN})_4^+\text{BF}_4^-$  gave the double helical complex **66** which was not isolated. Macrocyclisation under high dilution conditions yielded a mixture of products and the metallo-knot **67** was isolated in 3% yield after careful chromatography. Demetallation gave the free knot **68**. Also isolated was a small amount of the unknotted topological isomer.

Although the yield was low and the procedure difficult (Sauvage reported that even a repeat synthesis to make a further 100mg would take several months),<sup>87</sup> this route had finally given access to a molecular knot. Later work illustrated the importance of the group linking the two phenanthroline units<sup>88</sup> and saw improved yields, culminating in 1994 with a yield of 30%.<sup>89</sup> Some yields for different linker groups are illustrated in Table 1.1.

**Table 1.1. Yields for Sauvage's knot formation with different linker groups.**

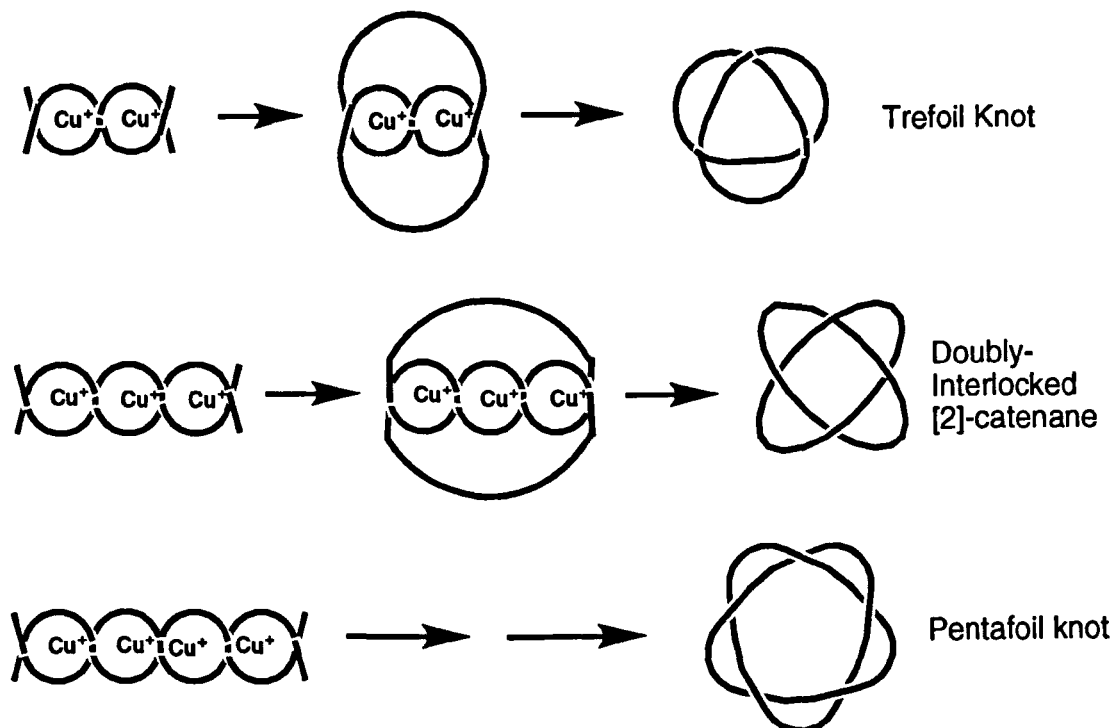
Linker Unit	$-\text{CH}_2(\text{CH}_2\text{OCH}_2)_n\text{CH}_2-$	Macrocyclisation Yield
$-(\text{CH}_2)_2-$	n=6	0.5%
$-(\text{CH}_2)_4-$	n=5	0.7%
$-(\text{CH}_2)_4-$	n=6	3%
$-(\text{CH}_2)_6-$	n=5	8%
$-(\text{CH}_2)_6-$	n=6	2.5%
1,3-phenylene	n=6	30%



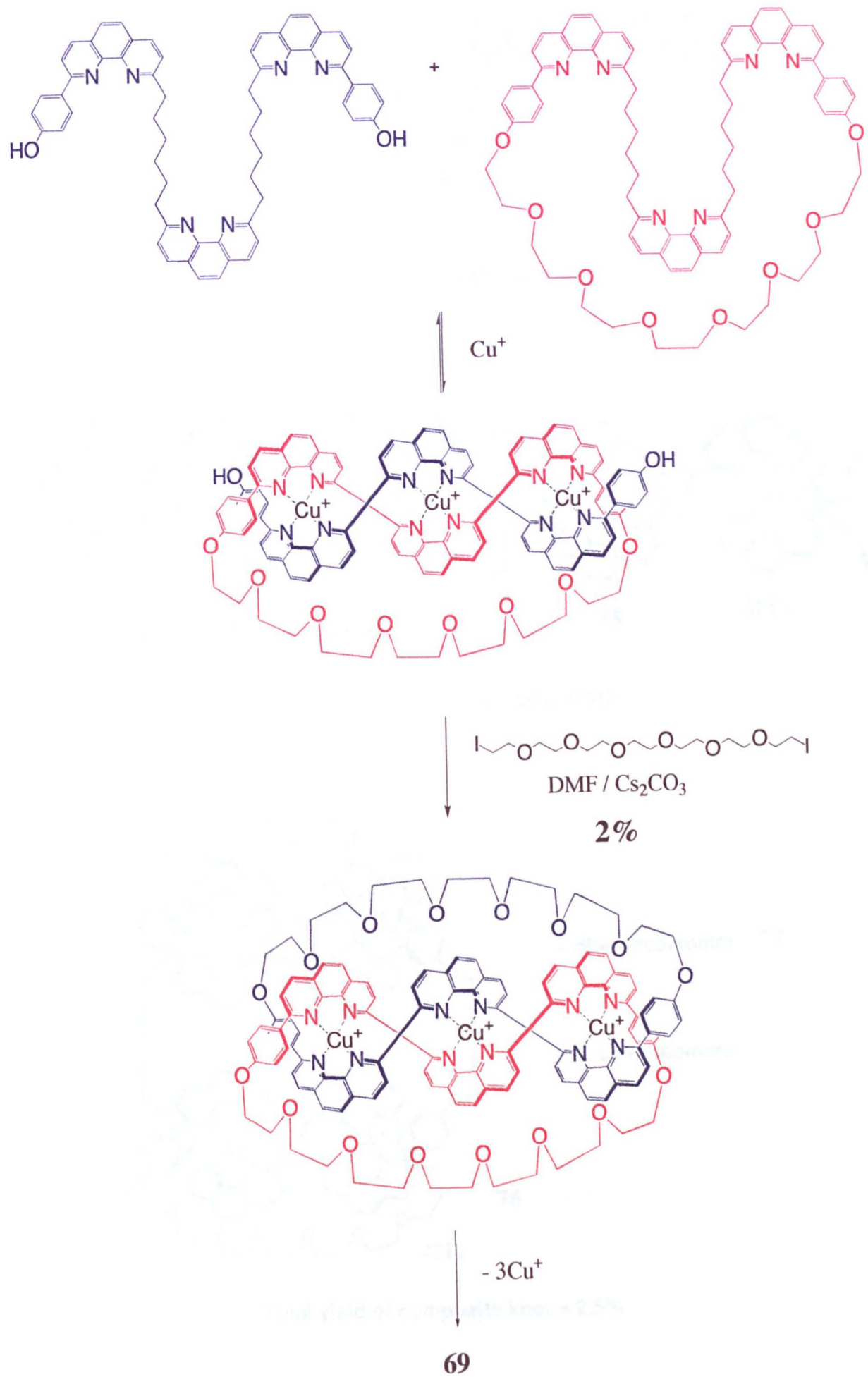
**Scheme 1.21.** Sauvage's initial trefoil knot synthesis.

### 1.7.4 Extension to More Complex Topologies

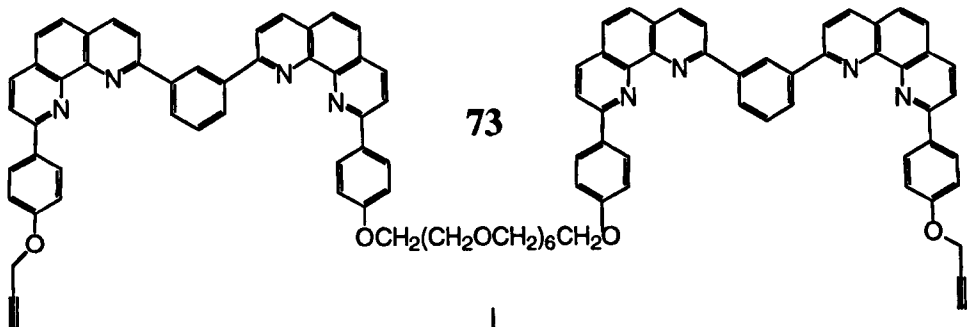
Sauvage has proposed that this knot is just the second in a series of topologies available using this strategy, the first member being the catenane discussed earlier. Some early members of the series are illustrated in Scheme 1.22.<sup>87</sup> Recently, the group has indeed published the first synthesis of a doubly interlocked [2]-catenane in 2% yield using this strategy (Scheme 1.23).<sup>90</sup> Doubly interlocked **69** exhibits remarkably different properties to its singly interlocked isomer. For example, the two compounds have remarkably different  $R_f$  values and undergo different fragmentation in FAB MS due to the more highly strained nature of the doubly interlocked system.<sup>91</sup> It remains to be seen if the group is now engaged in extending this methodology further to a pentafoil knot!



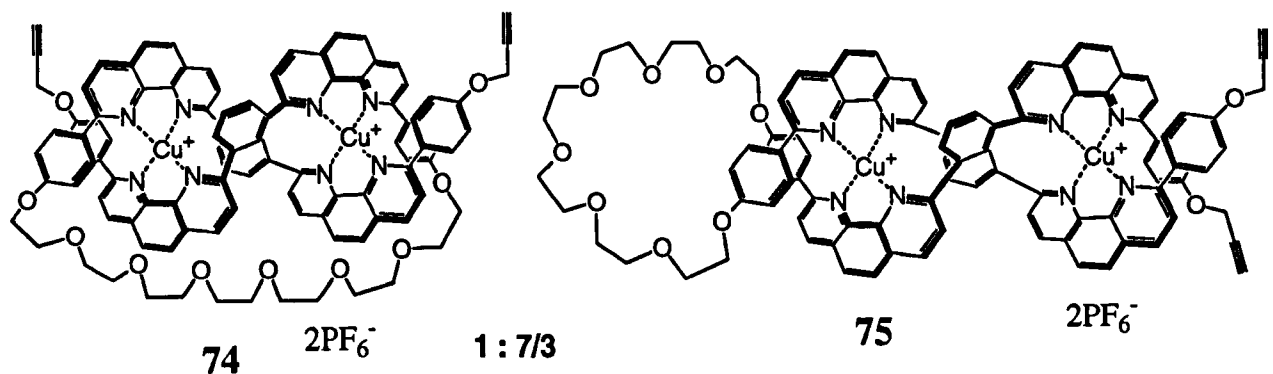
**Scheme 1.22.** A series of interesting topologies available from Sauvage's templated helix strategy.



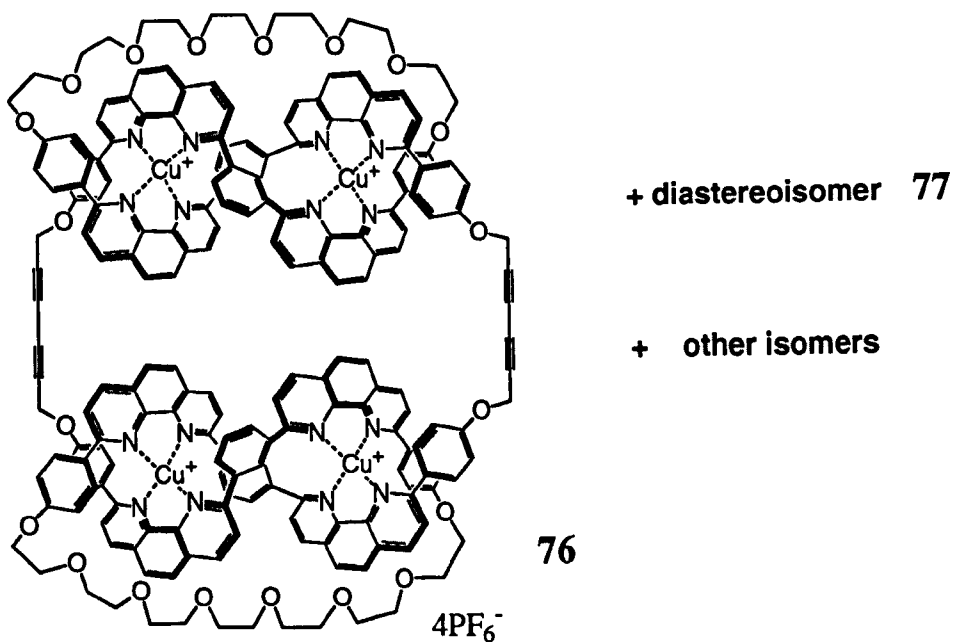
**Scheme 1.23.** Sauvage's synthesis of a doubly-interlocked [2]-catenane.



Cu(MeCN)<sub>4</sub><sup>+</sup> PF<sub>6</sub><sup>-</sup>



CuCl, CuCl<sub>2</sub>, DMF



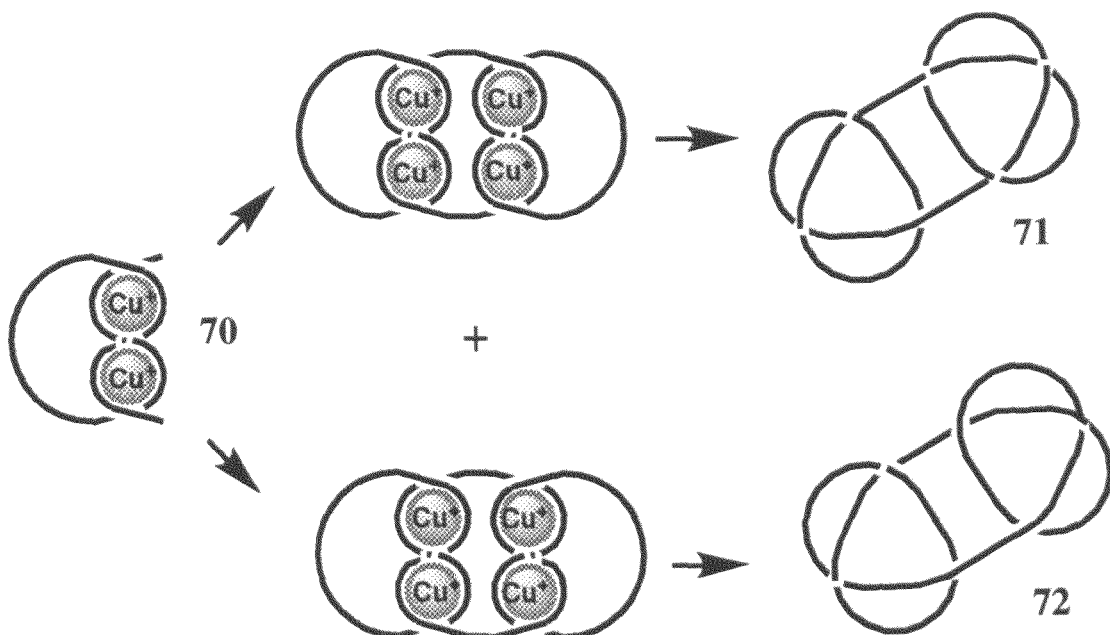
Total yield of composite knot = 2.5%

Scheme 1.25. Sauvage's synthesis of the first composite molecular knot.

### 1.7.5 Composite Molecular Knots

Most recently, the Sauvage group have extended their methodology to the synthesis of composite knots - that is to say knots made up of more than one subunit as opposed to the "prime" trefoil knot. The basic strategy for such a synthesis is illustrated schematically in Scheme 1.24.<sup>92</sup>

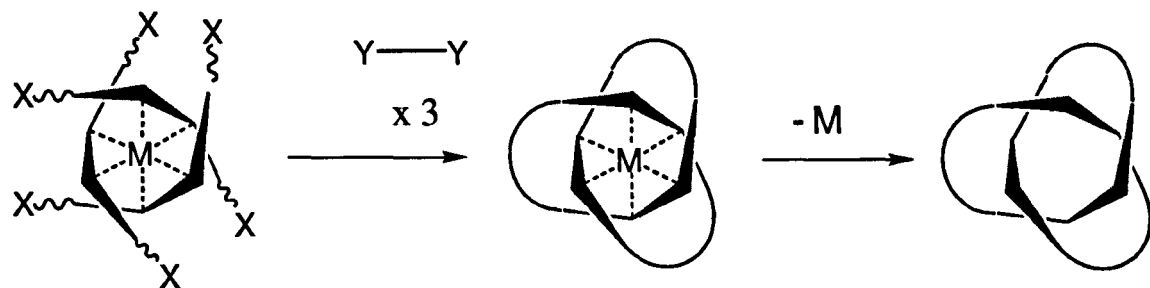
The open chain fragment **70** is structurally similar to the trefoil knot already reported but with two groups not cyclised. Dimerising two such units together followed by removal of the metal ion templates would give the composite knots **71** and **72** which are related as diastereoisomers, reflecting the fact that the sub-unit **70** is a mixture of two enantiomers.



Sauvage has successfully used this strategy and has recently reported the preparation of a mixture of molecules corresponding to **71** and **72**. The key points in the synthesis are outlined in Scheme 1.25. The final low yield of knot and production of other isomers is due mainly to the fact that the precursor **74** cannot be isolated pure but is the minor component in an inseparable mixture with **75**. Other products arise from the coupling of **74** with **75** (this is in fact a trefoil knot) and from coupling of **75** with itself (a topologically trivial macrocycle). The proportion of composite knots **76** and **77** in the product mixture compared to these by-products is actually larger than would be expected from a simple statistical analysis and Sauvage proposes that this may be due to a more suitable spatial arrangement of the terminal acetylinic functions of the more rigid **74** compared to **75**.

### 1.7.6 A Trefoil Knot Templated by an Octahedral Metal Ion

In 1973, Sokolov suggested a templating strategy based upon an octahedral metal centre with three coordinated bidentate ligands.<sup>93</sup> If three functionalised ligands are arranged around an octahedral metal ion, they are disposed in such a way that connection of the ends could lead to a trefoil knot (Scheme 1.26). X and Y represent groups that can react together to form a new bond.



**Scheme 1.26.** Sokolov's strategy for a trefoil knot synthesis via an octahedral metal ion template.

However, it seems that the probability of the ends linking two-by-two in the correct manner is fairly remote when one considers the numerous "wrong" connections that could be made. Not surprisingly, nearly 25 years after the original proposal, no experimental results have been reported using such a strategy.

This thesis concerns my work to take this initial idea and build in extra template effects to favour only the required connections to give access to not only a trefoil knot but also some other novel knotted structures. The adaptation of this strategy is described in Chapter 2.

---

# *Chapter 2*

---

## **Design Strategy**

## 2.1 Approach

### 2.1.0 Tris-Bipyridine Complexes

The proposed synthetic route requires the use of an octahedral metal complex containing three coordinated bidentate ligands. The ligands require functionality that can be used to form new bonds via a linker such that two ligands can be joined together in the required sequence. A number of ligands exist for incorporation into octahedral tris-complexes, but in our initial design it was decided to utilise 2,2'-bipyridine (bipy) ligands because of their versatility.

2,2'-bipyridine ligands are highly stable and their chemistry has been extensively studied.<sup>94</sup> Literature routes are available to ligands containing a wide range of substituents at a variety of positions. Models suggested that 5,5'-disubstitution would provide the optimum geometry for the system of interest and the literature here is particularly extensive.<sup>95</sup> As well as the possibility of using literature syntheses as a starting point for the required ligands, these synthetic methods are also straightforward and inexpensive to carry out on large scale.

Secondly, the metal complexes themselves are extremely versatile.  $M(\text{bipy})_3^{n+}$  complexes are known in at least one oxidation state for virtually every d-block metal ion, and indeed in several different oxidation states for a significant number.<sup>96</sup> The complexes have widely differing properties depending upon the metal ion and oxidation state - for example, some complexes are extremely stable while others are rather labile. It may also be possible to fine-tune the geometry of the system by the choice of the ionic radius of the metal ion. This ability to control the properties of the complex merely by changing the metal ion is attractive in a template-directed synthesis.

It is also worth noting that bipyridine complexes of many metal ions have extremely interesting properties in their own right: for example, complexes of  $\text{Ru}^{2+}$  and  $\text{Os}^{2+}$  have interesting photochemical and electrochemical properties and have been extensively investigated.<sup>97</sup> This raises the possibility of interesting modifications of these properties in preorganised, encapsulating ligands such as this: Sauvage has already demonstrated that an "encapsulation effect" can modify oxidation states of metal ions in his catenand systems.<sup>98</sup>

The final design point is that bipyridine is an aromatic system. It has already been stated that to modify the original Sokolov strategy to produce a working system, it will be necessary to introduce a second template effect to favour the formation of only the correct connections. As will be discussed shortly, it is necessary for the "linker" between two bipyridine units to "bridge" across a third such unit in order to give the correct connection pattern (Figure 2.1). If we use bipyridine complexes and also have an aromatic component in the bridging unit, it is possible that we may be able to use aromatic interactions to direct this bridging process and hence template the correct connections.

Terminal groups of  
bridging unit and bipyridine  
held in close proximity

Bridging Unit  
(Non-covalent interaction  
holds bridging unit in  
correct orientation)

3x correct connection

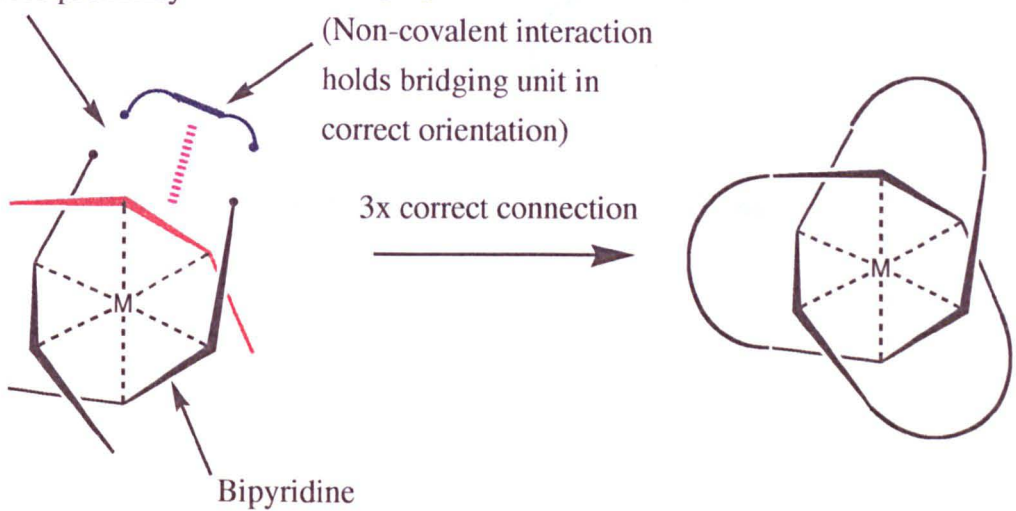


**Figure 2.1.** Proposed use of a secondary template effect to favour the formation of the correct bipyridine- bipyridine connections.

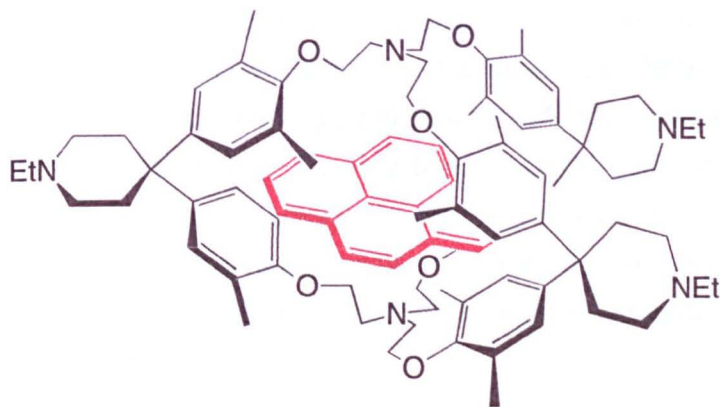


**Figure 2.2.** Diederich's host binding pyrene via aromatic interactions.

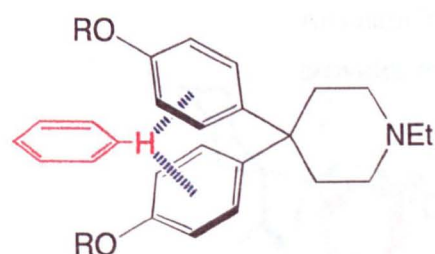


**Figure 2.3.** An expansion of the type of interactions involved in the host-guest complex of Figure 2.2. Aromatic interactions (-----) between the protons on the edge of the red aromatic guest and the face of the phenyl rings of the diarylmethane unit of the host provide the attractive interactions.

### 2.1.1 A Secondary Template Effect

Models of tris-bipyridine metal complexes reveal that the edge of the bipyridine unit is presented towards the exterior of the molecule. Since a linker unit needs to bridge across each bipyridine unit it is necessary to design an interaction between the bridging unit and the edge of the bipyridine unit to direct the correct bridging geometry. Aromatic interactions between the edge of one aromatic ring and the face of another have been well documented and explained in terms of favourable electrostatic contacts.<sup>99</sup> The outcome of much theoretical study is that the edge of an aromatic ring bears a slight positive charge on the sigma framework which can interact favourably with the  $\pi$ -cloud above the face of another aromatic ring which bears a slight negative charge due to the  $\pi$ -electrons. Such an effect should be enhanced in this system due to increased polarisation of the bipyridine system by its close proximity to a charged metal ion.

An interesting system exhibiting such an interaction has been reported by Diederich.<sup>100</sup> He found that the host molecule in Figure 2.2 can bind strongly to planar aromatic molecules such as pyrene. The recognition and binding are a result of aromatic interactions of the type shown in Figure 2.3. Here, we can clearly see the favourable interaction between the face of the two aromatic rings in the diarylmethane unit of the host and the edge of the guest molecule. If we could use such a recognition motif in our system then it quickly becomes apparent that the terminal phenolic groups of the diarylmethane unit would be held in close proximity to both bipyridine units which they are required to connect to give the desired product (Figure 2.4).

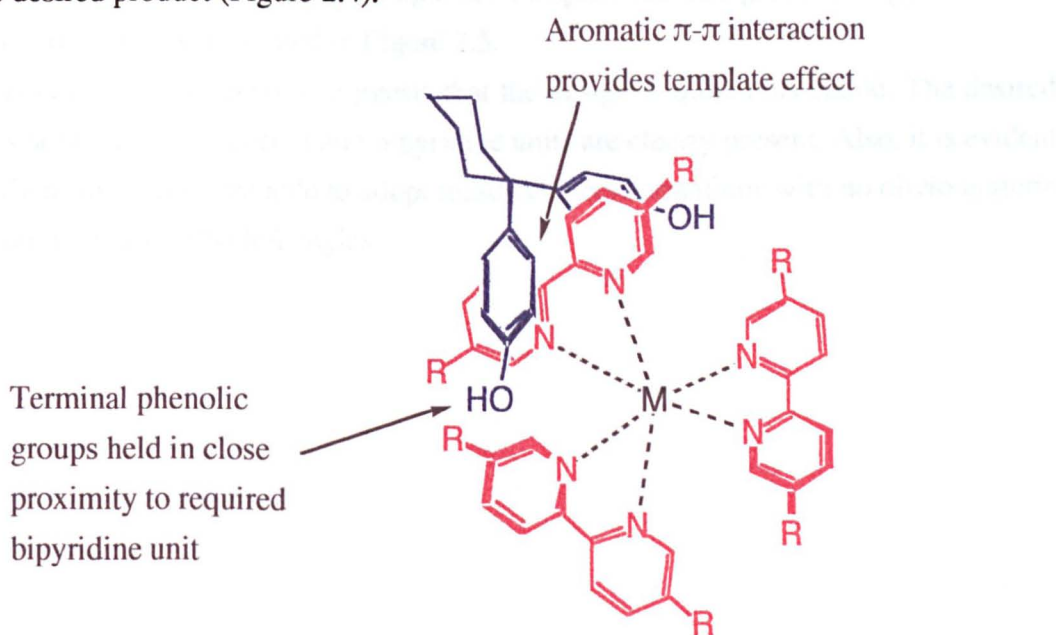


**Figure 2.4.** Proposed secondary template effect. R represents functionality to form a new bond with the phenolic groups of the linker unit.

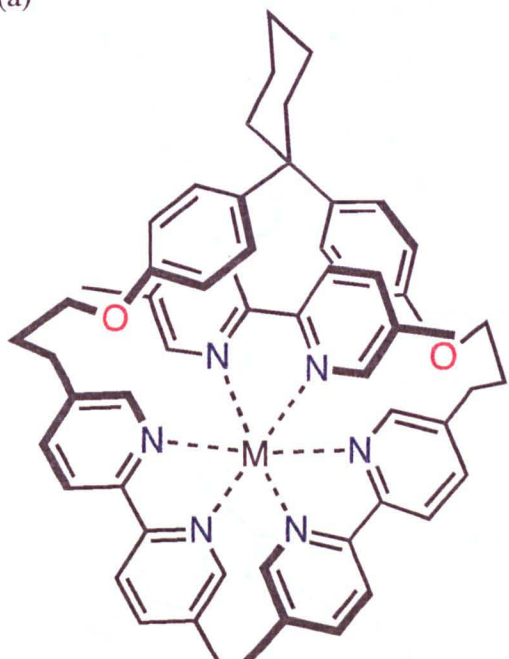
## 2.1.2 Molecular Modelling and Final Design

The use of CPK models suggested that a three carbon side-chain between each bipyridine and bisphenol unit would provide the optimum geometry. Clearly if these side-chains are too short then the desired product can not form. Equally, if the side-chains are unnecessarily long then cyclisation will be entropically less favoured and other intermolecular reactions may become more dominant. The only remaining question was the reactions required to form new bonds. Since we have decided to use bisphenol type linker units because of their ready accessibility, the two most obvious bond-forming reactions are displacement of a leaving group at the terminus of the three carbon side-chain to give ethers or the formation of esters via coupling with a terminal acid group. Molecular modelling studies were used to evaluate the suitability of both linker units.

Since the complete knot structure contained a large number of atoms and would be difficult to investigate using molecular mechanics calculations, the simpler partial structure illustrated in Figure 2.5 was used. The crystal structure of tris-bipyridine ruthenium (II) was obtained from the Cambridge Crystallographic Database and the macrocyclic component consisting of the three carbon side-chains and bisphenol linker were built on. The MacroModel implementation of the MM2 forcefield used for energy minimisation is not parameterised for metal-nitrogen bonds so the tris-bipyridine core was constrained to its X-ray geometry. This approximation is reasonable since it seems unlikely that the core of the molecule will have much flexibility. Monte Carlo conformational searching was therefore limited to the flexible side-chains and bisphenol components. The global energy minimum conformation obtained is illustrated in Figure 2.5.

Inspection of this structure suggests that the design is quite reasonable. The desired interactions between the bisphenol and bipyridine units are clearly present. Also, it is evident that the carbon side-chains are able to adopt reasonable conformations with no obvious steric clashes or unfavourable dihedral angles.

(a)



(b)

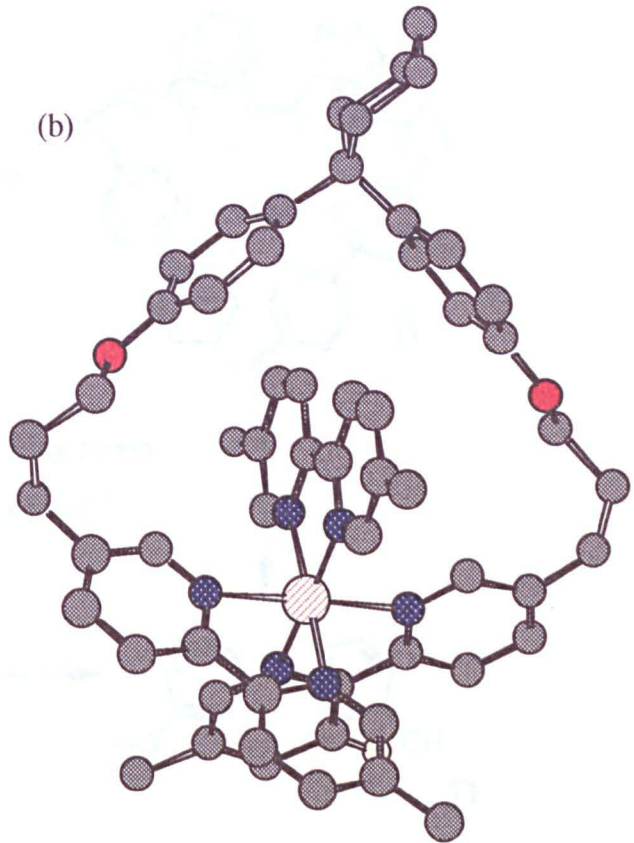


**Figure 2.5.(a)** A simple macrocyclic model complex for molecular modelling studies.

**(b)** The global energy minimum predicted by the MM2 forcefield.

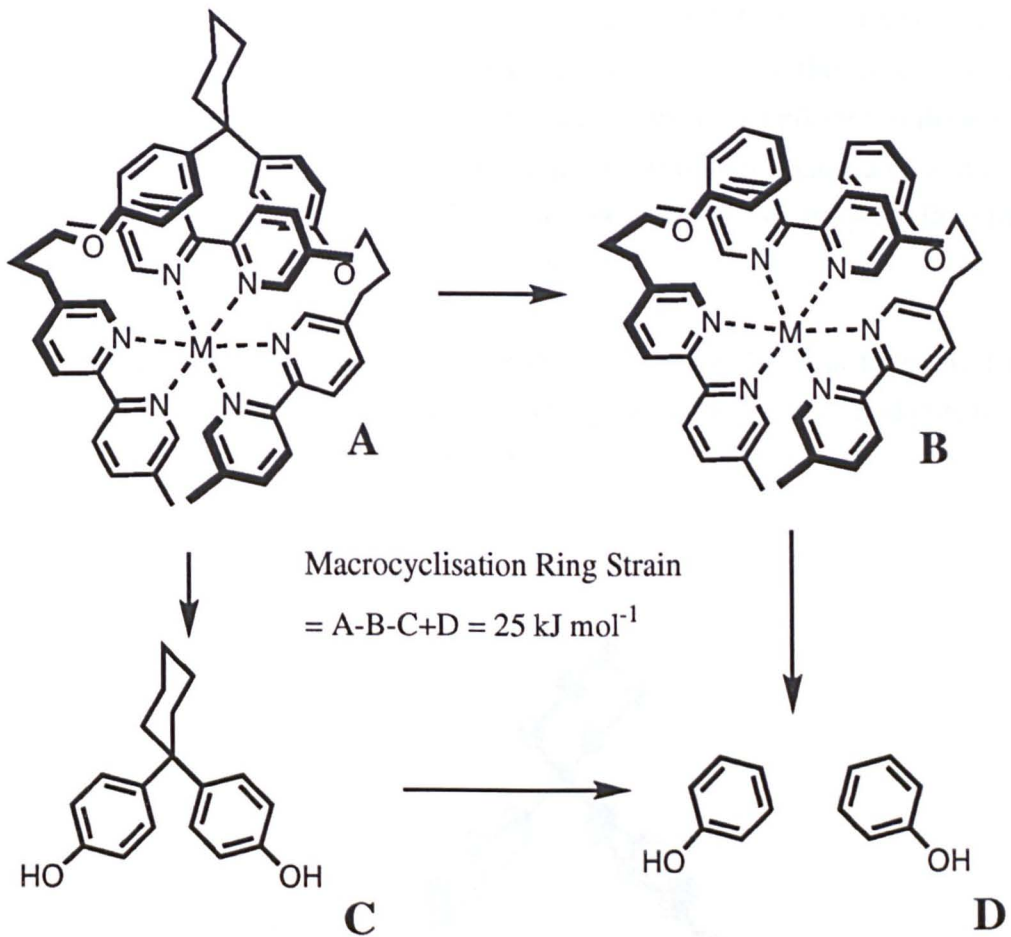


**Figure 2.6.** Cycle for the estimation of ring strain introduced by macrocyclisation.

The energy value obtained was also used to estimate the ring-strain introduced into the system by the macrocyclisation reaction using the cycle shown in Figure 2.6. As well as the energy for the structure in Figure 2.5 (A), an energy value was obtained for the related non-macrocyclic structure with the entire cyclohexyl ring removed and reminimised (B) as well as the energies for simple bisphenol (C) and phenol (D) units. Use of the equation A-B-C+D gave a value of approximately  $+25 \text{ kJ mol}^{-1}$  for the change in energy upon macrocyclisation. Since the aromatic interactions were still present in the non-macrocyclic structure (B), this energy change equates to the ring strain introduced upon macrocyclisation. This value is not unreasonably high and will be partially offset by the favourable aromatic interactions gained in the macrocyclic structure.

The minimum-energy conformation in Figure 2.5 was then used to obtain the structure of the entire knot by simply attaching two more bridges in identical conformations and reminimising the energy (Figure 2.7).

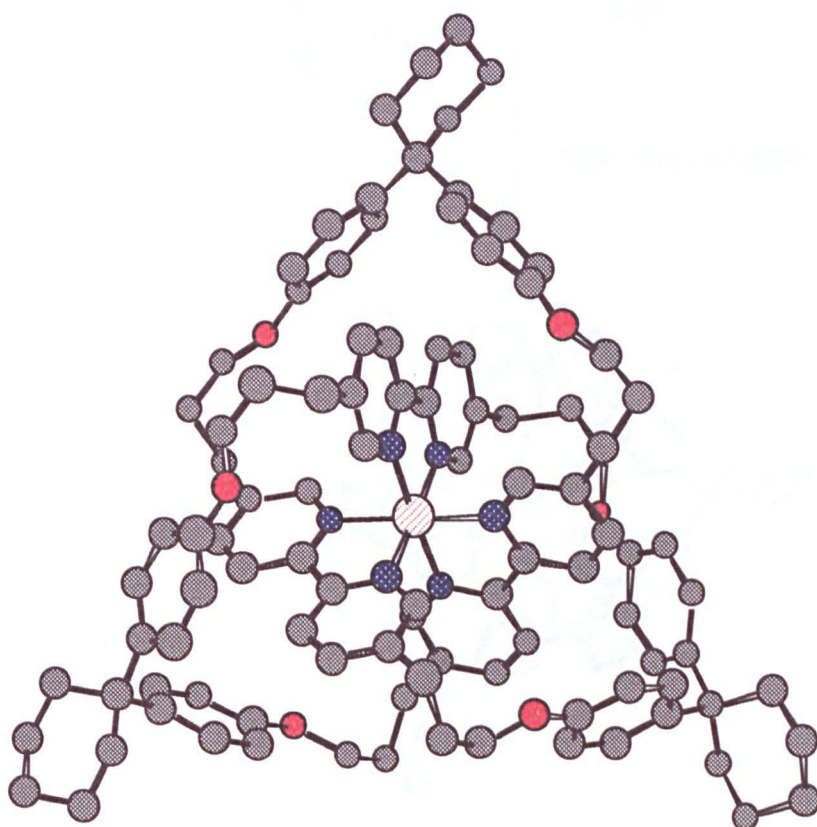


**Figure 2.7.** An energy-minimised conformation of the ether-linked trefoil knot.

On the basis of the molecular modelling results, the synthetic scheme illustrated in Figure 2.8 was adopted as a starting point for attempting macrocyclisation reactions. This design incorporates all the structural features discussed so far. The new ether bonds are formed via base-catalysed S<sub>N</sub>2 displacement reactions. The decision to use the N-acetyl piperidine bisphenol derivative was to provide a protected amine as a versatile site for further functionalisation on the surface of the knotted molecule.

Similarly, if one were to take the alcohols from which the tosyl groups are clearly derived and oxidise them to carboxylic acids, a second type of macrocyclisation reaction may be used: the formation of ester links after activation of the carboxylic acids.

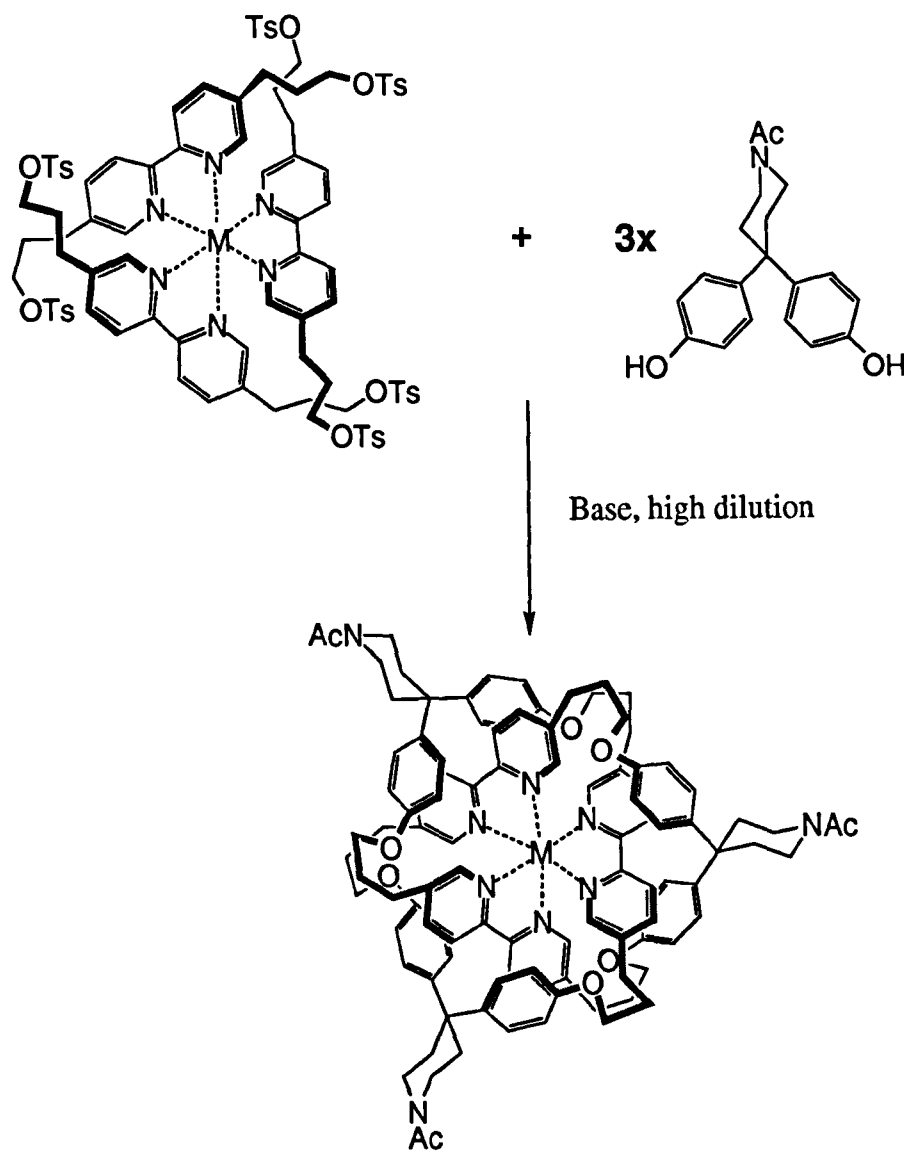


**Figure 2.8.** Proposed synthesis of the ether-linked trefoil knot.

## 2.2 Folding Strategy

The most obvious problem that may affect the strategy already discussed is the need to simultaneously form six new bonds in one macrocyclisation reaction. Clearly, even if each new bond is formed in relatively high yield, the final product yield may still be rather low. To overcome this problem, we have also worked on a second route to knotted molecules. In this strategy, the recognition components already discussed are linked into a linear molecule in the hope that in the presence of a metal ion they will "fold" into the open-knotted structure shown in Figure 2.9 which we have termed a *pseudo-overhand knot*.

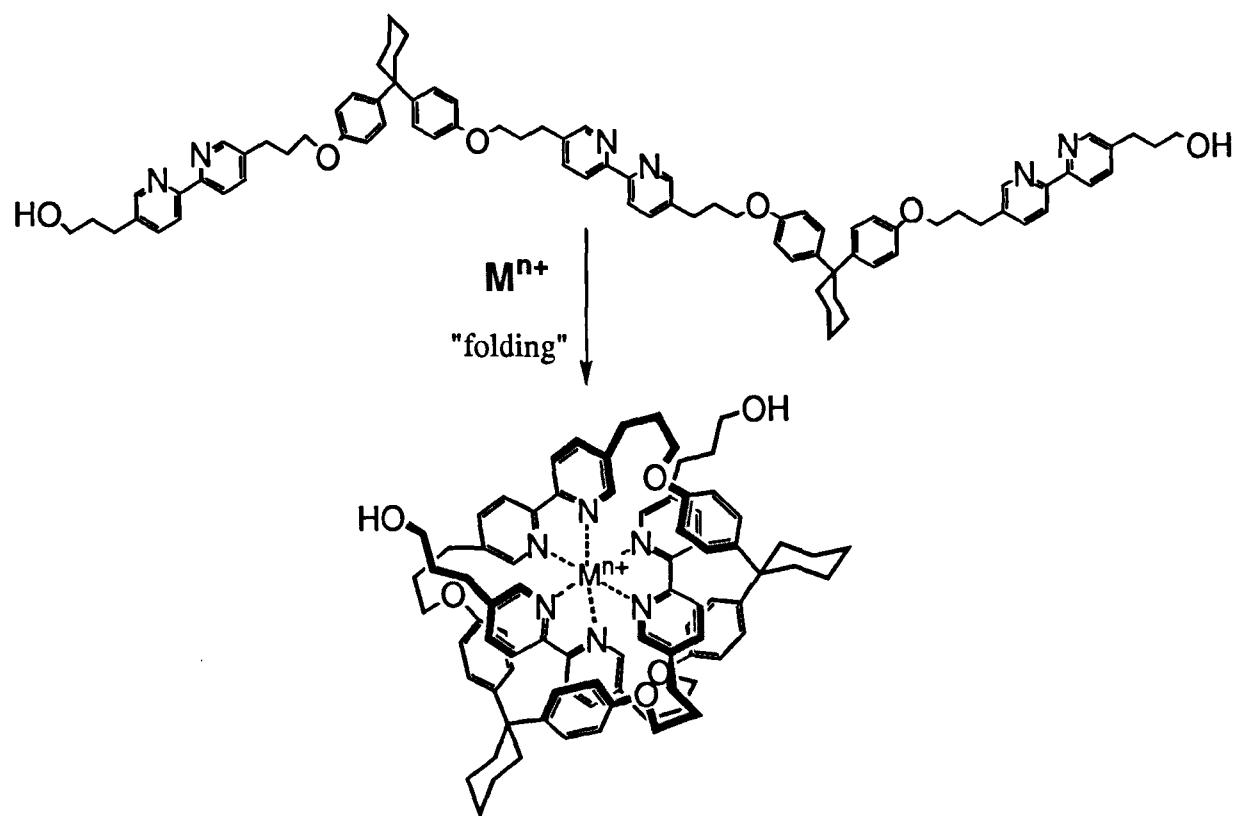


**Figure 2.9.** Approach to molecular knots via a "folding" strategy.

In fact, the pseudo-overhand knot makes an extremely versatile intermediate. Not only can a single macrocyclisation reaction convert it to the trefoil knot, but it could also be incorporated into more complex knotted structures as outlined schematically in Figure 2.10. The *overhand knot* where unthreading is prevented by bulky terminal groups (related to the trefoil knot in the same way that a rotaxane is related to a catenane) has not yet been reported in the literature. The composite knot structures such as the granny and reef knots have been reported by Sauvage<sup>92</sup> since we commenced this work but only in extremely low yield and it is clearly desirable to devise improved syntheses if such molecules are to be obtainable on preparative scale.

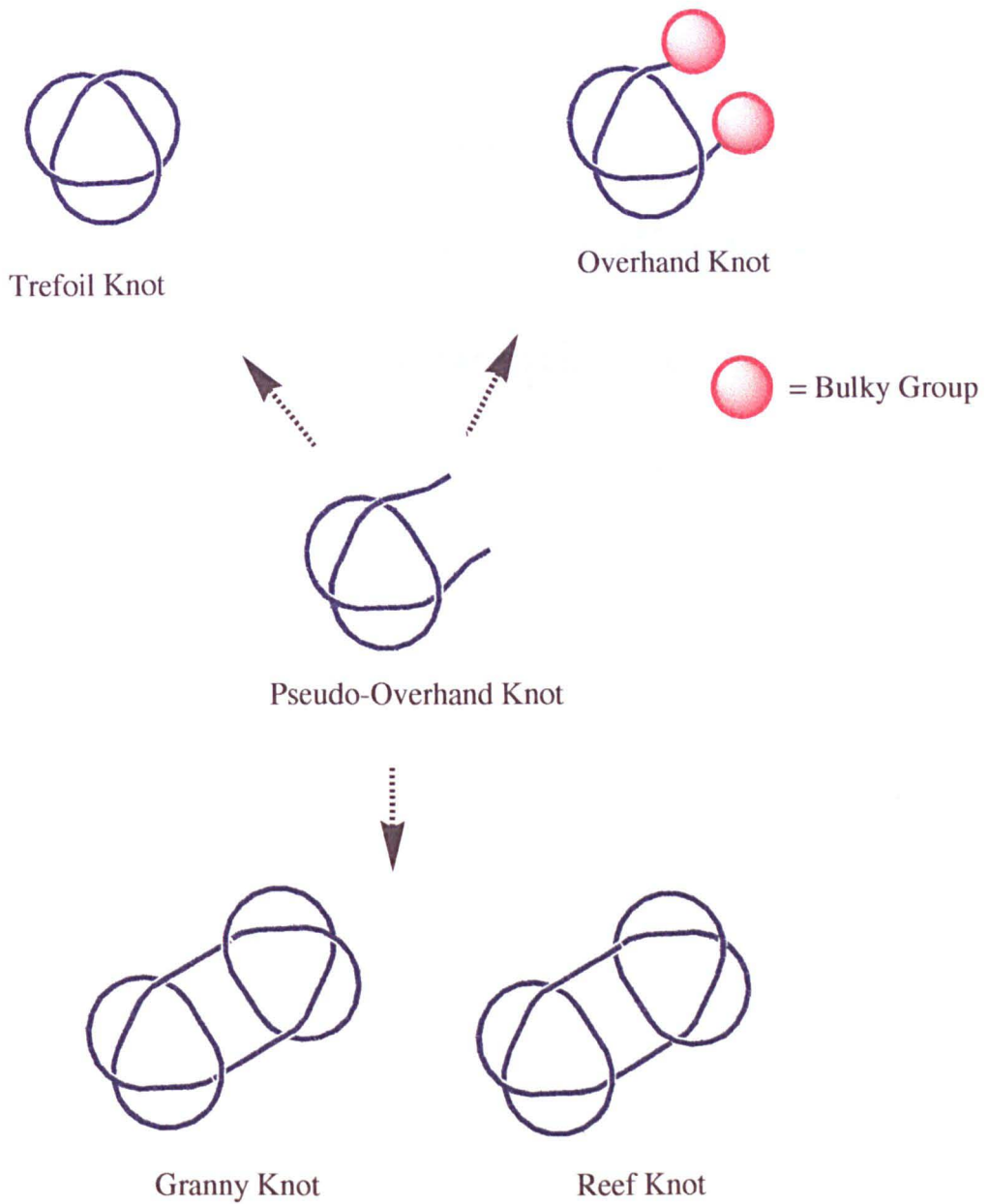


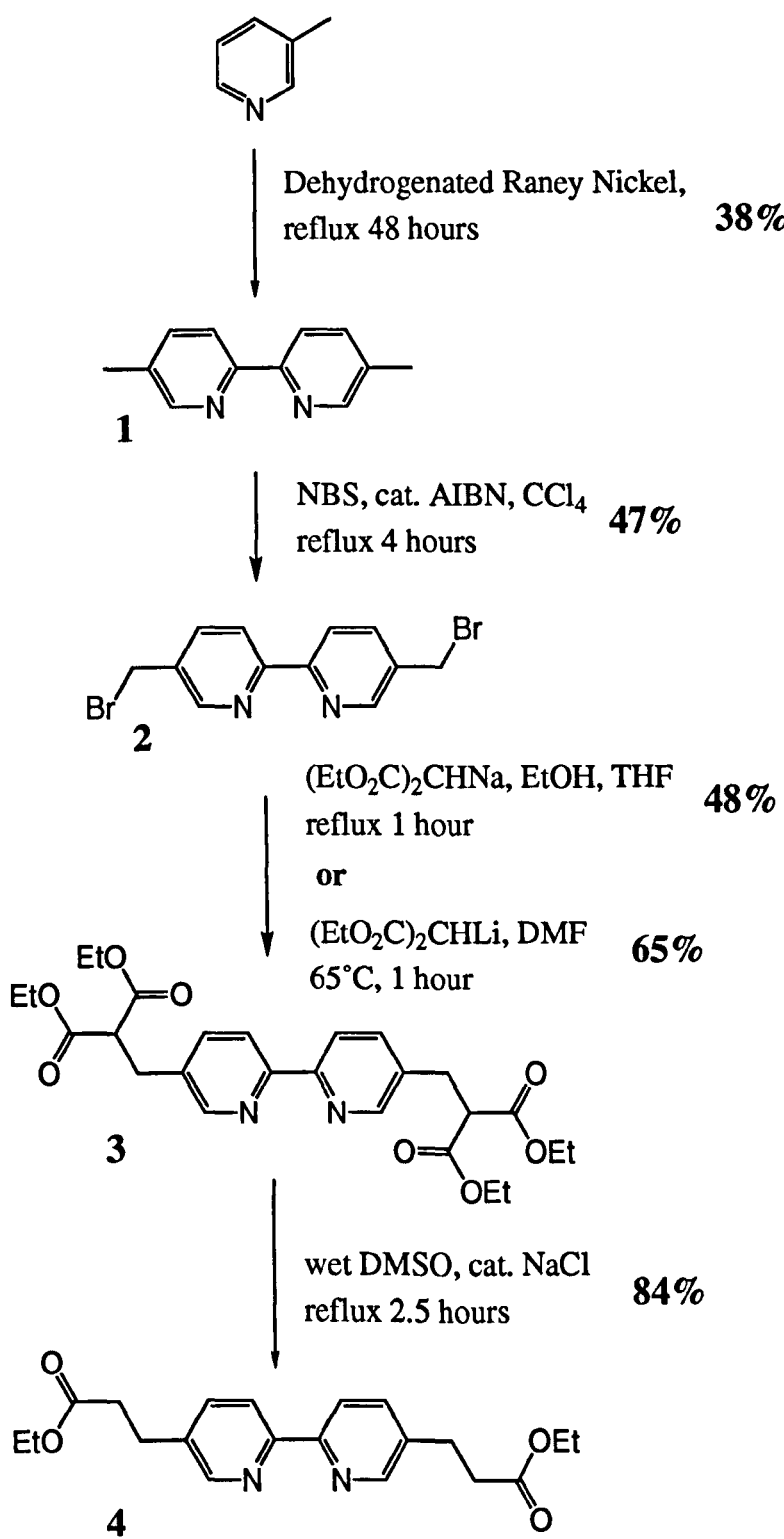
**Figure 2.10.** Schematics of some interesting topologies that may be accessible from the pseudo-overhand knot.

---

# *Chapter 3*

---

## **Synthesis and Macrocyclisation of Metal Complexes**



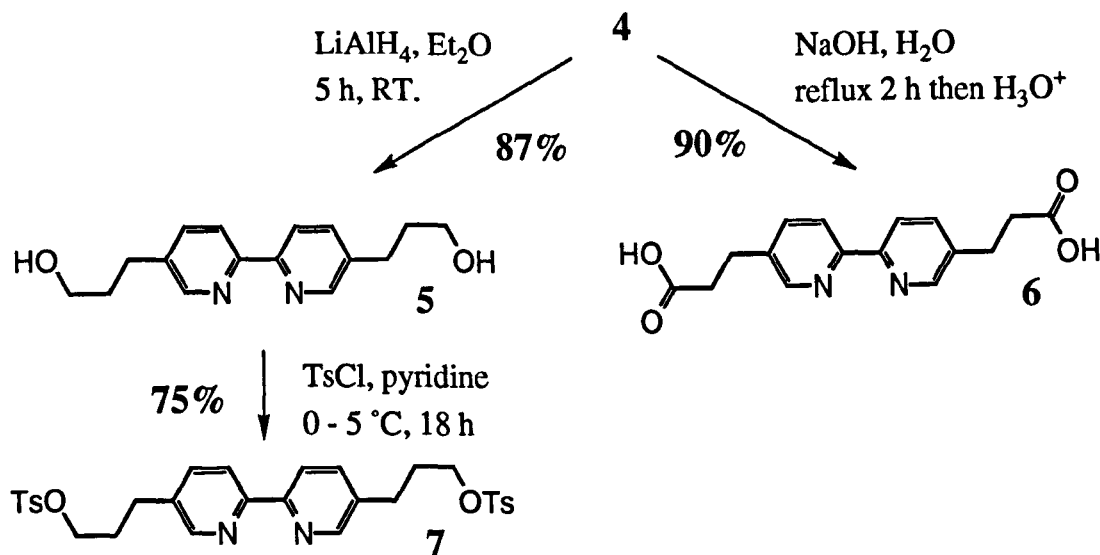
**Scheme 3.1.** *Synthesis of bipyridine diester 4.*

## 3.1 Synthesis of Building Blocks

### 3.1.0 The Bipyridine Unit

The key intermediate for the synthesis of the metal-coordinating component is the bipyridine-diester **4**<sup>†</sup>, the synthesis of which is outlined in Scheme 3.1. 5,5'-dimethyl-2,2'-bipyridine **1** was prepared from 3-methylpyridine in the presence of a dehydrogenated Raney nickel catalyst in 38% yield as reported in the literature.<sup>103, 104</sup> Bromination with N-bromosuccinimide in carbon tetrachloride under radical conditions gave the dibromide **2** (47%).<sup>105</sup>

The next step was considerably complicated by the extreme insolubility of **2**. Using the standard malonate-ester procedure (preparing the sodium anion of diethylmalonate followed by the addition of a hot, dilute solution of **2** in ethanol / THF<sup>‡</sup>) resulted in rather variable yields of **3** (up to 48% on small scale) and difficulty in scale-up of the reaction. It was found that superior results could be obtained by the addition of solid **2** to a solution of the lithium anion (prepared from diethylmalonate and lithium hydride) in DMF. This procedure gave the tetraester **3** in a reliable 65% yield even on large scale. **3** was then readily converted to diester **4** via the decarbethoxylation procedure of Krapcho *et al* in 84% yield.<sup>106</sup> **4** was readily elaborated to a number of useful bipyridine building blocks as outlined in Scheme 3.2.



Scheme 3.2. Conversion of diester **4** to **5**, **6** and **7**.

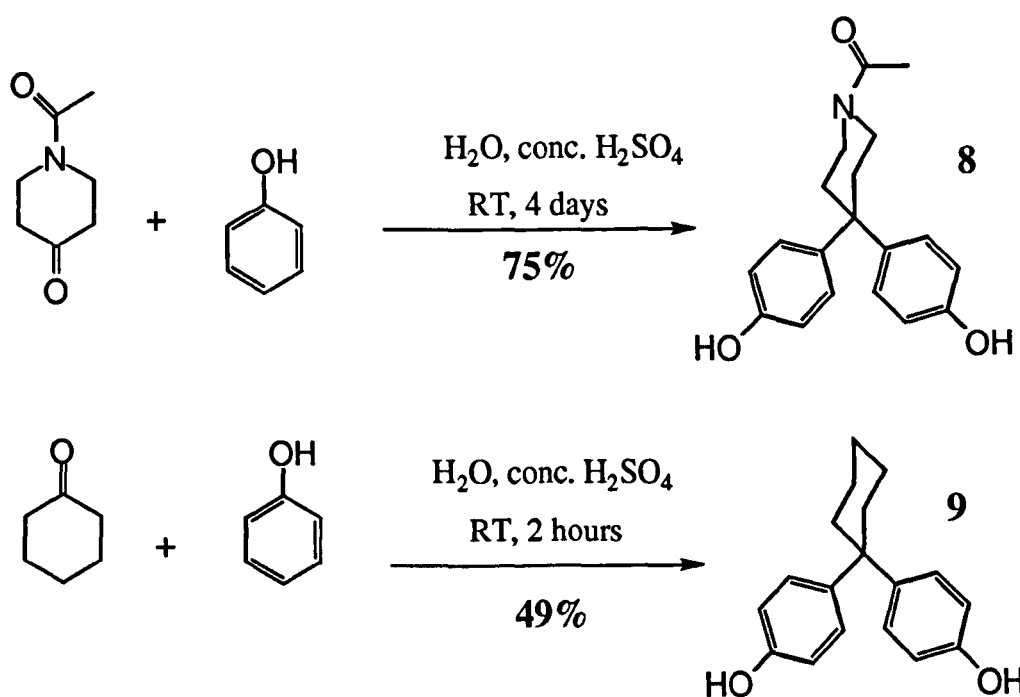
<sup>†</sup> Diester **4** and reduction product **5** have been reported by Hamilton<sup>101</sup> although prepared by a slightly different route. No experimental details were given and the synthesis of **4** was adapted from Hamilton's synthesis of related pyridyl compounds.<sup>102</sup>

<sup>‡</sup> **2** is only soluble at elevated temperature and even then only in dilute solution. Addition of THF to the more usual alcohol solvent is necessary since **2** is virtually insoluble in ethanol.

Reduction of **4** with lithium aluminium hydride in diethyl ether gave the diol **5** in 87% yield. Basic hydrolysis with aqueous sodium hydroxide in water followed by neutralisation with HCl gave the extremely insoluble diacid **6** (90%). **5** was also converted to the ditosylate **7** in 75% yield using tosyl chloride in pyridine.

### 3.1.1 The Bisphenol Unit

Two different bisphenol units were prepared. **8** was based upon an N-acetyl piperidine ring and **9** upon a cyclohexyl ring. The initial thinking was that target molecules incorporating **8** could be deprotected to give a secondary amine and hence provide a site for further functionalisation. However, **8** proved to be rather insoluble and compounds in which it was incorporated were difficult to purify by chromatography compared to the analogous compounds containing **9**. Both molecules were prepared by an acid catalysed condensation as outlined in Scheme 3.3. The preparation of **8** has been reported by Diederich<sup>107</sup>, and **9** was prepared by adapting this procedure rather than following a reported literature route.<sup>108</sup> The second reaction was terminated after only 2 hours because the reaction mixture became solid and this presumably accounts for the reduced yield.



Scheme 3.3. Preparation of bisphenol units.

## 3.2 Synthesis of Metal Complexes

### 3.2.0 General Procedures

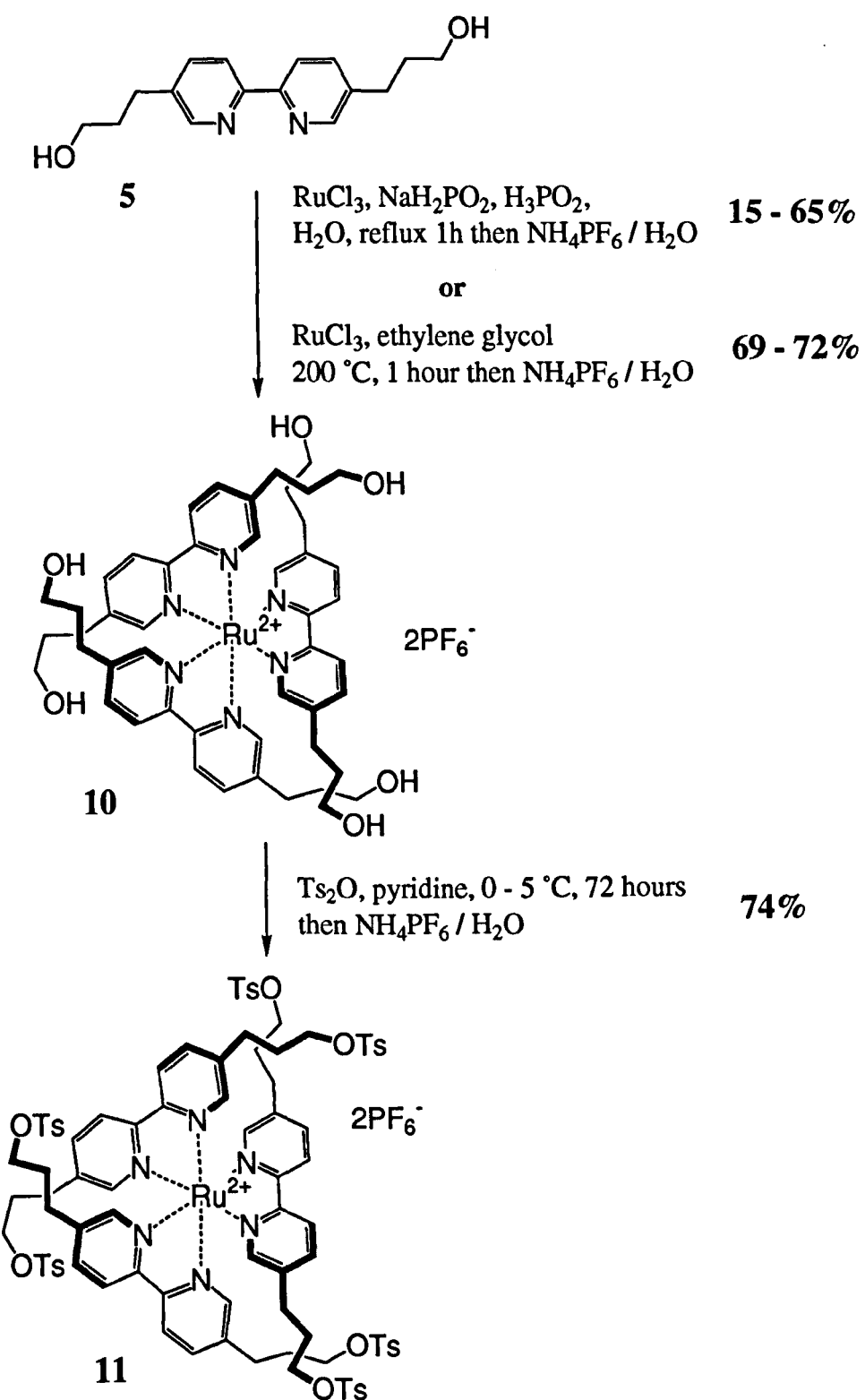
Orange Ru(bipy)<sub>3</sub><sup>2+</sup> complexes are extremely well known and the available literature is extensive. However, the majority of literature compounds feature only relatively simple ligands lacking any delicate functionality and the preparations generally utilise fairly vigorous conditions.<sup>109</sup> It was found that a number of modifications needed to be developed to prepare organic soluble complexes bearing the required ligands in high yield.

Bright red Fe(bipy)<sub>3</sub><sup>2+</sup> species have also been extensively studied. The standard procedure for their preparation involves the addition of an alcoholic solution of the required ligand to a solution of iron (II) chloride in water followed by the addition of a solution of the required counterion to precipitate the product.<sup>110</sup> Again, this approach proved impractical due to the insolubility of the ligands in such a solvent system and an alternative approach had to be developed.

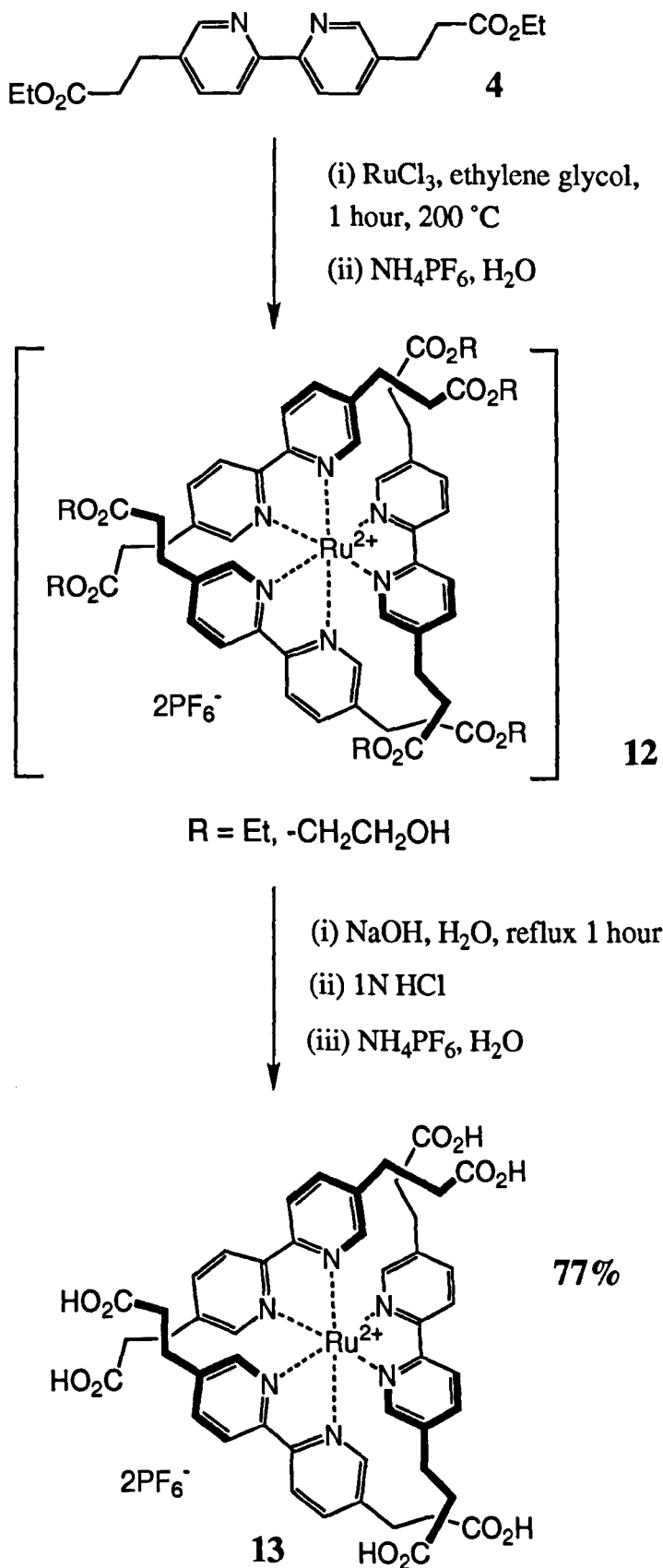
### 3.2.1 Synthesis of Ruthenium (II) Complexes

The first synthetic target was the hexa-tosylate ruthenium (II) complex **11** (Scheme 3.4). It quickly became apparent that direct coordination of ditosylate **7** was not feasible due to its instability and low solubility in the required solvents. Therefore, the alternative route involving coordination of diol **5** followed by conversion of all six hydroxyl groups of complex **10** to tosylates was adopted.

Two general methods were used for the preparation of **10**. The first involved a slight modification of a procedure reported by Broomhead and Young.<sup>111</sup> The ligand, dried ruthenium (III) chloride and freshly prepared NaH<sub>2</sub>PO<sub>2</sub> were heated at reflux for 30 minutes in water to obtain a bright orange solution. The product was precipitated as its hexafluorophosphate salt by the addition of NH<sub>4</sub>PF<sub>6</sub>. Yields in this reaction were found to be rather capricious, ranging from 15 - 65%. The higher yields could generally be obtained by maintaining a slight excess of hypophosphorous acid (H<sub>3</sub>PO<sub>2</sub>) when preparing the NaH<sub>2</sub>PO<sub>2</sub> solution, although the reason for this is not clear. The second procedure that was found to be far superior involved heating a mixture of the ligand and dried ruthenium (III) chloride in ethylene glycol at 200°C for 1 hour followed by the same precipitation procedure which gave the product in a reliable 69 - 72% yield.<sup>112</sup>



**Scheme 3.4.** Synthesis of hexa-tosyl ruthenium (II) complex **11**.



**Scheme 3.5.** *Synthesis of hexa-acid ruthenium (II) complex 13.*

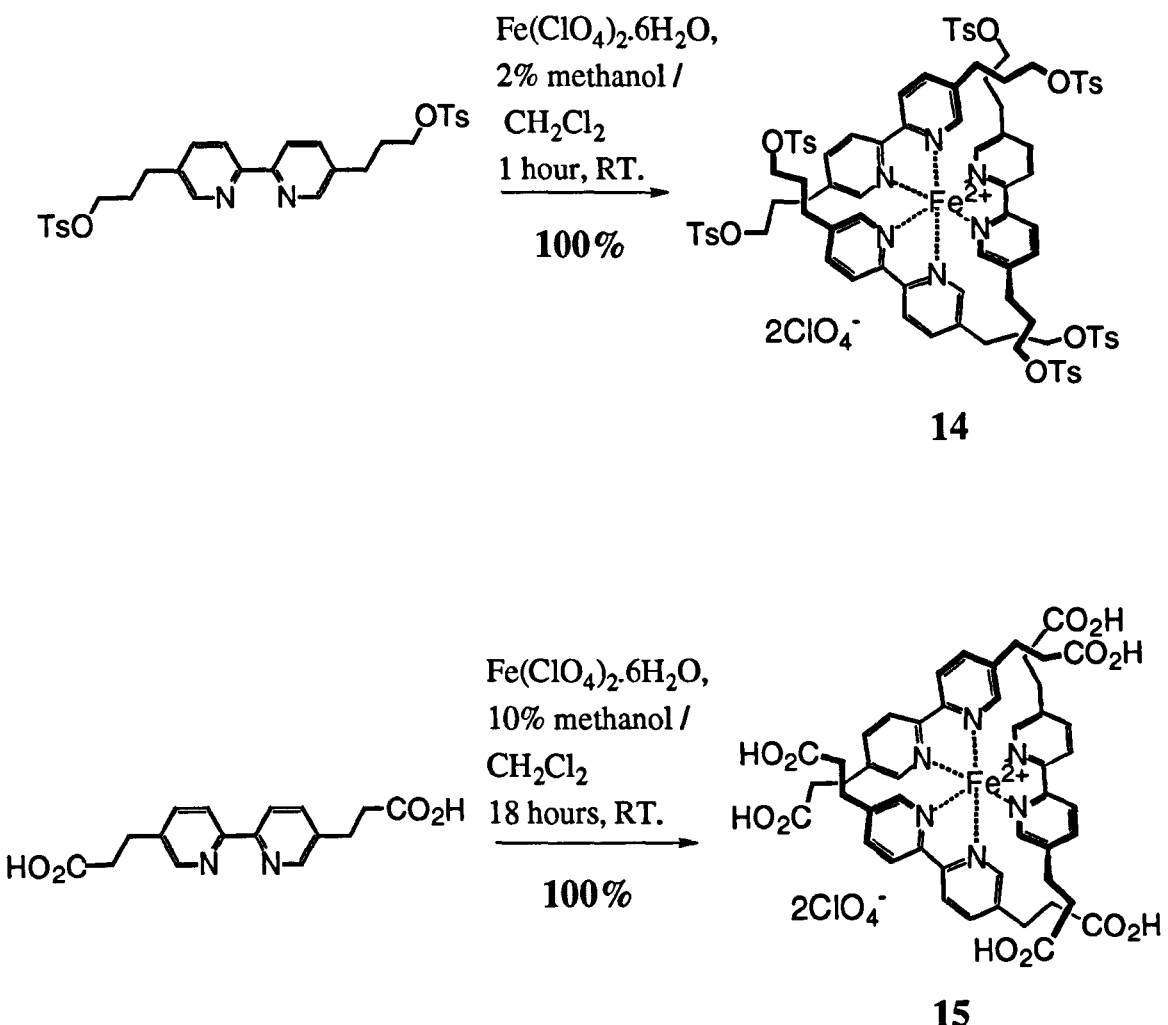
Complete tosylation of **10** proved rather difficult. Using the standard tosylation conditions of tosyl chloride in pyridine resulted in the isolation of only partially tosylated material. FAB<sup>+</sup> MS allowed the identification of mono-, di- and tri-tosylates only. It was eventually found that the use of the more powerful tosylating agent tosic anhydride gave the required product **11** in 74% yield.

Another target complex was the hexa-acid ruthenium (II) complex **13**, (Scheme 3.5). Direct coordination of the diacid failed to produce **13** due to the insolubility of the ligand. A way around this problem involved coordinating the diethyl ester **4** followed by hydrolysis of the hexaester intermediate. **12** was prepared by heating the ligand and dried ruthenium trichloride at 200 °C in ethylene glycol. **12** was actually shown by <sup>1</sup>H NMR and FAB<sup>+</sup> MS to be a mixture of ethyl and hydroxyethyl esters due to thermal transesterification caused by the vigorous reaction conditions. This was not a problem since the next step involved ester hydrolysis, and **13** can be produced by basic hydrolysis without isolation of the intermediate in an overall yield of 77% from **4**.

### 3.2.2 Iron (II) Complexes

Since only chlorinated solvents offered good solubility for the ligands used, it was necessary to find a way of working in these solvents. A good commercially available source of organic soluble iron (II) is the perchlorate hexahydrate salt Fe(ClO<sub>4</sub>)<sub>2</sub>.6H<sub>2</sub>O. Although this salt is not soluble in pure chloroform or dichloromethane, it is solubilised upon addition of 1-2% methanol. The required complexes can be prepared by the addition of one third of an equivalent of Fe(ClO<sub>4</sub>)<sub>2</sub>.6H<sub>2</sub>O in 2% methanol / CH<sub>2</sub>Cl<sub>2</sub> to a solution of the required ligand in CH<sub>2</sub>Cl<sub>2</sub>. In most cases the product was formed virtually instantaneously. Upon removal of solvent, the product was obtained in quantitative yield, usually as an extremely soluble red foam.

Iron (II) complexes required for cyclisation were the hexa-tosylate complex **14** and hexa-acid **15**. Both complexes were prepared in quantitative yield using the same procedure (Scheme 3.6). Even for the extremely insoluble diacid **6**, the correct product was formed quantitatively albeit somewhat more slowly.

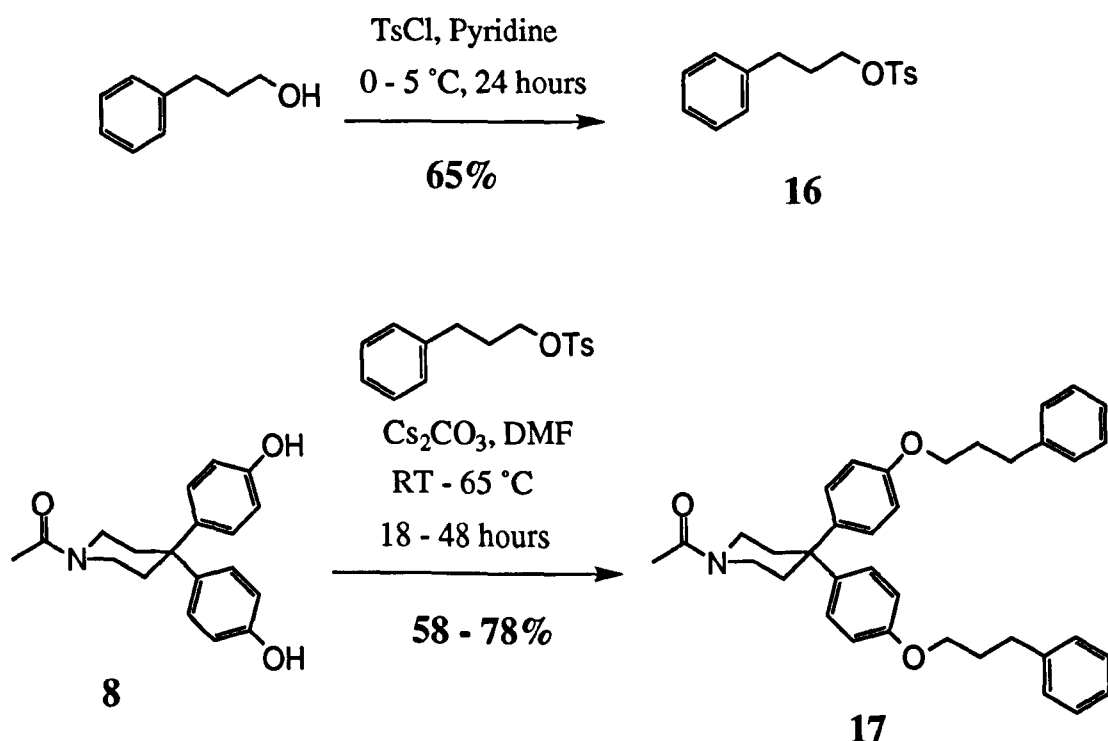


**Scheme 3.6.** Synthesis of iron (II) complexes.

### 3.3 Attempted Macrocyclisation via Formation of Ether Links

#### 3.3.0 Model Reactions

It was proposed to form new ether-links via the displacement of tosylate by a phenolic group in the presence of base. A simple model reaction was therefore carried out to determine the efficiency of this reaction. The model tosylate **16** was prepared from 3-phenyl-1-propanol and used to alkylate N-acetyl bisphenol **8** (Scheme 3.7).  $\text{Cs}_2\text{CO}_3$  was used as base<sup>‡</sup> and DMF as solvent, since it seemed likely that DMF would provide good solubility for all the required species and that its relatively polar nature may lead to reasonably efficient templating  $\pi$ - $\pi$  interactions. In fact, later investigations of the effect of solvent polarity on  $\pi$ - $\pi$  interactions indicated that this was the worst choice of solvent (see Chapter 4). At room temperature, the isolated yield of dialkylated product **17** was relatively low (58% after 48 hours) but was significantly improved by the use of an elevated temperature (78% after 18 hours at 60 - 65 °C). These conditions therefore seemed ideal for macrocyclisation of the hexa-tosylate metal complexes.



Scheme 3.7. Preparation of tosylate **16** and its use in a model alkylation reaction.

<sup>‡</sup> Similar conditions have been used extremely successfully by Sauvage in a number of macrocyclisation type reactions.<sup>113</sup> Several authors have reported a so-called "caesium effect" where caesium carbonate favours macrocyclisation reactions much more strongly than other bases.<sup>114, 115</sup>

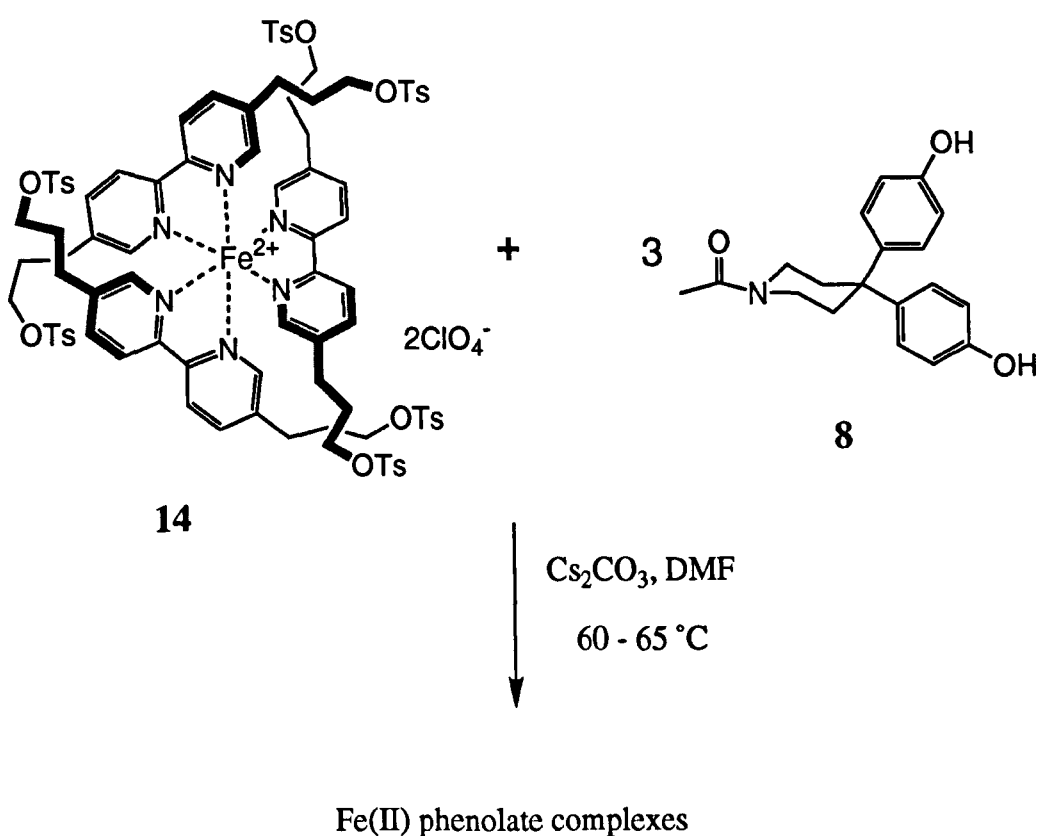
### 3.3.1 Iron (II) Complexes

Cyclisation of iron (II) complex **14** with three equivalents of N-acetyl bisphenol **8** was attempted in DMF using  $\text{Cs}_2\text{CO}_3$  as base as outlined in Scheme 3.8. Upon mixing **14** and **8** in DMF, a deep red solution was obtained. However, upon addition of  $\text{Cs}_2\text{CO}_3$  the red coloration was quickly lost and replaced by a yellow solution. Since species containing iron-oxygen bonds are yellow in colour, and the literature suggests that  $\text{Fe}(\text{bipy})_3^{2+}$  species are susceptible to attack by nucleophiles,<sup>109</sup> it seemed extremely likely that the generation of phenoxide ion had caused the decomposition of the complex and resulted in a complex containing Fe-O bonds. This was further evidenced by the fact that addition of  $\text{Fe}(\text{ClO}_4)_2 \cdot 6\text{H}_2\text{O}$  to an aliquot of this mixture resulted in the return of the characteristic red coloration.

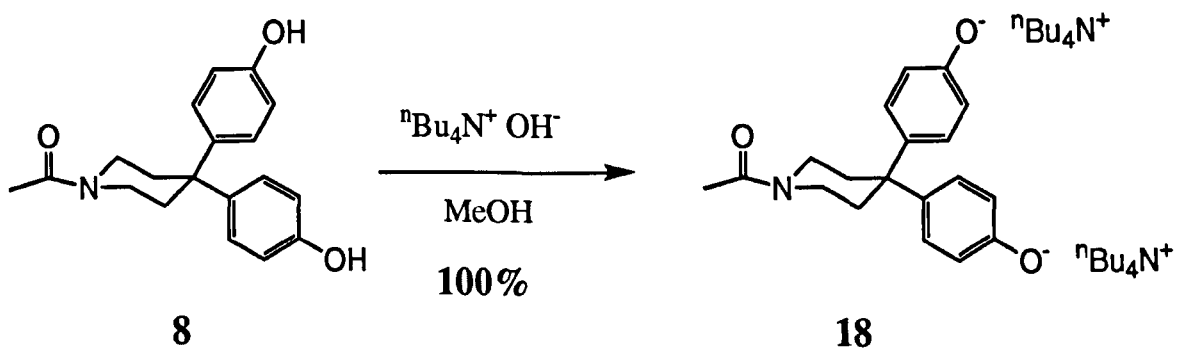
Since the difference between coordinated and free ligand is readily seen in the  $^1\text{H}$  NMR spectrum, it was decided to use a simple NMR experiment to determine if the presence of phenoxide was indeed the cause of the decomposition of the iron (II) bipyridine complex. Complex **14** has three  $^1\text{H}$  NMR signals due to the bipyridine unit at 7.23 ppm ( $\text{H}_6$ ), 7.82 ppm ( $\text{H}_4$ ) and 8.37 ppm ( $\text{H}_3$ ) in  $\text{CDCl}_3$ . The free ligand **7** exhibits a very different pattern:  $\text{H}_6$  at 8.39 ppm,  $\text{H}_4$  at 7.52 ppm and  $\text{H}_3$  at 8.22 ppm. The 1 ppm upfield shift of  $\text{H}_6$  (doublet,  $J = 2$  Hz) is a particularly distinctive change upon complexation.

The tetra *n*-butyl ammonium salt **18** was prepared as an organic soluble phenoxide anion by treatment of N-acetyl bisphenol **8** with  ${}^n\text{Bu}_4\text{N}^+ \text{OH}^-$  in methanol followed by removal of the solvent (Scheme 3.9).

Upon addition of bisphenol **8** to a  $\text{CDCl}_3$  solution of complex **14**, no change was observed in the chemical shifts of the signals due to the bipyridine protons. The resulting spectrum was a simple superimposition of the spectra of **8** and **14**. However, upon addition of dianion **18** to **14** a change was observed. Again, the colour changed from red to yellow, and the pattern of the bipyridine signals now resembled the free ligand: clearly complex decomposition had occurred. Somewhat surprisingly, no shifts in the phenolic signals were observed which might be expected with the formation of an  $\text{Fe}(\text{II})\text{OAr}$  species. It is clear from this result however that the iron (II) complexes are not stable in the presence of phenoxide, and hence displacement of tosylate groups is not a viable method for the macrocyclisation of iron (II) complexes. This approach was therefore abandoned.



**Scheme 3.8.** Attempted macrocyclisation of iron (II) hexa-tosylate complex **14**.



**Scheme 3.9.** Preparation of the organic soluble bisphenol dianion **18**.

### 3.3.2 Ruthenium (II) Complexes

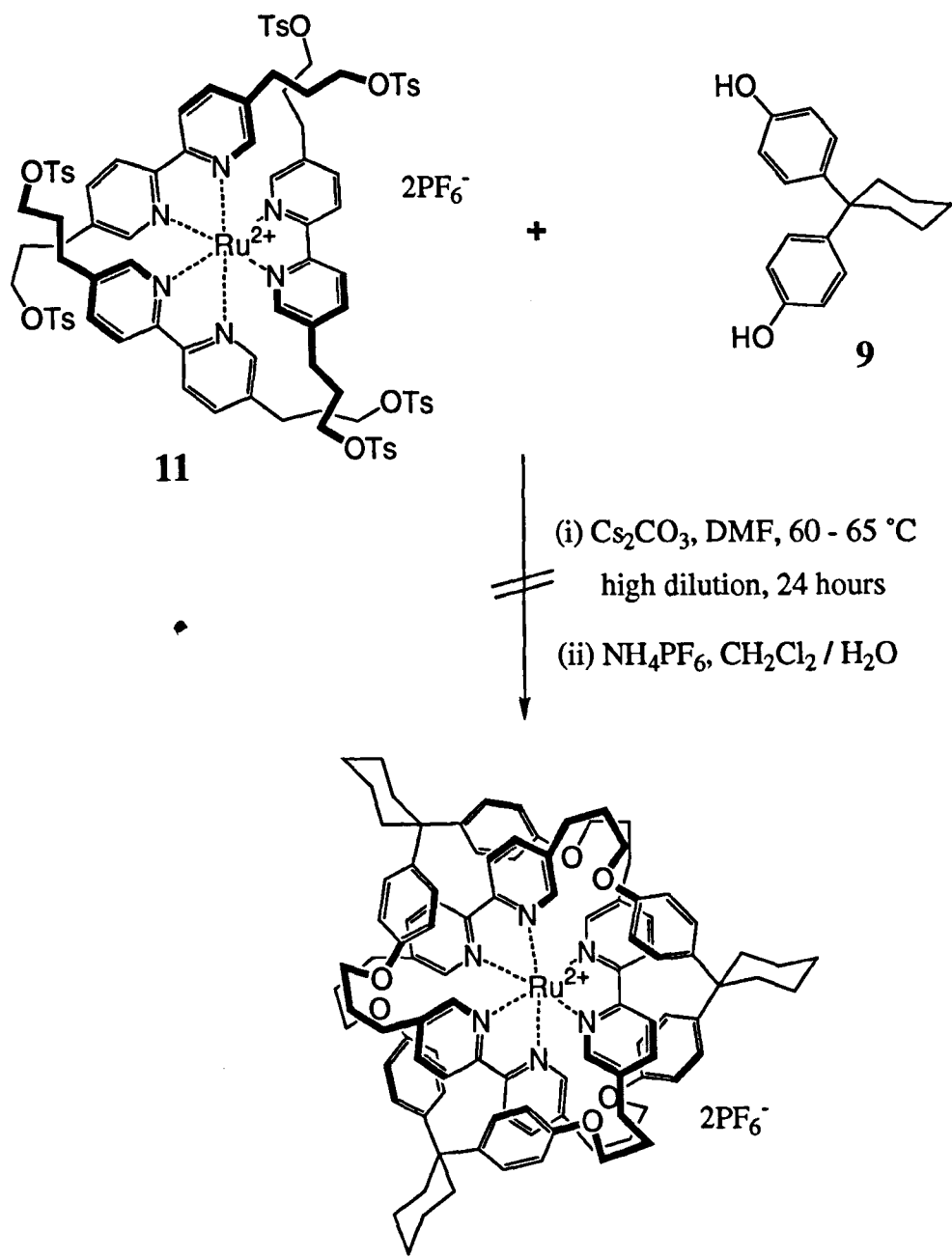
The literature suggests that ruthenium (II) tris-bipyridine complexes are extremely stable, so it seemed probable that such decomposition problems would not be experienced in this case. At this point, a switch was made from the N-acetyl bisphenol **8** to the cyclohexyl derivative **9**, since the latter had higher solubility, lower polarity (thereby facilitating chromatographic separation of products) and avoids possible side reactions of the N-acetyl functionality.

The ruthenium (II) hexatosylate complex **11** was therefore subjected to a high dilution reaction with **9** (Scheme 3.10). A solution of **11** and 3 equivalents of **9** in dry DMF was added dropwise over 5 hours to a stirred suspension of  $\text{Cs}_2\text{CO}_3$  in DMF at 60 - 65 °C. Upon addition, the orange solution became quickly dark brown and then black.

After completion of the reaction, the solvent was removed *in vacuo* and  $\text{CH}_2\text{Cl}_2$  added to the dark coloured residue. The vast majority of material produced was a dark brown solid insoluble in all organic solvents. No characterisation of this material was possible, and it seems likely that it is oligomeric in nature. This insoluble material was removed via filtration, and the  $\text{CH}_2\text{Cl}_2$  filtrate produced a small amount of a bright orange product: the colour was suggestive of the presence of tris-bipyridine ruthenium (II) complexes. The  $\text{CH}_2\text{Cl}_2$  solution was stirred overnight with a concentrated aqueous solution of  $\text{NH}_4\text{PF}_6$  to exchange any counterions present for  $\text{PF}_6^-$ .

TLC analysis of this product indicated the presence of three compounds which were separated by flash chromatography on silica. Attempts at characterisation were made by both  $^1\text{H}$  NMR and FAB $^+$  mass spectrometry without success. All three compounds contained the characteristic bipyridine signals but no other aromatic signals - i.e. no signals corresponding to the bisphenol component - and were therefore clearly not the desired product. No distinctive signals were observed in the FAB $^+$  mass spectrum and again no deductions could be made about the possible composition of these products.

In retrospect, it seems likely that the rather vigorous conditions, relatively high temperature and the use of DMF as solvent do not provide the optimum conditions for templating  $\pi$ - $\pi$  interactions (see Chapter 4 for a discussion of model complexes used to determine the effect of solvent and temperature upon  $\pi$ - $\pi$  interaction strength).

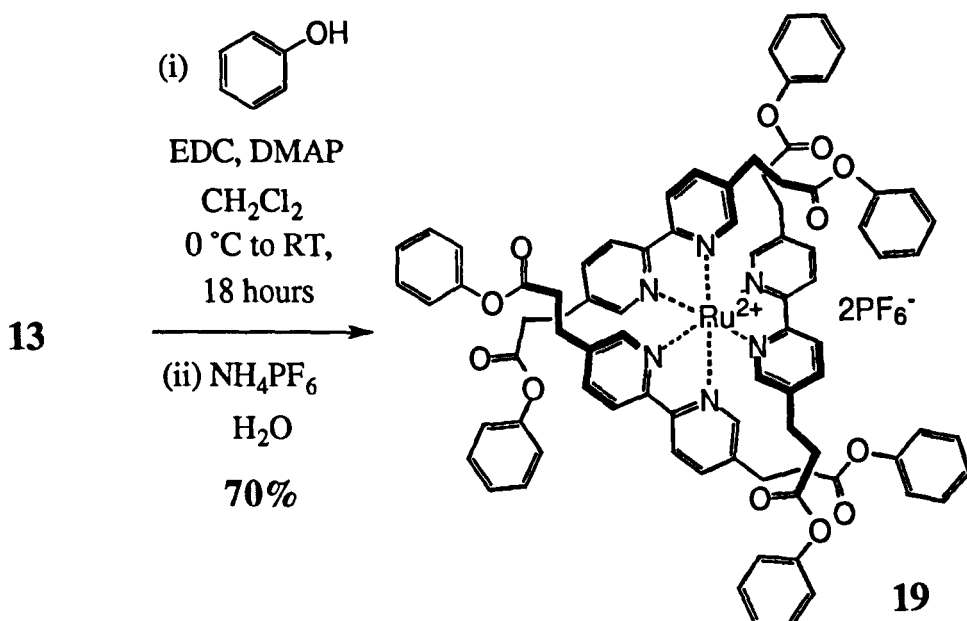


Scheme 3.10. Attempted macrocyclisation of ruthenium (II) hexa-tosylate complex **11**.

## 3.4 Macrocyclisation via Formation of Ester Links

### 3.4.0 Model Reactions

The main problem with the ether-linked strategy was the rather vigorous conditions required to form the new bonds in reasonable yield. It seemed likely however that ester links could be formed under much milder conditions. Direct coupling between terminal acid groups on the metal complexes and the bisphenol linker units could be achieved using a carbodiimide-type coupling agent without the need for the isolation of a complex containing activated acids. This type of reaction was tested for the coupling of ruthenium (II) hexa-acid **13** with phenol (Scheme 3.11). 1-(3-Dimethylaminopropyl)-1'-ethylcarbodiimide hydrochloride (EDC) was used as the coupling agent because the urea byproducts can be easily removed by aqueous acid in the workup. Catalytic DMAP was also added to the reaction and the hexa-phenyl ester **19** was isolated in an encouraging 70% yield.



Scheme 3.11. Model coupling of **13** and phenol using EDC.

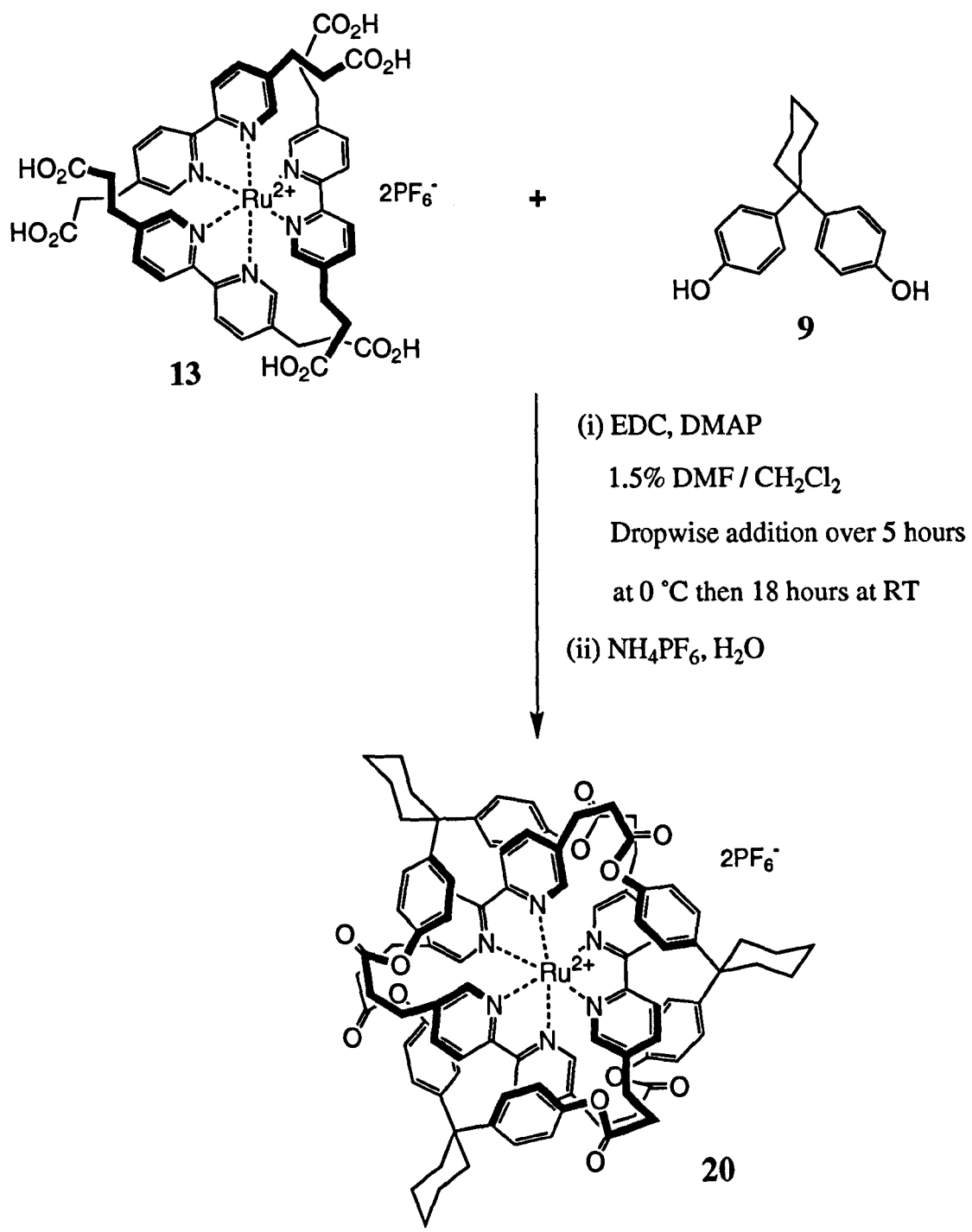
### 3.4.1 Ruthenium (II) Complexes

For the attempted macrocyclisation of ruthenium (II) hexa-acid complex **13**, it was decided to use  $\text{CH}_2\text{Cl}_2$  as solvent containing 1.5% DMF to provide the required solubility. A solution of **13** and 3 equivalents of bisphenol **9** in 1.5% DMF /  $\text{CH}_2\text{Cl}_2$  was added dropwise over 5 hours to a stirred solution of an excess of EDC and catalytic DMAP in  $\text{CH}_2\text{Cl}_2$  at 0 °C. After the addition was complete, the resulting solution was stirred at room temperature for a further 18 hours (Scheme 3.10). The solution produced was deep orange in colour indicating the presence of tris-bipyridine ruthenium (II) species. A small amount of an insoluble orange solid (accounting for approximately 5% of the starting material by mass) was removed by filtration. This solid could not be dissolved in any solvent and could not be characterised. This material is probably a mixture of oligomeric species.

The remaining solution was concentrated and washed with aqueous acid to removed the coupling agent and urea byproducts before being stirred with a concentrated aqueous solution of  $\text{NH}_4\text{PF}_6$  to effect counterion exchange. TLC analysis of the product on silica showed a complex mixture of products which failed to give any separation by flash chromatography using a variety of solvents.

Attempts were also made using HPLC (acetonitrile / water solvent, 1% TFA) on a variety of different column types but no resolution could be obtained and only extremely broad traces were produced.

The  $^1\text{H}$  NMR spectrum of the crude product was extremely broad and little information could be obtained (Figure 3.1). It is worth noting that the bipyridine signal usually observed at 8.5 ppm was absent which may indicate that it has been shifted upfield: this would be consistent with its position above the face of the aromatic rings of the bisphenol units in **20**. The use of high temperatures (100 °C in  $d_2$ -1,1,2,2-tetrachloroethane) or low temperatures (-60 °C in  $\text{CD}_2\text{Cl}_2$ ) failed to produce any sharpening of the signals in this spectrum.



**Scheme 3.12.** Attempted preparation of ester-linked knot **20**.

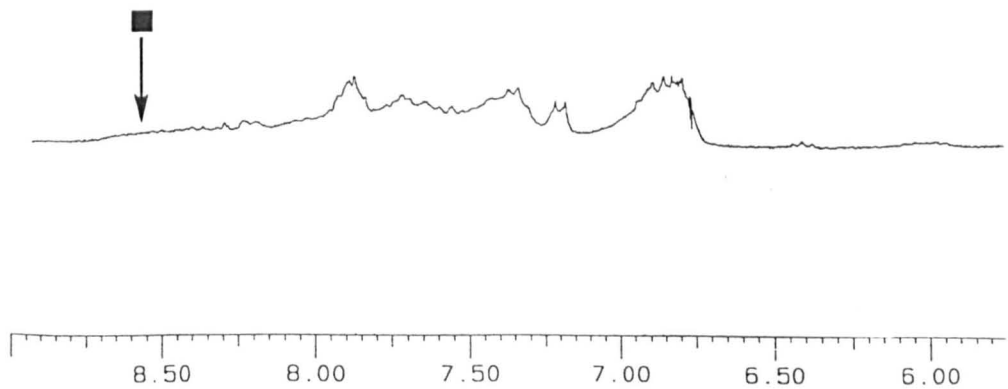


**Figure 3.1.** Aromatic region of the 250 MHz  $^1\text{H}$  NMR spectrum in  $d_6$ -acetone of the crude product from the reaction in Scheme 3.12. The region where the  $\text{H}_3$  bipyridine signal would be expected in a typical simple complex is indicated by the black square ( ■ ).

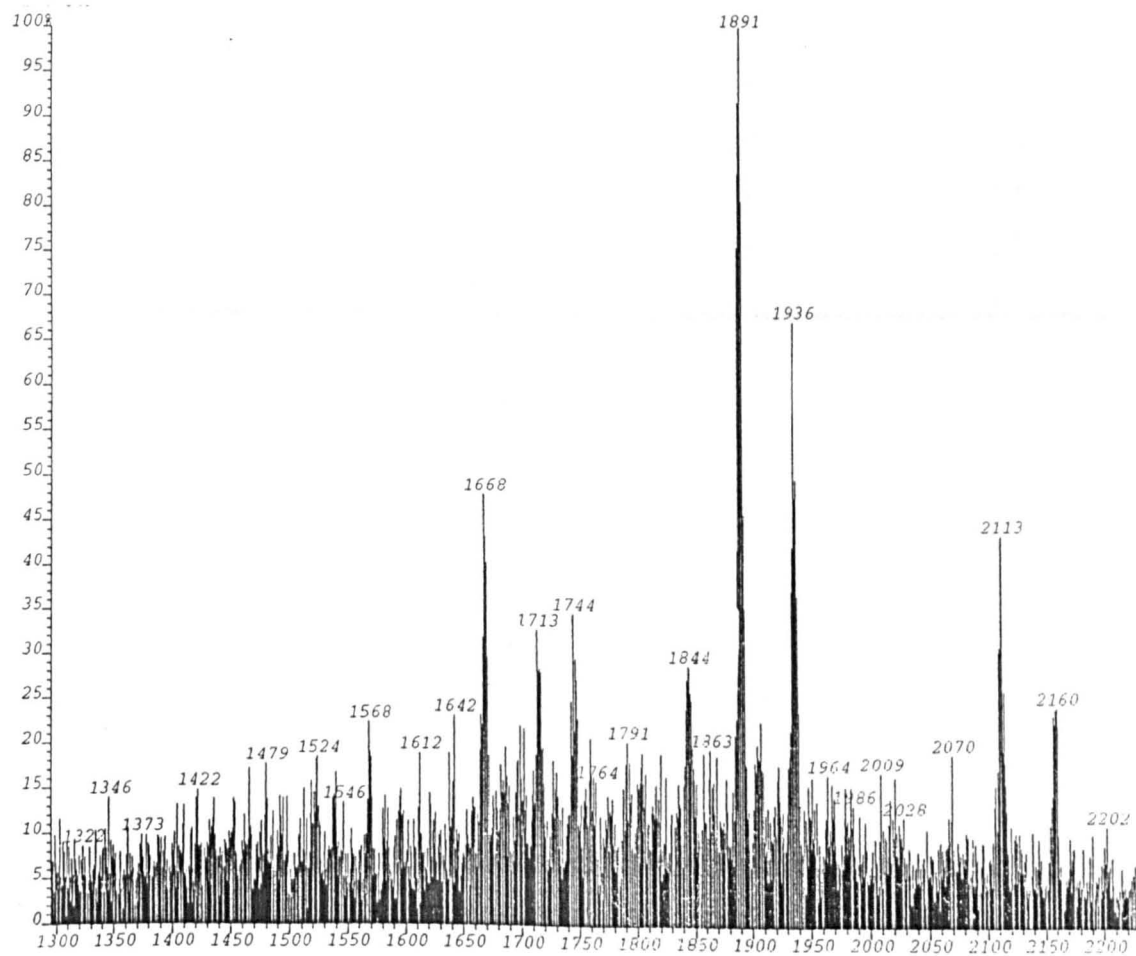


**Figure 3.2.** FAB $^+$  mass spectrum of the crude product from Scheme 3.12.

The FAB<sup>+</sup> mass spectrum of the crude product mixture was somewhat more informative (Figure 3.2). The peak at m/z 1844 corresponds to [20 - PF<sub>6</sub>]<sup>+</sup> and provides at least some evidence for the formation of the required product in the crude reaction mixture. A number of other signals appear in the same region of the spectrum as illustrated in Table 3.1. Structures corresponding to incomplete macrocyclisation products were tentatively assigned to these signals. The main cause of incomplete cyclisation seemed to be the formation of ethyl esters which was attributed to residual ethanol in the CH<sub>2</sub>Cl<sub>2</sub> solvent.<sup>‡</sup>

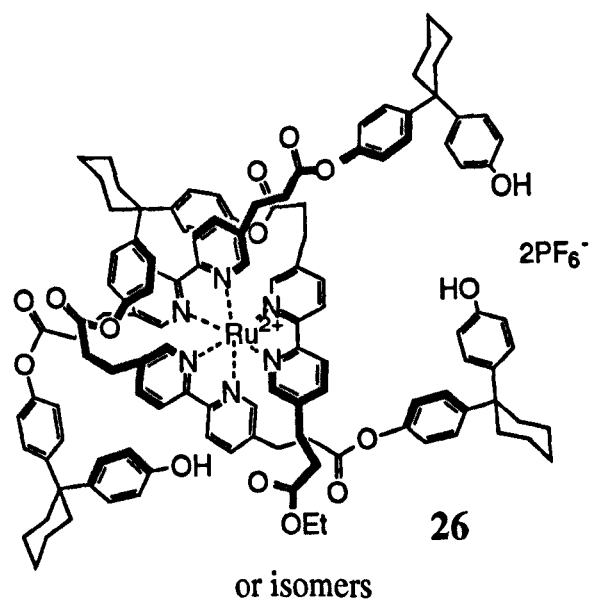
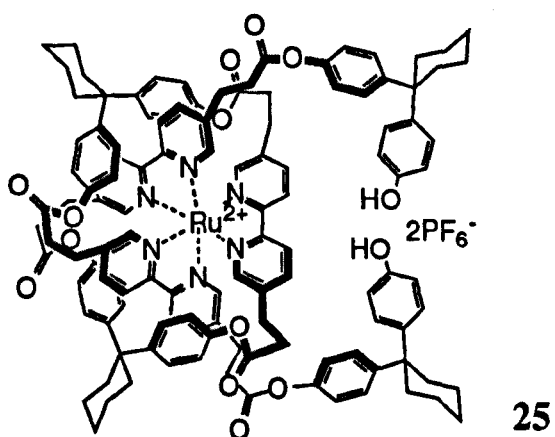
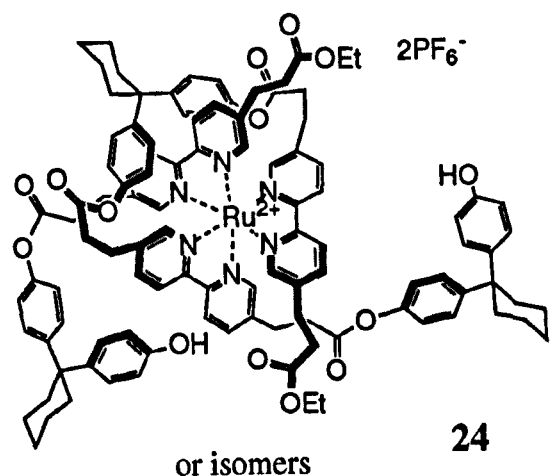
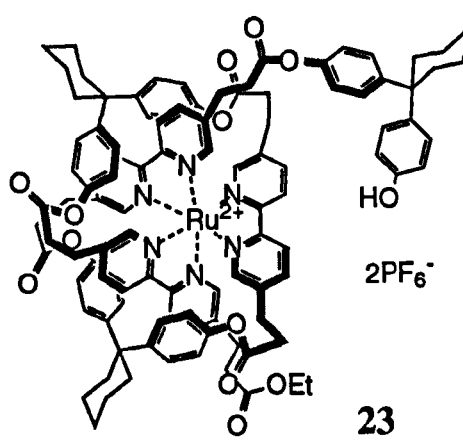
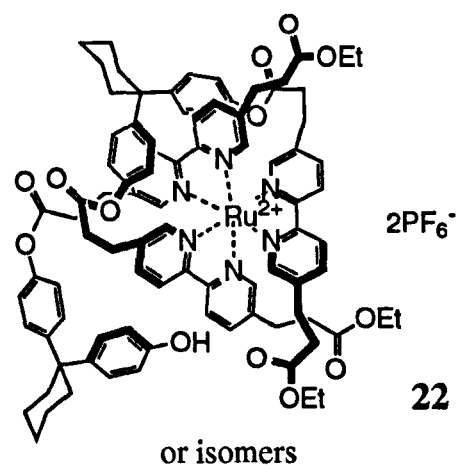
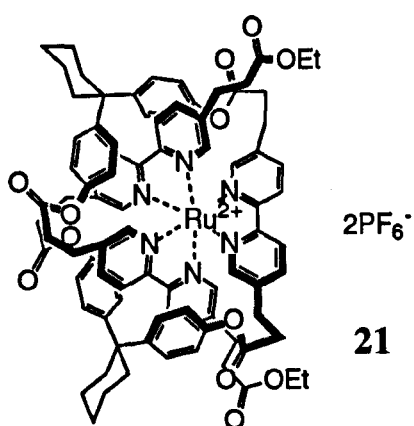
**Table 3.1.** FAB<sup>+</sup> MS signals observed for the crude macrocyclisation product from Scheme 3.12 along with their relative intensities and possible structures.

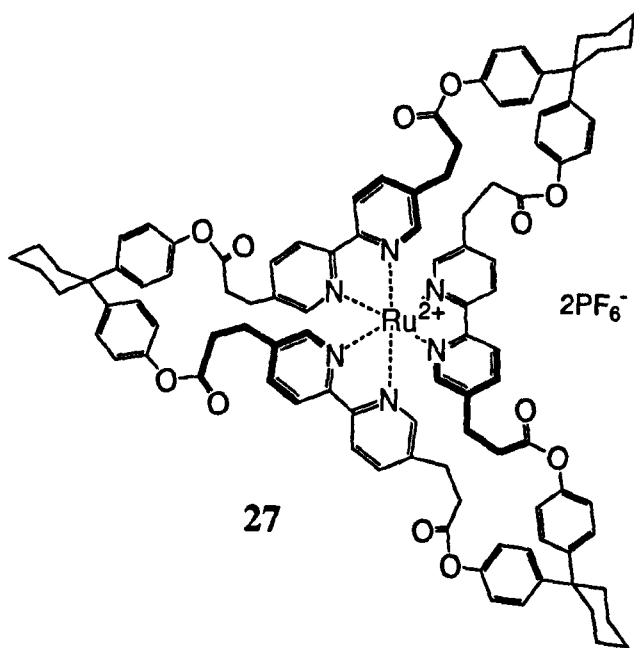
Signal Number	m/z	Intensity (%)	Structure <sup>b</sup>
1	1668	50	<b>21</b>
2	1713	30	<b>22</b>
3	1744	32	<sup>a</sup>
4	1844	30	<b>20</b>
5	1891	100	<b>23</b>
6	1936	65	<b>24</b>
7	2113	40	<b>25</b>
8	2160	20	<b>26</b>

<sup>a</sup> No reasonable structure could be proposed.

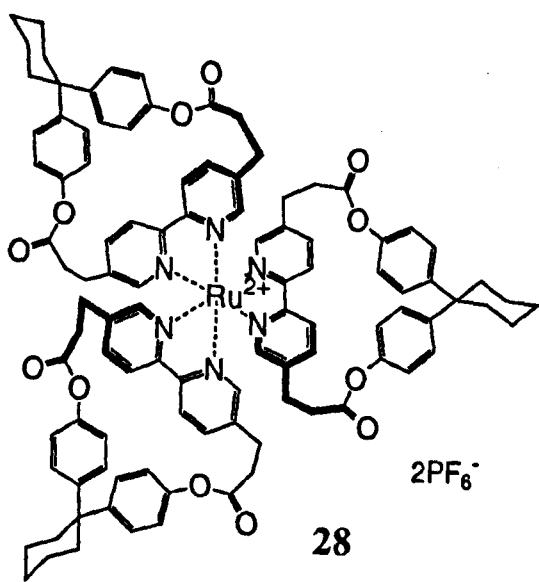
<sup>b</sup> All mass ions correspond to [M - PF<sub>6</sub>]<sup>+</sup>.

<sup>‡</sup> Dichloromethane used at this stage was obtained from the supplier containing 0.1% ethanol as a stabiliser. This was washed several times with water, pre-dried over MgSO<sub>4</sub> and 4 Å molecular sieves and distilled from calcium hydride before use. However, it seems likely that not all traces of ethanol were removed. This is of course particularly important in high-dilution reactions of this type. Subsequently, dichloromethane was obtained stabilised with amylene to avoid this problem.





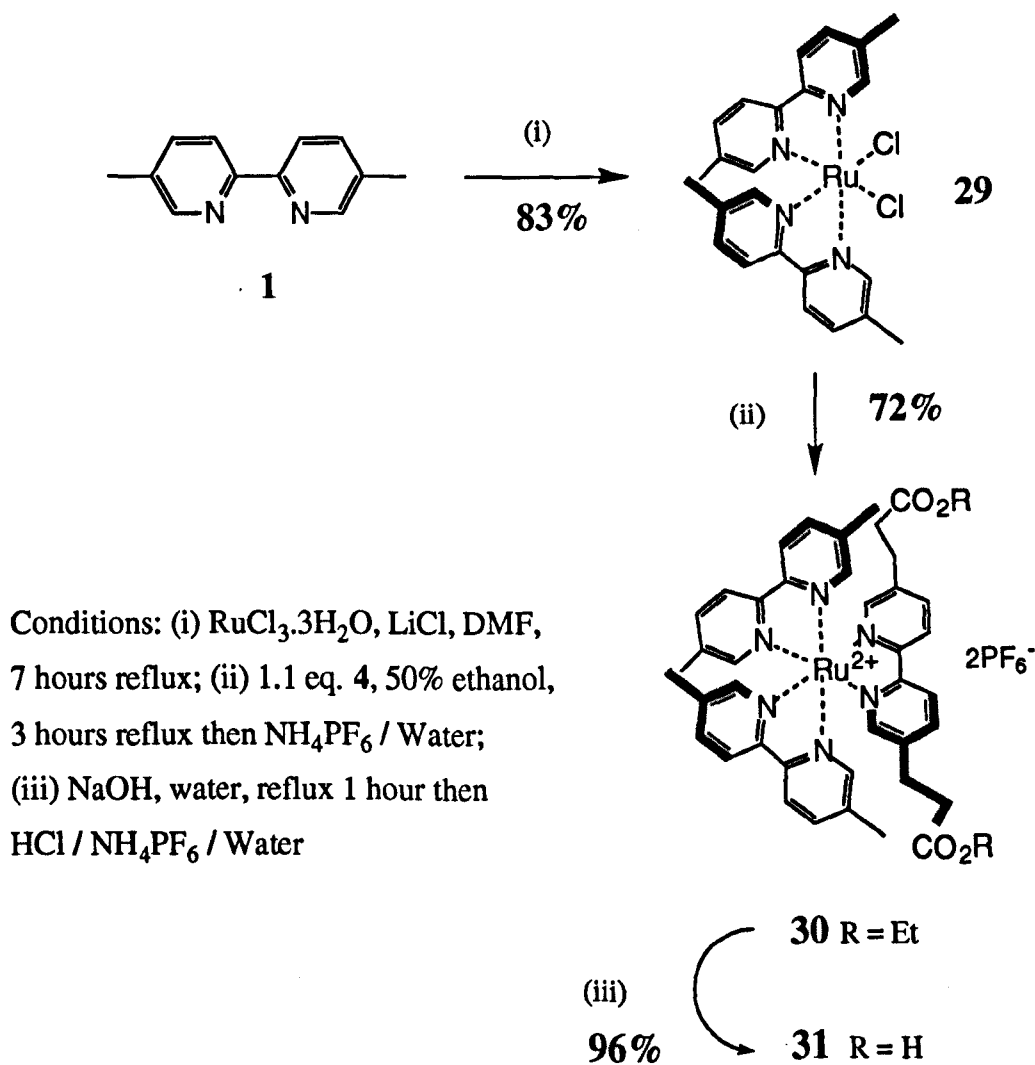
27



28

Of course, mass spectrometry can only suggest that the previously discussed structures are formed rather than providing definitive evidence. In particular, it is not possible to distinguish knot **20** from its two isomers **27** and **28** which would have identical molecular weights and hence the same FAB<sup>+</sup> signals. CPK models revealed that formation of the cyclic isomer **27** is not particularly favourable. Also, the bipyridine units are not in close proximity to the aromatic rings of the bisphenol linkers as in **20** and hence there is no explanation for the shift of the bipyridine signals in the <sup>1</sup>H NMR spectrum (Figure 3.1).

Formation of the tricyclic complex **28** also appeared rather unlikely and again, CPK models suggested that such a small ring would be extremely strained. However, in this case, the proximity of the bisphenol and bipyridine units would account for the upfield NMR shifts. To eliminate the possibility that **28** was being formed, a model reaction involving the ruthenium (II) diacid **31** was carried out. The synthesis of **31** is outlined in Scheme 3.13.

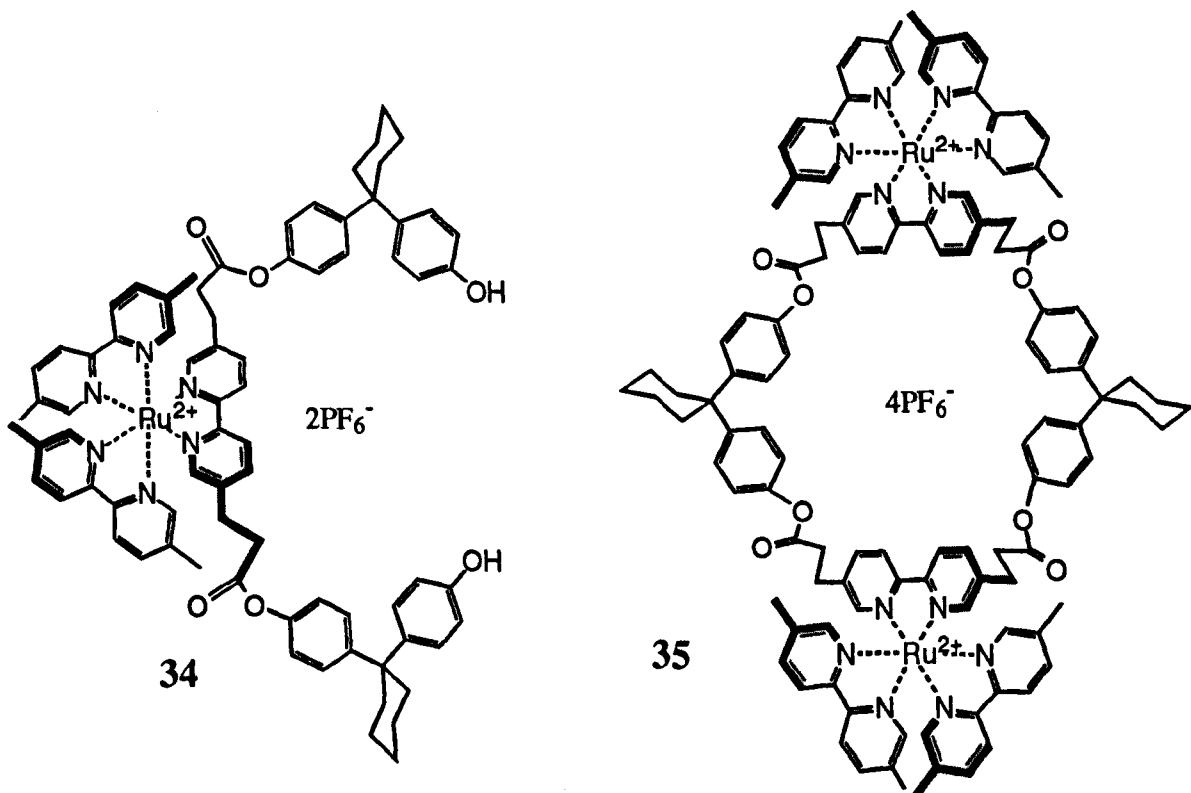


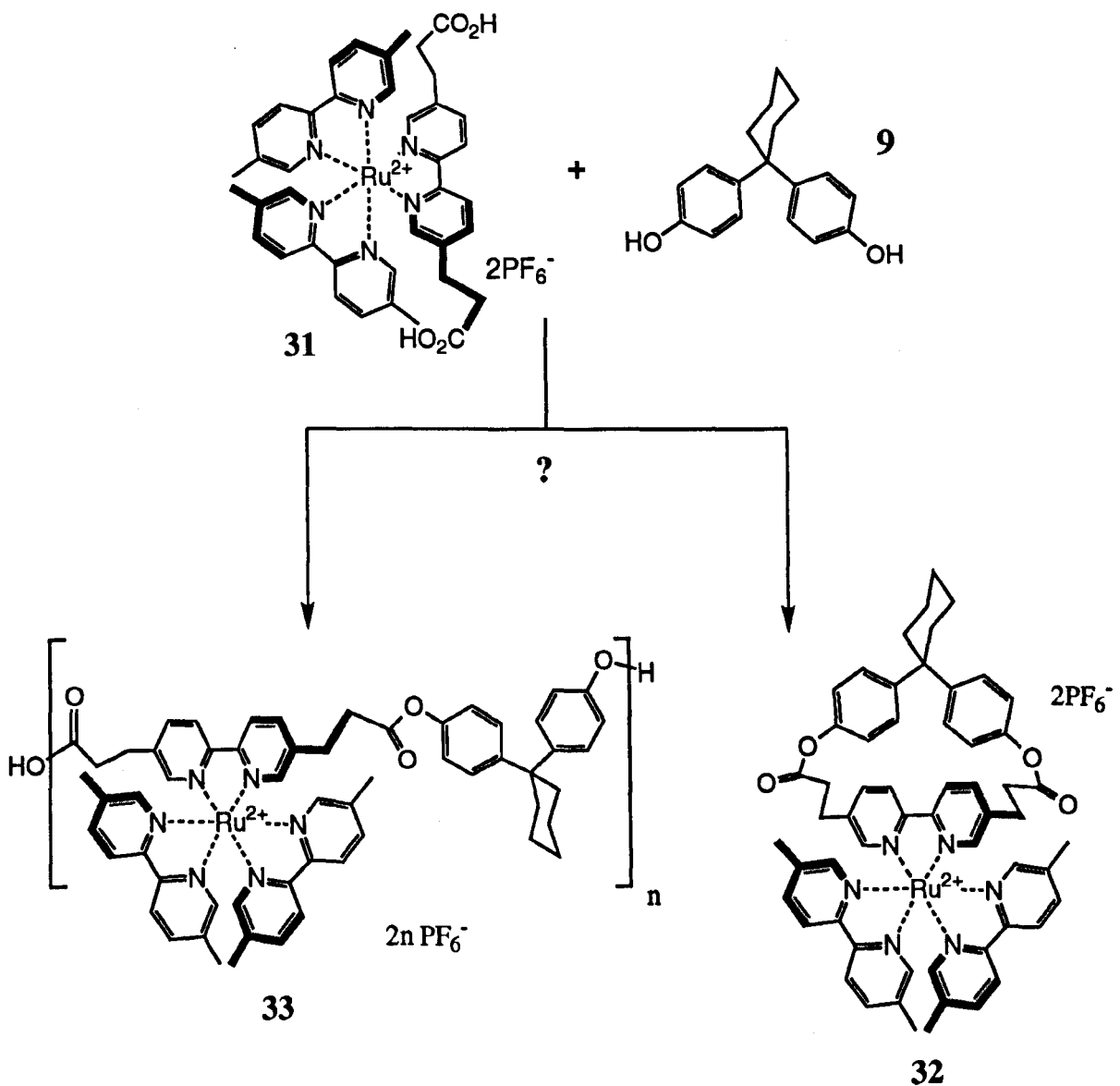
Scheme 3.13. Synthesis of model ruthenium (II) complex **31**.

Refluxing dimethylbipyridine with RuCl<sub>3</sub>.3H<sub>2</sub>O and lithium chloride in DMF gave a good yield of the *cis*-dichloro complex **29**, related to compounds reported in the literature.<sup>116</sup> The two chloride ligands were then displaced with the diester bipyridine ligand **4** in 72% yield by refluxing in 50% aqueous ethanol.<sup>117</sup> Finally, base hydrolysis of the esters gave **31** in 96% yield.

**31** was subjected to a macrocyclisation reaction with bisphenol **9** using identical conditions to those used in the attempted knot synthesis as outlined in Scheme 3.14. There are two possible types of product from this reaction. The formation of the cyclic compound **32** would indicate that the tricyclic structure **28** proposed as a possible product from the knot synthesis could account for the signals observed in the FAB<sup>+</sup> mass spectrum. If, however, no cyclic product was observed and the outcome of the reaction was the formation of oligomeric species of type **33** then this would be strongly suggestive that **28** could not be a product from the knot synthesis in Scheme 3.12.

In fact, when the reaction was carried out, the vast majority of product formed was baseline material by TLC analysis even in extremely polar solvent systems. This was strongly indicative that the major product was oligomeric in nature. A small amount of a higher running species was identified as **34**. Also tentatively identified in the FAB<sup>+</sup> mass spectrum of the crude reaction product was the 2:2 macrocycle **35** (peaks at m/z 2438 [35 - PF<sub>6</sub>]<sup>+</sup> and 2296 [35 - 2PF<sub>6</sub>]<sup>+</sup>). No peaks were observed for 1:1 macrocycle **32**. We are therefore confident that the formation of **28** in the knot synthesis reaction can be excluded.





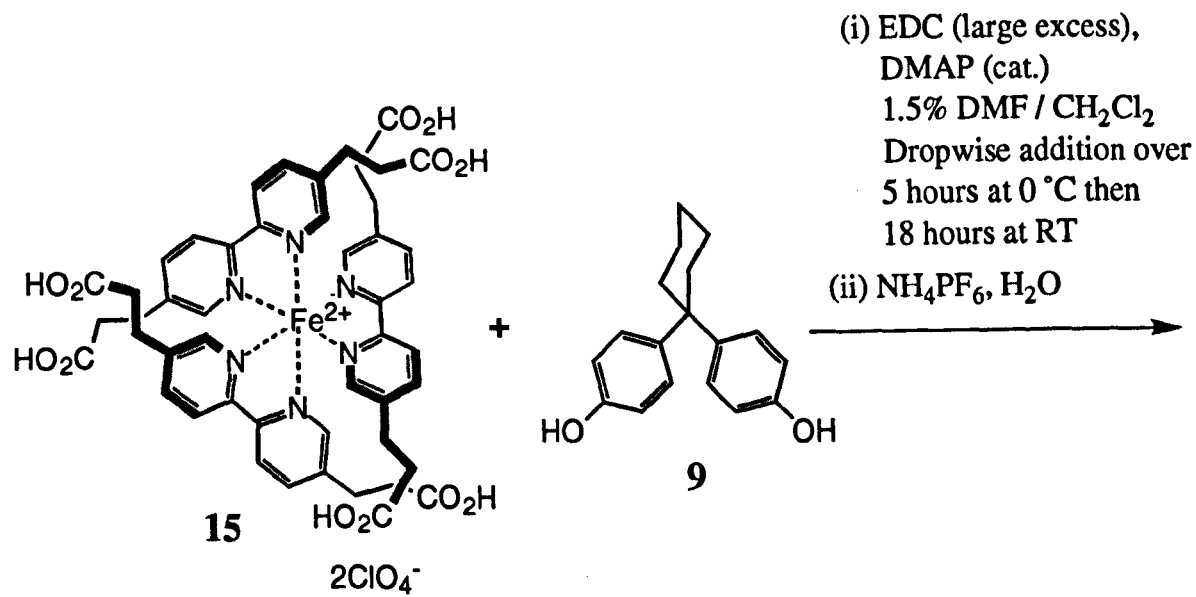
Conditions: (i) EDC, DMAP, 1.5% DMF /  $\text{CH}_2\text{Cl}_2$ , dropwise addition over 5 hours at 0 °C then 18 hours at RT; (ii)  $\text{NH}_4\text{PF}_6$  /  $\text{H}_2\text{O}$ .

**Scheme 3.14.** *Macrocyclisation of model complex **31**.*

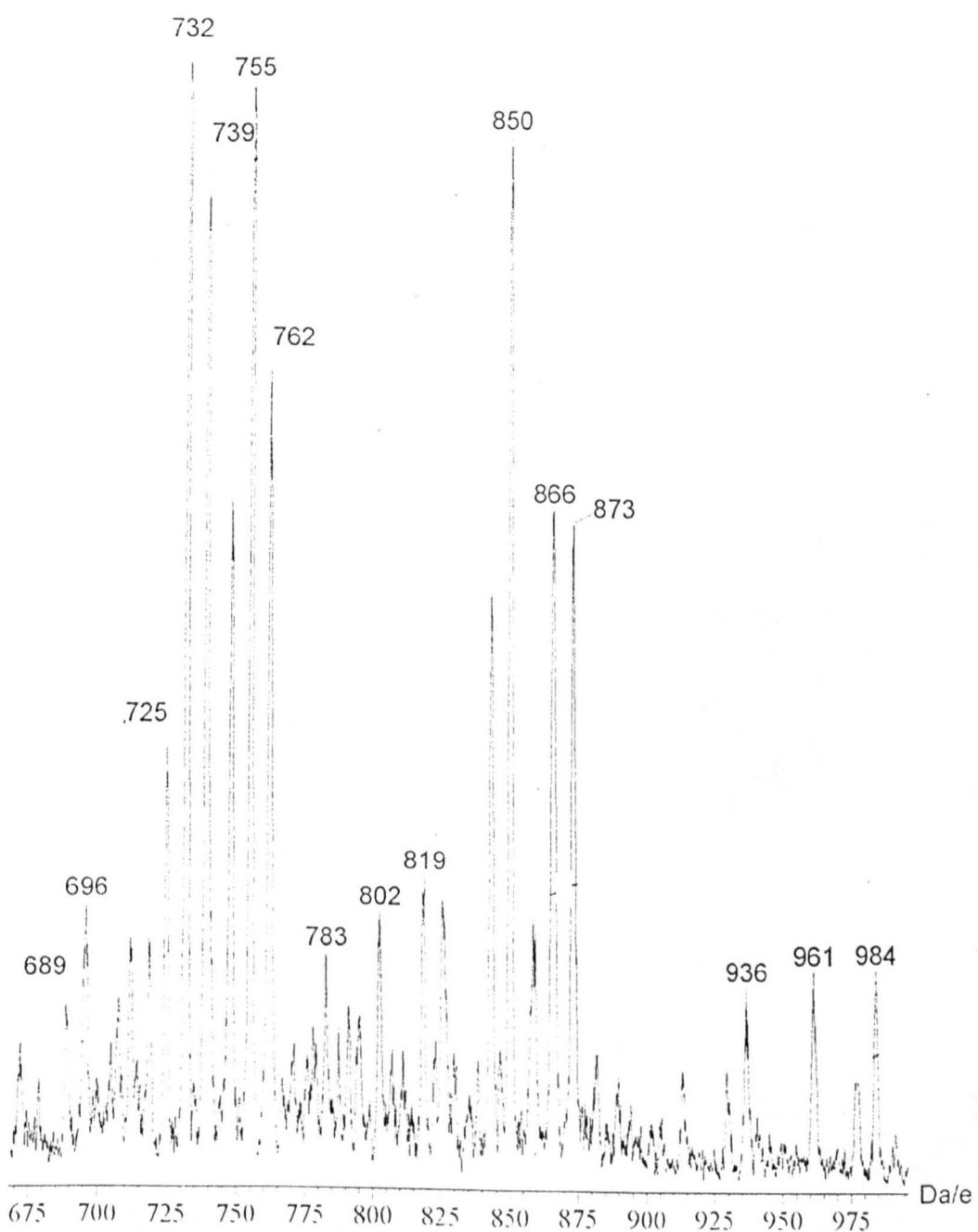
### 3.4.2 Iron (II) Complexes

Since the main problem with the ruthenium (II) complexes discussed in the previous section was the final chromatographic purification of the metal complexes, it seemed sensible to remove the metal ion from the crude product mixture, thereby reducing the problem to one of separating organic molecules rather than metal complexes. Such a strategy was not possible for the extremely stable ruthenium (II) species but looked much more feasible for the labile iron (II) complexes. As discussed in Section 3.3.1, this low stability can be a problem, resulting in decomposition of the complexes during attempted macrocyclisation. However, a simple model reaction suggested that iron (II) complexes were stable under the relatively mild conditions leading to ester formation.

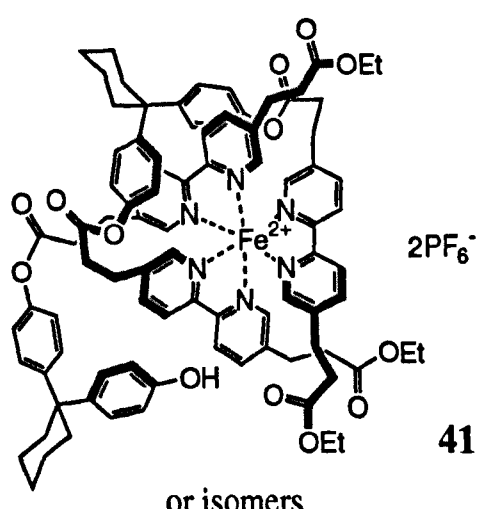
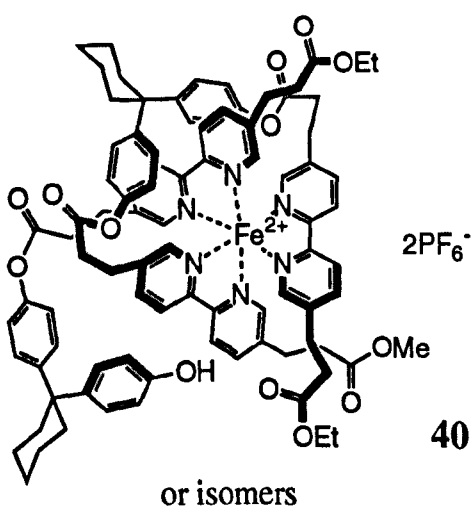
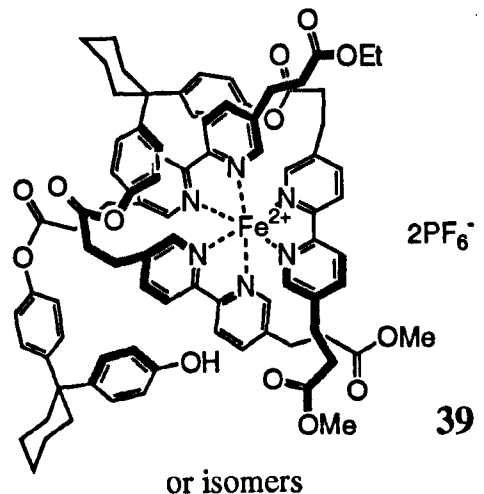
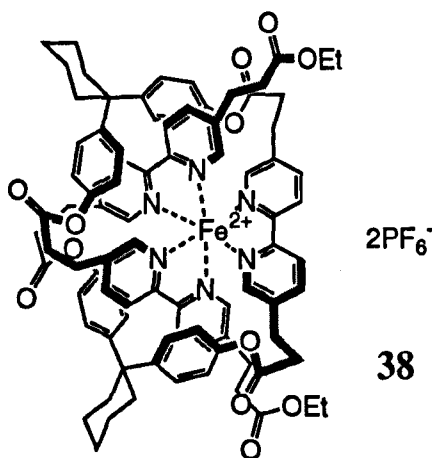
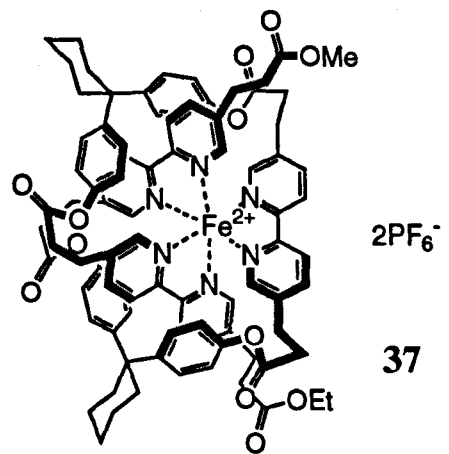
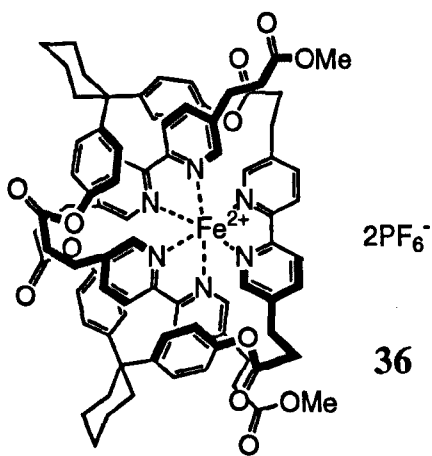
The iron (II) hexa-acid complex **15** was subjected to a high dilution reaction with three equivalents of bisphenol **9** as outlined in Scheme 3.15. **15**, 3 equivalents of **9** and catalytic DMAP were added dropwise over 5 hours to a  $\text{CH}_2\text{Cl}_2$  solution of EDC. The first attempt at this reaction was carried out in  $\text{CH}_2\text{Cl}_2$  that had been stabilised with 0.1% ethanol (see footnote to page 55). The crude product was characterised using ES<sup>+</sup> MS and as in the case of the ruthenium (II) complexes, the presence of a large number of species (tentatively assigned as structures **37 - 51**) could be inferred (Figure 3.3 and Table 3.2).



Scheme 3.15. Attempted macrocyclisation of iron (II) hexa-acid **15**.



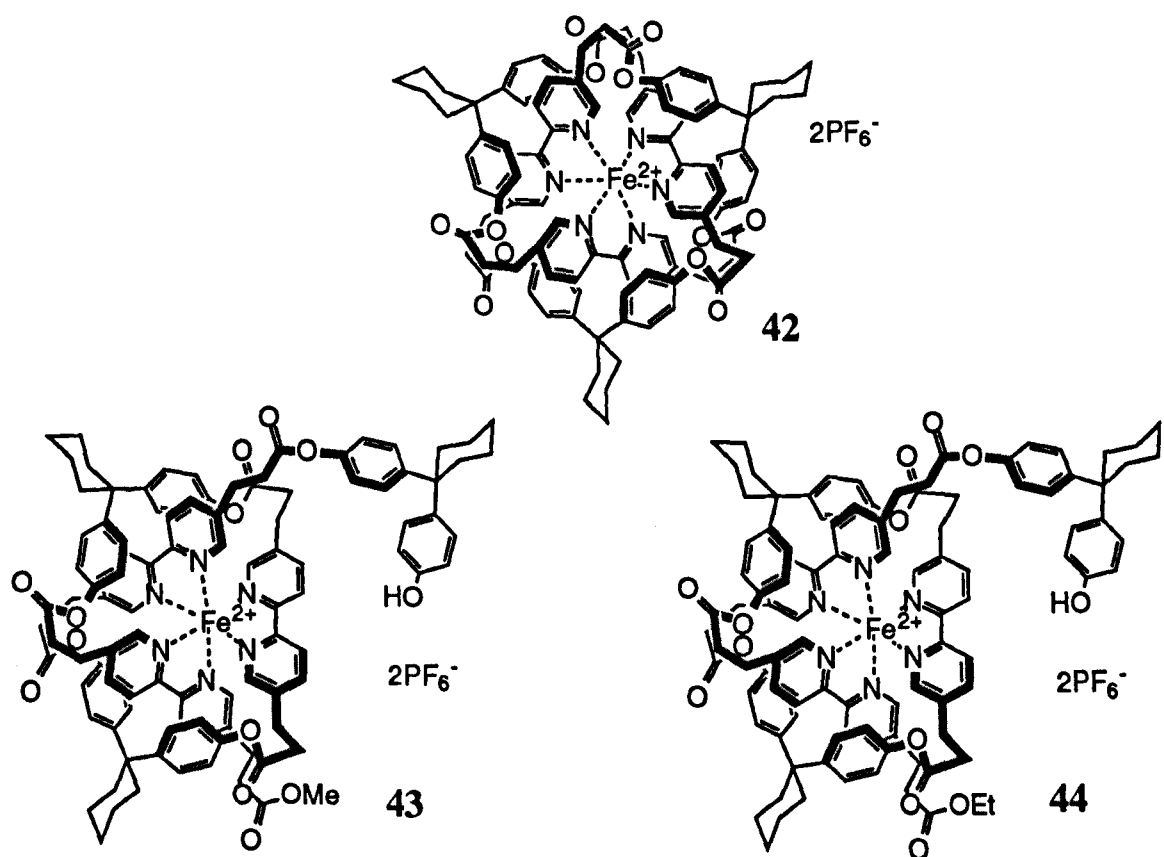
**Figure 3.3.** ES<sup>+</sup> mass spectrum of the crude product from the macrocyclisation reaction in Scheme 3.15.

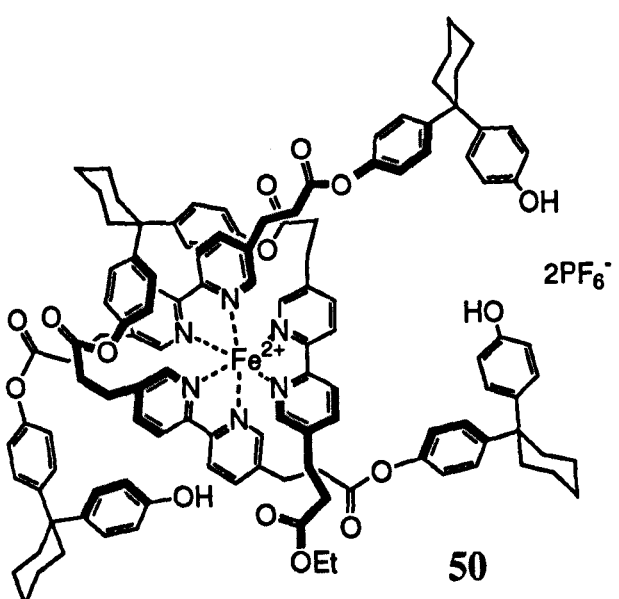
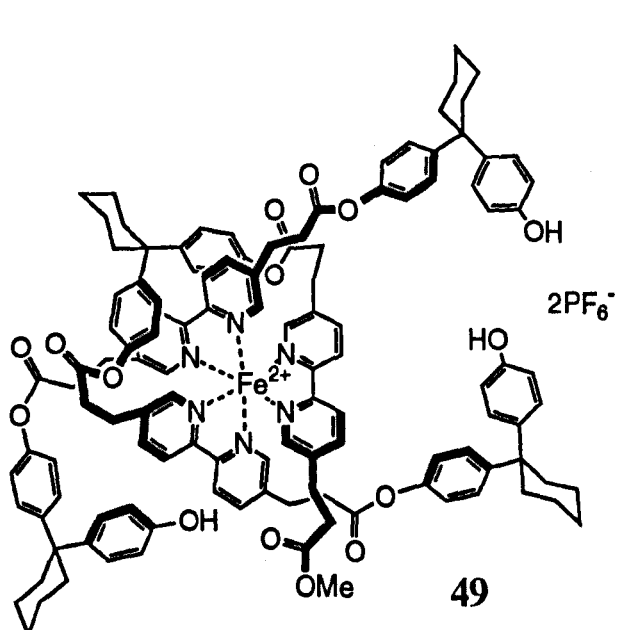
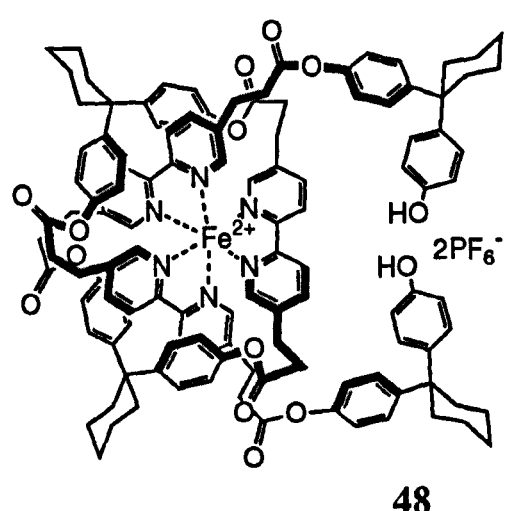
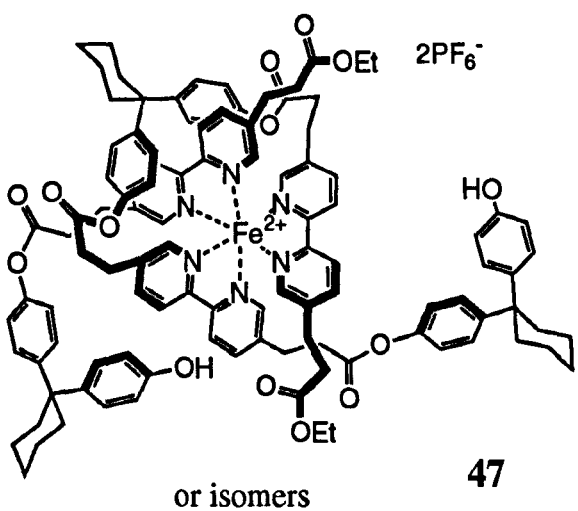
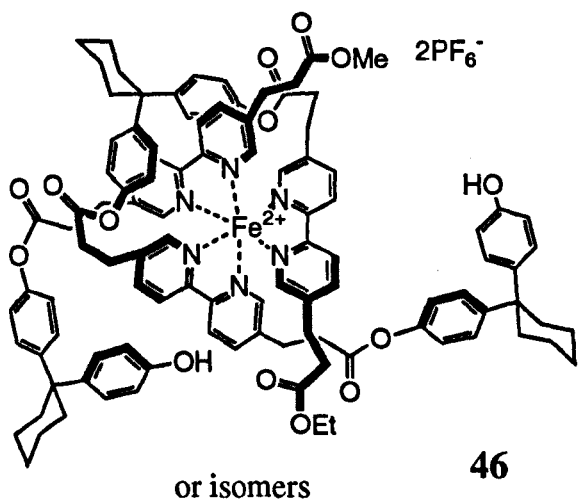
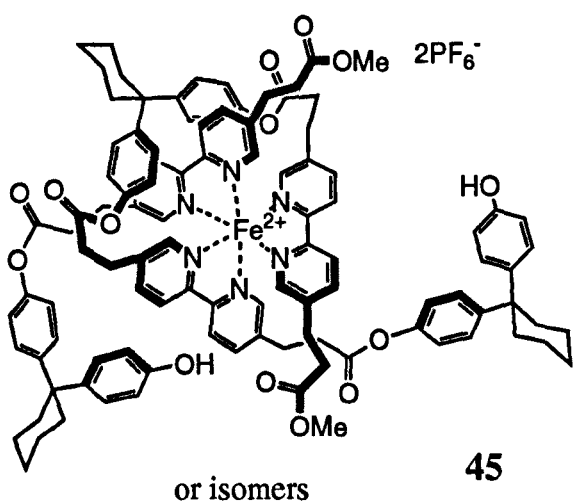


**Table 3.2.** Signals observed in the  $ES^+$  mass spectrum of the crude product from the macrocyclisation reaction outlined in Scheme 3.15.

Signal Number	m/z <sup>a</sup>	Intensity (%)	Possible Structure
1	725	32	36
2	732	100	37
3	739	85	38
4	748	55	39
5	755	95	40
6	762	65	41
7	826	25	42
8	843	50	43
9	850	90	44
10	859	20	45
11	866	55	46
12	873	55	47
13	961	20	48
14	977	10	49
15	984	20	50

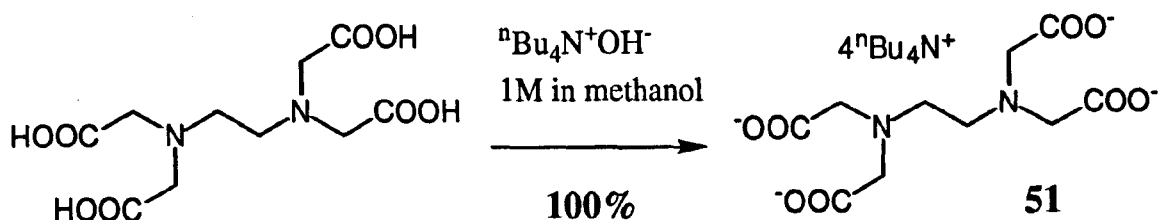
<sup>a</sup> All signals represent  $M^{2+}$  species formed by the loss of both counterions.





Again, as in the case of the ruthenium (II) complexes, the correct product can be tentatively identified from its peak in the mass spectrum, but as before the range of products is dominated by incompletely cyclised material. The same range of ethyl esters derived from the presence of small amounts of ethanol in the solvent can be seen, but also identified were many methyl esters. Since the only methanol used was in the reaction workup (the products are rather insoluble in  $\text{CH}_2\text{Cl}_2$  but extremely soluble in 1-2% methanol /  $\text{CH}_2\text{Cl}_2$ ) it seems that at the end of the reaction many of the acid groups remained activated by the EDC coupling reagent. Attempts to overcome this problem by using an increased reaction time still resulted in the same range of products.

As already discussed, the relative lability of the iron (II) complexes should in principle allow demetallation of the crude product thereby reducing the problem to one of separating organic molecules rather than metal complexes. Such a strategy is particularly attractive since one may envisage the desired knotted product having a significantly different  $R_f$  value to the linear molecules resulting from incomplete cyclisations. To remove the iron from the complexes an organic soluble derivative of EDTA was prepared (Scheme 3.16). Treatment of EDTA with a methanolic solution of  ${}^n\text{Bu}_4\text{N}^+\text{OH}^-$  followed by removal of solvent and prolonged drying gave the tetrakis (tetra-n-butyl ammonium) salt **51**.



**Scheme 3.16.** Preparation of organic soluble EDTA derivative **51**.

The crude product from the macrocyclisation reaction was dissolved in 2% methanol and treated with an excess of **51**. Over a period of several hours the strong red coloration disappeared and was replaced by a yellow solution. After work-up, TLC analysis indicated a complex mixture of products that proved inseparable by flash chromatography. Attempts were therefore made to identify some of the components of the mixture using  $\text{FAB}^+$  mass spectrometry. Two  $\text{FAB}^+$  mass spectra of the crude demetallated product are illustrated in Figure 3.4. Table 3.3 summarises the mass ions identified and structures attributed to them. As can be seen, almost all the ligands that one would expect to be derived from the demetallation of **36-50** can be identified. Unfortunately, no signal corresponds to the demetallation product of knot **42**.

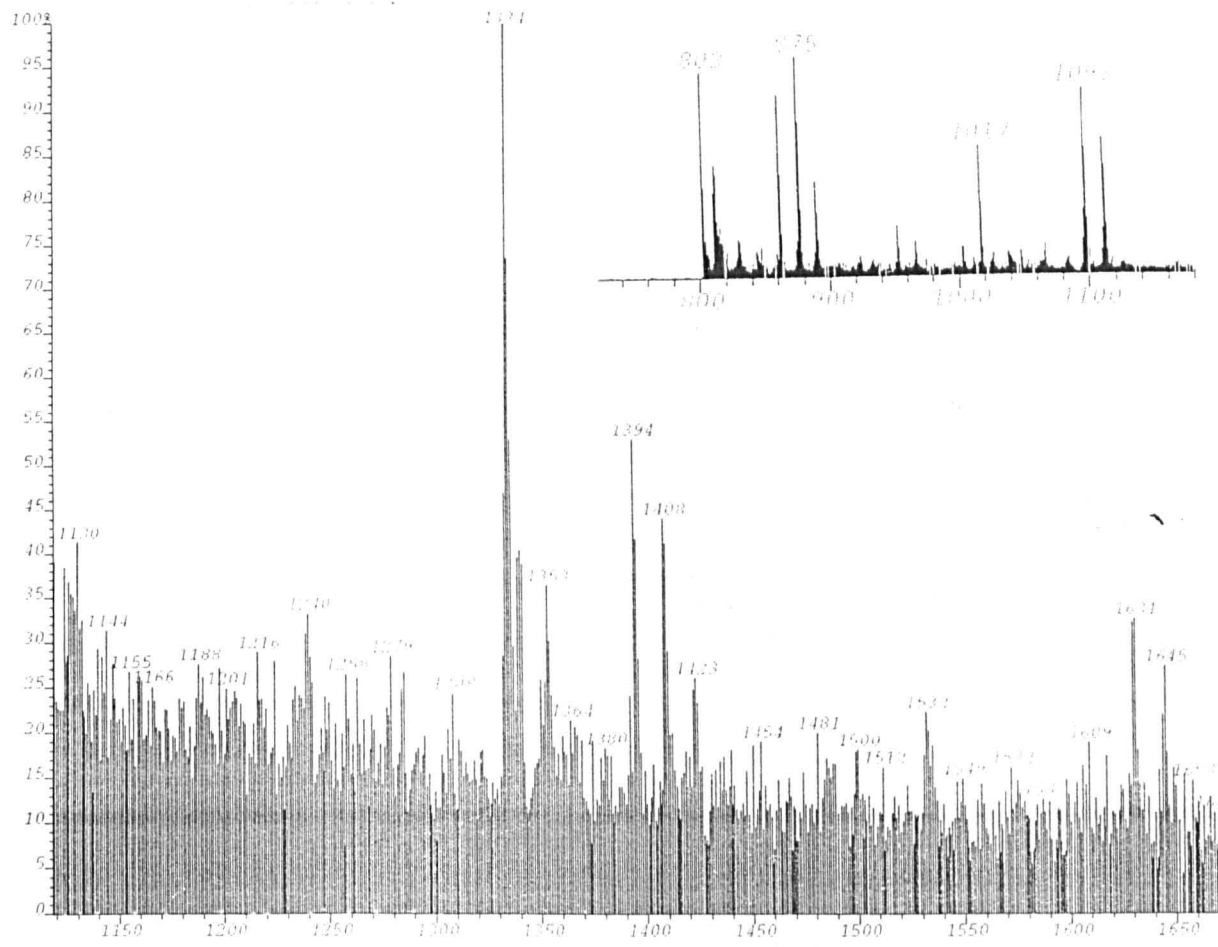
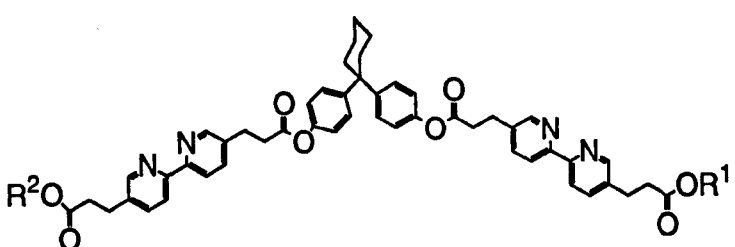
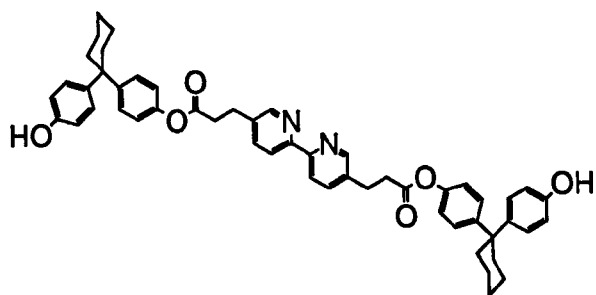


**Figure 3.4.** FAB<sup>+</sup> MS of the product from demetallation of the crude reaction mixture from macrocyclisation of iron (II) complex 15.

**Table 3.3.** Summary of signals observed in Figure 3.4. and proposed structures.

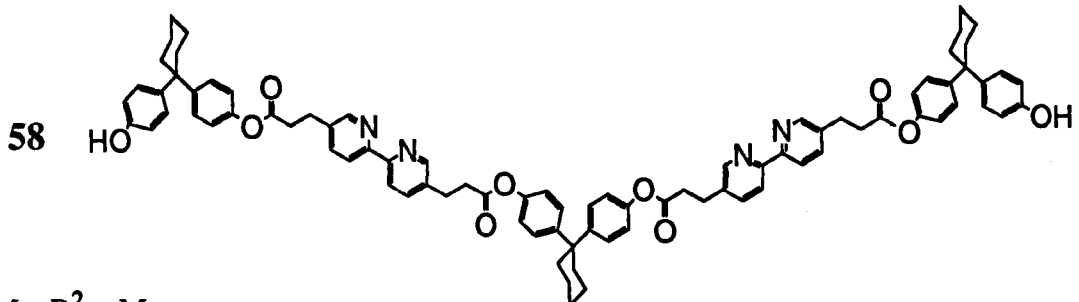
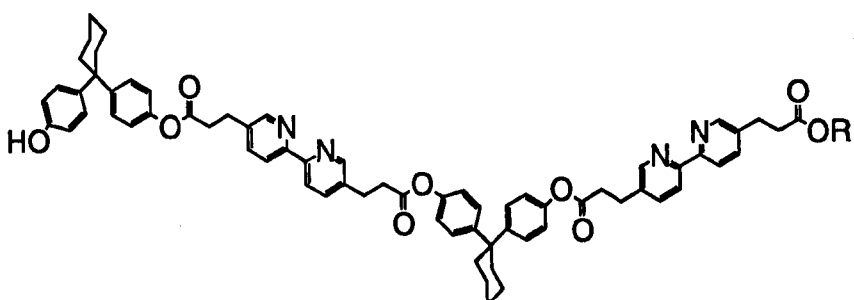
Signal Number	m/z	Structure
1	802	<b>52</b>
2	861	<b>53</b>
3	875	<b>54</b>
4	889	<b>55</b>
5	1098	<b>56</b>
6	1112	<b>57</b>
7	1334	<b>58</b>
8	1394	<b>59</b>
9	1408	<b>60</b>
10	1423	<b>61</b>
11	1631	<b>62</b>
12	1645	<b>63</b>

**52**



- 53**  $R^1 = \text{Me}, R^2 = \text{Me}$   
**54**  $R^1 = \text{Me}, R^2 = \text{Et}$   
**55**  $R^1 = \text{Et}, R^2 = \text{Et}$

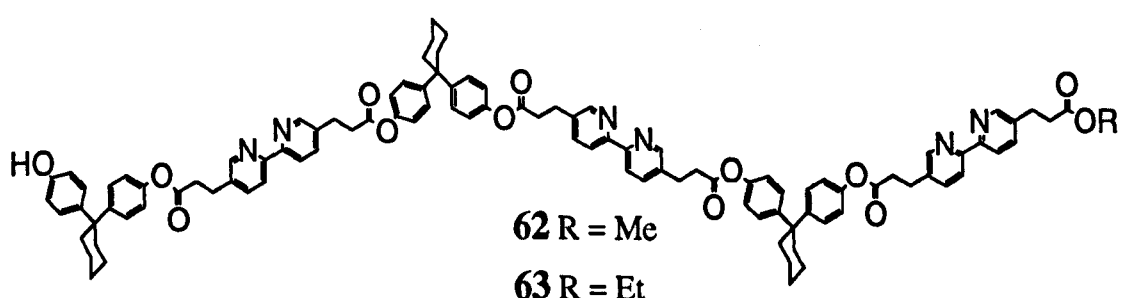
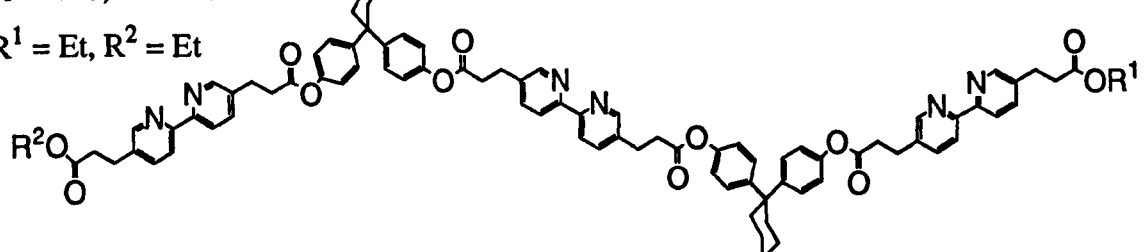
**56**  $R = \text{Me}$   
**57**  $R = \text{Et}$



**59**  $R^1 = \text{Me}, R^2 = \text{Me}$

**60**  $R^1 = \text{Me}, R^2 = \text{Et}$

**61**  $R^1 = \text{Et}, R^2 = \text{Et}$



- 62**  $R = \text{Me}$   
**63**  $R = \text{Et}$

Clearly, this result tells us that the ester-links are being formed in the required manner and that demetallation of the crude product prior to further purification is a feasible strategy. All that remained was to optimise the reaction to reduce the formation of incompletely cyclised byproducts. In particular, the formation of ethyl esters should readily be avoided, and in a second attempt at the reaction, dichloromethane stabilised with 0.005% amylene was used in place of the original solvent. The iron (II) complex **15** and bisphenol **9** were again added to the EDC, but this time the DMAP catalyst was pre-mixed with the EDC rather than with **9** and **15**. Again the product was dissolved in a methanol / dichloromethane solution during the final stages of the work-up. This time, a very different range of products was identified.

A high running spot on TLC was isolated in 32% yield and identified as the hexa-methyl ester **64** from its  $^1\text{H}$  NMR spectrum and ES $^+$  MS ( $\text{M}^{2+}$  ion at m/z 520). The remaining mixture of products accounting for approximately a further 50% of starting material could not be further separated. The dominant peak in the ES $^+$  MS was at m/z 725 corresponding to structure **36** also formed in the earlier reaction. The majority of signals in the product from the earlier reaction were absent. The  $^1\text{H}$  NMR of this crude mixture (Figure 3.5) is complex and clearly a mixture of products but is generally consistent with products such as **36** as the majority of the bipyridine signals have been shifted upfield. This upfield shift is consistent with the structural motif where the edge of the bipyridine unit is in close proximity to the face of the aromatic rings of the bisphenol unit.

Clearly, in this reaction the ester coupling is not proceeding as efficiently as before. The hexa-methyl ester **64** must be formed during work-up which implies that the product of the reaction itself must have all six acid groups activated by EDC. This raises the question of why bisphenol **9** does not react in the required manner. A possible solution to this may be provided by two further intense signals in the mass spectrum at m/z 424 and 579. These seem to correspond to the two EDC adducts **65** and **66**. Such structures would appear to be relatively unstable, and cannot be isolated but their formation during the reaction would account for the lack of nucleophilicity of **9**. These products seem to result purely from the change in order of addition of reactants, and we have no explanation for this effect.

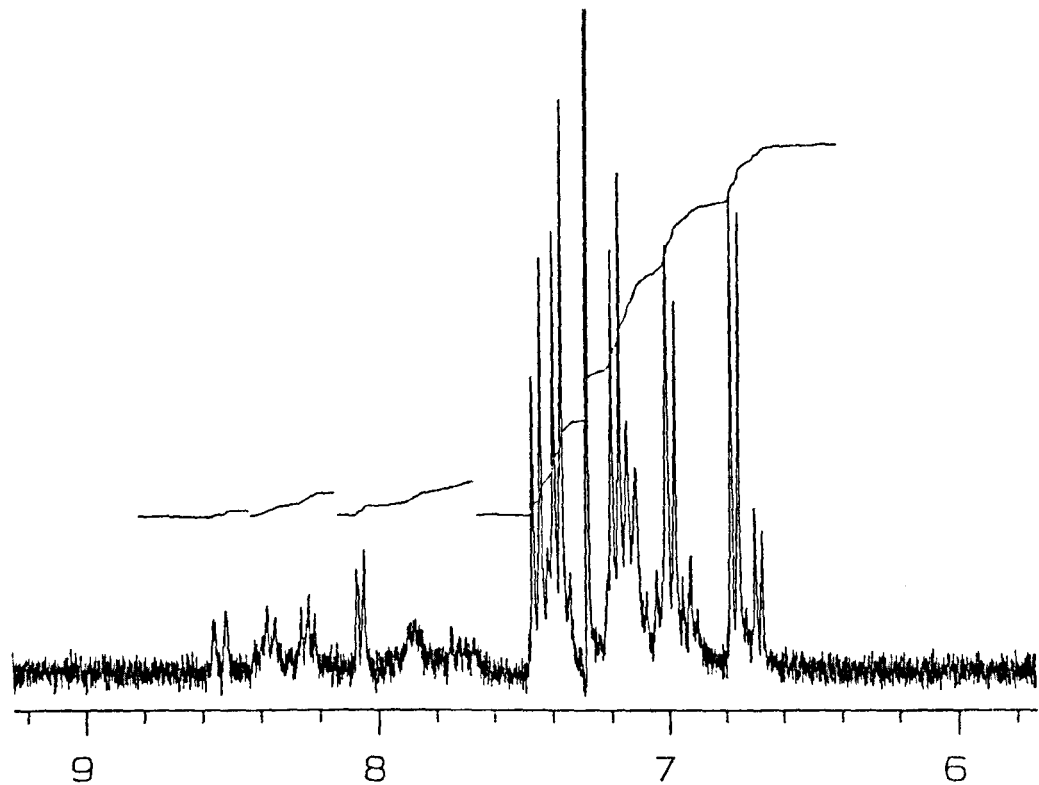
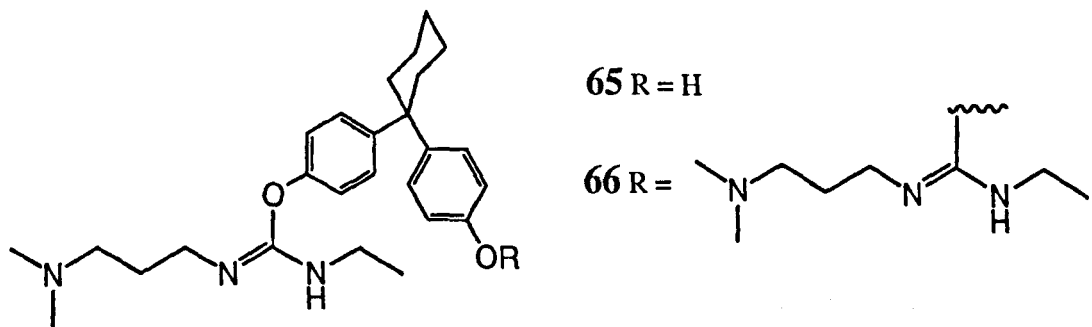
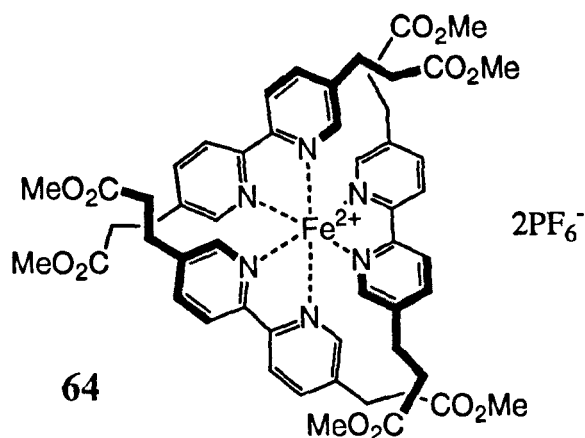
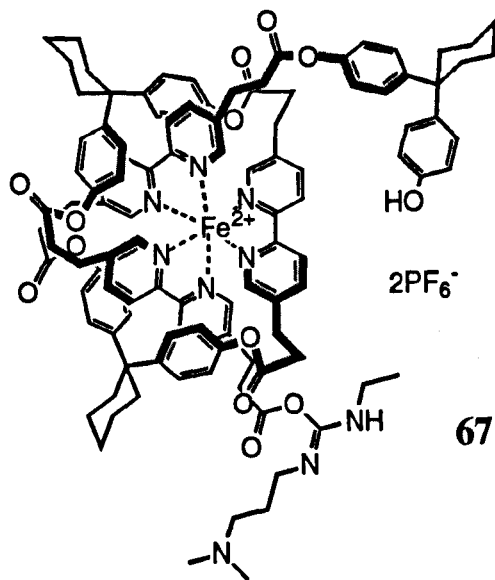


**Figure 3.5.** Aromatic region of the 300 MHz  $^1\text{H}$  NMR spectrum of the mixture of products derived from a second attempt at the macrocyclisation reaction in Scheme 3.15.

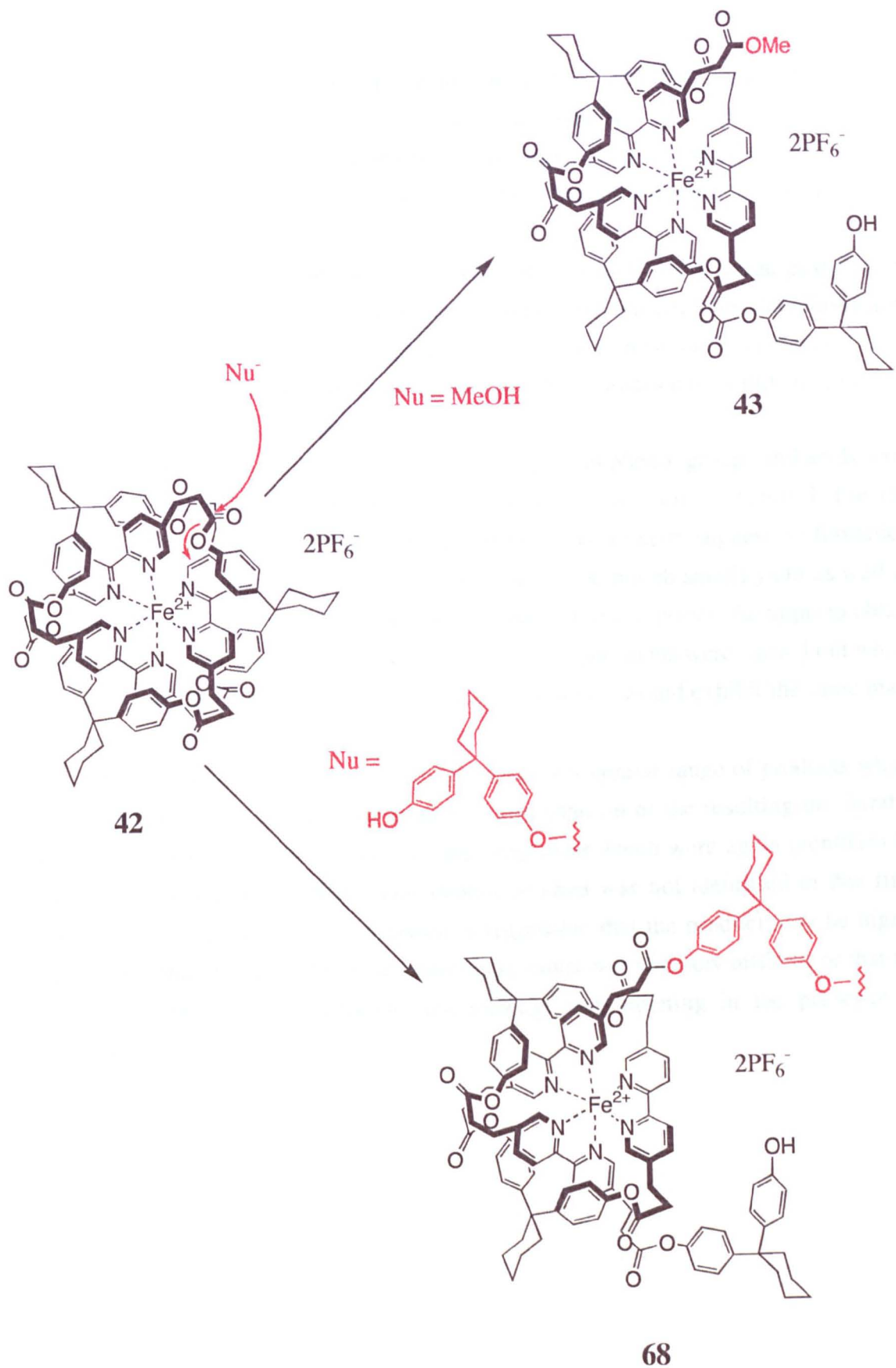


Since the order of addition used in the first reaction was clearly preferable, it was decided to repeat this reaction using amylene-stabilised  $\text{CH}_2\text{Cl}_2$ . The product derived from this reaction was again analysed by ES<sup>+</sup> MS and the range of signals observed was much reduced. A weak signal corresponding to the required product was found, but the dominant signal corresponded to structure **43** where only the final cyclisation is prevented by the presence of a single methyl ester. If we assume that the tris-bipyridine iron (II) core of the molecule is rigid, then there seems to be no reason why this final macrocyclisation reaction should not proceed just as efficiently as the other two identical cyclisations required to form **43**. This seems to suggest that the core is not rigid and there is a much larger degree of strain introduced when completing the final ring closure.<sup>‡</sup>

There are two possible reasons why **43** rather than knot **42** may be the dominant product, both linked to ring strain in the final macrocyclisation. The first possibility is that activated ester **67** cannot cyclise because the ring formed would be too strained. The second possibility is that although **42** may form during the reaction, the strain makes the esters more reactive and hence susceptible to nucleophilic attack. Attack by methanol during work-up would lead to **43** or by a phenolic group during the reaction would lead on to oligomeric species such as **68** (Scheme 3.17). No attempt was made to investigate this reaction further.



<sup>‡</sup> In view of later work (Chapter 5) it does seem extremely likely that complexes such as **43** would be significantly distorted from the ideal octahedral arrangement about the metal ion and that the final macrocyclisation may be much more difficult or indeed impossible.



**Scheme 3.17.** Possible decomposition of knot **42** due to ring strain.

### 3.5 Conclusions

A range of octahedral tris-bipyridine complexes of both ruthenium (II) and iron (II) have been prepared containing two different functionalities upon the bipyridine units to allow formation of new bonds in macrocyclisation reactions - terminal tosylate groups for displacement by phenoxide anions to form ethers and acids to form esters via the use of a coupling agent.

Attempted cyclisations via the formation of ether links were unsuccessful. Iron (II) complexes were unstable to the reaction conditions and complex decomposition occurred to yield iron (II) phenolate species. Although the ruthenium (II) complexes were stable, no characterisable products were isolated and it would seem that the majority of products were oligomeric in nature.

Cyclisations via the formations of ester links from phenol groups and acids with the use of a carbodiimide coupling agent were somewhat more successful. For the ruthenium (II) complexes,  $^1\text{H}$  NMR spectra and mass spectrometry suggest the formation of the desired knotted macrocycle in an indeterminate (although small) yield as well as allowing tentative identification of some incompletely cyclised species. Attempts to obtain the product in a pure form were unsuccessful. Model experiments were carried out which suggest that the formation of other isomeric species which would exhibit the same mass spectra is unlikely to occur.

Macrocyclisation of iron (II) complexes gave a similar range of products which were identified using the same procedures. Demetallation of the resulting inseparable mixture of complexes gave a series of short oligomers which were again identified by mass spectrometry. The demetallated knotted product was not identified in this final mixture. The range of products obtained is suggestive that the product may be highly strained and that the final macrocyclisation may either be extremely difficult or that the cyclised product may be unstable and undergo ring opening in the presence of nucleophiles.

---

# *Chapter 4*

---

## **Model Studies of $\pi$ - $\pi$ Interactions**

## 4.1 A Model System to Investigate $\pi$ - $\pi$ Interactions

### 4.1.0 Background

It was decided that this would make a good point to further investigate the nature of the  $\pi$ - $\pi$  interactions that were required to provide the secondary template effect to direct the macrocyclisation reactions in the knot syntheses. Would the interactions really exist in such a system and if so, how would they vary with solvent and temperature? Knowing the answers to these questions would hopefully enable us to optimise the conditions used in future work.

### 4.1.1 Previous Studies

Many workers have designed systems that enable the qualitative or quantitative investigation of the strength of weak aromatic interactions. A number of different approaches have been invoked for these investigations. Much work has utilised the effect that such interactions can have upon the conformation of flexible molecules containing two aromatic systems capable of interacting with each other.<sup>118</sup> Information has been obtained in the solid state via X-ray crystallography and in solution via NMR shifts induced by ring currents<sup>119</sup> as well as the relative intensities of NMR signals corresponding to different conformations.<sup>120</sup>

Other approaches utilise the effect of interactions upon dynamic properties of a molecule. For example, the energy barrier to rotation about a particular bond can be determined and equated to the strength of interaction between a group on that bond and another part of the molecule.<sup>121</sup>

Finally, host-guest chemistry has provided a valuable means for the qualitative determination of interaction strength trends as well as the quantitative measurement of  $\Delta G$  values for aromatic interactions. Our group has recently reported the use of "Double-Mutant" thermodynamic cycles involving host-guest complexes to directly measure interactions between various aromatic systems in chloroform.<sup>122</sup>

Although much attention has been directed towards determining the effect of the nature of the aromatic system and substituents upon interaction strength, little work has been reported on the effect of solvent. The most comprehensive study has been carried out by Diederich who has reported a number of host molecules that complex planar aromatic molecules via  $\pi$ - $\pi$  interactions.<sup>123</sup>  $\Delta G_{\text{complexation}}$  values have been determined from NMR binding experiments in various solvents and linear free energy relationships used to equate these values to solvent polarity. In such systems there is a clear relationship between polar solvents and strong binding constants (i.e. strong aromatic interactions) and between non-polar solvents and weak binding.

## 4.1.2 Design of a Model System

The system designed to allow the investigation of  $\pi$ - $\pi$  interactions relevant to our reactions made use of the effect that favourable interactions would have on the conformation of metal tris-bipyridine complexes containing pendant phenyl esters (Figure 4.1). We reasoned that the phenyl esters could interact with the edge of a nearby bipyridine unit in an edge-face manner. Such an interaction would have an almost identical geometry to the bisphenol bridging effect required for the templated macrocyclisation reactions (see Chapter 2). In the model system it should be possible to detect this interaction via the resulting shielding effect upon the bipyridine protons owing to their proximity to the face of the phenyl ring. This shift could be detected by comparison to a reference complex where the phenyl esters have been mutated to alkyl groups.

## 4.1.3 Synthesis of Simple Model Complexes

The tris-bipyridine complexes of both iron (II) and ruthenium (II) were prepared. The iron (II) complexes were prepared with both perchlorate and chloride counterions to extend the available range of solvents in which the complexes were soluble.

The preparation of the hexa-phenyl ruthenium (II) complex **19** has already been discussed (Chapter 3, page 53). The hexa-*n*-pentyl analogue **69** was prepared in an identical manner but replacing phenol with *n*-pentanol. (Scheme 4.1). Also prepared were the unsymmetrical ruthenium (II) complexes. The diphenyl ruthenium (II) complex **70** was prepared from the diacid **31** (Chapter 3, page 57) via a simple EDC coupling reaction in 75% yield (Scheme 4.2). The reference complex where phenyl is mutated to ethyl is an intermediate in the synthesis of **31** as discussed in Chapter 3.

The precursor for synthesis of the iron (II) complexes was the diphenyl ester **71** which was prepared in 73% yield from diacid **6** via an EDC coupling reaction with phenol. Iron (II) complexes were prepared quantitatively by treatment of **71** with a solution of 0.33 equivalents of the required iron salt ( $\text{Fe}(\text{ClO}_4)_2 \cdot 6\text{H}_2\text{O}$  in 5% methanol /  $\text{CH}_2\text{Cl}_2$  for the perchlorate salt **72**,  $\text{FeCl}_2 \cdot 4\text{H}_2\text{O}$  in methanol for the chloride salt **73**). The hexa-ethyl ester iron (II) reference complexes **74** and **75** were prepared in an identical manner substituting diethyl ester **4** for **71** (Scheme 4.3).

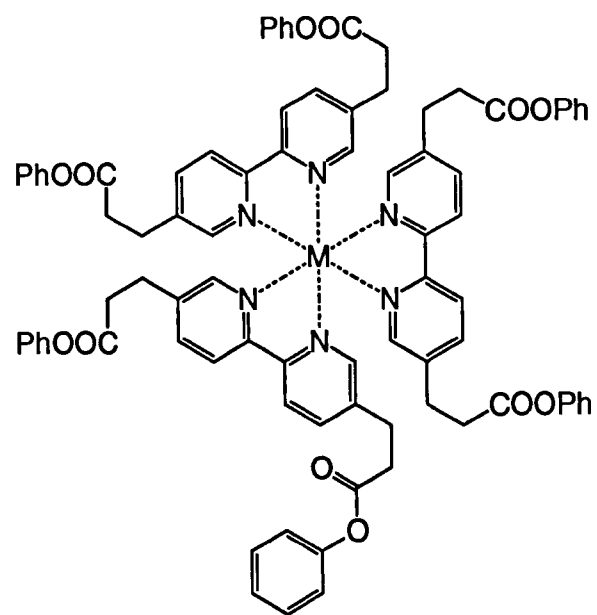
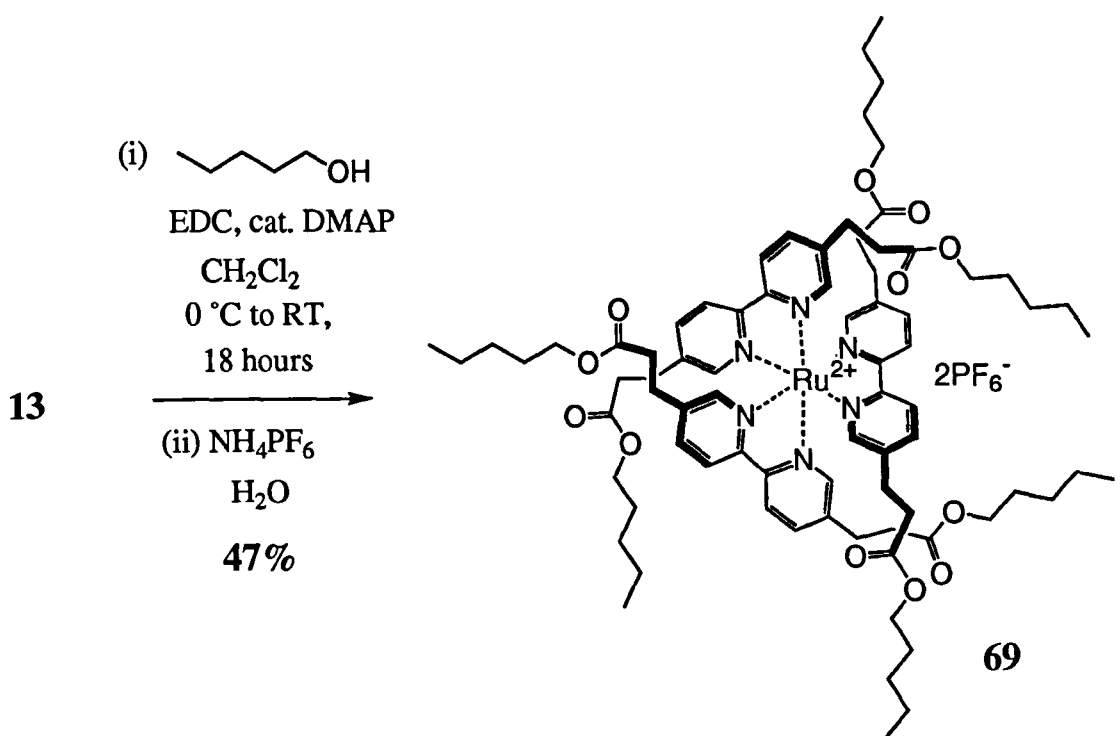
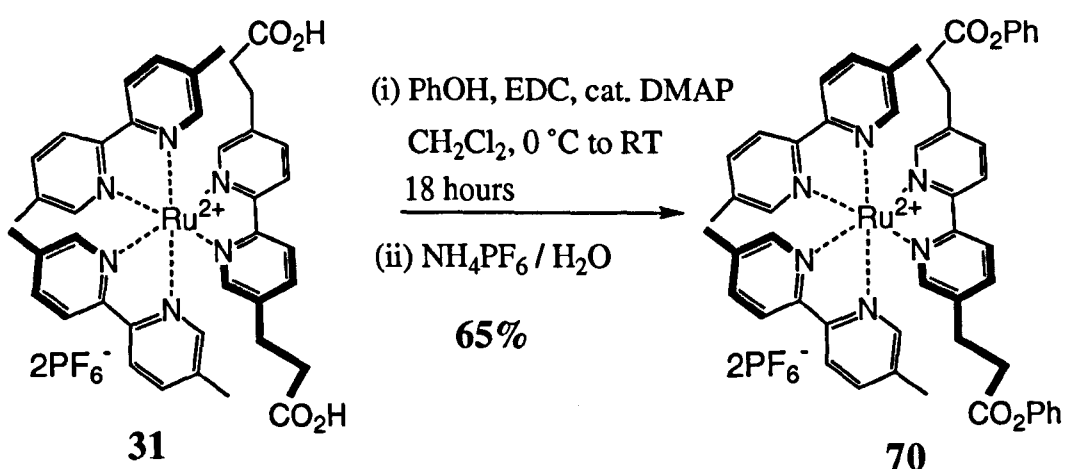


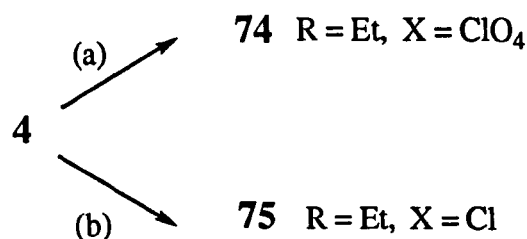
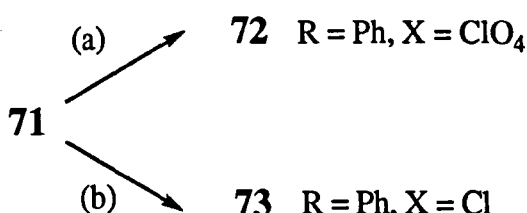
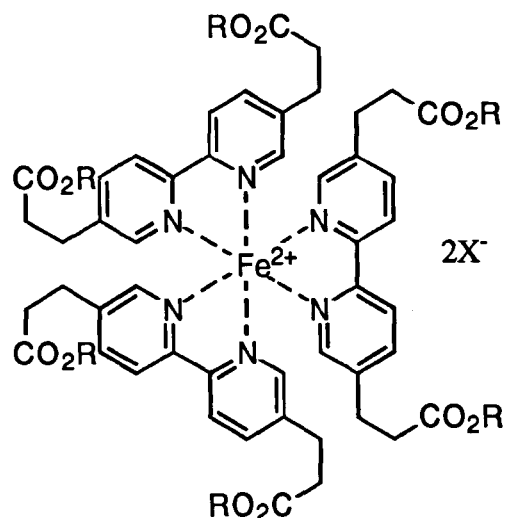
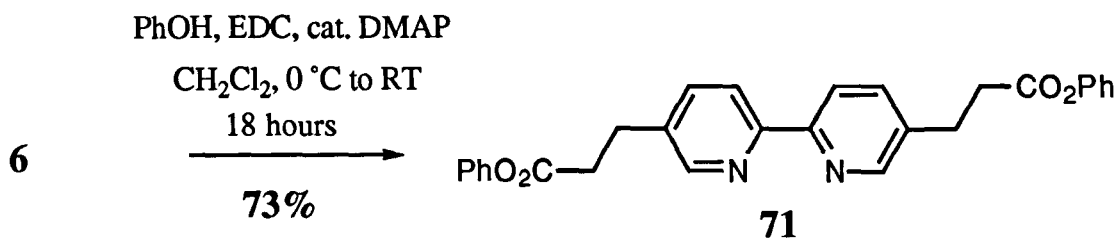
**Figure 4.1.** Model Complexes of the type required for the investigation of  $\pi$ - $\pi$  interactions in the systems of interest.



**Scheme 4.1.** Preparation of ruthenium (II) reference 69. See Chapter 3, page 53 for preparation of the phenyl derivative 19.



**Scheme 4.2.** Preparation of unsymmetrical ruthenium (II) complex 70. Preparation of reference 30 having phenyl mutated to ethyl is discussed in Chapter 3.



*Reagents, conditions and yields:* (a) 0.33 eq. Fe(ClO<sub>4</sub>)<sub>2</sub>.6H<sub>2</sub>O, 5% methanol / CH<sub>2</sub>Cl<sub>2</sub>, 30 minutes (quantitative); (b) 0.33 eq. FeCl<sub>2</sub>.4H<sub>2</sub>O, methanol, 30 minutes (quantitative).

**Scheme 4.3.** Preparation of iron (II) complexes **72-75**.

#### 4.1.4 Conformation-Induced Differences in Chemical Shift

It is indeed the case that large changes in chemical shift are induced in the bipyridine units of the tris-bipyridine complexes containing pendant phenyl esters. Figure 4.2 illustrates the changes for the hexa-phenyl iron (II) complex **72** in chloroform as well as the equivalent changes in the uncoordinated phenyl diester **71**. The signal due to H<sub>3</sub> is shifted 0.54 ppm upfield in **72** relative to the signal due to the same proton in reference **74**. In contrast, comparing the <sup>1</sup>H NMR spectra of the uncomplexed free ligands **71** and **4**, there is a 0.09 ppm downfield shift of H<sub>3</sub>, so the very large difference observed in the metal complexes is clearly not due to through bond effects.

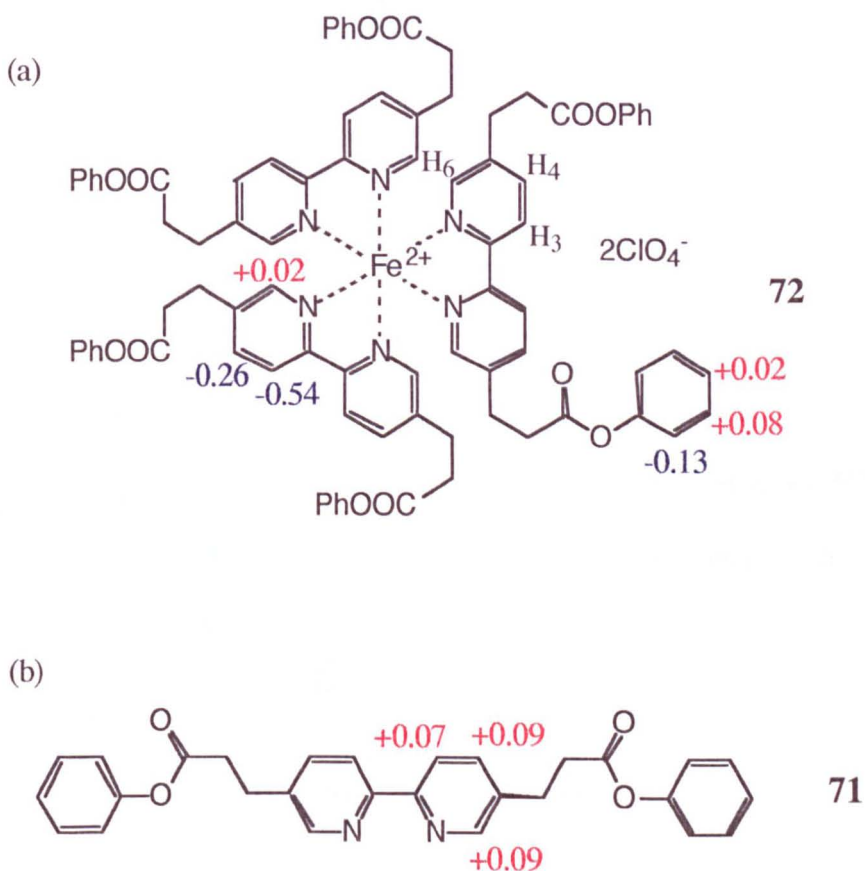
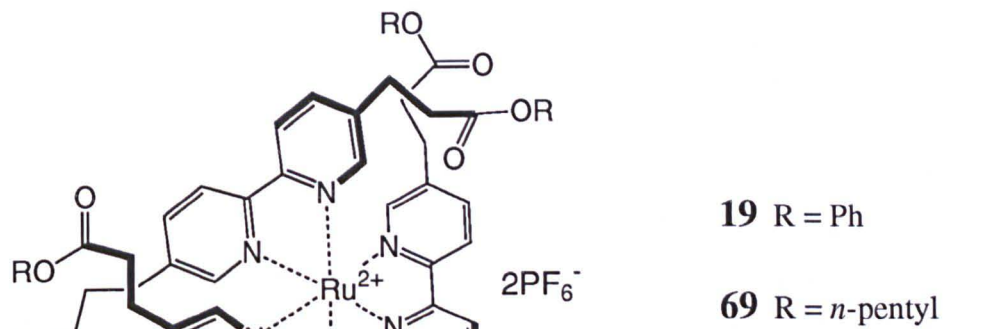


**Figure 4.2.(a)** Changes in chemical shift in complex **72** (bipyridine protons are relative to alkyl reference **74** and phenyl ester protons are relative to uncomplexed **71**).

**(b)** Changes in chemical shift in **71** relative to alkyl ester **4**.



**69** R = *n*-pentyl

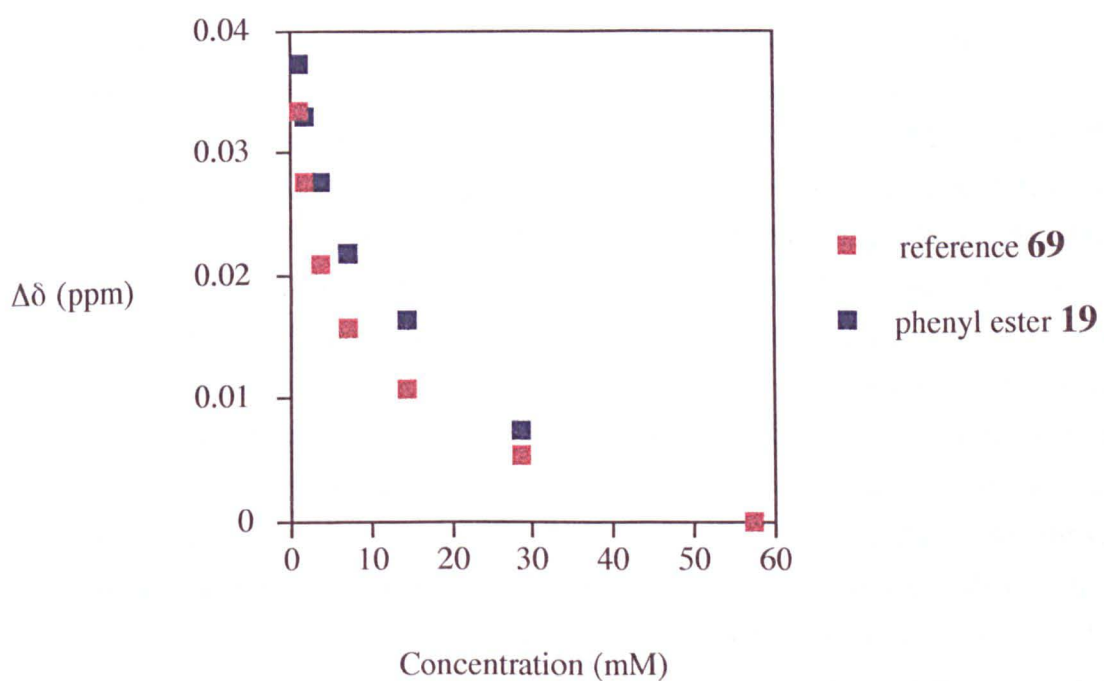


**Figure 4.3.** Concentration dependent changes in chemical shift for H<sub>3</sub> of hexa-phenyl ruthenium (II) complex **19** and reference **69**. Values shown indicate change relative to the value recorded at the highest concentration (57.2 mM).

One possibility is that the large shifts are caused by ion-pairing interactions with the counterions. However,  $^1\text{H}$  NMR dilution studies revealed very small concentration dependent changes in the  $^1\text{H}$  NMR chemical shift. Typical results are shown for the signal due to proton  $\text{H}_3$  in hexa-phenyl ruthenium (II) complex **19** and hexa-*n*-pentyl ruthenium (II) complex **69** in  $d_6$ -acetone (Figure 4.3). For this system, the difference between chemical shift of the signal due to  $\text{H}_3$  in **19** and the corresponding proton in the alkyl ester reference compound **69** is -0.37 ppm, but dilution of the complexes results in changes in chemical shift of less than 0.05 ppm for both complexes. In addition, both complexes exhibit an almost identical change in the chemical shift of the signal due to  $\text{H}_3$  over the same concentration range. Thus the small concentration dependent changes in chemical shift which are observed are not related to the large difference observed between the aromatic and alkyl esters. This indicates that even if ion pairing does take place to a significant extent in this system, it has a negligible effect on the observed differences in  $^1\text{H}$  NMR chemical shift in which we are interested.

A more likely interpretation of these observations is that the large shifts observed for the aromatic esters are caused by intramolecular aromatic interactions in the complex. These interactions lead to close proximity of the phenyl esters and the bipyridine groups in the metal complex which in turn causes ring current induced changes in chemical shift. The bipyridine protons  $\text{H}_3$  and  $\text{H}_4$  experience large upfield shifts in **72** relative to **73** whereas the phenol protons are not significantly shifted relative to free ligand **71**, which implies that the bipyridine protons lie over the face of the phenol rings. Figure 4.4 illustrates the conformational equilibria which are consistent with the NMR data. In conformation A, the ester group is directed away from the complex and there are no aromatic interactions. Conformations B and C show two different types of geometry in which there is an interaction between the bipyridine protons and the face of a phenol ring. Large differences in chemical shift are not observed between the uncomplexed free ligands **4** and **71** which implies that bending back of the phenyl ester onto its own bipyridine unit as in conformation C is not very probable. However, it is possible that complexation of the bipyridine by the metal cation significantly polarises protons  $\text{H}_3$  and  $\text{H}_4$  which increases the electrostatic interaction of these protons with the  $\pi$ -electrons on the face of the phenol ring. Therefore in order to distinguish conformations B and C, the unsymmetrical complex **70** was used.

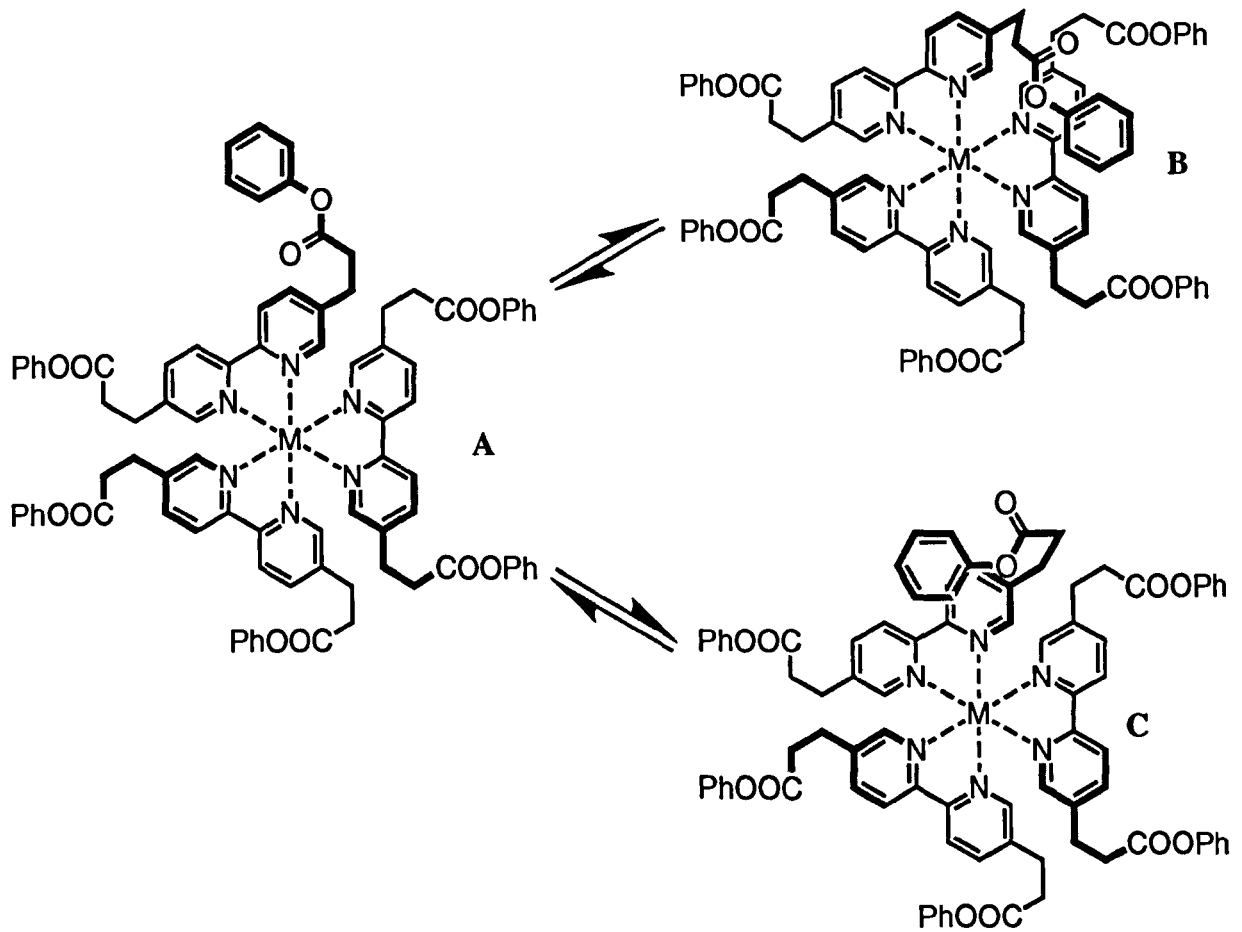


**Figure 4.4.** Possible conformational equilibria for hexa-phenyl ester tris-bipyridine metal complexes.

The differences in  $^1\text{H}$  NMR chemical shift between the bipyridine protons of **70** and the corresponding alkyl ester reference compound **30** in  $d_6$ -acetone are shown in Figure 4.5.  $\text{H}_3$  and  $\text{H}_4$  of the bipyridine unit containing the pendant phenyl esters are shifted slightly downfield: the shifts are in fact very similar to those observed for the uncomplexed free ligands **71** and **4**. The analogous  $\text{H}_3$  and  $\text{H}_4$  protons on the dimethylbipyridine units however show significant upfield shifts. The values in Figure 4.5 are averaged, since the two protons on opposite sides of each bipyridine unit are non-equivalent and their absolute assignment is not possible with certainty. The upfield shifts on one type of bipyridine unit and absence of shifts on the other prove that the aromatic interaction in the hexa-phenyl ester system is due to type B conformations rather than type C conformations (Figure 4.4). The magnitudes of the shifts observed in **70** (-0.15 and -0.09 ppm) are approximately half those observed in **19** (-0.37 and -0.12 ppm), because only one phenol group can interact with each set of dimethylbipyridine protons whereas in complex **19** in conformation B, two phenol groups interact with each set of bipyridine protons.

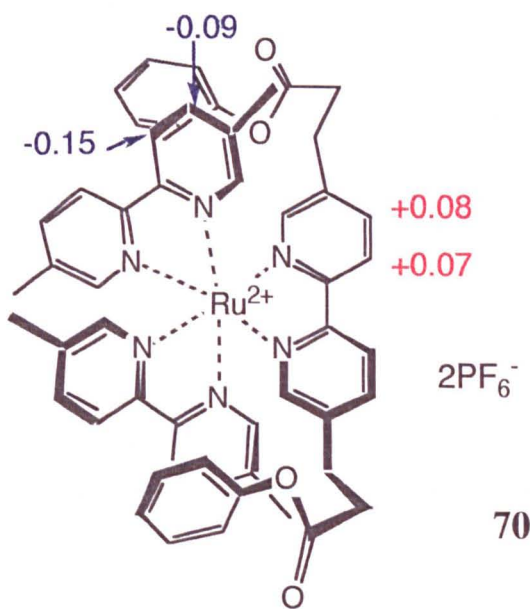


**Figure 4.5.** Changes in chemical shift for diphenyl ester **70** relative to the reference complex **30** where phenyl is mutated to ethyl.

#### 4.1.5 2D NMR Studies

Further evidence for the folded conformation of the aromatic esters was obtained from two-dimensional ROESY experiments. NOEs observed in a 400 MHz ROESY spectrum of **72** in  $CDCl_3$  are illustrated in Figure 4.6. Cross-peaks connecting the signals due to the bipyridine protons  $H_3$  and  $H_4$  and the signal due to the *ortho*-phenol protons indicate that these two parts of the molecule are close in space. These observations are clearly consistent with the folded conformation B shown in Figure 4.4.

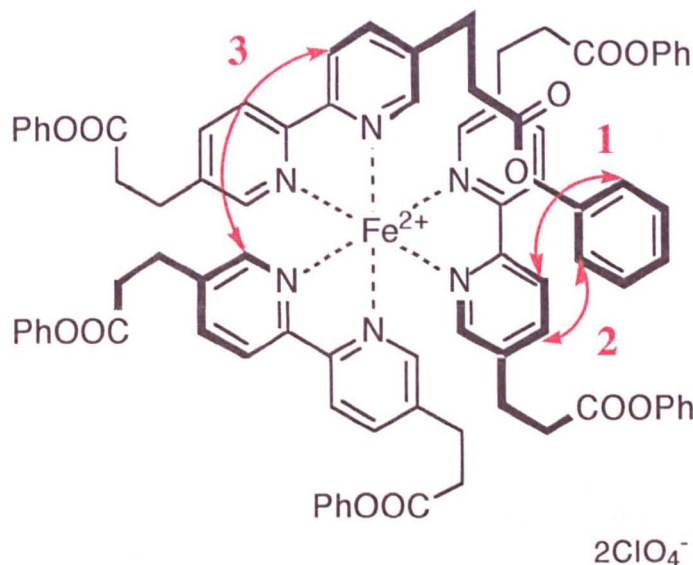


**Figure 4.6.** NOEs observed in a 400 MHz ROESY spectrum of **72** in  $CDCl_3$ . Numbered NOEs refer to those discussed on page 79.

#### 4.1.6 Molecular Modelling

The conformational properties of this system have also been investigated using molecular mechanics calculations. The X-ray crystal structure of ruthenium(II) tris-bipyridine was retrieved from the Cambridge Crystallographic Database and used as a starting point for molecular modelling studies. One phenyl ester side-chain was built onto this, and a Monte Carlo conformational search was carried out using the MacroModel implementation of the MM2 force-field with chloroform solvation and constraining the ruthenium(II) tris-bipyridine core to the X-ray structure geometry. In other words, the conformational properties of the flexible side-chain only were investigated. Not surprisingly, a large number of different low energy conformations were obtained. However, a number of these structures corresponded to conformation B, and none of the low energy structures were in conformation C, which is consistent with the experimental observations. A representative type B conformation is shown in Figure 4.7. It is not suggested that this is the optimal or most populated conformation, it simply illustrates one of the conformations which is populated to a significant extent and which is responsible for the large ring current shifts observed in this system.

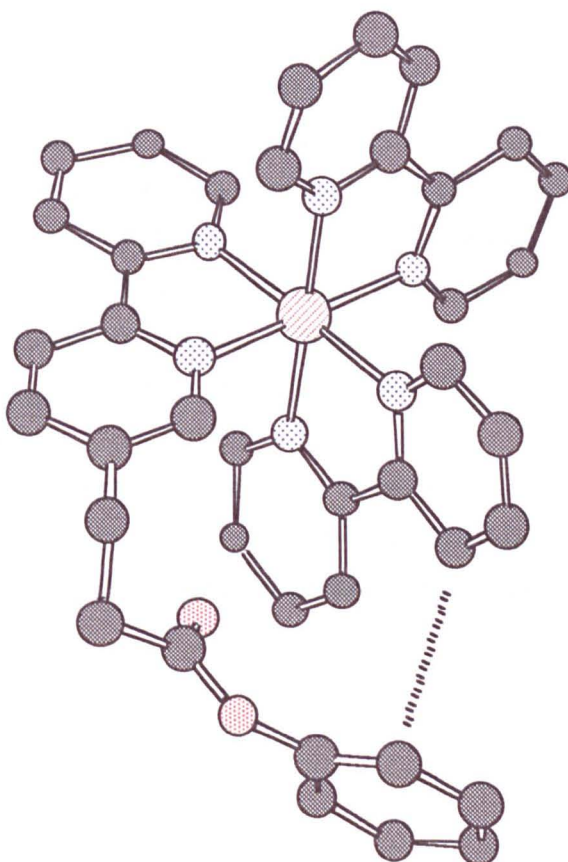


**Figure 4.7.** A typical low energy conformation of a simple model complex. The edge-face  $\pi$ - $\pi$  interaction (               ) can be clearly seen.

#### 4.1.7 Prediction of Chemical Shifts

Using the program SHIFTY<sup>‡</sup> it was possible to take the energy minimised structure illustrated in Figure 4.7 and calculate the expected ring current induced chemical shifts from the close proximity of the aromatic systems. These predicted shifts are illustrated in Figure 4.8.

The predictions are qualitatively in good agreement with experimental results. As expected, the predicted values are significantly larger than those observed experimentally because the "folded" conformation of Figure 4.7 represents an extreme situation in a series of conformational equilibria such as those illustrated in Figure 4.4. It should also be noted that one would expect the shifts observed in the actual complex to be twice as large because there are two phenyl rings interacting with each bipyridine unit whereas in the calculation there is only one ring inducing the shifts.

One significant failure in the predicted values is the H<sub>3</sub> / H<sub>4</sub> ratio. The predicted shift for H<sub>4</sub> (-0.20 ppm) is rather less than one fifth of the value for H<sub>3</sub> whereas experimentally the value is almost half that for H<sub>3</sub>. This suggests that in reality the phenyl ester ring is much more mobile in proximity of H<sub>3</sub> and H<sub>4</sub> than the MM2 forcefield predicts. Again this is not unreasonable in view of the large number of low energy conformations in such a system.

If we take the *average* observed shift for H<sub>3</sub> and H<sub>4</sub> (-0.40 ppm) and compare this with the *average* predicted shift of -1.32 ppm (the average value -0.66 ppm is doubled to estimate the effect of having two such rings on opposite sides of the bipyridine unit both inducing the same change in chemical shift), we estimate that each phenyl ester of complex 72 spends approximately one third of its time in a position where it is participating in an edge-face interaction with the bipyridine ring. Thus in complex 72, at any one time, on average two phenyl esters adopt the folded-type conformation while the other four groups do not.

These predictions must of course be regarded as approximations due to the flexibility of the system but it does suggest that edge-face interactions have a very significant effect on the conformational properties of the system.

---

<sup>‡</sup> C.A. Hunter, unpublished results. SHIFTY allows the prediction of ring current induced chemical shifts owing to the close proximity of an aromatic system to a particular proton.

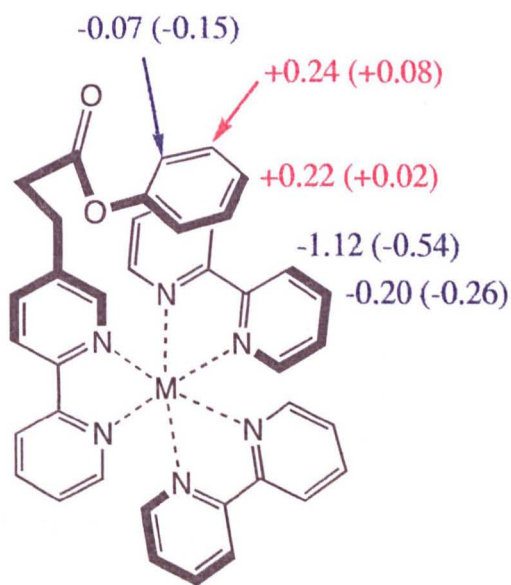


**Figure 4.8.** Shifts (in ppm) predicted by the SHIFTY program for the energy minimised structure in Figure 4.7. Values in parentheses are those observed experimentally in iron (II) complex **72** in  $\text{CDCl}_3$ .

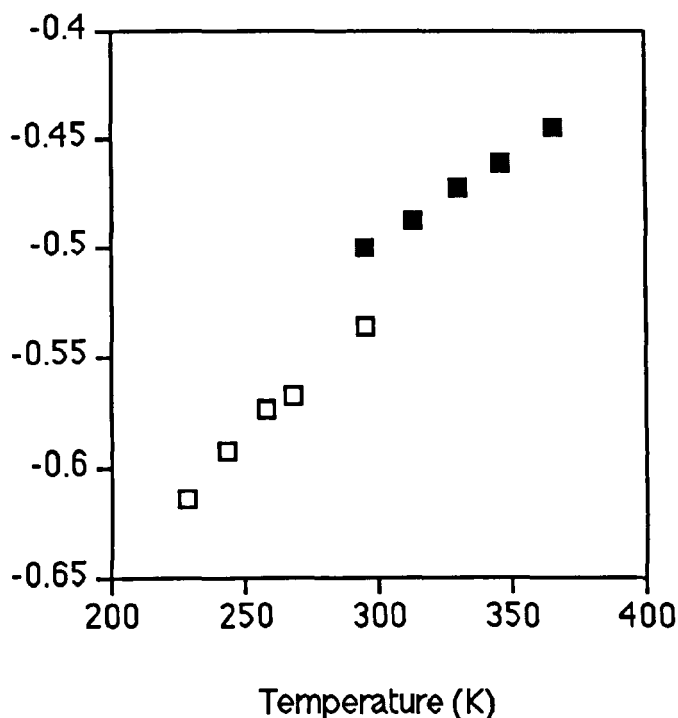


**Figure 4.9.** Changes in chemical shift difference with temperature for bipyridine  $H_3$  of iron (II) complex **72** relative to **74** in  $\text{Cl}_2\text{DCCDCl}_2$  ( ■ ) and  $\text{CDCl}_3$  ( □ ). The discontinuity at 295K is due to the change of solvent.

### 4.1.8 Temperature Dependent Effects

The temperature dependence of this effect was also investigated for hexa-phenyl iron (II) complex **72** and reference **74** in d<sub>2</sub>-1,1,2,2-tetrachloroethane (for high temperatures) and CDCl<sub>3</sub> (for low temperatures). The results are shown in Table 4.1 and Figure 4.9. At higher temperatures, the differences in chemical shift between the aromatic and alkyl esters are significantly reduced, while at low temperatures the differences increase. This is consistent with the model in Figure 4.4 where there is an equilibrium between a folded conformation (B) stabilised by attractive aromatic interactions and an unfolded disordered conformation (A). High temperatures shift the equilibrium towards the disordered conformation (A) and low temperature favour the more ordered state (conformation B). It seems that the two extreme conformations illustrated in Figure 4.4 are never fully populated within the temperature range studied.

**Table 4.1. Temperature dependent changes in chemical shift<sup>a</sup> of **72** relative to **74**.**

High Temperature (Cl <sub>2</sub> DCCDCl <sub>2</sub> )		Low Temperature (CDCl <sub>3</sub> )	
Temperature (K)	$\Delta\delta$ (H <sub>3</sub> ) (ppm)	Temperature (K)	$\Delta\delta$ (H <sub>3</sub> ) (ppm)
295	-0.500	295	-0.537
313	-0.488	268	-0.568
330	-0.473	258	-0.574
346	-0.462	243	-0.593
366	-0.445	228	-0.614

<sup>a</sup> All spectra were recorded at a concentration of 8.2 mM.

### 4.1.9 Summary

These experiments demonstrate that there is a strong intramolecular aromatic interaction in this system. The differences between the chemical shifts of the <sup>1</sup>H NMR signals due to the bipyridine protons H<sub>3</sub> and H<sub>4</sub> in the aromatic esters and the corresponding alkyl ester control compounds provide a simple measure of the position of the equilibrium between conformation A and conformation B (Figure 4.4) and hence a direct measure of the strength of the intramolecular aromatic interaction. The solubility of metal complexes of this type can easily be controlled by choice of counterions, so this represents an ideal system for investigating the influence of solvent on the magnitude of aromatic interactions.

## 4.2 Solvent Dependence of $\pi$ - $\pi$ Interactions

### 4.2.0 Changes in Chemical Shift

Perchlorate and chloride salts of the iron(II) complexes and the hexafluorophosphate salt of the ruthenium (II) complexes allowed us to record  $^1\text{H}$  NMR spectra in a wide range of solvents. The results are summarised in Table 4.2 and Figure 4.10.

**Table 4.2a.** Changes in chemical shift of complexes 72 and 73 relative to 74 and 75.<sup>a</sup>

Solvent	Z kcal mol <sup>-1</sup>	$\Delta\delta$ H <sub>3</sub> (ppm)	$\Delta\delta$ H <sub>4</sub> (ppm)	$\Delta\delta$ H <sub>6</sub> (ppm)	Counterion
CDCl <sub>3</sub>	63.2	-0.54	-0.26	+0.02 <sup>c</sup>	ClO <sub>4</sub> <sup>-</sup>
CD <sub>2</sub> Cl <sub>2</sub>	64.2	-0.48	-0.20	<sup>b</sup>	ClO <sub>4</sub> <sup>-</sup>
d <sub>6</sub> -acetone	65.7	-0.34	-0.15	<sup>b</sup>	ClO <sub>4</sub> <sup>-</sup>
d <sub>7</sub> -DMF	68.5	-0.25	-0.07	<sup>b</sup>	ClO <sub>4</sub> <sup>-</sup>
d <sub>6</sub> -DMSO	71.1	-0.12	-0.08	+0.03	ClO <sub>4</sub> <sup>-</sup>
CD <sub>3</sub> CN	71.3	-0.32	-0.12	+0.01	ClO <sub>4</sub> <sup>-</sup>
d <sub>7</sub> -iPrOD	76.3	-0.51	-0.18	<sup>b</sup>	Cl <sup>-</sup>
CD <sub>3</sub> OD	83.6	-0.56	-0.23	-0.06	Cl <sup>-</sup>
D <sub>2</sub> O	94.6	-0.81	-0.31	-0.09	Cl <sup>-</sup>

**Table 4.2b.** Changes in chemical shift of ruthenium (II) complex 19 relative to 69.<sup>a</sup>

Solvent	Z (kcal mol <sup>-1</sup> )	$\Delta\delta$ H <sub>3</sub> (ppm)	$\Delta\delta$ H <sub>4</sub> (ppm)	$\Delta\delta$ H <sub>6</sub> (ppm)
CDCl <sub>3</sub>	63.2	-0.61	-0.23	-0.01
CD <sub>2</sub> Cl <sub>2</sub>	64.2	-0.45	-0.21	-0.02
d <sub>6</sub> -acetone	65.7	-0.37	-0.12	-0.02
d <sub>7</sub> -DMF	68.5	-0.21	-0.05	+0.06
d <sub>6</sub> -DMSO	71.1	-0.20	-0.04	-0.06
CD <sub>3</sub> CN	71.3	-0.30	-0.11	+0.02

<sup>a</sup> All spectra were recorded at a concentration of 8.2 mM with the sole exception of D<sub>2</sub>O where a slightly lower concentration was necessitated for reasons of solubility.

<sup>b</sup> Values could not be obtained due to overlapping signals in 72 or 73.

<sup>c</sup> Signal obscured by overlapping signals. Value was obtained from the position of an NOE cross-peak in a 2D ROESY experiment.

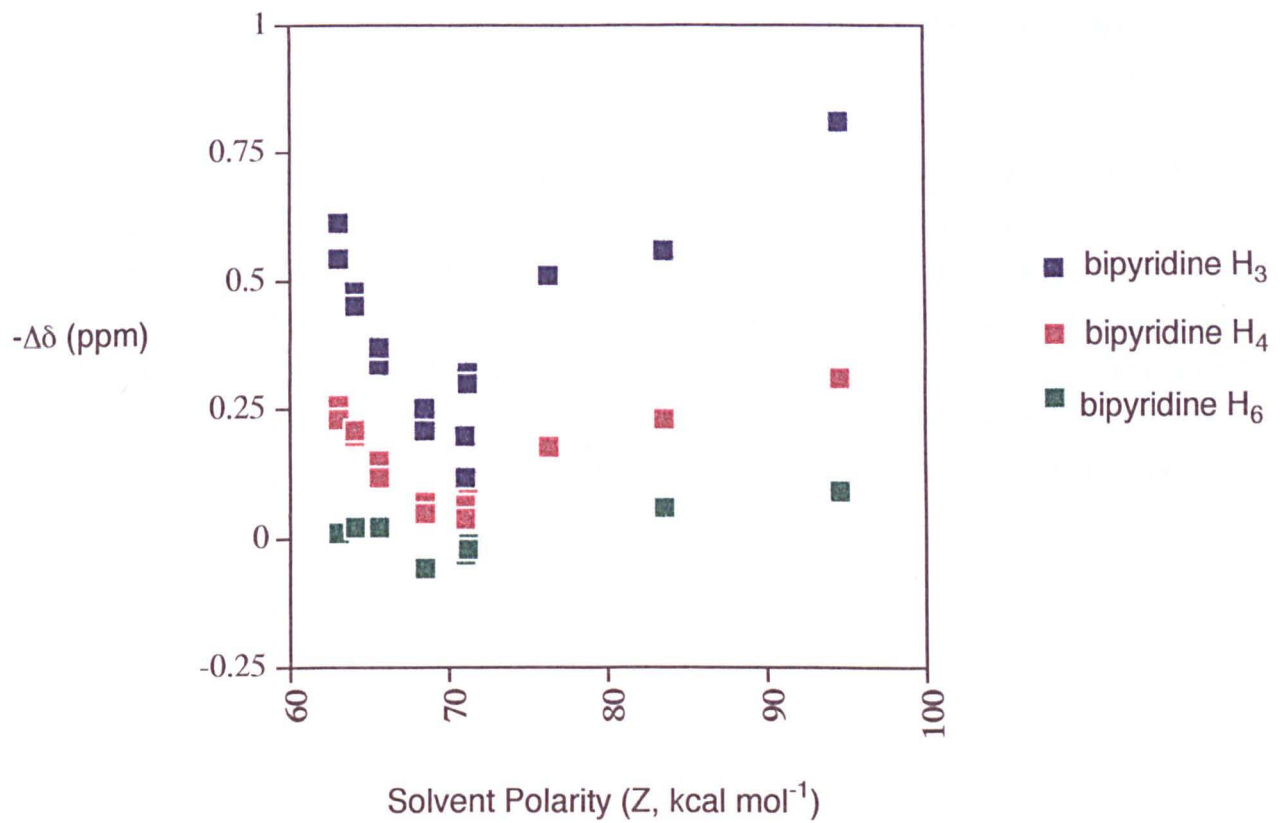


**Figure 4.10.** Solvent dependent changes in chemical shift for hexa-phenyl iron (II) complexes **72** and **73** and ruthenium (II) complex **19** relative to their respective references **74**, **75** and **69**.

The shifts observed in H<sub>3</sub> and H<sub>4</sub> of **72** and **73** relative to **74** and **75** show an interesting variation with solvent polarity as quantified by the parameter Z.<sup>124</sup> Since such aromatic interactions are generally considered to be solvophobic in nature, it was expected that a strong interaction (and hence a large upfield shift) would be observed in polar solvents such as water. It was also expected that this effect would reduce with decreasing polarity of the solvent which is indeed observed at first. However, after a certain point, the effect reverses and again we see an increase in the extent of shielding (and hence infer an increase in interaction strength). We believe that this represents a changeover from a solvophobic dominated interaction to one where electrostatic factors play a more important role so that as we decrease solvent polarity still further, the strength of interaction increases.

Experiments have also been carried out with the analogous ruthenium (II) complexes **19** and **69** where an almost identical effect was observed for those solvents that were available (chloride salts giving alcohol and water solubility were not prepared for the ruthenium (II) complexes). The points are almost superimposable and are all represented on the single graph in Figure 4.10. For both iron (II) and ruthenium (II) complexes, changes in chemical shift for H<sub>6</sub> were very small, indicative of its location in the interior of the molecule far away from possible interactions with the phenyl esters.

#### 4.2.1 2D NMR Studies

Further attempts to investigate the relative strengths of interactions were made using 2D ROESY NMR experiments which were carried out on **72** in  $\text{CDCl}_3$  and  $d_6$ -DMSO and **73** in  $\text{CD}_3\text{OD}$ . The NOEs discussed previously (Figure 4.6, page 73) were observed in all three solvents. The crosspeaks between the bipyridine  $\text{H}_3$  and  $\text{H}_4$  protons and the *ortho*-phenolic protons are strong in  $\text{CD}_3\text{OD}$  and  $\text{CDCl}_3$  but somewhat weaker in  $d_6$ -DMSO. This is consistent with the strong interaction proposed in the former solvents and the rather weaker interaction in the latter.

This effect was quantified by integration of the NOE crosspeaks to give a qualitative measure of the average relative distance between the two interacting units. The integrals for the crosspeaks between the bipyridine  $\text{H}_3$  and  $\text{H}_4$  signals and the *ortho*-phenolic signal (NOEs 1 and 2 respectively) were compared to that between  $\text{H}_6$  and  $\text{H}_3$  of an adjacent bipyridine unit (NOE 3) (Table 4.4). Since the latter interatomic distance is constrained by the coordination bonds and may be considered to remain constant in all solvents, the ratio of the two values provides a good qualitative indication of the average relative separation of the bipyridine and phenyl ester units.

**Table 4.4. Relative NOE Intensities.**

Solvent	ratio NOE 1 / NOE 3	ratio NOE 2 / NOE 3
$\text{CDCl}_3$	1.46	1.24
$\text{CD}_3\text{OD}$	0.95	0.78
$d_6$ -DMSO	0.54	0.66

In both  $\text{CDCl}_3$  and  $\text{CD}_3\text{OD}$ , this ratio was significantly larger than in  $d_6$ -DMSO indicating that in  $d_6$ -DMSO the average distance between the phenyl ring and bipyridine unit is larger than in  $\text{CDCl}_3$  or  $\text{CD}_3\text{OD}$  and we can assume that the interaction between the two is rather weaker.

## 4.3 A Model System Incorporating Bisphenol Units

### 4.3.0 Conformation-Induced Chemical Shifts

The model complex **77** was also prepared (Scheme 4.4). Based upon the interactions observed in the simpler complexes, it was hoped that this more realistic model of the knot-forming macrocyclisations would exhibit similar effects. The conformation-induced differences in chemical shift compared to the diethyl reference **30** are shown in Figure 4.11.

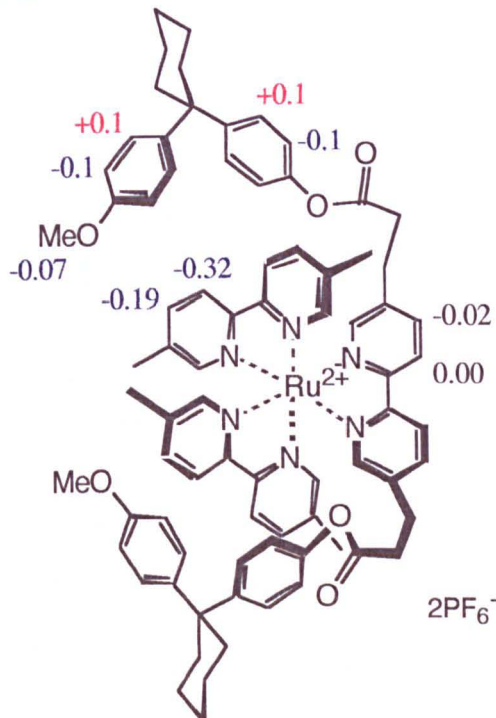
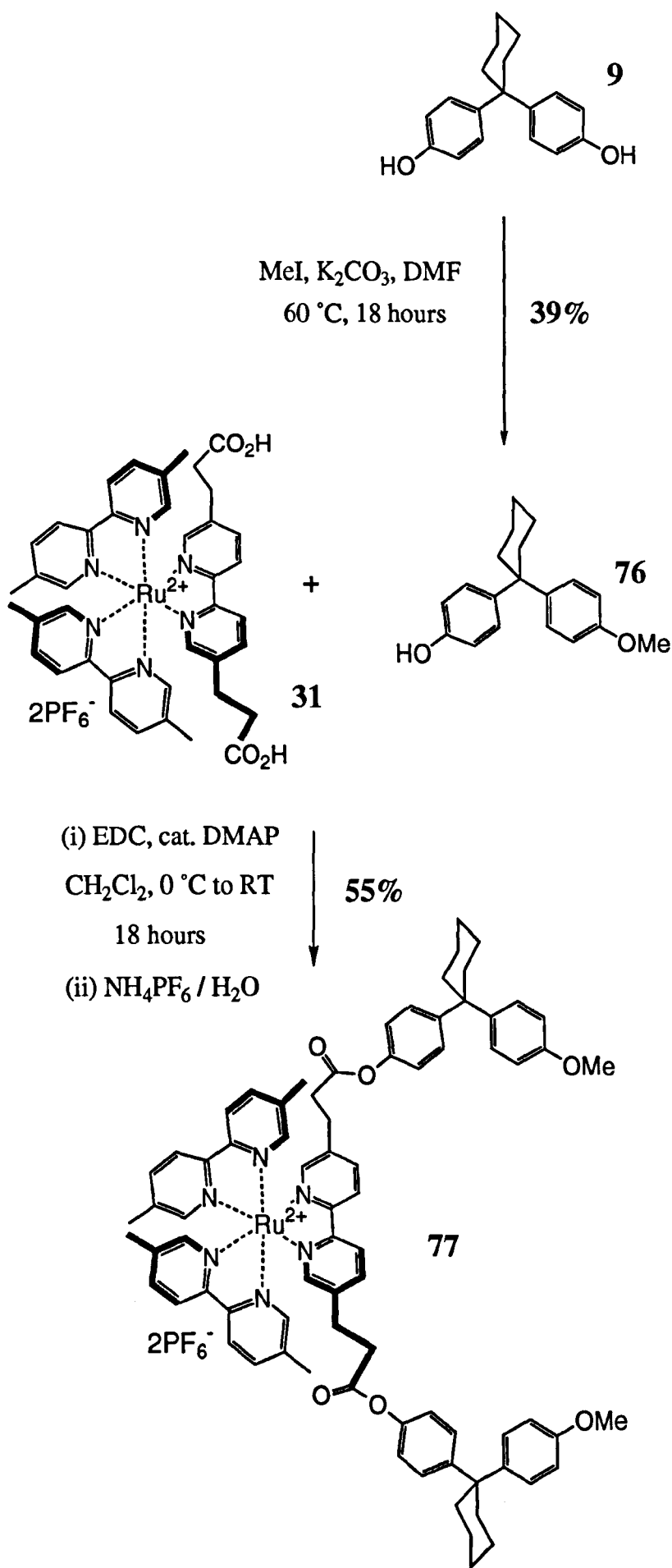


**Figure 4.11.** Conformation-induced changes in chemical shift (in ppm) for model complex **77** in  $CDCl_3$  relative to reference **30**.

As before, the upfield shifts of the dimethylbipyridine units are indicative of a significant time spent in a conformation where they are adjacent to the face of the neighbouring diarylmethane unit. It is interesting to note that although the shifts are larger than those observed in the diphenyl ester **70** (Figure 4.5) as would be expected from the fact that two phenyl groups rather than one are interacting with each dimethylbipyridine unit, the shifts are not as large as in hexa-phenyl complex **19**. At first sight, we might expect the shifts to be larger in **77** than in **19**. In both complexes, there are two aromatic rings interacting with the edge of the bipyridine unit. In **77**, because the two rings are joined via an  $sp^3$  carbon linker, this should result in a cooperative effect owing to smaller entropy loss on forming the conformation where both interactions occur. Clearly this is not observed.



**Scheme 4.4.** Preparation of ruthenium (II) model complex 77.

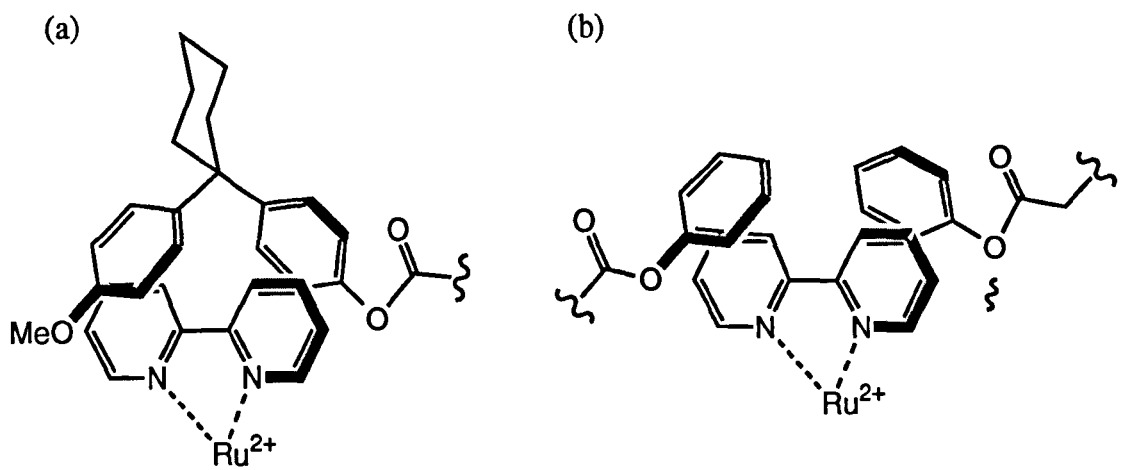


**Figure 4.12.** Interactions between the face of phenyl rings and the edge of a coordinated bipyridine unit. (a) Orientation of two phenyl rings with respect to each other is rigidly defined by the  $sp^3$  linker. (b) Unlinked phenyl rings are both free to adopt the optimum position to maximise interactions.

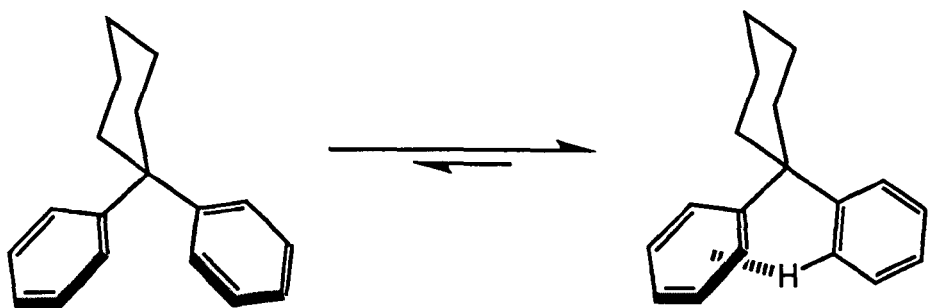


**Figure 4.13.** Possible intramolecular interaction in diarylmethane systems.

One possible explanation is that the  $sp^3$  tetrahedral carbon does not provide the optimum geometry for both phenyl rings to interact simultaneously with the edge of the bipyridine unit. In complex **19** where there is no link between the phenyl esters, the aromatic rings are both free to adopt the optimum position to interact with the edge of the bipyridine ligand (Figure 4.12). Another factor likely to contribute to a reduced interaction is the fact that diarylmethane type structures may adopt a conformation where they contain an intramolecular interaction which must be lost before interactions of the type in which we are interested can occur (Figure 4.13).

### 4.3.1 2D NMR Studies

The existence of folded conformations in this system is confirmed by 2D NMR experiments. Some NOEs observed in a 2D ROESY experiment in  $CDCl_3$  are illustrated in Figure 4.14. NOEs which give conformational information are shown in red and other NOEs are shown in blue. In general, the red NOEs are rather weak as would be expected for a complex in conformational equilibrium.

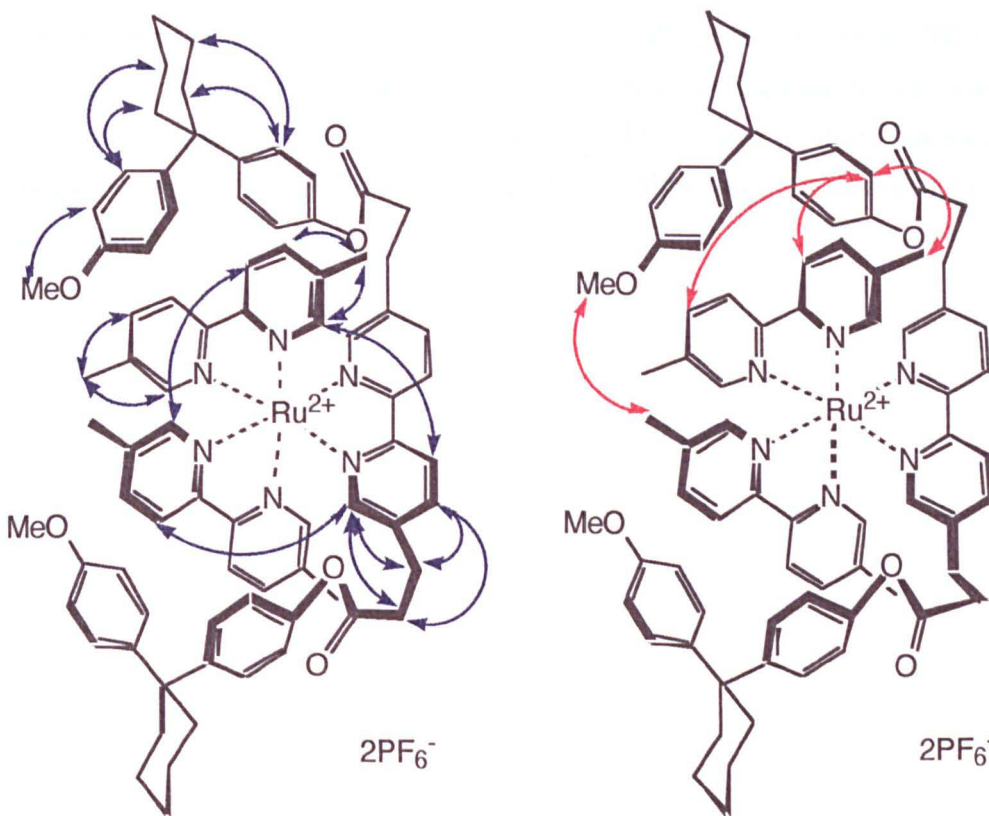


**Figure 4.14.** NOEs observed for complex 77.

## 4.4 Conclusions

A simple model system has been prepared based upon tris-bipyridine metal complexes where the faces of pendant phenyl ester groups exhibit aromatic interactions with the edge of the coordinated bipyridine unit. We have illustrated qualitatively how the strength of these interactions vary with solvent and hence have shown that such interactions possess electrostatic as well as the more usually considered solvophobic components, with the dominant effect depending upon the polarity of the solvent. The expected temperature dependence has also been illustrated.

Many lessons from these experiments can be applied to future attempts at the knot syntheses. In particular, the effect of solvent is extremely important. Traditional thinking on such "solvophobic" interactions would suggest that a highly polar solvent such as water would be required to optimise interaction strengths and this would have its associated problems of using large organic molecules in such a solvent. However, these results suggest that the use of solvents like chloroform may lead to interactions almost as strong. Equally important are those solvents of intermediate polarity that should be avoided. In particular DMSO and to a lesser extent DMF or acetonitrile are likely to lead to extremely weak templating interactions. As expected, the interactions are enhanced at low temperature and reduced at high temperature. However, it seems that temperature effects are much less important than solvent effects where the biggest change in relative interaction strength is observed.

---

*Chapter 5*

---

## **The Linear Oligomer Strategy**

## 5.1 Introduction

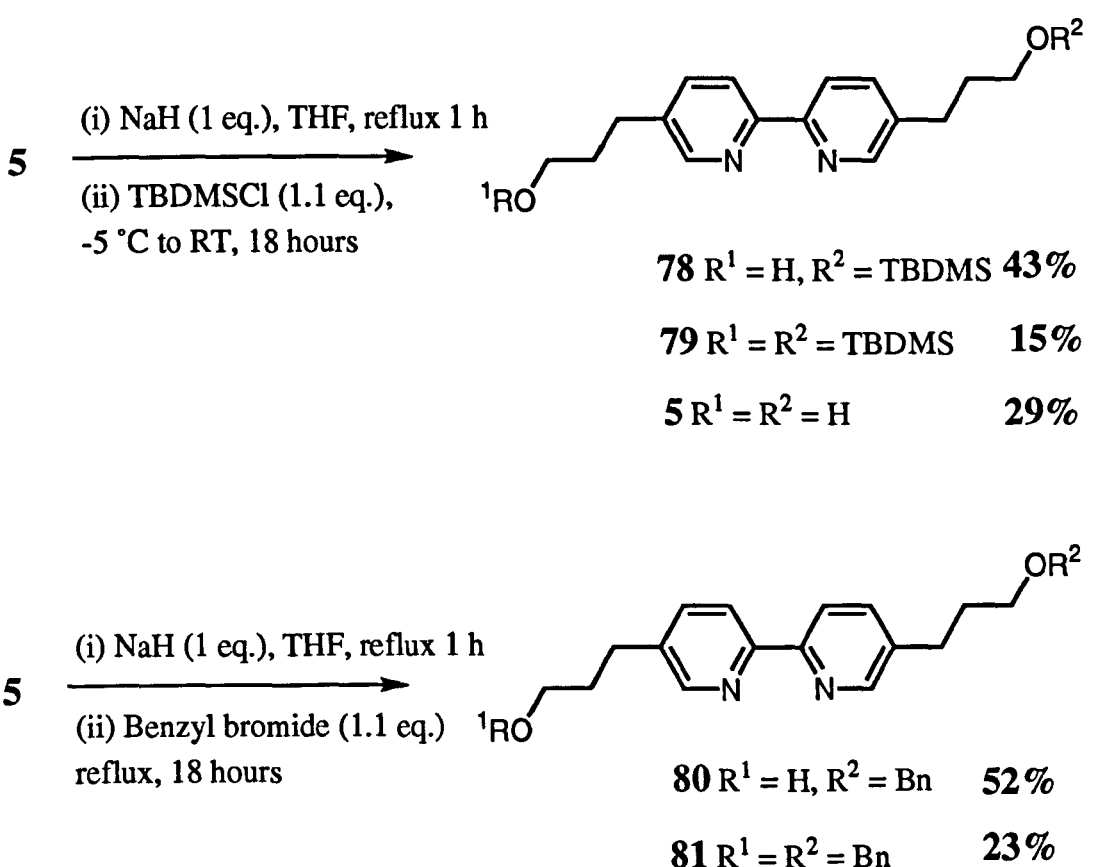
As discussed in Chapter 2, the second strategy proposed for the synthesis of knotted molecules was the preparation of a linear molecule containing all the required recognition components and attempting to induce a "folding" process in the presence of a suitable metal ion. Having already shown in Chapter 4 that the required templating aromatic interactions do exist in this system, this strategy would hopefully overcome the main problems found in the direct macrocyclisations discussed in Chapter 3, namely the requirement to form six new bonds in one reaction with the inevitable low yields and by-product formation.

This chapter describes the synthesis of a linear oligomer in which the components are joined by ether or ester links. The interactions of the molecules with several different metal ions and subsequent preparation of a pseudo-overhand knot are discussed.

## 5.2 Synthesis of an Ether-linked Oligomer

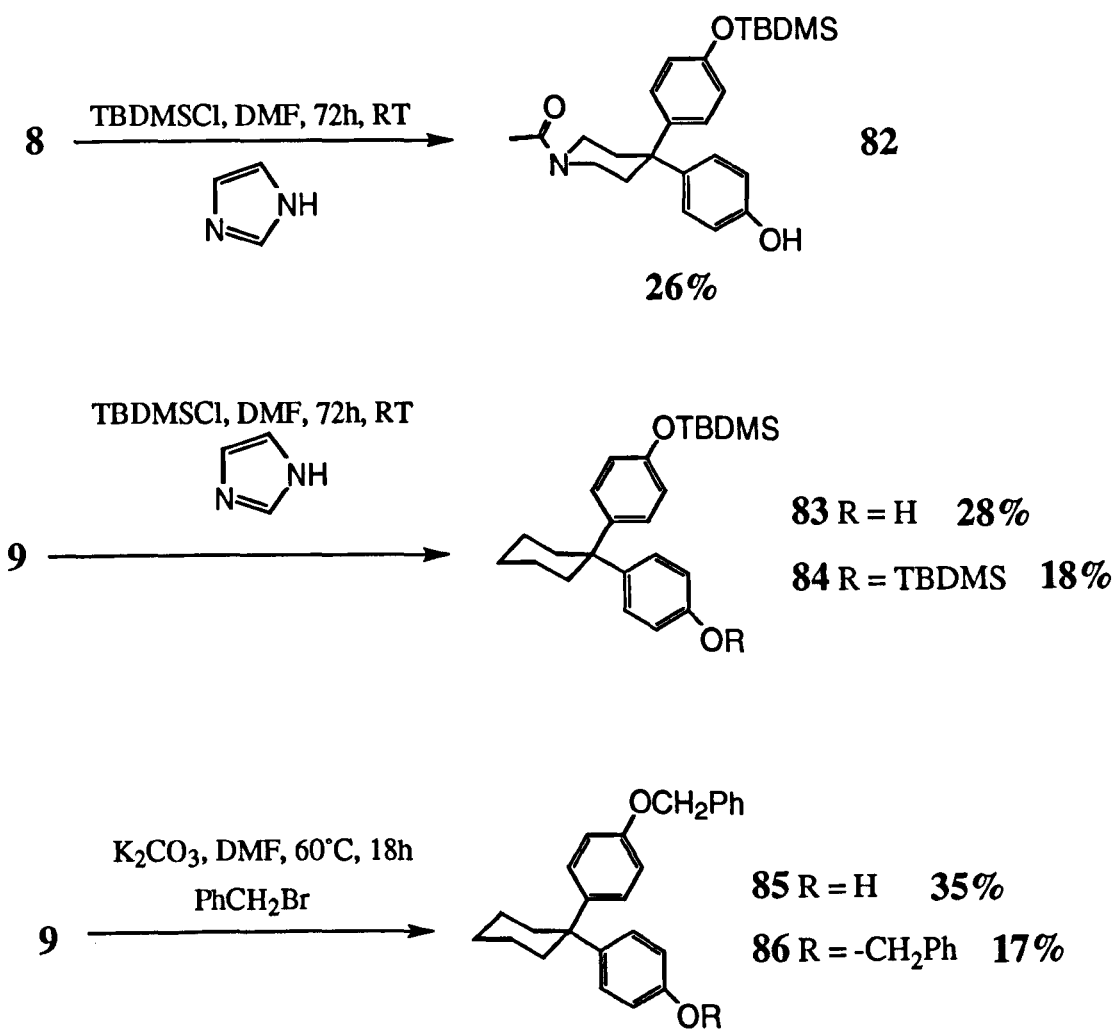
### 5.2.0 Synthesis of Mono-protected Building Blocks

Components required for preparation of the molecular strands are mono-protected derivatives of both the bipyridine diol **5** and bisphenols **8** and **9**. TBDMS and benzyl derivatives of **5** were prepared as outlined in Scheme 5.1. Alcohol **5** was deprotonated by refluxing for 1 hour with 1 equivalent of sodium hydride in THF. Quenching with TBDMSCl gave the mono TBDMS derivative **78** in 43% yield in addition to some di-TBDMS compound **79** (15%).<sup>125</sup> Unreacted starting material (29%) was also recovered. The use of benzyl bromide in place of TBDMSCl led to the mono-benzyl compound **80** (52%) and di-benzyl compound **81** (23%).



**Scheme 5.1.** Preparation of mono-protected diol derivatives.

Mono-protected derivatives of bisphenols **8** and **9** were prepared as outlined in Scheme 5.2. Treatment of N-acetyl piperidyl bisphenol **8** with TBDMSCl and imidazole in DMF<sup>126</sup> followed by flash chromatography to separate the statistical mixture of products gave mono-TBDMS derivative **82** in 26% yield. An identical procedure converted cyclohexyl bisphenol **9** to mono-TBDMS derivative **83** in 28% yield. The di-TBDMS compound **84** was also isolated in 18% yield. Benzyl protected derivatives of **9** were also prepared by treatment with benzyl bromide and potassium carbonate in DMF.<sup>127</sup> Both mono-benzyl **85** (35%) and di-benzyl **86** (17%) were isolated. No attempts were made to recover unreacted starting material due to the ready availability of large quantities of both **8** and **9**.



**Scheme 5.2.** Preparation of protected bisphenol derivatives.

### 5.2.1 Attempted Oligomer Synthesis via S<sub>N</sub>2 Reactions

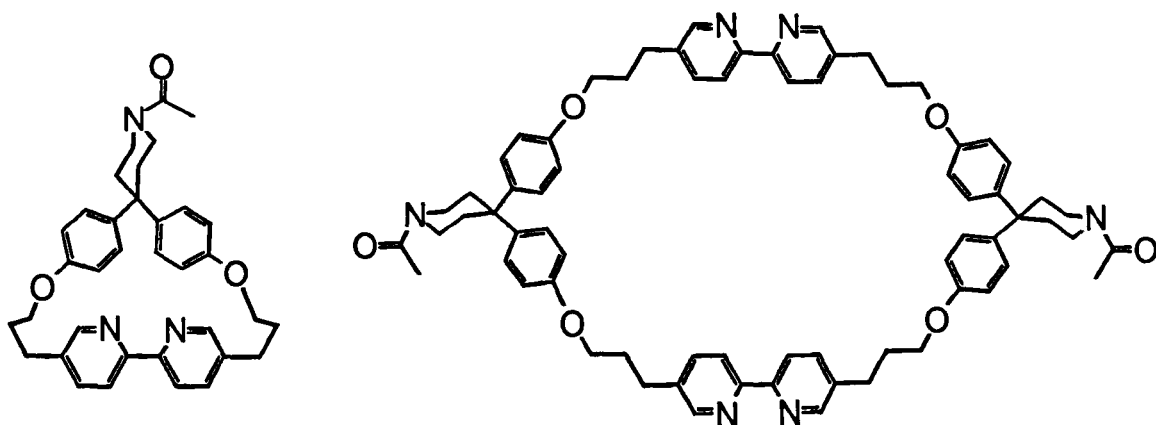
The first attempts at the preparation of **87** used the protected N-acetyl piperidine bisphenol **82** and ditosylate **7** as shown in Scheme 5.3. Various conditions were used without success (Table 5.1).

**Table 5.1.** Conditions for attempted synthesis of **87**

Reaction	Conditions
1	DMF, Cs <sub>2</sub> CO <sub>3</sub> , 60°C overnight. <sup>128</sup>
2	DMF, NaH, Room Temperature, 2 days.
3	Acetone, K <sub>2</sub> CO <sub>3</sub> , reflux. <sup>129</sup>
4	Toluene, NaH, Room Temperature, 18 hours. <sup>130</sup>
5	Toluene, NaH, Reflux, 12 hours.

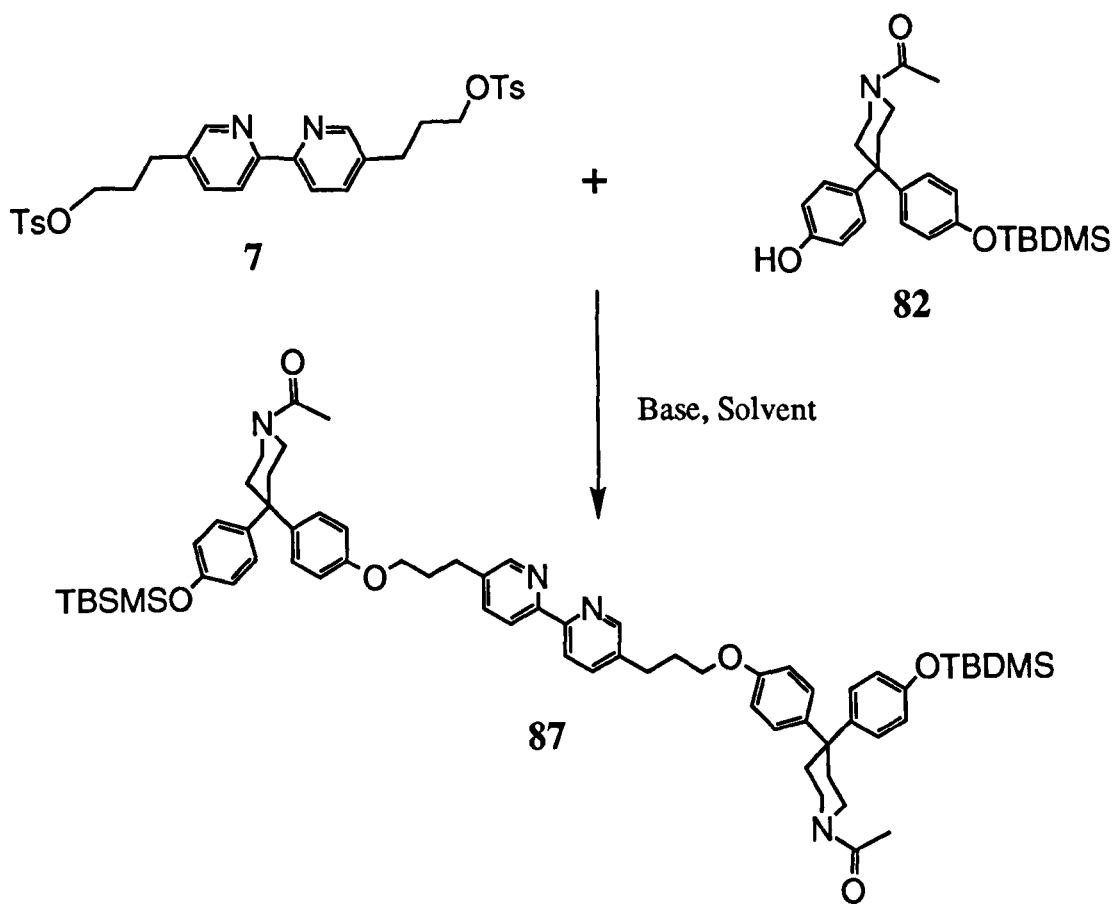
None of the required product was isolated under any of these conditions. In all cases the main product was baseline material by TLC analysis on silica. It therefore seemed likely that such material was polymeric in nature, and since this could only arise from the presence of unprotected bisphenol, the TBDMS protecting group was probably cleaved under the reaction conditions.

This was confirmed by a simple model experiment stirring mono-TBDMS bisphenol **82** with sodium hydride in DMF. The main products isolated were the free bisphenol and the di-TBDMS compound arising from migration of the protecting group. Further evidence for the formation of unprotected bisphenol during the coupling reactions was provided by the identification of macrocyclic products **88** and **89** in the FAB<sup>+</sup> MS (*m/z* 505 and 1010 respectively) of the crude product from several reactions.



**88**

**89**



**Scheme 5.3.** Attempted synthesis of 87 via  $S_N2$  displacement reactions between diotosylate 7 and mono-TBDMS bisphenol 82.  
Reagents and conditions: See Table 6.1.

## 5.2.2 Oligomer Synthesis using Mitsunobu Conditions

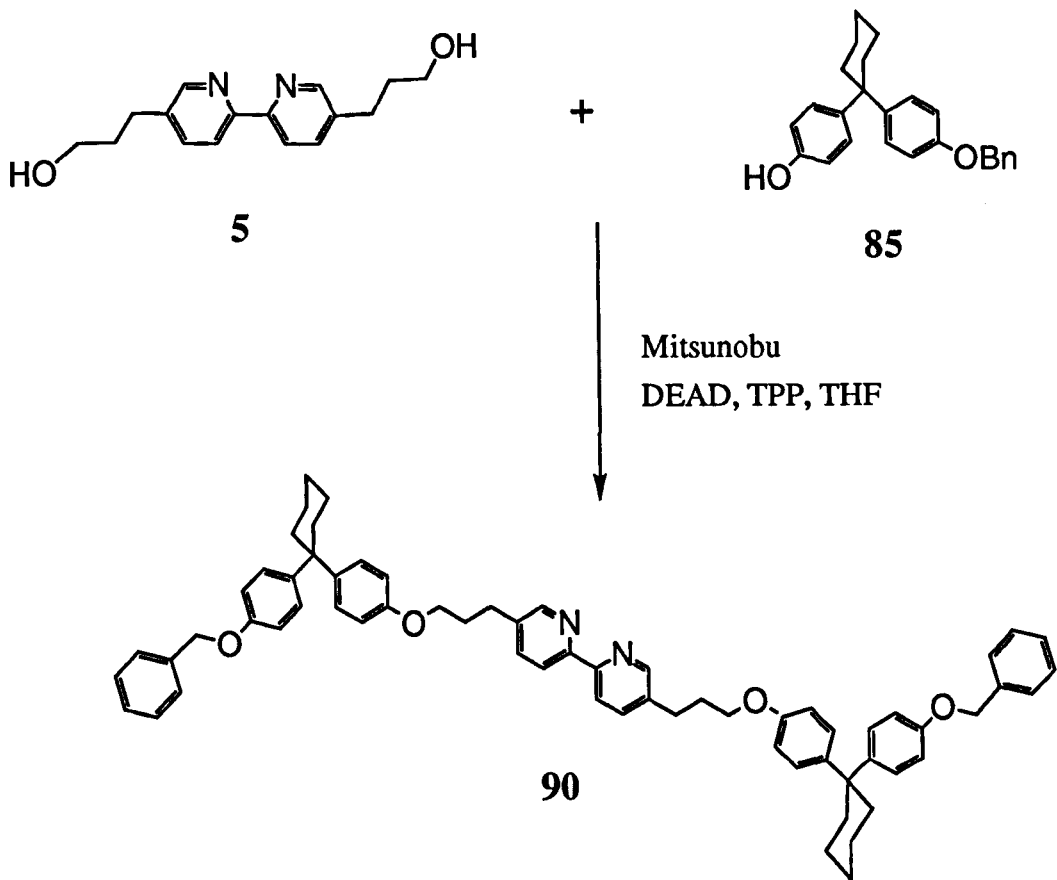
A second approach involved the use of Mitsunobu chemistry to form the alkyl-aryl ether links. At this point, a switch was made from the N-acetyl piperidine bisphenol **8** to the cyclohexyl derivative **9** due to its greater solubility and lower polarity making purification of products by column chromatography more straightforward.

Following the standard Mitsunobu procedure,<sup>131</sup> diethylazodicarboxylate (DEAD) and triphenylphosphine (TPP) were used as the coupling agents as shown in Scheme 5.4. Some yields obtained under different reaction conditions are summarised in Table 5.2.

**Table 5.2. Some yields obtained for the Mitsunobu coupling shown in Scheme 5.4.**

Reaction	Conditions:	Yield
1	DEAD, TPP (3 eq.), THF, reflux 4.5 h.	33%
2	DEAD, TPP (3 eq.), THF, RT, 4 hours.	44%
3	DEAD, TPP (2 eq.), THF, RT, 2 hours.	54%
4	DEAD, TPP (5 eq.), THF, RT, 4 hours.	0%
5	DEAD, TPP (3 eq.), THF, addition over 20 minutes, 0°C to RT , 24 hours.	0%

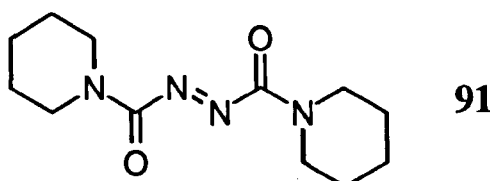
The yield of this reaction was extremely sensitive to reaction conditions: the optimum yield was obtained by rapid mixing of the reagents at room temperature. The use of higher or lower temperature or slower addition of the coupling reagent resulted in significantly lower yield or no isolable product at all. The yield was also very much scale dependent. The yields quoted above are based upon *ca.* 100 mg of diol **5**: on larger scale, the yield is again reduced and rather capricious. In view of this it was decided to try alternative coupling agents, since it was vitally important that this reaction could be completed with a good, reliable yield on reasonable scale for subsequent use in building up longer oligomers.



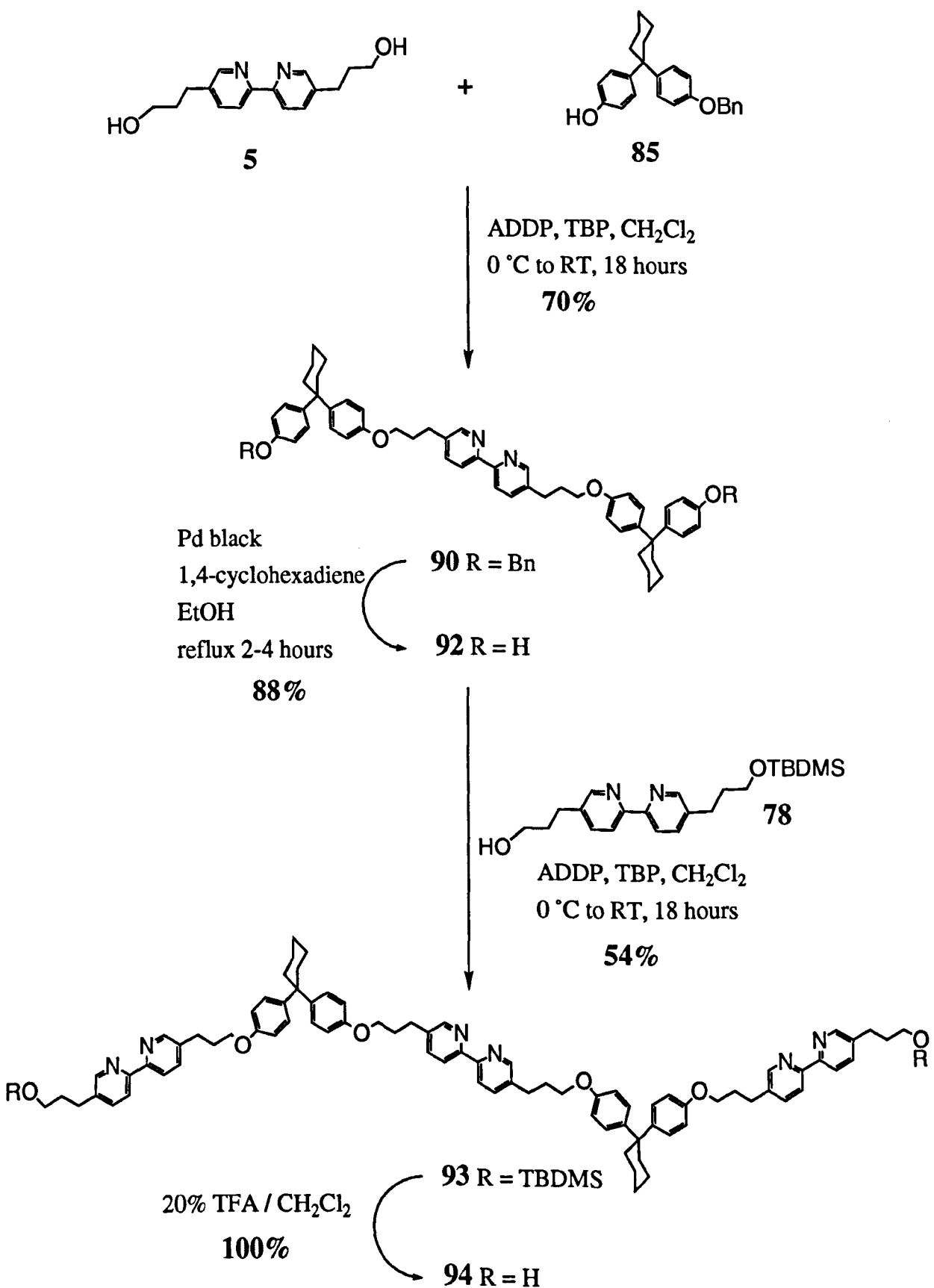
**Scheme 5.4.** *Synthesis of 2:1 protected oligomer using Mitsunobu conditions.  
Reagents, conditions and yields: see Table 5.2.*

### 5.2.3 Oligomer Synthesis Using Modified Mitsunobu Conditions

A number of new reagents for the Mitsunobu reaction have been reported over the last few years offering improvements over the traditional DEAD / TPP system. One of the better systems utilising a commercially available reagent is that reported by Tsunoda - 1,1'-(azodicarbonyl)-dipiperidine (ADDP) **91** / tributylphosphine (TBP).<sup>132</sup> This system has several advantages - for example with DEAD the pK<sub>a</sub> of the acidic component must be smaller than 11 for the reaction to give optimum yields, but ADDP works with pK<sub>a</sub>s in the range 11 - 13. Since the pK<sub>a</sub> of a phenol is rather borderline for the DEAD reagent, ADDP would be expected to offer a significant improvement. A further advantage is the fact that the hydrazine by-product of ADDP is extremely insoluble and therefore readily removed from the reaction product.



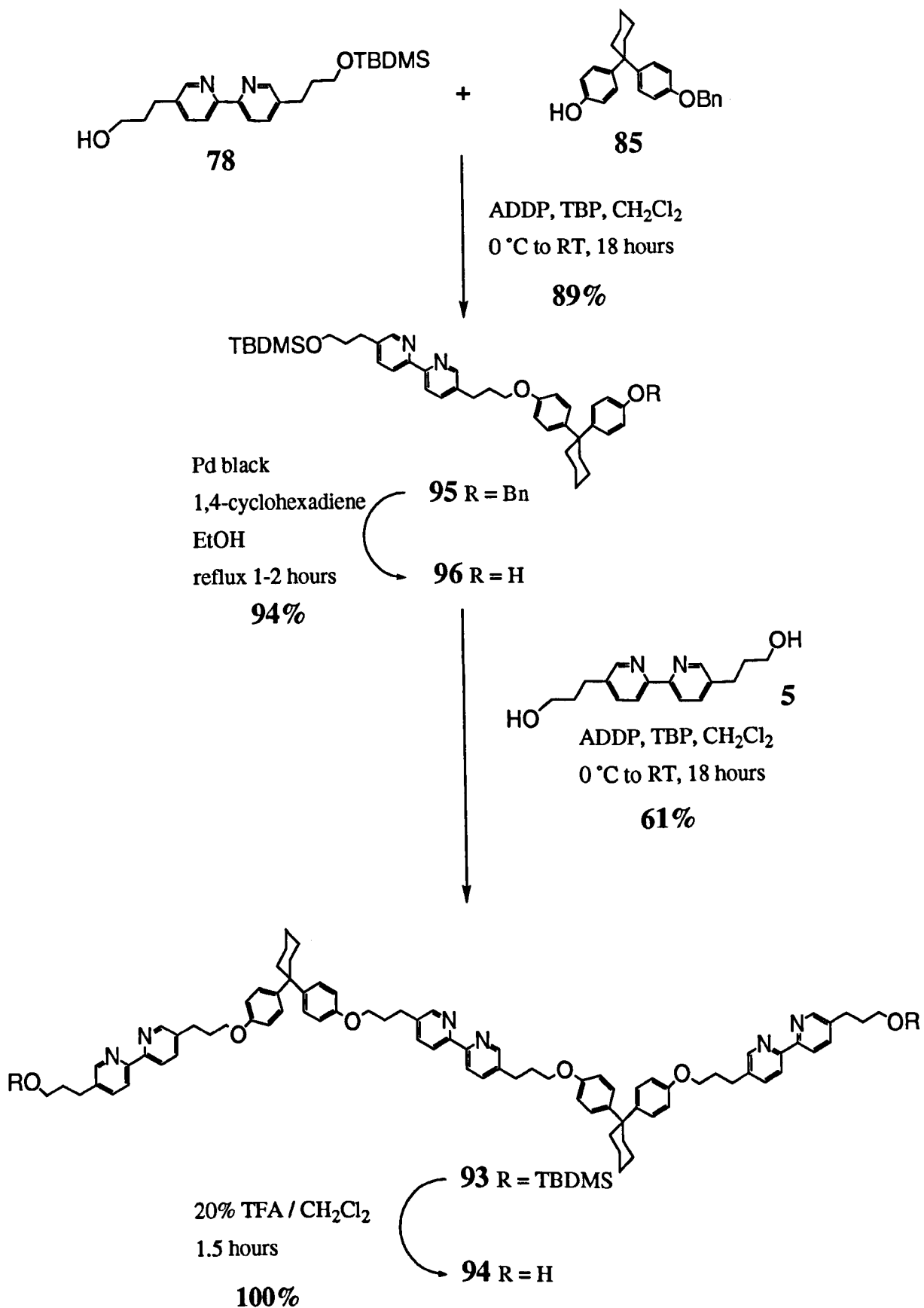
Applying this new methodology to our system resulted in improved and reliable yields which were readily carried out on larger scale. This quickly led to the complete synthesis of the 3:2 ether linked oligomer **94** as outlined in Scheme 5.5. Mono-benzyl bisphenol **85** and diol **5** were coupled to give the protected 2:1 adduct **90** in 70% yield using the ADDP / TBP system in CH<sub>2</sub>Cl<sub>2</sub>. The benzyl protecting group was removed to give **92** in 88% yield via a catalytic transfer hydrogenation reaction using a palladium black catalyst in ethanol with 1,4-cyclohexadiene as a hydrogen source.<sup>133</sup> Initial attempts using a 10% palladium on carbon catalyst resulted in significantly lower yields although TLC analysis suggested that the reaction had gone to completion. It seems likely that the product was becoming absorbed onto the carbon support of this catalyst. In both cases, a small amount of a brightly coloured impurity was formed which was removed by flash chromatography. Although this was not characterised, it is suspected that it may be a palladium-bipyridine coordination complex. Having obtained the deprotected 2:1 adduct **92**, a further Mitsunobu-type coupling with the mono-TBDMS protected diol **78** gave the protected 3:2 oligomer **93** in 54% yield. Cleavage of the TBDMS protecting group to give **94** was effected quantitatively by stirring in a 20% solution of TFA in CH<sub>2</sub>Cl<sub>2</sub>. This was found to be preferable to the more conventional procedure of TBAF in THF<sup>134</sup> due to the insolubility of the substrate in the required solvent. TBAF in CH<sub>2</sub>Cl<sub>2</sub> gave no reaction.



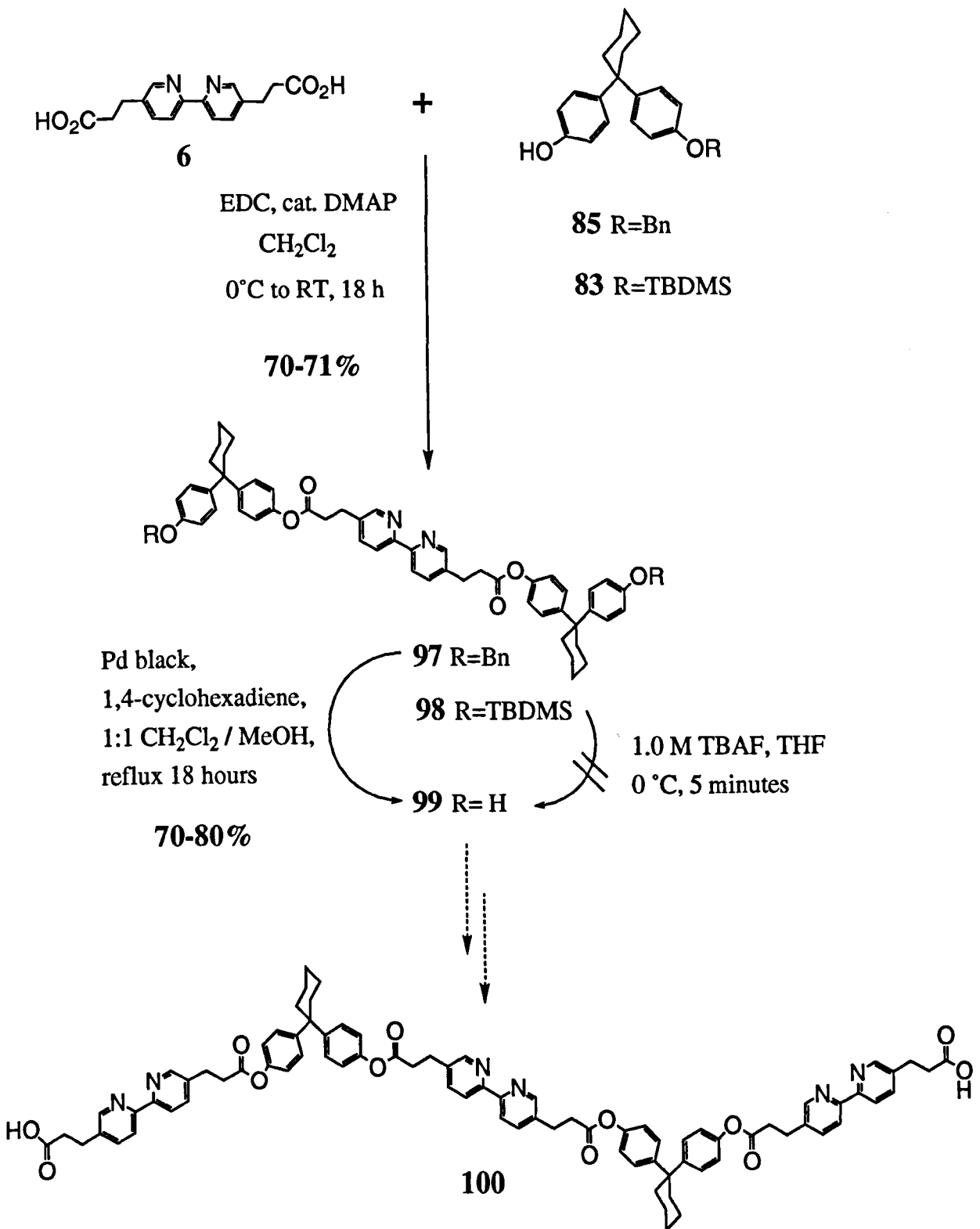
**Scheme 5.5.** Synthesis of 94 using the ADDP / TBP system.

Although this procedure gave access to **94** on reasonable scale, the overall yield was rather low and a number of problems still existed. Intermediate **92** was very insoluble which probably contributed to a low yield in the subsequent coupling reaction as well as complicating its isolation and purification. Also, a total of four steps in the scheme feature reactions at two sites in the molecule. This resulted in difficult chromatographic separation to remove mono-reacted material, particularly in the coupling to give **93**. These problems can be overcome by changing the order in which the components of the final oligomer are coupled together leading to the synthetic route in Scheme 5.6 which is now the method of choice for large scale synthesis of **94** (batches of up to 5 g were readily prepared).

Coupling of the mono-TBDMS diol **78** and mono-benzyl bisphenol **85** with ADDP / TBP gave the protected 1:1 compound **95**. Hydrogenolysis of the benzyl group gave the phenol **96** in 94% yield and a final Mitsunobu coupling with diol **5** gave the protected oligomer **93** in 61% yield. Deprotection as before gave **94** in quantitative yield.



**Scheme 5.6.** Alternative order of assembly for 3:2 oligomer **94**



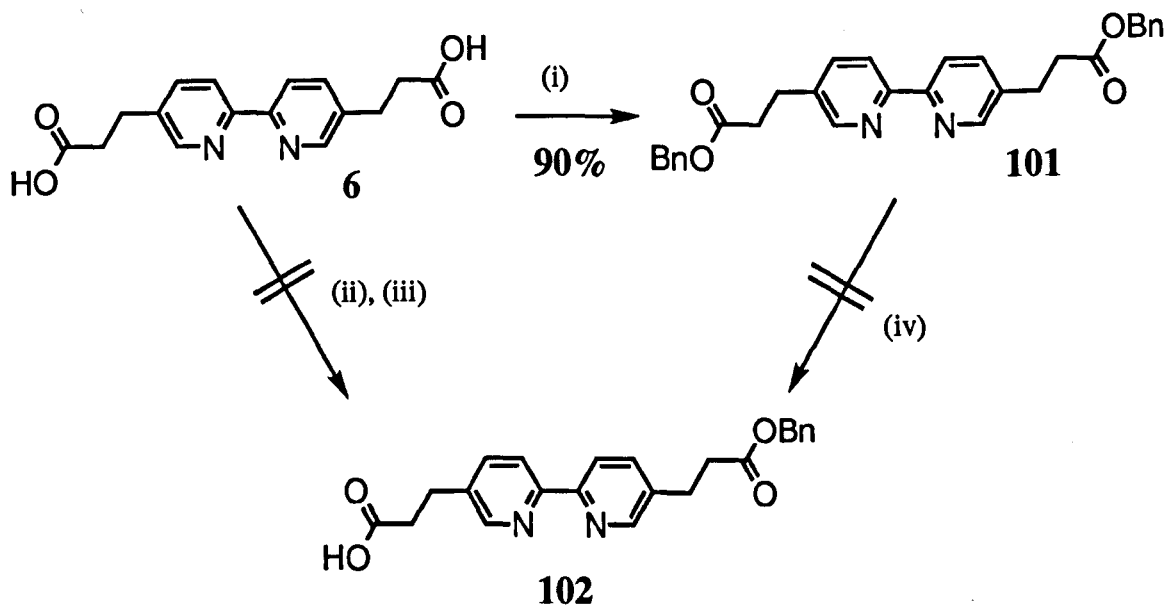
**Scheme 5.7.** Towards the synthesis of ester-linked oligomer 100.

## 5.3 Oligomers With Other Linker Units

### 5.3.0 Attempted Synthesis of an Ester Linked Oligomer

In order to investigate the effect of different linker groups on the folding process, an attempt was made to prepare **100**: an ester-linked variant to compare with the ether-linked oligomer. The 2:1 ester linked intermediate was readily prepared as shown in Scheme 5.7. Coupling of mono-benzyl bisphenol **85** and diacid **6** using EDC / DMAP in  $\text{CH}_2\text{Cl}_2$  gave the benzyl protected 2:1 adduct **97** in 71% yield. Catalytic transfer hydrogenation then gave **99**. Also prepared in an identical manner was the TBDMS derivative **98**. Attempts to deprotect **98** using TBAF in THF were unsuccessful and it seems likely that the basic fluoride ion causes decomposition of the ester links. TBDMS was therefore abandoned as a protecting group.

To complete the synthesis it was necessary to prepare the mono-protected acid derivative **102** which proved extremely difficult. A number of attempts to prepare this molecule were made without success (Scheme 5.8).‡



*Reagents and conditions:* (i)  $\text{BnOH}$  (excess), EDC, DMAP,  $\text{CH}_2\text{Cl}_2$ , RT, 18 hours  
(ii)  $\text{BnBr}$ ,  $\text{K}_2\text{CO}_3$ , DMF,  $60^\circ\text{C}$ , 18 hours; (ii)  $\text{BnOH}$  (1.1 eq), EDC, DMAP,  $\text{CH}_2\text{Cl}_2$  / DMF, RT, 18 hours; (iv) Pd black, cyclohexene, methanol /  $\text{CH}_2\text{Cl}_2$ , 30 mins - 18 hours, RT - reflux.

**Scheme 5.8.** Attempted preparation of mono-benzyl protected diacid **102**.

‡ Further attempts to synthesise **102** were also carried out by my colleague M. Simpson as part of an undergraduate project, without success.

Obtaining and purifying a statistical mixture of protected diacids proved much more difficult than for diol **5** (page 84) due to the extreme insolubility of acid **6** and high polarity of the products containing free acid groups which stuck to silica during chromatography.

Dibenzyl ester **101** was readily prepared in 90% yield using an EDC coupling reaction with an excess of benzyl alcohol. Attempts to carry out this reaction using just one equivalent of benzyl alcohol, followed by separation of the statistical mixture of benzyl esters were unsuccessful. Similarly, attempts to use benzyl bromide in the presence of  $K_2CO_3$  in DMF in a statistical manner were unsuccessful. It is likely that work-up and isolation are the problem rather than the reactions themselves: the desired product **102** is extremely polar and the statistical product mixture necessitates the use of chromatography for purification.

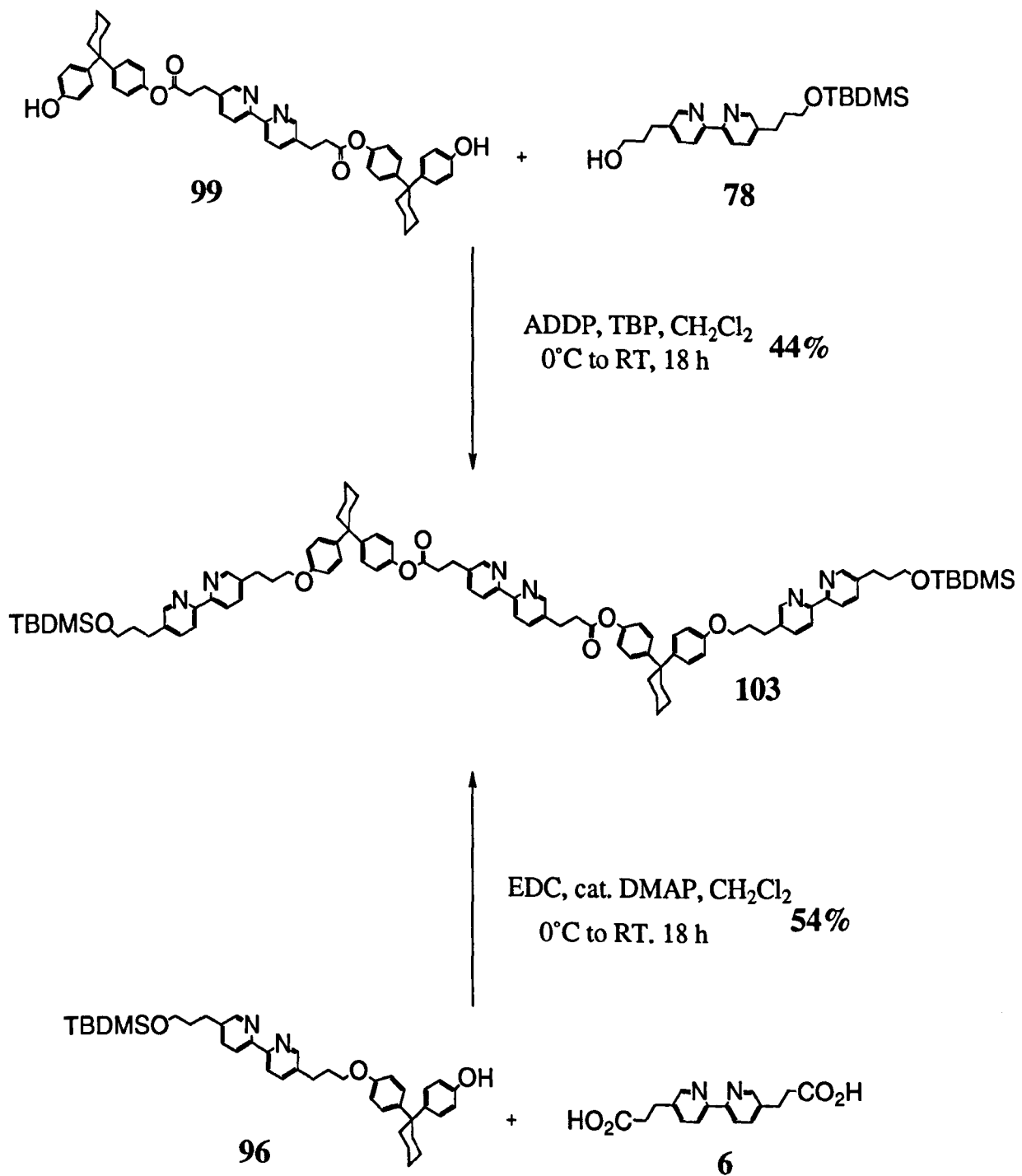
Attempts to statistically deprotect dibenzyl ester **101** using transfer hydrogenation conditions were also unsuccessful. Following the reaction by TLC suggested that although deprotection was slow at first, once the reaction started it proceeded extremely quickly, and it was not possible to stop the reaction at an intermediate stage when a significant amount of **102** was present.

Attempts to prepare the acid chloride of **6** using oxalyl chloride / catalytic DMF in  $CH_2Cl_2$  followed by addition of 1 equivalent of benzyl alcohol / triethylamine were also unsuccessful, resulting in an extremely complex mixture of products that could not be characterised.

### 5.3.1 Synthesis of a Mixed Ether-Ester Linked Oligomer

Rather than pursue the synthesis of the ester linked oligomer, the 2:1 ester-linked intermediate **99** was used to prepare the mixed linker oligomer **103** using the mono-protected diol and Mitsunobu chemistry already established. Such an oligomer containing two ether links and two ester links would still enable a relationship between linker group geometries and tendency to fold into a knotted structure to be determined.

In fact, two routes were utilised as outlined in Scheme 5.9. **99** and mono-TBDMS diol **78** were coupled using the ADDP / TBP system to give the TBDMS protected mixed oligomer **103**. Alternatively, **103** was prepared from the TBDMS 1:1 compound **96** and diacid **6** using an EDC coupling reaction in 54% yield. No attempts were made to remove the TBDMS protecting groups of **103** due to the earlier problems experienced with TBDMS deprotection in the presence of esters.

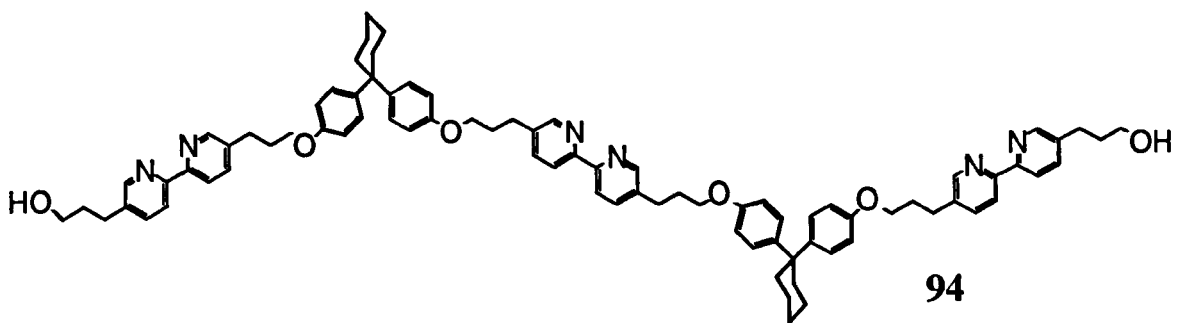


**Scheme 5.9.** Two routes to the mixed ether / ester oligomer 103.

## 5.4 Folding of the Ether Linked Oligomer

### 5.4.0 Folding Around Iron (II)

The first test of the interaction of strand **94** with a metal ion was carried out using iron (II). A solution of **94** in 5% methanol / CH<sub>2</sub>Cl<sub>2</sub> was treated with one equivalent of iron (II) perchlorate hexahydrate in the same solvent system.



After stirring for 2 hours, the solvent was removed and a <sup>1</sup>H NMR spectrum of the crude product was obtained. The spectrum was very broad and complex. TLC on silica indicated a complex mixture of products dominated by baseline material. It seemed possible that the relatively stable nature of the iron (II) tris-bipyridine complexes resulted in the trapping of kinetic oligomeric products rather than equilibration to the desired 1:1 complex. Several attempts were therefore made to induce an equilibration process.

Heating the product at reflux for 2 hours produced no improvement in the <sup>1</sup>H NMR spectrum or the complexity of the TLC. Due to the known acid lability of such complexes, it also seemed possible that the addition of catalytic acid may aid the equilibration process. Addition of *p*-toluenesulphonic acid (*ca.* 1 equivalent) produced no significant change, but trifluoroacetic acid (1 drop) did produce a sharpening of the broad signals in the <sup>1</sup>H NMR spectrum while a high running spot became somewhat more intense relative to the baseline material by TLC analysis on silica.

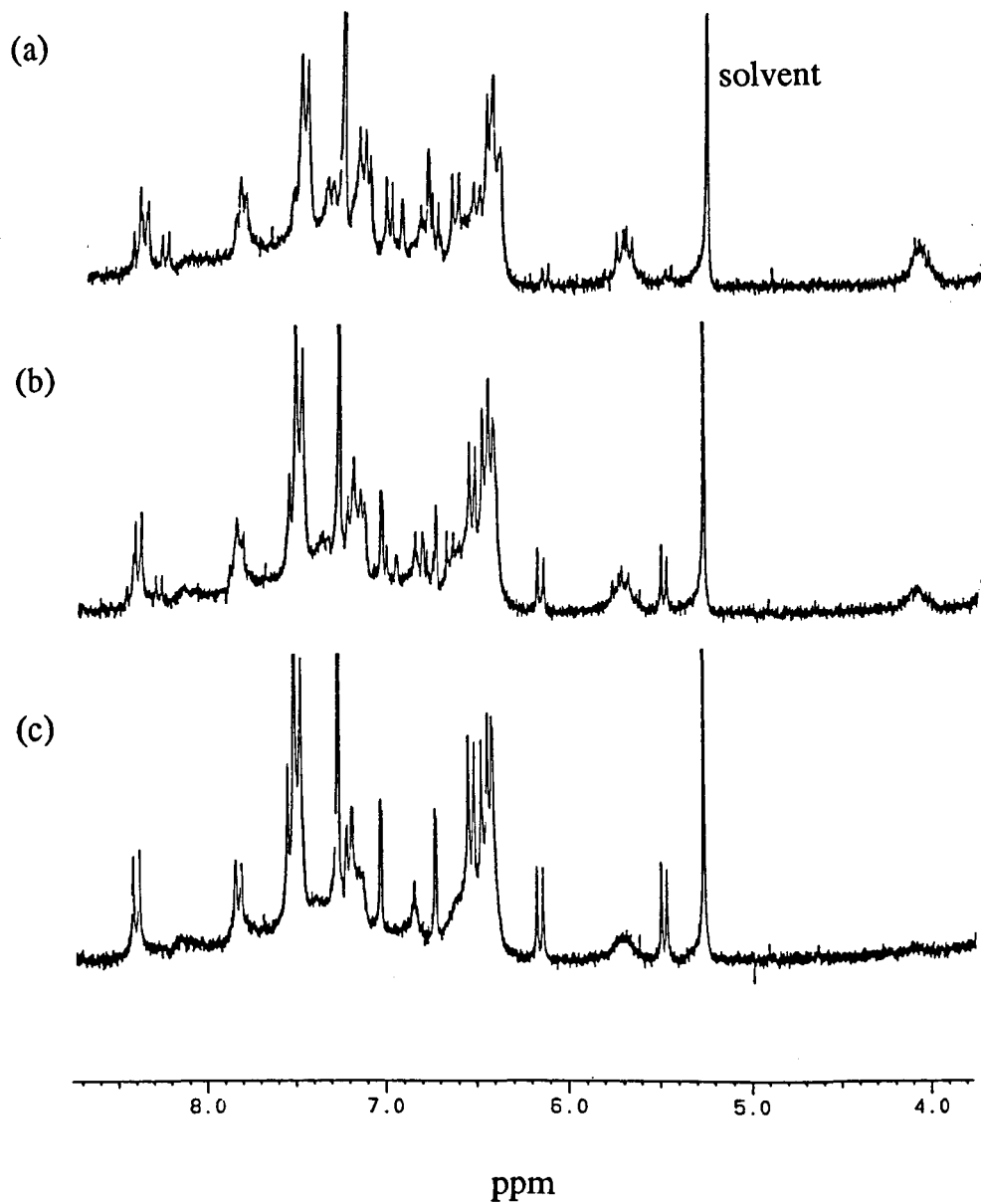


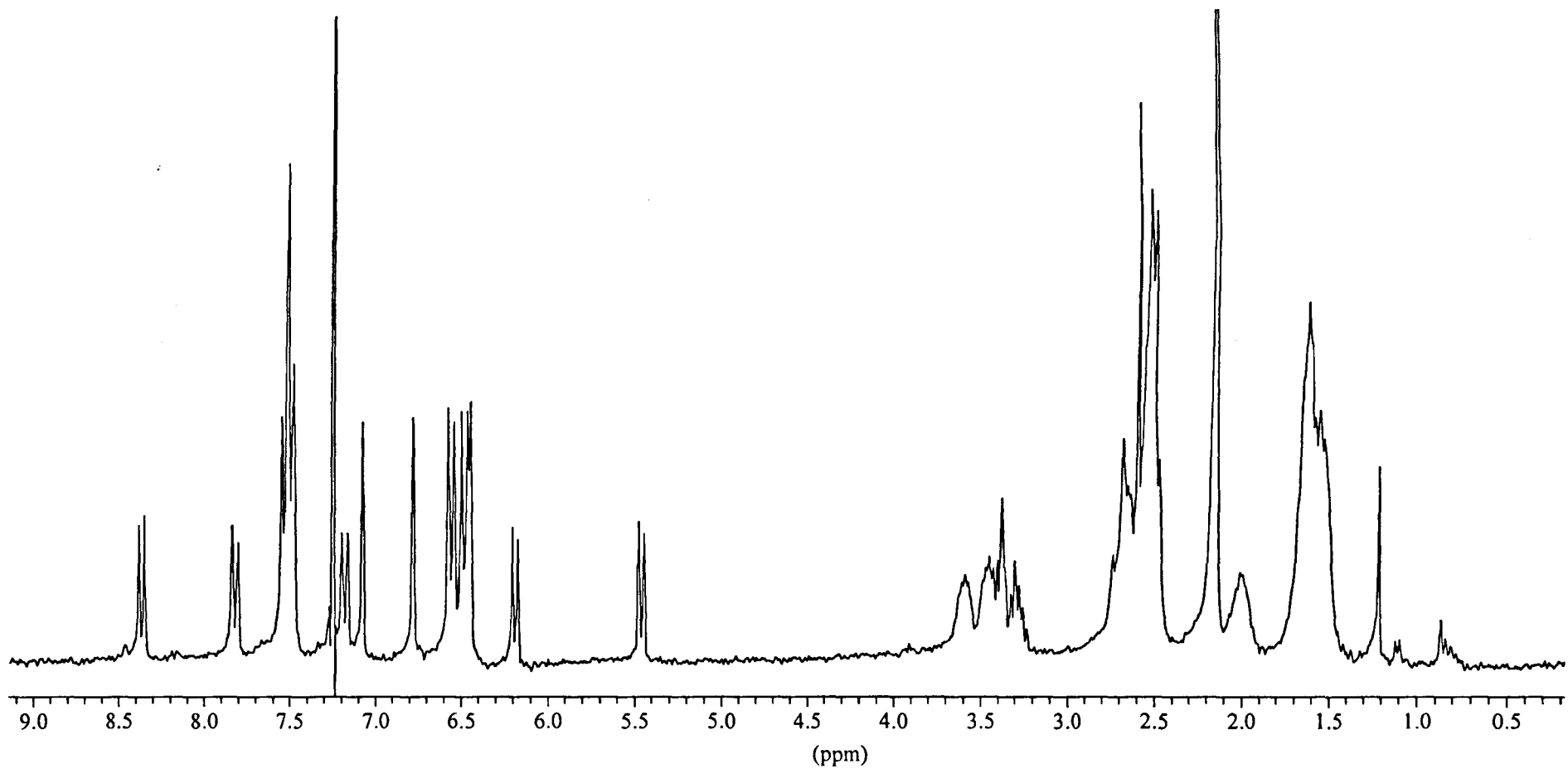
**Figure 5.1.** Aromatic region of the 250 MHz  $^1\text{H}$  NMR spectrum of the complex between **94** and iron (II) after (a) 10 minutes, (b) 6 hours and (c) 24 hours in 5%  $\text{CD}_3\text{OD} / \text{CDCl}_3$ .

At this point, it was observed that if the  $\text{CH}_2\text{Cl}_2$  solution was washed with aqueous  $\text{NaHCO}_3$  to remove the TFA and the solvent switched to  $\text{CDCl}_3 / 5\% \text{ CD}_3\text{OD}$  then a rearrangement process gradually takes place that leads to a considerable simplification in the  $^1\text{H}$  NMR spectrum. This was somewhat surprising, because when the original mixing of the metal ion and **94** was carried out in 5% methanol /  $\text{CDCl}_3$ , only an insoluble red precipitate was formed. The changes over a period of 24 hours are illustrated in Figure 5.1.

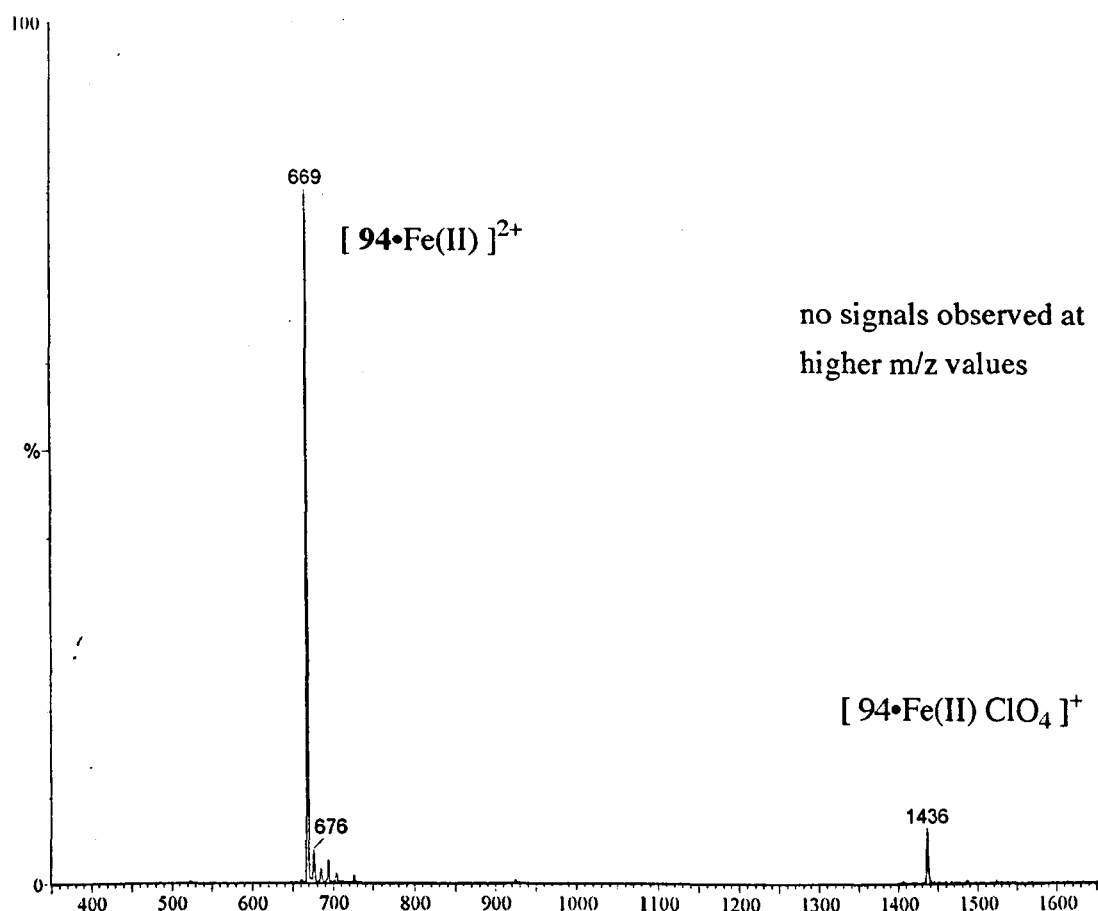
As well as the general simplification of the spectrum with time, the most striking feature is the emergence of two doublets at 5.5 ppm and 6.2 ppm. These signals are in an unusual chemical shift range for aromatic protons suggesting that there are strong ring-current shielding effects in the complex. Also of note is the rather broad signal at 5.7 ppm. This shows a reduction in intensity but does not disappear completely which implies that the signal corresponds to two distinct species, one of which rearranges to the product containing the new doublets and one of which is unchanged. Since the remaining signal is rather broad, this implies that it is oligomeric material that remains unchanged at the end of the rearrangement process.

TLC of the rearranged product is unchanged, consisting of a high running spot and baseline material. This is consistent with the final  $^1\text{H}$  NMR spectrum in Figure 5.1 (c) which seems to show the sharp signals of a discrete complex superimposed upon the broad signals of oligomeric material. This mixture was readily separated by flash chromatography on a short silica column. The only material to emerge from the column was the high running complex. The baseline material remained on the silica even when a very polar eluant was used (25% methanol /  $\text{CH}_2\text{Cl}_2$ ). The complex was obtained in 30% yield from starting material from which it is inferred that the oligomeric material that remains on the column accounts for the other 70%.

The isolated complex has a  $^1\text{H}$  NMR spectrum with a simple aromatic region but an extremely complex aliphatic region (Figure 5.2). The aromatic region shows a remarkable chemical shift dispersion with signals spread across a 3 ppm range. ES<sup>+</sup> MS revealed an intense signal at m/z 669 which corresponds to an  $\text{M}^{2+}$  ion from a 1:1 complex between **94** and iron (II). The only other peak present was a very weak signal at m/z 1436 corresponding to  $[\text{94}\bullet\text{Fe(II)} \text{ ClO}_4]^+$  (Figure 5.3).



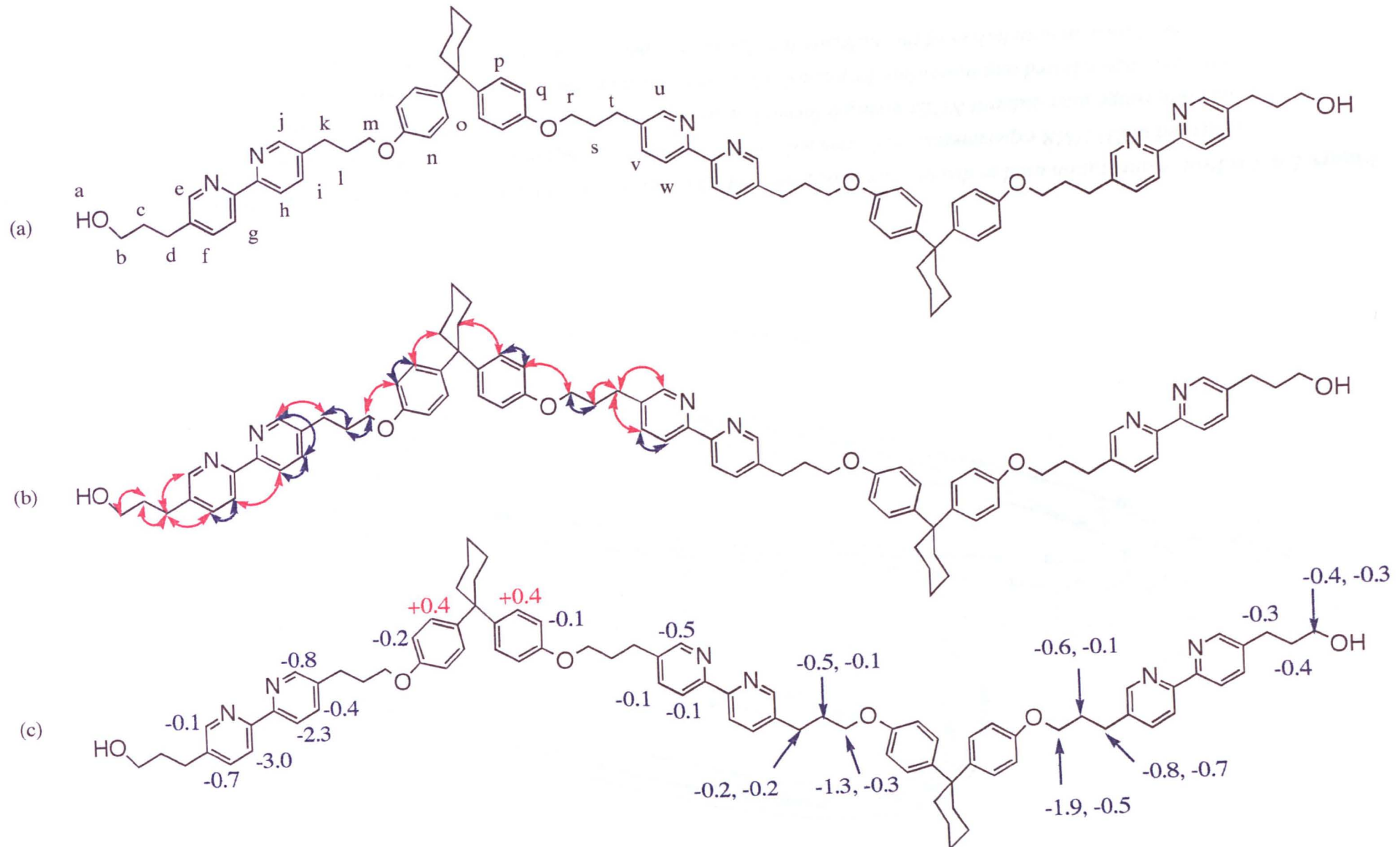
**Figure 5.2.** 250 MHz  $^1\text{H}$  NMR spectrum in  $\text{CDCl}_3$ /5%  $\text{CD}_3\text{OD}$  of  $\text{Fe}(\text{II}).94$  complex after chromatography.



**Figure 5.3.** ES<sup>+</sup> MS of the 94•Fe(II) complex.

#### 5.4.1 NMR Structure Determination

Assignment of the <sup>1</sup>H NMR spectrum of the Fe(II)•94 complex was achieved via 2D ROESY and COSY experiments. Starting from the methylene group adjacent to the terminal hydroxyl function of the oligomer 94, it was possible to sequentially assign all the <sup>1</sup>H NMR signals using NOE and COSY coupling connectivities along the chain (Figure 5.4 (b)).



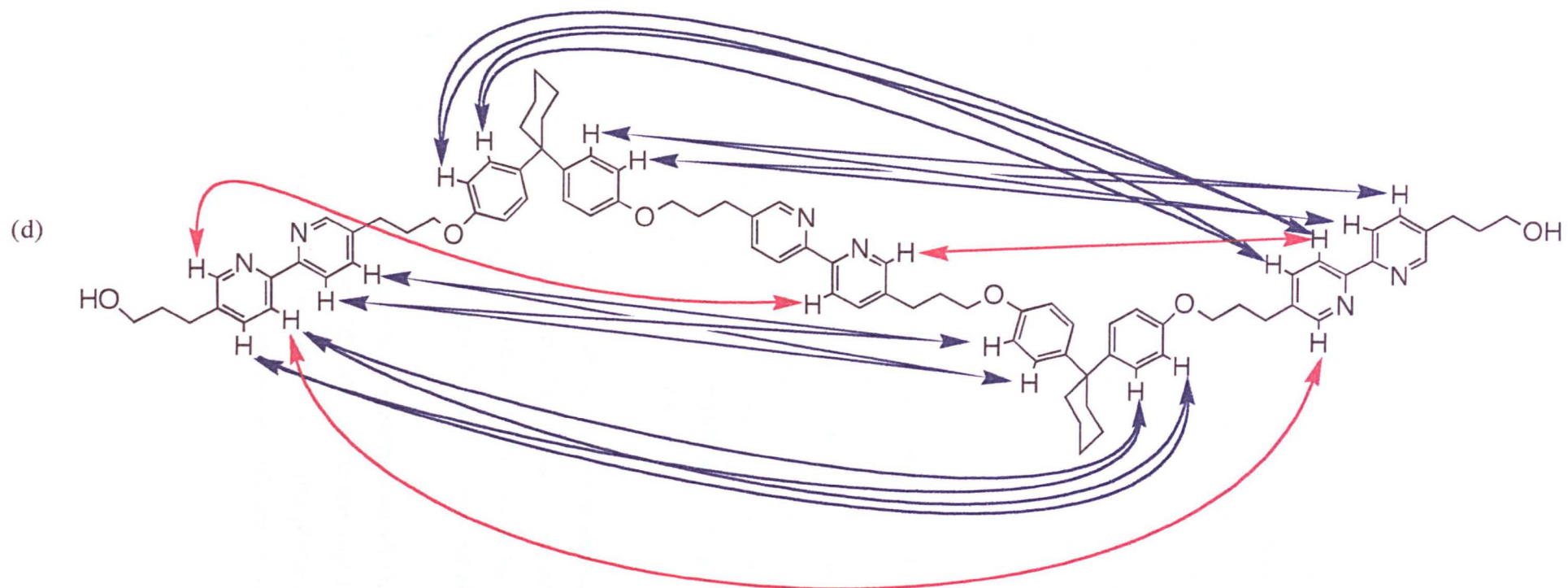


**Figure 5.4.** (a) Proton annotation used in discussions of oligomer 94. (b) Short range ROESY cross-peaks ( $\longleftrightarrow$ ) and COSY couplings ( $\longleftrightarrow$ ) observed in 2D NMR experiments. (c) Corrected changes in chemical shift observed for 94 in the presence of iron (II). (d) Long range inter-subunit NOEs giving information about the 3D structure of the 94•Fe (II) complex formed. Bipyridine-bipyridine NOEs are shown in red and bipyridine-bisphenol NOEs are shown in blue. 94 has 2-fold symmetry but the NOEs are shown only once and drawn on both halves of the molecule for clarity. All spectra were recorded in 5%  $CD_3OD / CDCl_3$ .

As stated previously, the signals in the aromatic region of the  $^1\text{H}$  NMR spectrum exhibit a remarkable chemical shift dispersion, and this also gives invaluable information about the 3-D structure of the complex. A full assignment of all the protons in **94** along with their equivalent values in the iron (II) complex **104** and the shifts induced upon complexation are given in Table 5.1.

Many of the signals are significantly shifted from their positions in the free oligomer **94**. Protons which are situated in close proximity to the face of another aromatic ring experience a strong shielding effect and hence are shifted significantly upfield. Conversely, protons situated close to the edge of another aromatic ring experience a downfield shift. These changes in chemical shift are illustrated in Figure 5.4 (c). The shifts on the bisphenol protons are relative to uncomplexed **94** and the shifts on the bipyridine protons are relative to tris-bipyridine iron (II) complex **74**. In this way, the changes in chemical shift of the signals due to the bipyridine protons are corrected for the effects produced by coordination to the metal ion and reflect purely the effects due to the folded conformation of the complex.

Many long-range inter-subunit NOEs are also observed connecting the bipyridine units to each other and to the bisphenol units as shown in Figure 5.4 (d). Due to the symmetrical nature of the molecule, there is a possible ambiguity as to which bisphenol unit is close to which terminal bipyridine. However, CPK models indicate that due to the short length of the three carbon linker, it is not possible to obtain a conformation where the bipyridine is close to its neighbouring bisphenol unit in an orientation that is consistent with all of the NOEs obtained.

Both the NOE data and the changes in chemical shift indicate that the bisphenol units bridge across the terminal bipyridine units, causing the bipyridine protons  $\text{H}_f$ ,  $\text{H}_g$ ,  $\text{H}_h$  and  $\text{H}_i$  to be in close proximity to the face of the aromatic rings of the bisphenol. In contrast, there are no changes in chemical shift or any long-range NOEs for the central bipyridine.

The only 1:1 structure consistent with all the data is the pseudo-overhand knot **104**. The pronounced upfield shifts on the terminal bipyridine units (shown in blue) can now be clearly seen to be due to their close proximity to the bridging bisphenol units (Figure 5.5). The reason for the lack of shifts on the central bipyridine is also clear.

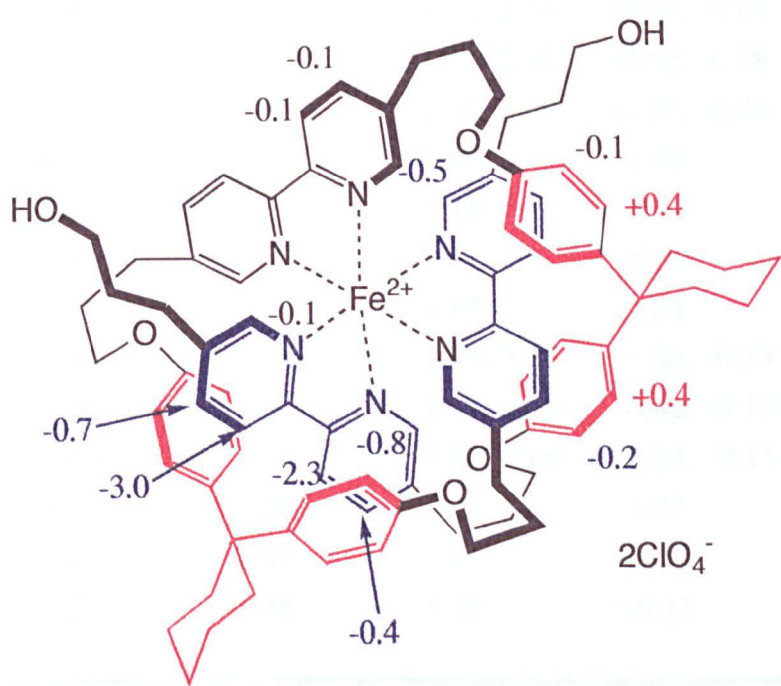
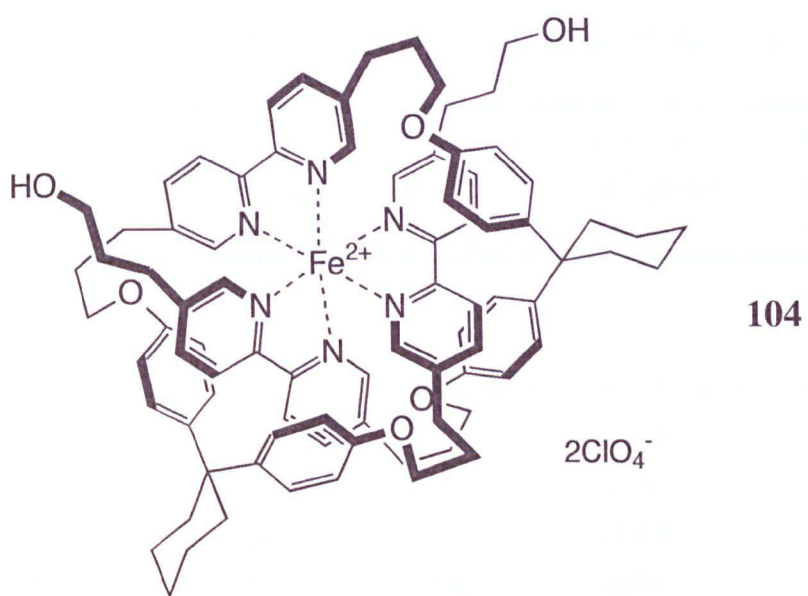


**Figure 5.5.** Changes in chemical shift induced upon folding of free ligand **94** into pseudo-overhand knot **104**. Changes in the chemical shift of the signals due to the bipyridine protons are corrected for the effects of metal ion coordination.

**Table 5.1.** Assignment of the 400 MHz  $^1\text{H}$  NMR spectrum of **104** in 5%  $\text{CD}_3\text{OD} / \text{CDCl}_3$  together with the equivalent chemical shifts for free oligomer **94**, chemical shifts of iron (II) complex **74** used to correct for the effects of metal ion coordination and complexation-induced changes in chemical shift.

Proton	Chemical Shift in <b>94</b> (ppm)	Chemical Shift in <b>74</b> (ppm)	Chemical Shift in <b>104</b> (ppm).*	Complexation $\Delta\delta$ (ppm).	Corrected Complexation $\Delta\delta$ (ppm).
$\text{H}_\text{a}$	not determined		not determined	-	-
$\text{H}_\text{b}$	3.69		3.30, 3.39	-0.39, -0.30	-0.39, -0.30
$\text{H}_\text{c}$	1.91		1.55	-0.36	-0.36
$\text{H}_\text{d}$	2.76		2.50	-0.26	-0.26
$\text{H}_\text{e}$	8.50	7.20	7.07	-1.43	-0.13
$\text{H}_\text{f}$	7.63	7.91	7.18	-0.45	-0.73
$\text{H}_\text{g}$	8.25	8.48	5.46	-2.79	-3.02
$\text{H}_\text{h}$	8.25	8.48	6.19	-2.06	-2.29
$\text{H}_\text{i}$	7.63	7.91	7.55	-0.08	-0.36
$\text{H}_\text{j}$	8.50	7.20	6.45	-2.05	-0.75
$\text{H}_\text{k}$	2.84		2.05, 2.15	-0.79, -0.69	-0.79, -0.69
$\text{H}_\text{l}$	2.09		1.54, 2.00	-0.55, -0.09	-0.55, -0.09
$\text{H}_\text{m}$	3.93		2.06, 3.47	-1.87, -0.46	-1.87, -0.46
$\text{H}_\text{n}$	6.78		6.48	-0.30	-0.30
$\text{H}_\text{o}$	7.15		7.48	+0.33	+0.33
$\text{H}_\text{p}$	7.15		7.51	+0.36	+0.36
$\text{H}_\text{q}$	6.78		6.55	-0.23	-0.23
$\text{H}_\text{r}$	3.93		2.63, 3.63	-1.30, -0.33	-1.30, -0.33
$\text{H}_\text{s}$	2.09		1.57, 1.96	-0.52, -0.13	-0.52, -0.13
$\text{H}_\text{t}$	2.84		2.60, 2.69	-0.24, -0.15	-0.24, -0.15
$\text{H}_\text{u}$	8.50	7.20	6.78	-1.72	-0.42
$\text{H}_\text{v}$	7.63	7.91	7.82	-0.19	-0.09
$\text{H}_\text{w}$	8.25	8.48	8.36	+0.11	-0.12

\* Two values listed for the aliphatic protons of **104** signify that the two protons in each methylene unit become inequivalent in the complex.

The inequivalence of the bipyridine protons H<sub>e</sub>, H<sub>j</sub> and H<sub>u</sub> indicates that the product does not have a perfect octahedral arrangement about the metal ion. This is also confirmed by the inequivalence of the H<sub>f</sub> / H<sub>i</sub> and H<sub>g</sub> / H<sub>h</sub> protons on opposite sides of the "bridged" bipyridine units. The significantly larger upfield shifts of H<sub>f</sub> and H<sub>g</sub> compared to H<sub>i</sub> and H<sub>h</sub> suggest that the bisphenol does not bridge across the centre of the bipyridine unit but is actually offset towards the H<sub>f</sub> / H<sub>g</sub> side. In reality, it is likely that the bisphenol unit has some freedom to move between the H<sub>g</sub> and H<sub>h</sub> side of the bipyridine unit but spends more time in close proximity to H<sub>g</sub>. Presumably this is because the aromatic edge-face interaction in the product can be maximised in this way.

This interpretation is supported by solvent effects on the chemical shift of H<sub>g</sub> and H<sub>h</sub> as shown in Figure 5.6. In chloroform, the difference in chemical shift between the two protons is 0.74 ppm indicating that the bisphenol has a strong preference to sit closer to H<sub>g</sub> and hence cause an enhanced shielding effect relative to H<sub>h</sub>. However, in acetone (weaker  $\pi$ - $\pi$  interactions, see Chapter 4) the difference is only 0.26 ppm (Table 5.2, Figure 5.6). In DMSO, which gives the weakest interactions of all, the protons are almost equivalent indicating that there is no driving force to direct the bisphenol bridge to maximise its edge-face interaction with either H<sub>h</sub> or H<sub>g</sub>.

**Table 5.2. Complexation-induced changes in chemical shift in different solvents.\***

Proton	Chloroform	Acetone	DMSO
H <sub>g</sub>	-3.0	-2.8	-3.0
H <sub>h</sub>	-2.3	-2.6	-3.0
H <sub>j</sub>	-0.8	-0.8	-0.7
H <sub>n</sub>	-0.3	-0.2	-0.3
H <sub>q</sub>	-0.2	-0.2	-0.2
H <sub>u</sub>	-0.4	-0.4	-0.4
H <sub>e</sub>	-0.1	-0.1	0.0
H <sub>f</sub>	-0.7	-0.4	-0.5
H <sub>o</sub>	+0.3	+0.6	+0.6
H <sub>p</sub>	+0.4	+0.6	+0.6
H <sub>i</sub>	-0.4	-0.2	-0.3
H <sub>v</sub>	-0.1	-0.1	0.0
H <sub>w</sub>	-0.1	-0.1	0.0

\* Bipyridine protons are corrected for the effects of metal ion coordination as discussed previously. Corrected values are relative to iron (II) complex **74** in the same solvent. NMR data for **74** in all three solvents is provided in the experimental section.

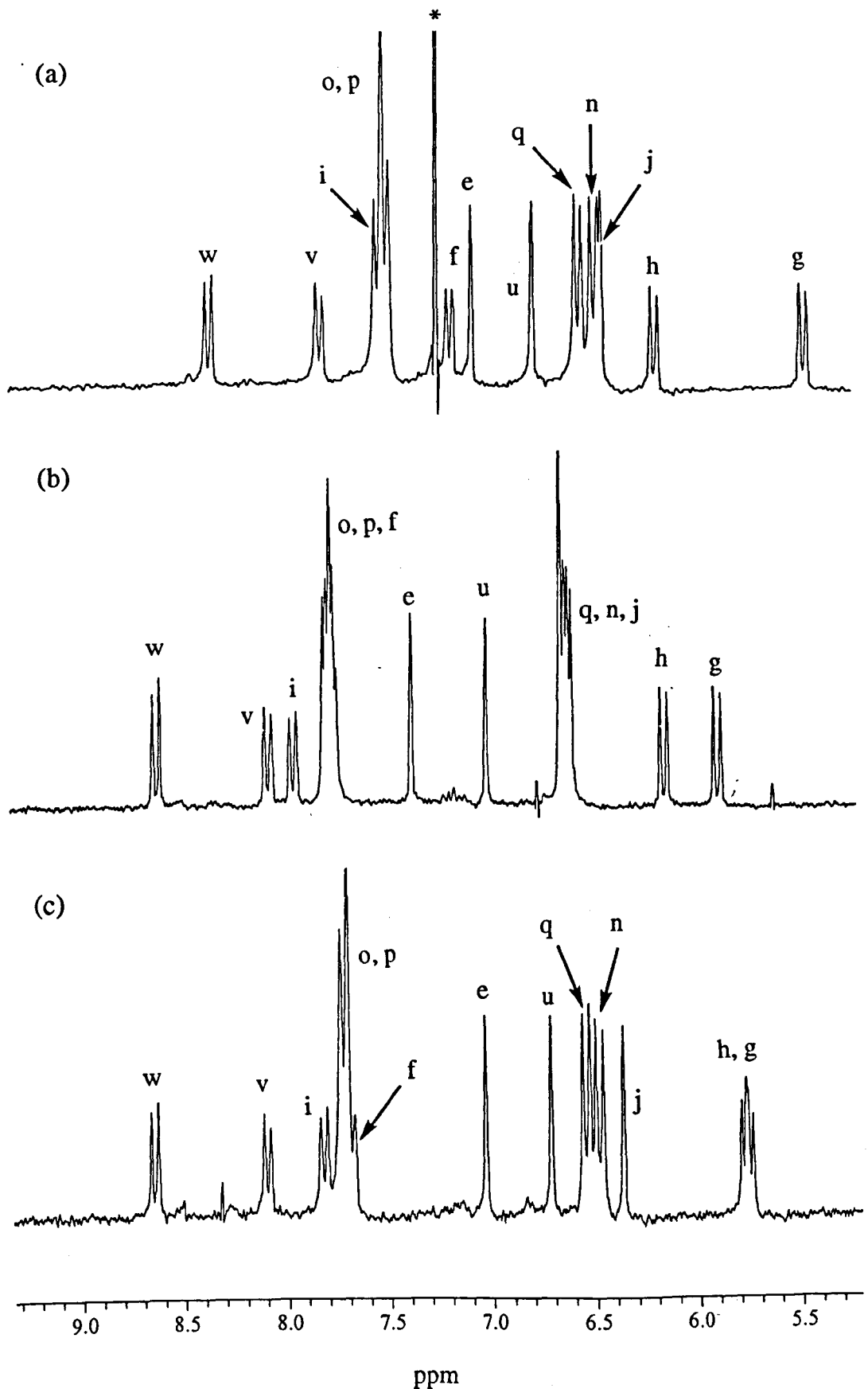


**Figure 5.6.**  $^1\text{H}$  NMR spectra of iron (II) pseudo-overhand knot 104 in (a) chloroform, (b) acetone and (c) DMSO. \* Denotes residual solvent peaks.

### 5.4.2 Summary of Folding Around Iron (II)

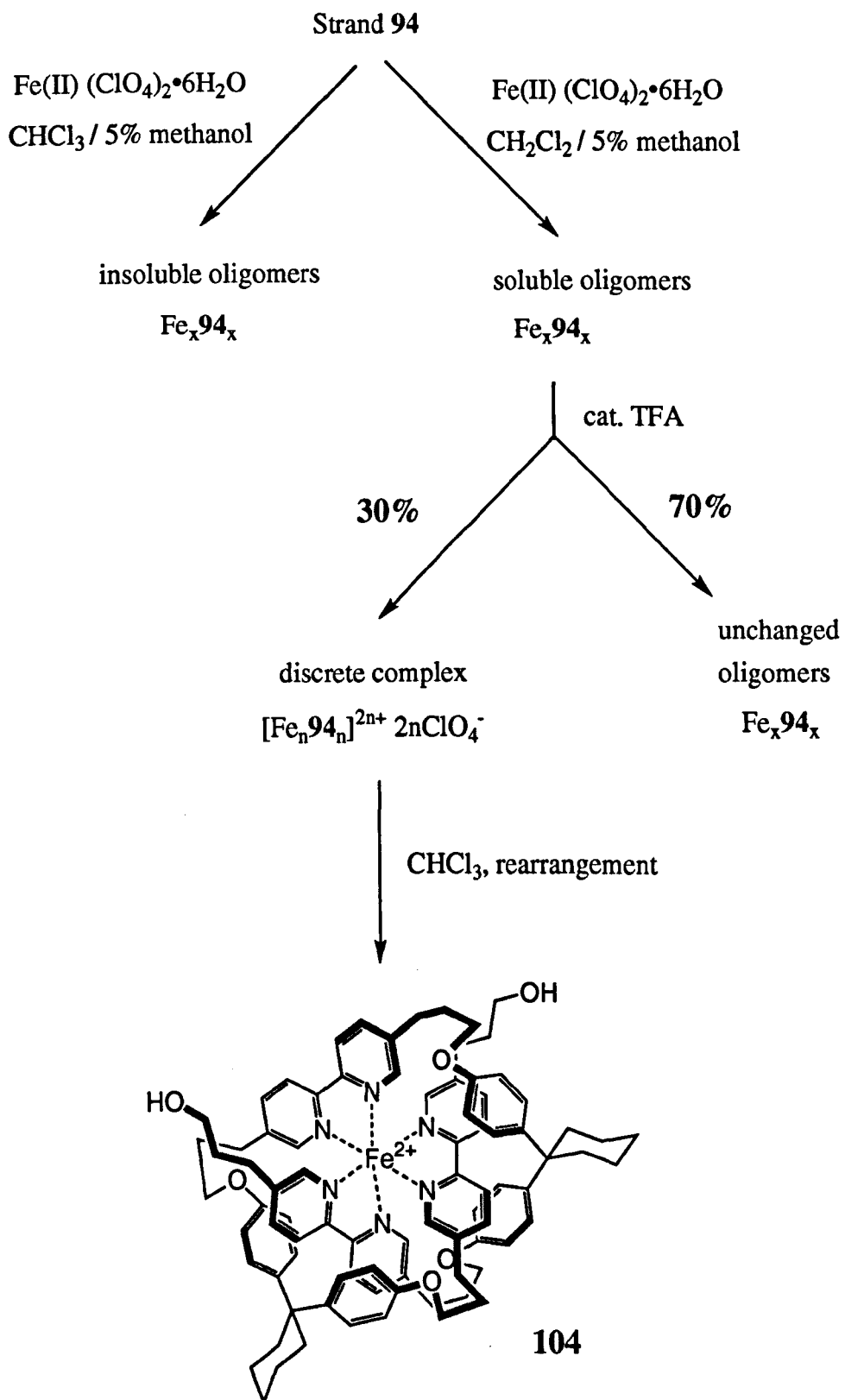
The overall sequence of events leading to the iron (II) pseudo overhand knot is illustrated in Scheme 5.10. Reaction of **94** with one equivalent of iron (II) in CH<sub>2</sub>Cl<sub>2</sub> leads to almost exclusively oligomeric species that are soluble in CH<sub>2</sub>Cl<sub>2</sub>. An identical reaction in CHCl<sub>3</sub> however leads to insoluble oligomeric species. Upon removal of solvent, these products cannot be redissolved in CH<sub>2</sub>Cl<sub>2</sub>. It seems possible that the oligomer solubility may depend upon length, *i.e.* shorter (soluble) oligomers are the initial kinetic product in CH<sub>2</sub>Cl<sub>2</sub> while longer (insoluble) oligomers are formed in CHCl<sub>3</sub>. The reason for this is not clear.

Addition of catalytic TFA to the soluble mixture of oligomers in CH<sub>2</sub>Cl<sub>2</sub> leads to the equilibration of 30% of the material present to some sort of discrete complex. This material may be a 1:1 **94**•Fe(II) complex or may have some higher stoichiometry. However, it is reasonable to infer that the material is not oligomeric in nature since it runs high on TLC and produces a relatively sharp, well defined spot. The <sup>1</sup>H NMR spectrum of this complex is sharp and well defined but different from that of **104** (Figure 5.1 (a)).

After removal of the CH<sub>2</sub>Cl<sub>2</sub> solvent and TFA catalyst from the discrete complex followed by redissolving in CHCl<sub>3</sub>, a slow rearrangement over a period of 24 hours results in the formation of pseudo-overhand knot **104** while the remaining 70% oligomeric material is unchanged. There is no obvious explanation for this solvent effect, although one could propose that the π-π interactions templating the correct product are slightly stronger in CHCl<sub>3</sub> than CH<sub>2</sub>Cl<sub>2</sub> as shown in Chapter 4. This small difference may be sufficient to provide the driving force for the rearrangement.

Rearrangement of the first intermediate also took place when trying to isolate it from the oligomers by flash chromatography on silica (eluting with CH<sub>2</sub>Cl<sub>2</sub> / methanol). It is therefore also reasonable to propose that silica catalyses this rearrangement process. As a result this intermediate could not be isolated free of oligomeric material or rearranged product **104** for full characterisation.

The discrete intermediate complex and oligomer possess the same type of structure. This is strongly suggested by the NMR experiments already discussed. For example the signal at 5.7 ppm is clearly a superimposition of sharp signals due to the discrete complex and a broad signal due to oligomers as can be seen by the changes which take place over a period of 24 hours (Figure 5.1).



**Scheme 5.10.** Summary of proposed steps in the formation of iron (II) pseudo-overhand knot 104.

### 5.4.3 Folding Around Zinc (II)

In an attempt to improve the yield of knotted product and develop an improved and simpler knotting procedure, several different metal ions were tested. The most successful procedure involved the use of zinc (II). Replacement of iron (II) with zinc (II) produced a huge improvement in the knotting process. Initially, addition of 1 equivalent of zinc (II) perchlorate hexahydrate in either 5% CD<sub>3</sub>OD / CD<sub>2</sub>Cl<sub>2</sub> or d<sub>7</sub>-DMF to a solution of **94** in 5% CD<sub>3</sub>OD or d<sub>7</sub>-DMF / CD<sub>2</sub>Cl<sub>2</sub> gave an insoluble white precipitate. However upon stirring or gentle shaking, the precipitate redissolved to give a clear, colourless solution. The <sup>1</sup>H NMR spectrum suggests that this is **105**, the zinc (II) analogue of **104**. No other products were detectable by NMR, and hence it is assumed that **105** is formed quantitatively (Scheme 5.11).

The most likely explanation for the production of insoluble material in this reaction is that the initial kinetic product is an insoluble oligomer which equilibrates to the more thermodynamically favoured knotted 1:1 complex. The high lability of zinc (II) complexes compared to iron (II) ensures that this equilibration process occurs rapidly and that no oligomeric products remain. In contrast to the reaction with iron (II), TFA is not required to induce equilibration, and the switch of solvents from dichloromethane to chloroform is not required. The reason for this difference is not clear.

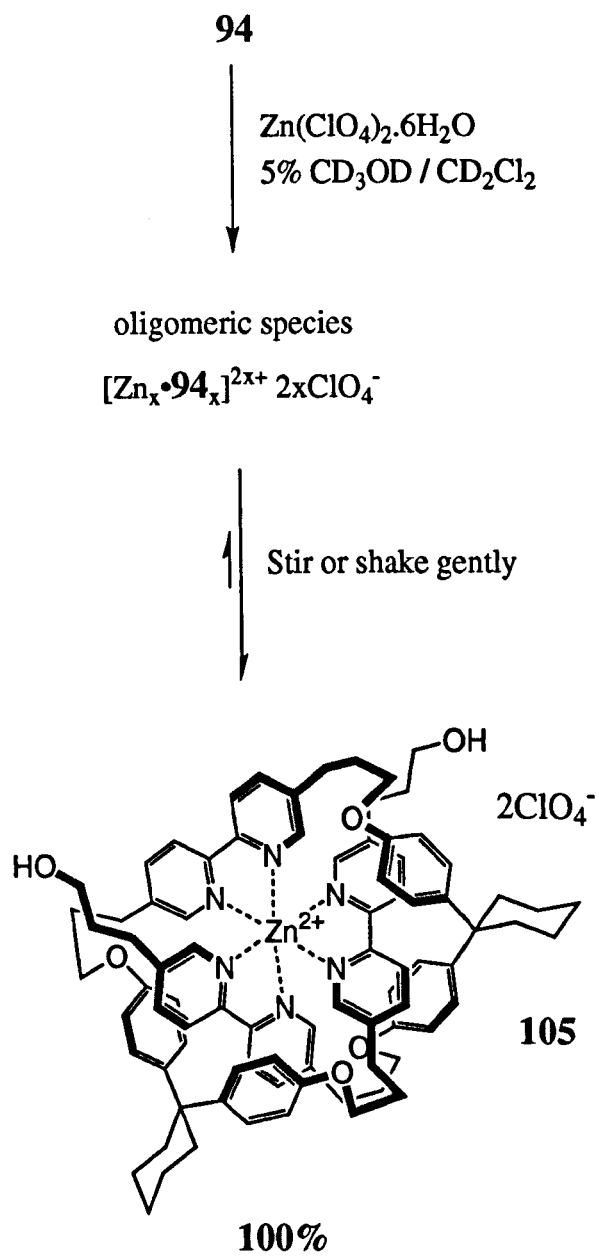
Since **94** can be readily accessed on reasonably large scale (batches of 5-6 g have been prepared) and knot **105** can be prepared quantitatively from **94**, this makes **105** an extremely versatile building block for the introduction of topological complexity into a variety of systems. The preparation of a number of interesting molecules incorporating **105** will be discussed in Chapter 6.

### 5.4.4 NMR Structure Determination of **105**

The structure of **105** was determined by 1D and 2D NMR techniques as for the iron (II) knot **104** already discussed in Section 5.4.1. All the spectra are in fact very similar. The aromatic region of the 250 MHz <sup>1</sup>H NMR spectrum is illustrated in Figure 5.7 along with the spectrum of **104** for comparison. Assignments of all protons are given in Table 5.3. Chemical shift changes induced on complexation are illustrated in Figure 5.8. The shifts on the bipyridine protons have again been corrected for the effects of metal ion coordination by quoting shifts relative to the tris bipyridine zinc (II) complex of the diester **4**<sup>‡</sup>. The 1:1 nature of the complex is illustrated by ES<sup>+</sup> MS (Figure 5.9). The NOEs observed in a 2D ROESY experiment are illustrated in Figure 5.10.

---

<sup>‡</sup> Prepared by addition of 3 equivalents of **4** to a solution of Zn(ClO<sub>4</sub>)<sub>2</sub>·6H<sub>2</sub>O in 5% CD<sub>3</sub>OD / CD<sub>2</sub>Cl<sub>2</sub>. <sup>1</sup>H NMR signals due to the bipyridine protons were observed at 7.79 ppm (H<sub>6</sub>), 8.03 ppm (H<sub>4</sub>) and 8.40 ppm (H<sub>3</sub>).



**Scheme 5.11.** Formation of zinc (II) pseudo-overhand knot 105.

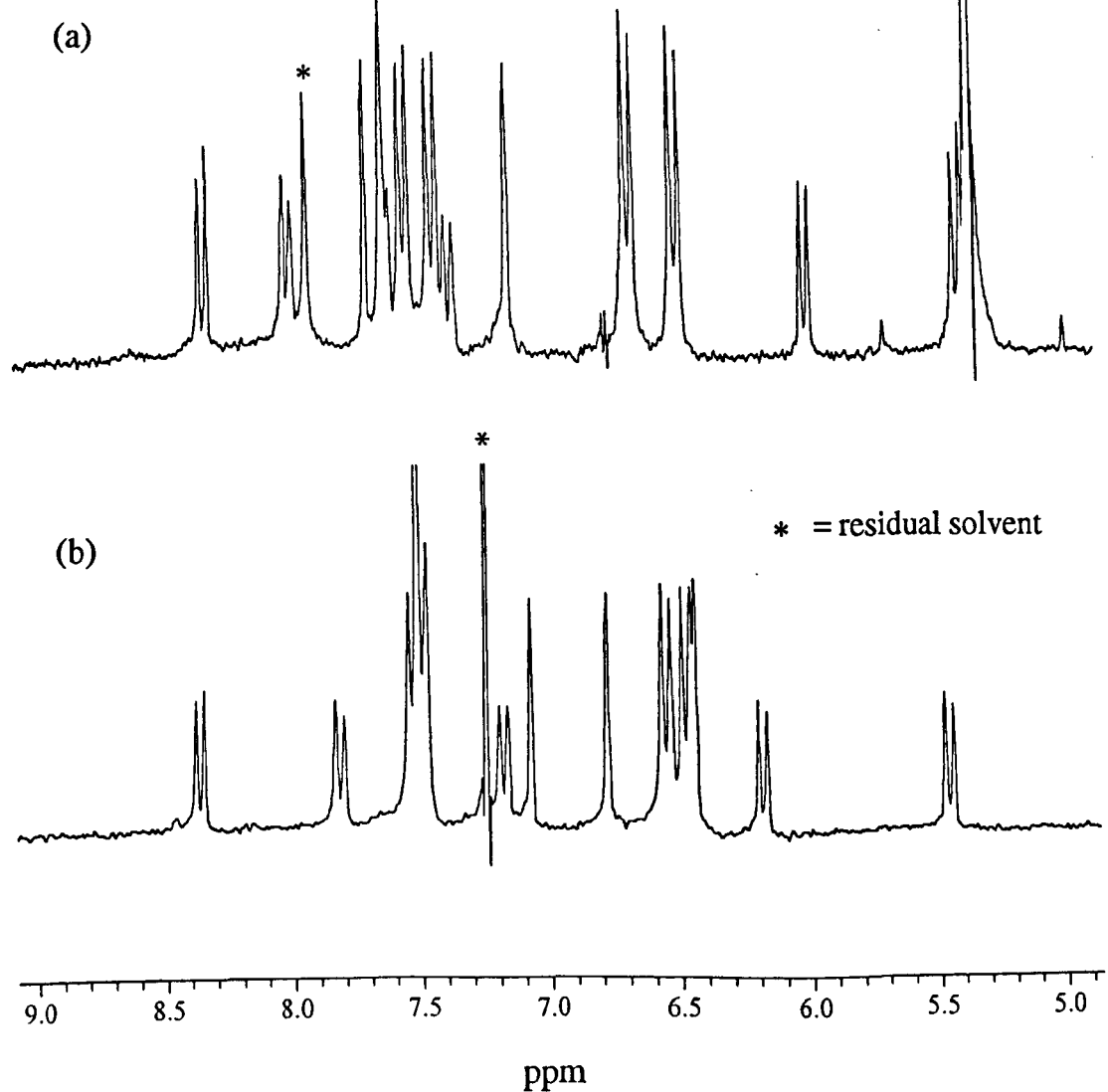
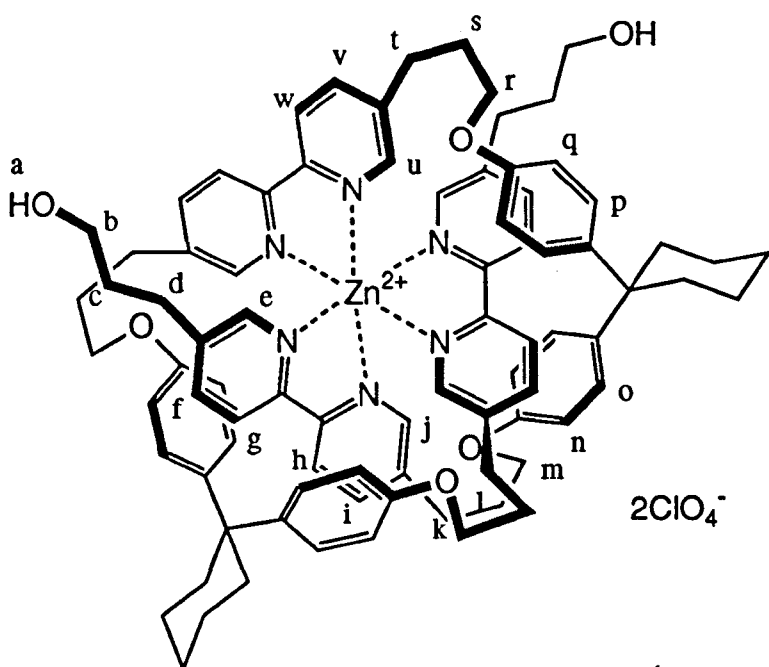


**Figure 5.7.** (a) Aromatic region of the 250 MHz  $^1H$  NMR spectrum of **105** in 5%  $d_7$ -DMF /  $CD_2Cl_2$  and (b) The aromatic region of iron (II) complex **104** in 5%  $CD_3OD$  /  $CDCl_3$  for comparison.

**Table 5.3.** Assignment of the 400 MHz  $^1\text{H}$  NMR spectrum of **105** in 5%  $\text{CD}_3\text{OD} / \text{CD}_2\text{Cl}_2$  together with the equivalent values for free oligomer **94** and complexation-induced changes in chemical shift.

Proton	Chemical Shift in <b>94</b> (ppm)	Reference Chemical Shift*	Chemical Shift in <b>105</b> (ppm)	Complexation $\Delta\delta$ .	Corrected Complexation $\Delta\delta$
$\text{H}_\text{a}$	not determined		not determined	-	-
$\text{H}_\text{b}$	3.69		3.32	-0.37	-0.37
$\text{H}_\text{c}$	1.91		ca. 1.50	-0.41	-0.41
$\text{H}_\text{d}$	2.76		2.52	-0.24	-0.24
$\text{H}_\text{e}$	8.50	7.79	7.66	-0.84	-0.13
$\text{H}_\text{f}$	7.63	8.03	7.36	-0.27	-0.67
$\text{H}_\text{g}$	8.25	8.40	5.40	-2.85	-3.00
$\text{H}_\text{h}$	8.25	8.40	5.94	-2.31	-2.46
$\text{H}_\text{i}$	7.63	8.03	7.56	-0.07	-0.47
$\text{H}_\text{j}$	8.50	7.79	7.13	-1.37	-0.66
$\text{H}_\text{k}$	2.84		1.48, 1.70	-1.36, -1.14	-1.36, -1.14
$\text{H}_\text{l}$	2.09		1.44, 1.93	-0.65, -0.16	-0.65, -0.16
$\text{H}_\text{m}$	3.93		2.71, 3.48	-1.22, -0.45	-1.22, -0.45
$\text{H}_\text{n}$	6.78		6.48	-0.30	-0.30
$\text{H}_\text{o}$	7.15		7.42	+0.27	+0.27
$\text{H}_\text{p}$	7.15		7.53	+0.38	+0.38
$\text{H}_\text{q}$	6.78		6.67	-0.11	-0.11
$\text{H}_\text{r}$	3.93		3.01, 3.67	-0.92, -0.26	-0.92, -0.26
$\text{H}_\text{s}$	2.09		1.41, 1.72	-0.68, -0.37	-0.68, -0.37
$\text{H}_\text{t}$	2.84		ca. 2.65	-0.19	-0.19
$\text{H}_\text{u}$	8.50	7.79	7.59	-0.91	-0.20
$\text{H}_\text{v}$	7.63	8.03	7.99	+0.36	-0.04
$\text{H}_\text{w}$	8.25	8.40	8.29	+0.04	-0.11

\* Chemical shifts observed in  $\text{Zn}(\text{II}) \cdot \text{4}_3 (\text{ClO}_4)_2$  (see footnote to page 100) are used to correct for the effects of coordination to the metal ion, and hence corrected changes in chemical shift reflect the environment of the proton in the 3D structure formed.

Two values listed for the aliphatic protons of **105** signify that the two protons of each methylene group become inequivalent in the complex.

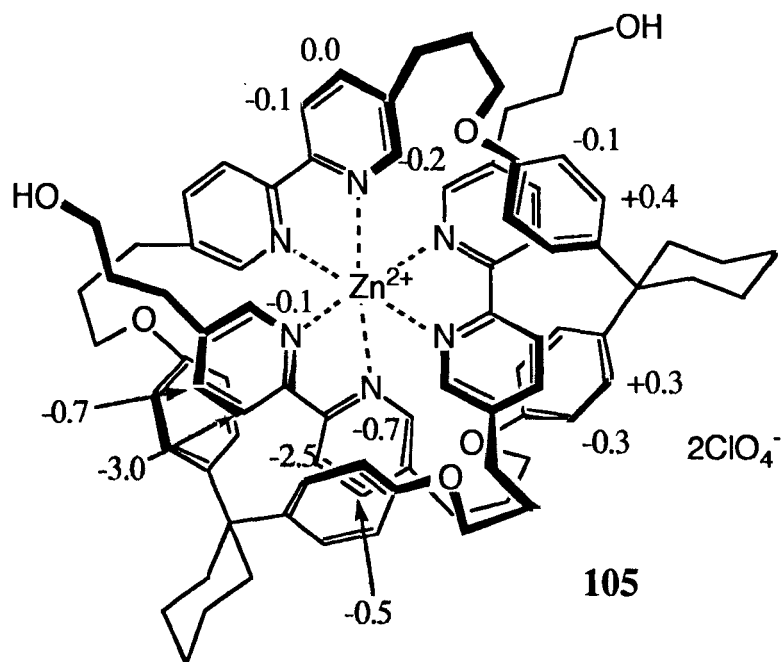


**Figure 5.8.** Conformation-induced chemical shifts for zinc (II) complex **105**.

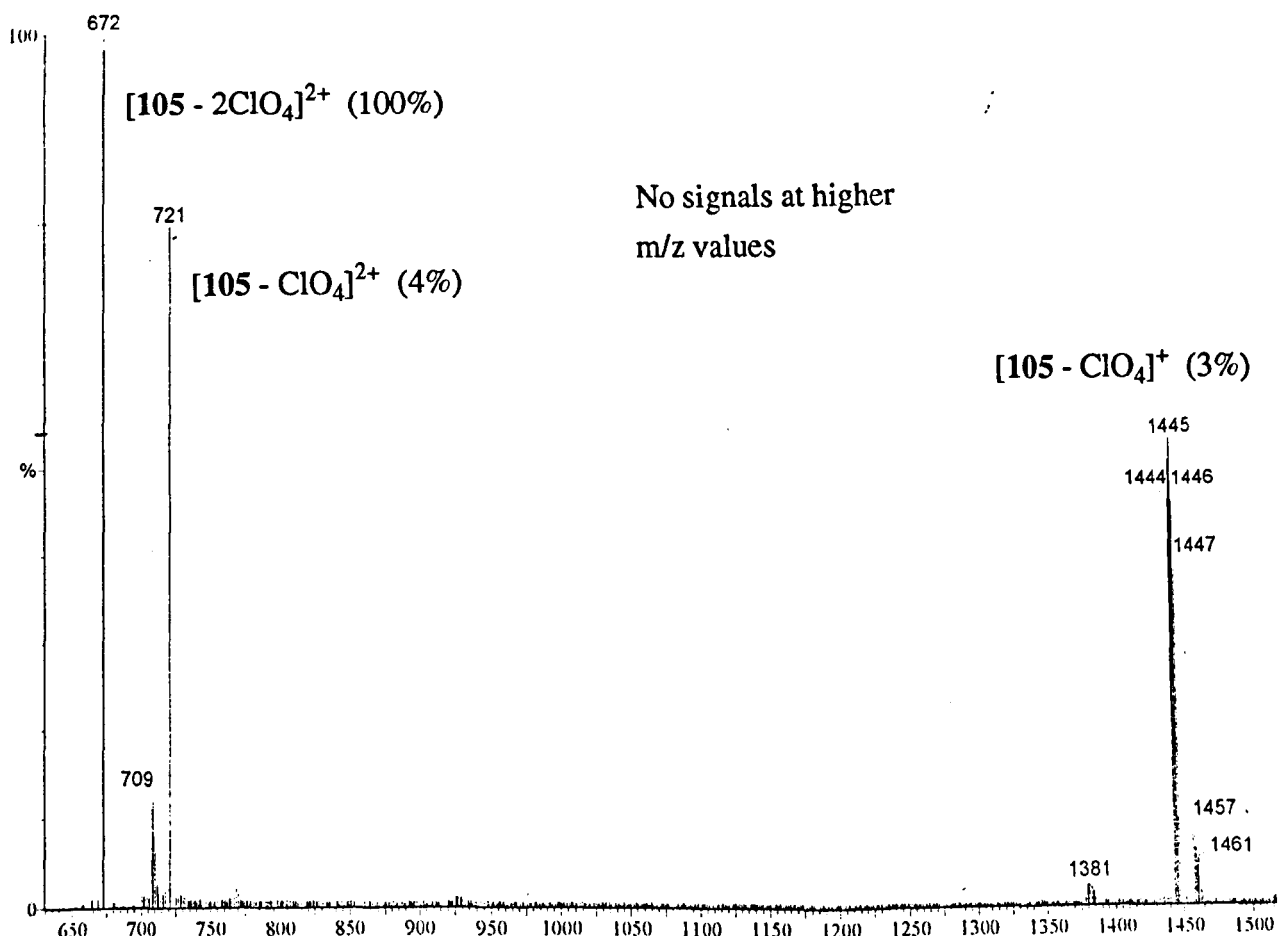


**Figure 5.9.** ES<sup>+</sup> mass spectrum of **105**

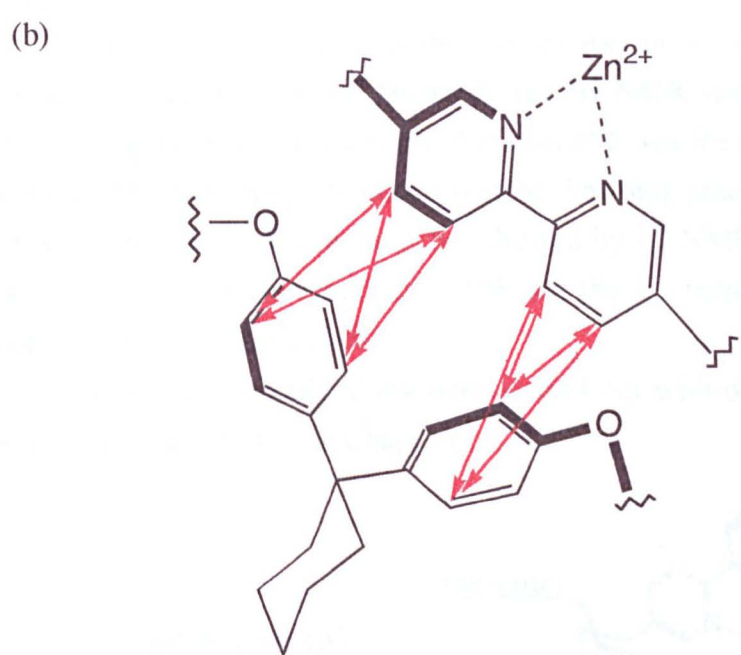
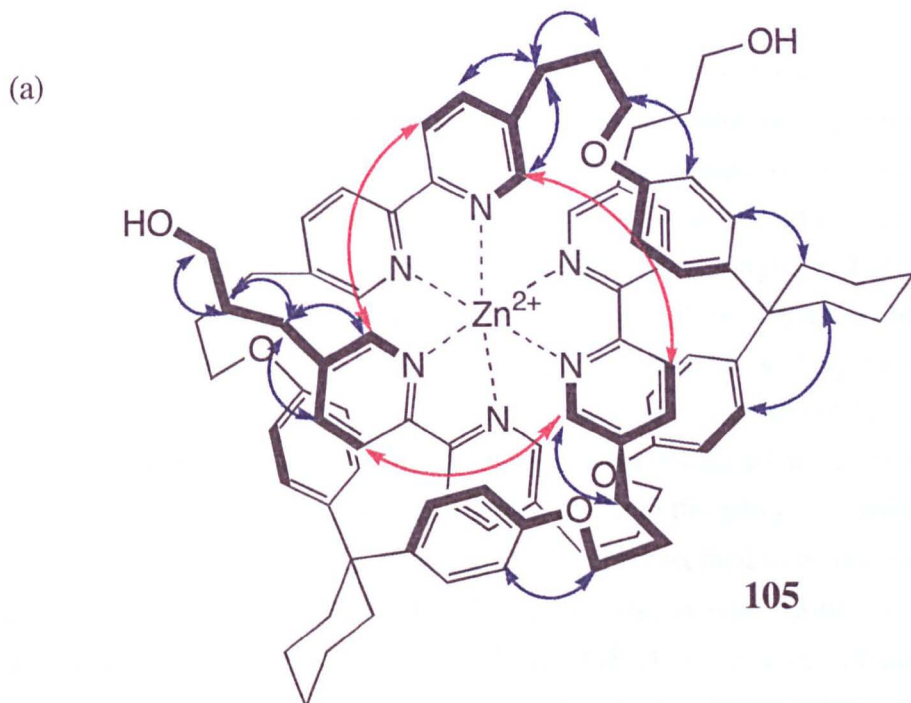


**Figure 5.10.** NOEs observed in a 400 MHz ROESY spectrum of **105** in 5%  $\text{CD}_3\text{OD} / \text{CDCl}_3$ . (a) bipyridine - bipyridine NOEs ( $\longleftrightarrow$ ) and aromatic - side chain NOEs ( $\longleftrightarrow$ ). (b) Expansion of bipyridine-bisphenol NOEs.

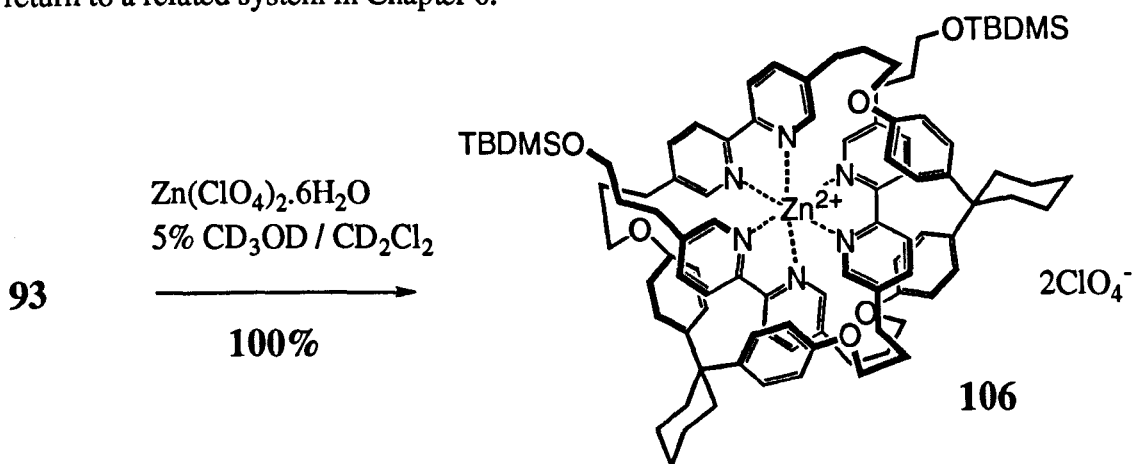
### 5.4.5 Effects of Terminal Groups

In the previous experiments, the terminal hydroxyl groups of oligomer **94** must "thread" through the partially formed  $Zn(II) \cdot \mathbf{94}$  coordination complex. Therefore, an interesting question arises concerning the effect of replacing the hydroxyl groups with something more bulky. Since the mechanism of formation of the knot seems likely to involve an initial coordination step followed by a threading step (Figure 5.11), this may slow down the rate of formation of the knot or prevent its formation altogether. Although this simplistic mechanism is likely to be greatly complicated by the fact that the third bipyridine unit (shown in red) will be involved in coordination to other zinc (II) ions (hence the formation of the oligomeric species discussed earlier), it does illustrate one key point: if the terminal group R is bulky, then the final threading step will be more difficult.

The ideal molecule to investigate this effect seemed to be intermediate **93** - i.e. the ligand prior to removal of the TBDMS protecting groups. **93** in 5%  $CD_3OD / CD_2Cl_2$  was treated with 1 equivalent of  $Zn(ClO_4)_2 \cdot 6H_2O$  in the same solvent system (Scheme 5.12). Unlike **94**, no insoluble material was produced which suggests that any oligomeric kinetic products formed are rendered soluble by the presence of the TBDMS groups.

Since in this reaction, all the species stay in solution, it should be possible to follow the reaction by NMR. However, the  $^1H$  NMR spectrum acquired immediately after mixing the reactants indicated that knot **106** was the only product present. Clearly the bulky TBDMS groups do not prevent the threading process occurring and do not slow it down to the extent where it can be followed by  $^1H$  NMR spectroscopy. **106** has a  $^1H$  NMR spectrum almost identical to **105** and the 1:1 nature of the complex was again confirmed by electrospray MS.

No further investigations were carried out with other terminal groups, but we return to a related system in Chapter 6.



**Scheme 5.12.** Preparation of knot **106** containing terminal TBDMS groups.

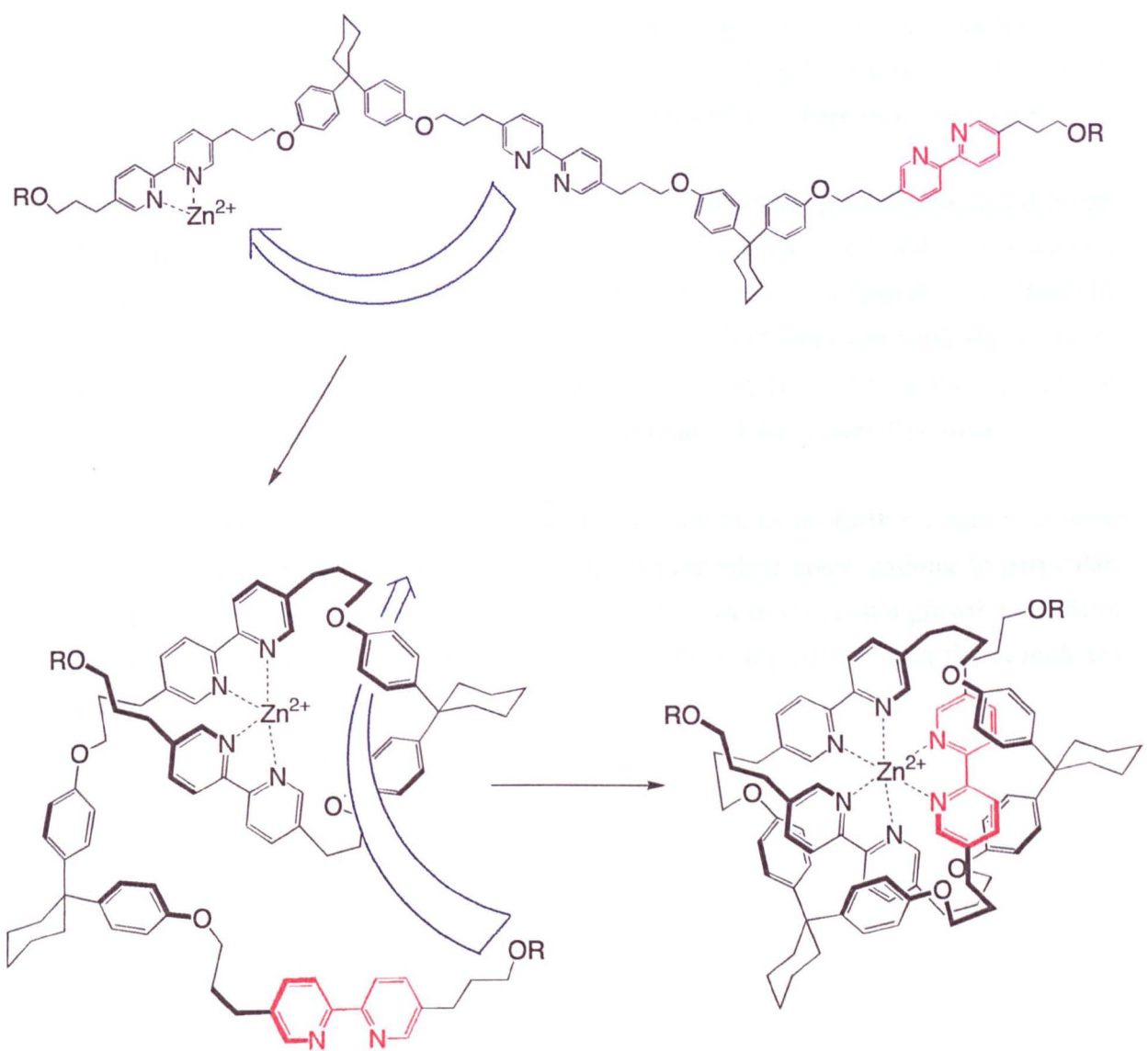


**Figure 5.11.** Proposed mechanism of formation of pseudo-overhand knots via subsequent coordination and threading steps.

### 5.4.6 Other Metal Ions

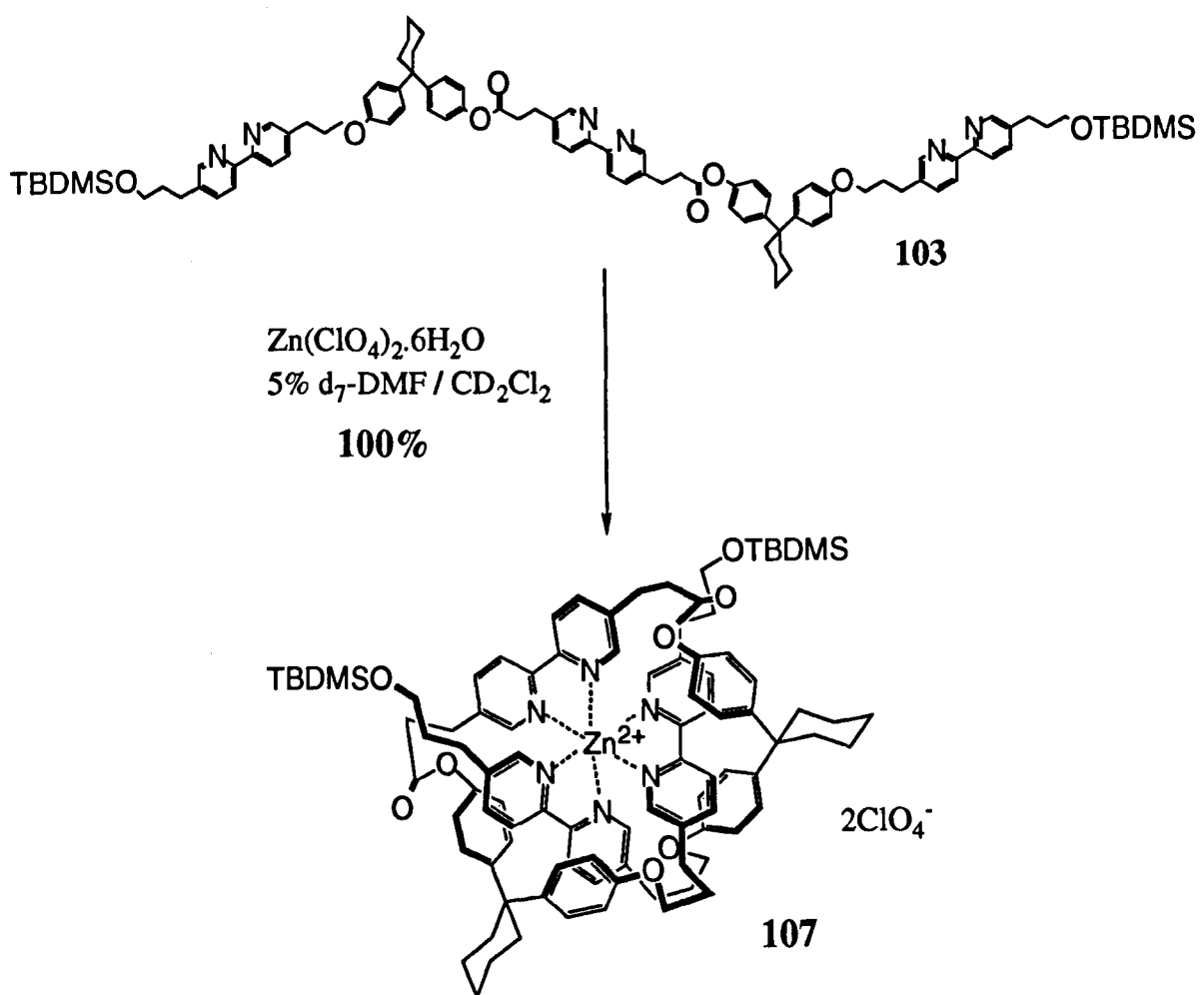
Having obtained good results with zinc (II), the obvious metal ion for comparison was cadmium (II), another Group 12 metal. However, Cd<sup>2+</sup> ions showed no interaction at all with ligand **94** and the <sup>1</sup>H NMR spectrum was completely unchanged upon addition of cadmium (II) perchlorate. A ligand which is completely selective for zinc (II) in the presence of cadmium (II) may also have potentially useful applications in the future.

Cobalt (II) was also investigated. The <sup>1</sup>H NMR of the product contained broad signals which had undergone significant shifts as would be expected in the presence of a paramagnetic metal ion. This made it impossible to determine conclusively if a cobalt (II) knot analogous to **104** had been produced although an ES<sup>+</sup> mass spectrum signal at m/z 670 (corresponding to Co(II)•**94**) and a major product on TLC with an almost identical R<sub>f</sub> to **104** were both highly suggestive of the formation of the required product.

As a result of the success of zinc (II) as a template, no further metal ions were studied although this may make an interesting area for future investigations. In particular, the variation of metal ion (and counterion) may help with single crystal growth to confirm the structure by X-ray diffraction which has not proved possible with the complexes studied to date.

## 5.5 Folding of the Mixed Ether-Ester Linked Oligomer

We turn now to the question of how critical the ether-linked structure of the oligomer is to the folding process. Mixed ether-ester linked oligomer **103** was used to investigate the effect of introducing two ester groups into the central section of the ligand. A solution of **103** in  $\text{CD}_2\text{Cl}_2$  was treated with 1 equivalent of  $\text{Zn}(\text{ClO}_4)_2 \cdot 6\text{H}_2\text{O}$  in a small volume of  $d_7\text{-DMF}$  with the immediate formation of knot **107** in quantitative yield (Scheme 5.13). The 1:1 nature of the complex was established from  $\text{ES}^+$  mass spectrometry. **107** was again characterised by NMR spectroscopy. Figure 5.12 illustrates the aromatic region of the 250 MHz  $^1\text{H}$  NMR spectrum along with assignments of all aromatic protons. Figure 5.13 shows the conformation induced differences in chemical shift. NOEs observed in a 2D ROESY experiment are illustrated in Figure 5.14.



**Scheme 5.13.** Preparation of knot **107** containing ether and ester linking groups.

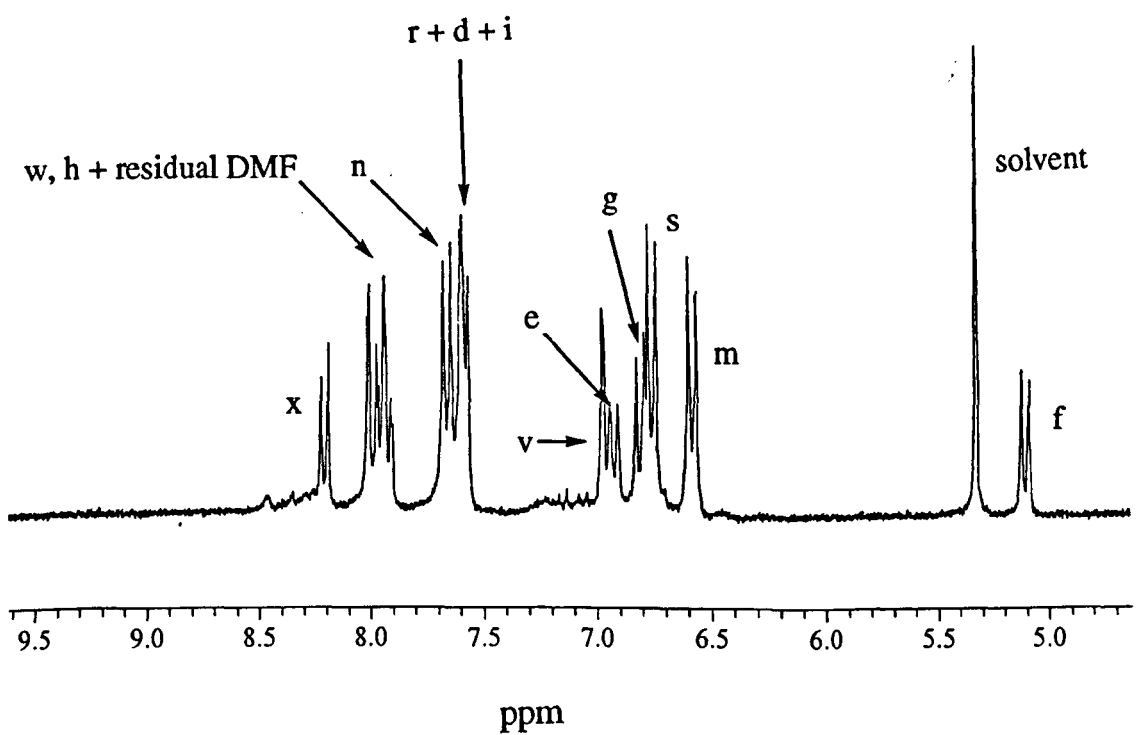
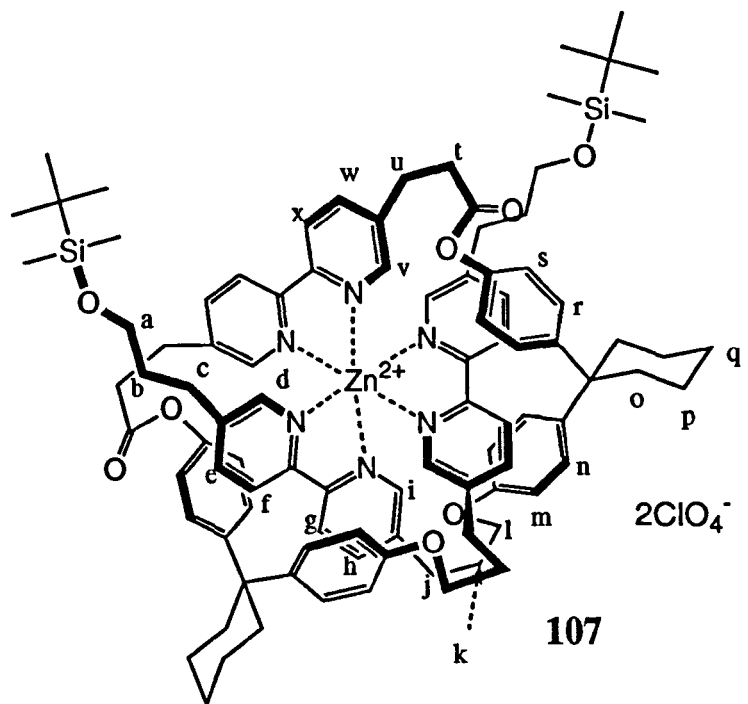


**Figure 5.12.** Aromatic region of the 250 MHz  $^1\text{H}$  NMR spectrum of 107.

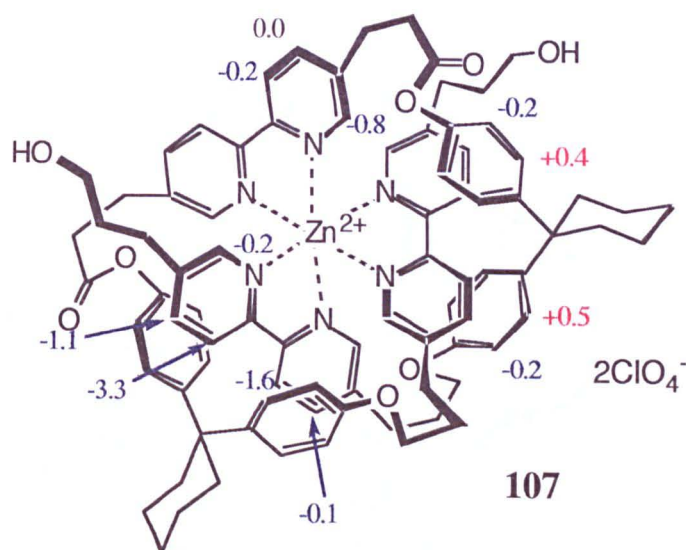


**Figure 5.13.** Conformation-induced changes in chemical shift upon folding of **103**. Bisphenol protons are relative to **103** and bipyridine protons are relative to  $Zn(II) \bullet 4_3(ClO_4)_2$  (see footnote to page 100).

Interestingly, the difference in chemical shift between the two bipyridine protons of the "bridged" bipyridine units  $H_f$  and  $H_g$  are enhanced relative to the ether-linked knots **105** and **106**. This presumably arises from the more rigid ester groups imposing a stricter control on the position of the bridging bisphenol unit.

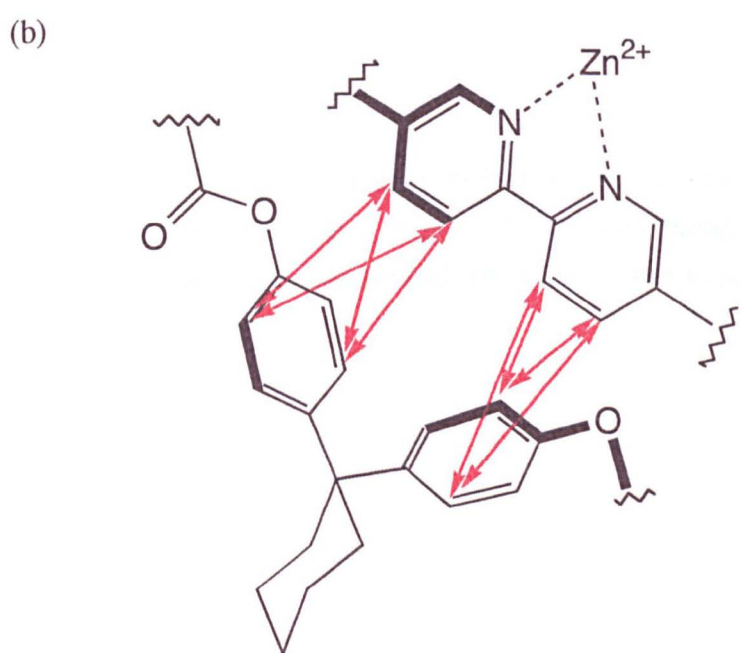
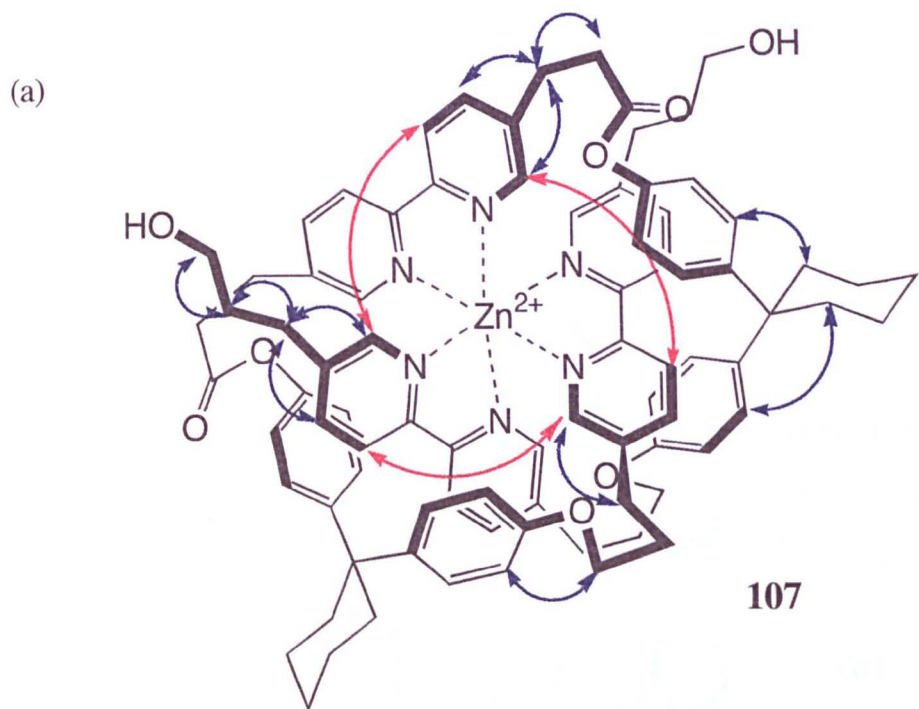


**Figure 5.14.** NOEs observed in a 400 MHz ROESY NMR spectrum of **107** in 5%  $d_7$ -DMF /  $CD_2Cl_2$ . (a) bipyridine - bipyridine NOEs ( $\longleftrightarrow$ ) and aromatic - side chain NOEs ( $\longleftrightarrow$ ). (b) Expansion of bipyridine-bisphenol NOEs.

Figure 5.15 shows the predicted ring-current induced changes in chemical shift for the bridged bisphenol-bipyridine motif. The chemical structure is shown with four specific atoms labeled M, each connected by a dashed line to a carbon atom. The predicted chemical shift values are: -0.28 (-0.27, -0.21) for the carbon atom connected to the bridging oxygen of the phenyl group; +0.30 (+0.35, +0.33) for the carbon atom connected to the bridging oxygen of the pyridine group; -3.01 (-2.66, -2.73) for the carbon atom connected to the bridging oxygen of the phenyl group; and -0.13 (-0.55, -0.57) for the carbon atom connected to the bridging oxygen of the pyridine group.

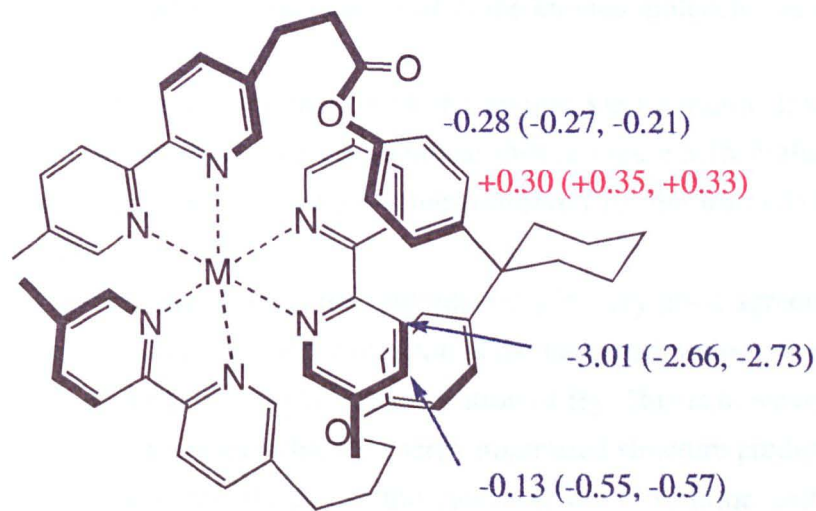


**Figure 5.15.** Predicted ring-current induced changes in chemical shift for the bridged bisphenol-bipyridine motif. Experimentally observed values (**104**, **105**) are shown in parentheses.

Figure 5.16 shows the predicted ring-current induced changes in chemical shift for the bisphenol-bipyridine motif.

The figure displays a complex organic molecule consisting of two bipyridine units linked by a central bridging group. The bridging group is a phenyl ring substituted with a carbonyl group (-C(=O)-) at one position and a methylene group (-CH<sub>2</sub>-) at another. A cyclohexane ring is attached to the methylene group. Dashed lines connect four specific atoms labeled 'M' to carbon atoms in the molecule. Predicted ring-current induced changes in chemical shift are indicated for these atoms:

- Atom M1 (top): -0.28 (-0.27, -0.21)
- Atom M2 (right): +0.30 (+0.35, +0.33)
- Atom M3 (bottom): -3.01 (-2.66, -2.73)
- Atom M4 (left): -0.13 (-0.55, -0.57)

## 5.6 Prediction of NMR Shifts

As discussed in the previous sections, the knotted structures exhibit very distinctive conformation-induced changes in chemical shift due to ring current effects. The use of the SHIFTY program (see Chapter 4, page 75) has already been described to enable the prediction of shifts based upon the relative orientations of aromatic rings in an energy-minimised structure of a simple model complex. This methodology has also been applied to the bipyridine-bisphenol structural motif of the knotted molecules as described below.

The energy-minimised conformation of the simple knot subunit described in Chapter 2 was used to predict the changes in chemical shift in Figure 5.15. Values shown in parentheses for comparison are average<sup>‡</sup> values observed for the iron (II) knot **104** and zinc (II) knot **105**.

It is evident that the predicted values are generally in very good agreement with those observed experimentally. The only exception is the underestimation of the upfield shift of bipyridine H<sub>4</sub> along with a slight overestimation of H<sub>3</sub>. This is however entirely consistent with the earlier observation that the energy minimised structure predicts that the bridging bisphenol unit sits directly across the centre of the bipyridine unit whereas experimental results suggest that it spends a significant proportion of time offset towards one of the bipyridine H<sub>3</sub> protons. Presumably the bridging bisphenol is "skewed" across the bipyridine unit (Figure 5.16(a)) rather than the predicted conformation of Figure 5.16 (b). It is also worth noting that since ring current effects exhibit a marked distance dependence, a very small error in predicting the conformation may lead to a relatively large error in prediction of chemical shift.

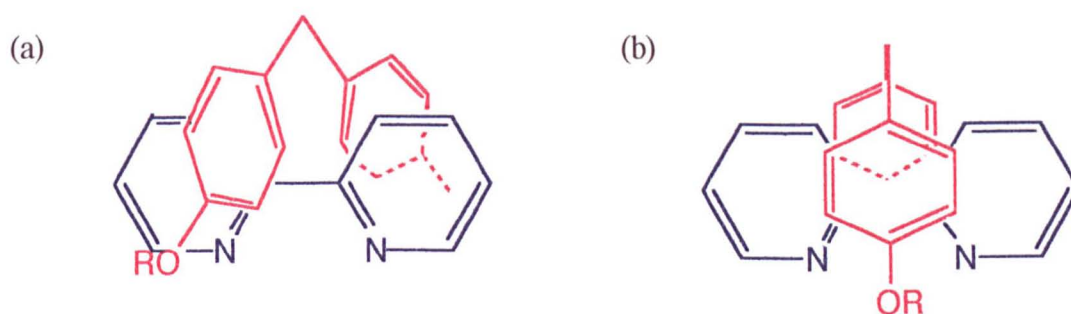


**Figure 5.16.** Possible conformations of the bridging bisphenol-bipyridine motif.

<sup>‡</sup> As stated previously, the H<sub>3</sub> and H<sub>4</sub> protons on opposite sides of each bipyridine unit actually exhibit slightly different chemical shifts which presumably arises from the "bridging" bisphenol unit not being exactly centred on each bipyridine unit but rather being offset to one side to allow a maximum  $\pi$ - $\pi$  interaction with H<sub>3</sub>. Since this effect is not predicted by the molecular modelling studies, values quoted here are an average of the two signals observed.

## 5.7 Conclusions

Linear molecules have been prepared that in the presence of a suitable octahedral metal ion can spontaneously fold into a knotted structure which we have termed a *pseudo-overhand knot*. This folding process is directed by metal-ligand and aromatic interactions. By judicious choice of metal ion, this folding process can be made to proceed in quantitative yield and has provided a simple route to the large scale preparation of a novel topological building block which via its incorporation into other structures will readily allow the introduction of topological complexity into a variety of systems.

We have demonstrated that there is some freedom for variation of the oligomer structure without any detrimental effects on the yield of the folding reaction. For example, incorporation of more bulky terminal groups or variation of the functionality linking the components of the oligomer does not inhibit the process.

---

---

# *Chapter 6*

---

---

## **Synthesis of Molecular Knots**

## 6.1 Introduction

As already discussed in Chapter 2, the pseudo-overhand knot structure could make an extremely versatile intermediate for the preparation of other knotted topologies. Some of those possibilities based upon the zinc (II) stabilised pseudo-overhand knot 105 are outlined in Figure 6.1.

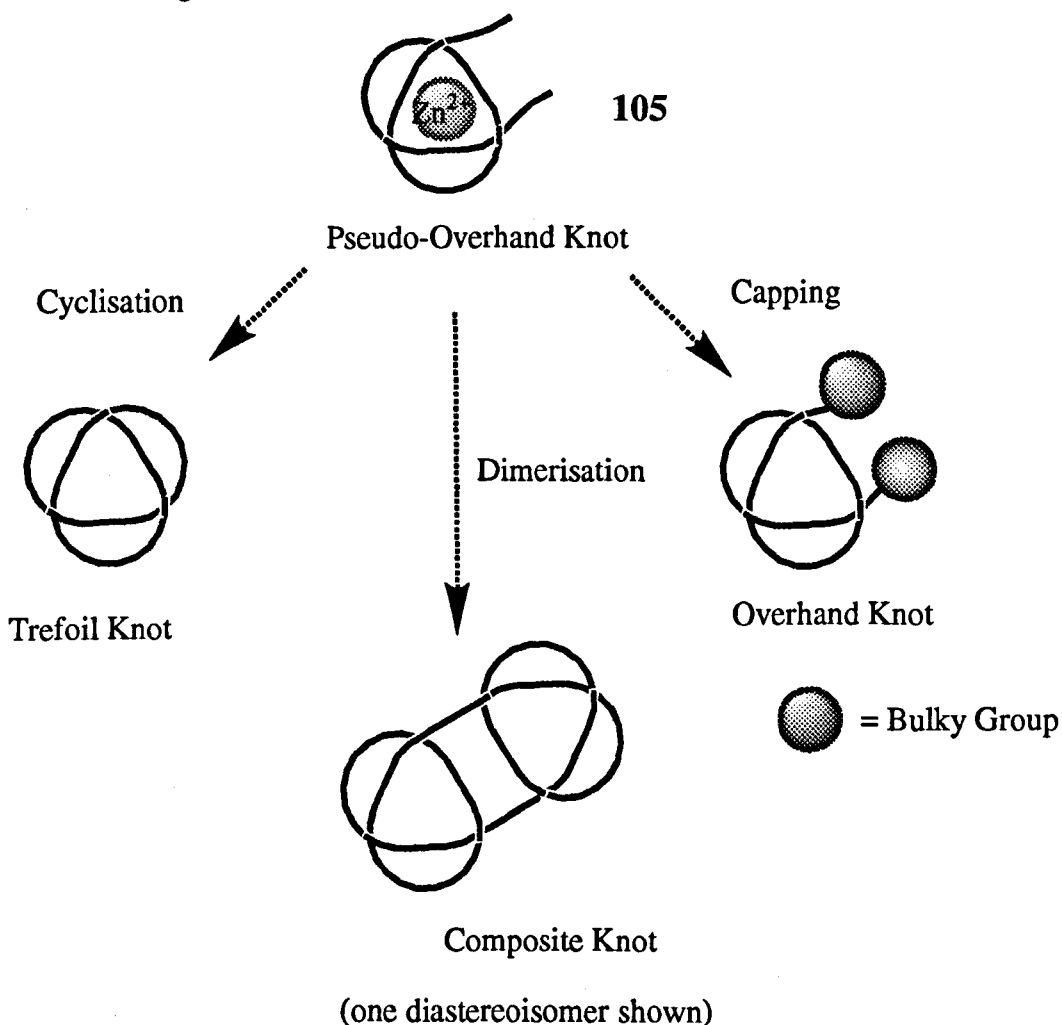


**Figure 6.1.** Schematic representation of the formation of three interesting topologies from the zinc (II) pseudo-overhand knot 105.

This chapter describes attempts to prepare two of these structures: the overhand knot via the attachment of bulky terminal groups and the trefoil knot via a macrocyclisation reaction. Lack of time precluded attempts at the preparation of composite knots. Firstly, we consider the choice of bond-forming reactions to join the units together. We then go on to discuss the design and preparation of a suitable terminal stopper group for use in the overhand knot synthesis and subsequently consider the preparation of an overhand knot. Finally, the synthesis of a trefoil knot is presented.

## 6.2 Choice of Bond-forming Reactions

### 6.2.0 Ether Links

Since the oligomer syntheses involved extensive use of Mitsunobu-type reactions to form alkyl-aryl ethers, this seemed a useful possibility for forming new bonds at the terminal hydroxyl groups of **105**. A model reaction between **105** and phenol using a large excess of ADDP and TBP<sup>‡</sup> in 5% d<sub>7</sub>-DMF / CD<sub>2</sub>Cl<sub>2</sub> (Scheme 6.1) was followed by <sup>1</sup>H NMR spectroscopy by successive acquisition of NMR spectra over a period of several hours. Not only was it important to follow the progress of the reaction, but it was also vital to confirm that the reaction conditions did not result in the decomposition (*i.e.* unknotting) of the labile zinc (II) complex.

The NMR experiments confirmed that **105** was stable under the reaction conditions, but the formation of the phenyl ethers did not occur. The only explanation that we can offer for this failure to react is that the terminal hydroxyl groups are too hindered. As can be seen from the structure in Figure 6.2 - a likely intermediate in the reaction - the electrophilic carbon centre that is attacked by the phenol nucleophile is hindered by both the bulk of the knot molecule and the ADDP / TBP adduct. Attempts to form ether links were therefore abandoned.

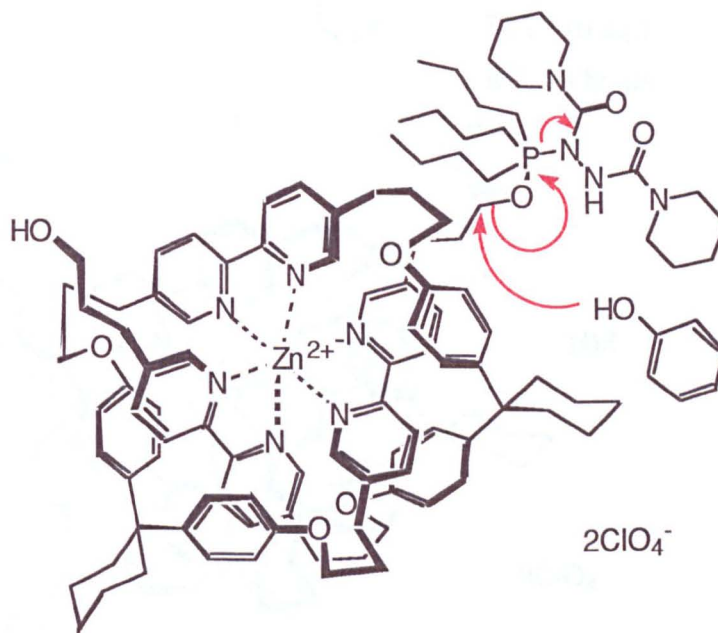
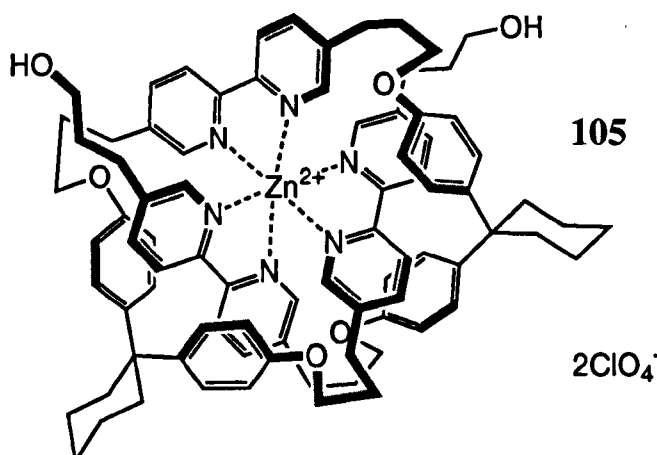


**Figure 6.2.** A possible intermediate in the reaction between **105** and phenol.

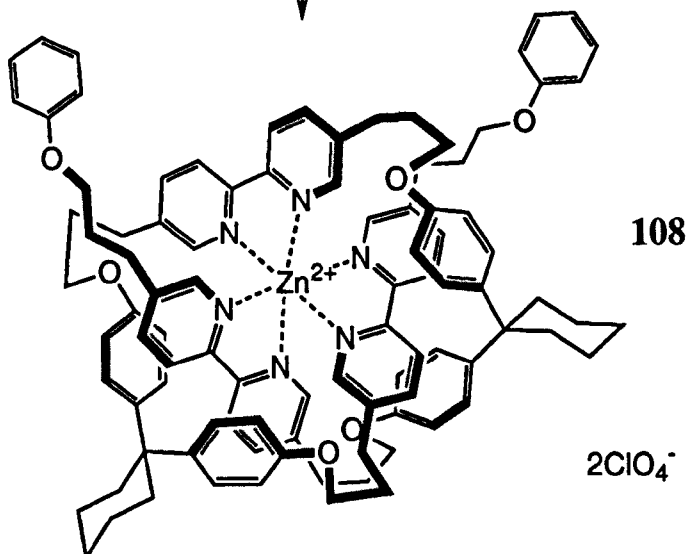
<sup>‡</sup> A large excess of the coupling reagent was necessary to compensate for the presence of approximately six molecules of water per molecule of **105** present in the mixture (derived from the hexahydrate zinc (II) salt used). Repetition of an earlier coupling reaction indicated that both the presence of a large excess of coupling reagent and 5-10% DMF in the solvent had no adverse effects on the yield obtained.

94

100%  
 $\downarrow$   
 $Zn(ClO_4)_2 \cdot 6H_2O$   
5% d<sub>7</sub>-DMF / CD<sub>2</sub>Cl<sub>2</sub>



$\downarrow$   
 $\text{C}_6\text{H}_5\text{OH}$  ADDP (10 eq.)  
TBP (10 eq.)  
RT, 18 hours



Scheme 6.1. Attempted preparation of 108 in a model reaction.

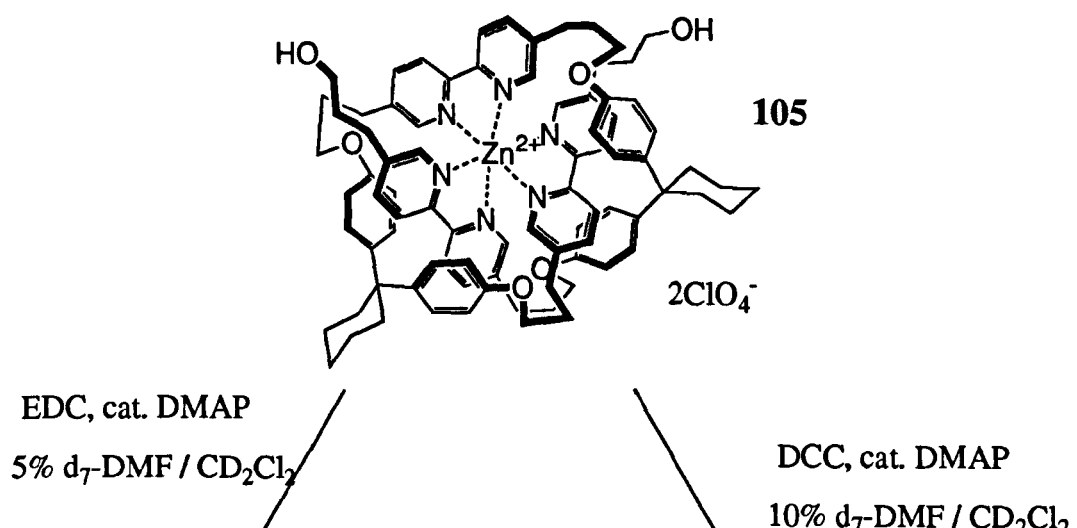
### 6.2.1 Ester Links

Another suitable reaction to form new bonds at the terminal hydroxyl groups of **105** is the use of activated acids to give esters. It was decided that the use of acid chlorides in this reaction would be impractical due to the presence of extraneous water in the reaction mixture that could not be removed. The best possibility therefore seemed to be the use of a carbodiimide coupling agent to facilitate a direct reaction with unactivated acids. The presence of extraneous water could then be compensated for by the use of a large excess of the coupling reagent. For initial work it was decided to use 1-(3-dimethylaminopropyl)-3-ethylcarbodiimide hydrochloride (EDC). As already discussed in Chapter 5, this reagent has the advantage that excess reagent and by-products can be removed by washing with aqueous acid - an important consideration since a large excess of the reagent is required in these reactions.

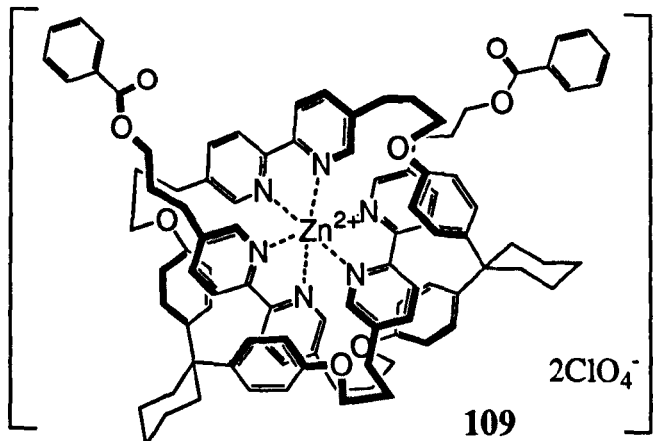
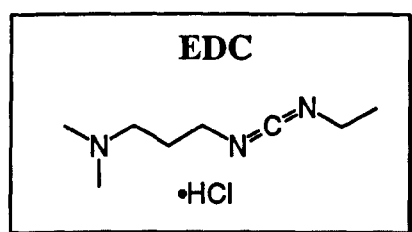
In an initial NMR experiment, a solution of **105** was prepared in 10% d<sub>7</sub>-DMF / CD<sub>2</sub>Cl<sub>2</sub>. The stability of the complex was found to be unaffected by addition of 2.2 equivalents of benzoic acid (as evidenced by the two characteristic doublets at 5.4 ppm and 6.0 ppm). However, upon addition of EDC, **105** decomposed immediately to give free **94**. The reason for this was not clear initially, and it was therefore decided to repeat the reaction using a simpler coupling agent: 1,3-dicyclohexylcarbodiimide (DCC).

Upon repetition of the reaction with DCC, no decomposition occurred on addition of the coupling reagent or a catalytic amount of DMAP. The product **109** seemed to form in good yield based on the <sup>1</sup>H NMR spectra. Upon washing the product with 1M aqueous HCl, the metal ion was removed and the diphenyl ester **110** was obtained. This product was however heavily contaminated with DCC and the N,N'-dicyclohexylurea (DCU) coupling by-product. Repeated chromatography on silica failed to produce pure **110** (Scheme 6.2).

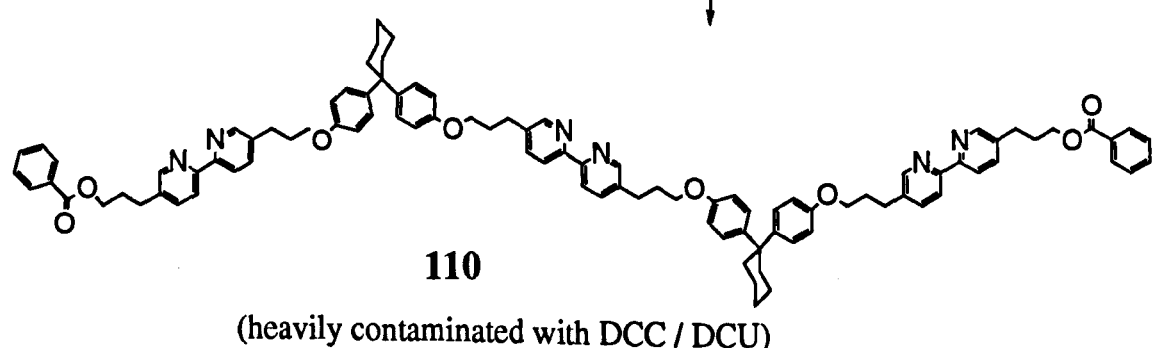
These initial experiments suggested that the use of a carbodiimide coupling agent to produce ester links was a viable procedure. However, the use of DCC was likely to result in extremely problematical purification of the products obtained. The use of EDC, a coupling agent that would alleviate this problem, was not possible because it caused decomposition of the zinc (II) complex. It was therefore important to answer the question: what structural feature of EDC is responsible for causing complex decomposition, and is it possible to change it?



Complex decomposes  
to **94**



aqueous HCl  
(removes  $\text{Zn}^{2+}$ )



**Scheme 6.2.** Preparation of **110** in a model ester-coupling reaction.

## 6.2.2 Stability Studies of complex 105

The only functionality present in EDC that is not found in DCC is the tertiary amine (responsible for conferring solubility in aqueous acid) and the fact that EDC is a hydrochloride salt. We therefore decided to implement some stability studies by adding various reagents to a solution of **105** in 10% d<sub>7</sub>-DMF / CD<sub>2</sub>Cl<sub>2</sub>. The results are outlined in Table 6.1. Stability was determined by the presence or absence of the two characteristic doublets at 5.4 ppm and 6.0 ppm approximately 10 minutes after addition.

**Table 6.1. Stability of **105** to various reagents.**

Reagent	105 stable?
Acetic acid (5 eq.)	Yes
Acetic acid (20 eq.)	Yes
Et <sub>3</sub> N (5 eq.)	Yes <sup>a</sup>
DMAP	Yes
<i>tert</i> -butylbenzoyl chloride (10 eq.)	No
Et <sub>4</sub> N <sup>+</sup> Cl <sup>-</sup> •H <sub>2</sub> O (5 eq.)	No
Et <sub>4</sub> N <sup>+</sup> Cl <sup>-</sup> •H <sub>2</sub> O (5 eq.) + AgOTf (5 eq.)	Yes <sup>b</sup>
AgOTf	No

<sup>a</sup> A small (and variable) amount of a white precipitate was produced on addition of Et<sub>3</sub>N. <sup>1</sup>H NMR spectra however confirm that **105** is unchanged. The most likely explanation is that Et<sub>3</sub>N removes any small excess of zinc (II) that may be present in the form of an insoluble zinc (II) amine complex.

<sup>b</sup> Although **105** is unstable in the presence of both Et<sub>4</sub>N<sup>+</sup>Cl<sup>-</sup>•H<sub>2</sub>O and AgOTf, when both are present in equal amounts, a white precipitate presumed to be AgCl is produced and **105** is stable. If **105** is decomposed by addition of one of these reagents, then it can be regenerated by addition of an equal amount of the other.

The experiments with acetic acid confirmed that **105** is stable in the presence of acid, and protonation from the hydrochloride present in EDC is probably not the cause of complex decomposition. Similarly, stability in the presence of triethylamine suggests that the tertiary amine functionality of EDC is not responsible for the decomposition of **105**. This suggested that the chloride ion of EDC was the most likely candidate for causing decomposition, and this was confirmed by the addition of Et<sub>4</sub>N<sup>+</sup>Cl<sup>-</sup>•H<sub>2</sub>O to **105** which resulted in immediate decomposition. The dramatic change in the aromatic region of the <sup>1</sup>H NMR spectrum upon decomplexation is illustrated in Figure 6.3.

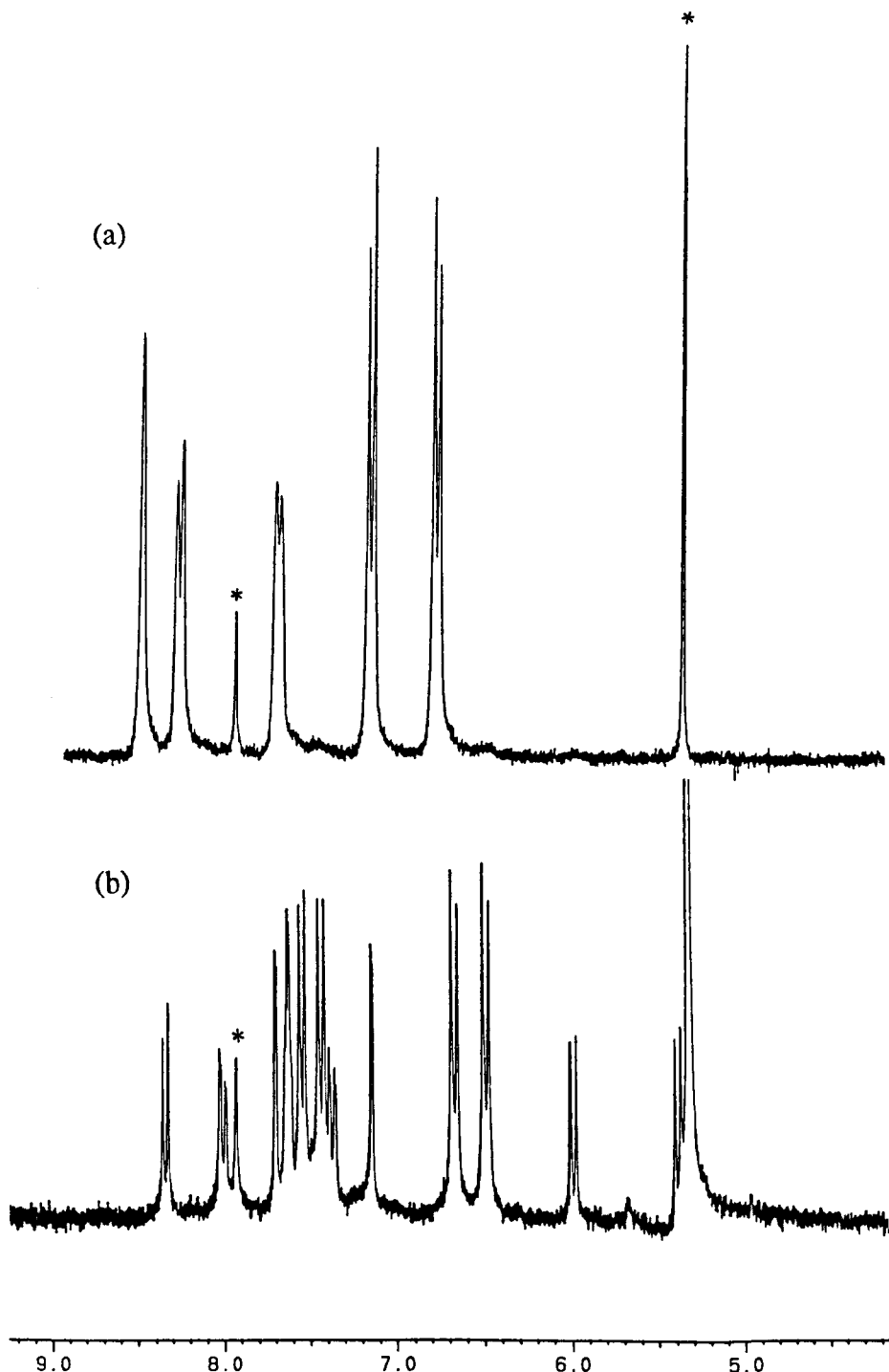
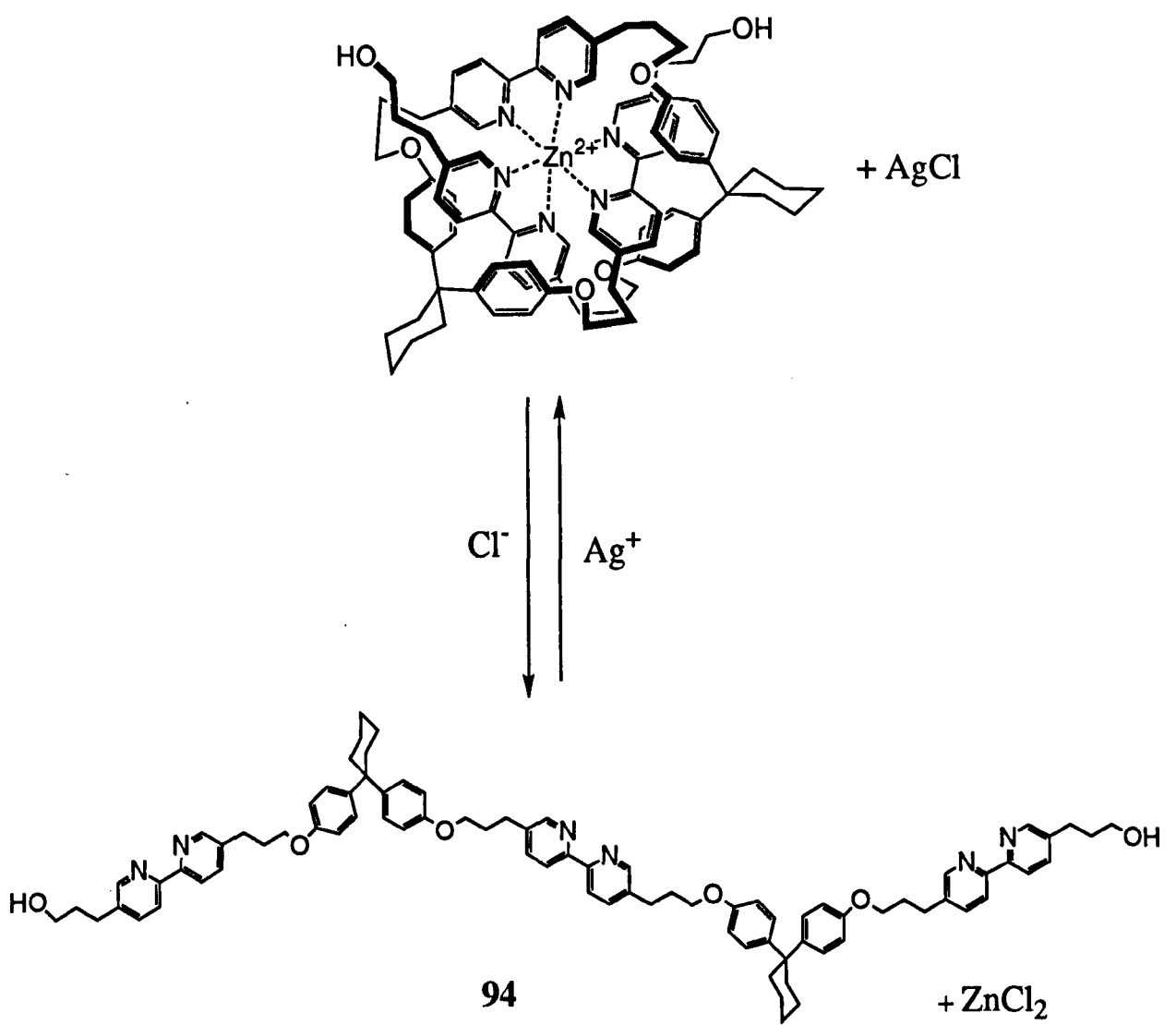


**Figure 6.3.** The change in the aromatic region of the  $^1\text{H}$  NMR spectrum of complex 105 upon decomplexation. (a) Free ligand 94 and (b) Complex 105. Both spectra were recorded in 10%  $d_7\text{DMF}/\text{CD}_2\text{Cl}_2$ . (\*) denotes residual solvent peaks.

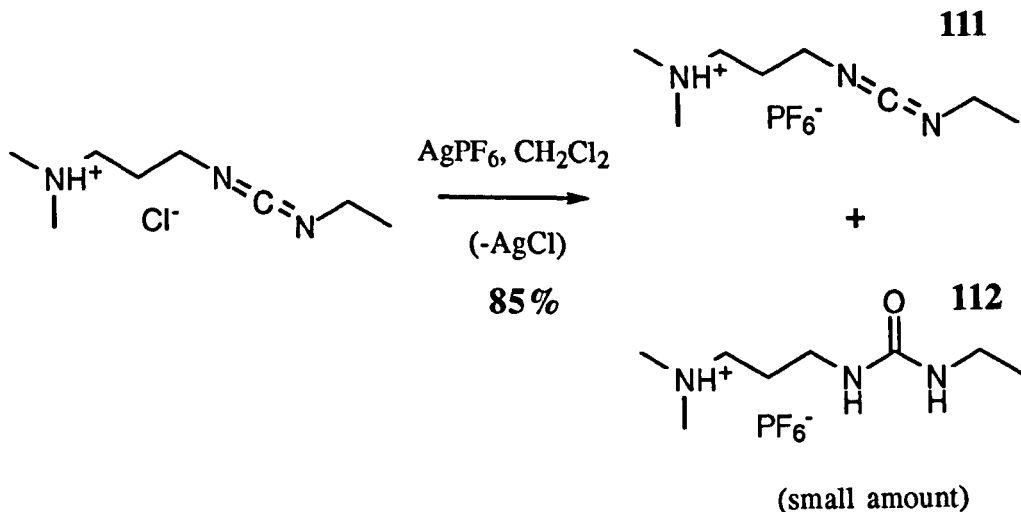


**Scheme 6.3.** Control of knotting and unknotting of strand 94 by the presence or absence of chloride.

As shown in Table 6.1, the presence / absence of chloride ions gives control over the knotting / unknotting of strand **94**. It was shown that unknotting by addition of chloride ions followed by a reknotted process upon addition of silver (I) triflate formed a cycle that could be repeated indefinitely (Scheme 6.3). This of course also indicates that **105** is stable in the presence of both  $\text{Et}_4\text{N}^+$  and  $\text{TfO}^-$ .

### 6.2.3 Development of a New Carbodiimide Coupling Reagent

Since the chloride ion in EDC had been shown to be responsible for causing decomposition of zinc (II) complex **105**, it was decided to prepare an EDC reagent bearing a non-nucleophilic counterion. Switching the counterion from chloride to hexafluorophosphate to give the new reagent 1-(3-dimethylaminopropyl)-3-ethylcarbodiimide hexafluorophosphate [EDC•PF<sub>6</sub>] **111** was achieved by stirring a CH<sub>2</sub>Cl<sub>2</sub> solution of EDC with silver (I) hexafluorophosphate and removing the AgCl precipitate formed (Scheme 6.4). The product was also shown by <sup>1</sup>H NMR to contain a small amount of the hydrolysis product **112** presumably arising from a reaction with extraneous water during the ion exchange reaction. Since EDC•PF<sub>6</sub> was to be used in a large excess in any coupling reactions performed, this was not considered a problem and no attempts at purification were made.

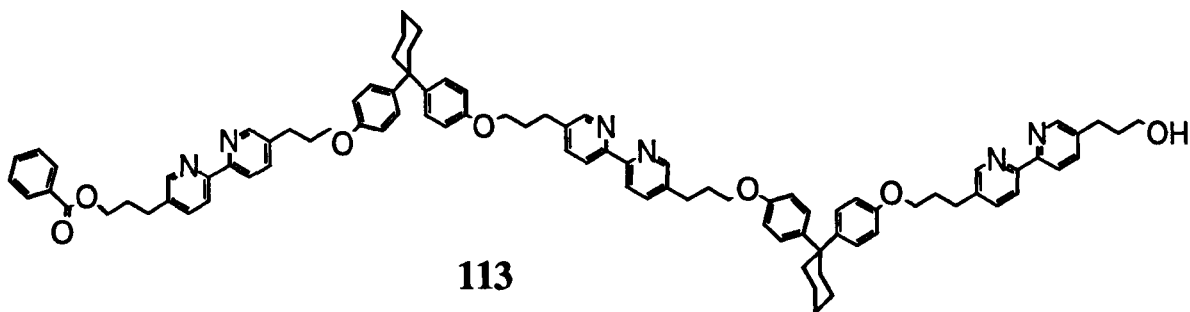


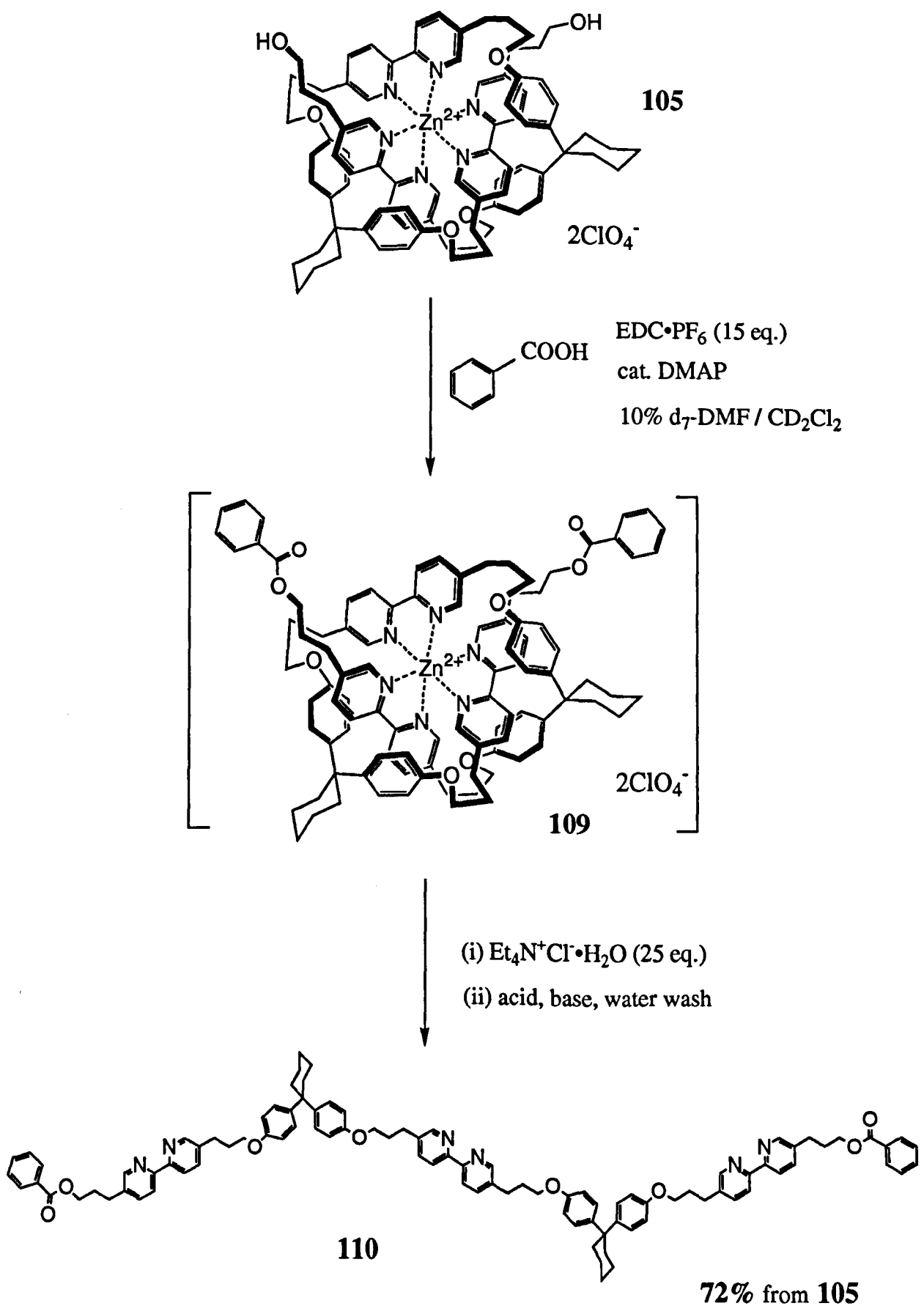
Scheme 6.4. Preparation of the new carbodiimide coupling reagent EDC•PF<sub>6</sub> **111**.

### 6.2.4 Model Reaction With EDC•PF<sub>6</sub>

The new EDC•PF<sub>6</sub> reagent was used in a repeat of the failed EDC coupling reaction discussed previously. **105** and 2.2 equivalents of benzoic acid were treated with 15 equivalents of EDC•PF<sub>6</sub> and 0.2 equivalents of DMAP in 10% d<sub>7</sub>-DMF / CD<sub>2</sub>Cl<sub>2</sub> (Scheme 6.5). The progress of the reaction was monitored by <sup>1</sup>H NMR spectroscopy. The fact that the knotted structure remained intact throughout the reaction was evidenced by the continued presence of the doublets at 5.4 ppm and 6.0 ppm.

The product was demetallated by treatment with 25 equivalents of Et<sub>4</sub>N<sup>+</sup>Cl<sup>-</sup>•H<sub>2</sub>O. Sequential washes with aqueous acid and base followed by water removed all excess coupling agent and urea by-products as well as the metal ions and Et<sub>4</sub>N<sup>+</sup>Cl<sup>-</sup>. The <sup>1</sup>H NMR spectra and TLC analysis of this crude product indicated that **110** was formed in good yield. An isolated yield of 72% was obtained after chromatography to remove a small amount of an impurity suspected to be the mono-benzoylated ligand **113**.



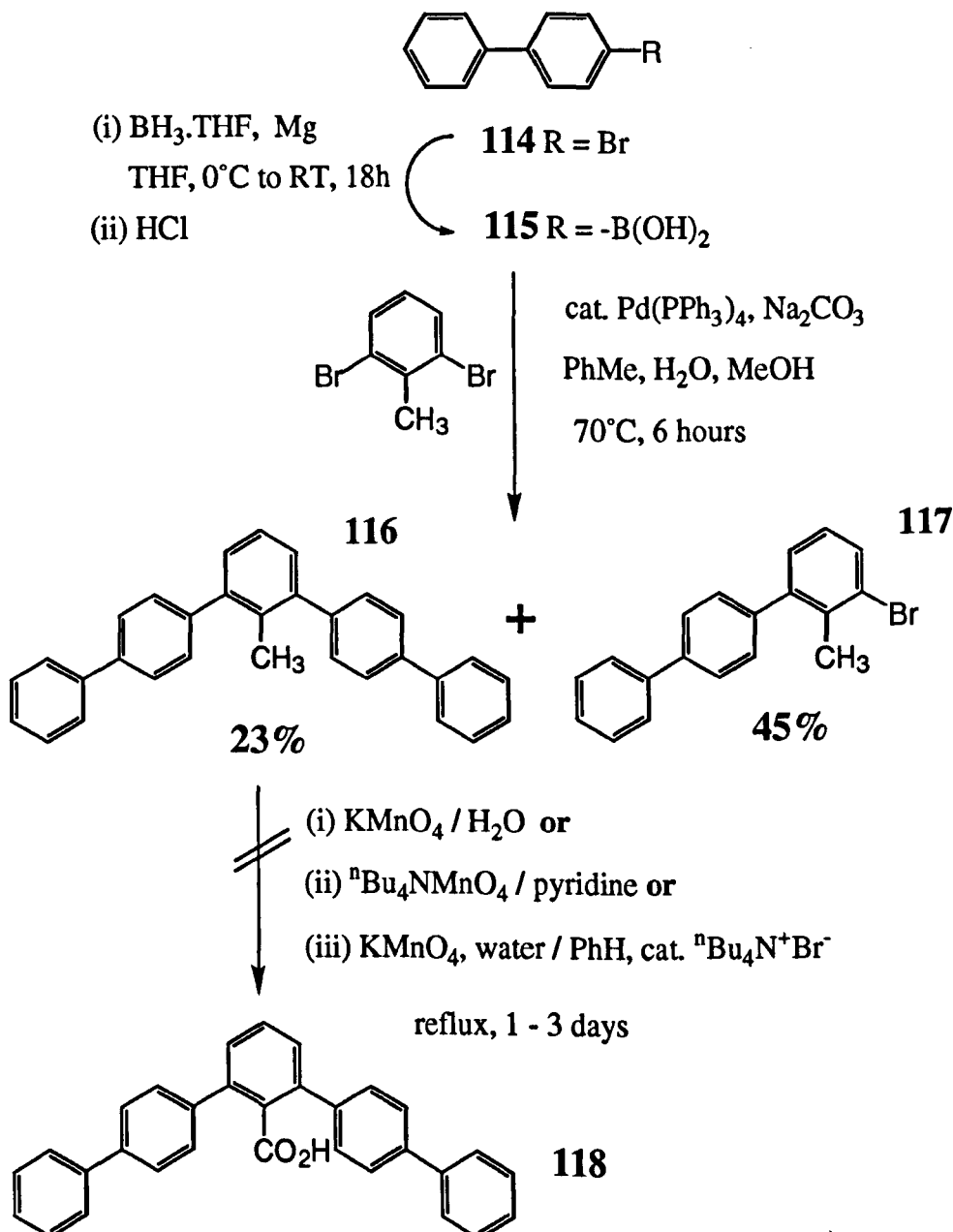


**Scheme 6.5.** Preparation of **110** using  $\text{EDC}\cdot\text{PF}_6$  coupling.

## 6.3 Synthesis of a Stopper Group

### 6.3.0 A Benzoic Acid Derived Stopper Group

CPK models suggested that the stopper group would need to be extremely large in order to prevent unthreading due to the relatively flexible nature of the knot structure after removal of the metal ion. The first target molecule proposed was the 2,6-diaryl benzoic acid **118**. This molecule seemed to possess the required bulk as well as the necessary functionality for ready attachment to the terminal hydroxyl groups of the pseudo-open knot via the formation of ester links. A first attempt at its synthesis is outlined in Scheme 6.6.



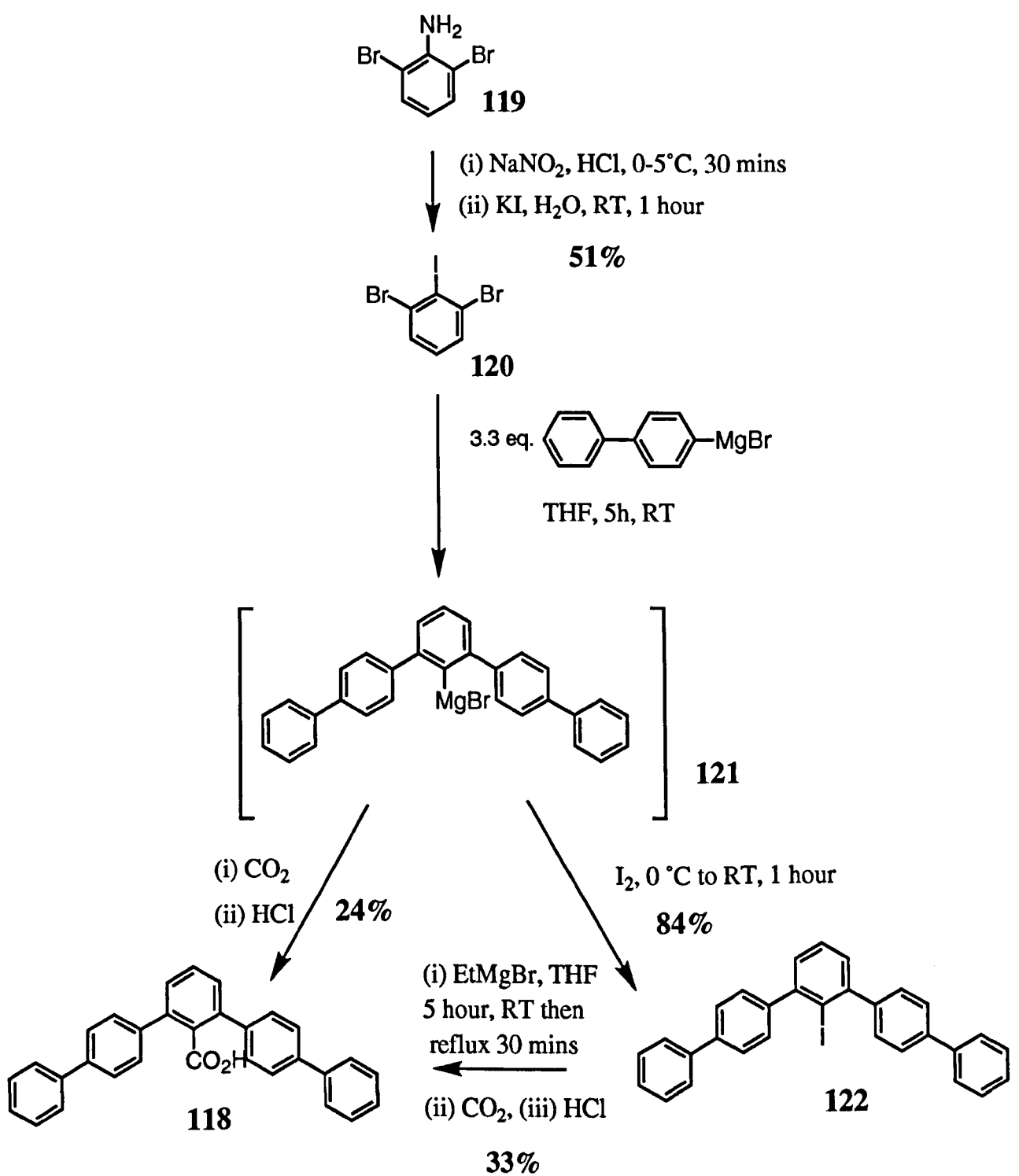
Scheme 6.6. Attempted synthesis of stopper **118** via Suzuki coupling / oxidation.

Commercially available bromide **114** was converted to boronic acid **115** using the procedure of Kabalka *et al.*<sup>135</sup> Slightly over 2 equivalents of **115** were then used in a Suzuki coupling reaction<sup>136</sup> with 2,6-dibromotoluene. The required product **116** was isolated in 23% yield with the major product being mono-reacted bromide **117**. It seems likely that a longer reaction time is required, but no attempt was made to optimise this reaction. To convert **116** to the required acid **118**, it was necessary only to oxidise the methyl group but this reaction proved impossible.

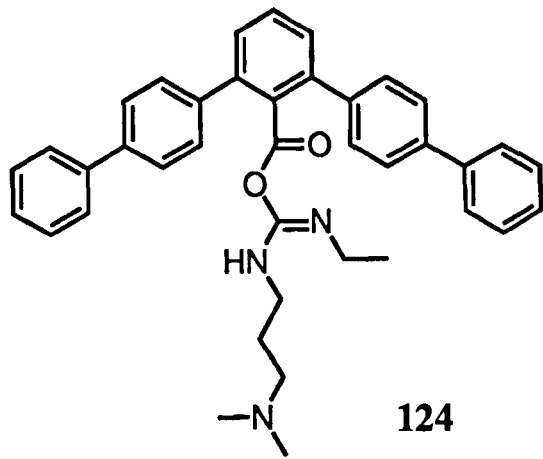
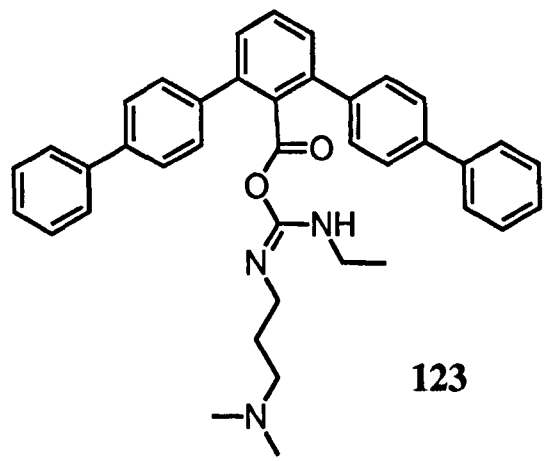
Using potassium permanganate in water as oxidant resulted in complete recovery of starting material. Since it seemed the likely problem was insolubility of the substrate, a switch to an organic based system was made. The use of either tetra-*n*-butylammonium permanganate in refluxing pyridine or KMnO<sub>4</sub> in a two phase water-benzene system, with <sup>n</sup>Bu<sub>4</sub>N<sup>+</sup>Br<sup>-</sup> as a phase transfer catalyst did not solve the problem. Again, only starting material was recovered after 3 days. Rather than pursue this reaction further, it was decided to use an alternative strategy based upon chemistry developed by Hart *et al*<sup>139</sup> (Scheme 6.7).

2,6-dibromoiodobenzene **120** was prepared from commercially available dibromoaniline **119** in moderate yield via diazotisation and subsequent treatment with potassium iodide.<sup>140</sup> **120** was then subjected to the Hart reaction with slightly over 3 equivalents of the Grignard reagent prepared from 4-bromobiphenyl. The intermediate formed during this procedure is reported to be Grignard reagent **121**. Quenching of **121** with powdered carbon dioxide followed by acidification with aqueous acid gave the required acid **118** (24% from **120**). The rather low yield was mainly due to difficult chromatographic purification and protonation of the Grignard intermediate by extraneous water during the CO<sub>2</sub> quench.

Hart reports that improved yields and more straightforward purification can generally be obtained by quenching with iodine to give the aryl iodide which can then be purified before the Grignard is reformed and quenched with the required electrophile. This is indeed the case - aryl iodide **122** was obtained in 84% yield and chromatographic purification is trivial. The Grignard is readily reformed by an exchange reaction with ethylmagnesium bromide and upon quenching with solid carbon dioxide, acid **118** was obtained in 33% yield (27% from **120**). Again, the yield was rather disappointing - the overall yield over two steps was only marginally better than the direct reaction with carbon dioxide. However, the simple chromatographic separation required makes this second route preferable for preparation of **118**. It seems that particular problems with protonation by adventitious water may be experienced due to the hindered nature of Grignard **121** rendering the reaction with carbon dioxide relatively slow.



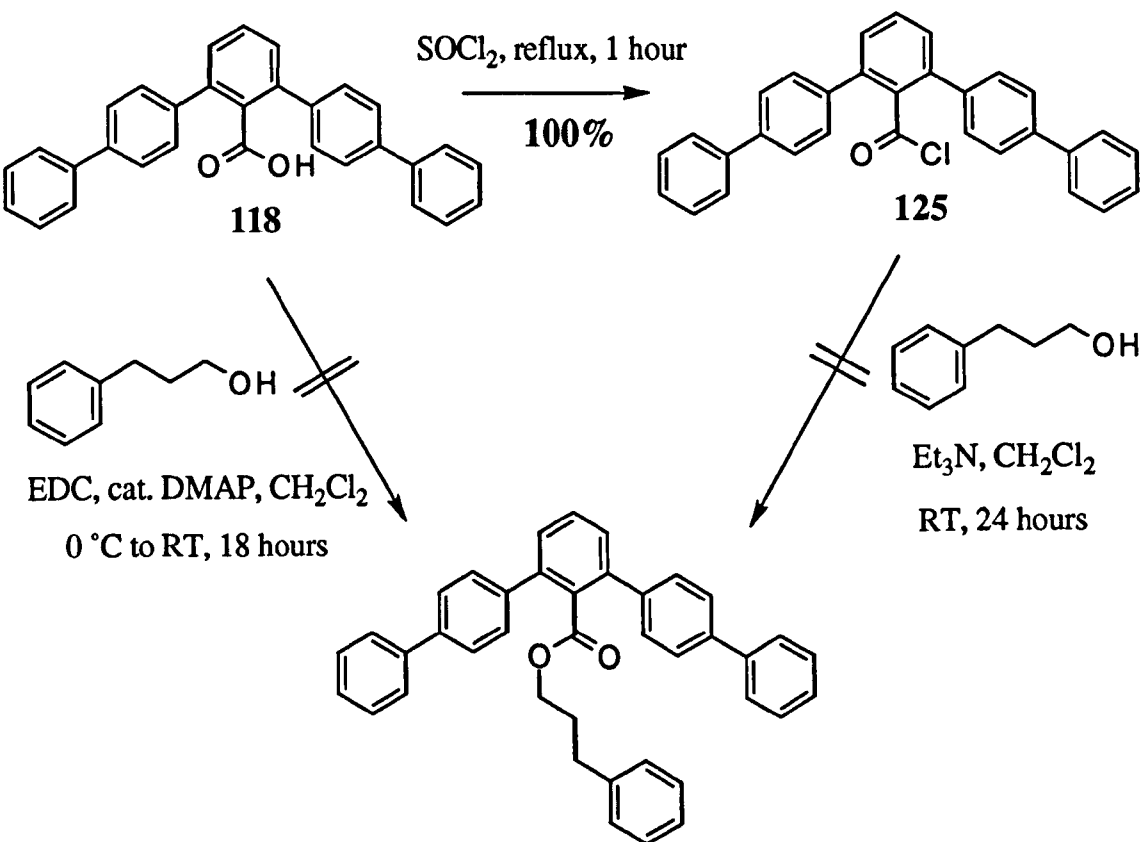
**Scheme 6.7.** Synthesis of stopper **118** using the Hart reaction.



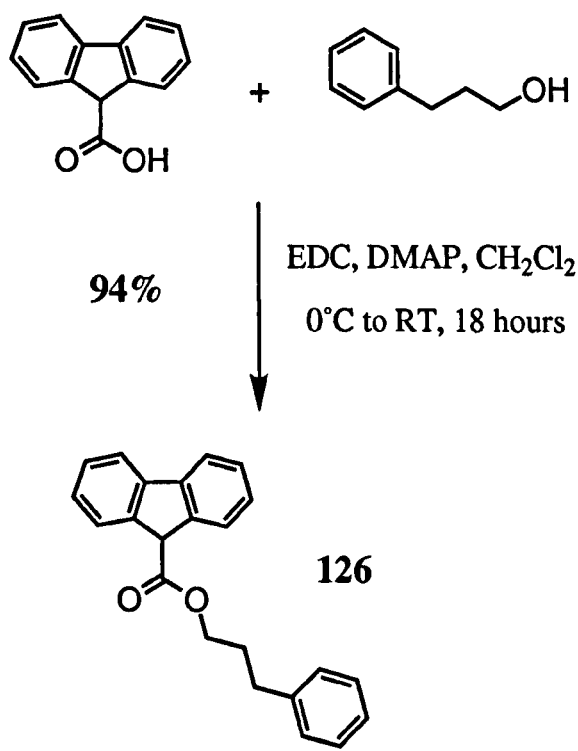
Due to the hindered nature of acid **118** and the fact that Siegel has reported that the properties of similar 2,6-diarylbenzoic acids are significantly modified by interactions with the adjacent  $\pi$  system,<sup>141</sup> it was decided to undertake a model reaction involving esterification of a simple alcohol (Scheme 6.8).

Unfortunately, the acid proved too hindered to react. Upon treatment of a mixture of **118** and 3-phenylpropanol in  $\text{CH}_2\text{Cl}_2$  with EDC and catalytic DMAP, none of the expected ester product was formed. The products isolated were identified as the stable EDC adducts **123** and **124**. These compounds survived chromatographic purification in a  $\text{CH}_2\text{Cl}_2$  / methanol mixture on silica with only slight conversion to the methyl ester!

**118** was readily converted to acid chloride **125** by refluxing in thionyl chloride in quantitative yield. Again, **125** and 3-phenylpropanol showed no reaction in the presence of base in  $\text{CH}_2\text{Cl}_2$  after 24 hours. It was therefore decided to abandon the benzoic acid derived stopper groups and design an alternative system.



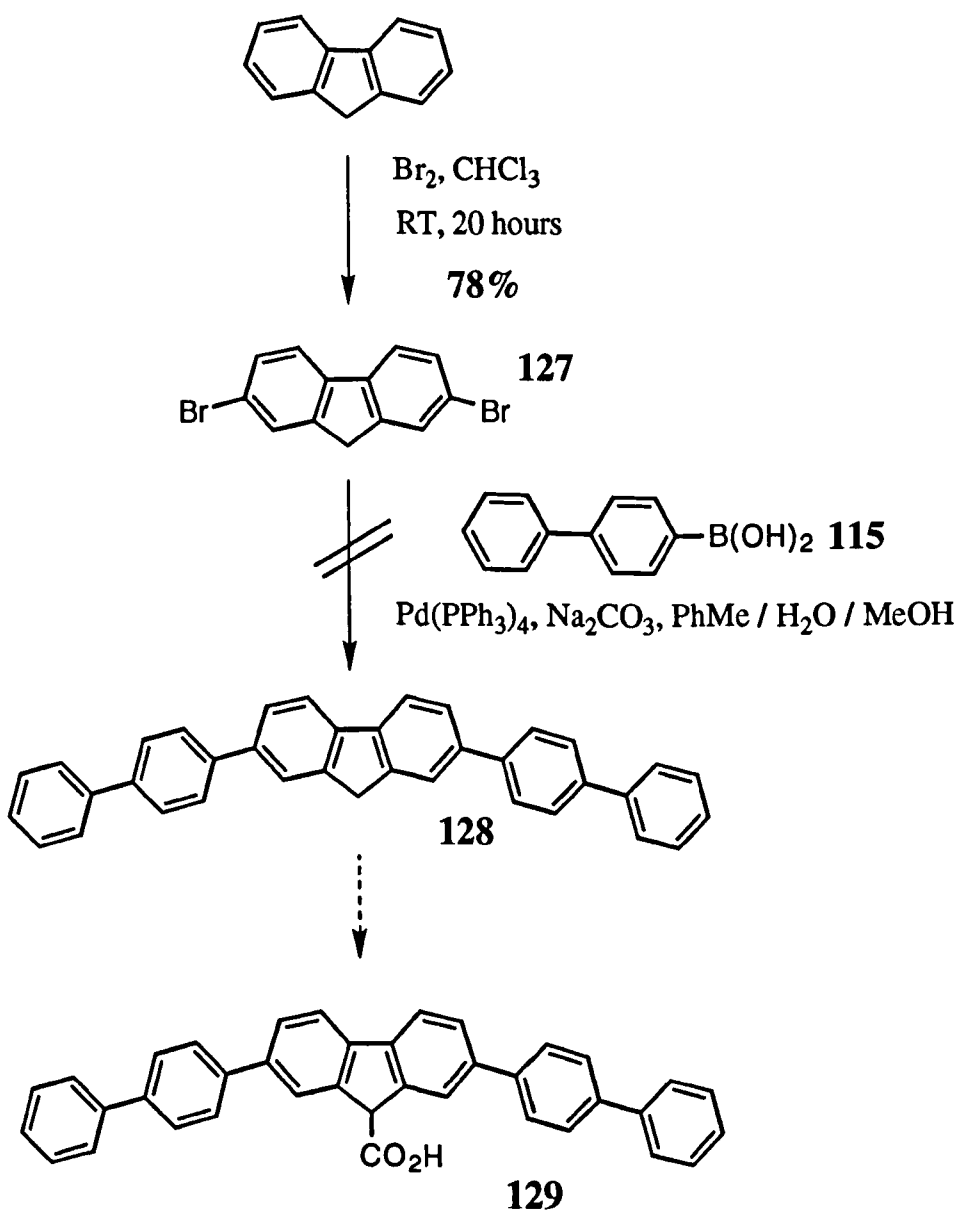
Scheme 6.8. Use of **118** in model acylation reactions with 3-phenylpropanol.



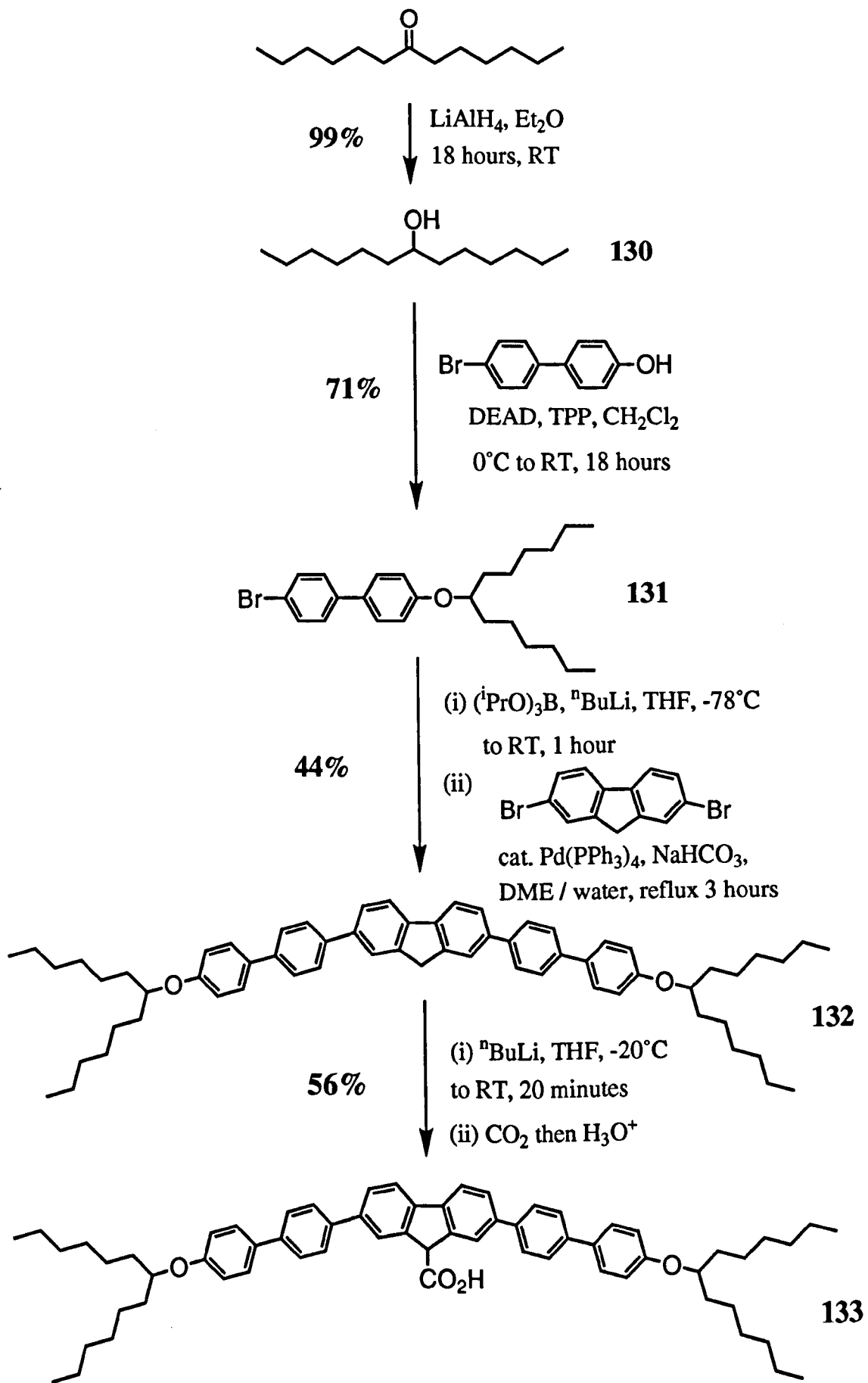
**Scheme 6.9.** Preparation of the 3-phenylpropyl ester of 9-fluorenecarboxylic acid.

### 6.3.1 A 9-Fluorenecarboxylic Acid Derived Stopper Group

The problem with the previous design was clearly steric hindrance caused by bulky substituents so close to the carboxylic acid functionality. The second strategy used was based upon a disubstituted 9-fluorenecarboxylic acid. It was shown that 9-fluorenecarboxylic acid itself coupled in good yield with 3-phenylpropanol using EDC as coupling agent to give the ester **126** (Scheme 6.9). Since the larger size of the fluorene system enables the introduction of bulky substituents at a site remote from the carboxylic acid functionality, this change should not greatly affect the reactivity of the acid. Thus the synthesis of acid **129** was attempted (Scheme 6.10).



Scheme 6.10. Attempted synthesis of 9-fluorenecarboxylic acid based stopper **129**.

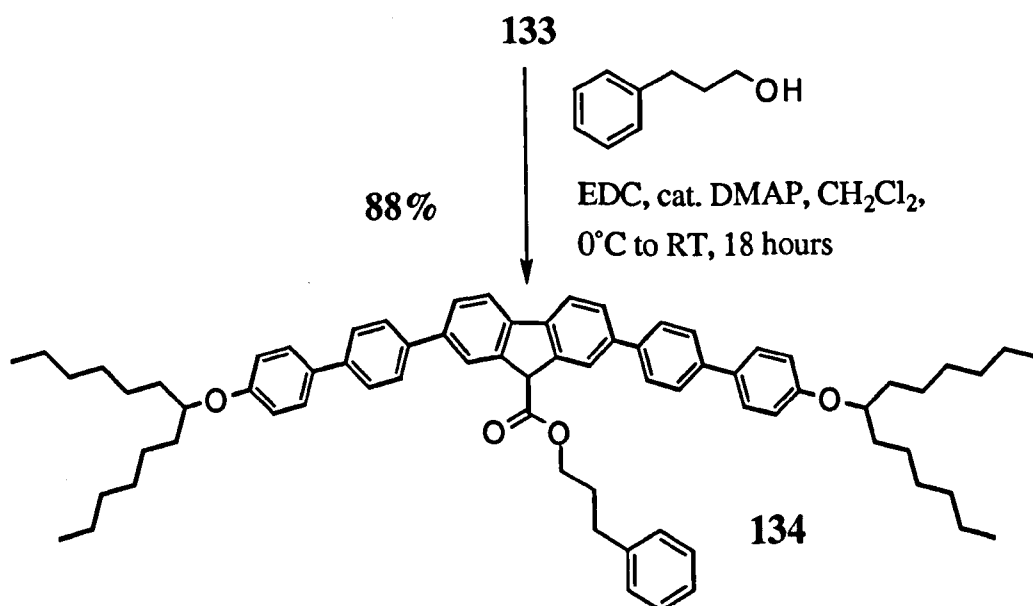


**Scheme 6.11. Synthesis of solubilised stopper group 133.**

2,7-dibromofluorene **127** was obtained by treatment of the parent hydrocarbon with bromine in chloroform<sup>142</sup> in good yield and is also commercially available. Attempts to prepare the hydrocarbon **128** via a Suzuki coupling lead to the formation of a completely insoluble product that could not be characterised. It is not unreasonable that such large planar aromatic molecules may be extremely insoluble and it was therefore decided to modify the design to include extra solubilising groups. This lead to the successful synthesis of stopper group **133** (Scheme 6.11).

Reduction of commercially available 7-undecanone with lithium aluminium hydride gave 7-undecanol **130**. A Mitsunobu reaction was then used to couple the alcohol and 4-bromo-4'-hydroxybiphenyl to give the solubilised bromobiphenyl **131**. Attempts to prepare the boronic acid derivative as discussed earlier were unsuccessful due to the lack of crystallinity of the product, so it was decided to prepare and react the boronic acid *in situ*. **131** was converted to the boronic acid diisopropyl ester by treatment with BuLi in the presence of triisopropyl borate and without isolation the product was coupled with 2,7-dibromofluorene using Suzuki-type conditions to give **132** in an overall 44% yield.<sup>143</sup> Attempts to incorporate a carboxylic acid group using the mild conditions reported by Chiba *et al* ( $\text{CO}_2$  gas,  $\text{K}_2\text{CO}_3$ , 18-crown-6 in DMSO)<sup>144</sup> were unsuccessful. The best procedure was found to be deprotonation with BuLi and quenching with carbon dioxide, which give the required acid **133** in 56% yield. The  $^1\text{H}$  NMR of **133** was extremely broad and not possible to assign. However, upon addition of 5 equivalents of acetic acid, a well-defined spectrum was obtained. We attribute this to the breaking down of H-bonded dimer structures.

In a model acylation reaction with 3-phenylpropanol and EDC as coupling agent, the ester **134** was produced in high yield (Scheme 6.12).

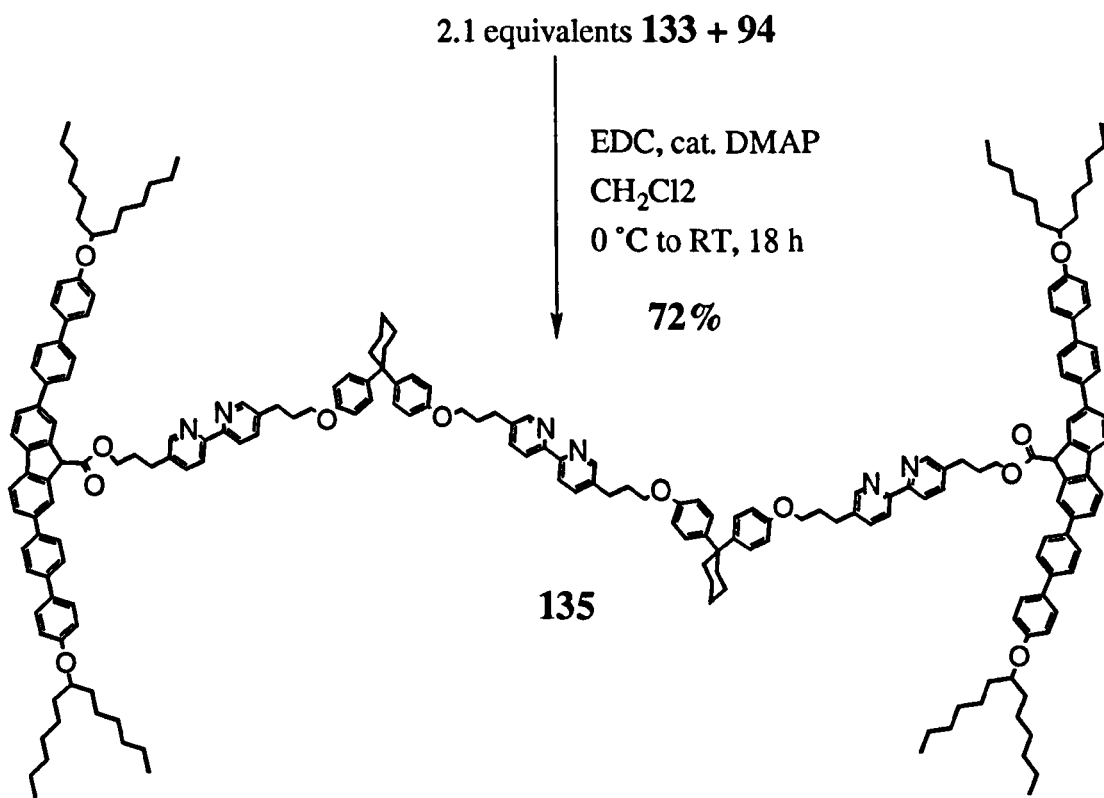


**Scheme 6.12.** Model acylation of 3-phenylpropanol with stopper **133**.

## 6.4 Towards the Synthesis of an Overhand Knot

### 6.4.0 Preparation of the Topologically Trivial Isomer

Prior to attempting the synthesis of the overhand knot, the unknotted topological isomer **135** was prepared for comparison. Treatment of **94** and 2.1 equivalents of stopper group **133** with EDC and catalytic DMAP gave the stoppered oligomer **135** in 72% yield (Scheme 6.13). The 250 MHz  $^1\text{H}$  NMR spectrum is illustrated in Figure 6.4. This spectrum was fully assigned via the cross-peaks observed in 2D COSY and ROESY experiments. The splitting of the bipyridine  $\text{H}_3$  and  $\text{H}_6$  signals to give the complex region of the spectrum between 8.0 and 8.5 ppm is a particularly distinctive characteristic of **135**. In the absence of the large terminal aromatic groups, these signals are almost degenerate despite the existence of three unique environments for both  $\text{H}_3$  and  $\text{H}_6$  in oligomer **94**. This is well illustrated by comparison of the aromatic region of the spectra of the two compounds (Figure 6.4).



Scheme 6.13. Preparation of the unknotted topological isomer of the overhand knot.

Unstoppered oligomer 94

\* = residual  $\text{CHCl}_3$

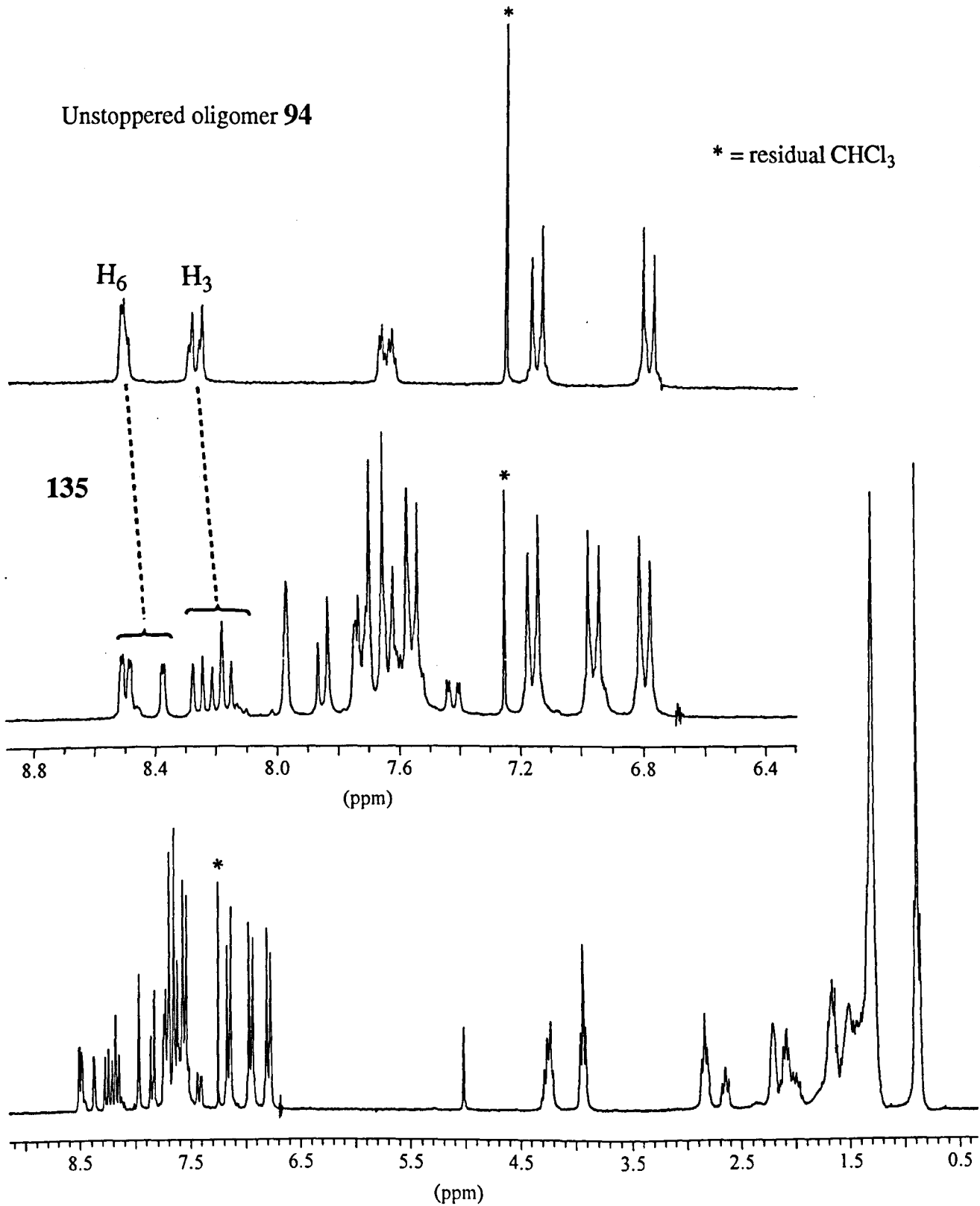


**Figure 6.4.** The 250 MHz  $^1\text{H}$  NMR spectrum of 135 in  $\text{CDCl}_3$ . An expansion of the aromatic region is shown as an inset along with the aromatic region of unstoppered oligomer 94. The characteristic complex splitting of the bipyridine  $\text{H}_3$  and  $\text{H}_6$  signals can be clearly seen.

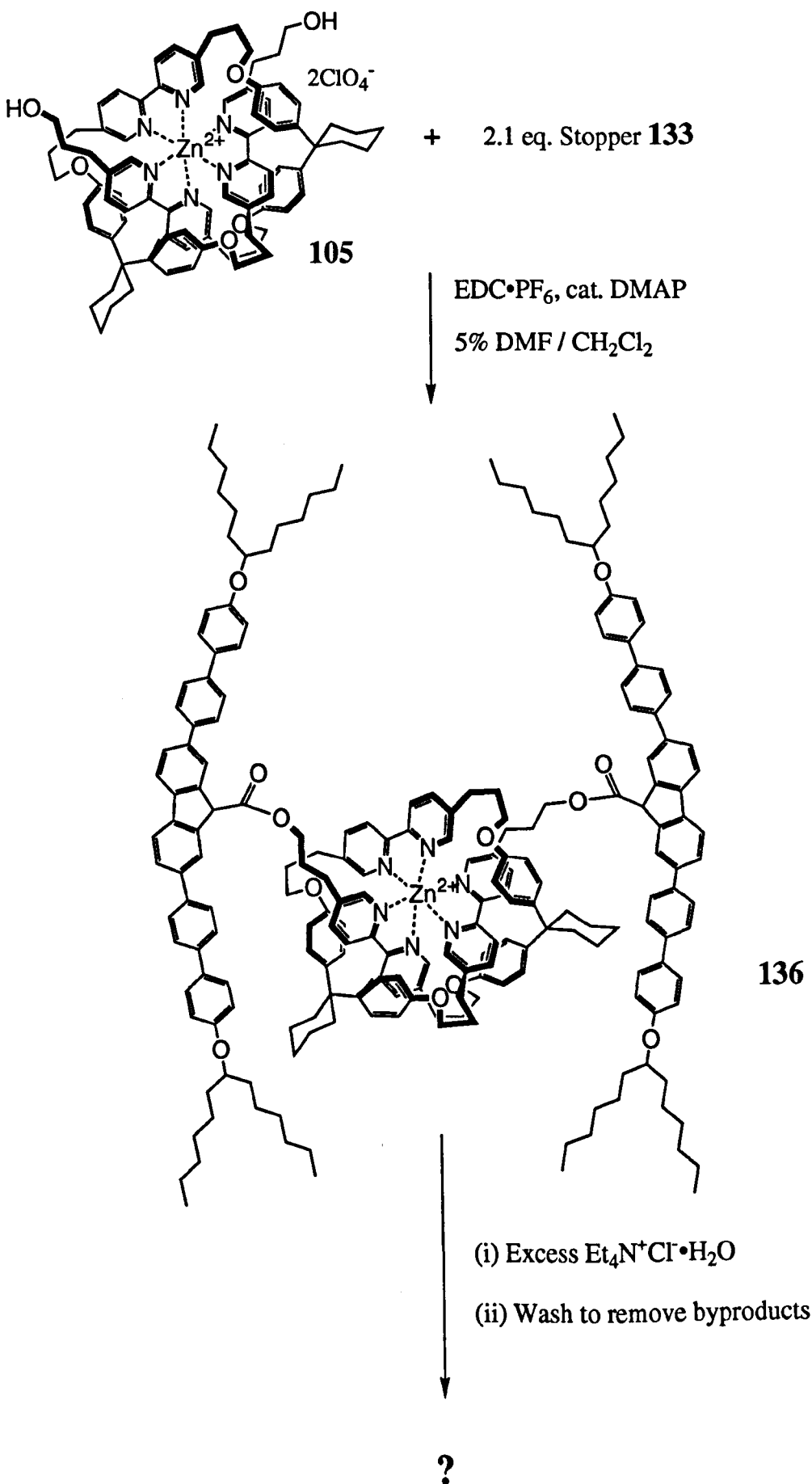
#### 6.4.1 Attempted Synthesis of an Overhand Knot.

The zinc (II) pseudo-overhand knot **105** was prepared as a solution in *ca.* 5% DMF / CH<sub>2</sub>Cl<sub>2</sub> as discussed previously in Chapter 5, and was treated with 2.1 equivalents of stopper **133**, a large excess of EDC•PF<sub>6</sub> and catalytic DMAP. Light was excluded from the reaction due to the potential photosensitivity of the fluorene unit. After 18 hours, the mixture which was assumed to contain the zinc (II) knot **136**, was treated with an excess of Et<sub>4</sub>N<sup>+</sup>Cl<sup>-</sup>•H<sub>2</sub>O to effect demetallation. The products were then washed successively with aqueous acid, aqueous base and water to remove the coupling and demetallation reagents (Scheme 6.14).

However, a <sup>1</sup>H NMR spectrum of the crude product of this reaction suggested that it was identical to the unknotted topological isomer **135** prepared previously. It was subsequently shown that the two materials were identical in every respect: R<sub>f</sub>, melting point, <sup>1</sup>H NMR spectra and FAB<sup>+</sup> mass spectra were all identical for both compounds. Clearly, there are two possible explanations for this result: an unknotting process occurred before the bulky stopper groups were attached or, an unknotting process occurred after attachment which would clearly indicate that the bulky stopper groups are not large enough to prevent unthreading of the overhand knot.

To distinguish these two possibilities it was necessary to establish the presence or absence of the zinc (II) stabilised knotted intermediate **136**. The reaction was therefore repeated in deuterated solvents (*ca.* 10 mg of pseudo-overhand knot **105** in 1 ml of CD<sub>2</sub>Cl<sub>2</sub>) and the <sup>1</sup>H NMR spectrum of the intermediate was recorded.

The <sup>1</sup>H NMR spectrum of this intermediate is rather broad and is dominated by signals corresponding to the EDC•PF<sub>6</sub> coupling agent which is present in a large excess. However, several features of the spectrum seemed to indicate the presence of a knotted structure: the upfield shifted signals at 5.10 ppm and 5.75 ppm although partially obscured by the EDC signals are consistent with the shielded H<sub>3</sub> signals. Also, the absence of signals above 7.8 ppm is consistent with the upfield shifts of the bipyridine H<sub>3</sub> and H<sub>4</sub> protons observed in the knotted starting material due to the bipyridine-bisphenol motif. Presumably the signals from the "outside" bipyridine unit which would usually be found in this region are now also shifted upfield due to their close proximity to the aromatic stopper groups.



**Scheme 6.14.** Attempted preparation of the overhand knot.

In order to be more certain about the nature of the metallated intermediate, it was necessary to obtain the compound pure. Since washing with aqueous acid to remove the coupling agent and by-products resulted in the partial demetallation of the material due to the labile nature of the zinc (II) complex, it was decided to attempt to effect a transmetallation reaction to produce the more stable iron (II) complex 137. The crude intermediate containing 136 was therefore treated with slightly over 1 equivalent of  $\text{Fe}(\text{ClO}_4)_2 \cdot 6\text{H}_2\text{O}$  with the immediate formation of a deep red solution. This solution was then washed with aqueous acid and base and finally purified by flash chromatography on silica to give 137 in 70% yield from 94 (Scheme 6.15). The success of this reaction indicates that the transmetallation reaction is faster than the unthreading process since the free knot must exist as a transient intermediate during the process. The  $^1\text{H}$  NMR spectrum of 137 is illustrated in Figure 6.5. The upfield shifted bipyridine signals at 5.1 and 5.75 ppm and the absence of signals above 7.8 ppm can now be clearly seen. In addition, an identical sample was prepared by treatment of the stable iron (II) pseudo-overhand knot 104 with 2 equivalents of stopper 133 in the presence of EDC and catalytic DMAP.

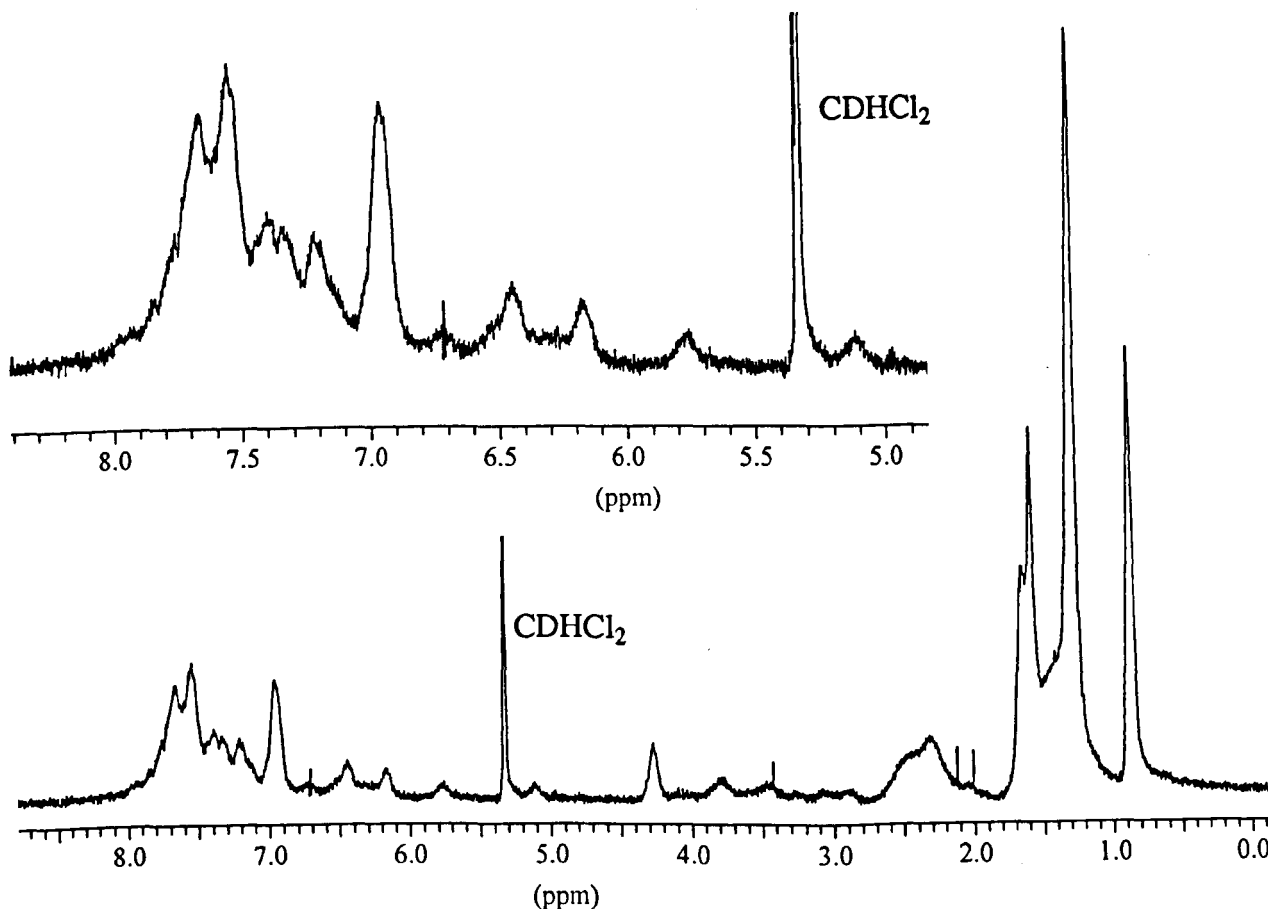


**Figure 6.5.** The 250 MHz  $^1\text{H}$  NMR spectrum of 137 in  $\text{CD}_2\text{Cl}_2$ . An expansion of the aromatic region is shown as an inset.

We attribute the broadness of this spectrum to restricted rotation of the large stopper groups which results in tumbling of the entire molecule being the only mechanism for relaxation of the protons in solution. The linear molecule **135** exhibits a sharp, well-defined spectrum (Figure 6.4) because the components are free to rotate individually. It has already been noted that stopper **133** itself exhibits an extremely broad  $^1\text{H}$  NMR spectrum due to its existence as a hydrogen-bonded dimer. Since knots **136** and **137** are effectively covalently linked dimers of **133**, it is not unreasonable that they may exhibit similar broad spectra. Attempts to produce better resolved spectra at high temperature were unsuccessful. The  $^1\text{H}$  NMR spectrum of **137** at 100 °C in  $\text{d}_2$ -tetrachloroethane showed no improvement over the room temperature spectrum.

Also investigated was the interaction of the stoppered oligomer **135** with zinc (II). A  $\text{CDCl}_3$  solution of **135** and 1 equivalent of  $\text{Zn}(\text{ClO}_4)_2 \cdot 6\text{H}_2\text{O}$  was stirred at room temperature for one day before heating at reflux for several days. The  $^1\text{H}$  NMR spectrum of the product is shown in Figure 6.6. The spectrum of the iron (II) knot **137** is also shown for comparison. The broad spectrum obtained and the lack of the distinctive signals at 5.1 ppm and 5.75 ppm indicated that the reverse of the unknotting process does not occur. So, although knot **136** readily unthreads when the zinc (II) ion is removed, the reverse process cannot occur. The failure of this reaction with such a bulky terminal group is consistent with the coordination and threading mechanism discussed in Chapter 5 (page 103).

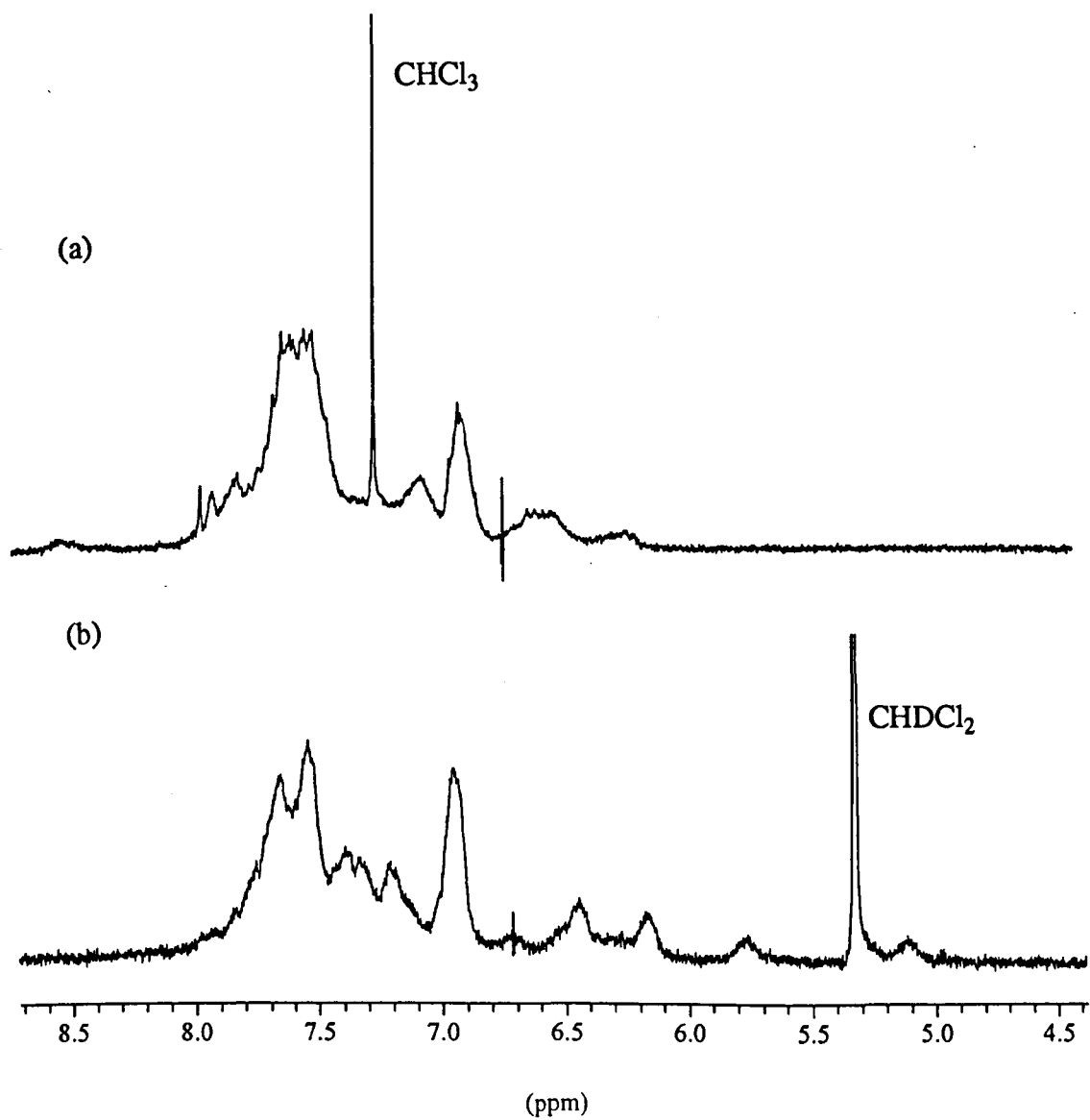


**Figure 6.6.** (a) Aromatic region of the 250 MHz  $^1\text{H}$  NMR spectrum in  $\text{CDCl}_3$  of the product of the reaction between stoppered oligomer **135** and zinc (**II**) after 2 days in refluxing  $\text{CDCl}_3$ . (b) The aromatic region of the  $\text{CD}_2\text{Cl}_2$  spectrum of iron (**II**) stabilised overhand knot **137** for comparison. The absence of the distinctive upfield shifted signals in (a) can be clearly seen.

#### 6.4.2 Conclusions and Future Possibilities

The conclusion from these experiments is clear: the terminal stopper groups are not large enough to prevent unthreading occurring to yield the unknotted isomer. We can conjecture that the required overhand knot is produced upon demetallation of the zinc (II) stabilised intermediate **136** but this compound then unknots quickly to give **135**. We propose that the various knotted and unknotted species may be related by an energy profile such as that illustrated in Figure 6.7.

Here we can clearly see that the metal-stabilised knot **136** and the unknotted ligand-metal complex **135•Zn(II)** are stable species that cannot readily inter-convert because of the large energy barrier between them. This is consistent with the stability of **136** with respect to unknotting, and the failure to generate **136** from the reaction between **135** and zinc (II). However, the zinc knot **136** has only a relatively small energy barrier to overcome to lose the zinc (II) ion and give the free knot. This is consistent with the facile demetallation reaction upon treatment of **136** with chloride ion. Upon formation of the free knot, we propose that there is only a small energy barrier to overcome to allow the unknotting process to give **135**. However, in the presence of iron (II), an alternative pathway can lead from this intermediate to the "trapped" iron (II) knot **137**.

The size of the energy barrier for the unknotting process is directly related to the bulk of the stopper groups, and the use of a large enough group should render this barrier insurmountable. Clearly however, stopper group **133** is not sufficiently large to achieve this. The synthesis of the more bulky group **138** is being undertaken by my colleague D. James.

No attempts were made to investigate the rate of the unknotting process and if it may be slowed or stopped completely at reduced temperature. This may make an interesting possibility for future work.

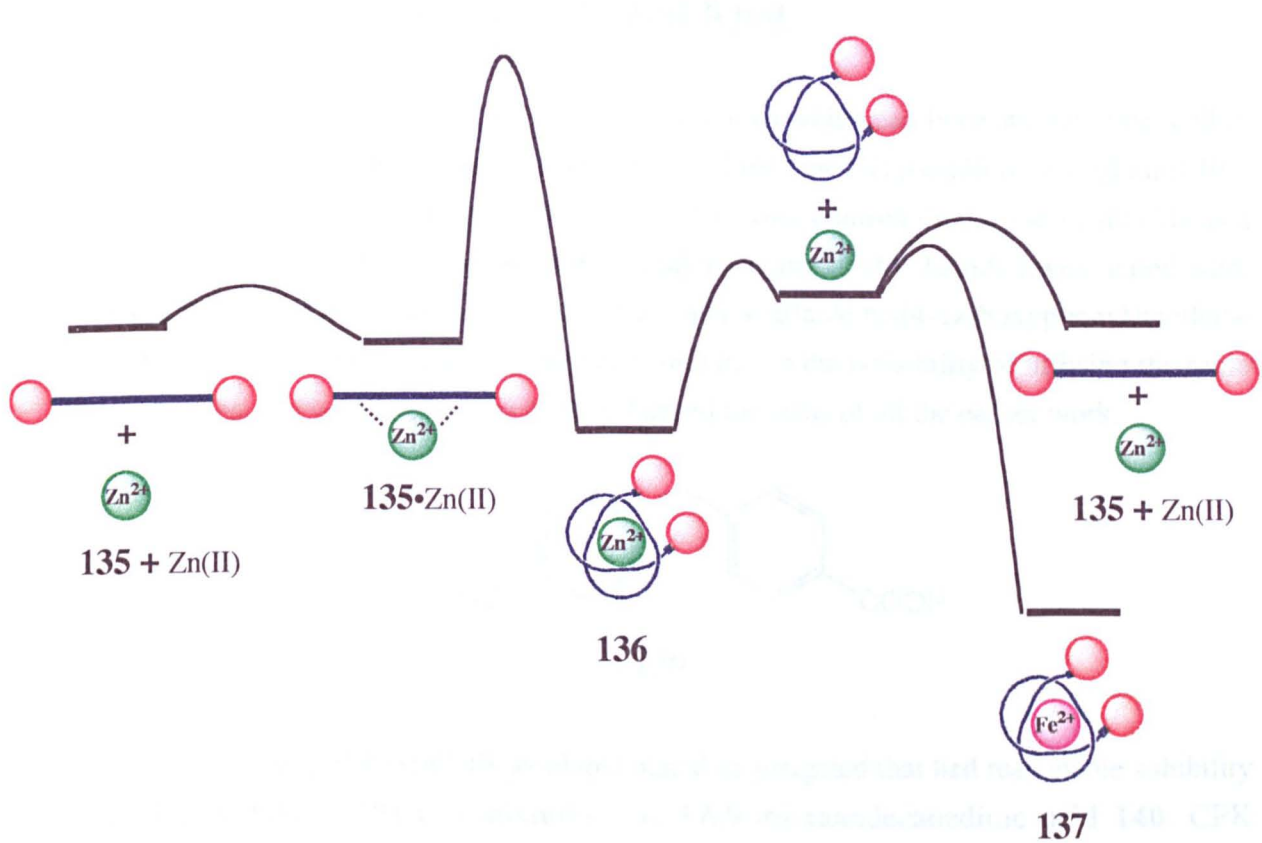
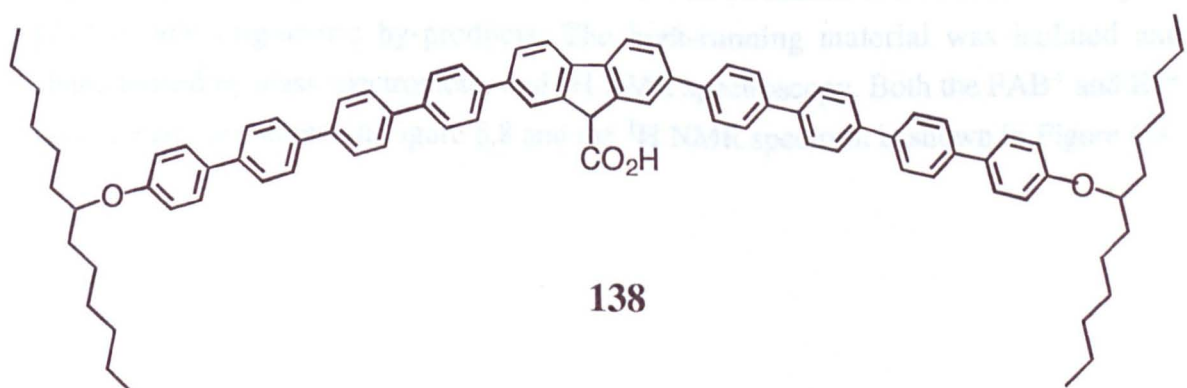
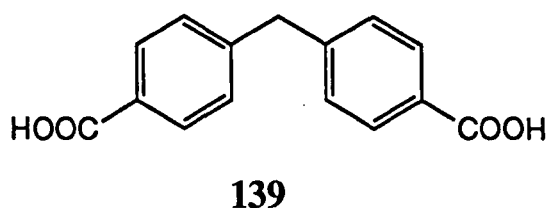


**Figure 6.7** A schematic energy diagram reflecting possible relationships between the different species of knotted / unknotted and metallated / demetallated overhand knots.



## 6.5 Macrocyclisation to a Trefoil Knot

Since ester couplings were the only reactions which had been shown to be readily achievable upon the terminal hydroxyl groups of the zinc (II) pseudo-overhand knot **105**, attempts to achieve macrocyclisation to a trefoil knot centred on the use of diacids as a unit to link the hydroxyl groups. Unfortunately, many of the diacids investigated were extremely insoluble, including the commercially available bis(4-carboxyphenyl)methane **139**. This would have made an ideal linker unit due to the possibility of utilising the same templating aromatic interactions as have formed the basis of all the earlier work.

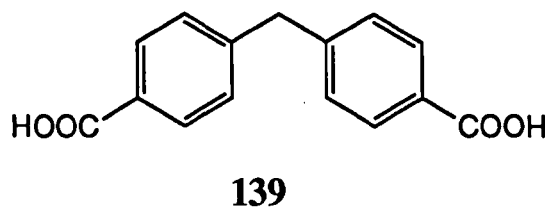


The only commercially available diacid investigated that had reasonable solubility in 5-10% DMF / CH<sub>2</sub>Cl<sub>2</sub> mixtures was 3,6,9-trioxaundecanedioic acid **140**. CPK models also confirmed that the ethylene glycol linker between the two acid groups was sufficiently long to allow the macrocyclisation reaction to occur. Although this strategy would lack the templating aromatic interactions that should ideally be present, it was hoped that the macrocyclisation may be directed to a certain extent by favourable electrostatic interactions between the oxygen atoms of the ethylene glycol chain and the edge of the bipyridine unit. A high dilution macrocyclisation reaction was therefore carried out as shown in Scheme 6.16.

A solution of **105** and 1 equivalent of the diacid **140** in 10% DMF / CH<sub>2</sub>Cl<sub>2</sub> was added dropwise over several hours to an ice-cooled solution of EDC•PF<sub>6</sub> and DMAP in CH<sub>2</sub>Cl<sub>2</sub>. After stirring for 18 hours, Et<sub>4</sub>N<sup>+</sup>Cl<sup>-</sup> (*ca.* 25 equivalents) was added in an attempt to demetallate the crude product. After work up, TLC on silica indicated a high running spot and baseline material consistent with the formation of a discrete macrocyclic product and oligomeric by-products. The high-running material was isolated and characterised by mass spectrometry and <sup>1</sup>H NMR spectroscopy. Both the FAB<sup>+</sup> and ES<sup>+</sup> mass spectra are shown in Figure 6.8 and the <sup>1</sup>H NMR spectrum is shown in Figure 6.9.

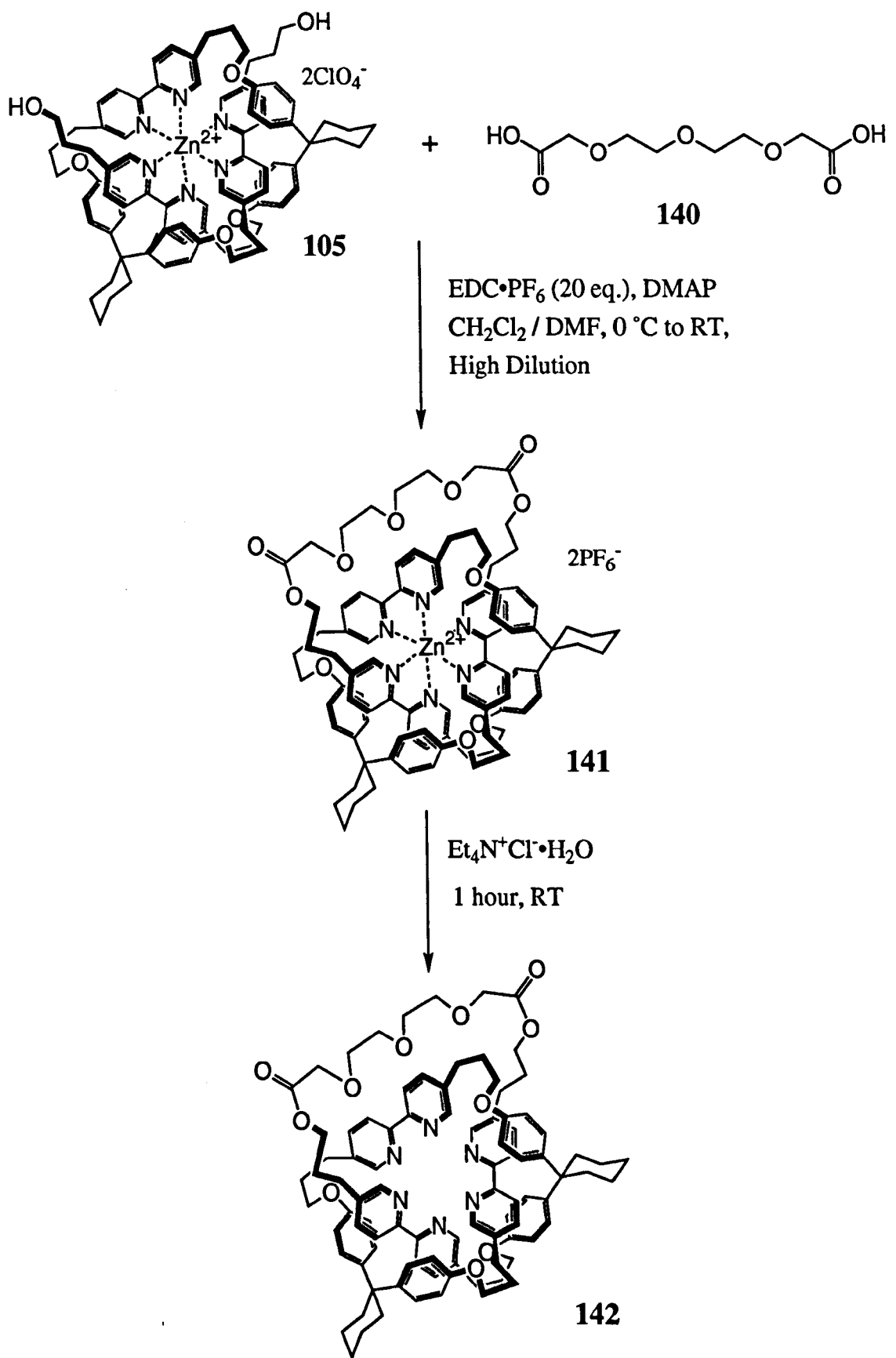
## 6.5 Macrocyclisation to a Trefoil Knot

Since ester couplings were the only reactions which had been shown to be readily achievable upon the terminal hydroxyl groups of the zinc (II) pseudo-overhand knot **105**, attempts to achieve macrocyclisation to a trefoil knot centred on the use of diacids as a unit to link the hydroxyl groups. Unfortunately, many of the diacids investigated were extremely insoluble, including the commercially available bis(4-carboxyphenyl)methane **139**. This would have made an ideal linker unit due to the possibility of utilising the same templating aromatic interactions as have formed the basis of all the earlier work.



The only commercially available diacid investigated that had reasonable solubility in 5-10% DMF / CH<sub>2</sub>Cl<sub>2</sub> mixtures was 3,6,9-trioxaundecanedioic acid **140**. CPK models also confirmed that the ethylene glycol linker between the two acid groups was sufficiently long to allow the macrocyclisation reaction to occur. Although this strategy would lack the templating aromatic interactions that should ideally be present, it was hoped that the macrocyclisation may be directed to a certain extent by favourable electrostatic interactions between the oxygen atoms of the ethylene glycol chain and the edge of the bipyridine unit. A high dilution macrocyclisation reaction was therefore carried out as shown in Scheme 6.16.

A solution of **105** and 1 equivalent of the diacid **140** in 10% DMF / CH<sub>2</sub>Cl<sub>2</sub> was added dropwise over several hours to an ice-cooled solution of EDC•PF<sub>6</sub> and DMAP in CH<sub>2</sub>Cl<sub>2</sub>. After stirring for 18 hours, Et<sub>4</sub>N<sup>+</sup>Cl<sup>-</sup> (*ca.* 25 equivalents) was added in an attempt to demetallate the crude product. After work up, TLC on silica indicated a high running spot and baseline material consistent with the formation of a discrete macrocyclic product and oligomeric by-products. The high-running material was isolated and characterised by mass spectrometry and <sup>1</sup>H NMR spectroscopy. Both the FAB<sup>+</sup> and ES<sup>+</sup> mass spectra are shown in Figure 6.8 and the <sup>1</sup>H NMR spectrum is shown in Figure 6.9.



**Scheme 6.16.** High dilution macrocyclisation reaction between zinc (II) pseudo-overhand knot **105** and 3,6,9-trioxaundecanedioic acid **140**.

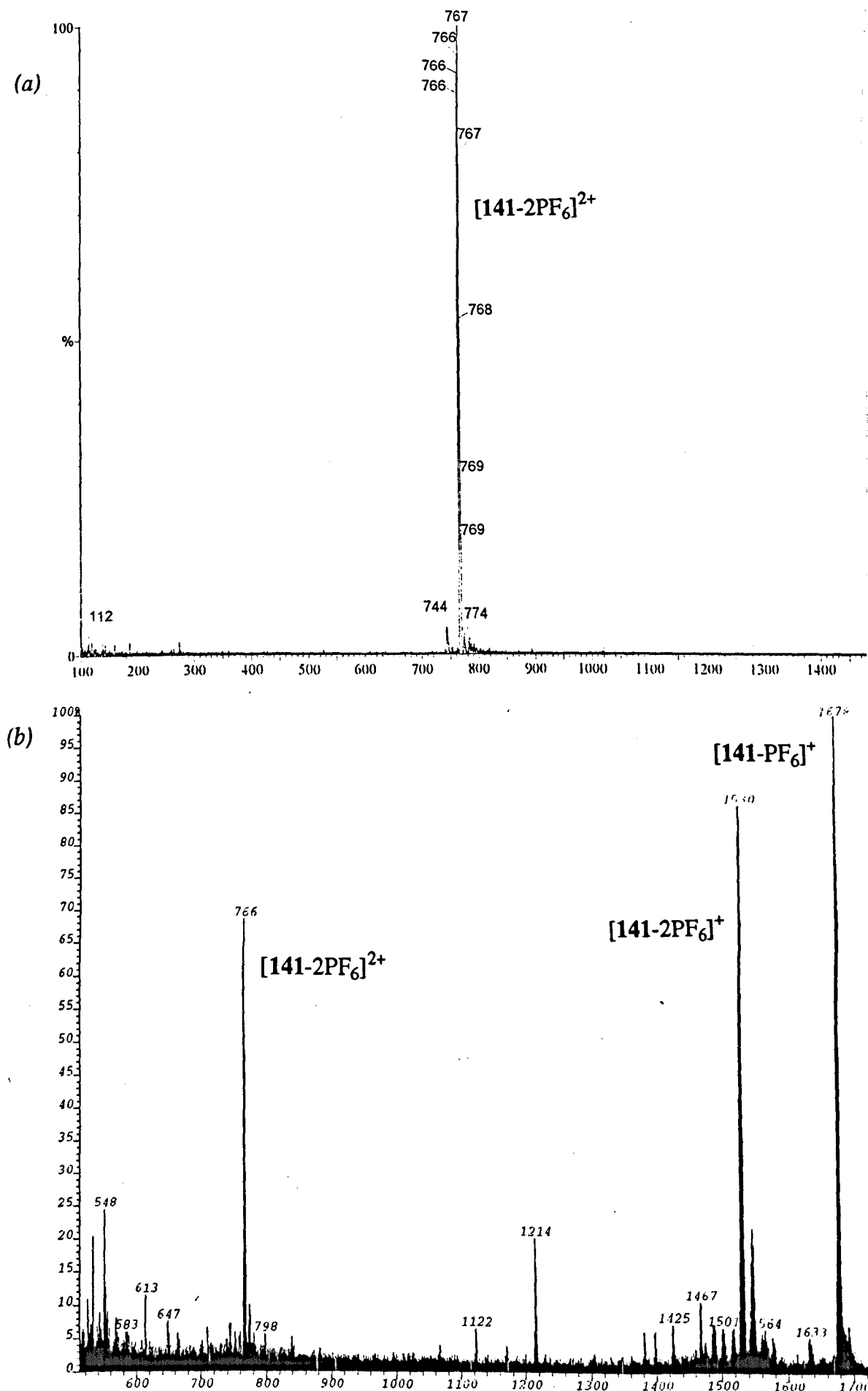


**Figure 6.8.** Mass spectra of the product from the macrocyclisation reaction in Scheme 6.16  
(a)  $\text{ES}^+$  spectrum and (b)  $\text{FAB}^+$  spectrum.

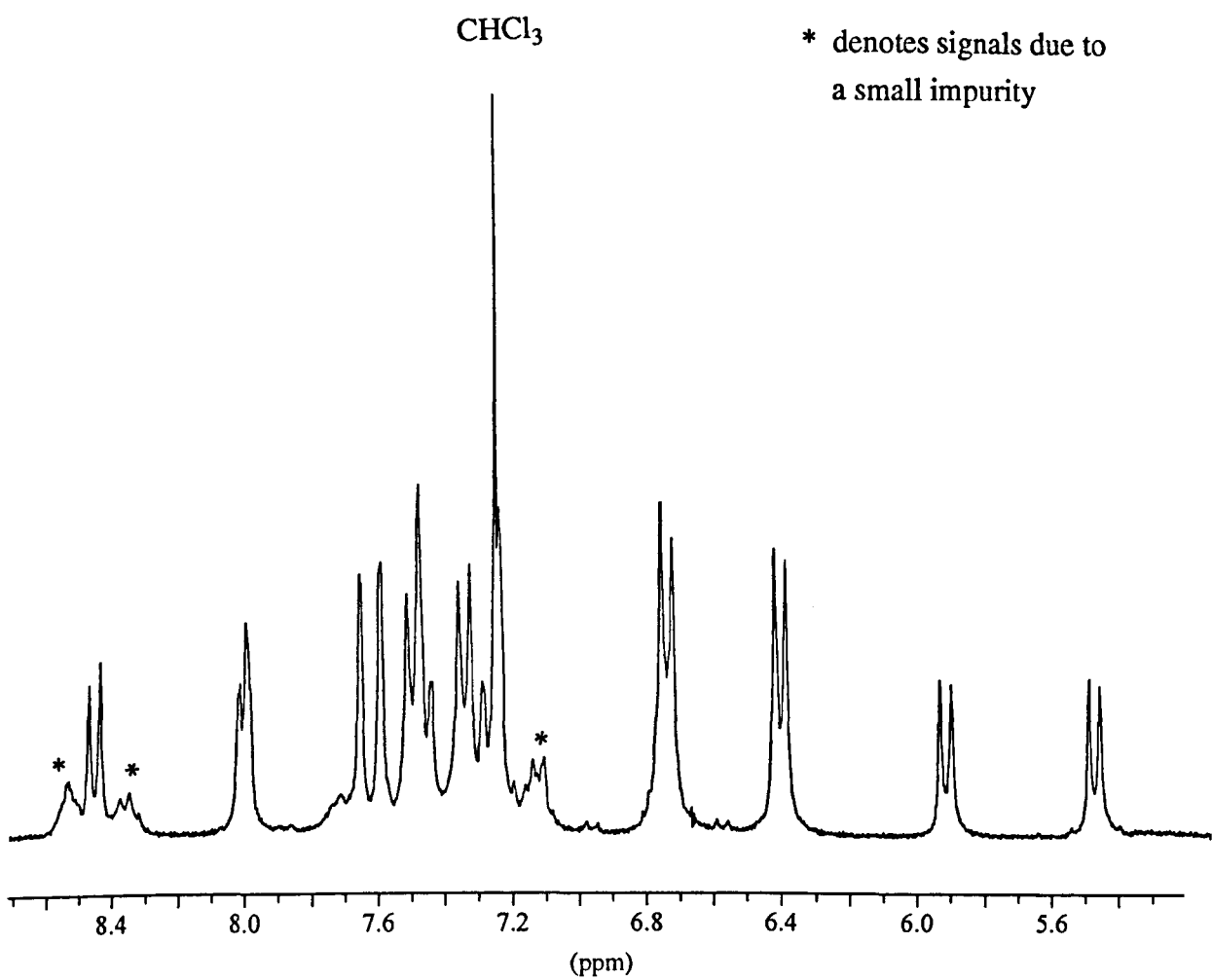


**Figure 6.9.** Aromatic region of the  $^1\text{H}$  NMR spectrum of the product from Scheme 6.16.

The ES $^+$  MS signal at m/z 767 indicated that the product was in fact not the trefoil knot **142** but rather the metallated intermediate **141**. The signal at m/z 767 corresponds to the M $^{2+}$  ion formed by the loss of both counterions. Similarly, in the FAB $^+$  MS, the signal at m/z 1530 corresponds to the single positive ion formed on loss of two counterions. The signal at m/z 1678 corresponds to the singly charged species flying with one PF<sub>6</sub> counterion. This interpretation is confirmed by the aromatic region of the  $^1\text{H}$  NMR spectrum. The signals are almost unchanged from the starting material **105** indicating the continued presence of both the metal ion and the knotted structure. **141** was obtained in an overall yield of 25% from **94**. A lack of time has precluded any attempts to optimise this yield.

Work towards the full characterisation of **141** is not yet complete. In particular, the aliphatic region of the spectrum is extremely complex and difficult to interpret. A 2D ROESY experiment has however facilitated a complete assignment of the aromatic region of the  $^1\text{H}$  NMR spectrum (data is given in the experimental section). A selection of the NOEs observed are shown in Figure 6.10. Of particular importance in confirming the proposed structure are the NOE cross-peaks linking the bipyridine unit to the ethylene glycol chain (shown in red in Figure 6.10). In the starting material **105**, unlike the other two bipyridine units, this bipyridine shows no NOE cross-peaks indicating its position on the "outside" of the molecule. The observation of cross-peaks in **141** confirms that the macrocyclisation has proceeded in the desired manner to give the knotted structure.

Further attempts to demetallate **141** with chloride ion were unsuccessful. No change in the  $^1\text{H}$  NMR spectrum was observed after heating at reflux in chloroform for 2 days. It has already been noted (page 113) that the demetallation of the zinc (II) pseudo-overhand knot **105** in the presence of chloride ions is extremely facile and occurs readily upon addition of any reagent that contains free chloride ion. The enhanced stability of this complex may be attributed to its topology and is entirely consistent with the structure **141**. The highly preorganised hexadentate ligand **142** will clearly have a much higher binding affinity for metal ions than the free ligand **94** which must undergo an extensive conformational change in order to be able to bind an octahedral metal ion. Sauvage has also reported interesting kinetic effects in the demetallation of both his knot<sup>145</sup> and catenand<sup>146</sup> systems which encapsulate bound metal ions. Models suggest that the degree of encapsulation and preorganisation are higher still in our system.

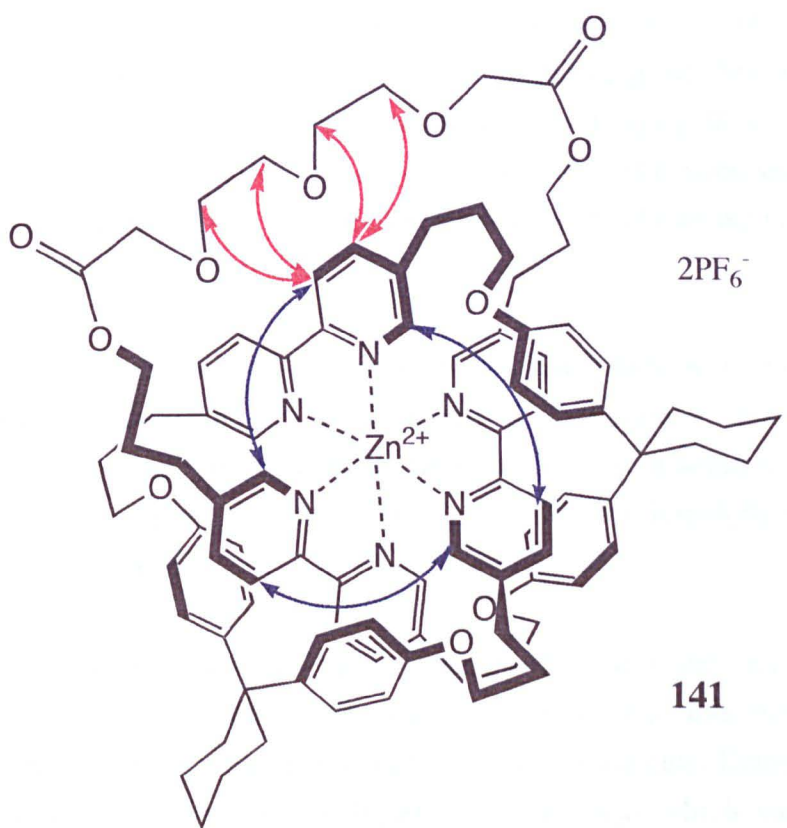


**Figure 6.10.** Some NOEs observed in a 2D ROESY experiment. The bipyridine-bipyridine NOEs ( $\longleftrightarrow$ ) again allow complete assignment of all the bipyridine protons. Good evidence for the knotted structure is provided by the intense bipyridine-ethylene glycol chain NOEs ( $\longleftrightarrow$ ). A full set of bisphenol-bipyridine NOEs are also observed as in complex 105 (page 102) but are omitted for clarity.

## 6.6 Conclusions

Preliminary work has been completed that illustrates the versatility of the zinc (II) pseudo-overhand knot **105** as a building block for the introduction of topological complexity into a variety of systems. The most significant problem in the use of **105** was shown to be its low stability and hence the limited range of chemistry which is accessible for bond-forming reactions with the terminal hydroxyl groups. We have demonstrated that this can be overcome by careful control of the species present in solution and have prepared a new coupling agent EDC•PF<sub>6</sub> that readily allows the incorporation of **105** into other molecules via ester links.

Attempts to prepare the novel overhand knot were unsuccessful due to an underestimation of the size of the stopper group required. This seems to illustrate that molecules of this type are actually far more flexible in solution than simple molecular models may suggest. A larger stopper group that will hopefully overcome this problem has been designed.

A simple macrocyclisation reaction has lead to the preparation of a metallated trefoil knot in 25% yield. To the best of our knowledge, this represents only the second distinct strategy that has given access to such a molecule. Demetallation of this metal-ligand complex has proved highly problematical which can be attributed to its preorganised structure. However, we do not envisage this being a significant problem in the majority of structures that **105** may be used to synthesise in future since they are likely to be considerably less preorganised than the macrocyclic knot. This is supported by the ready demetallation of structures such as the pseudo-overhand knot. It also seems likely that zinc (II) is the optimum choice of metal ions since its tris-bipyridine complexes are generally extremely labile compared to similar metal ions.

---

*Chapter 7*

---

## **Experimental**

## 7.1 General

### 7.1.0 Instrumentation

$^1\text{H}$  NMR spectra were recorded on Bruker AC-250 MHz or AM-250 MHz spectrometers operated in Fourier transform mode. Chemical shifts were referenced to TMS as an internal standard or residual solvent peaks ( $\text{CHCl}_3$  at 7.25 ppm in d-chloroform,  $\text{CD}_3\text{S(O)CHD}_2$  at 2.52 ppm in d<sub>6</sub>-DMSO,  $\text{CDHCl}_2$  at 5.32 ppm in d<sub>2</sub>-dichloromethane and  $\text{CD}_3\text{C(O)CHD}_2$  at 2.04 ppm in d<sub>6</sub>-acetone). 400 MHz spectra were recorded on a Bruker AMX-400 Spectrometer.

$^{13}\text{C}$  NMR spectra were also recorded on Bruker AC-250 or AM-250 spectrometers operated in J-Modulation mode. Chemical shifts were referenced to  $\text{CDCl}_3$  (77.0 ppm),  $(\text{CD}_3)_2\text{SO}$  (39.5 ppm) or  $(\text{CD}_3)_2\text{CO}$  (29.8 ppm).

The following abbreviations are used in the assignment of  $^1\text{H}$  NMR spectra: s singlet, d doublet, dd doublet of doublets, t triplet, q quintet, m multiplet, br broad signal. Other multiplicities are stated in full.

The numbering system used to annotate  $^{13}\text{C}$  NMR spectra refers to the structures on the facing page. The numbering system used is entirely arbitrary.

2D ROESY and COSY spectra were recorded on a Bruker AMX-400 spectrometer using a mixing time of 300 ms and a relaxation delay of 3 seconds.

Positive fast atom bombardment ( $\text{FAB}^+$ ) mass spectra were recorded on a Fisons VG ProSpec 8 using a matrix of *meta*-nitrobenzyl alcohol (NOBA) and a magnetic sector detection system. Positive electrospray ( $\text{ES}^+$ ) mass spectra were recorded on a Fisons VG Platform using a quadrupole detection system. Electrospray samples were injected as a solution in acetonitrile / methanol mixtures.

UV/visible spectra were recorded on a Phillips PU 8720 scanning spectrophotometer using 1 cm x 1 cm quartz cuvettes at a concentration of between  $2 \times 10^{-5}$  and  $3 \times 10^{-5}$  M in either dry  $\text{CH}_2\text{Cl}_2$  or spectroscopic grade methanol as specified.

IR spectra were recorded on a Perkin Elmer Paragon 1000 FT-IR spectrometer as Nujol mulls unless stated otherwise.

Melting points were recorded on a Reichert Kofler hot stage melting point apparatus and are uncorrected.

Microanalyses were performed using a Perkin-Elmer 2400 CHN elemental analyser operating at 975°C.

## 7.2 Synthetic Procedures

**5,5'-Dimethyl-2,2'-bipyridine (1).** To a solution of NaOH (160 g) in water (600 ml) cooled in an ice-bath was added nickel-aluminium alloy (125 g) portionwise with vigorous stirring to control frothing. When the exothermic reaction had subsided, the mixture was heated at 80°C for 40 minutes. Distilled water (600 ml) was added and the supernatant liquid decanted off. The catalyst was then washed with further distilled water (8 x 500 ml) before being transferred to a round-bottomed flask equipped with dropping funnel and connected to a water pump. As much water as possible was removed by pipette before the flask was slowly evacuated. The evacuated flask was heated at 90-100°C for 2 hours before 3-methylpyridine (150 ml) was added through the dropping funnel to the catalyst (caution: the dried catalyst is highly pyrophoric and all air must be excluded until it is thoroughly wetted). The mixture was then heated at reflux for 48 hours before the catalyst was filtered off and washed well with hot toluene. The combined filtrate and toluene extracts were distilled under reduced pressure to remove solvent and excess 3-methylpyridine. The solid residue was dissolved in a minimum of toluene and filtered through an 8 cm x 7 cm diameter column of basic alumina. The solvent was removed *in vacuo* and the residue recrystallised from a minimum of hot ethanol. The colourless crystals obtained were washed well with ice cold ethanol to yield the title compound (50.0 g, 38%).

m.p. 118-119°C (lit.<sup>103</sup> 114-115°C).

<sup>1</sup>H NMR (CDCl<sub>3</sub>, 250 MHz) δ2.35 (6H, s, -CH<sub>3</sub>), 87.58 (2H, dd, J = 8 Hz, 2 Hz, 4-pyridine H), 88.20 (2H, d, J = 8 Hz, 3-pyridine H), 88.45 (2H, d, J = 2 Hz, 6-pyridine H). <sup>13</sup>C NMR (CDCl<sub>3</sub>, 62.9 MHz) δ18.3 (C1), 120.3 (C4), 133.0 (C3), 137.4 (C5), 149.5 (C2), 153.7 (C6).

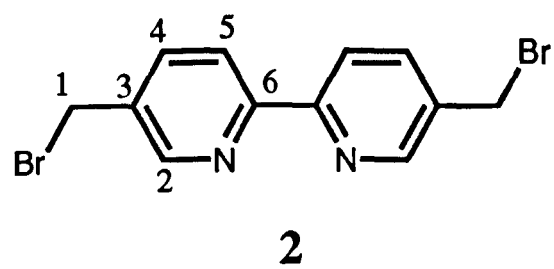
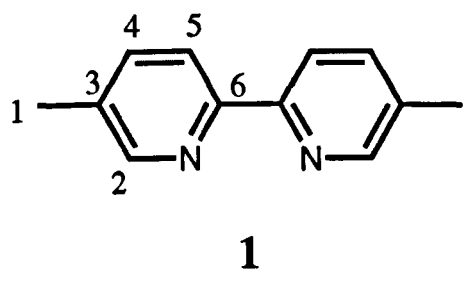
FAB<sup>+</sup> MS m/z=185 (100%, MH<sup>+</sup>). C<sub>12</sub>H<sub>12</sub>N<sub>2</sub> requires 184.2.

Calculated for C<sub>12</sub>H<sub>12</sub>N<sub>2</sub>: C 78.22, H 6.57, N 15.21;

Found C 78.32, H 6.59, N 15.27.

**5,5'-Bis(bromomethyl)-2,2'-bipyridine (2)** N-bromosuccinimide (23.18 g, 130.2 mmol) and **1** (12.00 g, 65.1 mmol) were suspended in carbon tetrachloride (500 ml). A spatula tip of AIBN was added and the mixture refluxed for 4 hours. The solvent was removed *in vacuo* and the residue dissolved in a minimum of CH<sub>2</sub>Cl<sub>2</sub> (approximately 700 ml). The organic layer was washed with saturated aqueous NaHCO<sub>3</sub> (3 x 200 ml), dried (Na<sub>2</sub>SO<sub>4</sub>), filtered and evaporated. The solid residue was washed with a little ice cold chloroform and dried *in vacuo* to yield the title compound as a slightly off-white powder (10.42 g, 47%).

R<sub>f</sub> = 0.65 (EtOAc). m.p. 201-202°C (dec.) (lit.<sup>105</sup> 211°C).



<sup>1</sup>H NMR (250 MHz, CDCl<sub>3</sub>) δ4.53 (4H, s, -CH<sub>2</sub>Br), δ7.84 (2H, dd, J = 8 Hz, 2 Hz, 4-pyridine H), δ8.40 (2H, d, J = 8 Hz, 3-pyridine H), δ8.67 (2H, d, J = 2 Hz, 6-pyridine H). <sup>13</sup>C NMR (62.9 MHz, CDCl<sub>3</sub>) δ31.2 (C1), 121.0 (C4), 135.1 (C3), 138.6 (C5), 150.2 (C2), 154.8 (C6).

FAB<sup>+</sup> MS m/z = 343 (100%, MH<sup>+</sup>). C<sub>12</sub>H<sub>10</sub>N<sub>2</sub>Br<sub>2</sub> requires 342.02.

Calculated for C<sub>12</sub>H<sub>10</sub>N<sub>2</sub>Br<sub>2</sub>: C 42.14, H 2.95, N 8.19, Br 46.72;

Found C 42.18, H 2.77, N 8.17, Br 46.49.

**5,5'-Bis(2,2-dicarbethoxyethyl)-2,2'-bipyridine (3).** *Method A:* Sodium metal (1.48 g, 64.3 mmol) was dissolved in dry ethanol (50 ml). Diethyl malonate (11.7 g, 64.3 mmol) was added over 4-5 minutes and refluxed for a further 10 minutes. To the clear solution produced was added a solution of **2** (2.00 g, 5.85 mmol) in hot THF / ethanol (54 ml : 36 ml) over 15 minutes followed by refluxing for 1 hour. The solvent was removed *in vacuo* and the residue taken up in water (15 ml) and extracted with diethyl ether (4 x 70 ml). The combined ether extracts were dried (K<sub>2</sub>CO<sub>3</sub>), filtered and evaporated. Flash chromatography on silica (4 x 25 cm) eluting with diethyl ether yielded an oil which crystallised upon standing overnight. The crystals were removed by filtration and washed well with petroleum ether (b.p 40 - 60°C) to yield the white crystalline title compound (1.41 g, 48%).

*Method B:* LiH (159 mg, 20 mmol) was added in one portion to a solution of diethyl malonate (5.86 g, 36.6 mmol) in dry DMF (10 ml) and stirred for 1 hour. Solid **2** (1.00 g, 2.92 mmol) was added in one portion and stirred for 30 minutes at 20°C followed by 1 hour at 50°C. Water (10 ml) was added to the mixture which was then extracted with Et<sub>2</sub>O (3 x 50ml). The combined extracts were washed with water (3 x 50 ml), dried (Na<sub>2</sub>SO<sub>4</sub>), filtered and evaporated to a yellow oil from which white crystals formed overnight. The crystals were removed by filtration, washed well with petroleum ether (b.p. 40-60°C) and dried *in vacuo* to yield the title compound (948 mg, 65%).

R<sub>f</sub> = 0.4 (Et<sub>2</sub>O). m.p. 123 - 124 °C.

<sup>1</sup>H NMR (250 MHz, CDCl<sub>3</sub>) δ1.22 (12H, t, J = 7 Hz, -CH<sub>3</sub>), δ3.26 (4H, d, J = 8 Hz, ArCH<sub>2</sub>-), δ3.66 (2H, t, J = 8 Hz, ArCH<sub>2</sub>CH-), δ4.16 (8H, m, -OCH<sub>2</sub>-), δ7.67 (2H, dd, J = 8 Hz, 2Hz, 4-pyridine H), δ8.27 (2H, d, J = 8 Hz, 3-pyridine H), δ8.52 (2H, d, J = 2 Hz, 6-pyridine H).

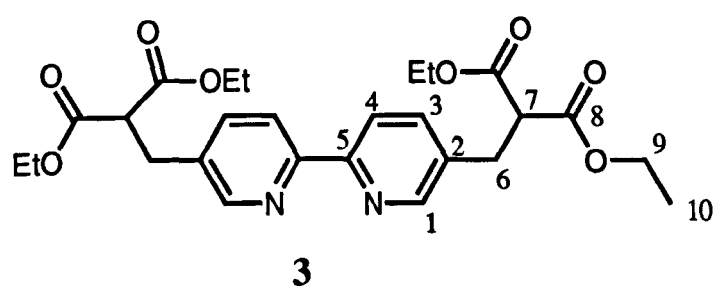
<sup>13</sup>C NMR (62.9 MHz, CDCl<sub>3</sub>) δ14.0 (C10), 31.7 (C6), 53.3 (C7), 61.7 (C9), 120.6 (C3), 133.5 (C2), 137.3 (C4), 149.6 (C1), 154.6 (C5), 168.4 (C8).

FAB<sup>+</sup> MS m/z = 501 (100%, MH<sup>+</sup>). C<sub>26</sub>H<sub>32</sub>N<sub>2</sub>O<sub>8</sub> requires 500.53.

ν = 1720 cm<sup>-1</sup> (C=O) and 1595, 1551 cm<sup>-1</sup> (aromatics).

Calculated for C<sub>26</sub>H<sub>32</sub>N<sub>2</sub>O<sub>8</sub>: C 62.39, H 6.44, N 5.60;

Found C 62.41, H 6.20, N 5.52.



**5,5'-Bis(2-carbethoxyethyl)-2,2'-bipyridine (4).** Tetraester **3** (7.50 g), water (2.0 ml) and sodium chloride (2.10 g) were refluxed in DMSO (100 ml) for 2.5 hours with the exclusion of light. After cooling, diethyl ether (400 ml) was added and the solution washed with water (5 x 150 ml) before being dried ( $\text{Na}_2\text{SO}_4$ ) and filtered. The ether solution was then filtered through 5 cm of silica and the solvent removed *in vacuo* to yield the title compound as a white crystalline solid (4.50 g, 84%).

$R_f = 0.50$  (10% methanol /  $\text{CH}_2\text{Cl}_2$ ). m.p. = 87-89 °C.

$^1\text{H}$  NMR (250 MHz,  $\text{CDCl}_3$ )  $\delta$  1.22 (6H, t,  $J = 7$  Hz, - $\text{CH}_3$ ), 2.55 (4H, t,  $J = 7.5$  Hz, - $\text{CH}_2-$ ), 2.98 (4H, t,  $J = 7.5$  Hz, - $\text{CH}_2-$ ), 4.12 (4H, q,  $J = 7$  Hz,  $\text{OCH}_2-$ ), 7.65 (2H, dd,  $J = 8$  Hz, 2 Hz, 4-pyridine H), 8.26 (2H, d,  $J = 8$  Hz, 3-pyridine H), 8.52 (2H, d,  $J = 2$  Hz, 6-pyridine H).

$^{13}\text{C}$  NMR (62.9 MHz,  $\text{CDCl}_3$ )  $\delta$  14.2 (C1), 28.0 (C5), 35.4 (C4), 60.6 (C2), 120.6 (C8), 135.9 (C7), 136.8 (C9), 149.2 (C6), 154.4 (C10), 172.4 (C3).

FAB<sup>+</sup> MS m/z = 357 (100%,  $\text{MH}^+$ ).  $\text{C}_{20}\text{H}_{24}\text{N}_2\text{O}_4$  requires 356.42.

$\nu = 1722 \text{ cm}^{-1}$  (C=O) and 1598, 1549  $\text{cm}^{-1}$  (aromatics).

Calculated for  $\text{C}_{20}\text{H}_{24}\text{N}_2\text{O}_4$ : C 67.40, H 6.79, N 7.86;

Found C 67.33, H 6.77, N 7.85.

**5,5'-Bis(3-hydroxypropyl)-2,2'-bipyridine (5).** A solution of **4** (0.973 g, 2.73 mmol) in dry diethyl ether (50 ml) was added dropwise over 30 minutes to a suspension of lithium aluminium hydride (0.228 g, 6.006 mmol) in dry ether (8 ml). The mixture was stirred for five hours before being quenched by the successive addition of water (0.23 ml), 15% aqueous sodium hydroxide (0.23 ml) and finally water (0.7 ml). The precipitate formed was removed by filtration and washed well with hot THF. The combined filtrate and THF washings were evaporated and the crude product purified by flash chromatography on silica (6 cm x 2 cm diameter) eluting with 5% MeOH increasing to 12.5% MeOH in dichloromethane to yield the title compound as a pale yellow solid (0.646 g, 87%).

$R_f = 0.05$  (10% methanol /  $\text{CH}_2\text{Cl}_2$ ). m.p 128-130°C.

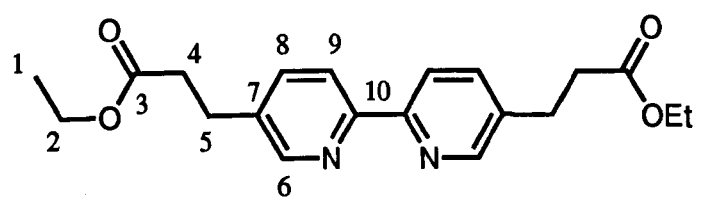
$^1\text{H}$  NMR (250 MHz,  $\text{CDCl}_3$ )  $\delta$  1.72 (2H, s, -OH), 1.90 (4H, quintet,  $J = 7$  Hz, - $\text{CH}_2\text{CH}_2\text{OH}$ ), 2.75 (4H, t,  $J = 7$  Hz, Ar $\text{CH}_2-$ ), 3.69 (4H, t,  $J = 7$  Hz, - $\text{CH}_2\text{OH}$ ), 7.64 (2H, dd,  $J = 8$  Hz, 2 Hz, 4-pyridine H), 8.27 (2H, d,  $J = 8$  Hz, 3-pyridine H), 8.50 (2H, d,  $J = 2$  Hz, 6-pyridine H).

$^{13}\text{C}$  NMR (62.9 MHz,  $\text{CDCl}_3$ )  $\delta$  29.0 (C3), 33.8 (C2), 61.7 (C1), 120.6 (C6), 137.0 (C5), 137.1 (C7), 149.3 (C4), 154.1 (C8).

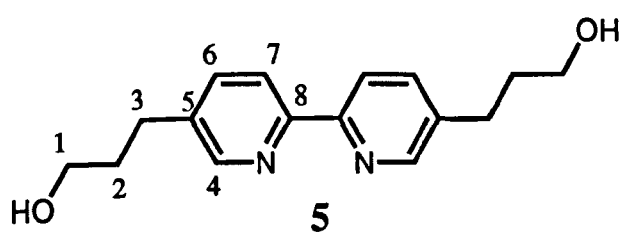
FAB<sup>+</sup> MS m/z = 273 (100%,  $\text{MH}^+$ ).  $\text{C}_{16}\text{H}_{20}\text{N}_2\text{O}_2$  requires 272.33.

Calculated for  $\text{C}_{16}\text{H}_{20}\text{N}_2\text{O}_2$ : C 70.56, H 7.40, N 10.29;

Found C 70.29, H 7.47, N 10.20.



4



**5,5'-Bis(2-carboxyethyl)-2,2'-bipyridine (6).** Sodium hydroxide (0.850 g, 21.25 mmol) and 4 (1.5 g, 4.208 mmol) were refluxed for 2 hours in water (10 ml). After cooling, concentrated HCl (36%, 2.15 g, 21.25 mmol) was added and the precipitate removed by filtration. After washing well with water and diethyl ether, the product was dried *in vacuo* at 60°C overnight to give the title compound as a white powder (1.13 g, 90%).  $R_f = 0.0$  (15% methanol / CH<sub>2</sub>Cl<sub>2</sub>).

m.p. 246 - 249 °C.

<sup>1</sup>H NMR (250 MHz, d<sub>6</sub>-DMSO) δ2.62 and δ2.89 (2 x 4H, 2t, J = 7 Hz, -CH<sub>2</sub>CH<sub>2</sub>-), δ7.79 (2H, dd, J = 8 Hz, 2 Hz, 4-pyridine H), δ8.27 (2H, d, J = 8 Hz, 3-pyridine H), δ8.54 (2H, d, J = 2 Hz, 6-pyridine H), δ12.25 (2H, br, -CO<sub>2</sub>H).

<sup>13</sup>C NMR (62.9 MHz, d<sub>6</sub>-DMSO) δ27.8 (C3), 35.1 (C2), 120.3 (C6), 137.1 (C5), 137.5 (C7), 149.6 (C4), 153.7 (C8), 174.0 (C1).

FAB<sup>+</sup> MS m/z = 301 (100%, MH<sup>+</sup>). C<sub>16</sub>H<sub>16</sub>N<sub>2</sub>O<sub>4</sub> requires 300.30.

Calculated for C<sub>16</sub>H<sub>16</sub>N<sub>2</sub>O<sub>4</sub>·0.25H<sub>2</sub>O: C 63.04 H 5.46, N 9.19;

Found C 62.91, H 5.18, N 9.17.

**5,5'-Bis(3-(*p*-toluenesulphonyl)oxypropyl)-2,2'-bipyridine (7).** TsCl (0.420 g, 2.20 mmol) was added portionwise to an ice-cooled solution of 5 (0.150 g, 0.55 mmol) in anhydrous pyridine (3 ml), stirring well and maintaining a temperature below 10°C. The flask was stoppered and refrigerated overnight before the contents were poured onto an ice / water mixture (*ca.* 8 ml) and stirred for 30 minutes. The precipitate formed was removed by filtration, washed well with water and dried *in vacuo*. Flash chromatography on silica (2 cm x 20 cm) eluting with 3% MeOH in CH<sub>2</sub>Cl<sub>2</sub> yielded the pure product as a white crystalline solid (0.240 g, 75%).

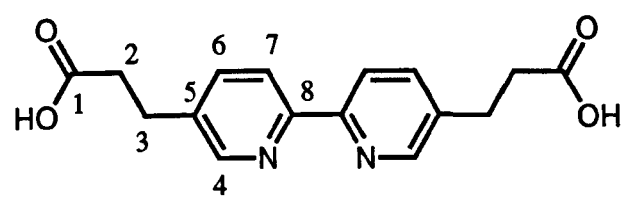
$R_f = 0.4$  (5% methanol / CH<sub>2</sub>Cl<sub>2</sub>). m.p. 171-172°C.

<sup>1</sup>H NMR (250 MHz, CDCl<sub>3</sub>) δ2.01 (4H, quintet, J = 7 Hz, ArCH<sub>2</sub>CH<sub>2</sub>-), δ2.44 (6H, s, -CH<sub>3</sub>), δ2.72 (4H, t, J = 7 Hz, ArCH<sub>2</sub>-), δ4.06 (4H, t, J = 7 Hz, -CH<sub>2</sub>SO<sub>3</sub>Ar), δ7.34 (4H, d, J = 9 Hz, *ortho*-toluene H), δ7.52 (2H, dd, J = 8 Hz, 2 Hz, 4-pyridine H), δ7.78 (4H, d, J = 9 Hz, *meta*-toluene H), δ8.22 (2H, d, J = 8 Hz, 3-pyridine H), δ8.39 (2H, d, J = 2 Hz, 6-pyridine H).

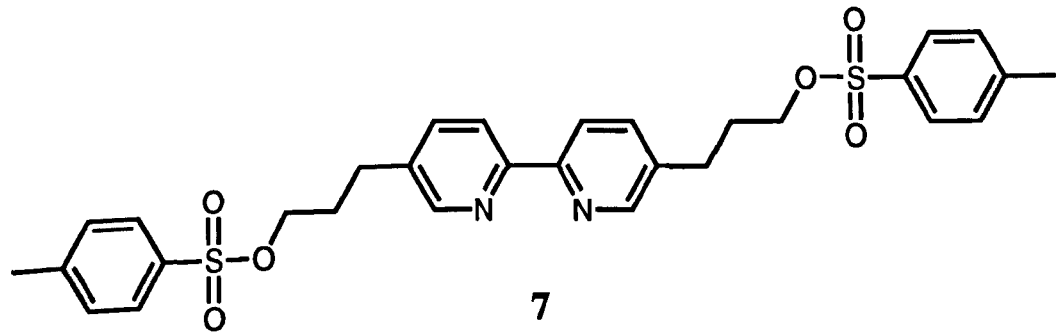
FAB<sup>+</sup> MS m/z = 581 (100%, MH<sup>+</sup>). C<sub>30</sub>H<sub>32</sub>N<sub>2</sub>O<sub>6</sub>S<sub>2</sub> requires 580.68.

Calculated for C<sub>30</sub>H<sub>32</sub>N<sub>2</sub>O<sub>6</sub>S<sub>2</sub>·H<sub>2</sub>O: C 60.18, H 5.72, N 4.68;

Found C 60.16, H 5.35, N 4.72.



**6**



**7**

**N-Acetyl-4,4-bis(4-hydroxyphenyl)piperidine (8).** To an ice-cooled suspension of phenol (20.52 g, 0.28 mol) in water (10 ml) was added N-acetyl-4-piperidone (14.93 g, 0.106 mol) with stirring. 98% sulphuric acid (40 g, 0.4 mol) was then added portionwise with stirring, maintaining a temperature below 25°C. The resulting mixture was left to stand for 4 days before being dissolved in hot acetone / methanol (7:3 v/v, 250 ml). The solution was neutralised with 1M aqueous Na<sub>2</sub>CO<sub>3</sub> and the total volume made up to 1L with water. The white precipitate was removed by filtration and washed well with water before being dried *in vacuo* at 120°C overnight to yield the title compound as a powdery white solid (24.71 g, 75%).

R<sub>f</sub> = 0.20 (10% methanol / CH<sub>2</sub>Cl<sub>2</sub>). m.p. 295-297°C (lit.<sup>107</sup> 301°C).

<sup>1</sup>H NMR (250 MHz, d<sub>6</sub>-DMSO) δ1.97 (3H, s, -CH<sub>3</sub>), δ2.18 and 2.29 (4H, 2br, -CH<sub>2</sub>-), δ3.39 (4H, m, N-CH<sub>2</sub>-), δ6.66 (4H, d, J = 9 Hz, *ortho*-phenol H), δ7.07 (4H, d, J = 9 Hz, *meta*-phenol H), δ9.22 (2H, s, phenol OH).

<sup>13</sup>C NMR (62.9 MHz, d<sub>6</sub>-DMSO) δ21.8 (C1), 35.8, 36.5, 38.6 (C3/4, 2 conformations), 43.4 and 43.5 (C5, 2 conformations), 115.5 (C8), 128.1 (C7), 137.8 (C6), 155.5 (C9), 168.5 (C2).

FAB<sup>+</sup> MS m/z = 312 (100%, MH<sup>+</sup>). C<sub>19</sub>H<sub>21</sub>NO<sub>3</sub> requires 311.4.

ν = 3335 cm<sup>-1</sup> (OH stretch), 1620 (C=O).

Calculated for C<sub>19</sub>H<sub>21</sub>NO<sub>3</sub>.H<sub>2</sub>O: C 69.28, H 7.03, N 4.25;

Found C 69.54, H 6.73, N 4.31.

**1,1-Bis(4-hydroxyphenyl)cyclohexane (9).** Cyclohexanone (10.40 g, 0.106 mol), phenol (20.52 g, 0.218 mol) and water (10 ml) were cooled in an ice-bath during the portionwise addition of conc. H<sub>2</sub>SO<sub>4</sub> (40 g, 0.40 mol). After stirring for a further 1.5 hours at room temperature, the mixture solidified and was added to water (200 ml). After neutralisation with solid NaHCO<sub>3</sub>, the precipitate was removed by filtration and dissolved in hot methanol (100 ml). Addition of water (700 ml) produced a precipitate which was filtered, washed well with water and sparingly with diethyl ether to yield the title compound as a pale pink solid (13.87 g, 49%).

R<sub>f</sub> = 0.4 (10% methanol / CH<sub>2</sub>Cl<sub>2</sub>). m.p. 184-186 °C.

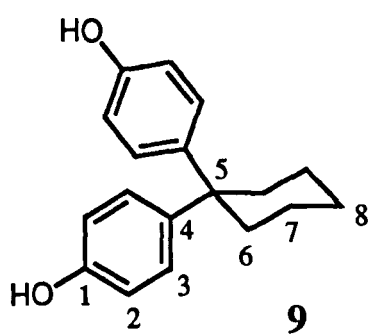
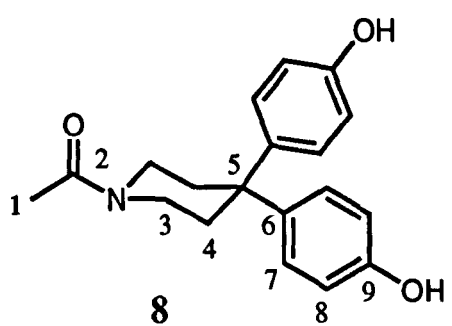
<sup>1</sup>H NMR (250 MHz, d<sub>6</sub>-acetone) δ1.50 (6H, br, 3,4-cyclohexyl H), δ2.20 (4H, br, 2-cyclohexyl H), δ6.72 (4H, d, J = 9 Hz, *ortho*-phenol H), δ7.10 (4H, d, J = 9 Hz, *meta*-phenol H), δ8.10 (2H, s, ArOH)

<sup>13</sup>C NMR (62.9 MHz, d<sub>6</sub>-acetone) δ23.6 (C7), 27.1 (C8), 38.0 (C6), 45.4 (C5), 115.6 (C2), 128.7 (C3), 140.8 (C4), 155.5 (C1).

FAB<sup>+</sup> MS m/z = 268 (100%, M<sup>+</sup>); C<sub>18</sub>H<sub>20</sub>O<sub>2</sub> requires 268.34.

Calculated for C<sub>18</sub>H<sub>20</sub>O<sub>2</sub>.0.25H<sub>2</sub>O: C 79.23, H 7.57;

Found C 78.9, H 7.5.



**Tris-(5,5'-bis(3-hydroxypropyl)-2,2'-bipyridine) ruthenium (II) hexafluorophosphate (10).** *Method A.* Sodium phosphinate was prepared by diluting hypophosphorus acid (50 wt% in water, 5 ml) with water (3 ml) and neutralising with sodium hydroxide pellets until a faint white precipitate appeared. The solution was then reacidified with hypophosphorus acid until a pH of 5-6 was obtained. Dried ruthenium trichloride (0.048 g, 0.23 mmol), **5** (0.188 g, 0.69 mmol) and freshly prepared sodium phosphinate solution (0.35 ml) were refluxed in water (5 ml) until a clear orange solution was obtained (approximately 1 hour). The solution was concentrated to *ca.* 2 ml and a solution of NH<sub>4</sub>PF<sub>6</sub> (0.300 g, 1.84 mmol) in a minimum volume of water was added with the immediate formation of a bright orange precipitate. This was removed by filtration, washed with a little water and dried *in vacuo* at 70°C overnight to yield the title compound as a bright orange solid (0.170 g, 61%).

*Method B.* Dried ruthenium trichloride (0.190 g, 0.918 mmol) and **5** (0.750 g, 2.754 mmol) were heated at reflux in ethylene glycol (3 ml) for 1 hour. A solution of NH<sub>4</sub>PF<sub>6</sub> (1.5 g, 9.20 mmol) in water (3 ml) was added and the crystals formed after refrigeration overnight were removed by filtration, washed sparingly with water and dried *in vacuo* at 95°C to yield the title compound as a bright orange solid (0.762 g, 69%).

R<sub>f</sub> = 0.0 (15% methanol / CH<sub>2</sub>Cl<sub>2</sub>). m.p. 150 - 152 °C.

<sup>1</sup>H NMR (250 MHz, d<sub>6</sub>-acetone) δ1.70 (12H, m, ArCH<sub>2</sub>CH<sub>2</sub>-), 82.64 (12H, m, ArCH<sub>2</sub>), 83.42 (12H, t, J = 7 Hz, -CH<sub>2</sub>OH), 87.77 (6H, d, J = 2 Hz, 6-pyridine H), 88.04 (6H, dd, J = 8 Hz, 2 Hz, 4-pyridine H), 88.64 (6H, d, J = 8 Hz, 3-pyridine H).

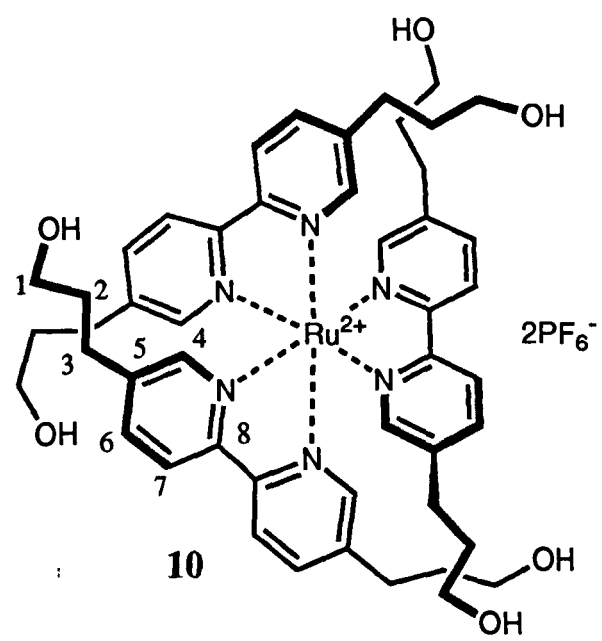
<sup>13</sup>C NMR (62.9 MHz, d<sub>6</sub>-DMSO) δ28.8 (C3), 33.1 (C2), 59.7 (C1), 124.1 (C6), 138.2 (C7), 142.2 (C5), 150.3 (C4), 155.0 (C8).

FAB<sup>+</sup> MS m/z=1063 (100%, [M-PF<sub>6</sub>]<sup>+</sup>), 917 (85%, [M-2PF<sub>6</sub>]<sup>+</sup>).

Calculated for C<sub>48</sub>H<sub>60</sub>N<sub>6</sub>O<sub>6</sub>P<sub>2</sub>F<sub>12</sub>Ru·4H<sub>2</sub>O: C 45.03, H 5.35, N 6.57;

Found: C 45.13, H 4.82, N 6.86.

λ<sub>max</sub> (ε) (CH<sub>2</sub>Cl<sub>2</sub>) 259.0 nm (34000), 265.1 nm (34000), 294.6 nm (89200), 425.6 nm (11500), 453.6 nm (14400).



**Tris(5,5'-bis(3-(*p*-toluenesulphonyl)oxypropyl)-2,2'-bipyridine) ruthenium (II) hexafluorophosphate (11).** Ts<sub>2</sub>O (0.540 g, 1.656 mmol) was added portionwise over 30 minutes to an ice-cooled solution of **10** (0.100 g, 0.083 mmol) in anhydrous pyridine (2 ml) under N<sub>2</sub>. The mixture was refrigerated for 72 hours before pouring onto ice / water (*ca.* 10 g) containing NH<sub>4</sub>PF<sub>6</sub> (1.0 g). The solid was filtered, washed well with water and dissolved in CH<sub>2</sub>Cl<sub>2</sub> (20 ml). The CH<sub>2</sub>Cl<sub>2</sub> layer was washed with aqueous NH<sub>4</sub>PF<sub>6</sub> (10 ml), 0.5 M HCl (10 ml) and water (2 x 10 ml) before being dried (Na<sub>2</sub>SO<sub>4</sub>), filtered and evaporated to give the title compound as an orange solid (131 mg, 74%). R<sub>f</sub> = 0.25 (10% methanol in CH<sub>2</sub>Cl<sub>2</sub>). m.p. 68–72 °C (dec.)

<sup>1</sup>H NMR (250 MHz, CDCl<sub>3</sub>). δ1.85 (12H, br, ArCH<sub>2</sub>CH<sub>2</sub>-), δ2.44 (18H, s, -CH<sub>3</sub>), δ2.65 (12H, br, ArCH<sub>2</sub>-), δ3.81 (12H, m, CH<sub>2</sub>OTs), δ7.33 (12H, d, J = 9 Hz, *ortho*-toluene H), δ7.56 (6H, d, J = 2 Hz, 6-pyridine H), δ7.65 (12H, d, J = 9 Hz, *meta*-toluene H), δ7.76 (6H, dd, J = 8 Hz, 2 Hz, 4-pyridine H), δ8.31 (6H, d, J = 8 Hz, 3-pyridine H). FAB<sup>+</sup> MS m/z = 1987 (100%, [M-PF<sub>6</sub>]<sup>+</sup>), 1842 (25%, [M-2PF<sub>6</sub>]<sup>+</sup>), 921 (30%, [M-2PF<sub>6</sub>]<sup>2+</sup>). Found for [M-PF<sub>6</sub>]<sup>+</sup>: m/z = 1987.3975; C<sub>90</sub>H<sub>96</sub>N<sub>6</sub>O<sub>18</sub>S<sub>6</sub>RuP<sub>2</sub>F<sub>12</sub> requires 1987.3791.

$\lambda_{\text{max}} (\varepsilon)$  (CH<sub>2</sub>Cl<sub>2</sub>) 256.2 nm (29500), 263.8 nm (30300), 295.4 nm (81800), 430.1 nm (10100), 446.1 nm (12200).

**Tris-(5,5'-bis(2-carboxyethyl)-2,2'-bipyridine) ruthenium (II) hexafluorophosphate (13).** Dried RuCl<sub>3</sub> (0.194 g, 0.935 mmol) and **4** (1.000 g, 2.806 mmol) were heated at reflux in ethylene glycol (6 ml) for 45 minutes. After cooling, NH<sub>4</sub>PF<sub>6</sub> (0.610 g, 3.74 mmol) in water (6 ml) was added and the mixture refrigerated overnight. The crystals that separated were removed by filtration and washed well with water to give a bright orange solid which was suspended in water (10 ml). NaOH (0.822 g, 20.55 mmol) was added and the mixture refluxed for 45 minutes until the solid dissolved to give a clear red solution. After cooling, 36% HCl (2.2 ml, 25 mmol) and NH<sub>4</sub>PF<sub>6</sub> (1.5 g, 9.20 mmol) were added and the solution returned briefly to reflux. The crystals that separated upon cooling were filtered, washed with water and dried *in vacuo* at 60 °C to give the title compound as an orange solid (0.925 g, 77%). m.p. 122 – 125 °C.

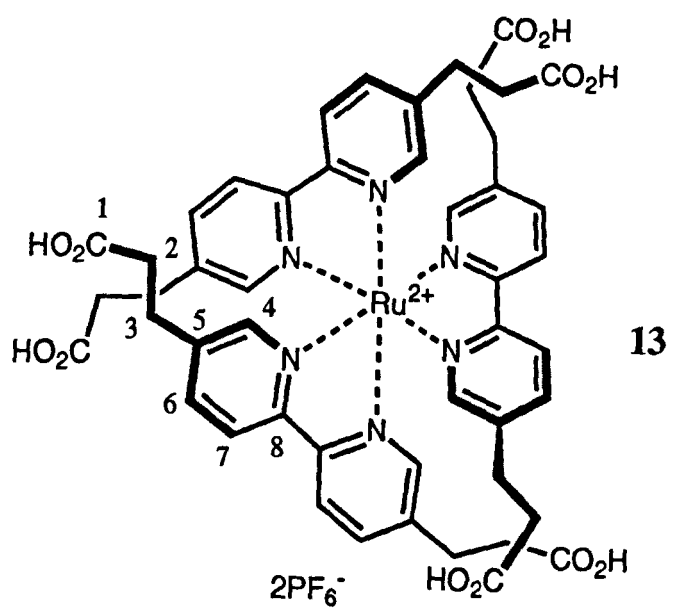
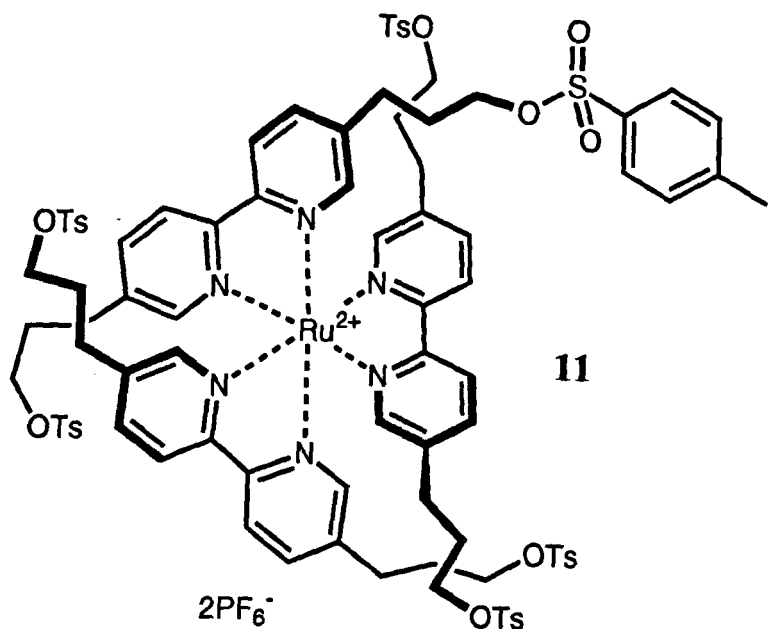
<sup>1</sup>H NMR (250 MHz, d<sub>6</sub>-acetone) δ2.61 and δ2.81 (2 x 12H, 2m, -CH<sub>2</sub>CH<sub>2</sub>-), δ7.78 (6H, d, J = 2 Hz, 6-pyridine H), δ8.09 (6H, dd, J = 8 Hz, 2 Hz, 4-pyridine H), δ8.63 (6H, d, J = 8 Hz, 3-pyridine H).

<sup>13</sup>C NMR (62.9 MHz, d<sub>6</sub>-acetone) δ28.2 (C3), 34.3 (C2), 124.6 (C6), 138.6 (C7), 142.0 (C5), 151.9 (C4), 156.2 (C8), 174.2 (C1).

FAB<sup>+</sup> MS m/z = 1147 [M - PF<sub>6</sub>]<sup>+</sup>, 1001 [M - 2PF<sub>6</sub>]<sup>+</sup>.  $\nu$  = 1706 cm<sup>-1</sup> (C=O).

Calculated for C<sub>48</sub>H<sub>48</sub>N<sub>6</sub>O<sub>12</sub>RuP<sub>2</sub>F<sub>12</sub>·3H<sub>2</sub>O: C 42.83, H 4.04, N 6.24;  
Found C 42.82, H 3.73, N 6.40.

$\lambda_{\text{max}} (\varepsilon)$  256.8 nm (28000), 294.3 nm (78000), 453.2 nm (13000).



**Tris(5,5'-bis(3-(*p*-toluenesulphonyl)oxypropyl)-2,2'-bipyridine) iron (II) perchlorate (14)** To a stirred solution of 7 (0.100 g, 0.172 mmol) in CH<sub>2</sub>Cl<sub>2</sub> (4 ml) was added a solution of Fe(ClO<sub>4</sub>)<sub>2</sub>.6H<sub>2</sub>O (20.8 mg, 0.0574 mmol) in 5% methanol / CH<sub>2</sub>Cl<sub>2</sub> (*ca.* 4 ml) with the immediate formation of a red coloration. Stirring was continued overnight before the solvent was removed *in vacuo* to give a quantitative yield of the title compound as a red foam.

m.p. *ca.* 170 °C (dec.)

<sup>1</sup>H NMR (250 MHz, CDCl<sub>3</sub>) δ1.84 (12H, br, ArCH<sub>2</sub>CH<sub>2</sub>-), δ2.43 (18H, s, -CH<sub>3</sub>), δ2.66 (12H, br, ArCH<sub>2</sub>-), δ3.82 (12H, br, -CH<sub>2</sub>OTs), δ7.23 (6H, br, 6-bipyridine H), δ7.32 (12H, d, J = 8.5 Hz, *ortho*-toluene H), δ7.66 (12H, d, J = 8.5 Hz, *meta*-toluene H), δ7.82 (6H, br, 4-bipyridine H), δ8.37 (6H, br, 3-bipyridine H).

FAB<sup>+</sup> MS m/z = 1897 (3%, [M - ClO<sub>4</sub>]<sup>+</sup>), 1795 (12%, [M - 2ClO<sub>4</sub>]<sup>+</sup>), 898 (100%, [M - 2ClO<sub>4</sub>]<sup>2+</sup>).

Calculated for C<sub>90</sub>H<sub>96</sub>N<sub>6</sub>O<sub>26</sub>S<sub>6</sub>FeCl<sub>2</sub>: C 54.12, H 4.85, N 4.21;

Found C 54.08, H 4.84, N 4.03.

λ<sub>max</sub> (ε) (CH<sub>2</sub>Cl<sub>2</sub>) 255.36 nm (75100), 308.0 nm (70600), 349.7 nm (5700), 513.8 nm (7600).

**Tris-(5,5'-bis(2-carboxyethyl)-2,2'-bipyridine) iron (II) perchlorate (15).** 6 (0.400 g, 1.332 mmol) was added to a solution of Fe(ClO<sub>4</sub>)<sub>2</sub>.6H<sub>2</sub>O (0.444 mmol) in 15% methanol / CH<sub>2</sub>Cl<sub>2</sub> (*ca.* 15 ml). The deep red solution formed was stirred for 18 hours before the solvent was removed *in vacuo* to give a quantitative yield of the title compound as a red foam.

m.p. *ca.* 140 - 150 °C.

<sup>1</sup>H NMR (250 MHz, d<sub>6</sub>-acetone) δ2.60 and 2.80 (2 x 12H, m, -CH<sub>2</sub>CH<sub>2</sub>-), δ7.42 (6H, d, J = 2 Hz, 6-pyridine H), δ8.14 (6H, dd, J = 8 Hz, 2 Hz, 4-pyridine H), δ8.65 (6H, d, J = 8 Hz, 3-pyridine H).

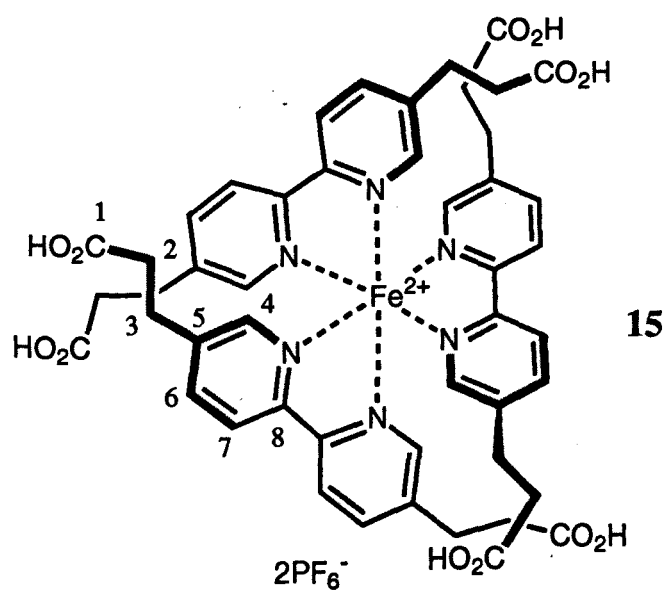
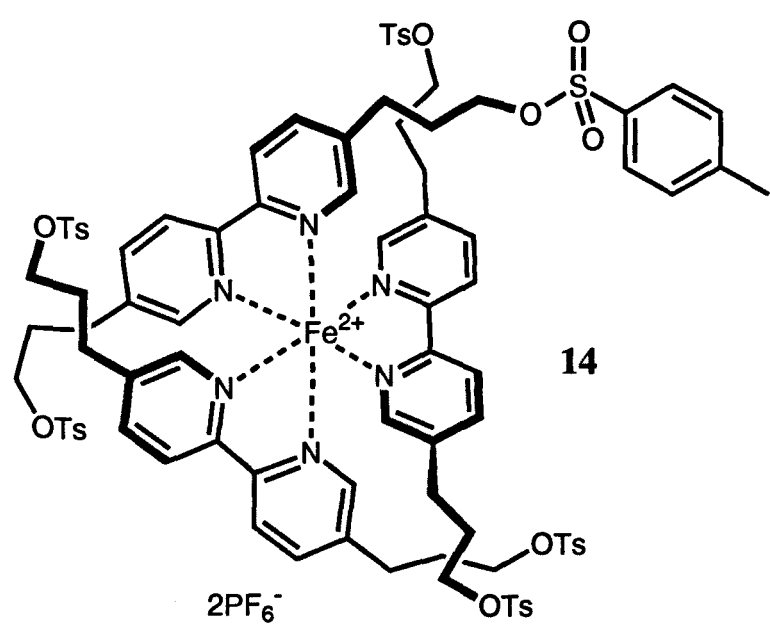
<sup>13</sup>C NMR (62.9 MHz, d<sub>6</sub>-DMSO) δ27.7 (C3), 34.0 (C2), 123.9 (C6), 139.0 (C7), 140.8 (C5), 153.2 (C4), 157.4 (C8), 173.5 (C1).

FAB<sup>+</sup> MS m/z = 1055 (20%, [M-ClO<sub>4</sub>]<sup>+</sup>), 955 (95%, [M-2ClO<sub>4</sub>]<sup>+</sup>), 755 (53%, [Fe(bipy)<sub>2</sub>ClO<sub>4</sub>]<sup>+</sup>), 655 (100%, [Fe(bipy)<sub>2</sub>]<sup>+</sup>).

Calculated for C<sub>48</sub>H<sub>48</sub>N<sub>6</sub>O<sub>20</sub>FeCl<sub>2</sub>.4H<sub>2</sub>O: C 46.96, H 4.60, N 6.85;

Found C 47.0, H 4.3, N 6.6.

λ<sub>max</sub> (ε) (CH<sub>2</sub>Cl<sub>2</sub>) 256.2 nm (31500), 268.0 nm (26000), 306.6 nm (62500), 514.6 nm (8900), 527.8 nm (8900).



**1-Phenyl-3-(*p*-toluenesulphonyloxy)-propane (**16**).** TsCl (9.53 g, 0.050 mol) was added portionwise to a stirred solution of 3-phenyl-1-propanol (3.405 g, 0.025 mol) in anhydrous pyridine (50 ml) at 0°C. After 15 minutes, the mixture was refrigerated overnight before quenching on ice (300 g) and warming to room temperature. The aqueous layer was extracted with Et<sub>2</sub>O (3 x 100 ml) and the extracts washed with aqueous HCl (2 x 50 ml, 1M) and water (2 x 50 ml) before being dried (K<sub>2</sub>CO<sub>3</sub> / Na<sub>2</sub>SO<sub>4</sub>), filtered and evaporated to a yellow oil which slowly solidified. The solid was washed with ice-cold petroleum ether (b.p. 40–60°C) and dried *in vacuo* to yield the title compound as a waxy yellow solid (4.75 g, 65%). m.p. *ca.* 15–20 °C.

<sup>1</sup>H NMR (250 MHz, CDCl<sub>3</sub>) δ1.95 (2H, quintet, J = 7 Hz, PhCH<sub>2</sub>CH<sub>2</sub>-), δ2.45 (3H, s, -CH<sub>3</sub>), δ2.65 (2H, t, J = 6.5 Hz, PhCH<sub>2</sub>-). δ4.06 (2H, t, J = 6.5 Hz, -CH<sub>2</sub>OTs), δ7.07 (2H, d, ArH), δ7.20 (3H, m, ArH), δ7.35 (2H, d, J = 8.5 Hz, *ortho*-toluene H), δ7.80 (2H, d, J = 8.5 Hz, *meta*-toluene H).

<sup>13</sup>C NMR (62.9 MHz, CDCl<sub>3</sub>) δ21.7 (C12), 30.5 and 31.5 (C5, 6), 69.9 (C7), 126.2, 127.9, 128.4, 128.5 and 129.9 (C1, 2, 3, 9, 10), 133.1 (C8), 140.4 (C11), 144.8 (C4).

EI<sup>+</sup> MS m/z = 290.0977; C<sub>16</sub>H<sub>18</sub>SO<sub>3</sub> requires 290.0978.

ν (thin film) = 1357, 1175 cm<sup>-1</sup> (-SO<sub>3</sub>-)

**N-Acetyl-4,4-bis(4-(3-phenylpropyloxy)phenyl)piperidine (**17**).** **8** (0.250 g, 0.81 mmol) and Cs<sub>2</sub>CO<sub>3</sub> (1.056 g, 3.24 mmol) in dry DMF (8 ml) were stirred for 0.5 hours before the addition of a DMF (7 ml) solution of **16** (0.466 g, 1.61 mmol). The mixture was stirred at room temperature for 48 hours before the solvent was removed *in vacuo*. The product was partitioned between water (10 ml) and CH<sub>2</sub>Cl<sub>2</sub> (10 ml). The CH<sub>2</sub>Cl<sub>2</sub> layer was separated, dried (Na<sub>2</sub>SO<sub>4</sub>), filtered and evaporated. Flash chromatography on silica (2 cm x 30 cm) eluting with 3% methanol / CH<sub>2</sub>Cl<sub>2</sub> gave the title compound as an off-white solid (0.257 g, 58%). Repetition of the reaction as above but at a temperature of 65 °C for 18 hours gave an identical product (0.346 g, 78%).

R<sub>f</sub> = 0.30 (5% methanol / CH<sub>2</sub>Cl<sub>2</sub>). m.p. 104 – 106 °C.

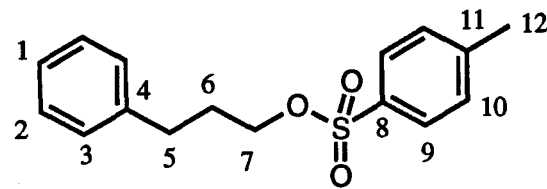
<sup>1</sup>H NMR (250 MHz, CDCl<sub>3</sub>) δ2.08 (7H, m, CH<sub>3</sub>CO- and ArOCH<sub>2</sub>CH<sub>2</sub>CH<sub>2</sub>Ph), δ2.35 (4H, br, AcNCH<sub>2</sub>CH<sub>2</sub>-), δ2.70 (4H, t, J = 7 Hz, -CH<sub>2</sub>Ph), δ3.48 and 3.66 (4H, br, AcNCH<sub>2</sub>-), δ3.94 (4H, t, J = 7 Hz, ArOCH<sub>2</sub>-), δ6.82 (4H, d, J = 9 Hz, *ortho*-ArOR), δ7.12 (4H, d, J = 9 Hz, *meta*-ArOR), δ7.20 – 7.32 (10H, m, -Ph).

<sup>13</sup>C NMR (62.9 MHz, CDCl<sub>3</sub>) δ21.5 (C1), 30.9 and 32.2 (C11, 12), 36.1, 37.0 and 38.7 (C3/4, two conformations), 43.7 and 43.8 (C5, two conformations), 66.9 (C10), 114.5 (C8), 126.0, 127.9, 128.5 and 128.6 (C7, 14, 15, 16), 138.6 (C6), 141.5 (C13), 157.2 (C9), 168.9 (C2).

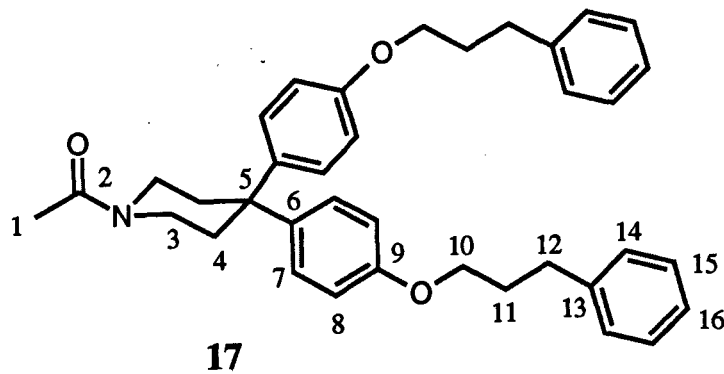
FAB<sup>+</sup> MS m/z = 548 (100%, M<sup>+</sup>). C<sub>37</sub>H<sub>41</sub>NO<sub>3</sub> requires 547.74. ν = 1628 cm<sup>-1</sup> (C=O).

Calculated for C<sub>37</sub>H<sub>41</sub>NO<sub>3</sub>·0.5H<sub>2</sub>O: C 79.81, H 7.60, N 2.52;

Found C 80.12, H 7.42, N 2.47.



16

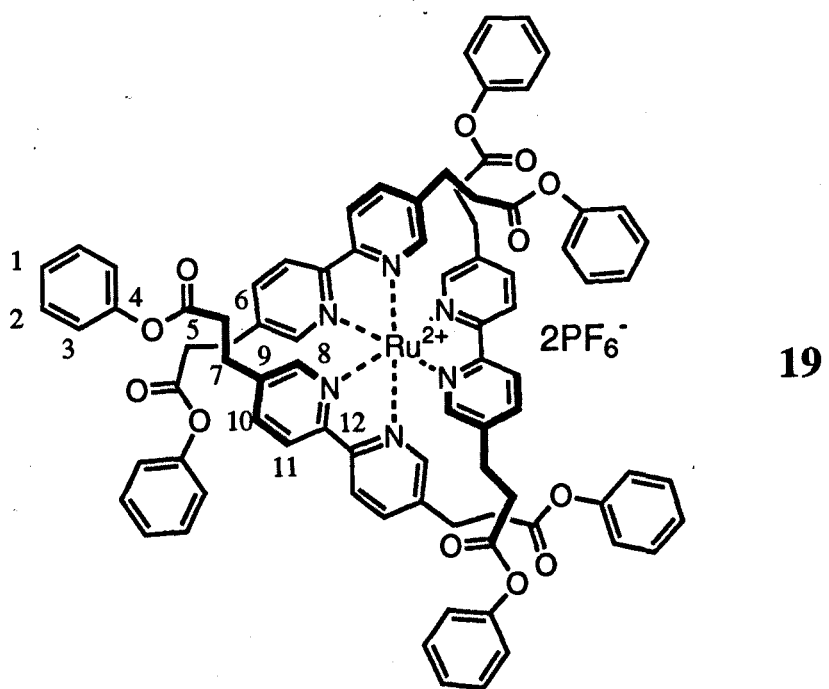
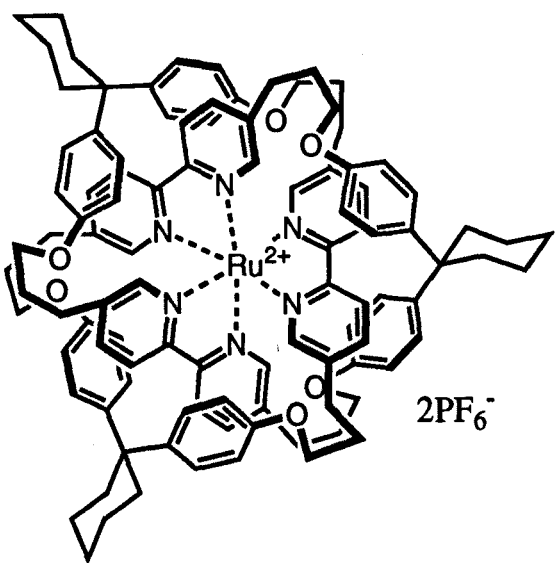
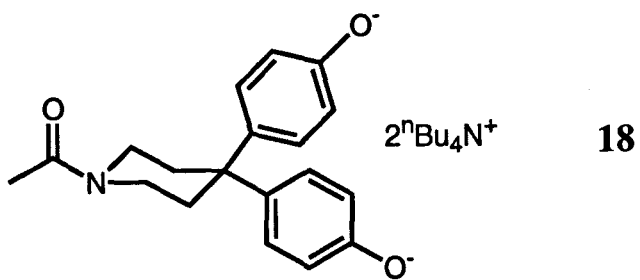


**N-Acetyl-4,4-bis(4-hydroxyphenyl)piperidine, bis(tetra-nbutyl ammonium) salt (18).** **8** (1 g, 3.21 mmol) was added to a solution of  $n\text{Bu}_4\text{N}^+\text{OH}^-$  (1.0M in MeOH, 6.5 ml, 6.5 mmol) and heated to reflux. The solution was cooled, filtered and evaporated before being dried thoroughly by gentle heat under high vacuum to give the title compound as a sticky brown solid in quantitative yield.

$^1\text{H}$  NMR (250 MHz,  $\text{CDCl}_3$ )  $\delta$  0.88 (24H, t, - $\text{CH}_2\text{CH}_3$ ), 1.28 (16H, m, - $\text{CH}_2\text{CH}_3$ ), 1.48 (16H, m, - $\text{CH}_2\text{CH}_2\text{CH}_3$ ), 1.99 (3H, s,  $\text{COCH}_3$ ), 2.15 (4H, br,  $\text{CH}_2\text{CAr}_2$ ), 3.50 (4H, br,  $\text{N}^+\text{CH}_2\text{C}_3\text{H}_7$ ), 6.70 and 6.80 (8H, br, ArH).

*Attempted macrocyclisation of 11 to a ruthenium (II) ether-linked trefoil knot.* A solution of **11** (0.500 g, 0.234 mmol) and **9** (0.189 g, 0.703 mmol) in dry DMF (50 ml) was added dropwise to a rapidly stirred suspension of  $\text{Cs}_2\text{CO}_3$  (0.915 g, 2.8 mmol) in DMF (80 ml) at 55 - 60 °C. The mixture quickly became very dark and stirring was continued for 18 hours. The solvent was removed under high vacuum and the residue partitioned between water (50 ml) and  $\text{CH}_2\text{Cl}_2$  (100 ml). The two-phase mixture was filtered to remove an insoluble brown product which was assumed to be oligomeric species. The deep orange / red  $\text{CH}_2\text{Cl}_2$  layer was separated and the aqueous layer further extracted with  $\text{CH}_2\text{Cl}_2$  (2 x 50 ml). The combined  $\text{CH}_2\text{Cl}_2$  layers were washed with water (3 x 50 ml) and concentrated *in vacuo* to ca. 25 ml. This solution was stirred vigorously for 18 hours with a solution of  $\text{NH}_4\text{PF}_6$  (2 g) in water (10 ml) before being separated, washed with water (2 x 25 ml), dried ( $\text{Na}_2\text{SO}_4$ ), filtered and evaporated. Flash chromatography on silica (1 cm x 20 cm) eluting with  $\text{CH}_2\text{Cl}_2$  increasing in 1% steps to 10% methanol /  $\text{CH}_2\text{Cl}_2$  gave 3 products in extremely small amounts with an  $R_f$  of 0.55, 0.40 and 0.15 in 10% MeOH /  $\text{CH}_2\text{Cl}_2$ . Attempts to characterise these products by  $^1\text{H}$  NMR and FAB $^+$  MS were unsuccessful.

**Tris-(5,5'-bis(2-carbophenoxyethyl)-2,2'-bipyridine) ruthenium (II) hexafluorophosphate (19).** Phenol (87.4 mg, 0.929 mmol) and **13** (0.100 g, 0.077 mmol) were cooled to 0 °C in dry  $\text{CH}_2\text{Cl}_2$  (15 ml) before the addition of DMAP (9.5 mg, 0.077 mmol) and EDC (89.0 mg, 0.464 mmol). After stirring for 48 hours, the  $\text{CH}_2\text{Cl}_2$  solution was washed with 1M HCl (2 x 15 ml), 1M NaOH (2 x 15 ml) and water (15 ml). The solution was then stirred vigorously with a saturated aqueous solution of  $\text{NH}_4\text{PF}_6$  (1 ml) for 5 hours before the  $\text{CH}_2\text{Cl}_2$  layer was separated, washed with water (15 ml), dried ( $\text{Na}_2\text{SO}_4$ ), filtered and evaporated. Flash chromatography on silica (20 cm x 1.5 cm) eluting with 2.5% methanol in  $\text{CH}_2\text{Cl}_2$  gave the title compound as an orange solid (94 mg, 70%).



$R_f = 0.60$  (5% methanol in  $\text{CH}_2\text{Cl}_2$ ). m.p. 175 - 176 °C.

$^1\text{H}$  NMR (250 MHz,  $\text{CDCl}_3$ )  $\delta$  2.69 (24H, br, Ar $\text{CH}_2\text{CH}_2\text{CO}_2\text{Ph}$ ), 86.88 (12H, d,  $J = 9$  Hz, *ortho*-phenol H), 87.24 (6H, m, *para*-phenol H), 87.35 (12H, m, *meta*-phenol H), 87.53 (6H, d,  $J = 2$  Hz, 6-bipyridine H), 87.55 (6H, dd,  $J = 8$  Hz, 2 Hz, 4-bipyridine H), 87.73 (6H, d,  $J = 8$  Hz, 3-bipyridine H).

$^{13}\text{C}$  NMR (62.9 MHz,  $\text{CDCl}_3 + 5\%$   $\text{CD}_3\text{OD}$ )  $\delta$  27.0 (C7), 33.6 (C6), 121.4 (C3), 123.4 (C10), 126.0 (C1), 129.4 (C2), 137.4 (C11), 140.4 (C9), 150.4 (C4), 151.2 (C8), 154.7 (C12), 170.6 (C5).

FAB<sup>+</sup> MS m/z = 1603 (100%, [M -  $\text{PF}_6$ ]<sup>+</sup>), 1459 (45%, [M - 2 $\text{PF}_6$ ]<sup>+</sup>).

Calculated for  $\text{C}_{84}\text{H}_{72}\text{N}_6\text{O}_{12}\text{RuP}_2\text{F}_{12}$ : C 57.70, H 4.15, N 4.81;

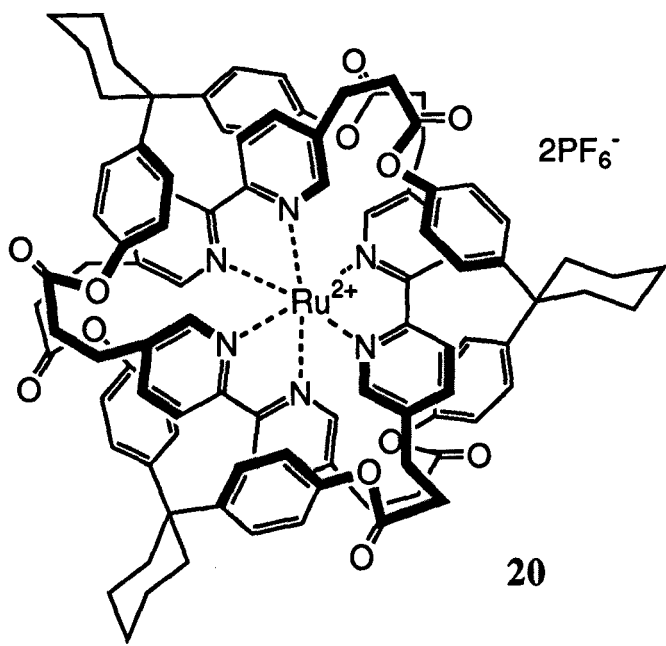
Found C 57.94, H 4.42, N 5.24.

$\lambda_{\text{max}} (\epsilon)$  ( $\text{CH}_2\text{Cl}_2$ ) 256.2 nm (37600), 265.4 nm (37100), 295.4 nm (102100), 422.8 nm (13800), 452.8 nm (16600).

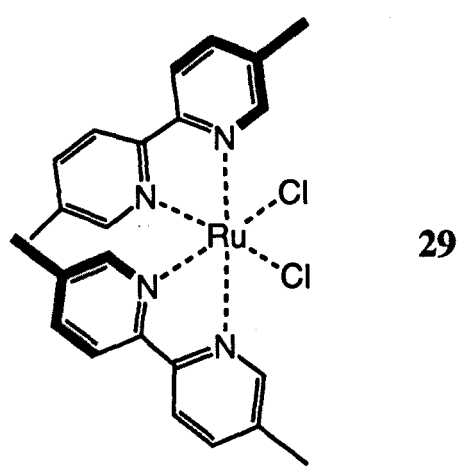
**Attempted macrocyclisation to ruthenium (II) ester-linked trefoil knot (20).** A solution of **13** (0.500 g, 0.386 mmol), **9** (0.311 g, 1.161 mmol) and DMAP (94 mg, 0.772 mmol) in dry  $\text{CH}_2\text{Cl}_2$  / DMF (98.25 : 1.75 v/v, 400 ml) was added dropwise over 5 - 6 hours at 0 °C to a stirred solution of EDC (1.100g, 5.79 mmol) in dry  $\text{CH}_2\text{Cl}_2$  (100 ml). After the addition, the solution was stirred for a further 18 hours at room temperature before filtering to remove an insoluble orange solid (32 mg) upon which no further characterisation was possible. The remaining solution was washed successively with 1M HCl (2 x 75 ml), saturated  $\text{NaHCO}_3$  (2 x 75 ml) and water (5 x 100 ml). The  $\text{CH}_2\text{Cl}_2$  layer was then stirred vigorously overnight with a solution of  $\text{NH}_4\text{PF}_6$  (5 g) in water (15 ml) to effect counterion exchange before being separated, washed with water (100 ml), dried ( $\text{Na}_2\text{SO}_4$ ), filtered and evaporated to give a bright orange solid (0.656 g). Attempts to characterise this product are discussed in Chapter 3.

**Cis-dichloro-bis(5,5'-dimethyl-2,2'-bipyridine) ruthenium (II) (29).** **1** (1.417g, 7.69 mmol),  $\text{RuCl}_3 \cdot 3\text{H}_2\text{O}$  (1.000 g, 3.82 mmol) and lithium chloride (1.100g, 25.9 mmol) were heated at reflux in HPLC grade DMF (8 ml) for 7 hours. The resulting dark solution was poured into acetone (25 ml) and after refrigeration overnight the precipitate was removed by filtration, washed with water (3 x 25 ml) and diethyl ether (3 x 25 ml) before being dried *in vacuo* to yield the title compound as a black solid (1.72 g, 83%) which was used directly in the subsequent step without characterisation.

FAB<sup>+</sup> MS m/z = 540 (100%,  $\text{M}^+$ ), 505 (58%, [M-Cl]<sup>+</sup>).



20



29

**Bis-[5,5'-dimethyl-2,2'-bipyridine]-[5,5-bis(2-carbethoxyethyl)-2,2'-bipyridine] ruthenium (II) hexafluorophosphate (30).** A solution of **29** (0.500 g, 0.868 mmol) and **4** (0.340 g, 0.955 mmol) in 50% ethanol / water (20 ml) was refluxed for 3 hours. After cooling, NH<sub>4</sub>PF<sub>6</sub> (1.4 g) in water (20 ml) was added and the orange precipitate was extracted into CH<sub>2</sub>Cl<sub>2</sub> (50 ml). The CH<sub>2</sub>Cl<sub>2</sub> layer was washed with 1M HCl (2 x 25 ml), 1M NaOH (2 x 25 ml) and water (25 ml), dried (Na<sub>2</sub>SO<sub>4</sub>), filtered and evaporated. Flash chromatography on silica (2 cm x 35 cm) eluting with 2% methanol / CH<sub>2</sub>Cl<sub>2</sub> gave the title compound as an orange solid (0.702 g, 72%).

R<sub>f</sub> = 0.70 (10% methanol / CH<sub>2</sub>Cl<sub>2</sub>). m.p. ca. 120 °C.

<sup>1</sup>H NMR (250 MHz, d<sub>6</sub>-acetone) δ1.10 (6H, t, J = 7 Hz, -OCH<sub>2</sub>CH<sub>3</sub>), 82.21 (2 x 6H, 2s, ArCH<sub>3</sub>), 82.57 and 82.82 (2 x 4H, 2m, ArCH<sub>2</sub>CH<sub>2</sub>CO<sub>2</sub>Et), 83.95 (4H, m, OCH<sub>2</sub>CH<sub>3</sub>), 87.61, 87.80 and 87.85 (3 x 2H, 3d, J = 2 Hz, 6-pyridine H), 87.95-8.09 (6H, m, 4-pyridine H), 88.62 (6H, m, 3-pyridine H).

<sup>13</sup>C NMR (62.9 MHz, d<sub>6</sub>-acetone) δ14.4 (C1), 18.4 (C13, 22), 28.1 (C5), 34.5 (C4), 60.9 (C2), 124.2, 124.3, 124.4 (C8, 14, 19), 138.6, 139.3 (C9, 15, 18), 139.0 (C7, 20, 13), 152.0, 152.1, 152.5 (C6, 12, 21), 155.7, 155.8, 156.1 (C10, 16, 17), 172.4 (C3).

FAB<sup>+</sup> MS m/z = 971 (100%, [M - PF<sub>6</sub>]<sup>+</sup>), 826 (75%, [M - 2PF<sub>6</sub>]<sup>+</sup>), 413 (86%, [M - 2PF<sub>6</sub>]<sup>2+</sup>). Calculated for C<sub>44</sub>H<sub>48</sub>N<sub>6</sub>O<sub>4</sub>RuP<sub>2</sub>F<sub>12</sub>: C 47.34, H 4.34, N 7.53; Found C 47.6, H 4.3, N 7.8.

λ<sub>max</sub> (ε) 265.0 nm (63000), 294.1 nm (140000), 446.4 nm (25000).

**Bis-[5,5'-dimethyl-2,2'-bipyridine]-[5,5'-bis(2-carboxyethyl)-2,2'-bipyridine] ruthenium (II) hexafluorophosphate (31).** **30** (0.112 g, 0.100 mmol) and NaOH (0.206 g, 5.15 mmol) in water (5 ml) were refluxed for 2.5 hours. After cooling, 36% HCl (0.608 g, 6 mmol) and NH<sub>4</sub>PF<sub>6</sub> (1.00 g) were added and the solution briefly returned to reflux. After cooling, the product was extracted into CH<sub>2</sub>Cl<sub>2</sub> (4 x 15 ml) and washed with water, dried (Na<sub>2</sub>SO<sub>4</sub>), filtered and evaporated to give the title compound as an orange solid (0.102 g, 96%). R<sub>f</sub> = 0.0 (10% methanol / CH<sub>2</sub>Cl<sub>2</sub>). m.p. 188-192 °C.

<sup>1</sup>H NMR (250 MHz, d<sub>6</sub>-acetone) δ2.20 (2 x 6H, 2s, -CH<sub>3</sub>), 82.57 and 82.83 (2 x 4H, 2m, ArCH<sub>2</sub>CH<sub>2</sub>COOH), 87.67, 87.80 and 87.87 (3 x 2H, 3d, J = 2 Hz, 6-pyridine H), 87.98 and 88.09 (4H and 2H, 2m, 4-pyridine H), 88.62 (6H, m, 3-pyridine H).

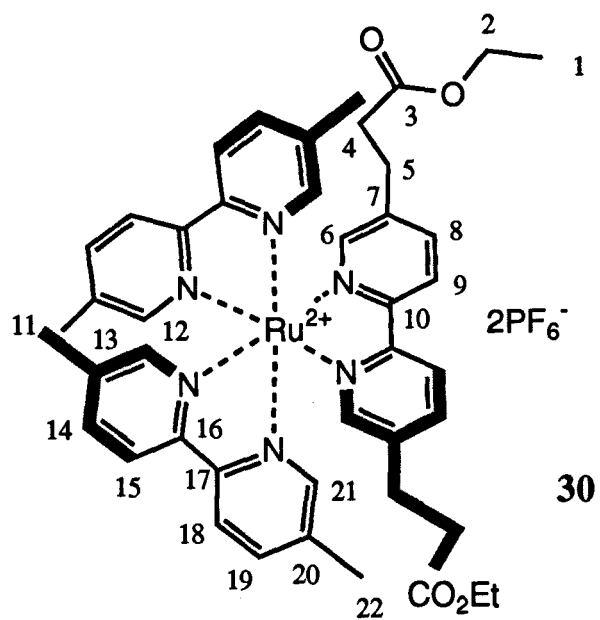
<sup>13</sup>C NMR (62.9 MHz, d<sub>6</sub>-acetone) δ18.5 (C11, 19), 28.1 (C3), 34.2 (C2), 124.3 and 124.5 (C6, 12, 17), 138.7, 139.1 and 139.2 (C7, 13, 16), 139.3 (C10, 18), 142.1 (C5), 152.0, 152.1 and 152.3 (C4, 9, 20), 155.8 and 156.1 (C8, 14, 15), 173.3 (C1).

FAB<sup>+</sup> MS m/z = 915 (85%, [M-PF<sub>6</sub>]<sup>+</sup>), 769 (100%, [M-2PF<sub>6</sub>]<sup>+</sup>), 385 (30%, [M-2PF<sub>6</sub>]<sup>2+</sup>).

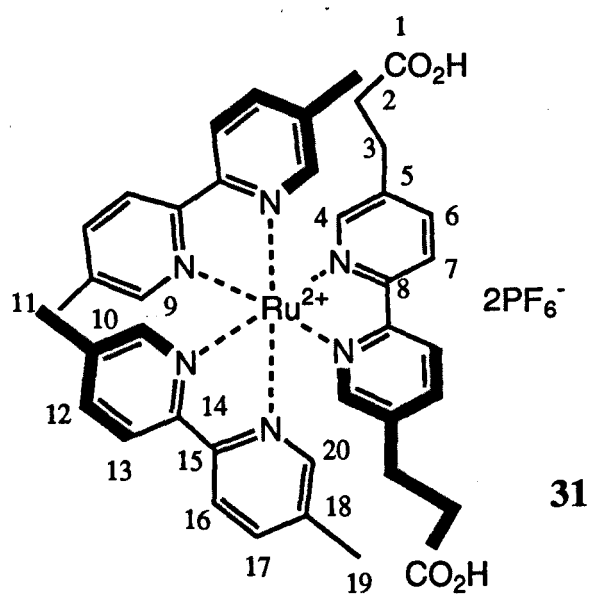
Calculated for C<sub>40</sub>H<sub>40</sub>N<sub>6</sub>O<sub>4</sub>RuP<sub>2</sub>F<sub>12</sub>: C 45.33, H 3.80, N 7.93;

Found: C 44.8, H 4.1, N 7.9.

λ<sub>max</sub> (ε) (CH<sub>2</sub>Cl<sub>2</sub>) 264.6 nm (32800), 294.6 nm (86300), 446.0 nm (13600).



30

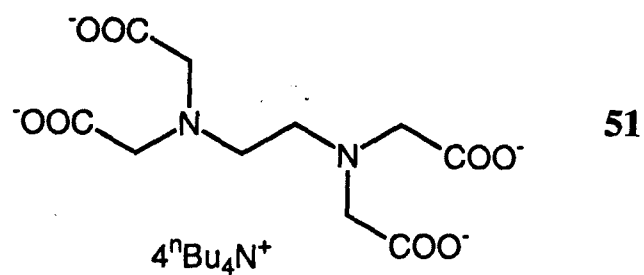
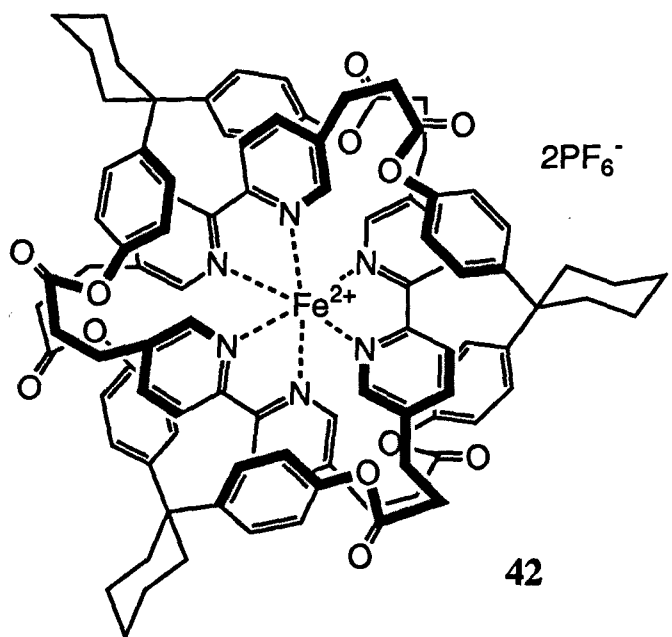


31

**Attempted macrocyclisation to iron (II) ester-linked trefoil knot (42).** A solution of **15** (0.467 g, 0.404 mmol), **9** (0.325 g, 1.212 mmol) and DMAP (98 mg, 0.808 mmol) in dry CH<sub>2</sub>Cl<sub>2</sub> / DMF (98.5 : 1.5 v/v, 360 ml) was added dropwise over 5 - 6 hours at 0 °C to a stirred solution of EDC (1.550g, 8.08 mmol) in dry CH<sub>2</sub>Cl<sub>2</sub> (90 ml). After the addition, the solution was stirred for a further 18 hours at room temperature before being washed successively with 1M HCl (2 x 50 ml), saturated NaHCO<sub>3</sub> (2 x 50 ml) and water (3 x 100 ml). Methanol (5 ml) was added to redissolve some precipitated red material. The CH<sub>2</sub>Cl<sub>2</sub> layer was then stirred vigorously overnight with a solution of NH<sub>4</sub>PF<sub>6</sub> (5 g) in water (20 ml) to effect counterion exchange before being separated, washed with water (6 x 100 ml), dried (Na<sub>2</sub>SO<sub>4</sub>), filtered and evaporated to give a dark red solid (0.646 g). Attempts to characterise this product are discussed in Chapter 3 as are some slight variations to the above procedure upon repetition of the reaction.

**Ethylenediaminetetraacetic acid (EDTA), tetrakis (*tetra-n*-butyl ammonium) salt (51).** EDTA (1.827 g, 6.25 mmol) was added to a 1M solution of *n*Bu<sub>4</sub>N<sup>+</sup> OH<sup>-</sup> in methanol (25 ml, 25 mmol) and refluxed for 0.5 hours. The solvent was removed *in vacuo* and the product dried for a prolonged period under high vacuum to give the title compound as a viscous yellow oil. The product was used directly to demetallate the crude product mixture from the above macrocyclisation.

**Demetallation of crude mixture containing iron (II) knot 42.** The crude macrocyclisation product (0.154 g) and **51** (0.300 g) were stirred for 12 hours in 2% methanol / CH<sub>2</sub>Cl<sub>2</sub> (15 ml) during which time the colour changed from deep red through brown and finally to yellow / brown. The CH<sub>2</sub>Cl<sub>2</sub> solution was washed with water (4 x 20 ml), dried (Na<sub>2</sub>SO<sub>4</sub>), filtered and evaporated. TLC (5% methanol / CH<sub>2</sub>Cl<sub>2</sub>) indicated a large number of products. Attempts to separate these products by flash chromatography on silica (1.5 cm x 30 cm) eluting with CH<sub>2</sub>Cl<sub>2</sub> containing 1 - 10% methanol were unsuccessful although this procedure readily removed the yellow/brown oxo-iron complexes. Tentative identification of the components of this mixture by FAB<sup>+</sup> mass spectrometry is discussed in Chapter 3.



**Tris(5,5'-bis(2-carbopentoxyethyl)-2,2'-bipyridine) ruthenium (II) hexafluorophosphate (69)** was prepared using an identical procedure to that used for **19** but substituting *n*-pentanol (0.450 g, 5.04 mmol) in place of phenol. The product was purified by flash chromatography on silica (20 cm x 1.5 cm) eluting with 2% methanol in CH<sub>2</sub>Cl<sub>2</sub> and collecting the fastest running band to give the title compound as an extremely hygroscopic orange solid (62 mg, 47%).

R<sub>f</sub> = 0.3 (5% methanol in CH<sub>2</sub>Cl<sub>2</sub>).

<sup>1</sup>H NMR (250 MHz, CDCl<sub>3</sub>) δ 0.86 (30H, m, -CH<sub>2</sub>CH<sub>3</sub>), 1.43 (12H, m, -OCH<sub>2</sub>CH<sub>2</sub>CH<sub>2</sub>-), 1.61 (12H, m, OCH<sub>2</sub>CH<sub>2</sub>-), 2.54 and 2.83 (2 x 12H, 2m, ArCH<sub>2</sub>CH<sub>2</sub>CO<sub>2</sub>R), 3.93 (12H, m, -OCH<sub>2</sub>-), 7.54 (6H, d, J = 2 Hz, 6-pyridine H), 7.81 (6H, dd, J = 8 Hz, 2 Hz, 4-pyridine H), 8.34 (6H, d, J = 8 Hz, 3-pyridine H).

FAB<sup>+</sup> MS m/z = 1567 (100%, [M - PF<sub>6</sub>]<sup>+</sup>), 1423 (75%, [M - 2PF<sub>6</sub>]<sup>+</sup>).

[M - PF<sub>6</sub>]<sup>+</sup> requires 1567.6710; Found m/z = 1567.6863.

λ<sub>max</sub> (ε) (CH<sub>2</sub>Cl<sub>2</sub>) 265.4 nm (35000), 295.5 nm (93000), 453.9 nm (16000).

**Bis-[5,5'-dimethyl-2,2'-bipyridine]-[5,5'-bis(2-carbophenoxyethyl)-2,2'-bipyridine] ruthenium (II) hexafluorophosphate (70).** To a solution of **31** (50.9 mg, 0.048 mmol), phenol (45.0 mg, 0.478 mmol) and DMAP (0.5 mg) in CH<sub>2</sub>Cl<sub>2</sub> (2 ml) at 0°C was added EDC (36.8 mg, 0.192 mmol) in one portion. The mixture was stirred a room temperature for 18 hours before diluting with CH<sub>2</sub>Cl<sub>2</sub> (10 ml) and washing with 1M HCl (10 ml), 1M NaOH (10 ml) and water (10 ml). After drying (Na<sub>2</sub>SO<sub>4</sub>), the solvent was removed *in vacuo* and the crude product purified by flash chromatography on silica (1 cm x 15 cm) eluting with 2% methanol in CH<sub>2</sub>Cl<sub>2</sub> to give the title compound as an orange solid (44.5 mg, 75%).

R<sub>f</sub> = 0.60 (10% methanol / CH<sub>2</sub>Cl<sub>2</sub>). m.p. ca. 150°C.

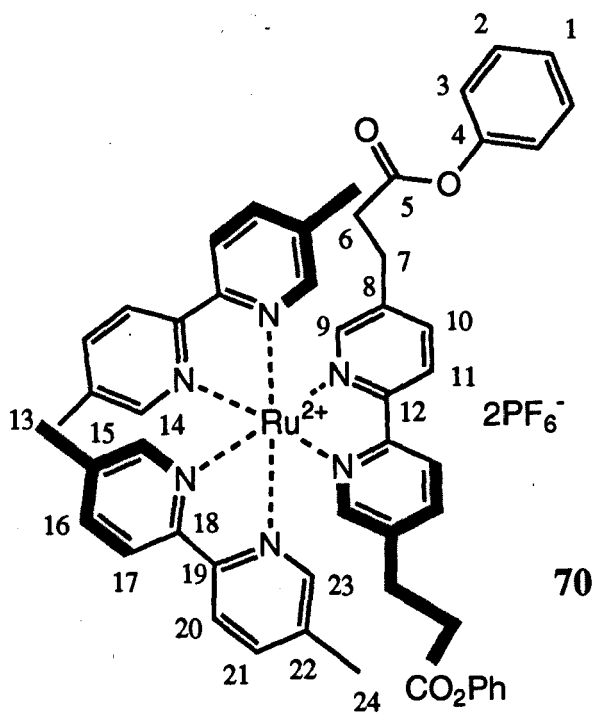
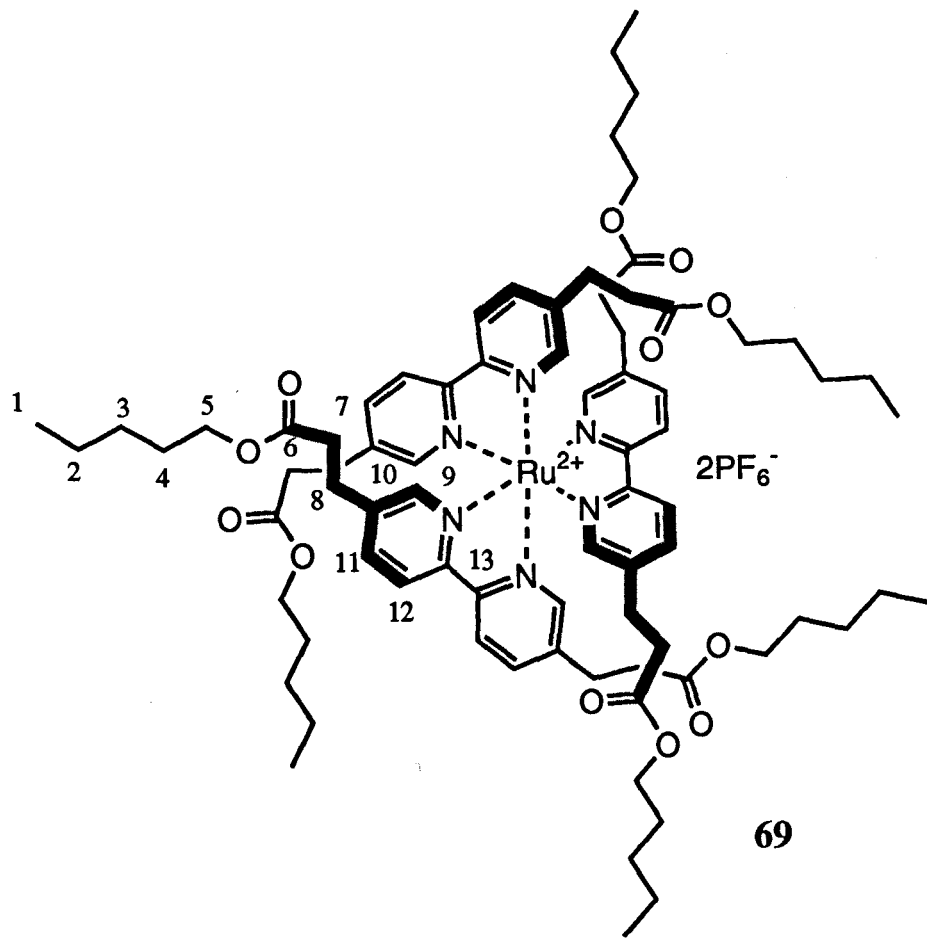
<sup>1</sup>H NMR (250 MHz, d<sub>6</sub>-acetone) δ 2.09 and 2.13 (2 x 6H, 2s, -CH<sub>3</sub>), 2.92 (8H, br, -CH<sub>2</sub>CH<sub>2</sub>-), 6.95 (4H, d, J = 8 Hz, *ortho*-phenol H), 7.27 (2H, t, J = 8 Hz, *para*-phenol H), 7.41 (4H, m, *meta*-phenol H), 7.70, 7.75 and 7.93 (3 x 2H, 2d, J = 2 Hz, 6-pyridine H), 7.88 and 7.95 (2 x 2H, 2dd, J = 8Hz, 2 Hz, 4 and 4' -dimethylbipy H), 8.15 (2H, dd, J = 8 Hz, 2 Hz, 4-bipyridine H), 8.43 and 8.51 (2 x 2H, 2d, J = 8 Hz, 3 and 3' -dimethylbipy H), 8.69 (2H, d, J = 8 Hz, 3-bipyridine H).

<sup>13</sup>C NMR (62.9 MHz, d<sub>6</sub>-acetone) δ 18.4 (C13, 24), 28.0 (C7), 34.5 (C6), 122.4 (C3), 124.2, 124.3 and 124.6 (C10, 16, 21), 126.7 (C1), 130.3 (C2), 138.7, 139.2 and 139.3 (C11, 17, 20), 139.0 and 139.1 (C15, 22, 9), 151.7 (C4), 151.9 and 152.6 (C8, 14, 23), 155.8 and 156.3 (C12, 18, 19), 171.3 (C5).

Calculated for C<sub>54</sub>H<sub>48</sub>N<sub>6</sub>O<sub>4</sub>RuP<sub>2</sub>F<sub>12</sub>·3H<sub>2</sub>O: C 50.27, H 4.22, N 6.51;

Found C 49.94, H 4.20, N 6.56.

λ<sub>max</sub> (ε) (CH<sub>2</sub>Cl<sub>2</sub>) 265.4 nm (38000), 295.5 nm (99000), 447.2 nm (16000).



**5,5'-Bis(2-carbophenoxyethyl)-2,2'-bipyridine (71).** **6** (0.195 g, 0.649 mmol) and phenol (0.306 g, 3.246 mmol) in dry  $\text{CH}_2\text{Cl}_2$  (10 ml) were cooled in ice before the addition of EDC (0.435 g, 2.27 mmol) and DMAP (8 mg, 0.0649 mmol). After stirring for 18 hours at room temperature, the organic layer was washed with 1M HCl (5 ml), 1M NaOH (10 ml) and water (2 x 10 ml). The  $\text{CH}_2\text{Cl}_2$  solution was dried ( $\text{Na}_2\text{SO}_4$ ), filtered and evaporated. The crude product was purified by flash chromatography on silica (2 cm x 15 cm) eluting with 1.5% methanol in  $\text{CH}_2\text{Cl}_2$  to give the title compound as a white solid (0.215 g, 73%).

$R_f$  = 0.3 (5% methanol in  $\text{CH}_2\text{Cl}_2$ ). m.p. 153.5 - 155°C.

$^1\text{H}$  NMR (250 MHz,  $\text{CDCl}_3$ )  $\delta$  2.94 (4H, t,  $J$  = 7.5 Hz,  $-\text{CH}_2-$ ), 31.14 (4H, t,  $J$  = 7.5 Hz,  $-\text{CH}_2-$ ), 87.03 (4H, d,  $J$  = 9 Hz, *ortho*-phenol H), 87.22 (2H, m, *para*-phenol H), 87.36 (4H, m, *meta*-phenol H), 87.74 (2H, dd,  $J$  = 8 Hz, 2 Hz, 4-pyridine H), 88.34 (2H, d,  $J$  = 8 Hz, 3-pyridine H), 88.61 (2H, d,  $J$  = 2 Hz, 6-pyridine H).

$^{13}\text{C}$  NMR (62.9 MHz,  $\text{CDCl}_3$ )  $\delta$  27.9 (C7), 35.5 (C6), 120.8 (C10), 121.5 (C3), 126.0 (C1), 129.5 (C2), 135.6 (C9), 137.0 (C11), 149.3 (C8), 150.5 (C4), 154.5 (C12), 170.9 (C5).

FAB<sup>+</sup> MS m/z = 453.1811;  $\text{C}_{28}\text{H}_{24}\text{N}_2\text{O}_4$  requires 453.1814.

Calculated for  $\text{C}_{28}\text{H}_{24}\text{N}_2\text{O}_4$ : C 74.32, H 5.35, N 6.19;

Found C 73.7, H 5.3, N 6.5.

#### *General procedure for the preparation of iron (II) complexes 72 - 75.*

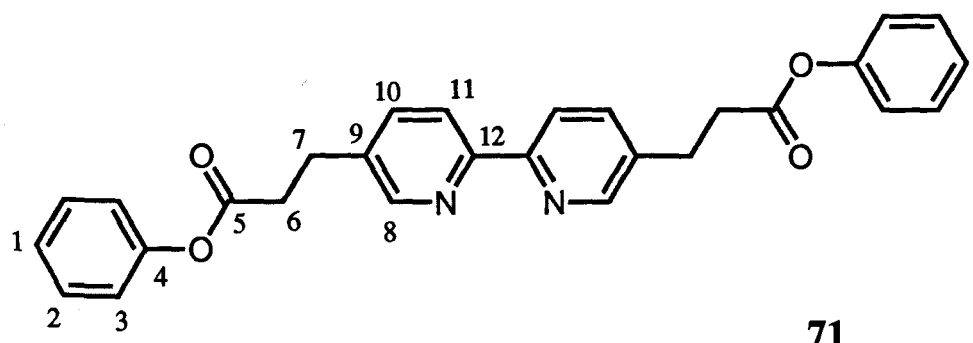
To a solution of the iron (II) salt with the required counterion ( $\text{Fe}(\text{ClO}_4)_2 \cdot 6\text{H}_2\text{O}$  or  $\text{FeCl}_2 \cdot 4\text{H}_2\text{O}$ ) (0.033 mmol) in the relevant solvent (5% methanol in  $\text{CH}_2\text{Cl}_2$  for  $\text{ClO}_4^-$  salts, methanol for  $\text{Cl}^-$  salts) was added ligand **4** or ligand **71** (1 mmol). After stirring for 30 minutes, the solvent was removed *in vacuo* to give a quantitative yield of the required product as a deep red solid.

#### **Tris(5,5'-bis(2-carbophenoxyethyl)-2,2'-bipyridine) iron (II) perchlorate (72)**

$^1\text{H}$  NMR (250 MHz,  $d_3\text{-MeCN}$ )  $\delta$  2.67 (24H, m,  $-\text{CH}_2\text{CH}_2-$ ), 66.88 (12H, d,  $J$  = 8 Hz, *ortho*-phenol H), 87.16 (6H, d,  $J$  = 1.5 Hz, 6-pyridine H), 87.25 - 7.43 (m, 18H, *meta*- and *para*-phenol H), 87.81 (6H, dd,  $J$  = 8 Hz, 1.5 Hz, 4-pyridine H), 88.05 (6H, d,  $J$  = 8 Hz, 3-pyridine H).

$^{13}\text{C}$  NMR (250 MHz,  $\text{CDCl}_3$ )  $\delta$  27.3 (C6), 33.7 (C7), 121.5 (C10), 123.1 (C3), 125.9 (C12), 129.4 (C11), 138.3 (C12), 140.0 (C4), 150.4 (C9), 154.2 (C5), 156.9 (C1), 170.5 (C8).

FAB<sup>+</sup> MS m/z = 1513 (15%,  $[\text{M} - \text{ClO}_4]^+$ ), 1414 (70%,  $[\text{M} - 2\text{ClO}_4]^+$ ), 960 (100%,  $[\text{M} - \text{bipy}]^{2+}$ ).



**71**

**Tris(5,5'-bis(2-carbophenoxyethyl)-2,2'-bipyridine) iron (II) chloride (73)**

m.p. ca. 180 °C.

<sup>1</sup>H NMR (250 MHz, CD<sub>3</sub>OD) δ2.63 (24H, m, -CH<sub>2</sub>CH<sub>2</sub>-), δ6.87 (12H, d, J = 7.5 Hz, *ortho*-phenol H), δ7.24 (6H, d, J = 1.5 Hz, 6-pyridine H), δ7.31 (6H, m, *para*-phenol H), δ7.42 (12H, m, *meta*-phenol H), δ7.81 (6H, dd, J = 8 Hz, 1.5 Hz, 4-pyridine H), δ8.04 (6H, d, J = 8 Hz, 3-pyridine H).

ES<sup>+</sup> MS m/z = 706 (100%, [M - 2Cl]<sup>2+</sup>).

Calculated for C<sub>84</sub>H<sub>72</sub>N<sub>6</sub>O<sub>12</sub>FeCl<sub>2</sub>·2H<sub>2</sub>O: C 66.36, H 5.04, N 5.53, Cl 4.66;

Found C 66.35, H 5.03, N 5.46, Cl 4.96.

λ<sub>max</sub> (ε) (methanol) 255.6 nm (39500), 265.7 nm (35100), 304.3 nm (76400), 394.0 nm (3100), 490.0 nm (7000), 518.3 nm (8100).

**Tris(5,5'-bis(2-carbethoxyethyl)-2,2'-bipyridine) iron (II) perchlorate (74)**

m.p. 112 - 115 °C.

<sup>1</sup>H NMR (250 MHz, d<sub>3</sub>-MeCN) δ1.08 (18H, t, J = 7 Hz, -CH<sub>3</sub>), δ2.46 and 2.72 (24H, br, -CH<sub>2</sub>CH<sub>2</sub>-), δ3.91 (12H, m, OCH<sub>2</sub>-), δ7.14 (6H, d, J = 1.5 Hz, 6-pyridine H), δ7.93 (6H, dd, J = 8 Hz, 1.5 Hz, 4-pyridine H), δ8.38 (6H, d, J = 8 Hz, 3-pyridine H).

FAB<sup>+</sup> MS m/z = 1223 (3%, [M-ClO<sub>4</sub>]<sup>+</sup>), 1125 (20%, [M-2ClO<sub>4</sub>]<sup>+</sup>), 562 (100%, [M-2ClO<sub>4</sub>]<sup>2+</sup>).

Calculated for C<sub>60</sub>H<sub>72</sub>N<sub>6</sub>O<sub>20</sub>FeCl<sub>2</sub>: C 54.43, H 5.48, N 6.35, Cl 5.36;

Found C 54.32, H 5.52, N 6.51, Cl 5.65.

**Tris(5,5'-bis(2-carbethoxyethyl)-2,2'-bipyridine) iron (II) chloride (75)**

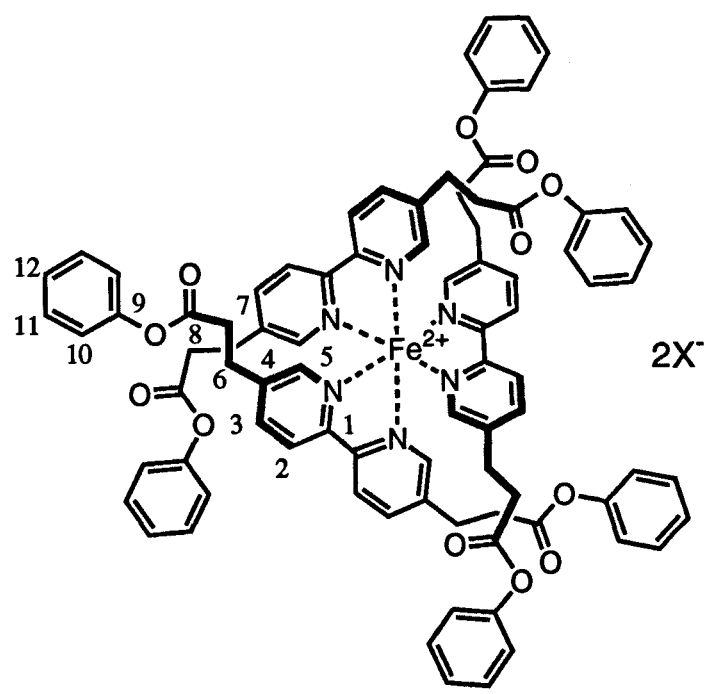
m.p. 105-106 °C.

<sup>1</sup>H NMR (250 MHz, CD<sub>3</sub>OD) δ1.11 (18H, t, J = 7 Hz, -CH<sub>3</sub>), δ2.58 and δ2.78 (2 x 12H, 2t, J = 6.5 Hz, -CH<sub>2</sub>CH<sub>2</sub>-), δ3.94 (12H, q, J = 7 Hz, -OCH<sub>2</sub>-), δ7.30 (6H, d, J = 1.5 Hz, 6-pyridine H), δ8.05 (6H, dd, J = 8 Hz, 1.5 Hz, 4-pyridine H), δ8.60 (6H, d, J = 8 Hz, 3-pyridine H).

<sup>13</sup>C NMR (62.9 MHz, CD<sub>3</sub>OD) δ14.5 (C10), 28.6 (C6), 34.8 (C7), 61.6 (C9), 124.6 (C3), 139.9 (C2), 142.2 (C4), 155.2 (C5), 158.9 (C1), 173.5 (C8).

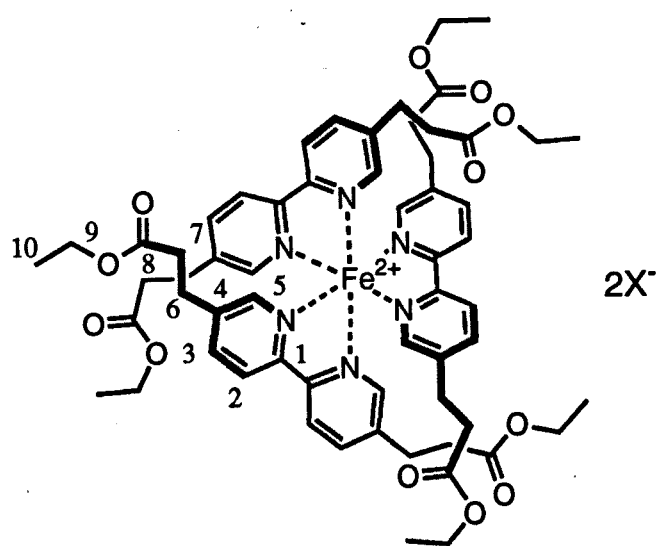
ES<sup>+</sup> MS m/z = 562 (100%, [M - 2Cl]<sup>2+</sup>).

λ<sub>max</sub> (ε) (methanol) 254.8 nm (30700), 267.1 nm (25700), 304.6 nm (62800), 354.5 nm (3000), 490.0 nm (4200), 520.0 nm (5200).



**72**  $X = \text{ClO}_4$

**73**  $X = \text{Cl}$



**74**  $X = \text{ClO}_4$

**75**  $X = \text{Cl}$

**1-(4-Hydroxyphenyl)-1-(4-methoxyphenyl)cyclohexane (76)** was prepared as for **85** replacing benzyl bromide with MeI (3.468 g, 24.4 mmol). Flash chromatography on silica (4 cm x 25 cm) eluting with 5:1 petroleum ether (b.p. 40 - 60 °C) : EtOAc and collecting the second band gave the title compound as a white solid (2.445 g, 39%).

$R_f = 0.3$  (25% EtOAc / 75% petroleum ether b.p. 40-60°C). m.p. 125 - 126 °C.

$^1\text{H}$  NMR (250 MHz,  $\text{CDCl}_3$ )  $\delta$  1.54 (6H, br, 3,4-cyclohexyl H), 82.23 (4H, br, 2-cyclohexyl H), 83.79 (3H, s, OMe), 84.80 (1H, s, OH), 86.75 (2H, d,  $J = 9$  Hz, *ortho*-ArOH), 86.82 (2H, d,  $J = 9$  Hz, *ortho*-ArOMe), 87.09 - 7.20 (4H, m, *meta*-ArOR).

$^{13}\text{C}$  NMR (62.9 MHz,  $\text{CDCl}_3$ )  $\delta$  23.0 (C8), 26.5 (C7), 37.5 (C6), 45.1 (C5), 55.3 (C13), 113.6 (C11), 115.1 (C2), 128.2 and 128.3 (C3, 10), 141.2 and 141.3 (C4, 9), 153.1 (C1), 157.0 (C12).

FAB<sup>+</sup> MS m/z = 282 (100%,  $\text{M}^+$ );  $\text{C}_{19}\text{H}_{22}\text{O}_2$  requires 282.37.

Calculated for  $\text{C}_{19}\text{H}_{22}\text{O}_2$ : C 80.81, H 7.85;

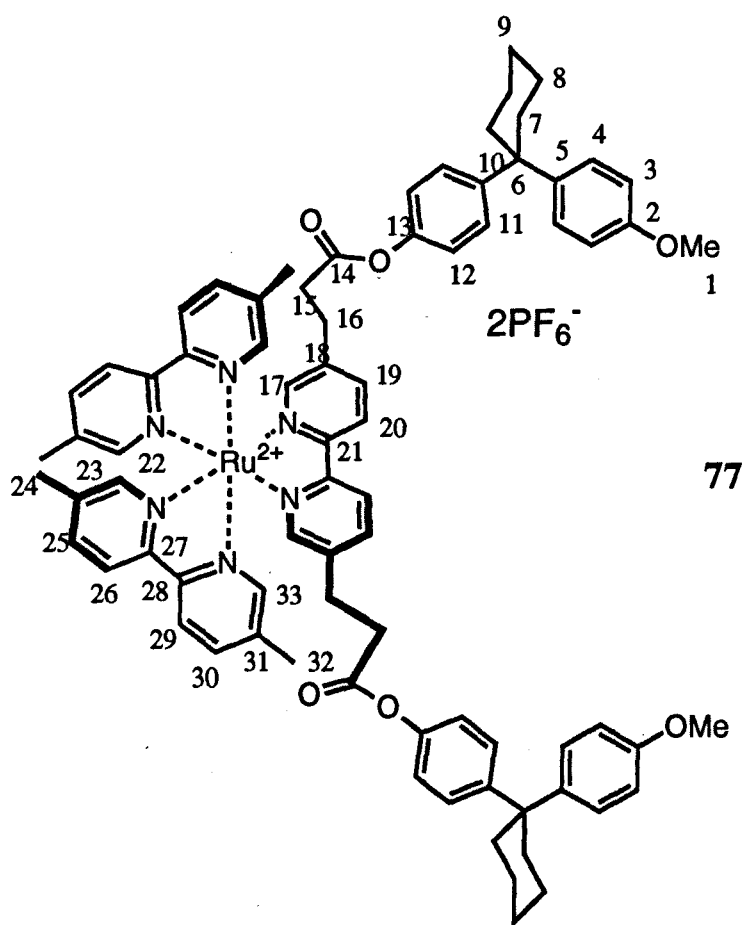
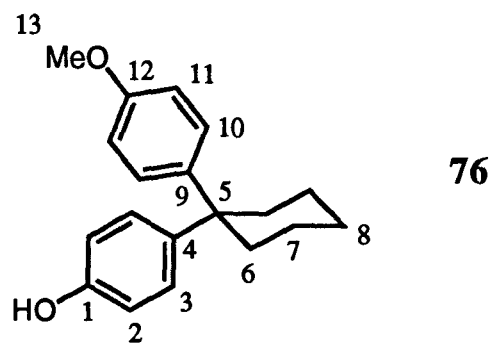
Found C 81.0, H 8.1.

**Bis-[5,5'-dimethyl-2,2'-bipyridine]-[5,5'-bis(2-carbo(4-(1-(4-methoxyphenyl)cyclohexyl)phenoxyethyl))-2,2'-bipyridine] ruthenium (II) hexafluorophosphate (77).** To a solution of **31** (0.098 g, 0.092 mmol), **76** (0.052 g, 0.185 mmol) and DMAP (1 mg) in  $\text{CH}_2\text{Cl}_2$  (5 ml) at 0°C was added EDC (0.071 g, 0.368 mmol). After stirring for 18 hours at room temperature, the orange solution was diluted with  $\text{CH}_2\text{Cl}_2$  (10 ml) and washed successively with 1M HCl (10 ml), 1M NaOH (10 ml) and water (2 x 10 ml) before stirring vigorously with a solution of  $\text{NH}_4\text{PF}_6$  (1 g) in water (2 ml) for 5 hours. Following a further wash with water (10 ml), drying ( $\text{Na}_2\text{SO}_4$ ), filtration and evaporation, flash chromatography on silica (1 cm x 20 cm) eluting with 2% methanol in  $\text{CH}_2\text{Cl}_2$  gave the title compound as an orange solid (0.080 g, 55%).

$^1\text{H}$  NMR (250 MHz,  $\text{CDCl}_3$ )  $\delta$  1.54 (12H, br, 3,4-cyclohexyl H), 82.04 and 82.19 (2 x 6H, 2s, -CH<sub>3</sub>), 82.30 (8H, br, 2-cyclohexyl H), 82.62-3.02 (8H, m, -CH<sub>2</sub>CH<sub>2</sub>-), 83.71 (6H, s, -OCH<sub>3</sub>), 86.72 (4H, d,  $J = 9$  Hz, *ortho*-ArOMe), 86.80 (4H, d,  $J = 9$  Hz, *ortho*-ArO<sub>2</sub>C-), 87.25 (8H, m, *meta*-ArOMe and *meta*-ArO<sub>2</sub>C-), 87.47 (4H, d,  $J = 2$  Hz, 6-pyridine H), 87.54 (2H, s, 6-pyridine H), 87.63 (4H, dd,  $J = 8$  Hz, 2 Hz, 4-(Me<sub>2</sub>-bipyridine) H), 87.80 (2H, dd,  $J = 8$  Hz, 2 Hz, 4-pyridine H), 87.89 (4H, d,  $J = 8$  Hz, 3-(Me<sub>2</sub>-bipyridine) H), 88.22 (2H, d,  $J = 8$  Hz, 3-pyridine H).

$^{13}\text{C}$  NMR (62.9 MHz,  $\text{CDCl}_3$ )  $\delta$  18.4 (C24, 32), 22.8 (C8), 26.3 (C9), 27.7 (C16), 33.5 (C15), 37.1 (C7), 45.2 (C6), 55.2 (C1), 113.8 (C3), 118.5 (C12), 121.0 (C25, 30, 19), 127.6 and 128.0 (C4, 11), 137.8 and 138.0 (C20, 26, 29), 138.4 (C5), 140.0 and 140.6 (C18, 23, 31), 147.3 and 147.9 (C10, 13), 150.3 (C17, 22, 33), 153.8, 154.0 and 154.4 (C21, 27, 28), 157.4 (C2), 170.6 (C14).

FAB<sup>+</sup> MS m/z = 1444 (70%,  $[\text{M} - \text{PF}_6]^+$ ), 1299 (85%,  $[\text{M} - 2\text{PF}_6]^+$ ), 649 (100%,  $[\text{M} - 2\text{PF}_6]$ ).  $\text{C}_{78}\text{H}_{80}\text{N}_6\text{O}_6\text{RuP}_2\text{F}_{12}$   $[\text{M}-\text{PF}_6]^+$  requires 1443.4824; Found 1443.4921.



**5-(3-Hydroxypropyl)-5'-(3-(*tert*-butyldimethylsilyloxy)propyl)-2,2'-bipyridine (78).** Sodium hydride (60% dispersion in oil, 73.4 mg, 1.836 mmol) and **5** (0.500 g, 1.836 mmol) were heated at reflux in dry THF (10 ml) for 75 minutes. After cooling to -5 °C, TBDMSCl (0.332 g, 2.203 mmol) was added and stirring continued for 18 hours. The product was filtered and the solvent removed *in vacuo* before being purified by flash chromatography on silica (2 cm x 18 cm) eluting with 2% methanol in CH<sub>2</sub>Cl<sub>2</sub>. The title compound was obtained as the second band (0.306 g, 43%). The higher running band was **5,5'-bis(3-(*tert*-butyldimethylsilyloxy)propyl)-2,2'-bipyridine (79)** (0.136 g, 15%). The solvent polarity was increased to 15% methanol to elute a third band which was recovered **5** (0.145 g, 29%).

#### Mono-TBDMS compound (78).

R<sub>f</sub> = 0.2 (10% methanol in CH<sub>2</sub>Cl<sub>2</sub>). m.p. 108 - 109 °C.

<sup>1</sup>H NMR (250 MHz, CDCl<sub>3</sub>) δ0.04 (6H, s, Si(CH<sub>3</sub>)<sub>2</sub>), δ0.89 (9H, s, SiC(CH<sub>3</sub>)<sub>3</sub>), δ1.72 (1H, br, OH), δ1.89 (4H, m, 2 x ArCH<sub>2</sub>CH<sub>2</sub>-), δ2.76 (4H, m, 2 x ArCH<sub>2</sub>-), δ3.65 (4H, m, -CH<sub>2</sub>OH and -CH<sub>2</sub>OTBDMS), δ7.63 (2H, m, 4-bipyridine H), δ8.26 (2H, m, 3-bipyridine H), δ8.49 (2H, m, 6-bipyridine H).

<sup>13</sup>C NMR (62.9 MHz, CDCl<sub>3</sub>) δ18.3 (C18), 25.9 (C19), 29.0 (C3, 14), 33.8 and 33.9 (C2, 15), 61.5 (C1), 61.9 (C16), 120.6 (C6, 11), 136.9 and 137.0 (C7,10), 137.2 and 137.5 (C5, 12), 149.2 and 149.3 (C4, 13), 153.9 and 154.1 (C8, 9).

FAB<sup>+</sup> MS m/z = 387 (100%, MH<sup>+</sup>). C<sub>22</sub>H<sub>34</sub>N<sub>2</sub>O<sub>2</sub>Si requires 386.59

Calculated for C<sub>22</sub>H<sub>34</sub>N<sub>2</sub>O<sub>2</sub>Si: C 68.35, H 8.87, N 7.25;

Found: C 68.1, H 9.1, N 7.5.

#### Bis-TBDMS compound (79).

R<sub>f</sub> = 0.55 (10% methanol in CH<sub>2</sub>Cl<sub>2</sub>). m.p. 137 - 139 °C.

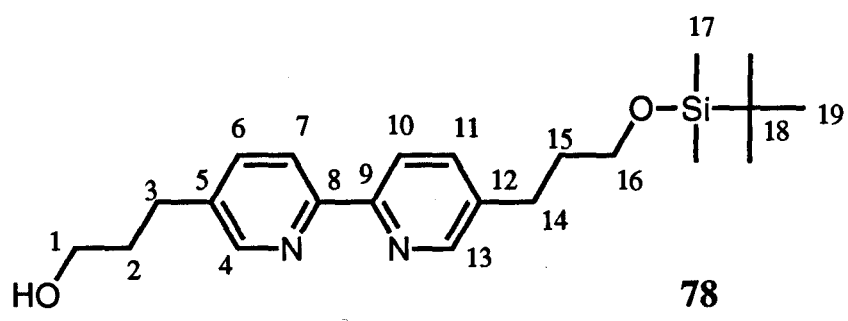
<sup>1</sup>H NMR (250 MHz, CDCl<sub>3</sub>) δ0.05 (12H, s, Si(CH<sub>3</sub>)<sub>2</sub>), δ0.91 (18H, s, SiC(CH<sub>3</sub>)<sub>3</sub>), δ1.85 (4H, quintet, J = 7 Hz, ArCH<sub>2</sub>CH<sub>2</sub>-), δ2.25 (4H, t, J = 7 Hz, ArCH<sub>2</sub>-), δ3.66 (4H, t, J = 7 Hz, -CH<sub>2</sub>OTBDMS), δ7.61 (2H, dd, J = 8 Hz, 2 Hz, 4-bipyridine H), δ8.26 (2H, d, J = 8 Hz, 3-bipyridine H), δ8.50 (2H, d, J = 2 Hz, 6-bipyridine H).

<sup>13</sup>C NMR (62.9 MHz, CDCl<sub>3</sub>) δ18.2 (C2), 25.9 (C1), 29.0 (C6), 33.9 (C5), 61.8 (C4), 120.3 (c9), 136.7 (C10), 137.2 (C8), 149.3 (C7), 154.0 (C11).

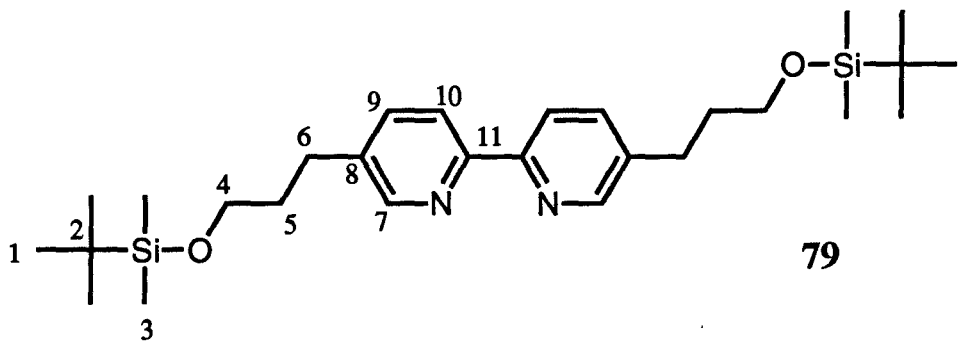
FAB<sup>+</sup> MS m/z = 501 (100%, MH<sup>+</sup>). C<sub>28</sub>H<sub>48</sub>N<sub>2</sub>O<sub>2</sub>Si<sub>2</sub> requires 500.85.

Calculated for C<sub>28</sub>H<sub>48</sub>N<sub>2</sub>O<sub>2</sub>Si<sub>2</sub>: C 67.14, H 9.66, N 5.59;

Found: C 66.8, H 9.6, N 5.8.



**78**



**79**

**5-(3-Hydroxypropyl)-5'-(3-(benzyloxy)propyl)-2,2' bipyridine (80).** Sodium hydride (60% dispersion in oil, 0.161 g, 4.037 mmol) and 5 (1.00 g, 3.67 mmol) were heated at reflux in dry THF (20 ml) for 1 hour. After cooling to -5 °C benzyl bromide (0.690 g, 4.037 mmol) was added and the solution refluxed for 18 hours. After cooling, CH<sub>2</sub>Cl<sub>2</sub> (30 ml) was added and the solution filtered and evaporated. The crude product was purified by flash chromatography on silica (2 cm x 20 cm) eluting with 1% methanol in CH<sub>2</sub>Cl<sub>2</sub>. The title compound was obtained as the second band (0.689 g, 52%). The higher running band was **5,5'-bis(3-(benzyloxy)propyl)-2,2'-bipyridine (81)** (0.387 g, 23%). No attempt was made to recover unreacted starting material.

#### Mono-benzyl compound (80).

m.p. 41-42°C.

<sup>1</sup>H NMR (250 MHz, CDCl<sub>3</sub>) δ1.87 (4H, m, HOCH<sub>2</sub>CH<sub>2</sub>- and BnOCH<sub>2</sub>CH<sub>2</sub>-), δ2.70 (4H, m, 2 x ArCH<sub>2</sub>-), δ2.83 (1H, br, OH), δ3.45 (2H, t, J = 7 Hz, BnOCH<sub>2</sub>-), δ3.62 (2H, t, J = 7 Hz, HOCH<sub>2</sub>-), δ4.45 (2H, s, benzylic CH<sub>2</sub>), δ7.29 (5H, m, benzyl), δ7.58 (2H, m, 4 and 4'-bipyridine H), δ8.20 (2H, m, 3 and 3'-bipyridine H), δ8.44 (2H, m, 6 and 6'-bipyridine H).

<sup>13</sup>C NMR (62.9 MHz, CDCl<sub>3</sub>) δ29.0 (C19), 29.3 (C8), 31.0 (C7), 33.8 (C20), 61.5 (C21), 69.0 (C5), 73.0 (C6), 120.6 (C11, 16), 127.6, 127.7, 128.4 (C1, 2, 3), 136.9 and 137.0 (C12, 15), 137.2 (C10, 17), 138.4 (C4), 149.2 and 149.3 (C9, 18), 154.0 (C13, 14).

FAB<sup>+</sup> MS m/z = 363 (100%, MH<sup>+</sup>). C<sub>23</sub>H<sub>26</sub>N<sub>2</sub>O<sub>2</sub> requires 362.45.

Calculated for C<sub>23</sub>H<sub>26</sub>N<sub>2</sub>O<sub>2</sub>: C 76.21, H 7.23, N 7.73;

Found C 76.25, H 7.35, N 7.68.

#### Bis-benzyl compound (81).

m.p. 43-44 °C.

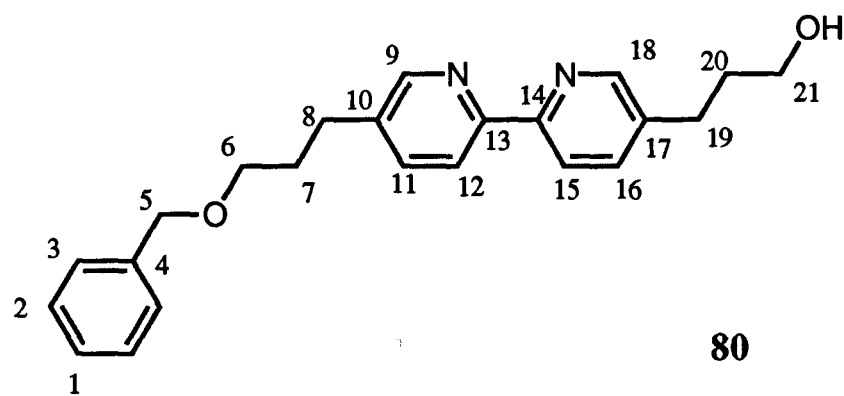
<sup>1</sup>H NMR (250 MHz, CDCl<sub>3</sub>) δ1.90 (4H, quintet, J = 7 Hz, ArCH<sub>2</sub>CH<sub>2</sub>-), δ2.71 (4H, t, J = 7 Hz, ArCH<sub>2</sub>-), δ3.45 (4H, t, J = 7 Hz, BnOCH<sub>2</sub>-), δ4.45 (2H, s, benzylic CH<sub>2</sub>), δ7.26 (10H, m, benzyl), δ7.55 (2H, dd, J = 8 Hz, 2 Hz, 4-pyridine H), δ8.22 (2H, d, J = 8 Hz, 3-pyridine H), δ8.46 (2H, d, J = 2 Hz, 6-pyridine H).

<sup>13</sup>C NMR (62.9 MHz, CDCl<sub>3</sub>) δ29.4 (C8), 31.1 (C7), 69.0 (C5), 73.1 (C6), 120.5 (C11), 127.6, 127.7 and 128.4 (C1, 2, 3), 136.9 (C12), 137.1 (C10), 138.4 (C4), 149.4 (C9), 154.1 (C13).

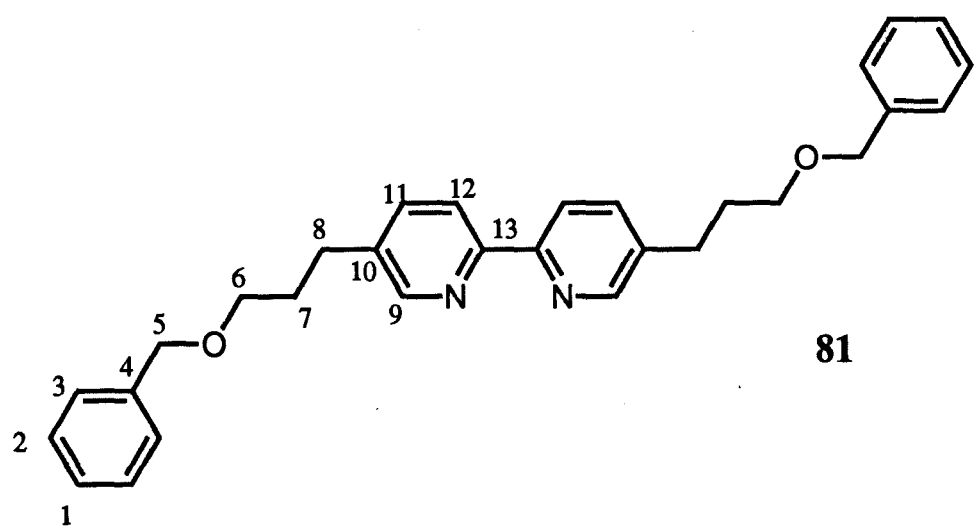
FAB<sup>+</sup> MS m/z = 453 (100%, MH<sup>+</sup>). C<sub>30</sub>H<sub>32</sub>N<sub>2</sub>O<sub>2</sub> requires 452.57.

Calculated for C<sub>30</sub>H<sub>32</sub>N<sub>2</sub>O<sub>2</sub>: C 79.61, H 7.13, N 6.19;

Found C 79.51, H 7.24, N 6.11.



**80**



**81**

**N-Acetyl-4-(4-hydroxyphenyl)-4-((*tert*-butyldimethylsilyloxy)phenyl)piperidine (82).** 8 (2.00 g, 6.42 mmol), TBDMSCl (1.250 g, 8.30 mmol), and imidazole (2.18 g, 32.1 mmol) were dissolved in dry DMF (15 ml) and stirred for 72 hours. The solution was then diluted with diethyl ether (200 ml) and washed with water (3 x 125 ml). The ether layer was dried ( $\text{Na}_2\text{SO}_4$ ), filtered and evaporated. Purification by flash chromatography on silica (2 cm x 20 cm) eluting with 2% MeOH in  $\text{CH}_2\text{Cl}_2$ , collecting the second band, gave the title compound as a white crystalline solid (0.700 g, 26%).

$R_f$  = 0.3 (7.5% methanol /  $\text{CH}_2\text{Cl}_2$ ). m.p. 103 - 104 °C.

$^1\text{H}$  NMR (250 MHz,  $\text{CDCl}_3$ )  $\delta$  0.20 (6H, s,  $\text{SiCH}_3$ ), 1.00 (9H,  $\text{SiC(CH}_3)_3$ ), 2.13 (3H, s,  $\text{COCH}_3$ ), 2.33 (4H, br,  $\text{N-CH}_2\text{-CH}_2$ ), 3.48 and 3.68 (4H, br,  $\text{N-CH}_2\text{-}$ ), 6.77 (4H, m, *meta*-phenol H), 7.06 (4H, m, *ortho*-phenol H), 8.43 (1H, s, phenol OH).

$^{13}\text{C}$  NMR (62.9 MHz,  $\text{CDCl}_3$ )  $\delta$  18.2 (C2), 21.3 (C12), 25.7 (C1), 36.1, 37.0, 39.0 (C9/10, two conformations), 43.7 and 43.8 (C8, two conformations), 115.5 (C15), 119.9 (C5), 127.9 (C6, 14), 137.4 (C13), 139.2 (C7), 153.6 (C4), 154.9 (C16), 169.6 (C11).

FAB<sup>+</sup> MS m/z = 426 (100%,  $\text{MH}^+$ ).  $\text{C}_{25}\text{H}_{35}\text{NO}_3\text{Si}$  requires 425.6

$\nu$  = 1607  $\text{cm}^{-1}$  (C=O) and 1264  $\text{cm}^{-1}$  (Si-Me).

Calculated for  $\text{C}_{25}\text{H}_{35}\text{NO}_3\text{Si}$ : C 70.54, H 8.29, N 3.29;

Found: C 70.13, H 8.19, N 3.20.

**1-(4-Hydroxyphenyl)-1-(4-(*tert*-butyldimethylsilyloxy)phenyl)cyclohexane (83).** TBDMSCl (1.55 g, 10.29 mmol), imidazole (2.92 g, 42.86 mmol) and **9** (2.3 g, 8.57 mmol) in DMF (5 ml) were stirred at room temperature for 24 hours. After cooling, the resulting solution was diluted with diethyl ether (150 ml) and washed with water (6 x 100 ml), dried ( $\text{Na}_2\text{SO}_4$ ), filtered and evaporated. Flash chromatography on silica (2 cm x 15 cm) eluting with 1:1 petroleum ether (b.p. 40 - 60°C) /  $\text{CH}_2\text{Cl}_2$  increasing to 100%  $\text{CH}_2\text{Cl}_2$  and collecting the second band gave the title compound as an off-white solid (0.921 g, 28%). The higher running band was **1,1-bis(4-(*tert*-butyldimethylsilyloxy)phenyl)cyclohexane (84)** (0.778 g, 18%).

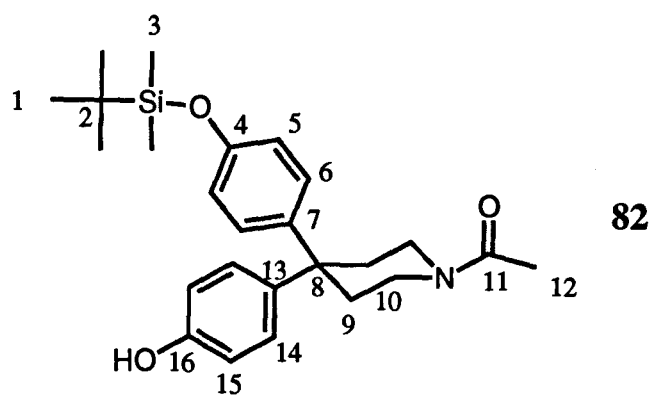
**Mono-TBDMS compound (83)**  $R_f$  = 0.6 ( $\text{CH}_2\text{Cl}_2$ ). m.p. 58 - 60 °C.

$^1\text{H}$  NMR (250 MHz,  $\text{CDCl}_3$ )  $\delta$  0.18 (6H, s,  $\text{SiCH}_3$ ), 0.97 (9H, s,  $\text{SiC(CH}_3)_3$ ), 1.51 (6H, br, 3,4-cyclohexyl H), 2.19 (4H, br, 2-cyclohexyl H), 4.69 (1H, s, ArOH), 6.82 (4H, m, *ortho*-ArOH and *ortho*-ArOTBDMS), 7.10 (4H, m, *meta*-ArOH and *meta*-ArOTBDMS).

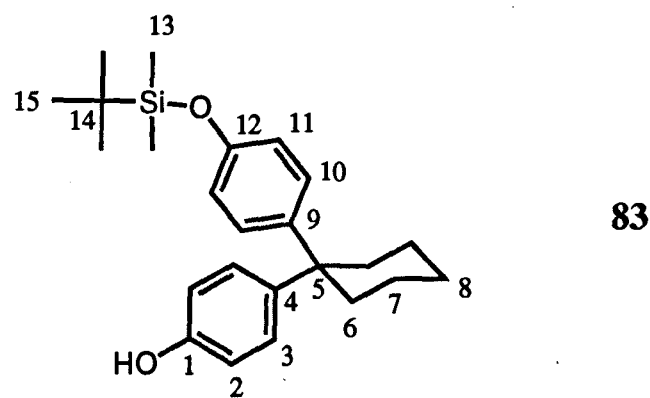
$^{13}\text{C}$  NMR (62.9 MHz,  $\text{CDCl}_3$ )  $\delta$  18.2 (C14), 22.9 (C7), 25.7 (C15), 26.5 (C8), 37.5 (C6), 45.1 (C5), 114.9 (C2), 119.5 (C11), 128.0 and 128.4 (C3, 10), 141.4 and 141.5 (C4, 9), 153.0 (C1, 12).

FAB<sup>+</sup> MS m/z = 382 (100%,  $\text{M}^+$ ).  $\text{C}_{24}\text{H}_{34}\text{O}_2\text{Si}$  requires 382.56.

Calculated for  $\text{C}_{24}\text{H}_{34}\text{O}_2\text{Si} \cdot 0.25\text{H}_2\text{O}$ : C 74.46, H 8.98; Found: C 74.58, H 8.95.



82



83

**Bis-TBDMS compound (84)**

$R_f = 0.95$  ( $\text{CH}_2\text{Cl}_2$ ). m.p. 65 - 67 °C.

$^1\text{H}$  NMR (250 MHz,  $\text{CDCl}_3$ )  $\delta$  0.17 (12H, s,  $\text{SiCH}_3$ ),  $\delta$  0.96 (18H, s,  $\text{SiC(CH}_3)_3$ ),  $\delta$  1.49 (6H, br, 3,4-cyclohexyl H),  $\delta$  2.17 (4H, br, 2-cyclohexyl H),  $\delta$  6.71 (4H, d,  $J = 9$  Hz, *ortho*- $\Delta r\text{OTBDMS}$ ),  $\delta$  7.08 (4H, d,  $J = 9$  Hz, *meta*- $\Delta r\text{OTBDMS}$ ).

$^{13}\text{C}$  NMR (62.9 MHz,  $\text{CDCl}_3$ )  $\delta$  18.2 (C2), 23.0 (C10), 25.7 (C1), 26.6 (C11), 37.6 (C9), 45.2 (C8), 119.4 (C5), 128.1 (C6), 141.6 (C7), 153.1 (C4).

FAB<sup>+</sup> MS m/z = 496 (100%,  $M^+$ ).  $\text{C}_{30}\text{H}_{48}\text{O}_2\text{Si}_2$  requires 496.85.

Calculated for  $\text{C}_{30}\text{H}_{48}\text{O}_2\text{Si}_2$ : C 72.52, H 9.74;

Found C 72.66, H 9.88.

**1-(4-Hydroxyphenyl)-1-(4-benzyloxyphenyl)cyclohexane (85).** Benzyl bromide (4.179 g, 24.43 mmol), potassium carbonate (3.376 g, 24.43 mmol) and **9** (5.96 g, 22.2 mmol) in DMF (50 ml) were heated at 60 °C for 24 hours. After cooling, the product was diluted with ethyl acetate (200 ml) and filtered before being washed with water (5 x 75 ml), dried ( $\text{Na}_2\text{SO}_4$ ), filtered and evaporated. Flash chromatography on silica (4 cm x 25 cm) eluting with 5:1 petroleum ether (b.p. 40 - 60 °C) : ethyl acetate and collecting the second band gave the title compound as a yellowish oil which solidified upon standing (2.75 g, 35%). The higher running band was **1,1-bis(4-benzyloxyphenyl)cyclohexane (86)** (1.728g, 17%).

**Mono-benzyl compound (85).**

$R_f = 0.40$  (3:1 petroleum ether : EtOAc). m.p. 124 - 125 °C.

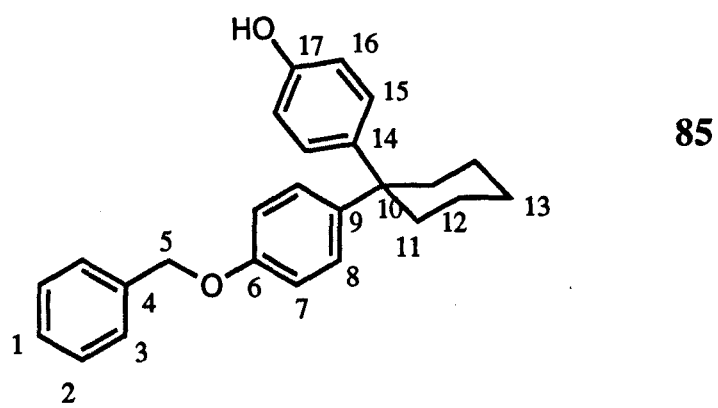
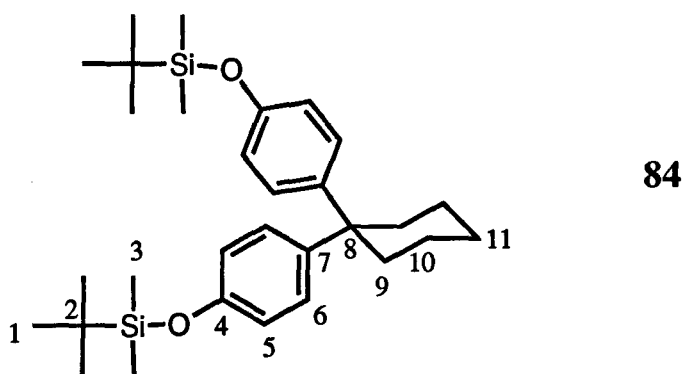
$^1\text{H}$  NMR (250 MHz,  $\text{CDCl}_3$ )  $\delta$  1.52 (6H, br, 3,4-cyclohexyl H),  $\delta$  2.22 (4H, br, 2-cyclohexyl H),  $\delta$  4.84 (1H, s, ArOH),  $\delta$  5.02 (2H, s, benzylic  $\text{CH}_2$ ),  $\delta$  6.74 (2H, d,  $J = 9$  Hz, *ortho*- $\Delta r\text{OH}$ ),  $\delta$  6.90 (2H, d,  $J = 9$  Hz, *ortho*- $\Delta r\text{OCH}_2\text{Ph}$ ),  $\delta$  7.15 (4H, m, *meta*- $\Delta r\text{OH}$  and *meta*- $\Delta r\text{OCH}_2\text{Ph}$ ),  $\delta$  7.39 (5H, m, - $\text{OCH}_2\text{Ph}$ ).

$^{13}\text{C}$  NMR (62.9 MHz,  $\text{CDCl}_3$ )  $\delta$  23.0 (C12), 26.5 (C13), 37.5 (C11), 45.1 (C10), 70.1 (C5), 114.5 and 115.1 (C7, 16), 127.6, 128.0, 128.2, 128.4, 128.6 (C1, 2, 3, 8, 15), 137.2 (C4), 141.2 (C14), 141.5 (C9), 153.1 (C17), 156.5 (C6).

FAB<sup>+</sup> MS m/z = 358 (100%,  $M^+$ );  $\text{C}_{25}\text{H}_{26}\text{O}_2$  requires 358.46.

Calculated for  $\text{C}_{25}\text{H}_{26}\text{O}_2$ : C 83.76, H 7.31;

Found: C 83.96, H 7.45.



**Bis-benzyl compound (86).**

$R_f$  = 0.70 (3:1 petroleum ether : EtOAc). m.p. 84 - 87 °C.

$^1\text{H}$  NMR (250 MHz, CDCl<sub>3</sub>)  $\delta$  1.56 (6H, br, 3,4-cyclohexyl H), 82.24 (4H, br, 2-cyclohexyl H), 85.03 (2H, s, benzylic CH<sub>2</sub>), 86.90 (4H, d, J = 9 Hz, *ortho*-ArOCH<sub>2</sub>Ph), 87.21 (4H, d, J = 9 Hz, 3-ArOCH<sub>2</sub>Ph), 87.39 (10H, m, -OCH<sub>2</sub>Ph).

$^{13}\text{C}$  NMR (62.9 MHz, CDCl<sub>3</sub>)  $\delta$  23.1 (C12), 26.6 (C13), 37.6 (C11), 45.2 (C10), 70.1 (C5), 114.5 (C7), 127.7, 128.0, 128.3, 128.7 (C1, 2, 3, 9), 137.4 (C4), 141.4 (C9), 156.6 (C6).

FAB<sup>+</sup> MS m/z = 448 (100%, M<sup>+</sup>). C<sub>32</sub>H<sub>32</sub>O<sub>2</sub> requires 448.58.

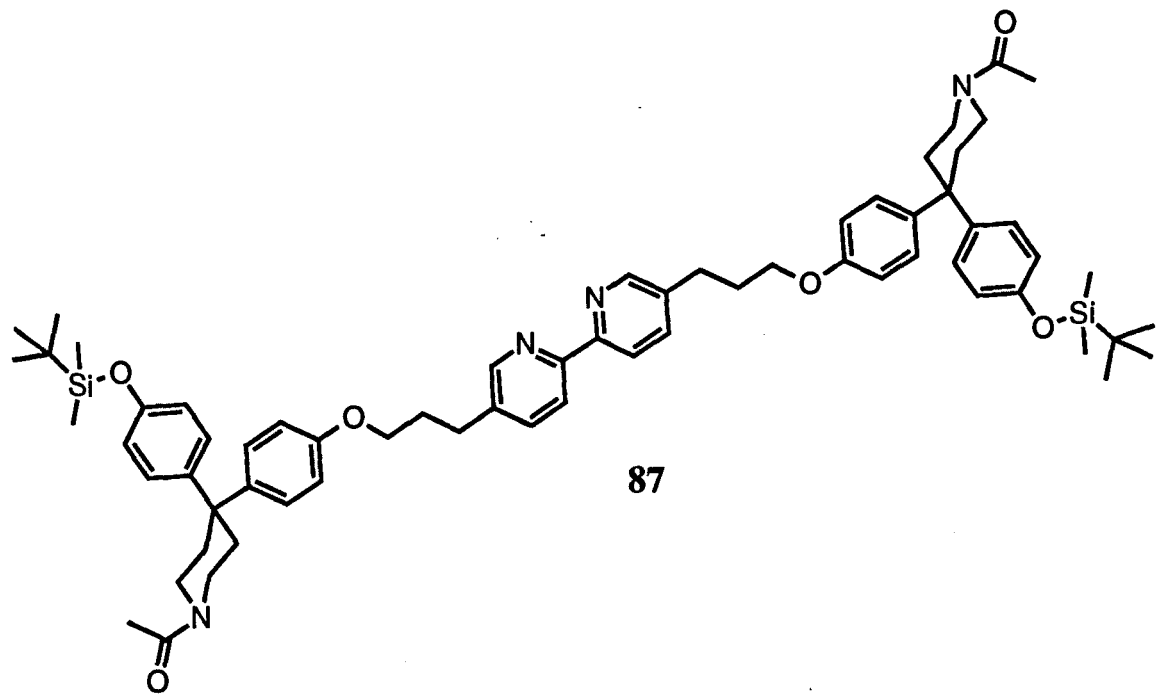
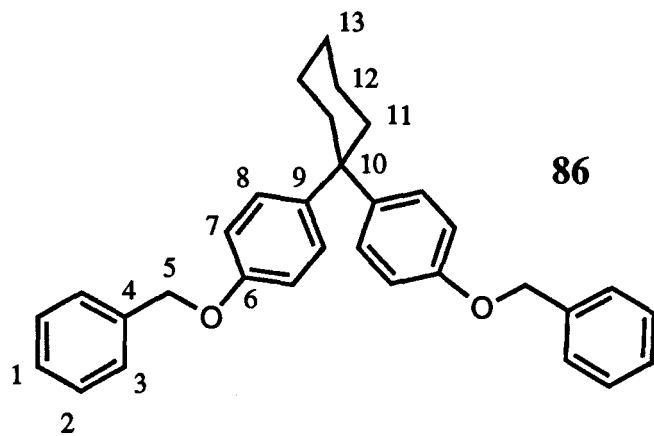
$\nu$  = 1604, 1577 cm<sup>-1</sup> (aromatics).

Calculated for C<sub>32</sub>H<sub>32</sub>O<sub>2</sub>: C 85.67, H 7.19;

Found C 85.63, H 7.21.

*Attempted synthesis of 5,5'-bis(3-(4-(4-(4-(4-(tert-butyldimethylsilyl)oxyphenyl)-N-acetyl piperidine)phenoxy)propyl)-2,2'-bipyridine (87)* In a typical procedure, **82** (0.183 g, 0.431 mmol) in toluene (3 ml) was added to a suspension of sodium hydride (80% dispersion in oil, 0.013 g, 0.431 mmol) in toluene (2 ml). The mixture was heated at reflux for 0.5 hours before addition of a suspension of **7** (0.100 g, 0.172 mmol) in toluene (10 ml). The mixture was heated at reflux for 18 hours before removal of the solvent *in vacuo*. TLC (5% methanol / CH<sub>2</sub>Cl<sub>2</sub>) indicated a complex mixture of products. Attempted purification by flash chromatography on silica (2 cm x 25 cm) eluting with CH<sub>2</sub>Cl<sub>2</sub> containing 1 - 5% methanol gave none of the required product. A number of attempts were made to vary base, solvent, reaction time and temperature using the same general procedure without success (see Chapter 5).

**5,5'-Bis(3-(4-(1-(4-benzyloxyphenyl)cyclohexyl)phenoxy)propyl)-2,2'-bipyridine (91).** **5** (0.191 g, 0.701 mmol), **85** (0.628 g, 1.754 mmol) and TBP (0.425 g, 2.103 mmol) were dissolved in dry CH<sub>2</sub>Cl<sub>2</sub> (8 ml). ADDP (0.530 g, 2.103 mmol) was added in one portion and the stoppered flask was stirred for 18 hours. The precipitate formed was removed by filtration. The filtrate was evaporated and purified by flash chromatography on silica (20 cm x 2 cm) eluting with 0.5% methanol / CH<sub>2</sub>Cl<sub>2</sub> to give the crude product as a yellow solid which was further purified by recrystallisation from a minimum of hot ethanol to give the pure title compound as a white solid (0.467 g, 70%).



$R_f = 0.55$  (10% methanol /  $\text{CH}_2\text{Cl}_2$ ). m.p. 158 - 160 °C.

$^1\text{H}$  NMR (250 MHz,  $\text{CDCl}_3$ )  $\delta$  1.51 (12H, br, 3,4-cyclohexyl H), 2.11 (4H, q,  $J = 7$  Hz,  $\text{ArCH}_2\text{CH}_2-$ ), 2.21 (8H, br, 2-cyclohexyl H), 2.85 (4H, t,  $J = 7$  Hz,  $\text{ArCH}_2\text{CH}_2\text{CH}_2\text{O}-$ ), 3.94 (4H, t,  $J = 7$  Hz,  $\text{ArCH}_2\text{CH}_2\text{CH}_2\text{OAr}$ ), 5.00 (4H, s, benzylic  $\text{CH}_2$ ), 6.78 and 6.86 (2 x 4H, 2d,  $J = 9$  Hz, *ortho*- $\text{ArO}(\text{CH}_2)_3\text{Ar}$  and *ortho*- $\text{ArOCH}_2\text{Ph}$ ), 7.15 (4H, m, *meta*- $\text{ArO}(\text{CH}_2)_3\text{Ar}$  and *meta*- $\text{ArOCH}_2\text{Ph}$ ), 7.38 (10H, m, - $\text{OCH}_2\text{Ph}$ ), 7.64 (2H, dd,  $J = 8$  Hz, 2 Hz, 4-bipyridine H), 8.26 (2H, d,  $J = 8$  Hz, 3-bipyridine H), 8.51 (2H, d,  $J = 2$  Hz, 6-bipyridine H).

$^{13}\text{C}$  NMR (62.9 MHz,  $\text{CDCl}_3$ )  $\delta$  23.0 (C12), 26.5 (C13), 29.2 (C20), 30.6 (C19), 37.4 (C11), 45.1 (C10), 66.4 (C18), 70.0 (C5), 114.1 and 114.4 (C7, 16), 120.6 (C23), 127.6, 127.9, 128.1, 128.6 (C1, 2, 3, 8, 14), 136.8 and 137.3 (C4, 21), 137.0 (C24), 141.1 and 141.4 (C9, 14), 149.4 (C22), 154.2 (C25), 156.5 (C6, 17).

FAB<sup>+</sup> MS m/z = 953;  $\text{C}_{66}\text{H}_{68}\text{N}_2\text{O}_4$  requires 953.22.

Calculated for  $\text{C}_{66}\text{H}_{68}\text{N}_2\text{O}_4$ : C 83.15, H 7.19, N 2.94;

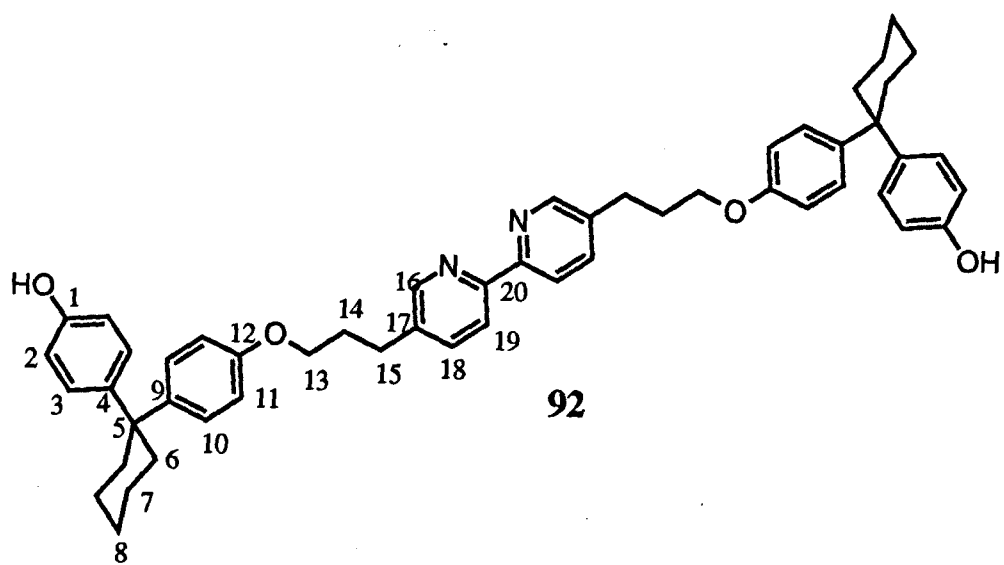
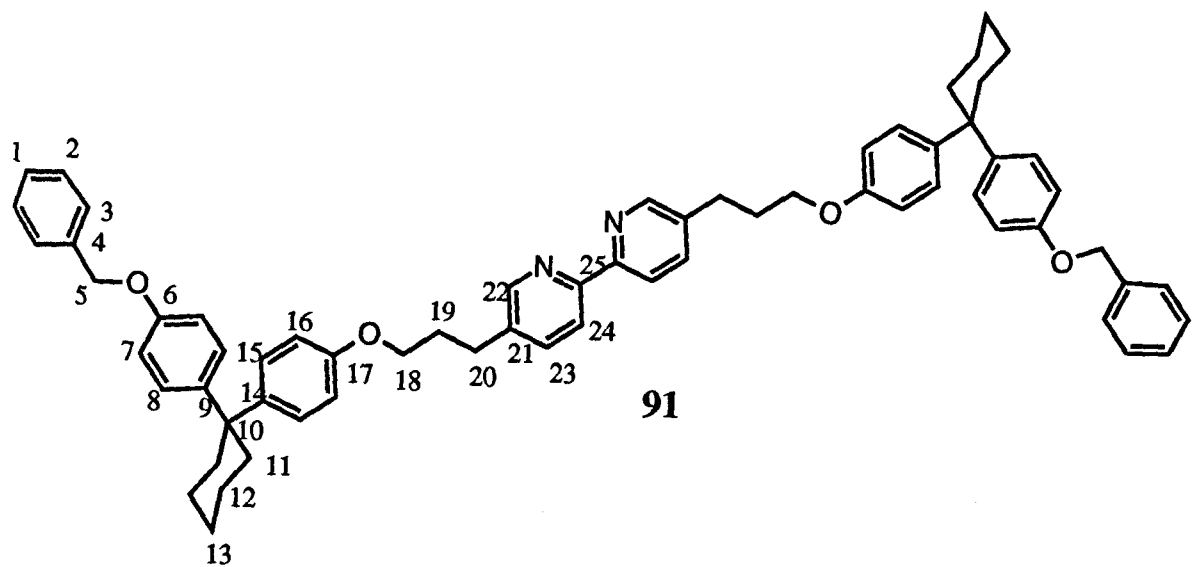
Found: C 83.3, H 7.2, N 3.1.

**5,5'-Bis(3-(4-(1-(4-hydroxyphenyl)cyclohexyl)phenoxy)propyl)-2,2'-bipyridine (92).** **91** (0.500 g, 0.525 mmol), palladium black (125 mg) and 1,4-cyclohexadiene (2 ml) were heated at reflux in ethanol (10 ml) for 4 hours. After cooling, the solution was filtered and the catalyst washed several times with hot 15% methanol /  $\text{CH}_2\text{Cl}_2$ . The combined filtrate and washings were evaporated and the crude product purified by flash chromatography on silica (2 cm x 15 cm) eluting with 4 - 6% methanol in  $\text{CH}_2\text{Cl}_2$  to yield the title compound as a white solid (0.358 g, 88%).

$R_f = 0.30$  (10% methanol /  $\text{CH}_2\text{Cl}_2$ ). m.p. 180 - 182 °C.

$^1\text{H}$  NMR (250 MHz, 95/5 v/v  $\text{CDCl}_3$  /  $\text{CD}_3\text{OD}$ )  $\delta$  1.40 (12H, m, 3,4-cyclohexyl H), 2.03 (4H, quintet,  $J = 7$  Hz,  $\text{ArCH}_2\text{CH}_2\text{CH}_2\text{OAr}$ ), 2.11 (8H, m, 2-cyclohexyl H), 2.80 (4H, t,  $J = 7$  Hz,  $\text{ArCH}_2\text{CH}_2\text{CH}_2\text{OAr}$ ), 3.87 (4H, t,  $J = 7$  Hz,  $\text{ArOCH}_2-$ ), 6.62 and 6.70 (2 x 4H, 2d,  $J = 8.5$  Hz, *ortho*- $\text{ArOH}$  and *ortho*- $\text{ArOR}$ ), 6.98 and 7.07 (2 x 4H, 2d,  $J = 8.5$  Hz, *meta*- $\text{ArOH}$  and *meta*- $\text{ArOR}$ ), 7.62 (2H, dd,  $J = 8$  Hz, 2 Hz, 4-pyridine H), 8.08 (2H, d,  $J = 8$  Hz, 3-pyridine H), 8.40 (2H, d,  $J = 2$  Hz, 6-pyridine H).

$\nu = 1608, 1509 \text{ cm}^{-1}$  (aromatics).



**5,5'-Bis(3-(4-(1-(4-(3-(5-(2-(5-(3-(*tert*-butyldimethylsilyl)oxypropyl)pyridine))pyridine)propyl)oxyphenyl)cyclohexyl)phenoxy)propyl)-2,2'-bipyridine (93).**

**Route A:** To a solution of **92** (0.300 g, 0.388 mmol), **78** (0.315 g, 0.815 mmol) and TBP (0.236 g, 1.164 mmol) in CH<sub>2</sub>Cl<sub>2</sub> (5 ml) at 0°C was added ADDP (0.294 g, 1.164 mmol) in one portion with the formation of a white precipitate. After stirring for 18 hours at room temperature, the product was filtered and evaporated. Flash chromatography on silica (2 cm x 25 cm) eluting with 0.5% methanol in CH<sub>2</sub>Cl<sub>2</sub> gave the title compound as a white solid (0.316 g, 54%).

**Route B.** To a solution of **5** (0.080 g, 0.293 mmol), **96** (0.421 g, 0.661 mmol) and TBP (0.178 g, 0.881 mmol) in CH<sub>2</sub>Cl<sub>2</sub> (4 ml) at 0°C was added ADDP (0.222 g, 0.881 mmol) in one portion with the formation of a white precipitate. After stirring for 18 hours at room temperature, the product was filtered and evaporated. Flash chromatography on silica (2 cm x 25 cm) eluting with 0.5% methanol in CH<sub>2</sub>Cl<sub>2</sub> gave the title compound as a white solid (0.272 g, 61%).

R<sub>f</sub> = 0.25 (10% methanol / CH<sub>2</sub>Cl<sub>2</sub>). m.p. 194 - 196°C.

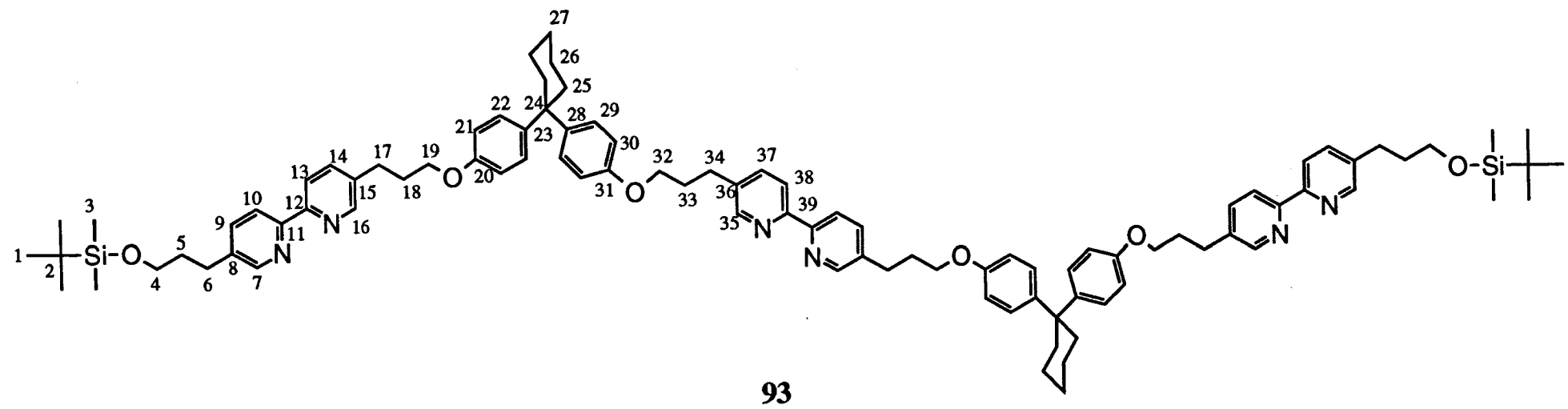
<sup>1</sup>H NMR (250 MHz, CDCl<sub>3</sub>) δ0.04 (12H, s, SiCH<sub>3</sub>), δ0.90 (18H, s, C(CH<sub>3</sub>)<sub>3</sub>), δ1.51 (12H, br, 3,4-cyclohexyl H), δ1.86 (4H, quintet, J = 7 Hz, TBDMSOCH<sub>2</sub>CH<sub>2</sub>-), δ2.09 (8H, quintet, J = 7 Hz, ArOCH<sub>2</sub>CH<sub>2</sub>-), δ2.15 (8H, br, 2-cyclohexyl H), δ2.74 (4H, t, J = 7 Hz, ArCH<sub>2</sub>(CH<sub>2</sub>)<sub>2</sub>OTBDMS), δ2.85 (8H, t, J = 7 Hz, ArCH<sub>2</sub>(CH<sub>2</sub>)<sub>2</sub>OAr), δ3.64 (4H, t, J = 7 Hz, -CH<sub>2</sub>OTBDMS), δ3.94 (8H, t, J = 7 Hz, -CH<sub>2</sub>OAr), δ6.79 (8H, d, J = 9 Hz, *ortho*-ArOR), δ7.15 (8H, d, J = 9 Hz, *meta*-ArOR), δ7.64 (6H, m, 4-pyridine H), δ8.27 (6H, m, 3-pyridine H), δ8.50 (6H, m, 6-pyridine H).

<sup>13</sup>C NMR (62.9 MHz, CDCl<sub>3</sub>) δ18.2 (C2), 22.9 (C26), 25.9 (C1), 26.4 (C27), 29.0 and 29.1 (C8, 17, 34), 30.5 (C18, 33), 33.9 (C5), 37.3 (C25), 45.0 (C24), 61.8 (C4), 66.3 (C19, 32), 114.0 (C21, 30), 120.4 (C9, 14, 37), 128.0 (C22, 39), 136.6 and 137.3 (C8, 15, 36), 136.8 (C10, 13, 38), 141.1 (C23, 28), 149.2 (C7, 16, 35), 153.9, 154.1 and 154.2 (C11, 12, 39), 156.4 (C20, 31).

FAB<sup>+</sup> MS m/z = 1510 (100%, M<sup>+</sup>); C<sub>96</sub>H<sub>120</sub>N<sub>6</sub>O<sub>6</sub>Si<sub>2</sub> requires 1510.13.

Calculated for C<sub>96</sub>H<sub>120</sub>N<sub>6</sub>O<sub>6</sub>Si<sub>2</sub>·0.5H<sub>2</sub>O: C 75.90, H 8.03, N 5.53;

Found C 75.9, H 7.9, N 5.7.



**5,5-Bis(3-(4-(1-(4-(3-(5-(2-(5-(3-hydroxypropyl)pyridine)))pyridine)propyl)oxyphenyl)cyclohexyl)phenoxy)propyl)-2,2'-bipyridine (94).** A solution of **93** (0.180 g) in 20% TFA / CH<sub>2</sub>Cl<sub>2</sub> (7 ml) was stirred at room temperature for 1.5 hours. After diluting with CH<sub>2</sub>Cl<sub>2</sub> (10 ml) the organic layer was washed with saturated aqueous NaHCO<sub>3</sub> (2 x 15 ml) before being dried (Na<sub>2</sub>SO<sub>4</sub>), filtered and evaporated. Recrystallisation by diffusion of a layer of petroleum ether b.p. 40-60 °C into a solution of the product in a minimum of 5% methanol / CH<sub>2</sub>Cl<sub>2</sub> gave the title compound as a white solid (0.153 g, 100%).

R<sub>f</sub> = 0.05 (10% methanol / CH<sub>2</sub>Cl<sub>2</sub>). m.p. 204 - 206 °C.

<sup>1</sup>H NMR (250 MHz, 5% CD<sub>3</sub>OD / CDCl<sub>3</sub>) δ1.55 (12H, br, 3,4-cyclohexyl H), δ1.91 (4H, quintet, J = 7 Hz, HOCH<sub>2</sub>CH<sub>2</sub>-), δ2.09 (8H, t, J = 6 Hz, ArCH<sub>2</sub>CH<sub>2</sub>CH<sub>2</sub>OAr), δ2.21 (8H, br, 2-cyclohexyl H), δ2.76 (4H, t, J = 7 Hz, HO(CH<sub>2</sub>)<sub>2</sub>CH<sub>2</sub>-), δ2.84 (8H, t, J = 7 Hz, ArCH<sub>2</sub>(CH<sub>2</sub>)<sub>2</sub>OAr), δ3.69 (4H, br, HOCH<sub>2</sub>-), δ3.93 (8H, t, J = 6 Hz, -CH<sub>2</sub>OAr), δ6.78 (8H, d, J = 9 Hz, *ortho*-ArOR), δ7.15 (8H, d, J = 9 Hz, *meta*-ArOR), δ7.63 (6H, dd, J = 8 Hz, 1.5 Hz, 4-pyridine H), δ8.25 (6H, d, J = 8 Hz, 3-pyridine H), δ8.50 (6H, d, J = 1.5 Hz, 6-pyridine H).

<sup>13</sup>C NMR (62.9 MHz, 5% CD<sub>3</sub>OD / CDCl<sub>3</sub>) δ22.8 (C23), 26.3 (C24), 28.8 and 29.0 (C5, 14, 31), 30.4 (C15, 30), 33.5 (C2), 37.2 (C22), 44.9 (C21), 61.0 (C1), 66.3 (C16, 29), 113.9 (C18, 27), 120.7 (C6, 11, 34), 128.0 (C19, 26), 137.0 and 137.4 (C5, 12, 33), 137.1 (C7, 10, 35), 141.1 (C20, 25), 149.0 (C4, 13, 32), 153.7 and 153.8 (C8, 9, 36), 156.2 (C17, 28).

FAB<sup>+</sup> MS m/z = 1282 (100%, MH<sup>+</sup>); C<sub>84</sub>H<sub>92</sub>N<sub>6</sub>O<sub>6</sub> requires 1281.62.

Calculated for C<sub>84</sub>H<sub>92</sub>N<sub>6</sub>O<sub>6</sub>·H<sub>2</sub>O: C 77.63, H 7.29, N 6.47;

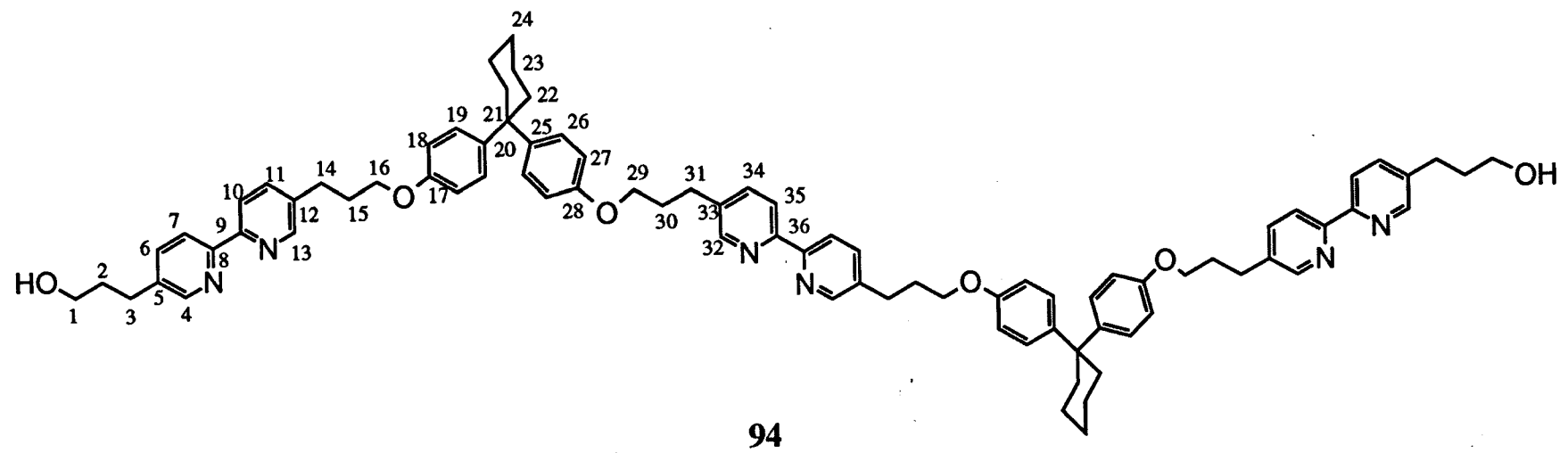
Found C 77.65, H 7.29, N 6.45.

### 1-(3-(5'-(3-(*Tert*-butyldimethylsilyl)oxypropyl)-2,2'-bipyridine))propyloxy

**phenyl)-1-benzyloxyphenylcyclohexane (95).** To a solution of **78** (0.405 g, 1.048 mmol), **85** (0.413 g, 1.152 mmol) and TBP (0.312 g, 1.571 mmol) in CH<sub>2</sub>Cl<sub>2</sub> (7 ml) at 0°C was added ADDP (0.397 g, 1.571 mmol) in one portion with the formation of a white precipitate. After stirring for 18 hours at room temperature, the product was filtered and evaporated. Flash chromatography on silica (2 cm x 25 cm) eluting with 0.5% methanol in CH<sub>2</sub>Cl<sub>2</sub> gave the title compound as a white solid (0.677 g, 89%).

R<sub>f</sub> = 0.15 (5% methanol / CH<sub>2</sub>Cl<sub>2</sub>). m.p. 118 - 119 °C.

<sup>1</sup>H NMR (250 MHz, CDCl<sub>3</sub>) δ0.05 (6H, s, Si(CH<sub>3</sub>)<sub>2</sub>), δ0.92 (9H, s, SiC(CH<sub>3</sub>)<sub>3</sub>), δ1.51 (6H, br, 3,4-cyclohexyl H), δ1.81 (2H, quintet, J = 7 Hz, TBDM<sub>3</sub>OCH<sub>2</sub>CH<sub>2</sub>-), δ2.10 (2H, quintet, J = 7 Hz, ArOCH<sub>2</sub>CH<sub>2</sub>-), δ2.21 (4H, br, 2-cyclohexyl H), δ2.73 (2H, t, J = 7 Hz, ArCH<sub>2</sub>CH<sub>2</sub>CH<sub>2</sub>OTBDMS), δ2.85 (2H, t, J = 7 Hz, ArCH<sub>2</sub>CH<sub>2</sub>CH<sub>2</sub>OAr), δ3.65 (2H, t, J = 7 Hz, -CH<sub>2</sub>OTBDMS), δ3.94 (2H, t, J = 7 Hz, ArOCH<sub>2</sub>-), δ5.00 (2H, s,



benzylic CH<sub>2</sub>), δ6.79 (2H, d, J = 9 Hz, *ortho*-ArOR), δ6.88 (2H, d, J = 9 Hz, *ortho*-ArOBn), δ7.17 (4H, m, *meta*-ArOR and *meta*-ArOBn), δ7.27 (5H, m, benzyl), δ7.64 (2H, m, 4-pyridine H), δ8.27 (2H, m, 3-pyridine H), δ8.50 (2H, m, 6-pyridine H).

<sup>13</sup>C NMR (62.9 MHz, CDCl<sub>3</sub>) δ18.2 (C2), 22.9 (C26), 25.9 (C1), 26.4 (C27), 29.0 and 29.1 (C6, 17), 30.5 (C18), 33.9 (C5), 37.3 (C25), 45.0 (C24), 61.8 (C4), 66.3 (C19), 69.9 (C32), 114.0 and 114.3 (C21, 30), 120.4 (C9, 14), 127.4, 127.8, 128.0 and 128.4 (C22, 29, 34, 35, 36), 136.6 and 137.3 (C8, 15), 136.8 (C10, 13), 141.0 and 141.3 (C23, 28), 149.3 (C7, 16), 154.0 and 154.2 (C11, 12), 156.4 (C20, 31).

ES<sup>+</sup> MS m/z = 727.6 (100%, MH<sup>+</sup>); C<sub>47</sub>H<sub>58</sub>N<sub>2</sub>O<sub>3</sub>Si requires 727.08.

Calculated for C<sub>47</sub>H<sub>58</sub>N<sub>2</sub>O<sub>3</sub>Si · 0.5H<sub>2</sub>O: C 76.70, H 8.08, N 3.81;

Found C 77.0, H 7.8, N 4.0.

**1-(3-(5'-(3-(*Tert*-butyldimethylsilyl)oxypropyl)-2,2'-bipyridine))propyloxy phenyl)-1-hydroxyphenylcyclohexane (96).** A suspension of **95** (0.577 g, 0.794 mmol), palladium black (0.150 g) and 1,4-cyclohexadiene (1.5 ml) in ethanol (7 ml) was heated at reflux for 1.5 hours. After cooling, the product was diluted with CH<sub>2</sub>Cl<sub>2</sub> (20 ml) and filtered. The catalyst was washed well with hot 10% methanol / CH<sub>2</sub>Cl<sub>2</sub> and the combined filtrate and washings concentrated *in vacuo*. Flash chromatography on silica (2 cm x 10 cm) eluting with 3% methanol in CH<sub>2</sub>Cl<sub>2</sub> gave the title compound as a white solid (0.466 g, 92%).

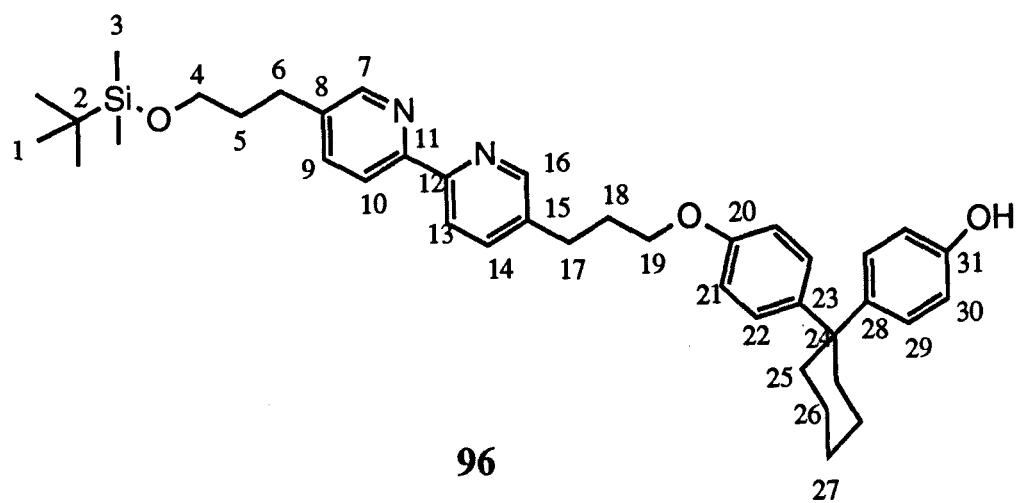
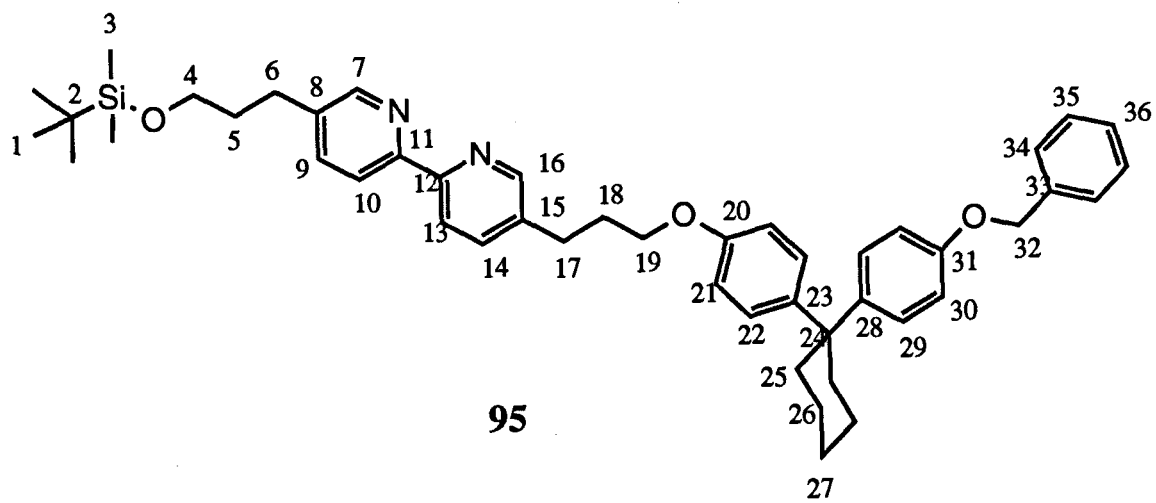
<sup>1</sup>H NMR (300 MHz, CDCl<sub>3</sub>) δ0.06 (6H, s, Si(CH<sub>3</sub>)<sub>2</sub>), δ0.92 (9H, s, SiC(CH<sub>3</sub>)<sub>3</sub>), δ1.33 (6H, br, 3,4-cyclohexyl H), δ1.87 (2H, quintet, J = 6.5 Hz, TBDMOSOCH<sub>2</sub>CH<sub>2</sub>-), δ2.09 (2H, quintet, J = 7 Hz, ArOCH<sub>2</sub>CH<sub>2</sub>-), δ2.20 (4H, br, 2-cyclohexyl H), δ2.75 (2H, t, J = 7 Hz, ArCH<sub>2</sub>CH<sub>2</sub>CH<sub>2</sub>OTBDMS), δ2.86 (2H, t, J = 7 Hz, ArCH<sub>2</sub>CH<sub>2</sub>CH<sub>2</sub>OAr), δ3.66 (2H, t, J = 7 Hz, -CH<sub>2</sub>OTBDMS), δ3.95 (2H, t, J = 6.5 Hz, ArOCH<sub>2</sub>-), δ5.22 (1H, br, -OH), δ6.72 (2H, d, J = 8.5 Hz, *ortho*-ArOH), δ6.79 (2H, d, J = 8.5 Hz, *ortho*-ArOR), δ7.13 (4H, m, *meta*-ArOR and *meta*-ArOH), δ7.61 (2H, m, 4-pyridine H), δ8.25 (2H, m, 3-pyridine H), δ8.51 (2H, m, 6-pyridine H).

<sup>13</sup>C NMR (62.9 MHz, CDCl<sub>3</sub>) δ-3.7 (C3), 18.2 (C2), 22.8 (C26), 25.8 (C1), 26.4 (C27), 28.8 and 28.9 (C6, 17), 30.4 (C18), 33.5 (C5), 37.2 (C25), 44.7 (C24), 61.8 (C4), 66.3 (C19), 113.9 (C21), 115.0 (C30), 120.9 (C9, 14), 127.7 (C22, 29), 137.0 and 137.4 (C8, 15), 137.1 and 137.2 (C10, 13), 139.9 and 141.2 (C23, 28), 148.9 and 149.0 (C7, 16), 153.5, 153.6 and 154.2 (C11, 12, 31), 156.2 (C20).

ES<sup>+</sup> MS m/z = 637.29 (100%, MH<sup>+</sup>); C<sub>40</sub>H<sub>52</sub>N<sub>2</sub>O<sub>3</sub>Si requires 636.96.

Calculated for C<sub>40</sub>H<sub>52</sub>N<sub>2</sub>O<sub>3</sub>Si : C 75.43, H 8.23, N 4.40;

Found: C 75.8, H 8.2, N 4.5.



**5,5'-Bis(2-carbo(4-(1-(4-benzyloxyphenyl)cyclohexyl)phenoxyethyl))-2,2'-bipyridine (97).** To a solution of **6** (0.100 g, 0.329 mmol), **85** (0.275 g, 0.823 mmol) and DMAP (8 mg, 20 mol%) in CH<sub>2</sub>Cl<sub>2</sub> (5 ml) at 0°C was added EDC (0.139 g, 0.723 mmol). The mixture was stirred at room temperature for 18 hours before the clear solution was diluted with CH<sub>2</sub>Cl<sub>2</sub> (10 ml) and washed with HCl (2 ml, 0.5 M), saturated NaHCO<sub>3</sub> (2 x 10 ml) and water (10 ml), dried (Na<sub>2</sub>SO<sub>4</sub>), filtered and evaporated. Flash chromatography on silica (15cm x 2cm) eluting with 10% petroleum ether (b.p. 40-60°C) in CH<sub>2</sub>Cl<sub>2</sub> increasing to 100% CH<sub>2</sub>Cl<sub>2</sub> then 1-3% methanol in CH<sub>2</sub>Cl<sub>2</sub> gave the title compound as a slightly off-white solid (0.230 g, 71%).

R<sub>f</sub> = 0.35 (10% MeOH in CH<sub>2</sub>Cl<sub>2</sub>). m.p. 194 - 196 °C.

<sup>1</sup>H NMR (250 MHz, CDCl<sub>3</sub>) δ1.53 (12H, br, 3,4-cyclohexyl H), δ2.22 (8H, br, 2-cyclohexyl H), δ2.91 and 3.13 (2 x 4H, 2t, J = 7.5 Hz, ArCH<sub>2</sub>CH<sub>2</sub>CO<sub>2</sub>-), δ5.02 (4H, s, benzylic CH<sub>2</sub>), δ6.90 (8H, m, *ortho*-ArO<sub>2</sub>C- and *ortho*-ArOCH<sub>2</sub>Ph), δ7.20 (8H, m, *meta*-ArO<sub>2</sub>C- and *meta*-ArOCH<sub>2</sub>Ph), δ7.39 (10H, m, -OCH<sub>2</sub>Ph), δ7.72 (2H, dd, J = 8 Hz, 2 Hz, 4-pyridine H), δ8.33 (2H, d, J = 8 Hz, 3-pyridine H), δ8.59 (2H, d, J = 2 Hz, 6-pyridine H).

<sup>13</sup>C NMR (62.9 MHz, CDCl<sub>3</sub>) δ22.9 (C12), 26.4 (C13), 27.9 (C20), 35.5 (C19), 37.3 (C11), 45.4 (C10), 70.0 (C10), 114.5 (C7), 120.7 (C23), 120.9 (C14), 127.6, 127.9, 128.1, 128.3 and 128.6 (C1, 2, 3, 8, 15), 135.6 (C22), 136.9 (C25), 137.2 (C4), 140.4 and 146.8 (C9, 14), 148.1 (C17), 149.3 (C21), 154.5 (C25), 156.6 (C6), 171.0 (C18).

FAB<sup>+</sup> MS m/z = 981 (100%, M<sup>+</sup>); C<sub>66</sub>H<sub>64</sub>N<sub>2</sub>O<sub>6</sub> requires 981.19.

ν = 1754 cm<sup>-1</sup> (C=O) and 1605, 1553 cm<sup>-1</sup> (aromatics).

Calculated for C<sub>60</sub>H<sub>64</sub>N<sub>2</sub>O<sub>6</sub>·H<sub>2</sub>O: C 79.32, H 6.66, N 2.80;

Found C 79.69, H 6.56, N 2.88.

**5,5'-Bis(2-carbo(4-(1-(4-(tert-butyldimethylsilyl)oxyphenyl)cyclohexyl)phenoxyethyl))-2,2'-bipyridine (98)** was prepared as for **97**, substituting **83** (0.276 g, 0.723 mmol) for **85** to yield the title compound as a white solid (0.237 g, 70%).

R<sub>f</sub> = 0.4 (10% methanol in CH<sub>2</sub>Cl<sub>2</sub>). m.p. 141 - 142 °C.

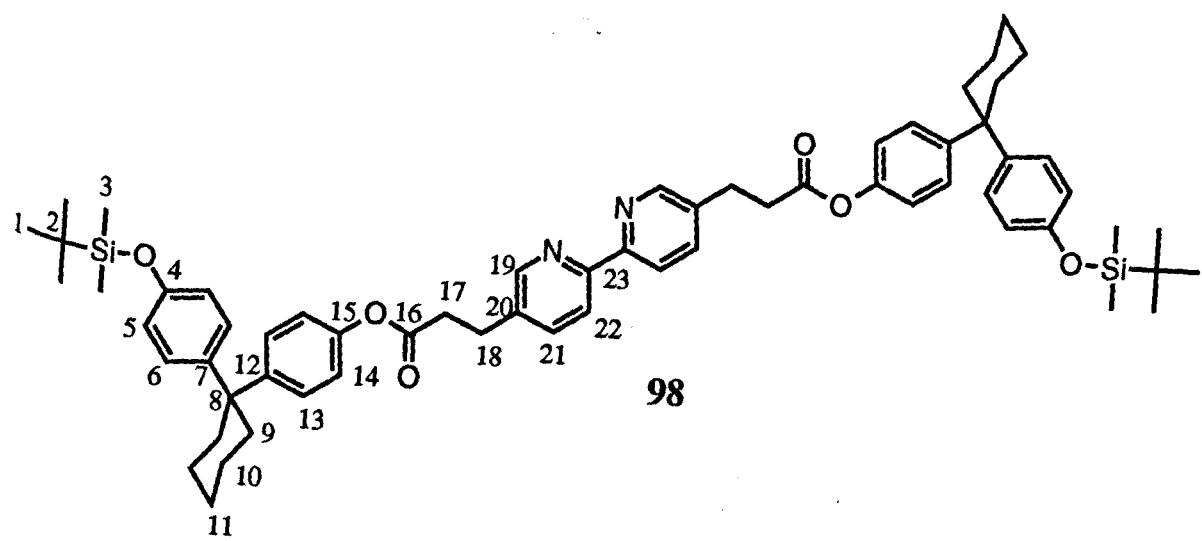
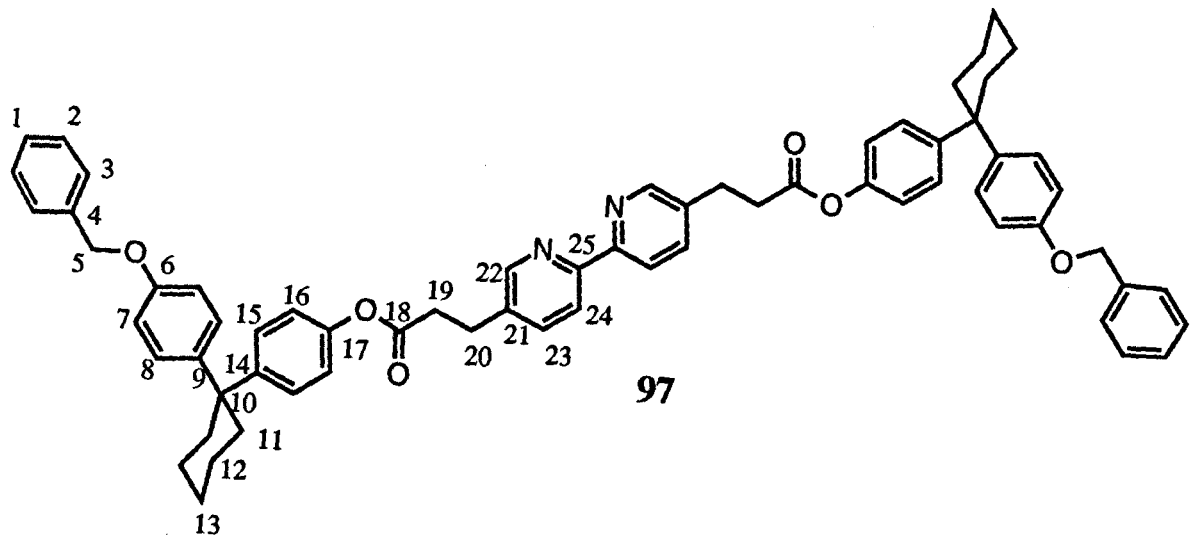
<sup>1</sup>H NMR (250 MHz, CDCl<sub>3</sub>) δ0.18 (12H, s, Si(CH<sub>3</sub>)<sub>2</sub>), δ0.95 (18H, s, SiC(CH<sub>3</sub>)<sub>3</sub>), δ1.50 (12H, br, 3,4-cyclohexyl H), δ2.20 (8H, br, 2-cyclohexyl H), δ2.80 and δ3.10 (2 x 4H, 2t, J = 7.5 Hz, ArCH<sub>2</sub>CH<sub>2</sub>CO<sub>2</sub>- and ArCH<sub>2</sub>CH<sub>2</sub>CO<sub>2</sub>-), δ6.71 and δ6.91 (2 x 4H, 2d, J = 9 Hz, *ortho*-ArOTBDMS and *ortho*-ArO<sub>2</sub>C-), δ7.08 and δ7.21 (2 x 4H, 2d, J = 9 Hz, *meta*-ArOTBDMS and *meta*-ArO<sub>2</sub>CR), δ7.70 (2H, dd, J = 8 Hz, 2 Hz, 4-pyridine H), δ8.30 (2H, d, J = 8 Hz, 3-pyridine H), δ8.57 (2H, d, J = 2 Hz, 6-pyridine H).

FAB<sup>+</sup> MS m/z = 1029 (100%, M<sup>+</sup>); C<sub>64</sub>H<sub>80</sub>N<sub>2</sub>O<sub>6</sub>Si<sub>2</sub> requires 1029.46.

ν = 1752 cm<sup>-1</sup> (C=O), 1606, 1552 and 1510 cm<sup>-1</sup> (aromatics), 1262 cm<sup>-1</sup> (Si-Me).

Calculated for C<sub>64</sub>H<sub>80</sub>N<sub>2</sub>O<sub>6</sub>Si<sub>2</sub>: C 74.66, H 7.83, N 2.72.

Found C 74.99, H 8.08, N 2.77.



**5,5'-Bis(2-carbo(4-(1-(4-hydroxyphenyl)cyclohexyl)phenoxyethyl))-2,2'-bipyridine (99) 97** (0.250 g, 0.255 mmol), palladium black (60 mg) and 1,4-cyclohexadiene (1 ml) were heated at reflux in 1:1 methanol / CH<sub>2</sub>Cl<sub>2</sub> (8 ml) for 18 hours - 2 days until TLC indicated that the reaction was complete. After cooling, the solution was filtered and the catalyst washed several times with hot 15% methanol / CH<sub>2</sub>Cl<sub>2</sub>. The combined filtrate and washings were evaporated and the crude product purified by flash chromatography on silica (2 cm x 15 cm) eluting with 5% methanol in CH<sub>2</sub>Cl<sub>2</sub> to yield the title compound as a white solid (0.163 g, 80%).

R<sub>f</sub> = 0.2 (10% methanol / CH<sub>2</sub>Cl<sub>2</sub>).

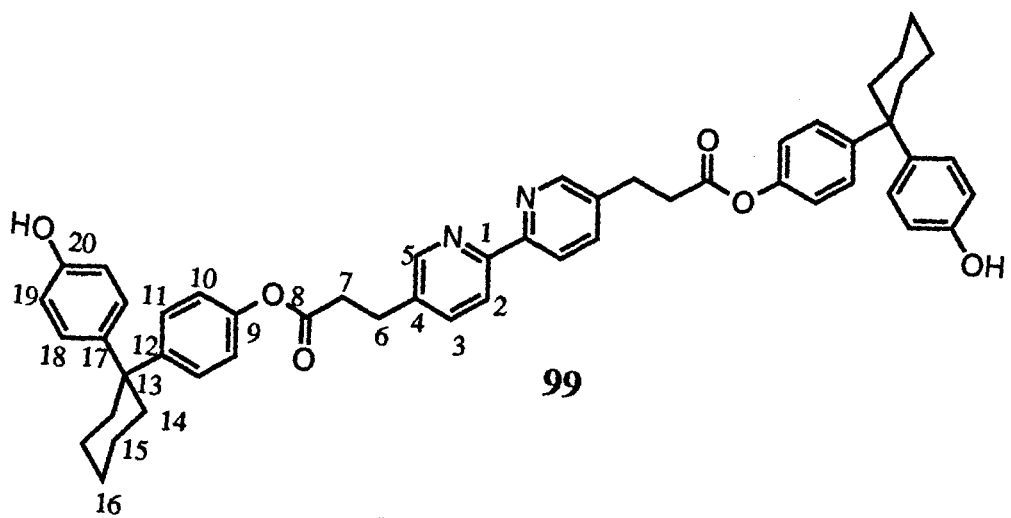
<sup>1</sup>H NMR (250 MHz, CDCl<sub>3</sub> + 5% CD<sub>3</sub>OD) δ1.48 (2H, br, 3,4-cyclohexyl H), δ2.18 (8H, br, 2-cyclohexyl H), δ2.90 and δ3.09 (2 x 4H, 2t, ArCH<sub>2</sub>CH<sub>2</sub>CO<sub>2</sub>Ar), δ6.69 and δ6.87 (2 x 4H, 2d, *ortho*-ArOH and *ortho*-ArO<sub>2</sub>C-), δ7.06 and δ7.20 (2 x 4H, 2d, *meta*-ArOH and *meta*-ArO<sub>2</sub>C-), δ7.72 (2H, dd, 4-pyridine H), δ8.24 (2H, d, 3-pyridine H), δ8.54 (2H, d, 6-pyridine H).

<sup>13</sup>C NMR (62.9 MHz, 5% CD<sub>3</sub>OD / CDCl<sub>3</sub>) δ22.8 (C16), 26.3 (C15), 27.8 (C6), 35.3 (C7), 37.3 (C14), 45.3 (C13), 115.0 (C19), 120.8 (C3), 121.1 (C10), 128.1 and 128.2 (C11, 18), 135.8 (C4), 137.3 (C2), 139.3 (C12, 17), 147.1 and 147.9 (C9, 20), 149.1 (C5), 154.2 (C1), 171.1 (C8).

FAB<sup>+</sup> MS m/z = 801 (100%, M<sup>+</sup>). C<sub>52</sub>H<sub>52</sub>N<sub>2</sub>O<sub>6</sub> requires 800.95.

Calculated for C<sub>52</sub>H<sub>52</sub>N<sub>2</sub>O<sub>6</sub>·H<sub>2</sub>O: C 76.26, H 6.65, N 3.42;

Found C 76.0, H 6.65, N 3.42.



**5,5'-Bis(2-carbo(benzyloxy)ethyl)-2,2'-bipyridine (101).** To a suspension of **6** (0.200 g, 0.666 mmol) and benzyl alcohol (0.360 g, 3.33 mmol) in dry CH<sub>2</sub>Cl<sub>2</sub> (25 ml) at 0°C was added DMAP (8 mg, 10 mol%) and EDC (0.447 g, 2.33 mmol). After stirring for 18 hours at room temperature the solution was washed with 1M HCl (2 x 25 ml), 1M NaOH (4 x 25 ml) and water (2 x 25 ml). The CH<sub>2</sub>Cl<sub>2</sub> solution was dried (Na<sub>2</sub>SO<sub>4</sub>), filtered and evaporated. The crude product was purified by flash chromatography on silica (2 cm x 20 cm) eluting with 2% methanol in CH<sub>2</sub>Cl<sub>2</sub> to give the title compound as a white solid (0.259 g, 81%).

R<sub>f</sub> = 0.30 (5% methanol / CH<sub>2</sub>Cl<sub>2</sub>). m.p. 104-105 °C.

<sup>1</sup>H NMR (250 MHz, CDCl<sub>3</sub>) δ2.64 (4H, t, J = 7 Hz, -CH<sub>2</sub>-), 82.94 (4H, t, J = 7 Hz, -CH<sub>2</sub>-), 85.03 (4H, s, benzyl CH<sub>2</sub>), 87.20 (10H, m, Ph), 87.53 (2H, dd, J = 8 Hz, 2 Hz, 4-pyridine H), 88.19 (2H, d, J = 8 Hz, 3-pyridine H), 88.43 (2H, d, J = 2 Hz, 6-pyridine H).

<sup>13</sup>C NMR (62.9 MHz, CDCl<sub>3</sub>) δ27.8 (C8), 35.2 (C7), 66.4 (C5), 120.5 (C11), 128.2 and 128.5 (C1, 2, 3), 135.6 and 135.7 (C4, 10), 136.6 (C12), 149.1 (C9), 154.3 (C13), 172.0 (C6).

EI<sup>+</sup> MS m/z = 480 (100%, M<sup>+</sup>); C<sub>30</sub>H<sub>28</sub>N<sub>2</sub>O<sub>4</sub> requires 480.54.

Calculated for C<sub>30</sub>H<sub>28</sub>N<sub>2</sub>O<sub>4</sub>: C 74.98, H 5.87, N 5.83;

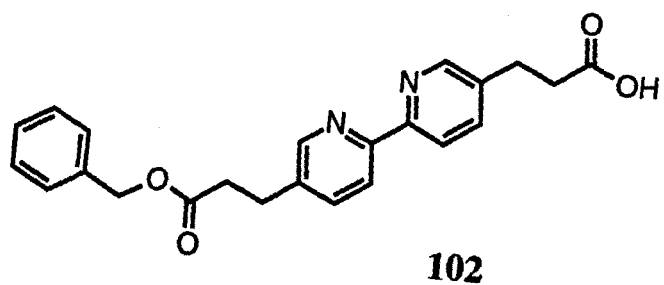
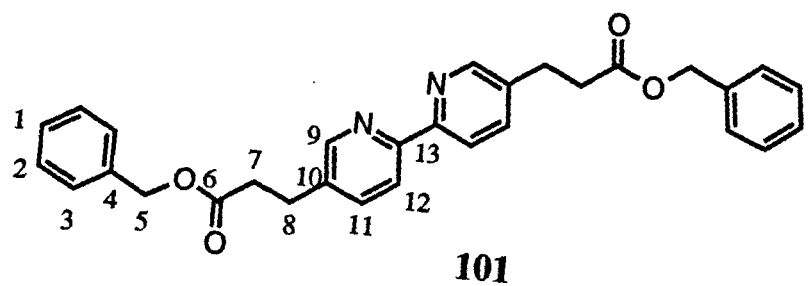
Found: C 74.93, H 5.77, N 5.72.

*Attempted preparations of 5-(2-carbo(benzyloxy)ethyl)-5'-(2-carboxyethyl)-2,2'-bipyridine (102).*

*Method A:* **6** (0.100 g, 0.33 mmol), K<sub>2</sub>CO<sub>3</sub> (0.046 g, 0.33 mmol) and benzyl bromide (0.057 g, 0.33 mmol) were stirred in DMF at 60 °C for 24 hours. EtOAc (30 ml) was added and the solution washed with water (3 x 10 ml), dried (Na<sub>2</sub>SO<sub>4</sub>), filtered and evaporated. TLC (10% methanol / CH<sub>2</sub>Cl<sub>2</sub>) indicated a mixture of products. Flash chromatography on silica (2 x 20 cm) eluting with CH<sub>2</sub>Cl<sub>2</sub> containing 1-10% methanol gave a small amount of dibenzyl compound **101** and no other products were eluted.

*Method B:* To a suspension of **6** (0.100 g, 0.33 mmol) and benzyl alcohol (0.039 g, 0.363 mmol) in 5% DMF / CH<sub>2</sub>Cl<sub>2</sub> (5 ml) was added EDC (1.65 mmol) and DMAP (5 mg). After stirring for 18 hours the CH<sub>2</sub>Cl<sub>2</sub> solution was washed with 1M HCl (2 x 2 ml) and water (5 ml), dried (Na<sub>2</sub>SO<sub>4</sub>), filtered and evaporated. TLC (10% methanol / CH<sub>2</sub>Cl<sub>2</sub>) indicated a mixture of products. Flash chromatography as above gave a small amount of **101** and no other products.

*Method C:* **101** (0.200 g, 0.416 mmol), palladium black (75 mg) and cyclohexene (2 ml) were refluxed in CH<sub>2</sub>Cl<sub>2</sub> (6 ml) and the reaction followed by TLC (10% methanol / CH<sub>2</sub>Cl<sub>2</sub>). The reaction was slow to begin but once initiated went extremely quickly to completely deprotected product **6**. The reaction could not be stopped at an intermediate stage to isolate **102**.



**5,5'-Bis(carbo(4-(1-(4-(3-(5-(2-(5-(3-*tert*-butyldimethylsilyloxy)propyl)pyridine)pyridine)propyl)phenyl)cyclohexyl)phenyl)oxyethyl)-2,2'-bipyridine (103).**

**Method A:** To a solution of **99** (0.104 g, 0.130 mmol), **78** (0.106 g, 0.273 mmol) and TBP (0.079 g, 0.390 mmol) in CH<sub>2</sub>Cl<sub>2</sub> (1 ml) at 0 °C was added ADDP (0.0985 g, 0.390 mmol). After stirring for 18 hours at room temperature, the product was filtered and evaporated. Flash chromatography on silica (1 cm x 20 cm) eluting with 1 - 2% methanol / CH<sub>2</sub>Cl<sub>2</sub> followed by a recrystallisation from hot ethanol gave the title compound as a white solid (88 mg, 44%).

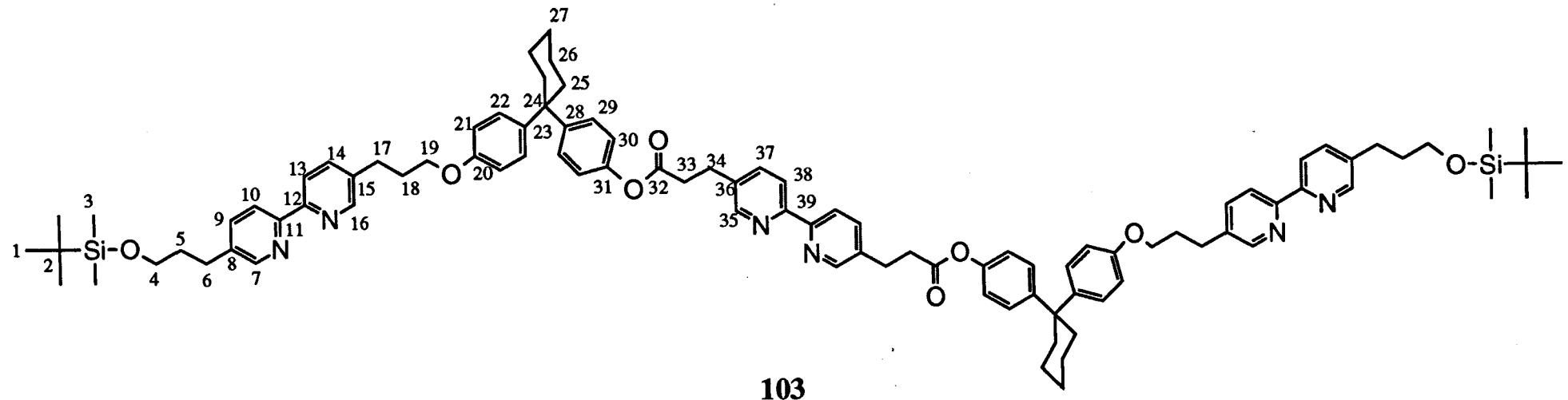
**Method B:** To a suspension of **6** (24.5 mg, 0.0816 mmol) and **96** (114 mg, 0.180 mmol) in CH<sub>2</sub>Cl<sub>2</sub> (4 ml) at 0°C was added EDC (62.6 mg, 0.326 mmol) and DMAP (2 mg). After stirring for 18 hours the product was diluted with CH<sub>2</sub>Cl<sub>2</sub> (10 ml) and washed successively with 1M HCl (5 ml), 1M NaOH (5 ml) and water (2 x 5 ml) before being dried (Na<sub>2</sub>SO<sub>4</sub>), filtered and evaporated. Purification as above gave the title compound (68 mg, 54%).

m.p. 179 - 181 °C.

<sup>1</sup>H NMR (250 MHz, CDCl<sub>3</sub>) δ0.04 (12H, s, Si(CH<sub>3</sub>)<sub>2</sub>), δ0.92 (18H, s, SiC(CH<sub>3</sub>)<sub>3</sub>), δ1.52 (12H, br, 3,4-cyclohexyl H), δ1.85 (4H, quintet, J = 6 Hz, TBDM<sub>2</sub>OCH<sub>2</sub>CH<sub>2</sub>-), δ2.08 (4H, quintet, J = 6 Hz, ArOCH<sub>2</sub>CH<sub>2</sub>-), δ2.20 (8H, br, 2-cyclohexyl H), δ2.74 (4H, t, J = 6 Hz, TBDM<sub>2</sub>OCH<sub>2</sub>CH<sub>2</sub>CH<sub>2</sub>-), δ2.85 (4H, t, J = 6 Hz, ArO(CH<sub>2</sub>)<sub>2</sub>CH<sub>2</sub>-), δ2.90 (4H, t, J = 7 Hz, ArCH<sub>2</sub>CH<sub>2</sub>CO<sub>2</sub>Ar), δ3.10 (4H, t, J = 7 Hz, -CH<sub>2</sub>CO<sub>2</sub>Ar), δ3.64 (4H, t, J = 6 Hz, TBDM<sub>2</sub>OCH<sub>2</sub>-), δ3.94 (4H, t, J = 6 Hz, ArOCH<sub>2</sub>-), δ6.79 (4H, d, J = 9 Hz, *ortho*-ArOCH<sub>2</sub>-), δ6.91 (4H, d, J = 9 Hz, *ortho*-ArOC(O)CH<sub>2</sub>-), δ7.14 (4H, d, J = 9 Hz, *meta*-ArOCH<sub>2</sub>-), δ7.22 (4H, d, J = 9 Hz, *meta*-ArOC(O)CH<sub>2</sub>-), δ7.64 (4H, m, 4-pyridine H), δ7.70 (2H, dd, J = 8 Hz, 2 Hz, 4-pyridine H), δ8.28 (6H, m, 3-pyridine H), δ8.51 (4H, m, 6-pyridine H), δ8.57 (2H, d, J = 2 Hz, 6-pyridine H).

<sup>13</sup>C NMR (62.9 MHz, CDCl<sub>3</sub>) δ18.3 (C2), 22.8 (C26), 25.9 (C1), 26.3 (C27), 27.9 (C34), 29.0 and 29.2 (C6, 17), 30.6 (C18), 33.9 (C5), 35.4 (C33), 37.3 (C25), 45.4 (C24), 61.9 (C4), 66.4 (C19), 114.2 (C21), 120.5, 120.6, 120.7 and 120.8 (C9, 14, 30, 37), 128.0 and 128.2 (C22, 29), 135.6, 136.9 and 137.5 (C8, 15, 36), 136.8 and 136.9 (C10, 13, 38), 140.2 (C23), 146.8 and 148.0 (C17, 28), 149.2 (C7, 16, 35), 153.8, 154.1 and 154.5 (C11, 12, 39), 156.6 (C20), 170.9 (C32).

FAB<sup>+</sup> MS m/z = 1537.8471. C<sub>96</sub>H<sub>116</sub>N<sub>6</sub>O<sub>8</sub>Si<sub>2</sub> requires 1537.8444.



**Iron (II) ether-linked pseudo overhand knot (104).** To a solution of **94** (10.0 mg, 0.0078 mmol) in 5% methanol / CH<sub>2</sub>Cl<sub>2</sub> (2 ml) containing 1 drop of TFA was added Fe(ClO<sub>4</sub>)<sub>2</sub>·6H<sub>2</sub>O (0.0078 mmol, 1.02 ml of an accurately made up 0.00769M stock solution in 5% methanol / CH<sub>2</sub>Cl<sub>2</sub>) with the immediate formation of a red coloration. After stirring for 2 hours, the solution was diluted with CH<sub>2</sub>Cl<sub>2</sub> (10 ml), washed with aqueous NaHCO<sub>3</sub> (5 ml), dried (Na<sub>2</sub>SO<sub>4</sub>), filtered and evaporated. Flash chromatography on silica (1 cm x 6 cm) eluting with 5% methanol / CH<sub>2</sub>Cl<sub>2</sub> removed baseline material. The CH<sub>2</sub>Cl<sub>2</sub> solution was evaporated and the residue dissolved in CHCl<sub>3</sub> / 2% methanol (1 ml) and stood for 24 hours before the solvent was removed *in vacuo* to give the title compound as a red solid (3.6 mg, 30%).

R<sub>f</sub> = 0.4 (10% methanol / CH<sub>2</sub>Cl<sub>2</sub>). m.p. 240-242 °C.

<sup>1</sup>H NMR (400 MHz, 5% CD<sub>3</sub>OD / CHCl<sub>3</sub>) δ1.49-1.72 (20H, m, 3,4-cyclohexyl H (12H), H<sub>c</sub> and H<sub>c'</sub> (4H), H<sub>l</sub> (2H) and H<sub>s</sub> (2H)), δ2.04 (4H, m, H<sub>l'</sub> and H<sub>s</sub>), δ2.46-2.75 (m, 24H including H<sub>k</sub> and H<sub>k'</sub> (4H, δ2.05 and δ2.15), H<sub>d</sub> and H<sub>d'</sub> (4H, *ca.* δ2.50), H<sub>r</sub> (2H, δ2.63), H<sub>t</sub> and H<sub>t'</sub> (4H, δ2.69 and *ca.* δ2.6), H<sub>m</sub> (2H, δ2.06), 2-cyclohexyl H (8H, *ca.* δ2.50)), δ3.30 (2H, m, H<sub>b</sub>), δ3.39 (2H, m, H<sub>b'</sub>), δ3.47 (2H, m, H<sub>m'</sub>), δ3.60 (2H, m, H<sub>r'</sub>), δ5.46 (2H, d, J = 8.2 Hz, H<sub>g</sub>), δ6.19 (2H, d, J = 8.4 Hz, H<sub>h</sub>), δ6.45 (2H, d, J = 1.5 Hz, H<sub>j</sub>), δ6.48 (4H, d, J = 8.9 Hz, H<sub>n</sub>), δ6.55 (4H, d, J = 8.9 Hz, H<sub>q</sub>), δ6.78 (2H, d, J = 1.5 Hz, H<sub>u</sub>), δ7.07 (2H, d, J = 1.5 Hz, H<sub>e</sub>), δ7.18 (2H, dd, J = 8.2 Hz, 1.5 Hz, H<sub>f</sub>), δ7.48 (4H, d, J = 8.9 Hz, H<sub>o</sub>), δ7.51 (4H, d, J = 8.9 Hz, H<sub>p</sub>), δ7.55 (2H, d, J = 1.5 Hz, H<sub>i</sub>), δ7.82 (2H, dd, J = 8.4 Hz, 1.5 Hz, H<sub>v</sub>), δ8.36 (2H, d, J = 8.4 Hz, H<sub>w</sub>).

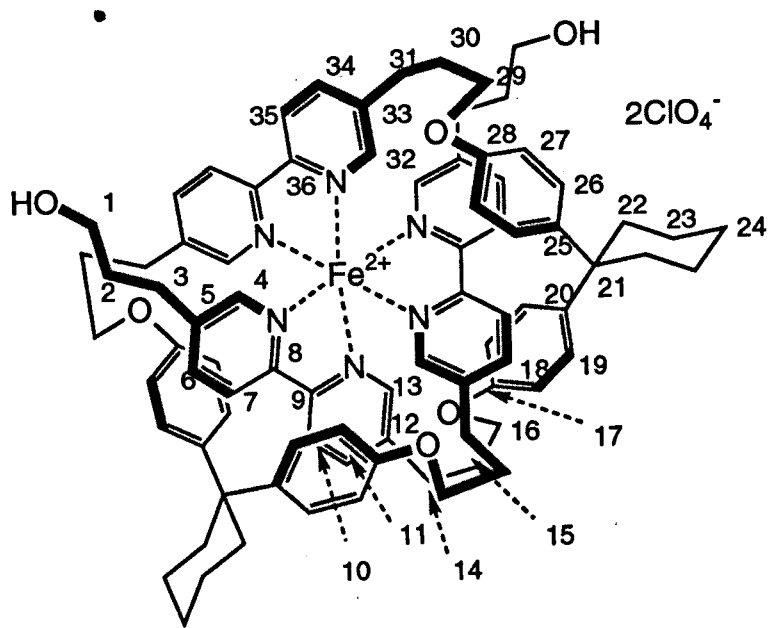
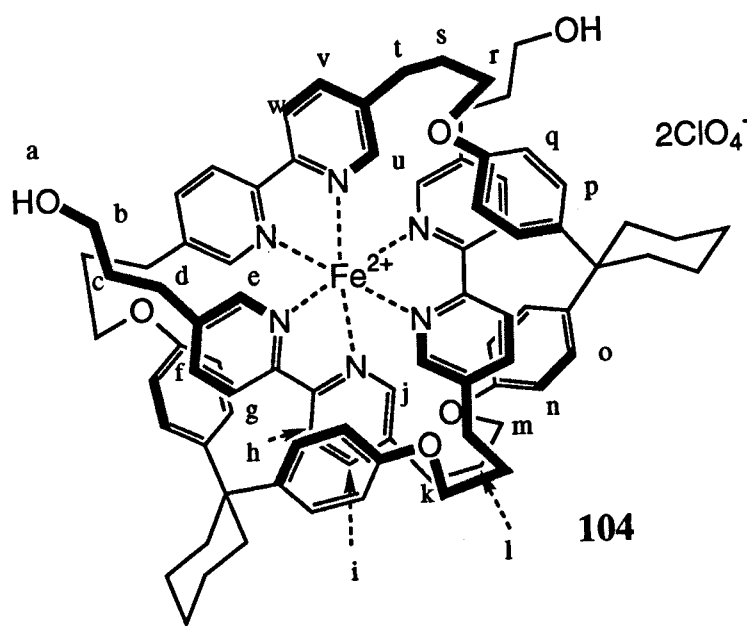
<sup>13</sup>C NMR (62.9 MHz, 5% CD<sub>3</sub>OD / CHCl<sub>3</sub>) δ22.7 (C23), 27.3, 28.8 and 29.1 (C5, 14, 31, 24), 32.7 (C2), 35.6 (C22), 44.3 (C21), 60.3 (C1), 63.6 and 63.8 (C16, 29), 114.9 (C18, 27), 123.2, 123.5 and 123.7 (C6, 11, 34), 126.9 (C19, 26), 137.9 and 139.0 (C7, 10, 35), 140.4, 140.6, 141.9 and 142.6 (C5, 12, 20, 25, 33), 152.2, 152.8 and 152.9 (C4, 13, 32), 154.9, 156.0, 156.1, 156.2 and 157.0 (C8, 9, 17, 28, 36).

ES<sup>+</sup> MS m/z = 669 (100%, [M-2ClO<sub>4</sub>]<sup>2+</sup>), 1436 (0.25%, [M-ClO<sub>4</sub>]<sup>+</sup>).

Calculated for C<sub>84</sub>H<sub>92</sub>N<sub>6</sub>O<sub>14</sub>FeCl<sub>2</sub>·5H<sub>2</sub>O: C 62.03, H 6.32, N 5.17;

Found: C 61.70, H 5.71, N 4.71.

λ<sub>max</sub> (ε) (CH<sub>2</sub>Cl<sub>2</sub>) 243.6 nm (49400), 266.3 nm (34900), 310.5 nm (71400), 358.1 nm (7600), 490.8 nm (8900), 519.7 nm (10900).



**Zinc (II) ether-linked pseudo overhand knot (105).** *Method A: Preparation of a solution in MeOH / CH<sub>2</sub>Cl<sub>2</sub>:* To a stirred solution of strand **94** (59.6 mg, 0.0465 mmol) in 5% methanol / CH<sub>2</sub>Cl<sub>2</sub> (5 ml) was added a solution of Zn(ClO<sub>4</sub>)·6H<sub>2</sub>O (1.40 ml of an accurately made up 0.0332 M solution in 5% methanol / CH<sub>2</sub>Cl<sub>2</sub>, 0.0465 mmol). A white precipitate formed and dissolved upon stirring for several minutes to give a solution of **105**.

*Method B: Preparation of a solution in DMF / CH<sub>2</sub>Cl<sub>2</sub>:* To a stirred suspension of strand **94** (0.100 g, 0.0781 mmol) in 5% DMF / CH<sub>2</sub>Cl<sub>2</sub> (10 ml) was added a solution of Zn(ClO<sub>4</sub>)·6H<sub>2</sub>O (0.423 ml of an accurately made up 0.1844 M solution in DMF, 0.0781 mmol). A white precipitate formed which dissolved upon stirring vigorously for 30 minutes - 1 hour.

The above solutions were used directly in subsequent reactions. Removal of the solvent *in vacuo* to give solid **105** resulted in the formation of a white solid which would not completely redissolve in DMF / CH<sub>2</sub>Cl<sub>2</sub> or methanol / CH<sub>2</sub>Cl<sub>2</sub> mixtures. It is likely that this material consists of oligomeric Zn(II)•**105** species.

Solutions for characterisation by NMR were prepared directly by substitution of deuterated solvents in the above procedures on a suitable scale and transfer of the resulting solution into an NMR tube. <sup>1</sup>H NMR spectra indicated that **105** was formed in quantitative yield.

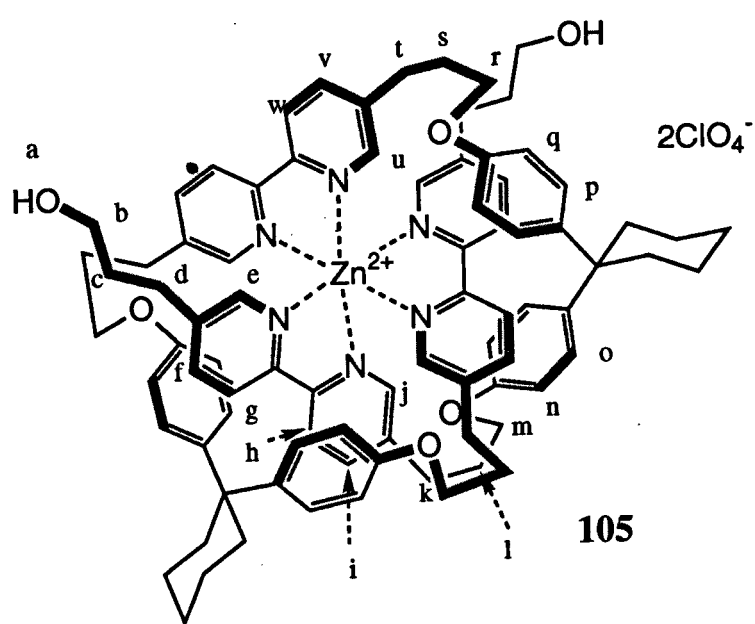
m.p. 234-236 °C (dec.)

<sup>1</sup>H NMR (400 MHz, 5% CD<sub>3</sub>OD / CD<sub>2</sub>Cl<sub>2</sub>) δ1.40-1.93 (28H, br, including H<sub>s</sub> (2H, δ1.41), H<sub>l</sub> (2H, δ1.44), H<sub>k</sub> (2H, δ1.48), H<sub>c</sub> and H<sub>c'</sub> (4H, *ca.* δ1.50), 3,4-cyclohexyl H (12H, δ1.68), H<sub>k'</sub> (2H, δ1.70), H<sub>s'</sub> (2H, δ1.72), H<sub>l'</sub> (2H, δ1.93)), δ2.40-2.80 (18H, m, including 2-cyclohexyl H (8H, δ2.50), H<sub>d</sub> and H<sub>d'</sub> (4H, δ2.52), H<sub>t</sub> and H<sub>t'</sub> (4H, *ca.* δ2.65), H<sub>m</sub> (2H, δ2.71)), δ3.01 (2H, m, H<sub>r</sub>), δ3.32 (4H, m, H<sub>b</sub> and H<sub>b'</sub>), δ3.48 (2H, m, H<sub>m'</sub>), δ3.67 (2H, m, H<sub>r'</sub>), δ5.40 (2H, d, J = 7.5 Hz, H<sub>g</sub>), δ5.94 (2H, d, J = 7.5 Hz, H<sub>h</sub>), δ6.48 (4H, d, J = 8.5 Hz, H<sub>n</sub>), δ6.67 (4H, d, J = 8.5 Hz, H<sub>q</sub>), δ7.13 (2H, d, J = 1.5 Hz, H<sub>j</sub>), δ7.36 (2H, dd, J = 1.5 Hz, J = 7.5 Hz, H<sub>f</sub>), δ7.42 (4H, d, J = 8.5 Hz, H<sub>o</sub>), δ7.53 (4H, d, J = 8.5 Hz, H<sub>p</sub>), δ7.56 (2H, dd, J = 1.5 Hz, J = 7.5 Hz, H<sub>i</sub>), δ7.59 (2H, d, J = 1.5 Hz, H<sub>u</sub>), δ7.66 (2H, d, J = 1.5 Hz, H<sub>e</sub>), δ7.99 (2H, dd, J = 1.5 Hz, J = 7.5 Hz, H<sub>v</sub>), δ8.29 (2H, d, J = 7.5 Hz, H<sub>w</sub>).

Calculated for C<sub>84</sub>H<sub>92</sub>N<sub>6</sub>O<sub>14</sub>ZnCl<sub>2</sub>·4H<sub>2</sub>O: C 62.36, H 6.23, N 5.19, Cl 4.38;

Found: C 62.41, H 6.08, N 5.17, Cl 4.66.

FAB<sup>+</sup> MS m/z = 672 (100%, [M-2ClO<sub>4</sub>]<sup>2+</sup>), 721 (4%, [M-ClO<sub>4</sub>]<sup>2+</sup>), 1445 (3%, [M-ClO<sub>4</sub>]<sup>+</sup>).



**Zinc (II) TBDMS capped ether linked pseudo-overhand knot (106)** was prepared as for **105** but substituting **93** in place of **94**.  $^1\text{H}$  NMR spectra indicated a quantitative yield.

$R_f = 0.4$  (10% methanol /  $\text{CH}_2\text{Cl}_2$ ) with some decomposition on silica.

$^1\text{H}$  NMR (400 MHz, 5%  $\text{CD}_3\text{OD} / \text{CD}_2\text{Cl}_2$ )  $\delta$  0.06 (12H, s,  $\text{SiCH}_3$ ), 0.91 (18H, s,  $\text{SiC(CH}_3)_3$ ), 1.37-1.95 (28H, br, including  $H_s$  (2H,  $\delta$  1.43),  $H_l$  (2H,  $\delta$  1.43),  $H_k$  (2H,  $\delta$  1.49),  $H_c$  and  $H_{c'}$  (4H,  $\delta$  1.50), 3,4-cyclohexyl H (12H,  $\delta$  1.68),  $H_{k'}$  (2H,  $\delta$  1.71),  $H_s'$  (2H,  $\delta$  1.74),  $H_{l'}$  (2H,  $\delta$  1.96)), 2.40-2.80 (18H, m, including 2-cyclohexyl H (8H,  $\delta$  2.51),  $H_d$  and  $H_{d'}$  (4H,  $\delta$  2.52),  $H_t$  and  $H_{t'}$  (4H,  $\delta$  2.66),  $H_m$  (2H,  $\delta$  2.71)), 3.03 (2H, m,  $H_r$ ), 3.32 (4H, m,  $H_b$  and  $H_{b'}$ ), 3.49 (2H, m,  $H_{m'}$ ), 3.69 (2H, m,  $H_r'$ ), 5.41 (2H, d,  $J = 7.5$  Hz,  $H_g$ ), 6.01 (2H, d,  $J = 7.5$  Hz,  $H_h$ ), 6.49 (4H, d,  $J = 8.5$  Hz,  $H_n$ ), 6.68 (4H, d,  $J = 8.5$  Hz,  $H_q$ ), 7.14 (2H, d,  $J = 1.5$  Hz,  $H_j$ ), 7.29 (2H, dd,  $J = 1.5$  Hz,  $J = 7.5$  Hz,  $H_f$ ), 7.43 (4H, d,  $J = 8.5$  Hz,  $H_o$ ), 7.54 (4H, d,  $J = 8.5$  Hz,  $H_p$ ), 7.61-7.65 (6H, m,  $H_i$ ,  $H_u$  and  $H_e$ ), 8.00 (2H, dd,  $J = 1.5$  Hz,  $J = 7.5$  Hz,  $H_v$ ), 8.29 (2H, d,  $J = 7.5$  Hz,  $H_w$ ).

$^{13}\text{C}$  NMR (62.9 MHz, 5%  $d_7\text{-DMF} / \text{CDCl}_3$ )  $\delta$  17.9 (C2), 22.5 (C26), 27.3 (C1), 28.7 (C6, 17, 34), ca. 29.5 (C25, 27 partially obscured by  $d_7\text{-DMF}$ ), 33.1 and 33.4 (C5, 18, 33), 44.0 (C24), 61.0 (C4), 64.0 and 64.4 (C19, 32), 113.8 and 114.7 (C21, 30), 122.6 and 122.8 (C9, 14, 37), 127.1 and 127.6 (C22, 29), 140.5, 140.9, 142.0 (C8, 15, 36, 23, 28), 145.2, 145.9 and 147.5 (C11, 12, 39), 155.8 and 155.9 (C20, 31). Signals for carbons (C10, 13, 38) and (C7, 16, 35) were not detected.

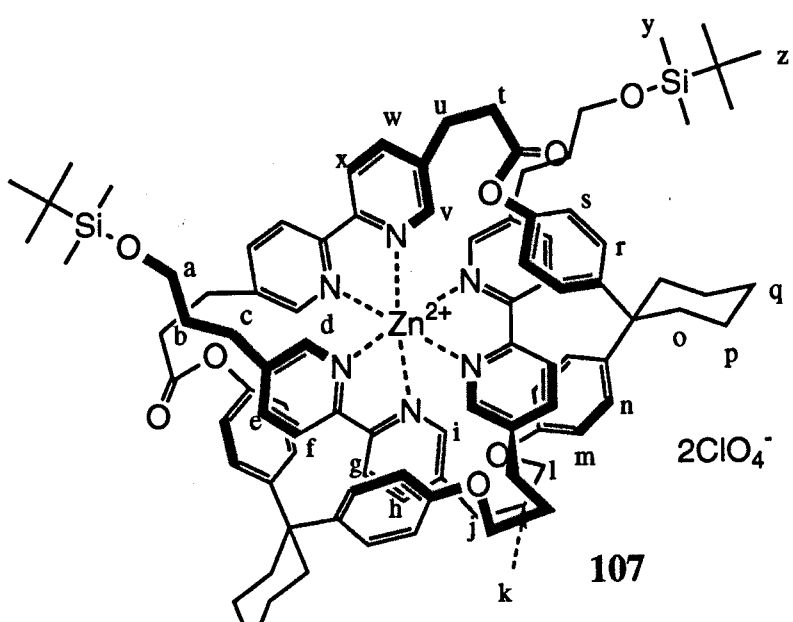
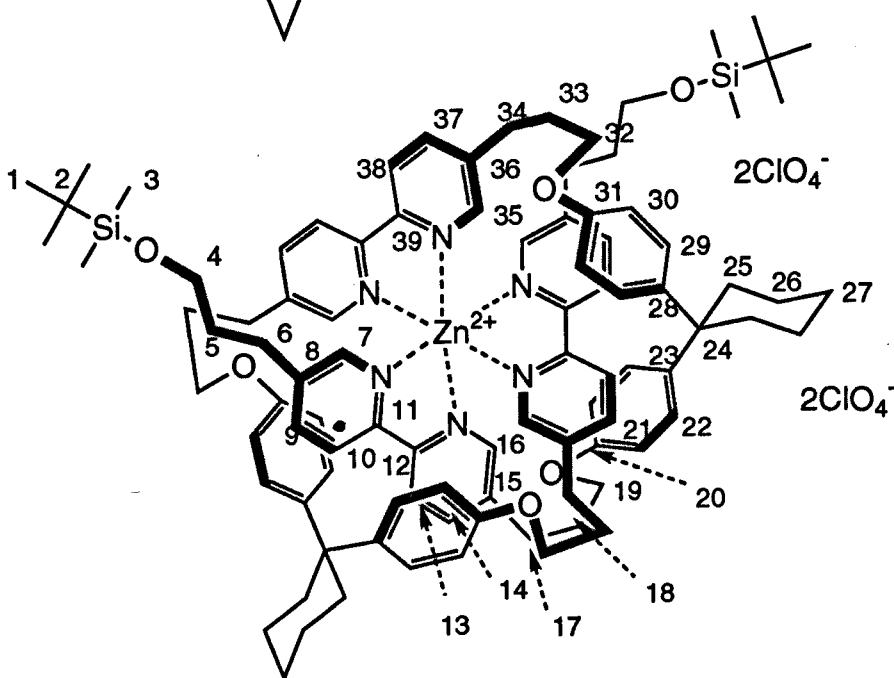
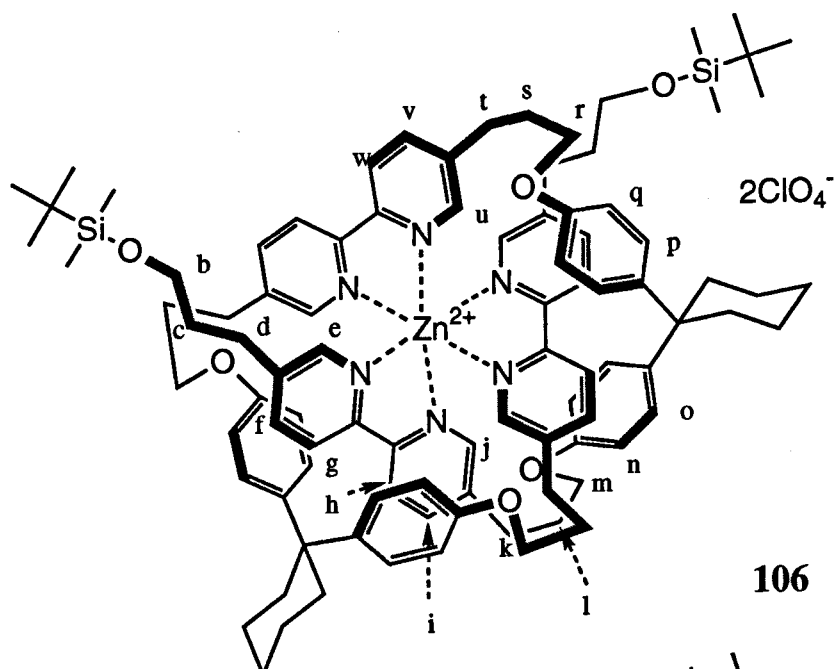
ES<sup>+</sup> MS m/z = 820 (100%,  $[\text{M}-2\text{ClO}_4]^{2+}$ ).

**Zinc (II) TBDMS capped ether-ester linked pseudo-overhand knot (107)** was prepared as for **105** but substituting **103** in place of **94**.  $^1\text{H}$  NMR spectra indicated a quantitative yield.

$R_f = 0.35$  (10% methanol /  $\text{CH}_2\text{Cl}_2$ ) with some decomposition on silica.

$^1\text{H}$  NMR (400 MHz, 5%  $d_7\text{-DMF} / \text{CD}_2\text{Cl}_2$ )  $\delta$  0.04 (12H, s,  $H_y$ ), 0.89 (18H, s,  $H_z$ ), 1.46-1.77 (16H, br, 3,4-cyclohexyl H ( $H_p$ ,  $q$ ) and  $H_b$  (t,  $J = 7$  Hz)), 2.06 (4H, m,  $H_k$  and  $H_{k'}$ ), 2.28-2.42 (4H, m,  $H_u$  and  $H_{u'}$ ), 2.42-2.89 (m, 24H, including  $H_c$  (4H, t,  $\delta$  2.70),  $H_j$  and  $H_{j'}$  (4H, ca.  $\delta$  2.75), 2-cyclohexyl H ( $H_o$ ) (8H, ca.  $\delta$  2.8),  $H_t$  and  $H_{t'}$  (4H,  $\delta$  2.66-2.89)), 3.43-3.55 (8H,  $H_a$  and  $H_{l/l'}$ ), 5.10 (2H, d,  $J = 8$  Hz,  $H_f$ ), 6.58 (4H, d,  $J = 9$  Hz,  $H_m$ ), 6.75 (4H, d,  $J = 9$  Hz,  $H_s$ ), 6.81 (2H, d,  $J = 8$  Hz,  $H_g$ ), 6.92 (2H, dd,  $J = 8$  Hz, 1.5 Hz,  $H_e$ ), 6.97 (2H, d,  $J = 1.5$  Hz,  $H_v$ ), 7.57 (4H, d,  $J = 9$  Hz,  $H_r$ ), 7.61 (2H, d,  $J = 1.5$  Hz,  $H_d$ ), 7.66 (4H, d,  $J = 9$  Hz,  $H_n$ ), 7.92 (2H, dd,  $J = 8$  Hz, 1.5 Hz,  $H_h$ ), 7.99 (2H, dd,  $J = 8$  Hz, 1.5 Hz,  $H_w$ ), 8.01 (2H + residual DMF peak, m,  $H_d$ ), 8.20 (2H, d,  $J = 8$  Hz,  $H_x$ ).

ES<sup>+</sup> MS m/z = 834 (100%,  $[\text{M}-2\text{ClO}_4]^{2+}$ ).



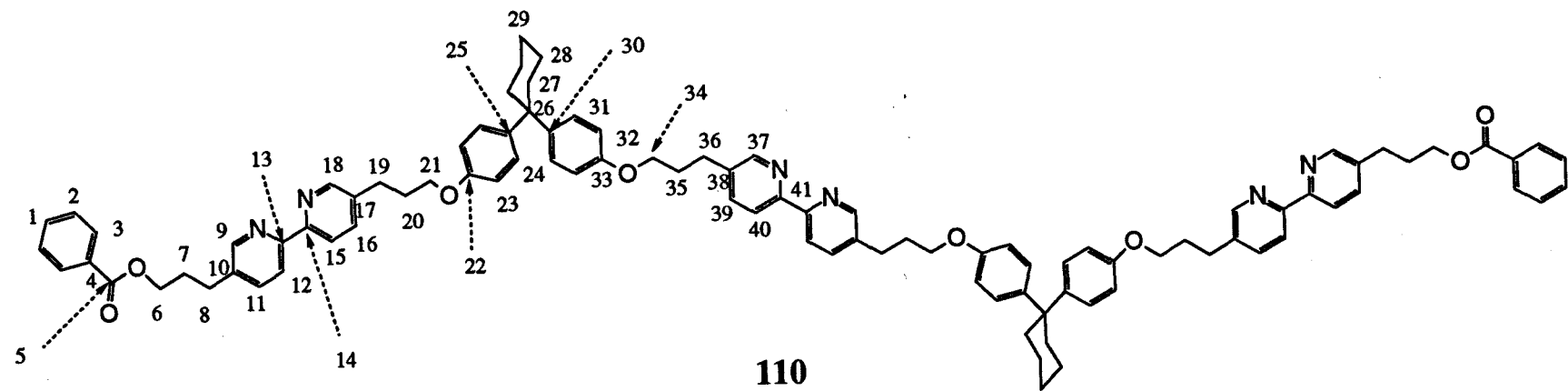
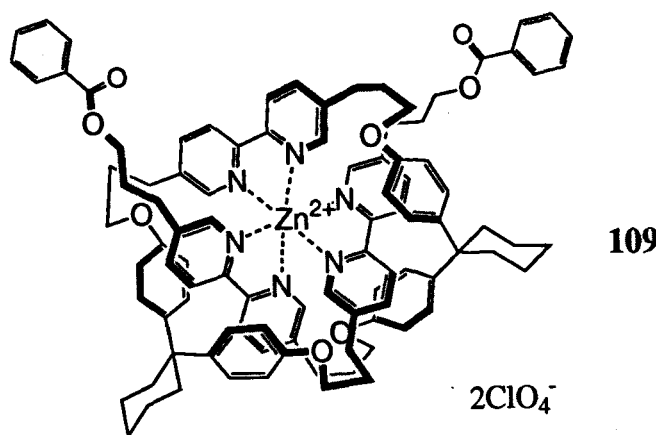
**Model ester coupling: The reaction of 105 with benzoic acid using EDC•PF<sub>6</sub>.** A solution of **105** in d<sub>7</sub>-DMF / CD<sub>2</sub>Cl<sub>2</sub> (ca. 2 ml) was prepared as discussed previously using 30.0 mg (0.0234 mmol) of **94**. The solution was cooled to 0°C before the addition of benzoic acid (6.0 mg, 0.049 mmol), EDC•PF<sub>6</sub> (**111**) (105.7 mg, 0.351 mmol) and DMAP (2.8 mg, 0.023 mmol). The solution was stirred at room temperature for 18 hours. A <sup>1</sup>H NMR spectrum of the solution confirmed the presence of the two doublets at 5.4 and 6.0 ppm, indicative of the continued presence of the knotted structure and hence an intermediate assumed to be **109**. Demetallation was effected by the addition of tetraethylammonium chloride monohydrate (86.0 mg, 0.468 mmol) and stirring for 1 hour. The product was diluted with CH<sub>2</sub>Cl<sub>2</sub> (10 ml) and washed successively with 1M HCl (2 x 10 ml), saturated aqueous NaHCO<sub>3</sub> (10 ml) and water (10 ml), dried (Na<sub>2</sub>SO<sub>4</sub>), filtered and evaporated. Flash chromatography on silica (1 cm x 20 cm) eluting with CH<sub>2</sub>Cl<sub>2</sub> containing 0-1% methanol gave the bis-benzoyl oligomer **110** as a white solid (25.1 mg, 72%).

R<sub>f</sub> = 0.40 (10% methanol / CH<sub>2</sub>Cl<sub>2</sub>). m.p. 147-149 °C.

<sup>1</sup>H NMR (250 MHz, CDCl<sub>3</sub>) δ1.50 (12H, br, 3,4-cyclohexyl H), δ2.07-2.20 (20H, m, 2-cyclohexyl H and -OCH<sub>2</sub>CH<sub>2</sub>CH<sub>2</sub>Ar), δ2.85 (12H, m, -CH<sub>2</sub>Ar), δ3.94 (8H, d, J = 6 Hz, -CH<sub>2</sub>OAr), δ4.37 (4H, d, J = 6 Hz, -CH<sub>2</sub>OBz), δ6.79 (8H, d, J = 9 Hz, *ortho*-ArOR), δ7.15 (8H, d, J = 9 Hz, *meta*-ArOR), δ7.42 (4H, t, J = 7 Hz, *meta*-benzoyl), δ7.55 (2H, m, *para*-benzoyl), δ7.66 (6H, m, 4-bipyridine H), δ8.03 (4H, d, J = 7 Hz, *ortho*-benzoyl), δ8.27 (6H, m, 3-bipyridine H), δ8.53 (6H, m, 6-bipyridine H).

<sup>13</sup>C NMR (62.9 MHz, CDCl<sub>3</sub>) δ22.9 (C28), 26.1 (C29), 29.3, 29.5, 30.0 and 30.5 (C7, 8, 19, 20, 26, 35), 37.3 (C27), 45.0 (C26), 63.9 (C6), 66.3 (C21, 34), 114.0 (C23, 32), 120.5, 120.6 and 120.7 (C11, 16, 39), 128.1 and 128.3 (C24, 31), 129.5 (C4), 129.5 130.1 and 132.9 (C1, 2, 3), 136.4 and 136.8 (C10, 17, 38), 136.8 and 136.9 (C12, 15, 40), 141.1 (C26, 30), 149.2 and 149.3 (C9, 18, 37), 154.0 and 154.2 (C13, 14, 41), 156.4 (C22, 33), 166.5 (C5).

FAB<sup>+</sup> MS m/z = 1490 (100%, MH<sup>+</sup>). C<sub>98</sub>H<sub>100</sub>N<sub>6</sub>O<sub>8</sub> requires 1489.82.



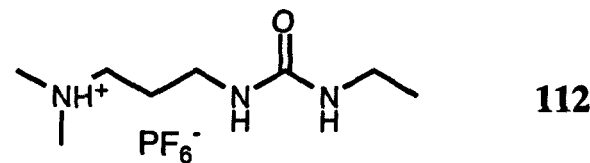
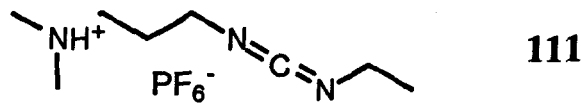
**1-(3-Dimethylaminopropyl)-3-ethyl carbodiimide hexafluorophosphate [EDC•PF<sub>6</sub>] (111).** To a suspension of EDC (0.416 g, 2.167 mmol) in dry CH<sub>2</sub>Cl<sub>2</sub> (10 ml) at 0°C was added silver hexafluorophosphate (0.548 g, 2.167 mmol). The mixture was stirred vigorously for 30 minutes at 0°C with the exclusion of light and moisture and then filtered to remove the precipitated AgCl. The filtrate was evaporated and thoroughly dried *in vacuo* to give the title compound as a white solid (0.552 g, 85%). The <sup>1</sup>H NMR spectrum indicated the presence of a small amount of the hydrolysis product **N-(3-dimethylaminopropyl)-N'-ethylurea hexafluorophosphate (112)** though no attempts were made at further purification.

m.p. 94–96°C.

<sup>1</sup>H NMR (250 MHz, CDCl<sub>3</sub>) δ1.09 (3H, t, J = 7 Hz, -CH<sub>2</sub>CH<sub>3</sub>), δ1.80–2.20 (2H, br, (CH<sub>3</sub>)<sub>2</sub>NCH<sub>2</sub>CH<sub>2</sub>-), δ3.01–3.15 and δ3.20–3.30 (4H, br, -CH<sub>2</sub>N=C=NCH<sub>2</sub>-), δ3.25 and δ3.38 (2 x 3H, 2s, (CH<sub>3</sub>)<sub>2</sub>N-), δ3.70 (2H, br, (CH<sub>3</sub>)<sub>2</sub>NCH<sub>2</sub>-).

Calculated for C<sub>8</sub>H<sub>18</sub>N<sub>3</sub>PF<sub>6</sub>: C 31.90, H 6.02, N 13.95;

Found: C 32.55, H 6.37, N 14.26.



**4-Biphenylboronic acid (115).** To a stirred suspension of magnesium turnings (250 mg, 10.30 mmol) in  $\text{BH}_3\text{-THF}$  complex (1M solution in THF, 34 ml, 34 mmol of  $\text{BH}_3$ ) at 0°C was added a solution of 4-bromobiphenyl **114** (2.000g, 8.58 mmol) in THF (7 ml) dropwise over 20 minutes under  $\text{N}_2$ . Stirring was continued for 18 hours and the pale green solution obtained was poured onto ice (*ca.* 200 g) with stirring followed by the addition of 10% aqueous HCl (7 ml). The aqueous layer was extracted with diethyl ether (4 x 100 ml) and the combined ether extracts dried ( $\text{Na}_2\text{SO}_4$ ), filtered and evaporated. The oil produced was triturated with petroleum ether (*ca.* 50 ml) to give a white solid which was removed by filtration and dried *in vacuo* to give the title compound (1.44 g, 85%).

m.p. 247 °C.

$^1\text{H}$  NMR (250 MHz,  $d_6$ -acetone)  $\delta$  7.35 (1H, m, 4'-ArH), 7.45 (2H, m, ArH), 7.67 (4H, m, ArH), 7.97 (2H, d, 3-ArH).

$^{13}\text{C}$  NMR (62.9 MHz,  $d_6$ -DMSO)  $\delta$  126.2, 127.2, 128.0 and 129.4 (C1, 2, 3, 6), 133.8 (C8), 135.3 (C7), 140.6 and 142.1 (C4, 5).

EI<sup>+</sup> MS m/z = 198 (100%, M<sup>+</sup>), 154 (35%, [M- B(OH)<sub>2</sub>]<sup>+</sup>).

$\nu$  = 3404 cm<sup>-1</sup> (OH stretch) and 1607, 1552, 1525 cm<sup>-1</sup> (aromatics).

Calculated for  $\text{C}_{12}\text{H}_{11}\text{BO}_2$ : C 72.78, H 5.60;

Found C 72.82, H 5.46.

**2"-Methyl-1, 1': 4', 1": 3", 1'": 4"": 1'"" - quinquephenyl (116).** To a stirred solution of 2,6-dibromotoluene (0.137 g, 0.549 mmol) and  $\text{Pd}(\text{PPh}_3)_4$  (37 mg, 0.032 mmol) in toluene (3 ml) was added 2M  $\text{Na}_2\text{CO}_3$  (1 ml) and a solution of **115** (0.250 g, 1.262 mmol) in methanol (1 ml). The mixture was heated at 80 °C for 6 hours and after cooling was partitioned between  $\text{CH}_2\text{Cl}_2$  (20 ml) and 2M  $\text{Na}_2\text{CO}_3$  (20 ml) containing 10% v/v concentrated ammonia solution. The  $\text{CH}_2\text{Cl}_2$  layer was separated, dried ( $\text{Na}_2\text{SO}_4$ ), filtered and evaporated. Flash chromatography on silica (2 cm x 25 cm) eluting with petroleum ether (b.p. 40 - 60 °C) gave **1-bromo-2-methyl-3, 1': 4', 1"-terphenyl (117)** (0.080 g, 45%) and then 75% ethyl acetate in petroleum ether gave the title compound as a white solid (49 mg, 23%).

#### Quinquephenyl (116)

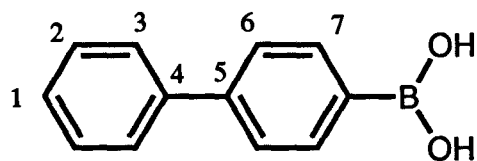
$R_f$  = 0.5 (10% EtOAc : 90% petroleum ether 40 / 60). m.p. 200 - 203 °C.

$^1\text{H}$  NMR (250 MHz,  $\text{CDCl}_3$ )  $\delta$  2.25 (3H, s, ArCH<sub>3</sub>), 7.28-7.52 and 7.68 (21H, m, ArH).

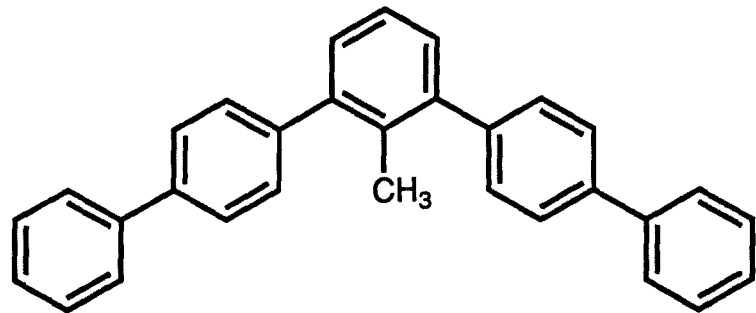
FAB<sup>+</sup> MS m/z = 396 (100%, M<sup>+</sup>);  $\text{C}_{31}\text{H}_{24}$  requires 396.50.

Calculated for  $\text{C}_{31}\text{H}_{24}$ : C 93.90, H 6.10;

Found C 92.20, H 6.05.



**115**



**116**

**Terphenyl (117)**

$R_f = 0.65$  (10% EtOAc : 90% petroleum ether 40 / 60). m.p. 94 - 96 °C.

$^1\text{H}$  NMR (250 MHz,  $\text{CDCl}_3$ )  $\delta$  2.38 (3H, s, ArCH<sub>3</sub>), 87.04-7.70 (12H, m, ArH).

$^{13}\text{C}$  NMR (62.9 MHz,  $\text{CDCl}_3$ )  $\delta$  21.2 (C15), 126.4 (C13), 126.9, 127.2, 127.5, 128.9, 129.1, 129.7 and 131.7 (C1, 2, 3, 6, 7, 10, 11, 12), 135.5, 140.1, 140.7 and 143.7 (C4, 5, 8, 9).

FAB<sup>+</sup> MS m/z = 322 / 324 (100%, M<sup>+</sup>);  $\text{C}_{19}\text{H}_{15}\text{Br}$  requires 323.21.

Calculated for  $\text{C}_{19}\text{H}_{15}\text{Br}$ : C 70.60, H 4.68, Br 24.72;

Found: C 71.13, H 4.83, Br 23.74.

*Attempted oxidation of quinquephenyl 116.* **Method A:** A solution of  $n\text{Bu}_4\text{NMnO}_4$  (0.397 g, 1.097 mmol) in anhydrous pyridine (5 ml) was added to a suspension of 116 (0.145 g, 0.366 mmol) in pyridine (3 ml). The mixture was heated at reflux and the progress of the reaction followed by TLC (10% EtOAc / petroleum ether b.p. 40-60 °C). After 48 hours, only starting material was present and the reaction was abandoned.

**Method B:** A solution of 116 (0.145 g, 0.366 mmol) in benzene (5 ml) was added to a solution of  $\text{KMnO}_4$  (0.173 g, 1.095 mmol) in water (5 ml).  $n\text{Bu}_4\text{N}^+\text{Br}^-$  (10 mg) was added and the solution stirred vigorously. TLC indicated that no reaction had occurred after 3 days and the reaction was abandoned.

**2,6-Dibromo-1-iodobenzene (120).** To a suspension of 2,6-dibromoaniline 119 (10.00g, 0.0399 mol) in concentrated HCl (36%, 20 ml) at 0°C was added dropwise a solution of sodium nitrite (2.845g, 0.0412 mol) in water (15 ml) maintaining a temperature below 5°C. The yellow solution formed was stirred at 0°C for 30 minutes before being poured cautiously with stirring into a solution of potassium iodide (66.2 g) in water (100 ml). Stirring was continued for 1 hour before the addition of  $\text{CH}_2\text{Cl}_2$  (150 ml) and 1N sodium sulphite (15 ml). The aqueous layer was separated and extracted with  $\text{CH}_2\text{Cl}_2$  (2 x 100 ml). The combined organic layers were washed successively with 10% NaOH (75 ml) and water (3 x 75 ml) before being dried ( $\text{MgSO}_4$ ), filtered and evaporated. The crude product was recrystallised from a minimum of hot ethanol to yield the title compound as a brownish solid (7.35 g, 51%).

m.p. 100 -101 °C (lit.<sup>139</sup> 99 - 99.5 °C).

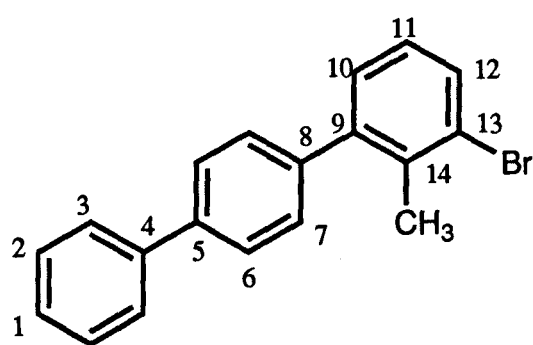
$^1\text{H}$  NMR (250 MHz,  $\text{CDCl}_3$ )  $\delta$  7.05 (1H, t, 4-ArH), 87.53 (2H, d, 3,5-ArH).

$^{13}\text{C}$  NMR (62.9 MHz,  $\text{CDCl}_3$ )  $\delta$  109.6 (C1), 130.4 and 131.1 (C3, 4), 131.4 (C2).

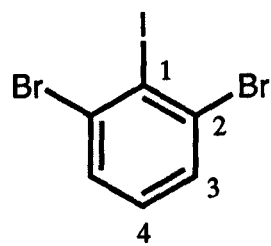
EI<sup>+</sup> MS m/z = 362 (100%, M<sup>+</sup>), 283 (6%, [M-Br]<sup>+</sup>), 235 (25%, [M-I]<sup>+</sup>), 154 (20%, [M-IBr]<sup>+</sup>).

Calculated for  $\text{C}_6\text{H}_3\text{Br}_2\text{I}$ : C 19.9, H 0.8, Br 44.2, I 35.1;

Found: C 19.8, H 0.8, Br 44.9, I 34.9.



**117**



**120**

**1, 1': 4', 1": 3", 1'''': 4'''': 1''''' - Quinquephenyl-2"-carboxylic acid (118).**

**Method A:** To a solution of 4-biphenylmagnesium bromide prepared from 4-bromobiphenyl (4.08 g, 17.5 mmol) and Mg turnings (0.496 g, 19.3 mmol) in dry THF (50 ml) was added a solution of **120** (1.809 g, 5 mmol) in THF (20ml) over 1 hour. After stirring for 4 hours a large excess of solid CO<sub>2</sub> was added followed 1 hour later by 1M HCl (40 ml). After extraction with CH<sub>2</sub>Cl<sub>2</sub> (4 x 150 ml), the combined organic layers were washed with 1M Na<sub>2</sub>SO<sub>3</sub> (100 ml) and water (100 ml), dried (Na<sub>2</sub>SO<sub>4</sub>), filtered and evaporated. Chromatography on silica (4 cm x 25 cm) eluting with CH<sub>2</sub>Cl<sub>2</sub> containing 0-10% methanol gave the title compound as a white solid (0.520 g, 24%).

**Method B:** To a stirred solution of **122** (2.060 g, 4.05 mmol) in dry THF (50 ml) was added a 1.0M solution of EtMgBr in THF (6.1 ml, 6.1 mmol). After stirring for 5 hours at room temperature and at reflux for 30 minutes the reaction was quenched by pouring onto a large excess of powdered CO<sub>2</sub>. The mixture was stirred vigorously until all the CO<sub>2</sub> had evaporated before the addition of 1M HCl (50 ml) and CH<sub>2</sub>Cl<sub>2</sub> (250 ml). The CH<sub>2</sub>Cl<sub>2</sub> layer was separated, dried (Na<sub>2</sub>SO<sub>4</sub>), filtered and evaporated. The crude product was purified by flash chromatography on silica (3 cm x 25 cm) eluting with 50% hexanes / CH<sub>2</sub>Cl<sub>2</sub> to remove a high-running byproduct and then 5% methanol / CH<sub>2</sub>Cl<sub>2</sub> to give the title compound as a white solid (0.570 g, 33%).

R<sub>f</sub> = 0.65 (5% methanol in CH<sub>2</sub>Cl<sub>2</sub>). m.p. 242-243 °C (dec.)

<sup>1</sup>H NMR (250 MHz, CDCl<sub>3</sub>) δ7.30-7.63 (21H, m, ArH).

<sup>13</sup>C NMR (62.9 MHz, d<sub>6</sub>-DMSO) δ114.7 (C11), 114.8 (C10), 127.1, 128.1 and 129.5 (C1, 2, 3, 6, 7, 12), 134.3 (C9), 138.9, 139.8 and 140.1 (C4, 5, 8), 170.7 (C13).

FAB<sup>+</sup> MS m/z = 426 (100%, M<sup>+</sup>). C<sub>31</sub>H<sub>22</sub>O<sub>2</sub> requires 426.49.

ν = 1736 cm<sup>-1</sup> (C=O).

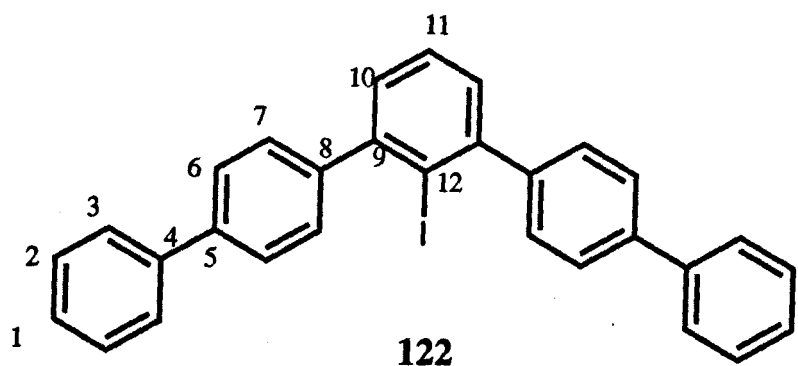
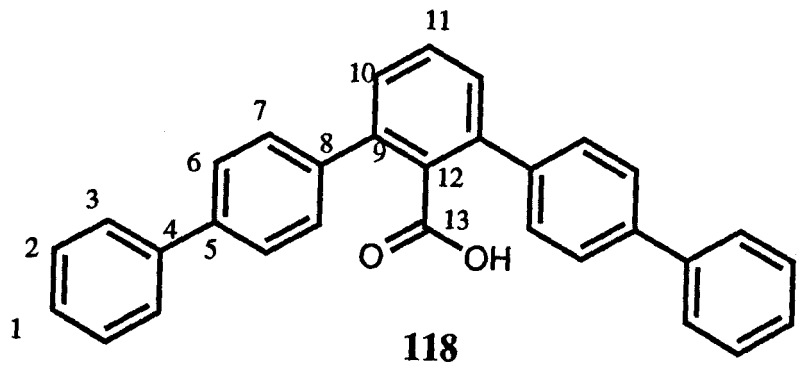
Calculated for C<sub>31</sub>H<sub>22</sub>O<sub>2</sub>·0.5H<sub>2</sub>O: C 85.49, H 5.32; Found: C 85.6, H 5.2.

**2"-Iodo-1, 1': 4', 1": 3", 1'''': 4'''': 1''''' - quinquephenyl (122)** was prepared as for **118** (*Method A*) but instead of quenching with CO<sub>2</sub>, iodine (1.904 g, 7.5 mmol) was added at 0 °C. After stirring for 1 hour at room temperature, the THF was removed *in vacuo* and the residue dissolved in CH<sub>2</sub>Cl<sub>2</sub> (400 ml). The organic layer was then washed with aqueous Na<sub>2</sub>SO<sub>3</sub> (100 ml), brine (2 x 100 ml) and water (100 ml) before being dried (MgSO<sub>4</sub>), filtered and evaporated. Flash chromatography on silica (4 cm x 20 cm) eluting with petroleum ether (b.p. 40 - 60 °C) and collecting the second band gave the title compound as a white solid (2.14 g, 84%).

R<sub>f</sub> = 0.75 (1:1 petroleum ether 40 / 60 : CH<sub>2</sub>Cl<sub>2</sub>). m.p. 219-220 °C,

<sup>13</sup>C NMR (62.9 MHz, CDCl<sub>3</sub>) δ103.5 (C12), 126.6, 127.1, 127.4, 127.6, 127.7, 128.8 and 129.9 (C1, 2, 3, 6, 7, 10, 11), 140.3, 140.7, 144.5, 147.8 (C4, 5, 8, 9).

EI<sup>+</sup> MS m/z = 508 (17%, M<sup>+</sup>), 382 (7%, [M-I]<sup>+</sup>), 306 (100%, [M-PhI]<sup>+</sup>). Calculated for C<sub>30</sub>H<sub>21</sub>I: 508.0688; Found: 508.0708.



**1, 1': 4', 1": 3", 1'''': 4'''': 1''''' - Quinquephenyl-2"-carbonoyl chloride (125).**

**118** (0.290 g, 0.680 mmol) in thionyl chloride (5 ml) was refluxed for 1 hour and then concentrated *in vacuo*. Addition of dry CH<sub>2</sub>Cl<sub>2</sub> (5 ml) and concentration *in vacuo* was used to azeotropically remove traces of thionyl chloride to give the title compound as a yellow solid (0.303 g, 100%). m.p. 207 - 210 °C (dec.)

ES<sup>+</sup> MS m/z = 444 (10%, M<sup>+</sup>), 408 ([M - Cl]<sup>+</sup>, 100%).

Calculated for C<sub>31</sub>H<sub>21</sub>OCl: C 83.67, H 4.76, Cl 7.98;

Found: C 83.6, H 4.9, Cl 7.6.

**9-Carbo-(3-phenylpropyloxy)-fluorene (126).** To a suspension of 9-fluorenecarboxylic acid (1.00 g, 4.757 mmol) and 3-phenyl-1-propanol (0.648 g, 4.757 mmol) in dry CH<sub>2</sub>Cl<sub>2</sub> at 0°C was added EDC (2.25 g, 11.74 mmol) and DMAP (58 mg, 20 mol%). The mixture was stirred at room temperature overnight before washing with 1M HCl (2 x 50 ml) and water (50 ml). The solution was then dried (Na<sub>2</sub>SO<sub>4</sub>), filtered and evaporated. Flash chromatography on silica (2 cm x 30 cm) eluting with 50% hexanes / CH<sub>2</sub>Cl<sub>2</sub> gave the title compound as a colourless oil (1.469, 94%).

R<sub>f</sub> = 0.50 (1:1 hexanes / CH<sub>2</sub>Cl<sub>2</sub>).

<sup>1</sup>H NMR (300 MHz, CDCl<sub>3</sub>) δ1.94 (2H, quintet, J = 6.5 Hz, -CH<sub>2</sub>CH<sub>2</sub>Ar), δ2.61 (2H, t, J = 6.5 Hz, -CH<sub>2</sub>Ar), δ4.15 (2H, t, J = 6.5 Hz, -CO<sub>2</sub>CH<sub>2</sub>-), δ4.86 (1H, s, 9-fluorene H), δ7.08-7.25 (9H, m, ArH), δ7.67 and 7.76 (2 x 2H, 2 x d, J = 8 Hz, 1 / 8 and 4 / 5 fluorene H).

<sup>13</sup>C NMR (62.9 MHz, CDCl<sub>3</sub>) δ30.1 and 31.9 (C10, 11), 53.5 (C7), 64.5 (C9), 120.0, 125.5, 125.9, 127.2, 128.0 and 128.3 (C2, 3, 4, 5, 13, 14, 15), 140.6, 140.9 and 141.3 (C1, 6, 12), 170.8 (C8).

EI<sup>+</sup> MS m/z = 328.1462; C<sub>23</sub>H<sub>20</sub>O<sub>2</sub> requires 328.1463.

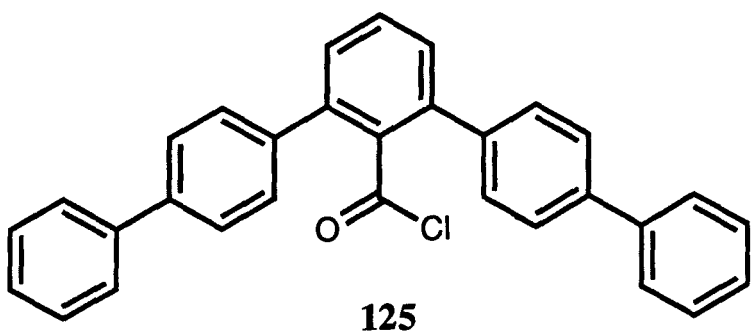
**2,7-Dibromofluorene (127).** To a solution of fluorene (8.00 g, 0.048 mol) in CHCl<sub>3</sub> (80 ml) was added a solution of bromine (4.95 ml, 0.096 mol) in CHCl<sub>3</sub> (30 ml) dropwise over 2 hours. Stirring was continued for 20 hours after which time evolution of HBr has ceased. The product mixture was diluted with CH<sub>2</sub>Cl<sub>2</sub> (100 ml), washed with water (3 x 100 ml), dried (Na<sub>2</sub>SO<sub>4</sub>), filtered and evaporated. Two successive recrystallisations from a minimum of hot ethanol gave the title compound as a white crystalline solid (12.20 g, 78%).

m.p. 164-165°C

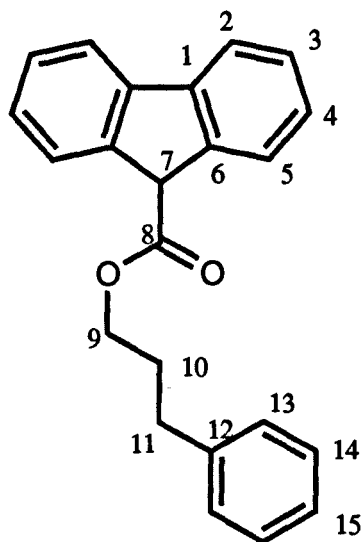
<sup>1</sup>H NMR (250 MHz, CDCl<sub>3</sub>) δ3.86 (2H, s, 9-Fluorene H), δ7.49 (2H, dd, J = 7.5 Hz, 1.5 Hz, 3,6-Fluorene H), δ7.59 (2H, d, 4,5-Fluorene H), δ7.66 (2H, d, J = 1.5 Hz, 1,8-Fluorene H).

Calculated for C<sub>13</sub>H<sub>8</sub>Br<sub>2</sub>: C 48.19, H 2.49, Br 49.32;

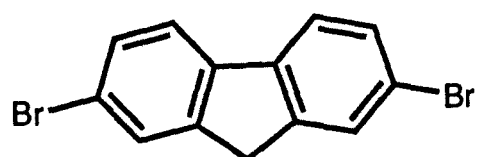
Found: C 48.29, H 2.48, Br 49.18.



**125**



**126**



**127**

**7-Tridecanol (130).** A solution of 7-tridecanone (7.17 g, 36.15 mmol) in dry diethyl ether (100 ml) was added dropwise to a stirred suspension of LiAlH<sub>4</sub> (1.372 g, 36.15 mmol) in ether (20 ml) over 1 hour. After stirring for 18 hours, the reaction was quenched by the successive addition of water (1.4 ml), 15% aqueous sodium hydroxide (1.4 ml) and water (4.2 ml). The precipitate was removed by filtration and washed well with hot THF. Combined filtrate and washings were dried (Na<sub>2</sub>SO<sub>4</sub>), filtered and evaporated to yield the title compound as a white solid (7.15 g, 99%).

m.p. 41-42°C.

<sup>1</sup>H NMR (250 MHz, CDCl<sub>3</sub>) δ0.87 (6H, t, J = 7 Hz, -CH<sub>3</sub>), δ1.20-1.46 (20H, n, -CH<sub>2</sub>CH<sub>2</sub>CH<sub>2</sub>CH<sub>2</sub>CH<sub>2</sub>CH<sub>3</sub>), δ3.56 (1H, q, J = 6.5 Hz, CHO<sub>H</sub>).

<sup>13</sup>C NMR (62.9 MHz, CDCl<sub>3</sub>) δ14.1 (C1), 22.6 (C2), 25.6 (C3), 29.4 (C4), 31.9 (C5), 37.5 (C6), 72.0 (C7).

EI+ MS m/z = 199 (2%, M<sup>+</sup>), 182 (48%, [M-OH]<sup>+</sup>).

Calculated for C<sub>13</sub>H<sub>28</sub>O: C 77.93, H 14.09;

Found C 78.12, H 14.34

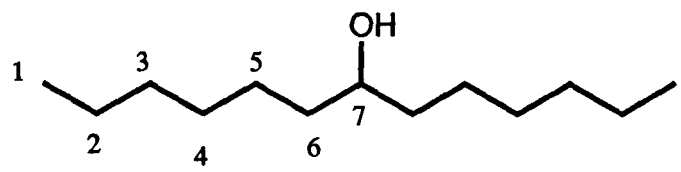
**4-Bromo-4'-(7-tridecyloxy)-biphenyl (131).** To an ice-cooled solution of 4-bromo-4'-hydroxybiphenyl (8.08 g, 32.44 mmol), 7-tridecanol **130** (6.50 g, 32.44 mmol) and PPh<sub>3</sub> (12.76 g, 48.66 mmol) in CH<sub>2</sub>Cl<sub>2</sub> (125 ml) was added diethylazodicarboxylate (8.47 g, 48.66) in CH<sub>2</sub>Cl<sub>2</sub> (15 ml) dropwise over 1.25 hours. After stirring at room temperature for 18 hours, the solvent was removed *in vacuo* and the crude product purified by flash chromatography on silica (8 cm x 20 cm) eluting with hexane and collecting the fastest running band to give the title compound as a colourless oil which slowly solidified (10.0 g, 71%).

R<sub>f</sub> = 0.75 (20% CH<sub>2</sub>Cl<sub>2</sub> / hexanes). m.p. 30-31 °C.

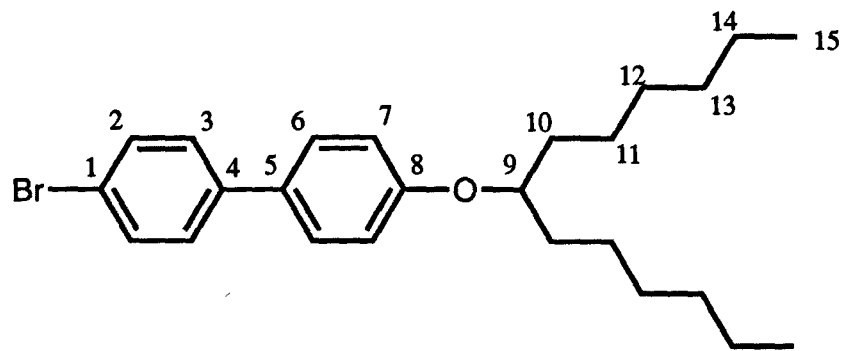
<sup>1</sup>H NMR (250 MHz, CDCl<sub>3</sub>) δ0.88 (6H, t, J = 7 Hz, -CH<sub>3</sub>), δ1.17-1.49 (16H, m, -CH<sub>2</sub>CH<sub>2</sub>CH<sub>2</sub>CH<sub>2</sub>CH<sub>3</sub>), δ1.65 (4H, q, J = 6.5 Hz, HOCHCH<sub>2</sub>-), δ4.26 (1H, q, J = 6.5 Hz, CHOAr), δ6.95 (2H, d, J = 8.5 Hz, 3'-biphenyl H), δ7.39-7.55 (6H, m, 2,2' and 3-biphenyl H).

<sup>13</sup>C NMR (62.9 MHz, CDCl<sub>3</sub>) δ14.0 (C15), 22.6 (C14), 25.4 (C11), 29.4 (C12), 31.8 (C13), 34.0 (C10), 78.1 (C9), 116.1 (C7), 120.6 (C1), 127.9 and 128.2 (C3, C6), 131.7 (C2), 132.0 (C5), 139.8 (C4), 158.6 (C8).

FAB<sup>+</sup> MS m/z = 430.1913. C<sub>25</sub>H<sub>35</sub>OBr requires 430.1871.



**130**



**131**

**2,7-Bis(4-(4'-(7-tridecyloxy)biphenyl))fluorene (132).** To a solution of **131** (1.338 g, 3.1 mmol) and triisopropyl borate (0.602 g, 3.2 mmol) in dry THF (10 ml) at -60°C was added <sup>n</sup>BuLi (2.0 ml of a 1.6M solution in hexanes, 3.2 mmol) dropwise over 10 minutes. After stirring at -60°C for 10 minutes, the solution was allowed to warm to room temperature over 1 hour. The solvent was removed *in vacuo* to give a white foam which was suspended in DME (5 ml). 2,7-dibromofluorene (0.454 g, 1.4 mmol) in DME (20 ml) and saturated aqueous NaHCO<sub>3</sub> (10 ml) were added and the solution degassed with argon for 10 minutes. Following the addition of Pd(PPh<sub>3</sub>)<sub>4</sub> (40 mg) the mixture was heated to reflux for 3 hours. After cooling, 5M NaOH (10 ml) was added and the mixture extracted with CH<sub>2</sub>Cl<sub>2</sub> (3 x 100 ml). The combined CH<sub>2</sub>Cl<sub>2</sub> extracts were dried (Na<sub>2</sub>SO<sub>4</sub>), filtered and evaporated to give the crude product which was purified by flash chromatography on silica (2.5 cm x 20 cm) eluting with petroleum ether b.p. 40 - 60°C containing 10-20% CH<sub>2</sub>Cl<sub>2</sub> to give the title compound as a slightly off-white solid which exhibited a strong fluorescence under UV light (0.530 g, 44%).

R<sub>f</sub> = 0.35 (30% CH<sub>2</sub>Cl<sub>2</sub> / petrouem ether b.p. 40 - 60°C). m.p. 222 - 224 °C.

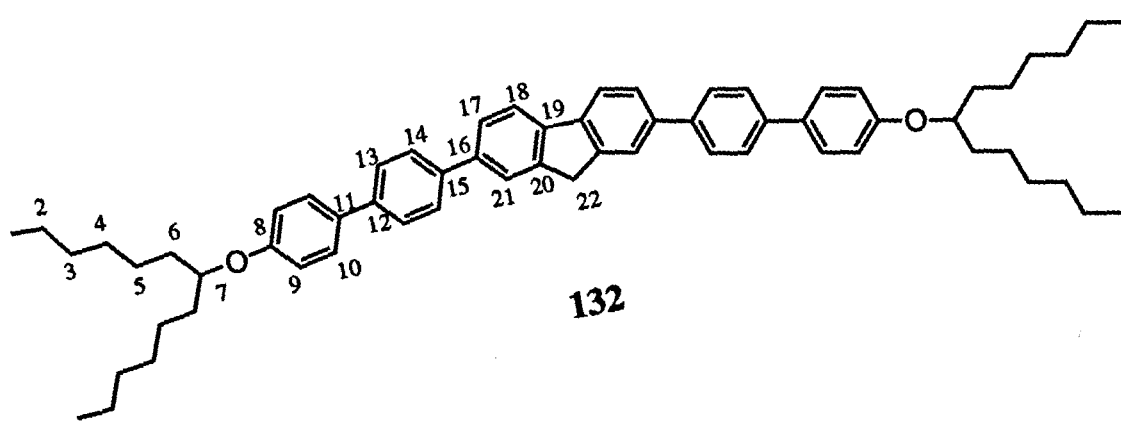
<sup>1</sup>H NMR (250 MHz, CDCl<sub>3</sub>) δ0.88 (12H, t, J = 7 Hz, -CH<sub>3</sub>), δ1.21-1.71 (20H, m, -(CH<sub>2</sub>)<sub>5</sub>CH<sub>3</sub>), δ4.06 (2H, s, 9-fluorene H), δ4.27 (2H, q, J = 6 Hz, CHOAr), δ6.96 (4H, d, J = 8.5 Hz, *ortho*-ArOR), δ7.56 (4H, d, J = 8.5 Hz, *meta*-ArOR), δ7.61-7.74 (10H, m, 3,6-fluorene H, ArH), δ7.83 (2H, s, 2,8-fluorene H), δ7.77 (2H, d, J = 7.5 Hz, 4,5-fluorene H).

<sup>13</sup>C NMR (62.9 MHz, CDCl<sub>3</sub>) δ14.1 (C1), 22.6 (C2), 25.4 (C5), 29.5 (C4), 31.8 (C3), 34.0 (C6), 37.1 (C22), 78.2 (C7), 116.1 (C9), 120.2 (C18), 123.6 (C21), 125.9, 127.0, 127.4 and 128.0 (C10, 13, 14, 17), 132.8, 139.4, 139.6, 139.7, 140.6 and 144.2 (C11, 12, 15, 16, 19, 20), 158.5 (C8).

FAB+ MS m/z = 866 (100%, [M-H]<sup>+</sup>).

Calculated for C<sub>63</sub>H<sub>78</sub>O<sub>2</sub>·H<sub>2</sub>O: C 85.47, H 9.11; Found C 85.67, H 9.17.

**2,7-Bis(4-(4'-(7-tridecyloxy)biphenyl))fluorene-9-carboxylic acid (133).** To a solution of **132** (1.47 g, 1.695 mmol) in THF (30 ml) at -20 °C was added <sup>n</sup>BuLi (1.6M in hexanes, 1.22 ml, 1.949 mmol) dropwise over 2 minutes with the immediate formation of a dark solution. Stirring was continued for 15 minutes while warming to room temperature before the solution was poured onto solid carbon dioxide (*ca.* 6 g) with vigorous stirring for 1 hour. 1M HCl (50 ml) was added and the product extrcted into CH<sub>2</sub>Cl<sub>2</sub> (2 x 200 ml). The CH<sub>2</sub>Cl<sub>2</sub> layer was dried (Na<sub>2</sub>SO<sub>4</sub>), filtered and evaporated. Flash chromatography on silica (4 cm x 25 cm) eluting with 3:1 CH<sub>2</sub>Cl<sub>2</sub> / petroleum ether (b.p. 40-60 °C) gradually increasing to pure CH<sub>2</sub>Cl<sub>2</sub> then 2-4% methanol in CH<sub>2</sub>Cl<sub>2</sub> gave the title compound as yellow solid that fluoresced strongly under UV light (0.863 g, 56%).



m.p. 224 - 225°C.

$^{13}\text{C}$  NMR (62.9 MHz,  $\text{CDCl}_3$ )  $\delta$  14.2 (C1), 22.7 (C2), 25.4 (C5), 29.5 (C4), 31.9 (C3), 34.0 (C6), 53.2 (C22), 78.1 (C7), 116.1 (C9), 120.4 and 124.3 (C13, 14), 126.9, 127.4 and 128.0 (C10, 17, 18, 21), 132.6 (C11), 138.9, 139.7, 139.9, 140.2 and 141.0 (C12, 15, 16, 19, 20), 158.4 (C8), 177.5 (C23).

FAB<sup>+</sup> MS m/z = 911 (60%, M<sup>+</sup>).

Calculated for  $\text{C}_{64}\text{H}_{78}\text{O}_4 \cdot 0.5\text{H}_2\text{O}$ : C 83.52, H 8.65;

Found C 83.53, H 8.68.

**2,7-bis(4'-(7-tridecyloxy)biphenyl)fluorene-9-carboxylic acid, (3-phenylpropyl)ester. (134).** To a solution of **133** (0.100 g, 0.110 mmol) and 3-phenylpropanol (16.4 mg, 0.121 mmol) in dry  $\text{CH}_2\text{Cl}_2$  (2 ml) at 0°C was added DMAP (1.3 mg, 0.011 mmol) and EDC (52.6 mg, 0.274 mmol). After stirring for 18 hours, the product was diluted with  $\text{CH}_2\text{Cl}_2$  (5 ml), washed with 1M HCl (5 ml) and water (5 ml), dried ( $\text{Na}_2\text{SO}_4$ ), filtered and evaporated. Flash chromatography on silica (1 cm x 12 cm) eluting with 1:1  $\text{CH}_2\text{Cl}_2$  / petroleum ether (b.p. 40-60 °C) gave the title compound as a yellow solid that showed a strong fluorescence under UV light (0.099 g, 88%).

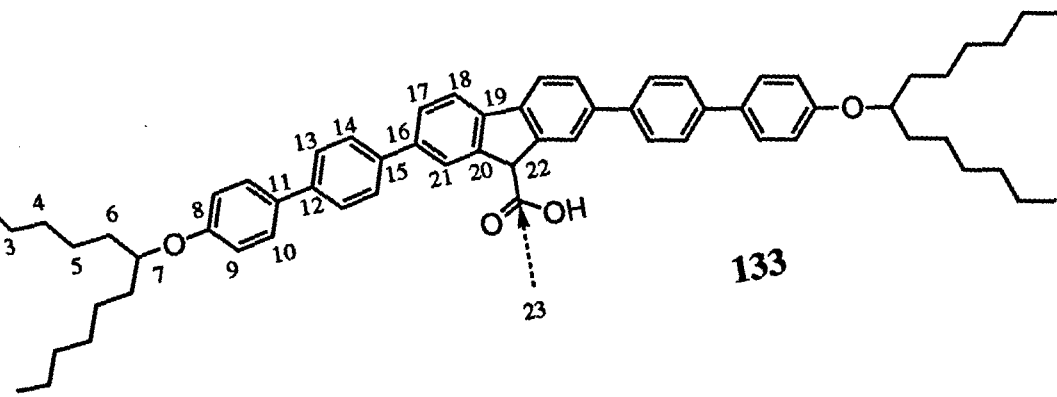
$R_f$  = 0.55 (50%  $\text{CH}_2\text{Cl}_2$  / petroleum ether b.p. 40 - 60°C). m.p. 95-98 °C.

$^1\text{H}$  NMR (250 MHz,  $\text{CDCl}_3$ )  $\delta$  0.92 (12H, t, J = 7 Hz, - $\text{CH}_3$ ), 1.24-1.76 (20H, m, -( $\text{CH}_2$ )<sub>5</sub> $\text{CH}_3$ ), 1.96 (2H, q, J = 6.5 Hz, - $\text{CO}_2\text{CH}_2\text{CH}_2-$ ), 2.63 (2H, t, J = 6.5 Hz, - $\text{CH}_2\text{Ar}$ ), 4.22 (2H, t, J = 6.5 Hz, - $\text{CO}_2\text{CH}_2-$ ), 4.28 (2H, q, J = 6 Hz,  $\text{CHOAr}$ ), 5.00 (1H, s, 9-fluorene H), 6.98 (4H, d, H<sub>9</sub>), 7.04 (2H, m, H<sub>28</sub>), 7.13-7.24 (3H, m, H<sub>29</sub>, 30), 7.58 (4H, d, J = 8.5 Hz, H<sub>10</sub>), 7.65 (4H, d, J = 8.5 Hz, H<sub>13</sub>), 7.72 (6H, m, H<sub>14</sub>, 17), 7.82 (2H, d, J = 7.5 Hz, H<sub>18</sub>), 8.00 (2H, s, H<sub>21</sub>).

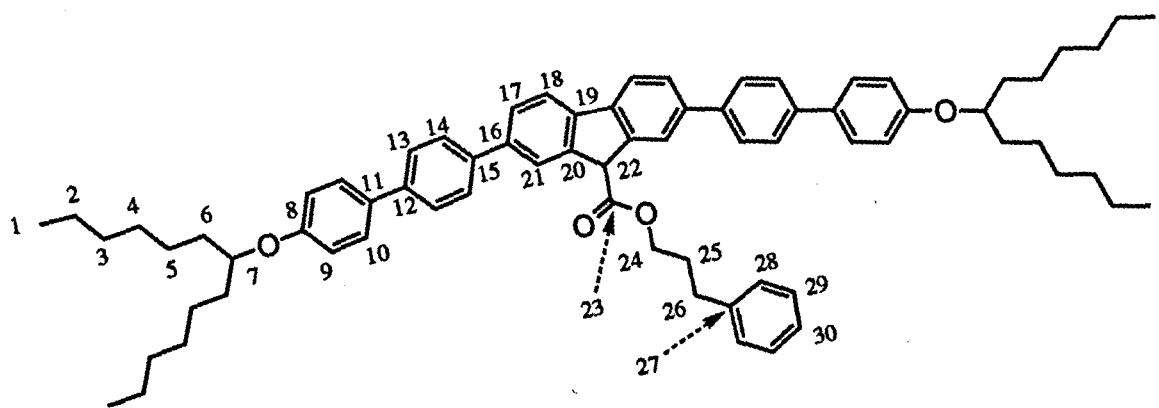
$^{13}\text{C}$  NMR (62.9 MHz,  $\text{CDCl}_3$ )  $\delta$  14.2 (C1), 22.7 (C2), 25.5 (C5), 29.5 (C4), 30.3 (C 26), 31.9 (C3), 32.2 (C25), 34.1 (C6), 53.8 (C22), 64.8 (C24), 78.2 (C7), 116.2 (C9), 120.5 and 124.2 (C13, 14), 126.0, 127.1, 127.2, 127.5, 128.1, 128.4 and 128.5 (C10, 17, 18, 21, 28, 29, 30), 132.7 (C11), 139.2, 139.9, 140.1, 140.3, 140.9 and 141.8 (C12, 15, 16, 19, 20, 27), 158.5 (C8), 170.8 (C23).

Calculated for  $\text{C}_{73}\text{H}_{88}\text{O}_4 \cdot \text{H}_2\text{O}$ : C 83.70, H 8.66;

Found C 83.88, H 8.73.



133



134

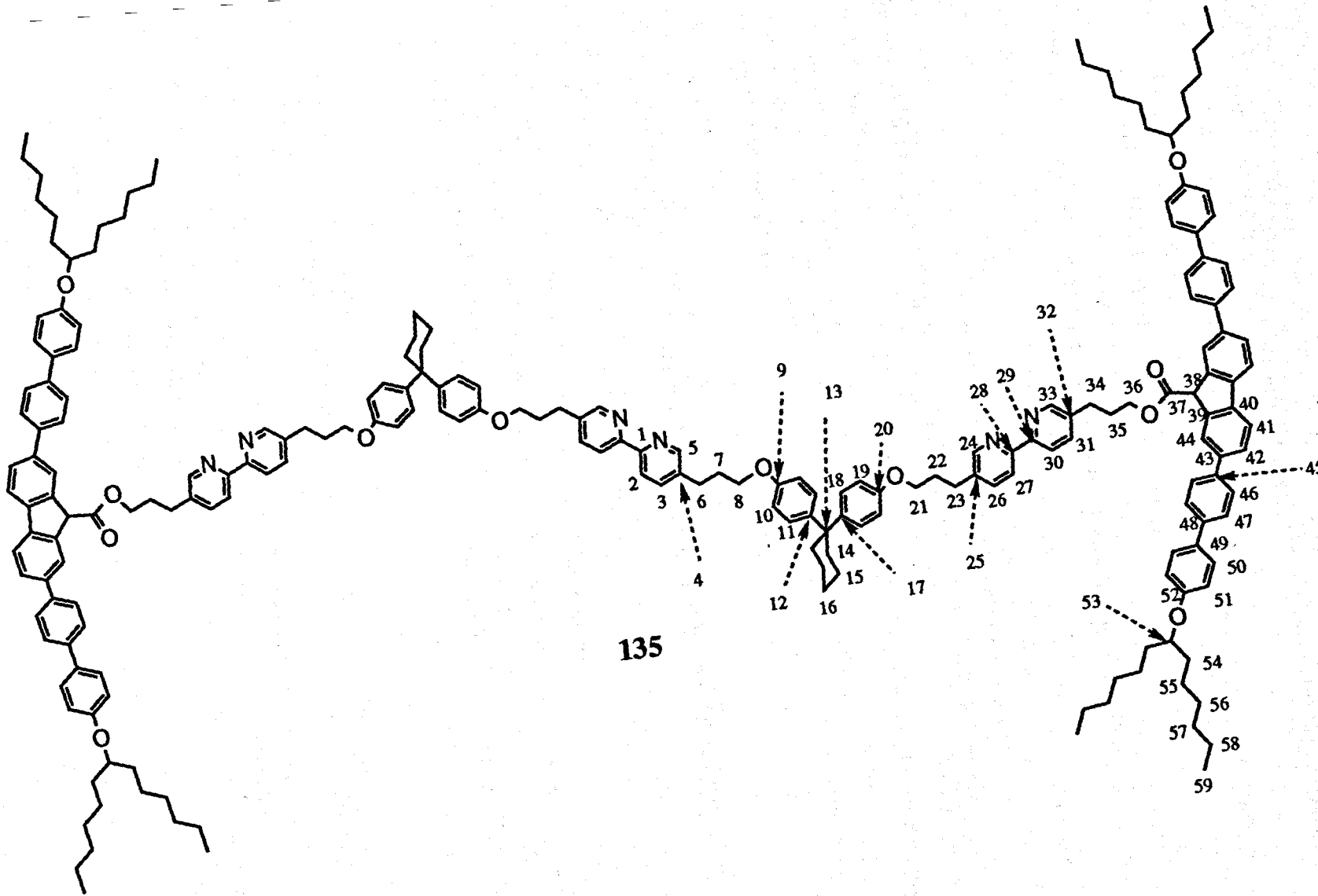
**O,O'-bis(2,7-bis(4-(4'-(7-tridecyloxy)biphenyl))fluorene-9-carboonyl)-[5,5-bis(3-(4-(1-(1-(4-(3-(5-(2-(5-(3-hydroxypropyl)pyridine)))pyridine)propyl)oxyphenyl)cyclohexyl)phenoxy)propyl]-2,2'-bipyridine] (135)** To a suspension of **94** (0.025 g, 0.0195 mmol) and **133** (0.039 g, 0.0429 mmol) in dry CH<sub>2</sub>Cl<sub>2</sub> (1 ml) at 0°C was added EDC (0.038 g, mmol) and DMAP (*ca.* 0.1 mg). The flask was sealed and stirred overnight before diluting with CH<sub>2</sub>Cl<sub>2</sub> (5 ml), washing with 1M HCl (2 ml) and water (2 ml), drying (Na<sub>2</sub>SO<sub>4</sub>), filtration and evaporation. Flash chromatography on silica (1 cm x 25 cm) eluting with 1% methanol in CH<sub>2</sub>Cl<sub>2</sub> gave the title compound as a pale yellow solid (0.035 g, 59%).

R<sub>f</sub> = 0.60 (10% methanol / CH<sub>2</sub>Cl<sub>2</sub>). m.p. 118-122 °C.

<sup>1</sup>H NMR (400 MHz, CD<sub>2</sub>Cl<sub>2</sub>) δ0.88 (24H, m, H<sub>59</sub>), δ1.25-1.56 (44H, br, H<sub>15</sub>, H<sub>16</sub>, H<sub>55</sub>, H<sub>56</sub>, H<sub>57</sub>, H<sub>58</sub>), δ1.66 (16H, m, H<sub>54</sub>), δ1.99-2.12 (12H, m, H<sub>7</sub>, H<sub>22</sub>, H<sub>35</sub>), δ2.21 (8H, br, H<sub>14</sub>), δ2.71 (4H, t, J = 7.6 Hz, H<sub>34</sub>), δ2.83 (8H, t, J = 7.6 Hz, H<sub>23</sub> and H<sub>6</sub>), δ3.93 (8H, t, J = 6.1 Hz, H<sub>8</sub> and H<sub>21</sub>), δ4.22-4.30 (8H, m, H<sub>36</sub> and H<sub>53</sub>), δ5.06 (2H, s, H<sub>38</sub>), δ6.79 and 6.80 (8H, 2 x d, J = 8.8 Hz, H<sub>10</sub> and H<sub>19</sub>), δ6.95 (8H, d, J = 8.8 Hz, H<sub>51</sub>), δ7.16 (8H, d, J = 8.8 Hz, H<sub>11</sub> and H<sub>18</sub>), δ7.49 (2H, dd, J = 8.0 Hz, 1.6 Hz, H<sub>31</sub>), δ7.57 (8H, d, J = 8.8 Hz, H<sub>50</sub>), δ7.58 and δ7.62 (2 x 2H, 2 x dd, J = 8.0 Hz, J = 1.6 Hz, H<sub>3</sub> and H<sub>26</sub>), δ7.66 (8H, d, J = 8.8 Hz, H<sub>47</sub>), δ7.74 (8H, d, J = 8.8 Hz, H<sub>46</sub>), δ7.76 (4H, d, J = 8.0 Hz, H<sub>42</sub>), δ7.88 (4H, d, J = 8.0 Hz, H<sub>41</sub>), δ7.99 (4H, s, H<sub>44</sub>), δ8.23, δ8.25 and δ8.29 (3 x 2H, 3 x d, J = 8.0 Hz, H<sub>2</sub>, H<sub>27</sub> and H<sub>30</sub>), δ8.38 (2H, d, J = 1.6 Hz, H<sub>35</sub>), δ8.46 and δ8.48 (2 x 2H, 2 x d, J = 1.6 Hz, H<sub>5</sub> and H<sub>24</sub>).

<sup>13</sup>C NMR (62.9 MHz, CDCl<sub>3</sub>) δ14.1 (C<sub>59</sub>), 22.6 (C<sub>58</sub>), 22.9 (C<sub>16</sub>), 25.4 (C<sub>55</sub>), 26.4 (C<sub>15</sub>), 29.1, 29.2, 29.4 and 29.8 (C<sub>6</sub>, 23, 34, 56), 30.6 (C<sub>6</sub>, 22, 35), 31.8 (C<sub>57</sub>), 34.0 (C<sub>54</sub>), 37.4 (C<sub>14</sub>), 45.1 (C<sub>13</sub>), 53.8 (C<sub>38</sub>), 64.3 (C<sub>36</sub>), 66.4 (C<sub>8</sub>, 21), 78.2 (C<sub>53</sub>), 114.1 (C<sub>10</sub>, 19), 116.1 (C<sub>51</sub>), 120.5 (C<sub>3</sub>, 26, 31), 124.1 (C<sub>46</sub>, 47), 127.0, 127.2, 127.4, 128.0 and 128.1 (C<sub>11</sub>, 18, 41, 42, 44, 50), 132.7 (C<sub>49</sub>), 136.0 and 136.8 (C<sub>4</sub>, 25, 32), 136.7, 136.8 and 136.9 (C<sub>2</sub>, 27, 30), 139.1, 140.0, 140.1, 140.3 and 141.2 (C<sub>43</sub>, 45, 48, 39, 40), 141.7 (C<sub>12</sub>, 17), 149.1 and 149.3 (C<sub>5</sub>, 24, 33), 154.1 and 154.2 (C<sub>1</sub>, 28, 29), 156.5 (C<sub>9</sub>, 20), 158.5 (C<sub>52</sub>), 170.8 (C<sub>37</sub>).

FAB+ MS m/z = 3065 (100%). C<sub>212</sub>H<sub>244</sub>N<sub>6</sub>O<sub>12</sub> requires 3068.11.



*Attempted preparation of the Overhand Knot: Reaction of 105 and stopper 133.*

A solution of **105** in  $\text{CH}_2\text{Cl}_2$  (2 ml) was prepared from **94** (32.5 mg, 0.025 mmol) and  $\text{Zn}(\text{ClO}_4)_2 \cdot 6\text{H}_2\text{O}$  (138  $\mu\text{L}$  of a 0.1844 M solution in DMF, 0.025 mmol) using the standard procedure. Stopper **133** (51 mg, 0.0558 mmol) was added and the solution cooled in an ice bath. EDC•PF<sub>6</sub> **111** (115 mg, 0.381 mmol) and DMAP (0.62 mg, 0.00507 mmol) were added and the mixture stirred at room temperature for 18 hours. Light was excluded due to the potential photosensitivity of the fluorene unit. Tetraethyl ammonium chloride monohydrate (114.8 mg, 0.625 mmol) was added and stirring continued for a further 2 hours. The solution was then diluted with  $\text{CH}_2\text{Cl}_2$  (10 ml) and washed successively with 1M HCl (3 x 10 ml), saturated aqueous  $\text{NaHCO}_3$  (10 ml) and water (10 ml), dried ( $\text{Na}_2\text{SO}_4$ ), filtered and evaporated. TLC of the crude product (10% methanol /  $\text{CH}_2\text{Cl}_2$ ) indicated a major product with an  $R_f$  of 0.6. <sup>1</sup>H NMR of the crude product suggested that it was identical to unknotted **135**.

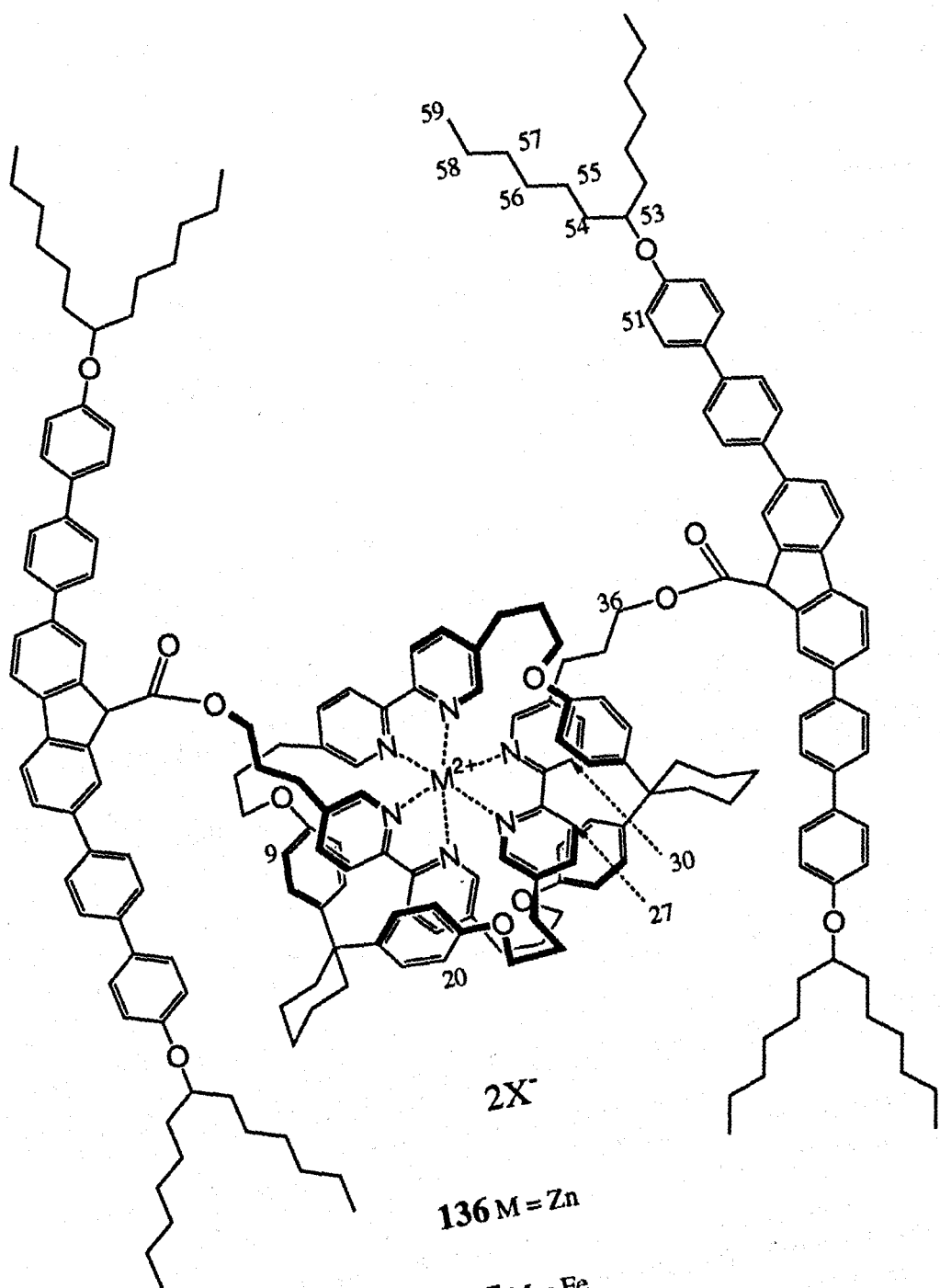
The crude product was further purified by flash chromatography on silica (25 cm x 1 cm) eluting with 1% methanol /  $\text{CH}_2\text{Cl}_2$ . The pure product was shown to be identical to the authentic sample of **135** prepared earlier by <sup>1</sup>H NMR, FAB<sup>+</sup> MS,  $R_f$  and m.p.

*Confirmation of the presence of knotted intermediate **136**.*

The reaction was repeated based upon **94** (12.8 mg, 0.00999 mmol), 32.8  $\mu\text{L}$  of a 0.3048 M solution of  $\text{Zn}(\text{ClO}_4)_2 \cdot 6\text{H}_2\text{O}$  in d<sub>7</sub>-DMF, **133** (20.0 mg), EDC•PF<sub>6</sub> (45 mg, 0.149 mmol) and DMAP (0.2 mg) in  $\text{CD}_2\text{Cl}_2$  (1 ml). A <sup>1</sup>H NMR spectrum of the intermediate prior to demetallation (i.e. before the addition of  $\text{Et}_4\text{N}^+\text{Cl}^- \cdot \text{H}_2\text{O}$ ) strongly suggested the presence of the knotted intermediate **136** as evidenced by the lack of signals above 7.8 ppm and the shielded signals at 5.10 ppm and 5.75 ppm. A full interpretation of this spectrum was precluded by the large number of signals produced by the excess of EDC•PF<sub>6</sub> present.

*Preparation of the iron (II) stabilised overhand knot (**137**) via transmetallation of **136**.*

The above solution of **136** in  $\text{CD}_2\text{Cl}_2$  was treated with  $\text{Fe}(\text{ClO}_4)_2 \cdot 6\text{H}_2\text{O}$  (1.19 ml of a 0.0092 M solution in 5% methanol /  $\text{CH}_2\text{Cl}_2$ , 0.010989 mmol) with the immediate formation of a red coloration. After stirring for 1 hour, the solution was diluted with  $\text{CH}_2\text{Cl}_2$  (5 ml) and washed successively with 1M HCl (3 x 5 ml), saturated aqueous  $\text{NaHCO}_3$  (5 ml), aqueous  $\text{NH}_4\text{PF}_6$  (5 ml) and water (5 ml), dried ( $\text{Na}_2\text{SO}_4$ ), filtered and evaporated. Flash chromatography on silica (1 cm x 15 cm) eluting with 1-2% methanol /  $\text{CH}_2\text{Cl}_2$  gave **137** as a red solid (23.8 mg, 70%).



$R_f = 0.40$  (10% methanol /  $\text{CH}_2\text{Cl}_2$ ).

The  $^1\text{H}$  NMR spectrum was extremely broad and the majority of signals could not be assigned with certainty. The following partial assignment was possible:  $\delta$ 0.80 ( $\text{H}_{59}$ ),  $\delta$ 1.05-1.70 ( $\text{H}_{54-58}$ ),  $\delta$ 4.25 ( $\text{H}_{36}$  and  $\text{H}_{53}$ ),  $\delta$ 5.08 and  $\delta$ 5.75 ( $\text{H}_{30}$ ,  $\text{H}_{27}$ ),  $\delta$ 6.14 and  $\delta$ 6.41 ( $\text{H}_9$  and  $\text{H}_{20}$ ),  $\delta$ 6.95 ( $\text{H}_{51}$ ).

**Zinc (II) trefoil knot hexafluorophosphate salt (141).** A solution of **105** was prepared from **94** (116.6 mg, 0.0910 mmol) and  $\text{Zn}(\text{ClO}_4)_2 \cdot 6\text{H}_2\text{O}$  (0.495 ml of a 0.1844 M solution in DMF, 0.0910 mmol) in  $\text{CH}_2\text{Cl}_2$  (25 ml) using the standard procedure. 3,6,9-Trioxaundecanedioic acid (20.2 mg, 0.0910 mmol) in DMF (1 ml) was added to the solution and thoroughly mixed. This solution was then added dropwise over 2.5 hours to a rapidly stirred, ice-cooled solution of EDC•PF<sub>6</sub> **111** (0.548 g, 1.82 mmol) and DMAP (42 mg). After the addition, the solution was allowed to warm to room temperature and stirring was continued for 18 hours.  $\text{Et}_4\text{N}^+\text{Cl}^- \cdot \text{H}_2\text{O}$  (0.500 g, 2.73 mmol) was added and the solution stirred for 2 hours before washing sequentially with 1M HCl (3 x 10 ml), aqueous NH<sub>4</sub>PF<sub>6</sub> (10 ml) and water (10 ml). The  $\text{CH}_2\text{Cl}_2$  solution was then dried ( $\text{Na}_2\text{SO}_4$ ), filtered and evaporated. Flash chromatography on silica (20 cm x 1.5 cm) eluting with 1-2% methanol in  $\text{CH}_2\text{Cl}_2$  gave the title compound as a slightly off-white solid (42 mg, 25%).

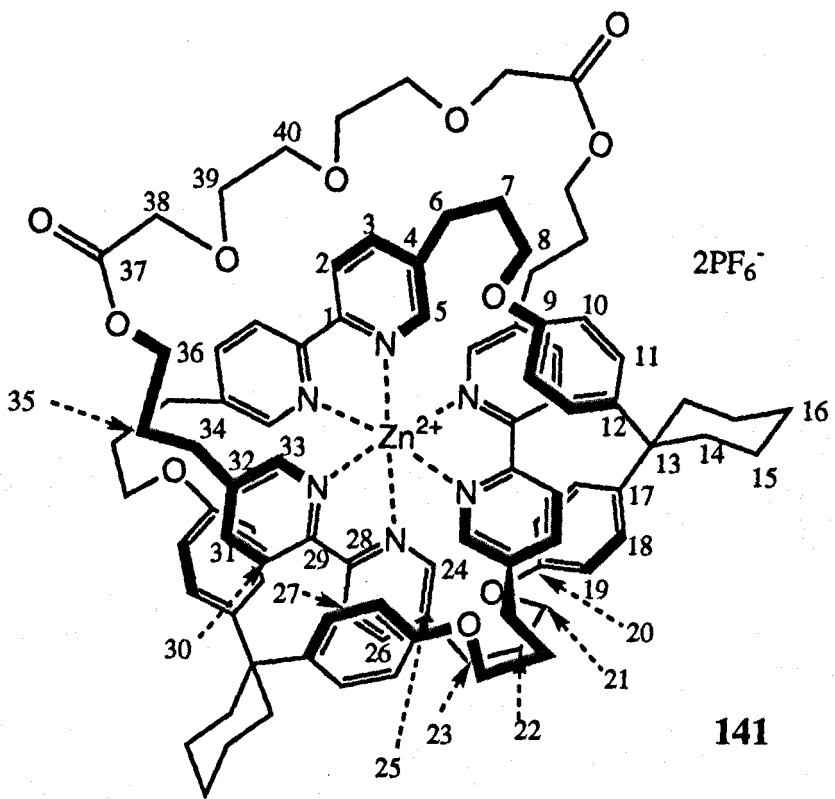
$R_f = 0.55$  (10% methanol /  $\text{CH}_2\text{Cl}_2$ ).

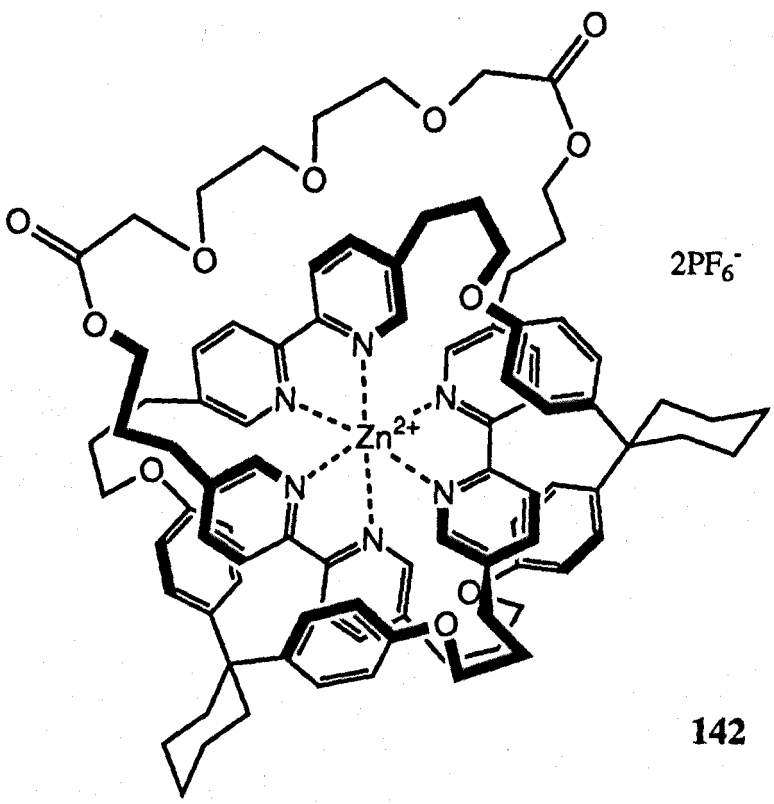
FAB<sup>+</sup> MS m/z = 766 (70%,  $[\text{M}-2\text{PF}_6]^{2+}$ ), 1530 (87%,  $[\text{M}-2\text{PF}_6]^+$ ), 1678 (100%,  $[\text{M}-\text{PF}_6]^+$ ). ES<sup>+</sup> MS m/z = 766 (100%,  $[\text{M}-2\text{PF}_6]^{2+}$ ).

$^1\text{H}$  NMR (400 MHz,  $\text{CDCl}_3$ ) Aromatic region:  $\delta$ 5.47 (2H, d,  $J = 8$  Hz,  $\text{H}_{30}$ ),  $\delta$ 5.91 (2H, d,  $J = 8$  Hz,  $\text{H}_{27}$ ),  $\delta$ 6.41 (4H, d,  $J = 8.5$  Hz,  $\text{H}_{19}$ ),  $\delta$ 6.22 (4H, d,  $J = 8.5$  Hz,  $\text{H}_{10}$ ),  $\delta$ 7.24 (2H, s,  $\text{H}_{33}$ ),  $\delta$ 7.28 (2H, d,  $J = 8$  Hz,  $\text{H}_{31}$ ),  $\delta$ 7.34 (4H, d,  $J = 8.5$  Hz,  $\text{H}_{18}$ ),  $\delta$ 7.46 (2H, d,  $J = 8$  Hz,  $\text{H}_{26}$ ),  $\delta$ 7.50 (4H, d,  $J = 8.5$  Hz,  $\text{H}_{11}$ ),  $\delta$ 7.61 (2H, s,  $\text{H}_{24}$ ),  $\delta$ 7.65 (2H, s,  $\text{H}_5$ ),  $\delta$ 8.01 (2H, d,  $J = 8$  Hz,  $\text{H}_3$ ),  $\delta$ 8.46 (2H, d,  $J = 8$  Hz,  $\text{H}_2$ ).

A full assignment of the aliphatic region of the spectrum has not yet been achieved. Two notable peaks that have been assigned from a 2D ROESY spectrum are  $\text{H}_{39}$  and  $\text{H}_{40}$  ( $\delta$ 3.65 and  $\delta$ 3.78).

$^{13}\text{C}$  NMR (62.9 MHz,  $\text{CDCl}_3$ )  $\delta$ 22.8 (C15), 27.4, 27.5, 28.6, 29.1, 29.6, 30.2, 35.3 and 35.4 (C6, 7, 14, 15, 16, 22, 23, 34, 35), 44.2 (C13), 61.2 (C36), 63.9 and 65.0 (C8, 21), 67.8 (C38), 70.5 and 70.8 (C39, 40), 114.1 and 114.7 (C10, 19), 123.0 (2 signals) and 123.7 (C3, 26, 31), 127.4 and 128.1 (C11, 18), 139.9, 140.2, 140.9, 141.2 and 142.4 (C4, 12, 17, 25, 32), 145.9, 146.3 and 147.4 (C1, 28, 29), 147.5 and 148.1 (C2, 27, 30), 156.1 (2 signals) (C9, 20), 169.3 (C37). No peaks detected for the  $\alpha$ -pyridyl carbons C5, 24 and 33.





142

*Attempted demetallation of 141 to give Trefoil knot 142.*

A solution of **141** (10.0 mg, 0.0055 mmol) and Et<sub>4</sub>N<sup>+</sup>Cl<sup>-</sup>•H<sub>2</sub>O (100 mg) in CDCl<sub>3</sub> (2 ml) was heated at reflux for 24 hours. After cooling, a <sup>1</sup>H NMR spectrum of the solution was recorded which showed that the characteristic pattern of signals in the aromatic region was unchanged. The solution was diluted with CH<sub>2</sub>Cl<sub>2</sub> (5 ml) and washed successively with water (2 x 5 ml), aqueous NH<sub>4</sub>PF<sub>6</sub> (10 ml) and water (10 ml), dried (Na<sub>2</sub>SO<sub>4</sub>), filtered and evaporated. The recovered material was identical to the metallated starting material **141**.

## References

- (1) For a general discussion of *cis-trans* isomerism, see March, J. *Advanced Organic Chemistry*, 4th Edition; Wiley: New York, 1992; pp127-138.
- (2) For a discussion of optical activity and stereoisomerism, see reference (1), pp94-
- (3) Wasserman, E. *J. Am. Chem. Soc.* **1960**, *82*, 4433.
- (4) Walba, D.M., *Tetrahedron* **1985**, *41*, 3161.
- (5) Turro, N.J. *Angew. Chem. Int. Ed. Engl.* **1986**, *25*, 882.
- (6) Arnold, B.H. *Intuitive Concepts in Elementary Topology*; Prentice-Hall: Englewood Cliffs, NJ, 1962.
- (7) Amabilino, D.B.; Stoddart, J.F. *Chem. Rev.* **1995**, *95*, 2725.
- (8) Hudson, B.; Vinograd, J. *Nature* **1967**, *216*, 647.
- (9) Clayton, D.A.; Vinograd, J. *Nature* **1967**, *216*, 652.
- (10) Liu, L.F.; Depew, R.E.; Wang, J.C. *J. Mol. Biol.* **1976**, *106*, 439.
- (11) Liu, L.F.; Perkocha, L.; Calendar, R.; Wang, J.C. *Proc. Natl. Acad. Sci. USA* **1981**, *78*, 5498.
- (12) Kreuzer, K.N.; Cozzarelli, N.R. *Cell* **1980**, *20*, 245.
- (13) Krasnow, M.A.; Stasiak, A.; Spengler, S.J.; Dean, F.; Koller, T.; Cozzarelli, N.R. *Nature* **1983**, *304*, 559.
- (14) Jaenisch, R.; Levine, A.J. *J. Mol. Biol.* **1973**, *73*, 199.
- (15) Wang, J.C. *J. Mol. Biol.* **1971**, *55*, 523.
- (16) Bates, A.D.; Maxwell, A. *DNA Topology*; Oxford University Press: Oxford, 1993.
- (17) Maxwell, A.; Gellert, M. *Adv. Prot. Chem.* **1986**, *38*, 69.

- (18) Hayashi, Y.; Hayashi, M. *Biochemistry* **1971**, *10*, 4212.
- (19) Tse-Dinh, Y.-C. *Nucleic Acids Res.* **1985**, *13*, 4751.
- (20) Drlica, K.; Franco, R.J. *Biochemistry* **1988**, *27*, 2253.
- (21) Liu, L.F.; Wang, J.C. *Proc. Natl. Acad. Sci. USA* **1987**, *84*, 7024.
- (22) Liang, C.; Mislow, K. *J. Am. Chem. Soc.* **1994**, *116*, 11189.
- (23) Liang, C.; Mislow, K. *J. Am. Chem. Soc.* **1995**, *117*, 4201.
- (24) Takusagawa, F.; Kamitori, S. *J. Am. Chem. Soc.* **1996**, *118*, 8945.
- (25) Du, S.M.; Stollar, B.D.; Seeman, N.C. *J. Am. Chem. Soc.* **1995**, *117*, 1194.
- (26) Chen, J.; Seeman, N.C. *Nature* **1991**, *350*, 631.
- (27) Zhang, Y.; Seeman, N.C. *J. Am. Chem. Soc.* **1994**, *116*, 1661.
- (28) Walba, D.M. *New J. Chem.* **1993**, *17*, 618.
- (29) Van Gulick, N. *New J. Chem.* **1993**, *17*, 619.
- (30) Wasserman, E. *Sci. Am.* **1962**, *207*, 94.
- (31) Lüttringhaus, A.; Cramer, F.; Prinzbach, H.; Henglein, F.M. *Liebigs Ann. Chem.* **1958**, *185*, 613.
- (32) Frisch, H.L.; Wasserman, E. *J. Am. Chem. Soc.* **1961**, *83*, 3789.
- (33) Harrison, I.T.; Harrison, S. *J. Am. Chem. Soc.* **1967**, *89*, 5723.
- (34) Agam, G.; Zilka, A. *J. Am. Chem. Soc.* **1976**, *98*, 5212.
- (35) Agam, G.; Zilka, A. *J. Am. Chem. Soc.* **1976**, *98*, 5214.

- (36) Walba, D.M.; Richards, R.M.; Haltiwanger, R.C. *J. Am. Chem. Soc.* **1982**, *104*, 3219.
- (37) Walba, D.M.; Armstrong, J.D.; Perry, A.E.; Richards, R.M.; Homan, T.C.; Haltiwanger, R.C. *Tetrahedron* **1986**, *42*, 1883.
- (38) Watson, J.D.; Crick, F.H.C. *Nature* **1953**, *171*, 737.
- (39) Busch, D.H. *J. Inclusion Phenom.* **1992**, *12*, 389.
- (40) Anderson, S.; Anderson, H.L.; Sanders, J.K.M. *Acc. Chem. Res.* **1993**, *26*, 469.
- (41) For a short review and further references, see Vögtle, F.; Hoss, R. *Angew. Chem. Int'l. Ed. Engl.* **1994**, *33*, 375.
- (42) Pedersen, C.J. *J. Am. Chem. Soc.* **1967**, *89*, 7017.
- (43) Greene, R.N. *Tetrahedron Lett.* **1972**, 1793.
- (44) McMurry, T.J.; Rodgers, S.J.; Raymond, K.N. *J. Am. Chem. Soc.* **1987**, *109*, 3451.
- (45) Anderson, H.L.; Sanders, J.K.M. *J. Chem. Soc. Chem. Commun.* **1992**, 1163.
- (46) Anderson, H.L.; Sanders, J.K.M. *Angew. Chem. Int'l. Ed. Engl.* **1990**, *29*, 1400.
- (47) Schill, G.; Lüttringhaus, A. *Angew. Chem. Int'l. Ed. Engl.* **1964**, *3*, 546.
- (48) Schill, G.; Rissler, K.; Fritz, H.; Vetter, W. *Angew. Chem. Int'l. Ed. Engl.* **1981**, *20*, 187.
- (49) Dietrich-Buchecker, C.O.; Sauvage, J.P. *Chem. Rev.* **1987**, *87*, 795.
- (50) Dietrich-Buchecker, C.O.; Sauvage, J.P. *Angew. Chem. Int'l. Ed. Engl.* **1989**, *28*, 289.
- (51) Mitchell, D.K.; Sauvage, J.P. *Angew. Chem. Int'l. Ed. Engl.* **1988**, *27*, 930.

- (52) Dietrich-Buchecker, C.O.; Hemmert, C.; Khémiss, A.-K.; Sauvage, J.P. *J. Am. Chem. Soc.* **1990**, *112*, 8002.
- (53) Bitsch, F.; Dietrich-Buchecker, C.O.; Hemmert, C.; Khémiss, A.-K.; Sauvage, J.P. *J. Am. Chem. Soc.* **1991**, *113*, 4023.
- (54) Wu, C.; Lecavalier, P.R.; Shen, Y.X.; Gibson, H.W. *Chem. Mater.* **1991**, *3*, 569.
- (55) Chambron, J.C.; Heitz, V.; Sauvage, J.P. *J. Am. Chem. Soc.* **1993**, *115*, 12378.
- (56) Diederich, F.; Dietrich-Buchecker, C.O.; Nierengarten, J.F.; Sauvage, J.P. *J. Chem. Soc. Chem. Commun.* **1995**, 781.
- (57) Chambron, J.-C.; Dietrich-Buchecker, C.O.; Nierengarten, J.F.; Sauvage, J.P. *J. Chem. Soc. Chem. Commun.* **1993**, 801.
- (58) Momenteau, M.; LeBras, F.; Loock, B. *Tetrahedron Lett.* **1994**, *35*, 3289.
- (59) Stoddart, J.F. *Chem. Brit.* **1991**, 714.
- (60) Stoddart, J.F. *Pure Appl. Chem.* **1988**, *60*, 467.
- (61) Odell, B.; Reddington, M.V.; Slawin, A.M.Z.; Spencer, N.; Stoddart, J.F.; Williams, D.J. *Angew. Chem. Int'l. Ed. Engl.* **1988**, *27*, 1547.
- (62) Ashton, P.R.; Goodnow, T.T.; Kaifer, A.E.; Reddington, M.V.; Slawin, A.M.Z.; Spencer, N.; Stoddart, J.F.; Vicent, C.; Williams, D.J. *Angew. Chem. Int'l. Ed. Engl.* **1989**, *28*, 1396.
- (63) Ashton, P.R.; Brown, C.L.; Chrystal, E.J.T.; Goodnow, T.T.; Kaifer, A.E.; Parry, K.P.; Slawin, A.M.Z.; Spencer, N.; Stoddart, J.F.; Williams, D.J. *Angew. Chem. Int'l. Ed. Engl.* **1991**, *30*, 1039.
- (64) Ashton, P.R.; Johnston, M.R.; Stoddart, J.F.; Tolley, M.S.; Wheeler, W. *J. Chem. Soc. Chem. Commun.* **1992**, 1128.
- (65) Ashton, P.R.; Belohradsky, M.; Philp, D.; Stoddart, J.F. *J. Chem. Soc. Chem. Commun.* **1993**, 1269.

- (66) (a) Ashton, P.R.; Brown, C.L.; Chrystal, E.J.T.; Parry, K.P.; Pietraszkiewicz, M.; Spencer, N.; Stoddart, J.F. *Angew. Chem. Int'l. Ed. Engl.* **1991**, *30*, 1042. (b) Stoddart, J.F. *Chem. Brit.* **1991**, 714.
- (67) (a) Ashton, P.R.; Ballardini, R.; Balzani, V.; Boyd, S.E.; Credi, A.; Gandolfi, M.T.; GomezLopez, M.; Iqbal, S.; Philp, D.; Preece, J.A.; Prodi, L.; Ricketts, H.G.; Stoddart, J.F.; Tolley, M.S.; Venturi, M.; White, A.J.P.; Williams, D.J. *Chem. Eur. J.* **1997**, *3*, 152-170. (b) Anelli, P.L.; Asakawa, M.; Ashton, P.R.; Bissell, R.A.; Clavier, G.; Gorski, R.; Kaifer, A.E.; Langford, S.J.; Mattersteig, G.; Menzer, S.; Philp, D.; Slawin, A.M.Z.; Spencer, N.; Stoddart, J.F.; Tolley, M.S.; Williams, D.J. *Chem. Eur. J.* **1997**, *3*, 1113-1135.
- (68) Li, Z.-T.; Stein, P.C.; Becher, J.; Jensen, D.; Mork, P.; Svenstrup, N. *Chem. Eur. J.* **1996**, *2*, 624.
- (69) Gunter, M.J.; Hockless, D.C.R.; Johnston, M.R.; Skelton, B.W.; White, A.H. *J. Am. Chem. Soc.* **1994**, *116*, 4810.
- (70) Hunter, C.A. *J. Am. Chem. Soc.* **1992**, *114*, 5303.
- (71) Carver, F.J.; Hunter, C.A.; Shannon, R.J. *J. Chem. Soc. Chem. Commun.* **1994**, 1277.
- (72) Adams, H.; Carver, F.J.; Hunter, C.A. *J. Chem. Soc. Chem. Commun.* **1995**, 809.
- (73) Vögtle, F.; Meier, S.; Hoss, R. *Angew. Chem. Int'l. Ed. Engl.* **1992**, *31*, 1619.
- (74) Ottens-Hildebrandt, S.; Nieger, M.; Rissanen, K.; Rouvinen, J.; Meier, S.; Harder, G.; Vögtle, F. *J. Chem. Soc. Chem. Commun.* **1995**, 777.
- (75) Vögtle, F.; Händel, M.; Meier, S.; Ottens-Hildebrandt, S.; Ott, F.; Schmidt, T. *Liebigs Ann. Chem.* **1995**, 739.
- (76) Johnston, A.G.; Leigh, D.A.; Pritchard, R.J.; Deegan, M.D. *Angew. Chem. Int'l. Ed. Engl.* **1995**, *34*, 1209.
- (77) Johnston, A.G.; Leigh, D.A.; Murphy, A.; Smart, J.P. *Bull. Soc. Chim. Belges* **1996**, *105*, 721.

- (78) Anderson, S.; Anderson, H.L. *Angew. Chem. Int'l. Ed. Engl.* **1996**, *35*, 1956.
- (79) Fujita, M.; Ibukuro, F.; Hagihara, H.; Ogura, K. *Nature* **1994**, *367*, 720.
- (80) Fujita, M.; Ibukuro, F.; Yamaguchi, K.; Ogura, K. *J. Am. Chem. Soc.* **1995**, *117*, 4175.
- (81) Schill, G.; Doerjer, G.; Logemann, E.; Fritz, H. *Chem. Ber.* **1979**, *112*, 3603.
- (82) Schill, G.; Tafelmair, F. *Synthesis* **1971**, *10*, 546.
- (83) Schill, G.; Keller, U.; Fritz, H. *Chem. Ber.* **1983**, *116*, 3675.
- (84) Walba, D.M. In *Graph Theory and Topology in Chemistry*, Ed. King, R.B.; Elsevier: Amsterdam, 1987; pp23-42.
- (85) Walba, D.M.; Zheng, Q.Y.; Schilling, K. *J. Am. Chem. Soc.* **1992**, *114*, 6259.
- (86) Lehn, J.M.; Pigault, A. *Angew. Chem. Int'l. Ed. Engl.* **1988**, *27*, 1095.
- (87) Dietrich-Buchecker, C.O.; Sauvage, J.P. *New. J. Chem.* **1992**, *16*, 277.
- (88) Dietrich-Buchecker, C.O.; Nierengarten, J.F.; Sauvage, J.P.; Armaroli, N.; Balzani, V.; De Cola, L. *J. Am. Chem. Soc.* **1993**, *115*, 11237.
- (89) Dietrich-Buchecker, C.O.; Sauvage, J.P.; De Cian, A.; Fischer, J. *J. Chem. Soc. Chem. Commun.* **1994**, 2231.
- (90) Nierengarten, J.F.; Dietrich-Buchecker, C.O.; Sauvage, J.P. *J. Am. Chem. Soc.* **1994**, *116*, 375.
- (91) Dietrich-Buchecker, C.O.; Leize, E.; Nierengarten, J.F.; Sauvage, J.P.; Van Dorsselaer, A. *J. Chem. Soc. Chem. Commun.* **1994**, 2257.
- (92) Carina, R.F.; Dietrich-Buchecker, C.; Sauvage, J.-P. *J. Am. Chem. Soc.* **1996**, *118*, 9110.
- (93) Sokolov, V.I. *Russ. Chem. Rev.* **1973**, *42*, 452.

- (94) (a) McKenzie, E.D. *Coord. Chem. Rev.* **1971**, *6*, 187. (b) Lindoy, L.F.; Livingstone, S.E. *Coord. Chem. Rev.* **1967**, *2*, 173. (c) Reedijk, J. in *Comprehensive Coordination Chemistry*, Ed. Wilkinson, G.; Permagon: Oxford, 1987; volume 2, pp89-92.
- (95) For the synthesis of 5,5'-disubstituted bipyridines bearing a wide range of substituents, see Whittle, C.P. *J. Heterocyclic Chem.* **1977**, *14*, 191.
- (96) Constable, E.C. *Adv. Inorg. Chem.* **1989**, *34*, 1-61.
- (97) (a) Schröder, M.; Stephenson, T.A. in *Comprehensive Coordination Chemistry*, Ed. Wilkinson, G.; Permagon: Oxford, 1987; volume 4, pp327-345. (b) Griffith, W.P. in *Comprehensive Coordination Chemistry*, Ed. Wilkinson, G.; Permagon: Oxford, 1987; volume 4, pp537-544.
- (98) Dietrich-Buchecker, C.O.; Kern, J.-M.; Sauvage, J.-P. *J. Chem. Soc. Chem. Commun.* **1985**, 760.
- (99) Hunter, C.A. *Chem. Soc. Rev.* **1994**, 101.
- (100) (a) Smithrud, D.B.; Diederich, F. *J. Am. Chem. Soc.* **1990**, *112*, 339. (b) Diederich, F., *Angew. Chem. Int. Ed. Engl.* **1988**, *27*, 362.
- (101) Hamilton, A.D.; Rubin, H.-D.; Bocarsly, A.B. *J. Am. Chem. Soc.* **1984**, *106*, 7255.
- (102) Hamilton, A.D., Private communication.
- (103) Sasse, W.H.F.; Whittle, C.P. *J. Chem. Soc.* **1961**, 1347.
- (104) Badger, G.M.; Sasse, W.H.F. *J. Chem. Soc.* **1956**, 616.
- (105) Ebmeyer, F.; Vögtle, F. *Chem. Ber.* **1989**, *122*, 1725.
- (106) Krapcho, A.P.; Lovey, A.J. *Tetrahedron Lett.* **1973**, 957.
- (107) Diederich, F.; Dick, K.; Griebel, D. *Chem. Ber.* **1985**, *118*, 3588.

- (108) McGreal, M.E.; Niederl, V.; Niederl, J.B. *J. Am. Chem. Soc.* **1939**, *61*, 345.
- (109) For example, Elliot, C.M.; Hershenhart, E.J. *J. Am. Chem. Soc.* **1982**, *104*, 7519. Also, see reference 97 (a).
- (110) Hawker, P.N. and Twigg, N.V. in *Comprehensive Coordination Chemistry*, Ed. Wilkinson, G.; Permagon: Oxford, 1987; volume 4, pp1214-1219.
- (111) Broomhead, J.A.; Young, C.G. *Inorg. Synth.* **28**, 338.
- (112) Thomas, J.A., University of Sheffield, private communication.
- (113) Sauvage, J.-P. *Acc. Chem. Res.* **1990**, *23*, 319.
- (114) Osbrowicki, A.; Koepp, E.; Vögtle, F. *Top. Curr. Chem.* **1991**, *37*, 161.
- (115) Galli, C. *Org. Prep. Proced. Int.* **1992**, *24*, 285.
- (116) Lay, P.A.; Sargeson, A.M.; Taube, H. *Inorg. Synth.* **1986**, *24*, 291.
- (117) Sprintschnik, G.; Sprintschnik, H.W.; Kirsch, P.P.; Whitton, D.G. *J. Am. Chem. Soc.* **1977**, *99*, 4947.
- (118) Eliel, E.L.; Allinger, N.L.; Angyal, S.J.; Morrison, G.A. *Conformational Analysis*; Interscience: New York, 1965.
- (119)(a) Gallo, E.A.; Gellman, S.H. *J. Am. Chem. Soc.* **1993**, *115*, 9774. (b) Newcomb, L.F.; Haque, T.S.; Gellman, S.H. *J. Am. Chem. Soc.* **1995**, *117*, 6509. (c) Newcomb, L.F.; Gellman, S.H. *J. Am. Chem. Soc.* **1994**, *116*, 4993.
- (120) Paliwal, S.; Geib, S.; Wilcox, C.S. *J. Am. Chem. Soc.* **1994**, *116*, 4497.
- (121)(a) Cozzi, F.; Cinquini, M.; Annunziata, R.; Dwyer, T.; Siegel, J.S. *J. Am. Chem. Soc.* **1992**, *114*, 5729. (b) Cozzi, F.; Cinquini, M.; Annunziata, R.; Siegel, J.S. *J. Am. Chem. Soc.* **1993**, *115*, 5330. (c) Cozzi, F.; Ponzini, F.; Annunziata, R.; Cinquini, M.; Siegel, J.S. *Angew. Chem. Int. Ed. Engl.* **1995**, *34*, 1019. (d) Cozzi, F.; Siegel, J.S. *Pure and Appl. Chem.* **1995**, *67*, 683.

- (122)(a) Adams, H.; Harris, K.D.M.; Hembury, G.A.; Hunter, C.A.; Livingstone, D.; McCabe, J.F. *J. Chem. Soc. Chem. Commun.* 1996, 2531. (b) Adams, H.; Carver, F.J.; Hunter, C.A.; Morales, J.C.; Seward, E.M. *Angew. Chem. Int. Ed. Engl.* 1996, 35, 1542. (c) Serrano, L.; Bycroft, M.; Fersht, A.R. *J. Mol. Biol.* 1991, 218, 465-475. (d) Kato, Y.; Conn, M.M.; Rebek, J. *J. Am. Chem. Soc.* 1994, 116, 3279. (e) Aoyama, Y.; Asakawa, M.; Yamagishi, A.; Toi, H.; Ogoshi, H. *J. Am. Chem. Soc.* 1990, 112, 3145. (f) Aoyama, Y.; Asakawa, M.; Matsui, Y.; Ogoshi, H. *J. Am. Chem. Soc.* 1991, 113, 6233.
- (123)(a) Ferguson, S.B.; Sanford, E.M.; Seward, E.; Diederich, F. *J. Am. Chem. Soc.* 1991, 113, 5410. (b) Smithrud, D.B.; Wyman, T.B.; Diederich, F. *J. Am. Chem. Soc.* 1991, 113, 5420. (c) Smithrud, D.B.; Diederich, F. *J. Am. Chem. Soc.* 1990, 112, 339.
- (124) Z values were obtained from Gordon, A.J.; Ford, R.A. *The Chemist's Companion*; Wiley: New York, 1972; pp 22-23 and references therein. Isotope effects for deuterated solvents were ignored. For a discussion of the derivation of Z values, see Kosower, E.M. *J. Am. Chem. Soc.* 1958, 80, 3253.
- (125) McDougal, P.G.; Rico, J.G.; Oh, Y.-I.; Condon, B.D. *J. Org. Chem.* 1986, 51, 3388.
- (126) Hansen Jr., D.W.; Pilipauskas, D. *J. Org. Chem.* 1985, 50, 945.
- (127) Venuti, M.C.; Loe, B.E.; Jones, G.H.; Young, J.M. *J. Med. Chem.* 1988, 31, 2132.
- (128) Dietrich-Buchecker, C.O.; Sauvage, J.-P. *Tetrahedron Lett.* 1983, 24, 5091.
- (129) For example, see Vyas, G.N.; Shah, N.M. *Org. Synth. Collect. Vol. IV* 1963, 836.
- (130) Wheatley, W.B.; Fitzgibbon, W.E.; Cheney, L.C.; Binkley, S.B. *J. Am. Chem. Soc.* 1950, 72, 1655.
- (131) For a comprehensive review, see Mitsunobu, O. *Synthesis* 1981, 1.
- (132) Tsunoda, T.; Yamamiya, Y.; Itô, S. *Tetrahedron Lett.* 1993, 34, 1639.

- (133) Felix, A.M.; Heimer, E.P.; Lambros, T.J.; Tzougraki, C.; Meienhofer, J. *J. Org. Chem.* **1978**, *43*, 4194.
- (134) Corey, E.J.; Venkateswarlu, A. *J. Am. Chem. Soc.* **1972**, *94*, 6190.
- (135) Kabalka, G.W.; Sastry, U.; Sastry, K.A.R.; Knapp Jr., F.F.; Srivastava, P.C. *J. Organomet. Chem.* **1983**, *259*, 269.
- (136) For a review, see Miyaura, N.; Suzuki, A. *Chem. Rev.* **1995**, *95*, 2457.
- (137) Sala, T.; Sargent, M.V. *J. Chem. Soc. Chem. Commun.* **1978**, 253.
- (138) Herriott, A.W.; Picker, D. *Tetrahedron Lett.* **1974**, 1511.
- (139) Du, C.-J. F.; Hart, H.; Ng, K.-K. D. *J. Org. Chem.* **1986**, *51*, 3162.
- (140) Bolton, R.; Sandall, J.P.B. *J. Chem. Soc., Perkin Trans. II* **1977**, 278.
- (141) Chen, C.-T.; Siegel, J.S. *J. Am. Chem. Soc.* **1994**, *116*, 5959.
- (142) Hodgkinson, W.R.; Matthews, F.E. *J. Chem. Soc.* **1883**, *43*, 163.
- (143) Maddaford, S.P.; Keay, B.A. *J. Org. Chem.* **1994**, *59*, 6501.
- (144) Chiba, K.; Tagaya, H.; Miura, S.; Karasu, M. *Chem. Lett.* **1992**, 923.
- (145) Meyer, M.; Albrecht-Gary, A.M.; Dietrich-Buchecker, C.O.; Sauvage, J.P. *J. Am. Chem. Soc.* **1997**, *119*, 4599.
- (146) Albrecht-Gary, A.M.; Saad, Z.; Dietrich-Buchecker, C.O.; Sauvage, J.P. *J. Am. Chem. Soc.* **1985**, *107*, 3205.

# *Appendices*

**Appendix One: A Monomer Unit for Knotted Polymers**

191

**Appendix Two: Macrocyclisation Reactions via  
Platinum Coordination**

196

## Appendix 1: A Monomer Unit for Knotted Polymers

There have been literature reports speculating on the properties of polymers consisting of linear units that are knotted or have mechanical cross-linking provided by knotting rather than the more usual covalent linkages.<sup>1</sup> This section outlines some preliminary work to develop a suitable monomer unit for the introduction of knotted substructures into a bulk polymer. Of course, the pseudo overhand knot structures already described in detail in Chapter 5 could be used directly to introduce knotting into a particular polymer strand as in Figure A1.1a. Of more interest is the design of a unit to introduce mechanical cross-linking. A possible design for such a unit is illustrated in Figure A1.1b.

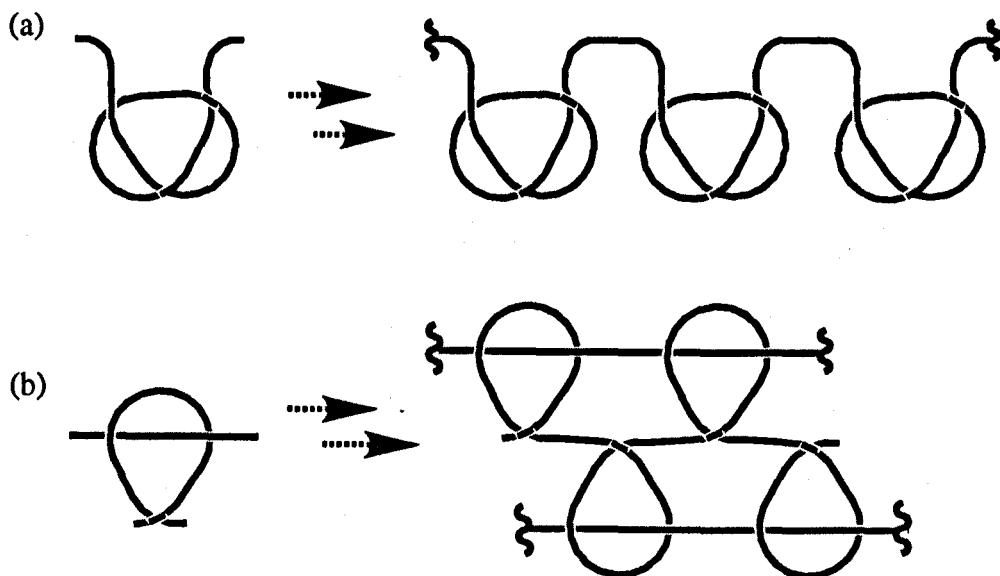
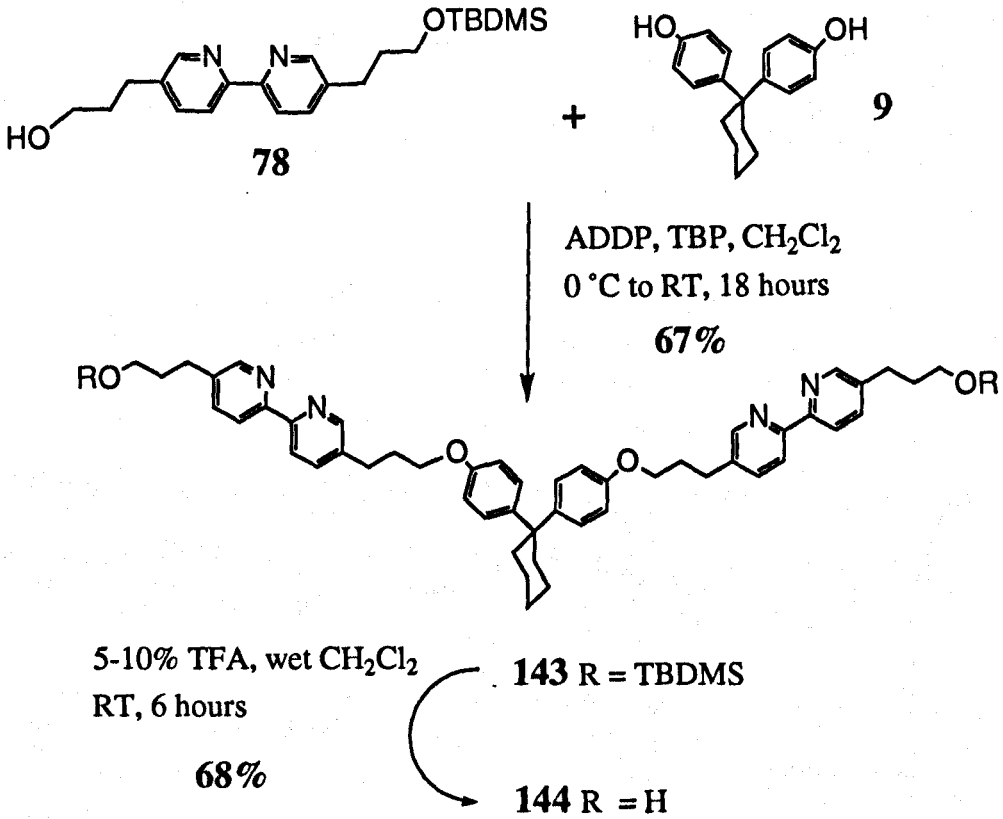


**Figure A1.1.** Possibilities for the incorporation of knotted substructures into polymers.  
 (a) into a single polymer strand and (b) mechanical cross-linking of polymer strands.

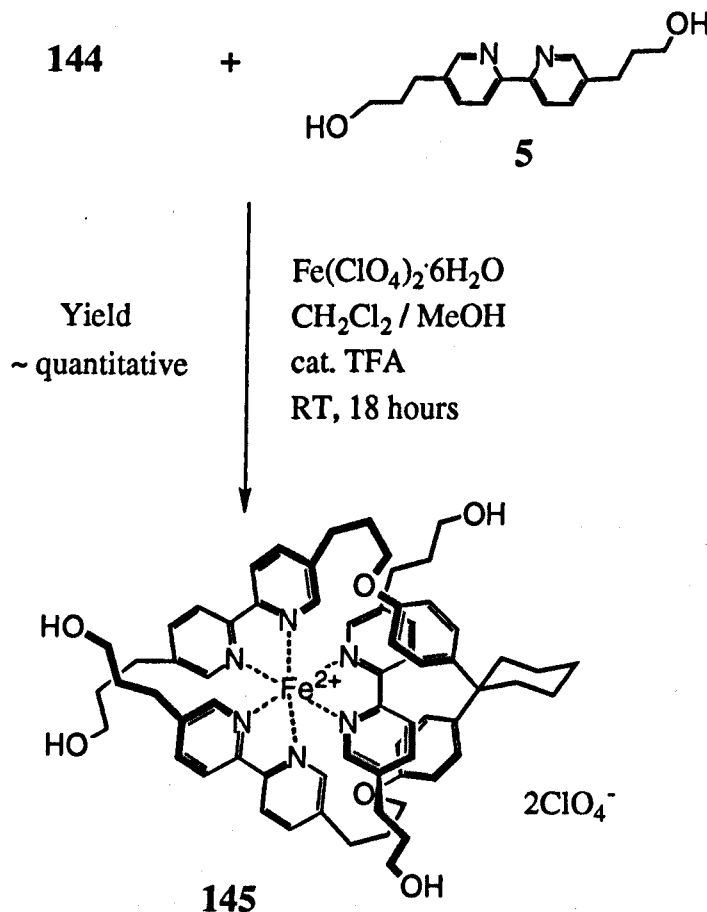
A monomer unit of this type could be assembled in principal in the same way and directed by the same interactions as the pseudo overhand knot already discussed. The synthesis of the new ligand required is outlined in Scheme A1.1.

<sup>1</sup> Y. Geerts, D. Muscat, K. Mullen, *Macromol. Chem. Phys.*, 1995, 196, 3425.



**Scheme A1.1.** *Synthesis of ligand 144.*

Coupling of bisphenol **9** and mono-TBDMS diol **78** using the Mitsunobu conditions discussed in Chapter 5 gave the protected 1:2 ligand **143** in 67% yield. Cleavage of the TBDMS protecting groups was achieved using 5-10% TFA in CH<sub>2</sub>Cl<sub>2</sub> to give **144** in 68% yield. Ligand **144** and diol **5** were then mixed with Fe(ClO<sub>4</sub>)<sub>2</sub>·6H<sub>2</sub>O in 2% methanol / CH<sub>2</sub>Cl<sub>2</sub> in a 1:1:1 ratio in the presence of catalytic TFA to aid equilibration as shown in Scheme A1.2.



**Scheme A1.2.** Assembly of a monomer unit for possible incorporation into polymers.

**145** is formed in almost quantitative yield as evidenced by the <sup>1</sup>H NMR spectrum of the crude product (Figure A1.2). Interestingly, **145** is formed almost instantaneously in contrast to the iron (II) pseudo overhand knot **104** discussed in Chapter 5. This can presumably be attributed to the fact that no "threading" process is required. Good evidence for the structure is again provided by the chemical shift changes induced on formation of **145** by shielding and deshielding effects of aromatic rings in close proximity (Figure A1.3). The distinctive upfield shift of bipyridine H<sub>3</sub> is clearly seen. Electrospray MS also indicates a 1:1 complex. The correct 1:1 complex is again presumably favoured due to  $\pi$ - $\pi$  interactions between the bipyridine and bisphenol units in **145**.

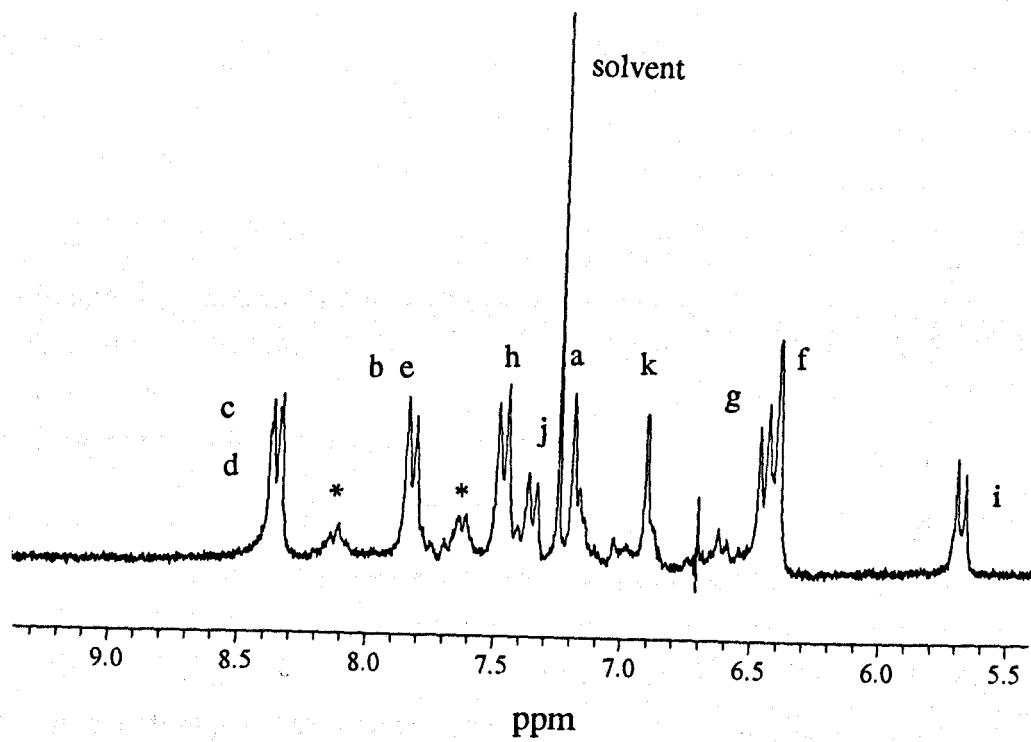
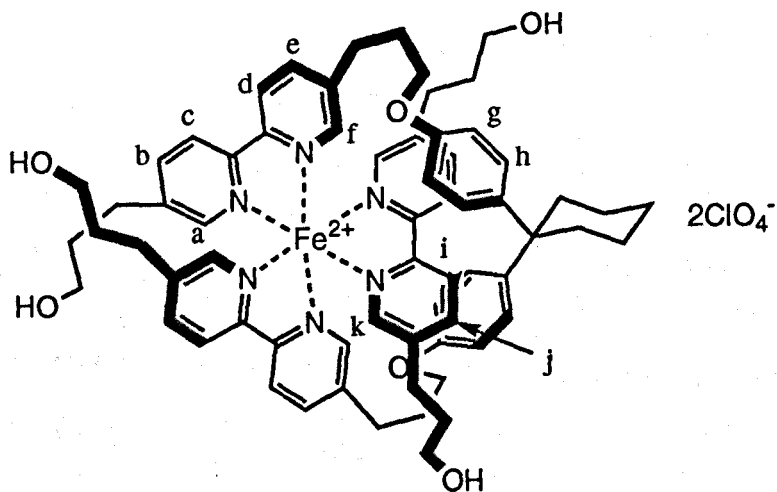


**Figure A1.2.** Aromatic region of the 250 MHz  $^1\text{H}$  NMR spectrum of **145** in 5% methanol /  $\text{CDCl}_3$ . Extraneous peaks indicated (\*) presumably arise from the presence of a small amount of other complexes or a slight mismatch in the required 1:1:1 stoichiometry due to difficulties in measuring the precise quantities required on small scale.

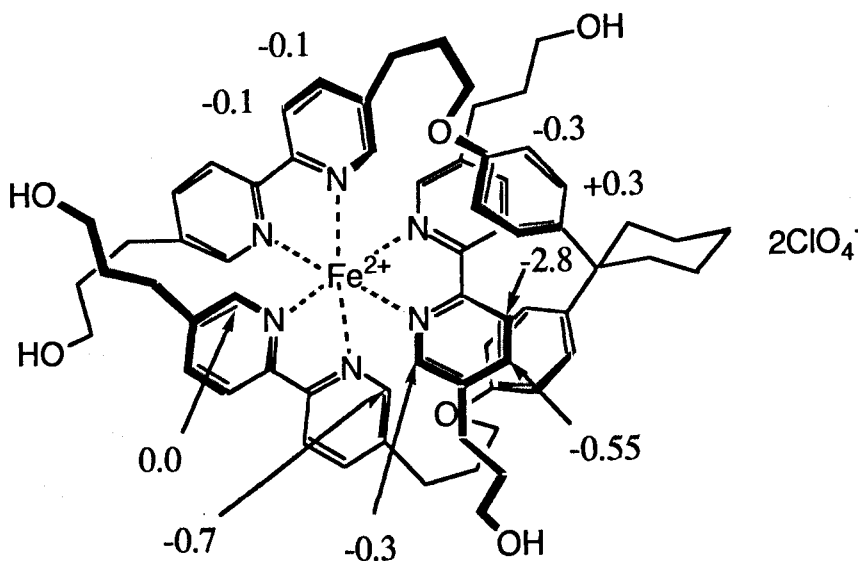


**Figure A1.3.** Changes in chemical shift induced upon formation of complex 145. Changes on the bipyridine unit have been corrected for the effect of coordination to the metal ion by comparison to iron (II) complex 74. Significant upfield shifts are shown in blue and downfield shifts in red.

In principle, it should be straightforward to alter the terminal hydroxyl groups to a wide variety of functionalities and hence provide a precise control of how derivatives of 145 become incorporated into polymer structures.<sup>‡</sup> Such structures may be interesting not only for the effects of topology on their properties but also for their ability to interact with metal ions. For example, it may be possible to alter the material properties of a given polymer by the presence or absence of various metal ions. Also, the geometry of the metal coordination sites may change under different physical conditions: for example, as a function of strain applied to the polymer.

<sup>‡</sup> Work to incorporate knotted subunits such as derivatives of 145 into polymer structures is being pursued by my colleague E. Ashworth.

## Appendix 1 Experimental Section

**1,1-Bis(3-(5'-(3-(*Tert*-butyldimethylsilyl)oxypropyl)-2,2'-bipyridine))propyloxyphenyl)cyclohexane (143).** To a solution of **78** (0.150 g, 0.388 mmol), **9** (0.052 g, 0.194 mmol) and tri-*n*-butyl phosphine (0.118 g, 0.582 mmol) in CH<sub>2</sub>Cl<sub>2</sub> (2 ml) at 0°C was added ADDP (0.147 g, 0.582 mmol) in one portion. The stoppered flask was stirred at room temperature for 18 hours before the product was filtered and evaporated. Flash chromatography on silica (2 cm x 25 cm) eluting with 0.5% methanol / CH<sub>2</sub>Cl<sub>2</sub> gave the title compound as a white solid (0.130 g, 67%).

m.p. 162 - 163°C.

<sup>1</sup>H NMR (250 MHz, CDCl<sub>3</sub>) δ0.04 (12H, s, Si(CH<sub>3</sub>)<sub>2</sub>), δ0.90 (18H, s, SiC(CH<sub>3</sub>)<sub>3</sub>), δ1.49 (6H, br, 3,4-cyclohexyl H), δ1.84 (4H, quintet, J = 7 Hz, -CH<sub>2</sub>CH<sub>2</sub>OTBDMS), δ2.10 (4H, quintet, J = 6.5 Hz, -CH<sub>2</sub>CH<sub>2</sub>OAr), δ2.20 (4H, br, 2-cyclohexyl H), δ2.73 (4H, t, J = 7 Hz, ArCH<sub>2</sub>CH<sub>2</sub>CH<sub>2</sub>OTBDMS), δ2.86 (4H, t, J = 6.5 Hz, ArCH<sub>2</sub>(CH<sub>2</sub>)<sub>2</sub>OAr), δ3.64 (4H, t, J = 7 Hz, -CH<sub>2</sub>OTBDMS), δ3.94 (4H, t, J = 6.5 Hz, -CH<sub>2</sub>OAr), δ6.79 (4H, d, J = 8.5 Hz, *ortho*-ArOR), δ7.16 (4H, d, J = 8.5 Hz, *meta*-ArOR), δ7.63 (4H, m, 4,4'-bipyridine H), δ8.27 (4H, m, 3,3'-bipyridine H), δ8.50 (4H, m, 6,6'-bipyridine H).

<sup>13</sup>C NMR (62.9 MHz, CDCl<sub>3</sub>) δ-5.3 (C3), 18.3 (C2), 22.9 (C27), 25.9 (C1), 26.4 (C26), 29.0 and 29.2 (C6, 17), 30.6 (C18), 33.9 (C5), 37.8 (C25), 45.0 (C24), 61.9 (C4), 66.4 (C19), 114.1 (C21), 120.5 and 120.6 (C9, 14), 128.1 (C22), 136.8 and 137.5 (C8, 15), 137.0 (C10, 13), 141.2 (C23), 149.2 (C7, 16), 153.8 and 154.1 (C11, 12), 156.4 (C20).

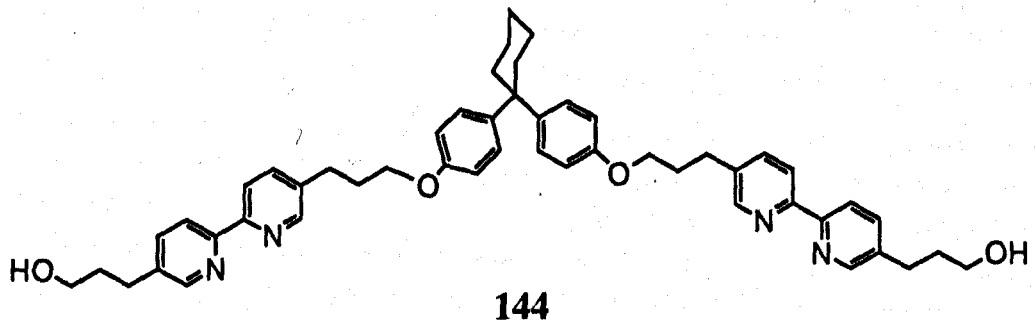
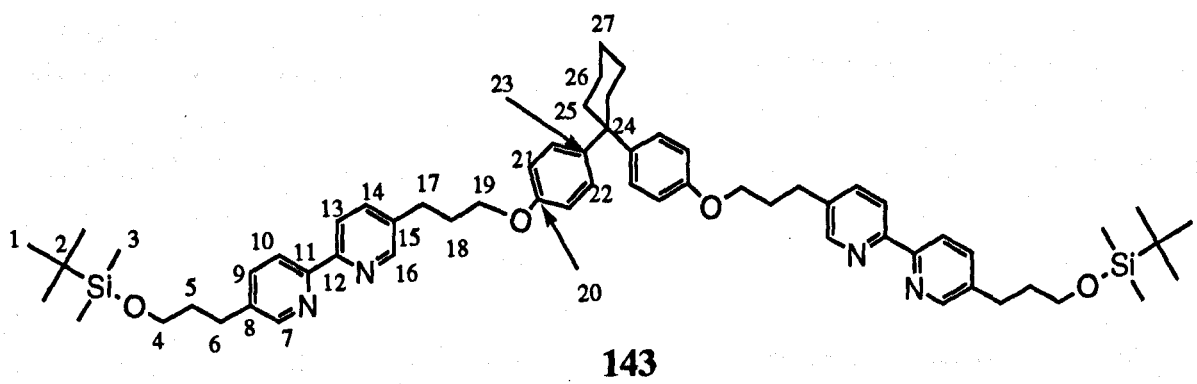
Calculated for C<sub>62</sub>H<sub>84</sub>N<sub>4</sub>O<sub>4</sub>Si<sub>2</sub>: C 74.06, H 8.42, N 5.57;

Found C 74.25, H 8.45, N 5.50.

**1,1-Bis(3-(5'-(3-hydroxypropyl)-2,2'-bipyridine))propyloxyphenyl)cyclohexane (144).** **143** (38 mg) in CH<sub>2</sub>Cl<sub>2</sub> (4 ml) containing water (1 drop) and TFA (15 drops) was stirred for 6 hours before being diluted with CH<sub>2</sub>Cl<sub>2</sub> (10 ml), washed with saturated aqueous NaHCO<sub>3</sub> (10 ml), dried (Na<sub>2</sub>SO<sub>4</sub>), filtered and evaporated. Flash chromatography on silica (1 cm x 18 cm) eluting with 5-10% methanol in CH<sub>2</sub>Cl<sub>2</sub> gave the product as a white powder (20 mg, 68%).

m.p. 178-180°C.

<sup>1</sup>H NMR (250 MHz, CDCl<sub>3</sub>) δ1.52 (6H, br, 3,4-cyclohexyl H), δ1.92 (4H, quintet, J = 6.5 Hz, HOCH<sub>2</sub>CH<sub>2</sub>-), δ2.11 (4H, quintet, J = 6.5 Hz, ArOCH<sub>2</sub>CH<sub>2</sub>-), δ2.21 (4H, br, 2-cyclohexyl H), δ2.80 (2 x 4H, 2t, J = 6.5 Hz, 2 x ArCH<sub>2</sub>-), δ3.68 (4H, t, J = 6.5 Hz, HOCH<sub>2</sub>-), δ3.95 (4H, t, J = 6.5 Hz, ArOCH<sub>2</sub>-), δ6.79 (4H, d, J = 8.5 Hz, *ortho*-ArOR), δ7.15 (4H, d, J = 8.5 Hz, *meta*-ArOR), δ7.64 (4H, dd, J = 8 Hz, J = 2 Hz, 4



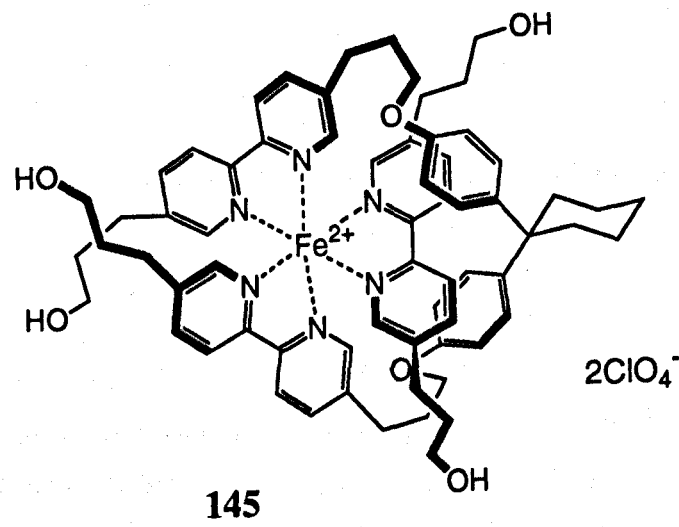
and 4'-bipyridine H),  $\delta$ 8.26 (4H, d, J = 8 Hz, 3 and 3'-bipyridine H),  $\delta$ 8.52 (4H, d, J = 2 Hz, 6 and 6'-bipyridine H).

FAB<sup>+</sup> MS m/z = 777.4346 (100%); C<sub>50</sub>H<sub>57</sub>N<sub>4</sub>O<sub>4</sub> requires 777.4380.

**[1,1-Bis(3-(5'-(3-hydroxypropyl)-2,2'-bipyridine))propyloxy phenyl)cyclohexane]-[5,5'-bis(3-hydroxypropyl)-2,2'-bipyridine] iron (II) perchlorate (145).** To a stirred solution of **144** (9.2 mg, 0.0118 mmol) and **5** (3.2 mg, 0.0118 mmol) in 10% methanol / CH<sub>2</sub>Cl<sub>2</sub> (10 ml) containing 2 drops of TFA was added Fe(ClO<sub>4</sub>)<sub>2</sub>.6H<sub>2</sub>O (0.0118 mmol) in 5% methanol / CH<sub>2</sub>Cl<sub>2</sub> (0.7 ml) over 5 minutes with the formation of a deep red coloration. Stirring was continued for 18 hours before washing with saturated aqueous NaHCO<sub>3</sub> (5 ml). The organic layer was then dried (Na<sub>2</sub>SO<sub>4</sub>), filtered and evaporated to give the title compound as a red solid. <sup>1</sup>H NMR spectroscopy indicated an almost quantitative yield with some small extraneous peaks that may correspond to other species in equilibrium with the desired product or may simply represent a small mismatch in the required stoichiometry.

<sup>1</sup>H NMR (250 MHz, CDCl<sub>3</sub>)  $\delta$ 5.69 (2H, d, J = 8 Hz, H<sub>i</sub>),  $\delta$ 6.60 (2H, s, H<sub>f</sub>),  $\delta$ 6.46 (4H, d, J = 8.5 Hz, H<sub>g</sub>),  $\delta$ 6.41 (2H, s, H<sub>k</sub>),  $\delta$ 7.19 (2H, s, H<sub>a</sub>),  $\delta$ 7.37 (2H, d, J = 8 Hz, H<sub>j</sub>),  $\delta$ 7.73 (4H, d, J = 8 Hz, H<sub>b</sub> and H<sub>e</sub>),  $\delta$ 8.38 (4H, d, J = 8 Hz, H<sub>c</sub> and H<sub>d</sub>). The complex aliphatic region of the spectrum could not be assigned completely by 1D NMR techniques.

ES<sup>+</sup> MS m/z = 553 (100%, [M-2ClO<sub>4</sub>]<sup>2+</sup>).



145

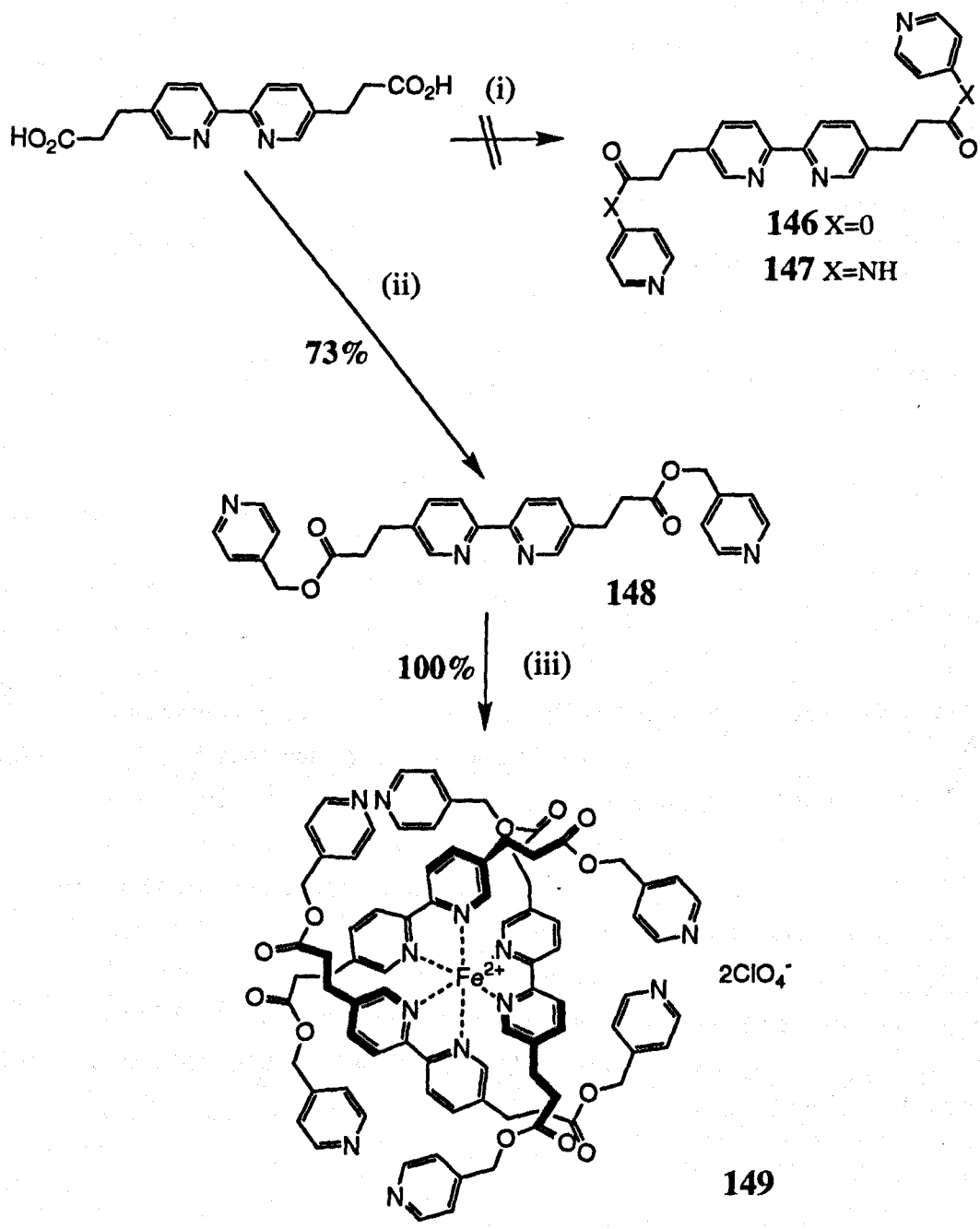
## Appendix Two: Macrocyclisation via Platinum Coordination

Many literature reports have discussed the use of platinum-pyridine bonding to form a variety of complex structures such as catenanes and molecular squares.<sup>1</sup> Some of the structures discussed in Chapter 4 such as the iron (II) hexaphenyl complex 74 (page 69) seemed good candidates to utilise in such an approach via conversion of the phenyl groups to pyridine. Macrocyclisation could then be attempted with the platinum complexes utilised by both Fujita and Stang. This led to the synthesis of the hexa-pyridyl iron (II) complex 149 (Scheme A2.1).

Attempts to convert diacid 6 to the diester 146 or diamide 147 were both unsuccessful. In the former case this was most likely due to the pyridone resonance form of 4-hydroxypyridine rendering it a poor nucleophile and in the latter case was most likely due to the extreme insolubility of the amide product. However, the reaction with 4-(hydroxymethyl)pyridine was successful and gave the diester 148 in 73% yield. Although this introduced an extra methylene group which was likely to reduce the required templating aromatic interactions between the pyridine ring and the coordinated bipyridine unit, this compromise seemed reasonable for initial feasibility studies.

Coordination of 148 to iron (II) was readily achieved using the standard procedure (see Chapter 3, page 48) and the pendant pyridyl esters resulted in no problems involving competing coordination reactions.

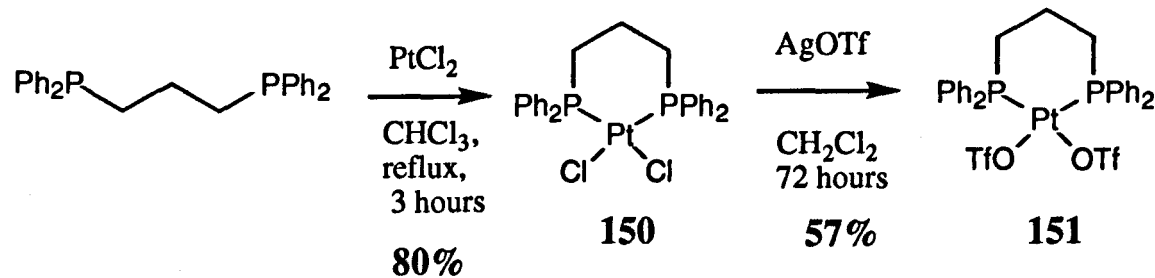
<sup>1</sup> Some recent examples: Stang, P.J.; Persky, N.E.; Manna, J. *J. Am. Chem. Soc.* 1997, 119, 4777. Manna, J.; Whiteford, J.A.; Stang, P.J.; Muddiman, D.C.; Smith, R.D. *J. Am. Chem. Soc.* 1996, 118, 8731. Fujita, M.; Sasaki, O.; Mitsuhashi, T.; Fujita, T.; Yazaki, J.; Yamaguchi, K.; Ogura, K. *J. Chem. Soc. Chem. Commun.* 1996, 1535. Fujita, M.; Ogura, K. *Coord. Chem. Rev.* 1996, 148, 249. Fujita, M.; Ibukuro, F.; Yamaguchi, K.; Ogura, K. *J. Am. Chem. Soc.* 1995, 117, 4175. Fujita, M.; Ibukuro, F.; Hagihara, H.; Ogura, K. *Nature* 1994, 367, 720.



*Conditions:* (i) 4-hydroxypyridine or 4-aminopyridine, EDC, DMAP,  $\text{CH}_2\text{Cl}_2$ , 0°C to RT, 18h; (ii) 4-(hydroxymethyl)pyridine, EDC, DMAP,  $\text{CH}_2\text{Cl}_2$ , 0°C to RT, 48h; (iii)  $\text{Fe}(\text{ClO}_4)_2$ , 5%  $\text{MeOH}$  in  $\text{CH}_2\text{Cl}_2$ , 30 mins, RT.

**Scheme A2.1. Preparation of iron (II) complex 149.**

The platinum complex **151** was prepared as outline in Scheme A2.2. *Cis*-dichloro-(1,3-bis(diphenylphosphino)propane platinum(II) **150** was prepared by refluxing the ligand with platinum (II) chloride.<sup>2</sup> Reaction with silver triflate then gave **151** in a procedure reported by Stang.<sup>3</sup>



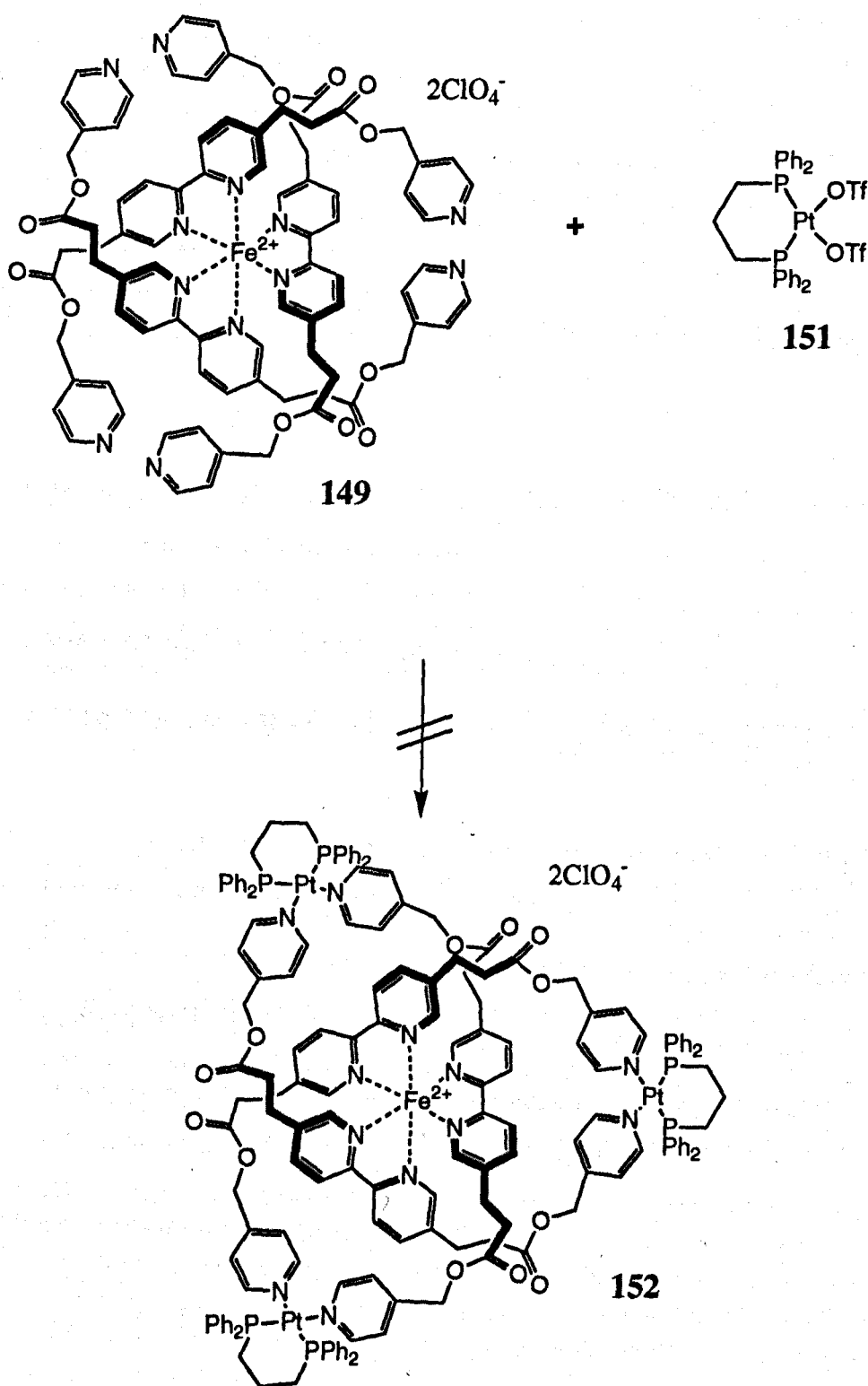
Scheme A2.2. Preparation of platinum (II) complex **151**.

Iron (II) complex **149** and 3 equivalents of platinum complex **151** were subjected to a high dilution reaction by addition of  $\text{CH}_2\text{Cl}_2$  solutions of both complexes to a flask containing vigorously stirred  $\text{CH}_2\text{Cl}_2$  over a period of several hours. After the reaction was complete, the solvent was removed and the product was obtained as a deep red solid.

Unfortunately, all attempts to characterise the solid by  $^1\text{H}$  NMR spectroscopy and mass spectrometry were unsuccessful, and no positive identification of any product was possible. This strategy was therefore not pursued any further. The results do however offer some encouragement. The fact that the pendant pyridyl esters do not have any adverse effect on the formation of the tris-bipyridine iron (II) complex and the bipyridine ligands clearly do not migrate from iron to platinum suggest that under the right conditions, this may still make a feasible strategy. In particular, the success of such reactions to produce a wide variety of structures in the literature, often in extremely high yield, suggests that this approach may still be worth pursuing in the future.

<sup>2</sup> Appleton, T.G., Bennett, M.A., Tompkins, I.B. *J. Chem. Soc. Dalton Trans.* 1976, 439.

<sup>3</sup> Stang, P.J., Cao, D.H., Saito, S. and Arif, A.M. *J. Am. Chem. Soc.* 1995, 117, 6273.



**Scheme A2.3.** Attempted preparation of knot 152 via macrocyclisation of 149 and 151.

## Appendix Two: Experimental Section

### **5,5'-Bis(2-carbo(4-pyridinemethoxy)ethyl)-2,2'-bipyridine (148).**

To a suspension of **6** (200 mg, 0.666 mmol) and 4-(hydroxymethyl)pyridine (363 mg, 3.33 mmol) in dry CH<sub>2</sub>Cl<sub>2</sub> (25 ml) at 0°C was added DMAP (8 mg, 10 mol%) and EDC (447 mg, 2.33 mmol). The solution was stirred for 18 hours at room temperature before washing with 1M sodium hydroxide (4 x 25 ml) and water (2 x 25 ml). The CH<sub>2</sub>Cl<sub>2</sub> solution was dried (Na<sub>2</sub>SO<sub>4</sub>), filtered and evaporated. The crude product was purified by flash chromatography on silica (2 cm x 20 cm) eluting with 5% methanol in CH<sub>2</sub>Cl<sub>2</sub> to give the title compound as a white solid (234 mg, 73%).

R<sub>f</sub> = 0.45 (10% methanol in CH<sub>2</sub>Cl<sub>2</sub>). m.p. 126 - 128 °C.

<sup>1</sup>H NMR (250 MHz, CDCl<sub>3</sub>) δ2.77 and δ3.03 (2 x 4H, 2t, J = 7 Hz, -CH<sub>2</sub>CH<sub>2</sub>-), δ5.09 (4H, s, ArCH<sub>2</sub>O<sub>2</sub>C-), δ7.13 (4H, d, J = 8.5 Hz, *meta*-pyridine H), δ7.64 (2H, dd, J = 8 Hz, 2 Hz, 4, 4'-bipyridine H), δ8.27 (2H, d, J = 8 Hz, 3,3'-bipyridine H), δ8.54 (6H, m, 6,6'-bipyridine H and *ortho*-pyridine H).

<sup>13</sup>C NMR (62.9 MHz, CDCl<sub>3</sub>) δ27.8 (C7), 35.1 (C6), 64.4 (C4), 120.6 (C10), 121.8 (C2), 135.5 (C9), 136.8 (C11), 144.6 (C3), 149.2 (C8), 150.0 (C1), 154.4 (C12), 171.8 (C5).

FAB<sup>+</sup> MS m/z = 483 (100%, MH<sup>+</sup>); C<sub>28</sub>H<sub>26</sub>N<sub>4</sub>O<sub>4</sub> requires 482.52.

**Tris-[5,5'-bis(2-carbo(4-pyridinemethoxy)ethyl)-2,2'-bipyridine] iron (II) perchlorate (149).** A solution of **148** (129 mg, 0.267 mmol) and Fe(ClO<sub>4</sub>)<sub>2</sub>.6H<sub>2</sub>O (0.089 mmol) in 5% methanol / CH<sub>2</sub>Cl<sub>2</sub> (4 ml) was stirred for 2 hours. The solvent was removed *in vacuo* to give the product as a red foam (152 mg, 100%).  
m.p. ca. 70 °C (dec.)

<sup>1</sup>H NMR (250 MHz, d<sub>6</sub>-acetone) δ2.63-2.88 (24H, m, ArCH<sub>2</sub>CH<sub>2</sub>-), δ5.07 (12H, s, -CO<sub>2</sub>CH<sub>2</sub>Py), δ7.26 (12H, d, *meta*-pyridine H), δ7.53 (6H, s, 6-bipyridine H), δ8.08 (6H, d, 4-bipyridine H), δ8.56 (12H, br, *ortho*-pyridine H), δ8.70 (6H, d, 3-bipyridine H).

ES<sup>+</sup> MS m/z = 751 (100%, [M-2ClO<sub>4</sub>]<sup>2+</sup>).

Calculated for C<sub>84</sub>H<sub>78</sub>N<sub>12</sub>O<sub>20</sub>FeCl<sub>2</sub>H<sub>2</sub>O: C 58.6, H 4.7, N 9.8;

Found: C 58.6, H 4.6, N 10.2.

**Pt(dPPP)Cl<sub>2</sub> (150).** 1,3-bis(diphenylphosphino)propane (0.31 g, 0.75 mmol) and platinum (II) chloride (0.20 g, 0.75 mmol) were heated at reflux in CHCl<sub>3</sub> (40 ml) under N<sub>2</sub> for 3 hours. Hexane (200 ml) was added to the hot solution and the white precipitate formed was removed by filtration and washed well with further hexane before drying *in vacuo* at 60 °C to yield the product as a fine white powder (0.410 g, 80%).

<sup>1</sup>H NMR (250 MHz, CDCl<sub>3</sub>) δ 2.05 (2H, br, PCH<sub>2</sub>CH<sub>2</sub>-), 2.52 (4H, br, -PCH<sub>2</sub>-), 7.32-7.82 (20H, m, ArH).

FAB<sup>+</sup> MS m/z = 678 (5%, M<sup>+</sup>), 643 (100%, [M-Cl]<sup>+</sup>).

**Pt(dPPP)(OTf)<sub>2</sub> (151).** To a solution of **150** (0.301 g, 0.444 mmol) in CH<sub>2</sub>Cl<sub>2</sub> (25 ml) in the absence of light was added AgOTf (0.912 g, 3.549 mmol). The mixture was stirred for 72 hours before filtering to remove precipitated AgCl. The filtrate was concentrated *in vacuo* to a volume of 5 ml and the product was precipitated by the addition of diethyl ether. The solid was removed by filtration, washed well with ether and dried *in vacuo* to give the title compound as a slightly off-white solid (0.230 g, 57%). m.p. > 250 °C.

<sup>1</sup>H NMR (250 MHz, CD<sub>2</sub>Cl<sub>2</sub>) δ 2.20 (2H, br, PCH<sub>2</sub>CH<sub>2</sub>), 2.66 (4H, br, -PCH<sub>2</sub>-), 7.4 - 7.6 (20H, m, ArH).

<sup>19</sup>F NMR (235 MHz, CDCl<sub>3</sub>) δ -78 ppm.

FAB<sup>+</sup> MS m/z = 756 (100%, [M - OTf]<sup>+</sup>), 606 (35%, [M - 2OTf]<sup>+</sup>), 302 (21%, [M - 2OTf]<sup>2+</sup>).

Calculated for C<sub>29</sub>H<sub>26</sub>S<sub>2</sub>O<sub>6</sub>P<sub>2</sub>F<sub>6</sub>Pt·2H<sub>2</sub>O: C 37.0, H 3.2, S 6.8;

Found: C 37.2, H 3.2, S 6.4.

**Attempted preparation of 152 via macrocyclisation of 149 and 151.** A solution of **149** (0.187 g, 0.110 mmol) in dry CH<sub>2</sub>Cl<sub>2</sub> (100 ml) and a solution of **151** (0.298 g, 0.3287 mmol) in dry CH<sub>2</sub>Cl<sub>2</sub> (100 ml) were simultaneously added dropwise at an equal rate to a flask containing rapidly stirred CH<sub>2</sub>Cl<sub>2</sub> (100 ml) over a period of 1 hour. After stirring for 48 hours, the deep red solution was concentrated *in vacuo* to ca. 75 ml and stirred vigorously with a solution of NH<sub>4</sub>PF<sub>6</sub> (6 g) in water (10 ml) for 24 hours to effect counterion exchange. The CH<sub>2</sub>Cl<sub>2</sub> layer was then separated, washed with water (2 x 50 ml), dried (Na<sub>2</sub>SO<sub>4</sub>), filtered and evaporated to give a red solid. TLC (10% methanol / CH<sub>2</sub>Cl<sub>2</sub>) indicated a major product with R<sub>f</sub> 0.50. Attempts to characterise the products by FAB<sup>+</sup> MS, ES<sup>+</sup> MS and <sup>1</sup>H NMR spectroscopy were unsuccessful.